

**Canopy transpiration of beech forests in Northern Bavaria –  
Structure and function in pure and mixed stands with oak  
at colline and montane sites**

Dissertation zur Erlangung der Doktorwürde (Dr. rer. nat.)  
der Fakultät für Biologie, Chemie und Geowissenschaften  
der Universität Bayreuth

vorgelegt von  
Markus W.T. Schmidt  
aus Düsseldorf

Bayreuth, November 2007



Die vorliegende Arbeit wurde zwischen Februar 1998 und November 2007 am Lehrstuhl für Pflanzenökologie der Universität Bayreuth unter Anleitung von Herrn Prof. John D. Tenhunen (Ph.D.) angefertigt.

Vollständiger Abdruck der von der Fakultät für Biologie, Chemie und Geowissenschaften der Universität Bayreuth genehmigten Dissertation zur Erlangung des akademischen Grades eines Doktors der Naturwissenschaften (Dr. rer. nat.).

Antrag auf Zulassung der Dissertation: 30. November 2007

Wissenschaftliches Kolloquium: 15. Februar 2008

Erstgutachter: Prof. J.D. Tenhunen (Ph.D.)

Zweitgutachter: Prof. Dr. E. Komor



---

## Table of contents

<b>Acknowledgements .....</b>	<b>iv</b>
<b>Abbreviations and symbols.....</b>	<b>vi</b>
<b>1 Introduction .....</b>	<b>1</b>
<b>2 Objectives .....</b>	<b>4</b>
<b>2.1. General objectives .....</b>	<b>4</b>
<b>2.2. Spatial levels of structure considered in the study .....</b>	<b>6</b>
<b>2.3. Review of the literature.....</b>	<b>7</b>
<b>2.3.1. Radial within-tree variations in wood anatomy and hydraulic properties .....</b>	<b>7</b>
<b>2.3.2. Influence of structure on whole-tree water use.....</b>	<b>13</b>
<b>2.3.3. Effects of stand structure on canopy transpiration and conductance .....</b>	<b>14</b>
<b>2.4. Hypotheses.....</b>	<b>16</b>
<b>3 Study sites .....</b>	<b>18</b>
<b>3.1. Steigerwald .....</b>	<b>18</b>
<b>3.2. Fichtelgebirge.....</b>	<b>21</b>
<b>3.3. Site characteristics .....</b>	<b>22</b>
<b>4 Methods.....</b>	<b>25</b>
<b>4.1. Measurements of sap flow with the thermal dissipation technique .....</b>	<b>25</b>
<b>4.1.1. Principles and conversions .....</b>	<b>25</b>
<b>4.1.2. Probe design .....</b>	<b>29</b>
<b>4.1.3. Field installations .....</b>	<b>29</b>
<b>4.1.4. Sample trees .....</b>	<b>30</b>
<b>4.1.5. Accuracy and errors .....</b>	<b>33</b>
<b>4.2. Tree and stand biometry.....</b>	<b>33</b>
<b>4.3. Sapwood area.....</b>	<b>34</b>

<b>4.4. Leaf area index of the canopy.....</b>	<b>38</b>
4.4.1. Direct estimates of LAI, allometric relationships .....	38
4.4.2. Semi-direct estimates of LAI, leaf area per unit dry mass .....	39
4.4.3. Indirect estimates of LAI .....	40
<b>4.5. Meteorological and soil measurements .....</b>	<b>41</b>
<b>5 Results.....</b>	<b>44</b>
<b>    5.1. Structural drivers of canopy transpiration.....</b>	<b>44</b>
5.1.1. Sapwood area.....	44
5.1.2. Stand structure .....	49
5.1.3. Leaf area index and related variables of tree and stand structure .....	53
5.1.3.1. Leaf area per unit dry mass.....	53
5.1.3.2. Leaf area index.....	54
5.1.3.3. Leaf area-to-sapwood area relationship.....	57
<b>    5.2. Atmospheric and soil conditions during the investigated years .....</b>	<b>60</b>
5.2.1. Steigerwald-sites Steinkreuz and Großebene .....	60
5.2.2. Fichtelgebirge-site Farrenleite .....	70
<b>    5.3. Radial within-tree variation of xylem sap flow density <math>J_s</math>.....</b>	<b>75</b>
<b>    5.4. Whole-tree water use <math>Q_t</math> of <i>Fagus sylvatica</i> and <i>Quercus petraea</i> .....</b>	<b>93</b>
<b>    5.5. Stand water use: Canopy transpiration and canopy conductance.....</b>	<b>100</b>
<b>6 Discussion .....</b>	<b>127</b>
<b>    6.1. Structural drivers of canopy transpiration.....</b>	<b>127</b>
<b>    6.2. Xylem sap flow density <math>J_s</math>.....</b>	<b>134</b>
6.2.1. Radial patterns of sap flow density $J_s$ in <i>Fagus sylvatica</i> .....	134
6.2.2. Sap flow density $J_s$ in <i>Quercus petraea</i> .....	138
6.2.3. General radial pattern of $J_s$ .....	140
6.2.4. Effects of soil conditions, and seasonal trends in general, on radial patterns of $J_s$ in <i>Fagus sylvatica</i> .....	143

---

<b>6.3. Whole-tree water use <math>Q_t</math></b> .....	<b>147</b>
6.3.1. $Q_t$ of European beech.....	147
6.3.2. $Q_t$ of sessile oak .....	151
<b>6.4. Canopy transpiration <math>E_c</math> and canopy conductance <math>g_c</math></b> .....	<b>157</b>
6.4.1. Structural controls on $E_c$ and $g_c$ .....	159
6.4.2. Comparison of beech in the Steigerwald and the Fichtelgebirge.....	166
6.4.3. Comparison of beech and oak in mixed stands in the Steigerwald .....	169
6.4.4. Variation of $E_c$ of beech and oak across Central Europe.....	176
<b>7 Conclusions</b> .....	<b>182</b>
<b>7.1. Review of hypotheses</b> .....	<b>182</b>
<b>7.2. Future perspectives</b> .....	189
<b>8 Summary</b> .....	<b>191</b>
<b>9 Zusammenfassung</b> .....	<b>193</b>
<b>10 References</b> .....	<b>196</b>
<b>11 Appendix</b> .....	<b>222</b>
11.1. Computer tomograms (Chapter 5.1.1).....	222
11.2. Allometric relationships (Chapter 5.1.2) .....	225
11.3. Atmospheric drivers and daily sap flow density (Chapter 5.3).....	227
11.4. Seasonal change of $J_s \text{ deep}/J_s \text{ 0-2cm}$ (Chapter 5.3) .....	228
11.5. Size classes of beech and oak for upscaling (Chapter 5.5) .....	229
11.6. Relationships of $E_c$ and atmospheric drivers (Chapter 5.5).....	230
11.7. Maximum daily $E_c$ of beech and oak stands (Chapter 6.4.1).....	234
11.8. Seasonal sums of $E_c$ (Chapter 6.4.4).....	236

## Acknowledgements

I am most sincerely grateful to Prof. John Tenhunen for entrusting me with this topic, for his invaluable, continuous support and numerous constructive discussions. I very much enjoyed the stimulating atmosphere at the Department of Plant Ecology and the opportunity to meet colleagues with diverse backgrounds which broadened my views and interests. I am very grateful for having had the chance to gain invaluable experience through teaching assignments, and through planning and carrying out fieldwork and research projects.

I am also greatly indebted to PD Dr. Barbara Köstner for the in-depth introduction to structure and function in forest ecophysiology and for many of the scientific ideas presented here, for inspiring discussions and constructive comments on an earlier version of the text. I am especially thankful to Dr. Reiner Zimmermann for sharing his invaluable experience in both the practical and theoretical aspects of sap flow and for sharing data from the Fichtelgebirge.

I am dearly indebted to Dr. Dennis Otieno for his support in Bayreuth and at remote field sites, for many stimulating discussions, and his friendship. I am deeply thankful to PD Dr. Eva Falge for creating an inspiring atmosphere at Plant Ecology and for always having had time for a question – and an answer, and to Stefan Fleck for his comradeship during joint fieldwork in the early days, for sharing biometric data, and the interesting exchange of ideas. I am greatly thankful to Marga Wartinger for her support in the lab and in the field and for her great companionship during countless field campaigns over the years. I am grateful to Annette Suske for manufacturing sap flow sensors and for introducing me to this discipline, for help in the field and in the lab; to Dr. Pedro Gerstberger for biometric data and for creating maps; to Wolfgang Faltin for sharing biometric data; to Barbara Scheitler for lots of help with field and lab work; to Ralf Geyer for carefully watching over data safety and permanency and for PC troubleshooting; and to all the colleagues I have met over the years at Plant Ecology for contributing to the warm atmosphere.

I am grateful to Gerhard Müller for invaluable advice on electronic questions, for logger maintenance and help with solar panels and the Hylipt, and to Gerhard Künfer for help with hardware, and to the former BITÖK (Bayreuth Institute for Terrestrial Ecosystem Research, now Bayreuth Center of Ecology and Environmental Research, BayCEER) for the excellent infrastructure provided.

My gratitude also extends to Prof. Y. Kakubari for the scientific cooperation, and Dr. Mitsumasa Kubota for sharing his software to calculate sap flow densities. I owe thanks to Dr. André Granier for very stimulating discussions, and to PD Dr. Gunnar Lischke for providing soil water and meteorological data from Steinkreuz.

I am grateful to the local forestry administration (formerly Forstamt Ebrach), particularly to Revierförster Geiz (Oberschwarzach), for their support, and to the regional forestry administration (formerly Oberforstdirektion Oberfranken) for access to literature and to forestry economic plans. Also I am much obliged to the Bavarian State Institute of Forestry (LWF) for meteorological data from their network of forest climate stations.

And last but not least I am most deeply indebted to my parents and my own family for their overwhelming help and the confidence they gave me, and in particular Mathilde and Claire who helped me to put matters into perspective, and for the sacrifices they all made over the years. This work would not have been possible without the tremendous support from Iris.

This study was funded by the Bundesministerium für Bildung und Forschung (BMBF), contracts PT BEO – 0339476 C and D.

## Abbreviations and symbols

$\alpha$	Absorption coefficient for $\gamma$ -radiation multiplied by $10^3$ , $\text{cm}^{-1}$
$\alpha_c$	Angle of crown opening, $^\circ$
$\Delta T_a$	Current temperature difference, K
$\Delta T_{\max}$	Maximum temperature difference
$\theta$	Soil water content, $\text{m}^3 \text{ m}^{-3}$
$\theta_e$	Relative extractable soil water
$\theta_F$	Soil water content at field capacity, $\text{m}^3 \text{ m}^{-3}$
$\rho_{wd}$	Wood density, $\text{g cm}^{-3}$
$\Psi_{\text{soil}}$	Soil water potential, kPa
$A_b$	Basal area of a stand, $\text{m}^2 \text{ ha}^{-1}$
$A_{bt}$	Basal area of a tree, $\text{m}^2$ or $\text{cm}^2$
$A_s$	Sapwood area of a stand, $\text{m}^2 \text{ ha}^{-1}$
$A_{st}$	Sapwood area of a tree, $\text{m}^2$ or $\text{cm}^2$
CBH	Circumference of a tree at breast height, i.e. 1.3 m above the ground, cm
CT	Computer (or computed or computerised) tomography
CV	Coefficient of variation (standard deviation/average of sample)
d	Diameter of a tree at a height different from breast height, cm
D	Vapour pressure deficit of the air, hPa
$D_{\text{avg}}$	D averaged over one day (24 h), hPa
$D_{\text{integr}}$	D integrated over a season, kPa
DBH	Diameter of a tree at breast height, i.e. 1.3 m above the ground, cm
$E_{c \max}$	Seasonal maximum of daily integrated canopy transpiration, $\text{mm d}^{-1}$
$E_{c \text{ season}}$	Seasonal sum of daily integrated canopy transpiration, $\text{mm season}^{-1}$
$E_c$	Canopy transpiration, $\text{mm s}^{-1}$
$g_{c \max}$	Maximum diurnal canopy conductance, $\text{mm s}^{-1}$
$g_c$	Canopy conductance, $\text{mm s}^{-1}$
$h_t$	Tree height, m
$J_s$	Sap flow density, $\text{g m}^{-2} \text{ s}^{-1}$
$J_{s \text{ 0-2cm}}$	Sap flow density in 0–2 cm radial sapwood depth
$J_{s \text{ day}}$	Daily integrated $J_s$ (24 h), $\text{kg m}^{-2} \text{ d}^{-1}$
$J_{s \text{ deep}}$	$J_s$ in 2–4 cm ( $J_{s \text{ 2-4cm}}$ ) or 4–6 cm ( $J_{s \text{ 4-6cm}}$ ) sapwood depth
$J_{st}$	Sapwood area-weighted average $J_s$ of a tree, i.e. $Q_t/A_{st}$ , $\text{g m}^{-2} \text{ s}^{-1}$ , $\text{kg m}^{-2} \text{ d}^{-1}$
LAI	Leaf area index, projected leaf area in $\text{m}^2$ per $\text{m}^2$ of ground area
PAI	Plant area index, projected area of all light-intercepting elements of a canopy
PCA	Plant Canopy Analyser, LAI-2000, optical instrument to estimate PAI, LAI, WAI
PFD	Photosynthetical photon flux density, $\mu\text{mol m}^{-2} \text{ s}^{-1}$
$PFD_{\text{day}}$	PFD integrated over a day (24 h), $\text{mol m}^{-2} \text{ d}^{-1}$
$PFD_{\text{integr}}$	PFD integrated over a season, $\text{mol m}^{-2} \text{ season}^{-1}$
$q_r$	$J_{s \text{ day deep}}/J_{s \text{ day 0-2cm}} \cdot J_{s \text{ day 0-2cm}}^{-1}$ , $\text{kg}^{-1} \text{ m}^2 \text{ d}$

---

$Q_r$	Sap flux in one annulus, $\text{g s}^{-1}$
$Q_{t \text{ avg}}$	Seasonally averaged daily tree water use, $\text{kg d}^{-1}$
$Q_{t \text{ day}}$	Daily (24 h) integrated tree water use, $\text{kg d}^{-1}$
$Q_{t \text{ hh max}}$	Maximum seasonal value of half-hourly tree water use, $\text{kg h}^{-1}$
$Q_{t \text{ max}}$	Maximum seasonal value of daily integrated tree water use, $\text{kg d}^{-1}$
$Q_{t \text{ sum}}$	Seasonally integrated tree water use, $\text{kg season}^{-1}$
$Q_t$	Sap flux in one tree, or tree water use, $\text{g s}^{-1}$
$R_w$	Relative water content, %
SAI	Stem hemi-surface area index
$T_{\text{air}}$	Air temperature, measured at 2 m above the ground, $^{\circ}\text{C}$
WAI	Wood area index, projected area of e.g. stems and branches per ground area
$W_f$	Water content, $\text{g cm}^{-3}$



## 1 Introduction

The natural vegetation of Central Europe is dominated by European beech (*Fagus sylvatica* L.) (Ellenberg 1996), its altitudinal distribution here ranging from the lowlands in the north to montane zones in the sub-Mediterranean (Meusel et al. 1965). Additional important species with overlapping distribution are pedunculate oak (*Quercus robur* L.) in lowlands and sessile oak (*Quercus petraea* (MATT.) LIEBL.) in colline to sub-montane regions in Central Europe (Walter and Breckle 1994). The dominance of sessile oak is confined to areas where soils are too dry for beech (Ellenberg 1996). Intensive human impacts on land cover began in the Neolithic Period and large-scale influences occurred since the Middle Ages (Firbas 1949). Forest cover in Germany was reduced from about 90 % around 700 AD to 15 % around 1300, and has increased again to 30 % over the last 400 years (Bork et al. 2001). Deforestation, afforestation and soil degradation have also changed the distribution and dominance of forest tree species. Today, forest management is the prime determinant of species composition. Of the  $10.7 \cdot 10^6$  ha forested area of Germany, only 34 % are broadleaved deciduous forests (BMVEL 2001a), 14 % are dominated by beech, 9 % by oak (BMVEL 2001b). It has been suggested that beech forests would naturally cover 66 % of Germany (Bohn et al. 2003). In Bavaria, where about one quarter of Germany's forests stock, coverages are slightly lower (25 %, 11 %, and 5 %, respectively), and Norway spruce (48 %) and Scots pine (23 %) clearly dominate (Bayerische Staatsforstverwaltung 2002). Under current climatological and pedological conditions, the proportion of beech in Bavaria's forests would naturally amount to 60–70 % (Kölling and Walentowski 2001). In Germany 13 % of all forests are “pure” broadleaved forests (< 10 % admixed conifers) and 43 % are mixed forests (> 10 % admixed species) (BMVEL 2001a), the latter increasing in importance over the last few decades (Smaltschinski 1990, Krüger and Mößmer 1993, Krüger et al. 1994).

Forests play a prominent role in terrestrial carbon and water cycles, and the water flux quantitatively is the most important flux in an ecosystem. Forests serve as water filters and reservoirs and about one fifth of Bavaria's forests are explicitly assigned to functions of water protection, stressing their importance in drinking water and ground-water management and in flood and erosion control. Forests are additionally a large source of water vapour, in the form of physically controlled, unproductive evaporation of intercepted precipitation and from the soil, and, due to the linking of carbon dioxide ( $\text{CO}_2$ ) and water fluxes via the plant leaves' stomata, of productive, biologically controlled transpiration. Exchange processes of water vapour and  $\text{CO}_2$  between the forest canopy and the atmosphere have gained wider interest in the context of research on global change and the function of forests as a source of, or sink for carbon, and knowledge on atmospheric gas exchange has increased significantly during the last two decades, a period during which micrometeorological eddy-covariance techniques were improved and employed in forest canopies (e.g. Baldocchi et al. 1988, Baldocchi 2003, Valentini 2003).

Besides the well-recognised influence of short-term atmospheric controls over forest canopy transpiration via available energy and vapour pressure deficit of the air, the structure of a stand also exerts long-term control over water fluxes (e.g. Shuttleworth 1989). In forest ecology, structure refers to the spatial and temporal distribution of trees in a stand (Oliver and Larson 1990). Also, patterns in stand structure can be described by the number, rate of change, or spatial distribution of trees or parts of

trees, by species, or age classes (Oliver 1992). The structural traits of forests relevant in water and carbon flux regulation include for instance stand density, basal area, sapwood area, tree height, crown length, projected crown area, leaf area index, leaf area density, and species composition. These characteristics, on the one hand, modify the atmospheric environment of a tree and its edaphic conditions. On the other hand, structure is also a feature that acts on plant water use on its own, independent of atmosphere and soil, e.g. via sapwood area and species composition. Structure in this sense can be regarded as a species-specific characteristic modulated by intra- and interspecific competition. The physiology and hydraulic architecture of the individual species then determines the integrated stand response.

In contrast to relationships between forest function and atmospheric and edaphic variables, comparatively little is known about the structural controls of transpiration (Peck and Mayer 1996, Ryan 2002), particularly of deciduous forests (Raulier et al. 2002). For coniferous forests our knowledge has improved during the last few years (e.g. Alsheimer et al. 1998, Köstner et al. 2001). There is a growing need for a more comprehensive understanding of the structure-function relationships of forests since forest policy e.g. in Germany currently aims at increasing the vertical and horizontal structural diversity of forests and at adopting the principles of sustainable and ecological, near-natural silviculture (BMVEL 2003, UBA 2003). This policy includes for instance small-scale harvesting and abandoning clear-cutting, natural regeneration in small canopy gaps, conversion of even-aged plantations, in particular of Norway spruce, into uneven-aged mixed species forests with special emphasis on beech and oak and other site-adjusted species (BMVEL 2003, UBA 2003). Ecological benefits expected from highly structured mixed forest stands are higher physical stability, better use of resources, higher resistance to pests and higher resilience towards environmental changes and extremes (e.g. Cannell et al. 1992, Kelty et al. 1992, Larson 1992, Thomasius 1992, König et al. 1995, Pretzsch 2003, UBA 2003). Beneficial effects are most apparent when specific resource limitations are compensated by an adapted species or when species differ in their ecological amplitude (Kelty 1992, Rothe and Kreutzer 1998, Pretzsch 2003). Demands on forests have increased also with respect to carbon pool accounting and management (Valentini 2003) and flood, water pollution and erosion control (UBA 2003). Thus understanding the regulation of the carbon and water fluxes at tree and stand level regarding structure should also help to improve quantitative management strategies (Tenhunen et al. 1998).

While micrometeorological techniques are used to determine spatially integrated net ecosystem fluxes of CO<sub>2</sub> and water vapour over extended forest canopies, it is not possible to discern physically from biologically controlled fluxes (see above) or fluxes from different ecosystem compartments. Thus, additional measurements and modelling are required to analyse and explain contributions to total fluxes at the ecosystem level (Ehman et al. 2002). Further, measurements of eddy covariance under non-ideal conditions (sloped terrain, non-turbulent atmospheric conditions, wet canopy) result in error-prone estimates (Balocchi 2003). Long established hydrological methodologies usually integrate to catchment level and derive canopy transpiration as the residual, with errors being propagated, and most do not distinguish between transpiration and evaporation (Wullschleger et al. 1998, Savenije 2004). Gas exchange measurements at the leaf level must be scaled-up to the tree crown or forest canopy level (Beyschlag et al. 1995, Balocchi and Amthor 2001, Tenhunen et al. 2001).

Between gas exchange measurements at small scales and micrometeorological and hydrological measurements at larger scales, sap flow measurements at the branch, tree and plot level have been used to validate gas exchange models (Falge et al. 2000, Fleck 2002) and to interpret total fluxes of eddy-covariance measurements (Köstner et al. 1992, Granier et al. 1996a, 2003, 2007). Sap flow measurements are the only technique providing continuous water fluxes at the whole-tree level in situ under (all) natural atmospheric conditions and in any type of terrain, separating tree water flux from other sources, and directly enabling its analysis with respect to tree size, age and species (e.g. Köstner et al. 1992, Granier et al. 1996b, Wilson et al. 2001, Catovsky et al. 2002).

Investigation of the effects of species composition as a structural feature influencing canopy transpiration is required in forest stands of *F. sylvatica* mixed with *Q. petraea*, because the two species naturally and potentially dominate and co-exist in large areas (e.g. Walentowski et al. 2001) and will be promoted as co-dominants in the future (BMVEL 2003, UBA 2003), while they have different physiological and morphological traits, which could lead to synergistic and/or antagonistic effects in mixed compared to pure stands.

## 2 Objectives

### 2.1. General objectives

The importance of beech for Central European forests and the increasing significance of mixed forests requires more knowledge of the relationships between water use and stand structure. **The overall goal of this study was therefore to quantify and analyse the function of beech forest stands, as a whole and of the individual trees composing it, regarding the water use of the canopy and its short-term control by environmental drivers of transpiration and its long-term control by structural characteristics.**

Given the longevity and temporal inertia of forests, especially of mature temperate hardwood forests (e.g. “lag” phase after silvicultural treatment during which competition is increased for the newly available resources until canopy closure and a new steady state is reached again), it is not possible to assess the effects of a changed structure on function in the same stand within the framework of a conventional study. Furthermore, it is not possible to find and to study a sufficient number of stands in the field with gradually differing structure under the same environmental conditions. Therefore, detailed gas exchange models depending on 3D-stand structure and related microclimate (e.g. Wang and Jarvis 1990a, Cescatti 1997, Falge et al. 1997, 2000) are appropriate analytical tools to study potential effects of structure on stand gas exchange. Simulation models on the other hand can only be as comprehensive as the set of input parameters, and models need to be calibrated and validated. These data are largely lacking, especially for deciduous forest trees and in particular for beech. **The present study thus was aimed at establishing functional relationships between transpiration at tree and canopy level and its controlling atmospheric and structural drivers from direct measurements, overcoming methodological shortcomings and uncertainties of other methods and studies** (see above and Tenhunen et al. 1998) and thus also laying the basis for spatially explicit modelling of canopy gas exchange of water and CO<sub>2</sub> (see Fleck 2002, Fleck et al. 2004).

These functional relationships were sought in a **regional context of beech stands distributed across Upper Franconia**, northern Bavaria. Therefore the sites selected for this study were on the one hand located in an area where *F. sylvatica* occurs in mixed stands with *Q. petraea*, in order to investigate the structural effects of species composition on water use: the Steigerwald (Fig. 3.1.1), a forest-rich, low-elevation (colline to sub-montane) hillside region in western Upper Franconia in northern Bavaria offers some unique opportunities in this respect due to its history of land-use and forest management. On the other hand water use in *F. sylvatica* was studied in the Fichtelgebirge, a mountain range in north-eastern Upper Franconia, where the species is at its current upper altitudinal limit of distribution in the whole region (north-eastern Bavaria, south-eastern Thuringia, south-western Saxony, eastern Czech Republic) and probably also close to its potential altitudinal limit in the region (Meusel et al. 1965). A comparison of beech in the Steigerwald and the Fichtelgebirge may reveal the **influence of climate and elevation on water use when considered at regional scale**. The selected sites also offered the rare chance to study autochthonous deciduous forest stands, unlike in many forest regions in Germany where the natural vegetation has been replaced by coniferous monoculture plantations.

To study water flux regulation in forest stands by atmospheric and structural drivers, selecting methodology which allows continuous access to tree-level transpiration in any terrain is imperative (see Chap.1). Sap flow techniques meet this requirement (e.g. Smith and Allen 1996, Köstner et al. 1998a) and the sap flow methodology best suited for the purpose of this study on mature forest trees (see Swanson 1994) was considered to be the thermal dissipation sap flow technique introduced by Granier (1985, 1987a). This steady-state, thermoelectric tissue heat balance method has been shown to be accurate by validation (Köstner et al. 1998a, Clearwater et al. 1999, Catovsky et al. 2002, Herbst et al. 2007a, b) and extension of the original (Granier 1985) calibration to higher sap flow rates as encountered e.g. in vines (Braun and Schmid 1999). The thermal dissipation sap flow technique compares with other methodologies such as eddy covariance (e.g. Granier et al. 1990, 1996a, 2000a, 2007; Diawara et al. 1991, Kelliher et al. 1992, Köstner et al. 1992, Berbigier et al. 1996, Hogg et al. 1997, Saugier et al. 1997, Oren et al. 1998, Catovsky et al. 2002), other sap flow techniques (Granier et al. 1994, 1996b, Köstner et al. 1996, 1998b, Alsheimer et al. 1998, Schaeffer et al. 2000, Lundblad et al. 2001), water absorption in cut trees (Granier et al. 1994), or with qualitative staining (Granier et al. 1994) and thermal imaging techniques (Anfodillo et al. 1993, Granier et al. 1994).

The thermal dissipation technique combines features important in continuous, plot-level and remote field use on large, adult forest trees with rather simple calculations of sap flow: It is suitable for monitoring sap flow over a whole season or longer (e.g. Granier et al. 1996b, Köstner et al. 1998a, Oliveras and Llorens 2001) since the wounding is minimal due to the small dimensions of the probes (2 mm diameter, typically 2 cm in radial length) and its electrical inertia from the tree. Installation in remote areas is greatly facilitated by the low power requirements of heaters and regulators, easily met by photovoltaic cells, as well as by the sturdy and rather simple electronic implementation and low data storage requirements of one data logger channel per gauge. Implanting the probes into trees is easily accomplished, though errors in sensor placement can lead to large errors when extrapolating readings to the whole tree (Nadezhina et al. 2002). The equipment is comparatively inexpensive, especially when self-manufactured, and thus makes quantitative sampling aimed at assessing and representing spatial heterogeneity in water fluxes affordable. Further, adaptations in design to accommodate specific experiments are easily carried out as a variety of modifications demonstrate (e.g. Granier et al. 1990, 1994, 1996a, 2000a, Lu et al. 2000, Brooks et al. 2002, James et al. 2002, Ford et al. 2004a, Geßler et al. 2005). Re-calibration or validation may be required, however, as e.g. exemplified by Goulden and Field (1994), Catovsky et al. 2002, Ford et al. (2004a), Herbst et al. (2007a, b) and McCulloh et al. (2007), depending on the extent of deviation from original construction, especially if the power supplied to the heater deviates from the original value of 200 mW (Granier 1985, Goulden and Field 1994, Lu et al. 2004).

Thermal dissipation probes of the original design (Granier 1985, 1987a) integrate over a radial length of 20 mm. This is a spatial resolution intermediate between the other widely used thermoelectric sap flow methods, namely the heat pulse velocity probes, which ideally would return “point” estimates but typically rather integrate over 7-8 mm (Swanson 1974), and the trunk sector heat balance gauges which usually integrate sap flow over the whole sapwood radius (Cermák et al. 1973, Kučera et al. 1977). The 20 mm-design of the Granier-type probes offers flexibility to study trees with small as well as with large water-conducting wood cross-sectional areas (i.e. sapwood area) with the same make of instruments by employing an appropriate

number of gauges in increasing radial depth from the sapwood-cambium to the sapwood-heartwood boundary. Also, the spatial integration of a standard thermal dissipation probe is large enough to reduce the additional uncertainty related to the spatial interpolation from individual probes to the whole tree (Hatton et al. 1995) to a statistically robust and practically sound level.

## 2.2. Spatial levels of structure considered in the study

Using the thermal dissipation technique to explicitly assess axial sap flow rates in incremental radial depths of the sapwood of trees with large sapwood area offers the opportunity to study the function of structure in water flux regulation on a within-tree level, and on hourly to seasonal time scales (cf. Phillips et al. 1996). Thus, in the context of regulation of forest canopy transpiration, the following spatial levels of structure were addressed in this study:

- The **tree-internal structure** of the xylem. The wood anatomy or hydraulic architecture of a tree or a tree species may exert control over transpiration at small spatial scales (in an order of magnitude of  $10^{-5}$  to  $10^{-2}$  m). For instance, a tree species with large sapwood area might use its sapwood area variably depending on environmental conditions.
- On a larger scale ( $10^{-1}$ – $10^1$  m), structure can relate to **individual trees and to the internal structure of a stand**, e.g. the leaf area of a tree, tree basal area, tree sapwood area, tree spacing, neighbouring species, and may constrain the water use of a single tree.
- At the stand level ( $10^2$ – $10^3$  m), the **structure of the whole stand** may control stand water use e.g. via stand density, species composition, basal area of the stand, sapwood area of the stand, leaf area index. At this scale new properties of a stand emerge, for instance the aerodynamic roughness of the canopy as an important structural determinant of gas exchange processes between canopy and atmosphere. The stand level is also the scale to which forest management, remote sensing, 3D-models of carbon and water fluxes, and micrometeorological methods integrate.

The three discerned levels of structural integration also reflect the steps of scaling-up water fluxes from the sap flow sensor to the forest canopy and will be introduced in more detail in the following chapters.

## 2.3. Review of the literature

### 2.3.1. Radial within-tree variations in wood anatomy and hydraulic properties

Wood anatomy. Sapwood as defined by the International Association of Wood Anatomists is the portion of the wood that, in the living tree, contains living cells and reserve materials (e.g. starch; Committee on Nomenclature 1964). Water, following gradients in water potential, is transported in the sapwood through conductive elements (mainly vessels and tracheids); these conduits consist of dead cells when fully functional in long-distance water transport. The cross-sectional sapwood area of a tree ( $A_{st}$ ) and of the whole stand ( $A_s$ ) need to be known if the tree and stand water use are to be scaled up from measurements of sap flow density (sap flow per unit of sapwood area) with thermal dissipation probes (Köstner et al. 1998a, see below). Heartwood is defined as the inner layers of wood which, in the growing tree, have ceased to contain living cells and in which reserve materials (e.g. starch) have been removed or converted into heartwood substances. It is generally darker in colour than sapwood, though not always clearly differentiated (Committee on Nomenclature 1964). Thus in tree species in which the colour of wood obligatorily changes upon heartwood formation through accumulation of phenolic compounds (Magel et al. 1997), the distinction between sapwood and heartwood is easily accomplished, as for instance in *Quercus*, *Juglans*, *Pinus* and *Larix* species. In some species, such as European beech (*Fagus sylvatica* L.), no coloured heartwood is formed, but a "ripenwood" is discernible by its lower water content (Grosser 1977, Hillis 1987) and by the almost complete absence of storage carbohydrates (Magel et al. 1997, Wagenführ 2000). In these species facultative heartwood formation, caused by external factors and not internally controlled, may occur (Magel et al. 1997). This "discoloured" wood is irregular and not strictly bound to annual rings, but similar to obligatorily formed and coloured heartwood in that it contains no living cells and in that it is darker than sapwood. Thus in contrast to regular heartwood, the area of discoloured wood and ripewood do not have to be congruent.

Sapwood is usually wider in diffuse-porous than in ring-porous angiosperm tree species (Huber 1935). The large radial dimension of sapwood encountered e.g. in mature diffuse-porous European beech requires the measurement of axial sap flow along the radius of sapwood if functional understanding and quantitative, defensible scaling-up to whole-tree and stand level is sought (Edwards and Booker 1984, Hatton et al. 1990, 1995, Phillips et al. 1996, Cermák and Nadezhina 1998, Köstner et al. 1998a, Oren et al. 1998), since it can be inferred from anatomical observations that resistance to axial sap flow in vessels and tracheids may vary considerably in radial direction: wood structure changes with the age of the cambium producing the wood (i.e. from pith to bark, from "juvenile" or "immature wood" to "adult" or "mature wood"). Conduit length and, more important in angiosperm tree species, conduit diameter generally increases with cambial age (e.g. Zobel and van Buijtenen 1989, Romberger et al. 1993):

The average vessel diameter increases with cambial age in *F. sylvatica* (Gasson 1985, 1987, Vollenweider et al. 1994), in *Quercus petraea* (Helinska-Raczkowska 1994) and in ring- and diffuse-porous tree species in general (Gartner and Meinzer 2005). Vessel length also increases with age like vessel diameter (Tyree and Zimmermann 2002; for beech: Buchmüller 1986) and long vessels are more efficient in water transport than short ones (Tyree and Zimmermann 2002), but there are always also small, short vessels for safety (Zimmermann 1983, Buchmüller 1986). Many tree species produce longer vessels in spring (earlywood) than in summer (latewood; Zimmermann and Potter 1982) and

vessel length is correlated with vessel diameter: wide vessels are generally long, narrow vessels short (Greenidge 1952, Zimmermann and Jeje 1981, Sperry et al. 2005; for beech: Buchmüller 1986). The earlywood serves primarily conducting functions, latewood more mechanical functions (Bosshard 1976, Tyree and Zimmermann 2002). In oak, the earlywood radius is almost constant ("endogenous control": Gasson 1987; but the climatic conditions during the previous year have an influence: Bouriaud et al. 2004, Lebourgeois et al. 2004, Skomarkova et al. 2006) and the latewood radius is dependent on (current-year) environmental variables such as soil water availability (Gasson 1987, Bréda and Granier 1996). A low proportion of latewood in ring-porous oaks results in a low wood density due to the large cross-sectional area of the wide earlywood vessels (Gasson 1987). Vessel formation at the beginning of cambial activity is mainly controlled by internal factors in beech as well and external factors only have a minor influence, which increases later during cambial activity (Sass and Eckstein 1995). There is no abrupt change between earlywood and latewood in *F. sylvatica* but a more gradual decline in vessel diameter (Gasson 1987), and whole-ring wood density proved to be less variable interannually than ring width (Bouriaud et al. 2004, see also Sass and Eckstein 1995). Wood density  $\rho_{wd}$  (in g cm<sup>-3</sup>) is determined primarily by conduit lumen area and conduit wall thickness (e.g. Swenson and Enquist 2007).

**Hydraulic conductivity.** Thus the resistance to axial water flow generally decreases from the pith to the youngest growth rings, or hydraulic conductivity increases (e.g. Zobel and van Buijtenen 1989, Romberger et al. 1993). The hydraulic conductivity  $K_h$  is the (sap) flow rate through a stem segment of a unit length per unit pressure gradient, and the specific conductivity  $K_s$  is  $K_h$  per unit cross-sectional sapwood area  $A_{st}$  (Tyree and Zimmermann 2002). The hydraulic conductivity of an ideal conduit (a capillary), according to the Hagen and Poiseuille law, increases with the fourth power of the radius of the conduit and makes wide vessels more efficient in water transport; vessels and other conduits, however, are not ideal capillaries (Tyree and Zimmermann 2002).  $K_h$  or  $K_s$  can either be calculated from conduit diameters as a theoretical value or measured destructively on branch or trunk segments by applying a (known) hydrostatic pressure to induce a volume flow of water through the segment. In an intact tree the pressure gradient is represented by the difference in xylem pressure between the considered end points, e.g. the soil and the leaves.

Theoretical  $K_h$  or  $K_s$  may deviate from real  $K_h$  or  $K_s$  (even if accounting for the non-circular cross-section of real conduits) due to additional resistances to flow along the path, introduced by conduit wall sculptures, perforation plates between vessel elements, conduit length, which in turn influences the number of intervessel pits, the number of pits in general and the type of pits (Tyree and Zimmermann 2002, Sperry et al. 2006). Recent observations by Jansen et al. (2007) in members of the *Rosales* demonstrated that there is more variation in angiosperm pit architecture than previously thought, with corresponding differences in functionality like the probability of air seeding through pit membranes (Choat et al. 2004). Additionally, conducting tissues undergo long-term changes that reduce the conductance to liquid water, such as cavitation and formation of tyloses, the latter typically leading to the formation of heartwood (Romberger et al. 1993, Tyree and Zimmermann 2002; but tyloses are also frequently found in the sapwood: Bamber and Fukazawa 1985, Tyree and Zimmermann 2002). Furthermore, pits may undergo long-term changes as well and become encrusted or aspirated (Mark and Crews 1973). Also,  $K_s$  measured on wood sections may not completely reflect the natural conditions since emboli may be removed, pits may be affected and their resistances as a consequence left altered. Seasonal changes in the hydration of pit membranes are currently discussed to influence  $K_h$  as well (e.g. López-Portillo et al. 2005, Gascó et al. 2006, 2007).

Conduit volume is not directly correlated with vulnerability to drought-induced cavitation, and not at all when comparing different species (Sperry and Sullivan 1992). It is

the size of the pores in the pit membranes that are directly correlated with vulnerability to drought-induced cavitation (Crombie et al. 1985, Tyree and Sperry 1989, Sperry et al. 1991, Sperry and Sullivan 1992), and larger conduits tend to have more permeable pit membranes than smaller conduits (Sperry and Sullivan 1992). More specifically, Choat et al. (2005) and Wheeler et al. (2005) suggested that, because in larger conduits the total pit membrane area increases, the range of pit membrane pore-diameters will increase and concurrently with this the number of larger pores which in turn are most vulnerable to cavitation. Embolisms are not static but can be repaired; the rapidly growing body of literature on the controversially discussed proposed mechanisms of embolism reversal was recently reviewed by Tyree and Zimmermann (2002) and Clearwater and Goldstein (2005).

Most of the literature on radial patterns of  $K_h$ , however, concerns conifers (e.g. Comstock 1965, Booker and Kininmonth 1978, Booker 1984, Shelburne and Hedden 1996, Spicer and Gartner 2001, Domec and Gartner 2001, 2003). In *F. sylvatica*, Schmidt (1954, cited in Huber 1956, p 555f) experimentally found a strong decrease in axial water permeability of the xylem at approx. 8 cm radial distance from cambium in a tree with a total radius of ca. 13 cm. Radial trends in xylem conducting properties have also been inferred from sapwood properties such as water content and wood density measured on increment cores or stem disks (e.g. Phillips et al. 1996, Cermák and Nadezhina 1998, Granier et al. 2000a, James et al. 2003) or with computer tomography (Raschi et al. 1995, Tognetti et al. 1996, Alsheimer et al. 1998, Schäfer et al. 2000).

**Sap flow.** Sap flow measurements can reveal how much water flows axially in which region of the sapwood of a tree, on the one hand as a consequence of the demand in the canopy and the supply by the roots, and on the other hand as facilitated by the tree's hydraulic architecture:

The hydraulic architecture in this respect may be defined as the distribution of hydraulic conductances across the sapwood (cf. Cruziat et al. 2002, Tyree and Zimmermann 2002). It is not static but varies in several temporal scales as detailed above. The magnitude of the pressure gradient (water potential) between leaves and roots in the SPAC (soil-plant-atmosphere-continuum) then determines how much resistance along the path from root to leaves can be surmounted. Also, liquid and vapour phase water transport in plants (sap flow and transpiration, respectively) must be co-ordinated to maintain hydraulic integrity. Plants regulate their stomatal conductance in order to prevent excessive embolism (Jones and Sutherland 1991). Transpiration from leaves is driven by the gradient between the vapour pressure deficit of the air ( $D$ ) inside the leaf (close to zero) and the atmosphere surrounding the leaf. Loss of water to the atmosphere causes the leaf tissue to dehydrate and the water potential to become (more) negative, building up a suction pressure within the water column in the plant which is transmitted through the leaf-soil continuum. Variable resistances along the path influence the amount of water that will be transported at a given driving force (water potential). Among the components that influence these resistances (or the hydraulic conductance) are the exchange of water between the transpiration stream and internal storage compartments via capacitive discharge and recharge, cavitation and its reversal, temperature-induced changes in the viscosity of water, direct effects of xylem sap composition on xylem hydraulic properties, and endogenous and environmentally induced variation in the activity of membrane water channels in the hydraulic pathway (Meinzer 2002). With decreasing (more negative) water potentials more and more vessels will cavitate and at a species-specific threshold of leaf water potential stomatal conductance will be reduced to prevent complete xylem dysfunction.

Radial variation of axial sap flow has been inferred from the application of dye staining techniques (Huber 1935, Ladefoged 1952, Edwards and Booker 1984, Ellmore and Ewers 1985, Cermák et al. 1992) and directly from measurements of heat pulse velocity (e.g. Swanson 1967, Mark and Crews 1973, Lassoie et al. 1977, Miller et al.

1980, Hirose et al. 2005) and more recently also with heat balance probes (e.g. Granier et al. 1994, Alsheimer et al. 1998, Cermák and Nadezhina 1998, Rouspard et al. 1999, Ewers and Oren 2000, Nadezhina and Cermák 2000, Jiménez et al. 2000, Lundblad et al. 2001, James et al. 2002, Ford et al. 2004a, Krauss et al. 2007, Nadezhina et al. 2007). Qualitative descriptions of radial sap flow patterns were obtained with thermal imaging techniques (Anfodillo et al. 1993, Granier et al. 1994). Edwards and Booker (1984) reported a radial decline of both hydraulic conductivity  $K_h$  and heat pulse velocity with distance from cambium in *Populus* species. Rust (1999) and Domec et al. (2006) showed  $K_h$  and sap flow density  $J_s$  (sap flow per unit sapwood area) to decline concurrently towards the pith in *Pinus sylvestris* and *P. menziesii*, respectively. James et al. (2003) could present a strong correlation of  $J_s$  with specific conductivity  $K_s$ , calculated from vessel diameters, for tropical deciduous and evergreen trees, both decreasing from outer to inner sapwood as well. Lang (1999) in contrast only found a weak radial decline in theoretical  $K_s$  calculated from vessel lumen areas of the earlywood in European beech, while the radial decline in  $J_s$  was pronounced. James et al. (2003) and Meinzer et al. (2006) documented an increasing  $J_s$  with increasing  $K_s$  across four tropical angiosperm and two temperate gymnosperm tree species, respectively.

Phillips et al. (1996) summarised their own data and published results on radial trends in sapwood hydraulic conductivity, heat pulse velocity and sap flow density  $J_s$ , mostly gathered on conifers. From the few studies conducted on broadleaved tree species at the time, a rather clear-cut general picture emerged, namely that in diffuse-porous trees (usually with wide sapwood) the sap flow radially decreases from outer to inner sapwood comparatively smoothly, whereas in ring-porous species (*Quercus* spec., *Ulmus americana*, with narrow sapwood) the decrease is rather steep (Phillips et al. 1996). Additional to the few works on ring-porous trees cited by these authors, there is a considerable body of older literature focussing on the physiological significance of this conduit system, mainly starting with Huber (1935), reviewed e.g. by Huber (1956) and Braun (1970). It is common ground today (e.g. Tyree and Zimmermann 2002) that the large, mostly without magnification visible vessels ("pores") in the earlywood of ring-porous trees, formed prior to leaf-unfolding, are very efficient in water transport but usually embolise and become dysfunctional during the first or second year after formation. The narrower latewood (and the few narrow earlywood) vessels of the current and older growth rings are then the only water-conducting elements providing a less effective but safe water supply to the leaves. Freezing during winter effectively disrupts most of the water columns in the large earlywood vessels if they have not been embolised during the vegetation period already.

In ring-porous North-American oak species Kozlowski and Winget (1963) observed the movement of dye solution to be confined to the outermost two annual rings. In another ring-porous species, *Ulmus americana*, fluid flow was found to be limited to the youngest six growth rings, the maximum flow rate (92 %) occurring in the outermost ring (early- and latewood; Ellmore and Ewers 1986); in the latewood, dyes were transported up to the 8<sup>th</sup> youngest ring (Ellmore and Ewers 1985). In accord with these observations Cochard and Tyree (1990) summarised that in their study on *Quercus alba* and *Q. rubra* most earlywood vessels were blocked by tyloses during the second growing season whereas less many latewood vessels were plugged by tyloses; the number of blocked latewood vessels increased slowly in older rings and some conduction was still evident in 6 year-old rings. Embolism in contrast can render vessels dysfunctional already during the growing season of their formation

(Cochard and Tyree 1990). Phillips et al. (2003b) noted a decrease of  $J_s$  from the outer 10 mm of sapwood to inner sapwood (ca. 10–30 mm depth) of 59 % and 70 % in short (young) and tall (old) trees of ring-porous *Q. garryana* in the north-western US, respectively. Schiller et al. (2007), measuring heat pulse velocity, found significant and radially decreasing sap flow in ring-porous eastern Mediterranean *Q. aegilops* in 4 mm, 12 mm and 20 mm sapwood depth and insignificant sap flow in 28 mm, 36 mm and 44 mm in trees of about 27 cm diameter. Poyatos et al. (2007) observed apparent sap flow with the heat field deformation sap flow method down to 35 mm sapwood depth in sub-mediterranean ring-porous *Q. pubescens*, the maximum flow mostly located in 3 mm or 11 mm depth for trees ranging 13–49 cm in stem diameter.

A preliminary study carried out at one of the sites investigated in the current study (Steinkreuz, Steigerwald) in 1996 on two representative oak trees, similar to the reports cited above, revealed insignificant sap flow in 2–4 cm xylem depth using the thermal dissipation technique (Schäfer 1997). A similar pattern emerged from a study on *Q. petraea* in France, where 80 % of the sap flow occurred in 0–1.1 cm and 93 % in 0–2.2 cm (Bréda et al. 1993a, Granier et al. 1994, thermal dissipation technique) and from a more qualitative investigation using dye staining in *Q. robur*, where dye velocity approached zero in 2 cm depth of a mature tree (stem diameter 30 cm; Cermák et al. 1992). The radial variability of axial water transport in the sapwood of mature sessile oak thus is on a spatial level smaller than that of the resolution of a standard thermal dissipation probe (2 cm). Given that the total sapwood radius of mature oak trees at the study sites was around 2 cm (Schäfer 1997), sap flow density could be expected to be adequately sampled in these oaks with one standard thermal dissipation probe.

Since the report by Phillips et al. (1996) a number of studies using sap flow methods have corroborated the general pattern in diffuse-porous tree species (e.g. Becker 1996, Zang et al. 1996, Cermák and Nadezhina 1998, Jiménez et al. 2000, Lu et al. 2000, Pausch et al. 2000, Wullschleger and King 2000, James et al. 2002, 2003, Nadezhina et al. 2002, Schiller et al. 2003). However, few publications so far have explicitly shown radial trends of sap flow with heat tracer techniques in *F. sylvatica* (Köstner et al. 1998a, Granier et al. 2000a, Schäfer et al. 2000, Patzner 2004, Geßler et al. 2005, Hölscher et al. 2005, Kolcun 2005) or closely related species (*F. crenata*: Kubota et al. 2005a, b; *Nothofagus* species: Kelliher et al. 1992), which commonly followed the pattern extracted by Phillips et al. (1996, see above). Only two studies have quantitatively assessed seasonal changes in the radial patterns of sap flow density  $J_s$  in *F. sylvatica* (Lang 1999, Lütschwager and Remus 2007), yet only on a small number of trees. Very few studies have detailed such season-long trends of  $J_s$  in other species (Oren et al. 1999, Schäfer et al. 2002, Schiller et al. 2003, Ford et al. 2004b, Kubota et al. 2005a, b, Fiora and Cescatti 2006). In most studies focussed on long-term stand-level canopy transpiration, radial sap flow profiles have only been observed on a few days or on a small sub-sample of trees. As was cautioned e.g. by Nadezhina et al. (2002), since these radial patterns may change over time, using short-term radial patterns to scale-up from single-sensor measurements to whole-tree transpiration for a longer period of time, e.g. a whole growing season, may introduce significant errors that could obscure functional changes in the conducting system which may evolve over the course of a season under a variety of climatic and edaphic conditions.

Indeed it has been shown that soil water conditions have an effect on radial sap flow patterns, namely a larger reduction of sap flow density  $J_s$  in inner sapwood compared to  $J_s$  in outer sapwood during a drying cycle (Phillips et al. 1996, Schäfer et al. 2002) or vice-versa (Nadezhina et al. 2002, Ford et al. 2004b), or complete cessation of inner  $J_s$  as found in several angiosperm trees species (Becker 1996, Schiller et al. 2003); in orchard-grown *Mangifera indica* trees, the trends were divergent (Lu et al. 2000). Among-tree variability was noted to be larger during dry periods as well (e.g. Bréda et al. 1995a, Cermák et al. 1995, Becker 1996). Sap flow in trees has commonly been observed to decrease with increasing soil drought (e.g. Schulze et al. 1985, Granier and Loustau 1994, Lu et al. 1995, David et al. 1997, Zimmermann et al. 2000, Bovard et al. 2005). Nadezhina et al. (2002) hypothesised that long-term records of radial patterns of sap flow could be used as an indicator of tree water status.

The vapour pressure deficit of the air D was also shown to influence the radial distribution of sap flow (Nadezhina et al. 2002). Furthermore, Granier et al. (2000a) noted that in *F. sylvatica* the proportion of  $J_s$  in inner sapwood had a tendency to increase with increasing tree transpiration. Highly variable patterns in radial sap flow among co-occurring trees in a laurel forest was observed by Jiménez et al. (2000), which they found was in part due to the canopy position of the trees. Between-tree variability in  $J_s$  (mostly assessed only in the outer 2 cm of the sapwood) has also been demonstrated to be larger in tropical rainforests (coefficient of variation, CV, 35–50 %; Granier et al. 1996c) than in temperate deciduous (CV 11 %, *Q. petraea*: Bréda et al. 1993a, 1995) or coniferous forest stands (CV 9–15 %: Granier et al. 1996b), the latter two types of forests having been monospecific and much more uniform in structure and also age. The coefficient of variation in  $J_s$  was larger in a thinned oak stand (37 %, Bréda et al. 1993a, 1995). Oren et al. (1998) summarised that to reduce the CV in  $J_s$  to 15 %, 23–48 trees would have had to be measured in three temperate North American deciduous broadleaved forests. In a 74 year-old beech stand Lang (1999) calculated a CV in  $J_s$  of 14 % (however, only 4 trees had been monitored). The CV of  $J_s$  reached up to 61 % in a young beech forest, due to very low rates of  $J_s$  in intermediate and suppressed trees (Granier et al. 2003). Accordingly, sap flow density  $J_s$  has been observed to be positively correlated with stem diameter e.g. in southern hemispheric temperate *Nothofagus* species (Kelliher et al. 1992), several tropical rainforest species (Granier et al. 1996c) and in *F. sylvatica* from a young stand (Granier et al. 2000a). Radial patterns of  $J_s$  were recently shown to compare among trees of different size when normalising for both  $J_s$  and sapwood depth in *Fagus* species (Granier et al. 2003: *F. sylvatica*; Kubota et al. 2005b: *F. crenata*).

As can be concluded from the above overview of the literature, a study of the water use of beech forests with heat tracer techniques consequently must critically assess axial sap flow along the sapwood radius. Monitoring the radial pattern of sap flow density  $J_s$  over the whole growing season is imperative for defensible seasonal estimates of tree and stand level transpiration under varying environmental conditions. It may also reveal changes in the hydraulic properties at the within-tree level in response to changed conditions like soil water supply, which so far has not been sufficiently quantified for European beech on seasonal scales. Furthermore, adequate sampling of the wide range of tree sizes found in mature forest stands could possibly uncover general relationships between tree size and radial patterns of sap flow density. And lastly, since systematic investigations of the radial variability of  $J_s$  across

stands with a common sampling strategy are lacking for *F. sylvatica*, strategies for applying radial patterns from one site to others could potentially be developed.

### 2.3.2. Influence of structure on whole-tree water use

Several studies using sap flow methodologies have addressed the issue of whole-tree water use and its relation to scalars of tree size, often in the context of extrapolating transpiration from single trees to forest stands. For instance, Ladefoged (1963) investigated young beech and oak trees and observed larger water use in trees with dominant crowns than in trees with intermediate crowns. Köstner et al. (1992) demonstrated that the maximum tree water use was significantly correlated with tree height, stem circumference and stem sapwood area in *Nothofagus* species in a pristine New Zealand forest. In their study daily sap flux varied by an order of magnitude between suppressed and emergent trees, and three emergent trees out of 14 trees in their small plot contributed > 50 % to the canopy transpiration of the plot. Vertessy et al. (1995, 1997) showed tree water use to increase with stem diameter and leaf area in *Eucalyptus regnans* in differently aged stands; sapwood area and stem diameter were also strongly correlated. Vertessy et al. (1997) also found that large trees contributed relatively more to the stand transpiration than small trees with the same sapwood area. Hatton and Wu (1995) and Hatton et al. (1995) demonstrated positive linear relationships of tree water use and stem diameter, sapwood area and leaf area in several other *Eucalyptus* species. Santiago et al. (2000) reported a significant correlation of tree water use with leaf area in *Metrosideros polymorpha* (Myrtaceae). A decrease in tree water use per unit of leaf area with increasing leaf area of a tree was noticed by Vertessy et al. (1995) in *E. regnans*.

With the aid of sap flow measurements it has also been demonstrated that co-occurring species respond differently to drought (e.g. Cienciala et al. 1998), with varying sensitivities to soil water content and vapour pressure deficit (Pataki et al. 1998, 2000, Moore et al. 2004, Hölscher et al. 2005). Different species may also access different soil water reserves (Cermák et al. 1995, Cienciala et al. 1998, Stratton et al. 2000, Moore et al. 2004). And species may also differ in their ratio of leaf area to sapwood area (Tyree and Zimmermann 2002, McDowell et al. 2002).

The two species of interest in this study, *F. sylvatica* and *Q. petraea*, differ in a number of traits. For instance, beech trees cast deep shade and their seedlings require little light (more light though than the amount which penetrates a mature beech trees' canopy), oak canopies in contrast absorb less radiation and oak seedlings require more light (beech could regenerate under oak but not vice-versa; Ellenberg 1996). Beech shows a strong sun-shade leaf dimorphism (Schulze 1970, Eschrich et al. 1989) and typically a sun and a shade crown differing in ecophysiological characteristics (Schulze 1970, Leuschner 1994, Backes 1996), with up to three layers of sun leaves and at least 3–4 layers of shade leaves, much more than pedunculate oak (Ellenberg 1996). Crowns of oak are umbrella-like in vertical cross-section and leaves concentrated in the periphery of the crown; the crown shape of beech is globular-cylindrical pear-shaped with leaves distributed more evenly (Leuschner 1994, Fleck 2002). Beech is more efficient in canopy space occupation than sessile oak in terms of costs for leaf and branch dry matter production and nitrogen investment, mainly a consequence of a low leaf area per canopy volume (leaf area density) and the same holds for the cost of shade production (Leuschner 2001). The fine root biomass of beech was found to be larger than that of oak in a mixed stand on acidic soil (Büttner and Leuschner 1994, Leuschner et al. 2001b) while oak is known to root deeper than

beech (Köstler et al. 1968). *Q. petraea* has been shown to be more drought tolerant than *F. sylvatica* in direct comparisons in mixed stands, based on a wide range of techniques on the leaf and the whole-tree level (Aranda et al. 1996, 2000, 2005, Backes and Leuschner 2000, Leuschner et al. 2001a).

To capture and explain the variation in water use between trees, particularly in heterogeneous stands with a wide range of tree sizes and canopy positions, it is desirable to sample a large number of individual trees for sap flow measurements concurrently with their structure and atmospheric and soil conditions. Systematic trends for the correlation of water use with scalars of tree size could be expected to emerge from such an effort.

### 2.3.3. Effects of stand structure on canopy transpiration and conductance

Systematic studies of the effect of differences in structure on whole-tree water use are relatively scarce to date (Ryan 2002). In contrast, the influence of canopy structure on radiation interception and carbon, water and energy exchange and vertical patterns of these and related leaf traits have received considerable attention (e.g. Wang and Jarvis 1990a, b, Ellsworth and Reich 1993, Falge et al. 1997, Law et al. 2001, Baldocchi et al. 2002, Niinemets et al. 2004). Structure controls stand water use or canopy transpiration ( $E_c$ ) on longer time scales and sets limits for the response of  $E_c$  to short-term atmospheric drivers. Structure itself is influenced by the atmospheric drivers through environmental forcing, i.e. by the feedback via the carbon cycle (e.g. Law et al. 2002; "carry-over effects", cf. Ma et al. 2007). For instance, a number of studies have shown a direct relationship between leaf area index (LAI) and water availability (e.g. Grier and Running 1977, Gholz 1982).

Running and Coughlan (1988) indicated the importance of LAI for processes of mass and energy exchange in forest canopies. Bréda and Granier (1996) demonstrated that canopy transpiration was positively correlated with LAI in a French stand of *Q. petraea*, also shown by Santiago et al. (2000) for a montane Hawaiian cloud forest. Köstner (2001) found a nearly linear relationship between  $E_c$  and LAI, independent of stand age, for five beech stands which was attributed to a high optimisation of the leaf area within the canopy. In several other coniferous and broadleaved forests the stand water use of the overstory decreased with age, in parallel with reductions in LAI and sapwood area (Dunn and Connor 1993, Alsheimer et al. 1998, Zimmermann et al. 2000, Köstner 2001, Law et al. 2001, Vertessy et al. 2001, Roberts et al. 2001, Köstner et al. 2002, Phillips et al. 2002, Moore et al. 2004, Delzon and Loustau 2005). Granier et al. (2000b) found LAI to explain the variability in canopy conductance between a range of tropical and temperate, broadleaved and coniferous forest stands. From these data and those presented by Granier and Bréda (1996) for sessile oak it was suggested that canopy conductance saturates at high values of LAI, around 6, due to increased self-shading and shading by neighbouring trees.

Differences in the contribution of ring-porous and diffuse-porous species to canopy transpiration of mixed stands based on their respective basal area have been described by Oren and Pataki (2001) and Wullschleger et al. (2001). Wullschleger et al. (2001) concluded that sapwood area represented the contribution of either wood anatomical group to  $E_c$  better than basal area. Oren and Pataki (2001) summarised that stands with a high proportion of diffuse-porous tree species had higher maximum rates of  $E_c$ , while a higher proportion of ring-porous species resulted in lower maximum rates of  $E_c$ .

The stomatal conductance ( $g_s$ ) of sessile oak has often been observed to be mostly higher than  $g_s$  in beech, diurnally and seasonally (e.g. Aranda et al. 2000, Backes and Leuschner 2000, Fleck 2002), both regarding sun and shade leaves (Aranda et al. 2000). However, differences between beech and oak seem to be reduced at the stand level, and maximum canopy conductance  $g_c \text{ max}$  scaled from sap flow measurements was only slightly smaller for pure beech stands compared to pure sessile oak stands as summarised by Granier et al. (2000b). For temperate North American deciduous forests Oren and Pataki (2001) suggested that stands with a high proportion of ring-porous species have a lower canopy conductance than stands with a high proportion of diffuse-porous species. However, the evaluation of Oren and Pataki (2001) was based on single-tree level canopy conductances and not on a whole-stand level. No values of  $g_c$  for mixed beech-oak stands seem to be documented in the literature.

At higher (montane) elevations, atmospheric conditions constrain the transpiration of plants more often than at lower elevations, due to lower temperatures, higher frequency of cloudy and rainy days, lower radiation and hence a lower vapour pressure deficit of the air (e.g. Körner et al. 1989). Consequently, season-long integrals of sap flow density and tree and stand level sap flux are expected to be lower at higher elevated sites (e.g. Körner 1999) as noted by Granier et al. (2000a) for European beech, whereas daily rates, particularly at the tree level, may be similar, shown e.g. for Japanese *F. crenata* by Kubota et al. (2005b) or for *Picea abies* by Kolcun (2005).

In mixed stands of beech and oak species-specific relationships between scalars like stand level sapwood area or leaf area and canopy transpiration are likely to exist. The distribution of individuals of each species across tree size classes or canopy positions can be expected to be crucial for the amount of stand level transpiration and also for the magnitude of drought effects, given the different drought tolerance of beech and oak. Thus, for each species, trees for the measurement of sap flow were selected according to canopy position or social class, and biased towards the classes with the largest basal area and hence sapwood area (e.g. Thorburn et al. 1993, Martin et al. 1997, Köstner et al. 1998a, Raulier et al. 2002).

## 2.4. Hypotheses

The following hypotheses can be formulated based on the reviewed literature, at the three spatial levels of structure considered in this study.

### Within-tree radial variation of sap flow in beech

1. The axial xylem sap flow density  $J_s$  of beech declines radially towards the sapwood-ripenwood boundary.
2. A relationship between tree diameter and  $J_s$  exists in beech and oak.
3. A general relationship of the decrease of  $J_s$  with radial sapwood depth can be described for trees of different size when normalising both the probed sapwood radius with total sapwood radius and  $J_s$  with  $J_{s,0-2cm}$ .
4. Beech trees growing at higher elevation are comparable to trees from lower elevations in their capacity of  $J_s$  (similar maximum  $J_s$ ).
5. Large overstory beech trees, due to their large sapwood area, differ from smaller sub-canopy trees in their ability to respond to increased transpirational water demand in the crown (increasing proportion of  $J_s$  in deeper sapwood).
6. The radial pattern of  $J_s$  changes seasonally with progressive soil water deficit in that the water conducting radius decreases.

### Whole-tree water use

1. Whole tree water use  $Q_t$  is related to scalars of tree size, in both beech and oak, and across stands.
2. Whole tree water per unit leaf area  $Q_t/A_{lt}$  decreases with increasing tree height, in both beech and oak.
3. Beech trees of similar size from higher and lower elevation stands reach similar values of  $Q_t$ .

### Stand water use

1. Because of the inferior ability to occupy crown space, the higher self-shading and smaller shade tolerance of oak compared to beech, canopy transpiration  $E_c$  in mixed stands of oak and beech is smaller than  $E_c$  in pure beech stands.
2. The contribution of beech and oak to stand level  $E_c$  in mixed stands can be assessed via contributions of stand structural characteristics of these species to stand level totals; relationships of maximum daily  $E_c$  and scalars, such as leaf area index or basal area, exist.
3. Maximum daily  $E_c$  is similar at low and high elevation sites under similar atmospheric conditions.

4. Seasonal canopy transpiration of beech stands is lower at higher elevation due to lower air temperatures, lower D and a shorter growing season than at lower elevation.
5. Critically low soil water supply reduces  $E_c$  more strongly in beech than in the more drought-tolerant oak, and is more frequently limiting  $E_c$  at lower elevation than at higher elevation.
6. The canopy conductance of mixed stands of beech and oak is only slightly higher or as high as in pure beech stands because of the larger dominance of beech in canopy space capture.

### 3 Study sites

Important historical aspects of the beech distribution in Upper Franconia relevant for the selection of the locations in this study include the following:

Human activities promoted oak in the **Steigerwald** since the late Middle Ages when the landowners, the bishops of Bamberg and Würzburg, restricted coppicing to the vicinity of villages and managed the forests in order to yield economically valuable, large oak and also pine stems (Sperber and Regehr 1983). This policy lay ground to single-stem harvest and selective logging which by creating small canopy gaps fostered natural regeneration and thus maintained a highly differentiated, near-natural structure of the forests, especially of the northwestern Steigerwald (Sperber and Regehr 1983, Oberforstdirektion Oberfranken 1999).

A once regionally common silvicultural practice was the “nursing” of oak under the crowns of beech which resulted in long-stemmed, strong oaks of high economic value (Göpfert 1950, Sperber and Regehr 1983). The local forestry administration has successfully reintroduced these practices since the 1970s (Sperber 1983), after a period of decreasing silvicultural skills since about 1900 (Sperber and Regehr 1983). The older deciduous forests found within the range of the forestry district Ebrach, where this study was carried out, can be regarded as autochthonous (Sperber 1983).

Within the forestry district Ebrach, comprising 50 km<sup>2</sup> of forests, beech is the most important species, holding 43 % of the total forested area, followed by oak with 20 %. The proportion of conifers, promoted by humans during former centuries, has been reduced since the 1970s to 26 % (13 % *Pinus sylvestris* L., 9 % *Picea abies* (L.) KARST.; Oberforstdirektion Oberfranken 1999). The most abundant stand types are beech-dominated ones, namely 34 % beech-oak and 24 % beech-conifer stands. Pure beech and pure oak stands in contrast account for less than 2 % each. Beech-oak stands (dominated by beech) are mainly found in older age classes (> 80 years), beech-conifer stands prevail in the age classes 41 to 80 years. Oak-beech stands (dominated by oak; 15 % of all stands) are mainly found in the age classes 121–140 years and > 160 years (Oberforstdirektion Oberfranken 1999).

The potential natural vegetation of the **Fichtelgebirge** is montane, mixed (*Acer pseudoplatanus*-*Fraxinus excelsior*)-*Picea abies*-*Abies alba*-*Fagus sylvatica* forest (Firbas 1952, Firbas and Rochow 1956, Kölling and Walentowski 2001, Walentowski et al. 2001). Norway spruce (*Picea abies*), in contrast to its present forest cover (> 80 % of the local forestry district; Forstamt Weißenstadt 2002; > 90 % coniferous forest in the whole region; Walentowski et al. 2001), is thought to only have occurred naturally very locally as a displaced species after the invasion of beech between ca. 700 BC and 1200 AD (Firbas 1952, Reif 1989). Fruiting beech trees have been found at the Schneeberg up to 1025 m a.s.l. and vigorous re-growth up to 980 m a.s.l. (Firbas 1952, Firbas and Rochow 1956 and own observations). Currently only 3 % of the forested area of the ridges of the Fichtelgebirge are covered by beech forests (Forstamt Weißenstadt 2002) and merely about 7 % of the whole region’s forests carry deciduous broadleaved trees (Walentowski et al. 2001). Deforestation of vast areas related to mining since the late Middle Ages and subsequent reforestation with Norway spruce, usually in even-aged monocultures, have changed most of the landscape.

#### 3.1. Steigerwald

Experimental work was mainly conducted in the Steigerwald (Fig. 3.1.1), a forested colline to sub-montane hillside area in northern Bavaria, Germany, located between the cities of Bamberg and Würzburg, and comprising approx. 1000 km<sup>2</sup>, with elevations of 300 m a.s.l. in the East to 500 m a.s.l. in the West (Meynen and Schmithüsen 1953–1962). The sites studied were located near the town of Ebrach in the middle to northern part of the Steigerwald and close to its steep western escarpment, composed of Late Triassic layers of sandstone, which rise 100–200 m above the western lower plains of Middle Triassic sediments (Tab. 3.3.1).

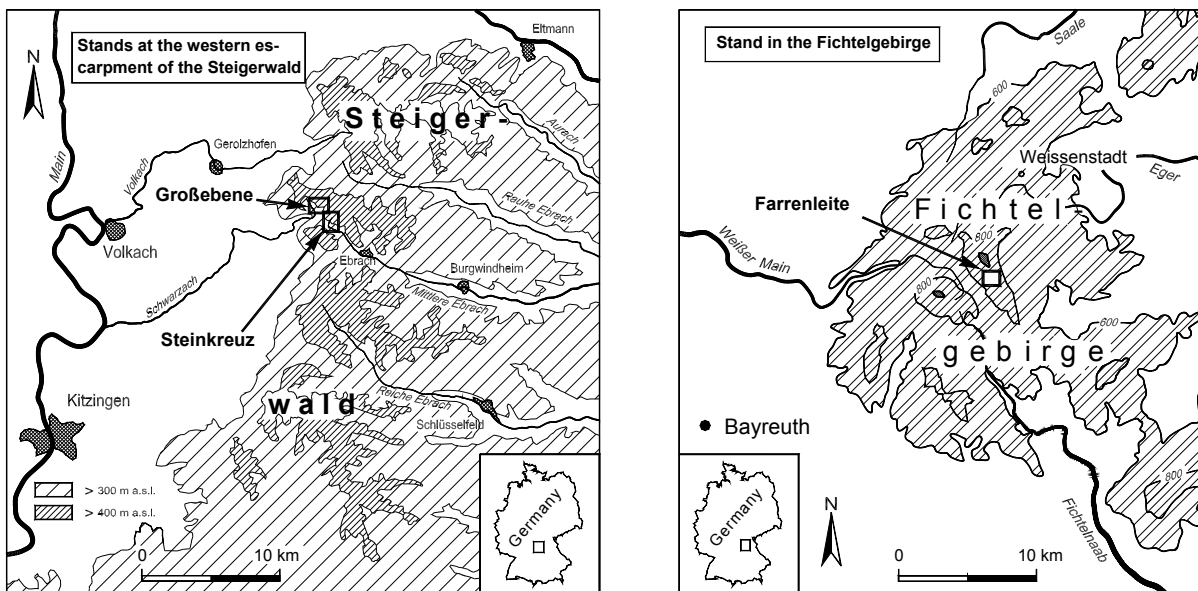


**Figure 3.1.1:** Location of the studied sites “Steinkreuz” and “Großebene” in the Steigerwald (**left**) and “Farrenleite” in the Fichtelgebirge (**right**). Maps courtesy of P. Gerstberger, Dept. of Plant Ecology, Univ. of Bayreuth.

The Steigerwald hillsides belong to a belt of moderately warm and relatively moist climate in the transition zone between maritime and continental climate (BayFOR-KLIM 1996). The long-term mean monthly air temperature near the study sites reaches a maximum of 16.7 °C in July and a minimum of -1.5 °C in January (DWD 1999–2000; Fig. 3.1.2a), and the mean annual air temperature is 7.7 °C (Fig. 3.1.2). The long-term pattern of monthly precipitation (Fig. 3.1.2a) is typical for foothills under a maritime influence and shows a pronounced peak in June (ca. 90 mm) and a secondary maximum in December (70 mm). The least precipitation is observed in February and October (approx. 55 mm month<sup>-1</sup>). The long-term mean annual precipitation amounts to ca. 800 mm (Fig. 3.1.2). These climatic conditions favour beech (*Fagus sylvatica*)-dominated hardwood forests in Central Europe (Ellenberg 1996) and the natural vegetation of the area are beech forests with additional canopy tree species such as *Q. petraea*, and oak-hornbeam forest on clayey soils (Welß 1985, Türk 1993, Walentowski et al. 2001, Kölling and Walentowski 2001).

The two mature beech-oak stands chosen for this study in the forestry district Ebrach lie close to each other within a large, contiguously forested area, at 440–460 m a.s.l. and in SE- to SSE-exposition (Tab. 3.3.1). Of these, the stand Steinkreuz has been monitored meteorologically, hydrologically and biogeochemically since 1995 by the Bayreuth Institute for Terrestrial Ecosystem Research (BITÖK, now BayCEER, Bayreuth Center of Ecology and Environmental Research) (e.g. Matzner and Köstner 2001, Gerstberger 2001, Matzner 2004) and is part of a small catchment (0.57 km<sup>2</sup>). The second stand, Großebene, was selected for its higher proportion of oak (Tab. 3.3.2) and in cooperation with S. Fleck, formerly Dept. of Plant Ecology, Univ. of Bayreuth, for concurrent investigations of gas exchange at leaf level and its spatially explicit representation in a simulation model (Fleck 2002). Both stands were established by natural regeneration around the same time (Steinkreuz ca. 1863–1872, Großebene ca. 1880).

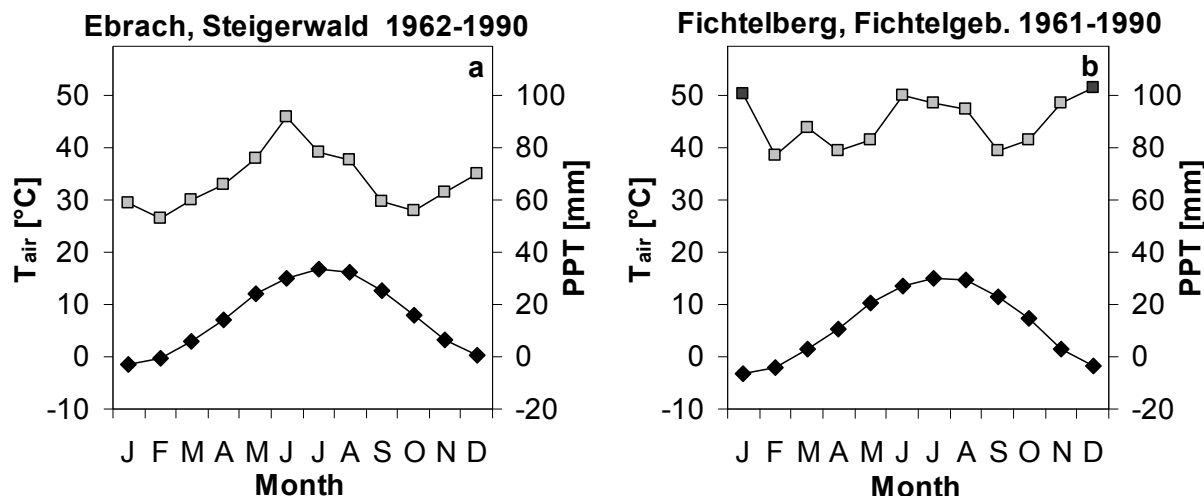


**Figure 3.1.2:** Climate diagrams, according to Walter and Lieth (1960–1967), for the German weather service (DWD) station Ebrach, Steigerwald, 360 m a.s.l. (a), and Fichtelberg-Hüttstadt, Fichtelgebirge, 659 m a.s.l. (b). Values are long-term (1962–1990 or 1961–1990, respectively) monthly averages of air temperature ( $T_{air}$ , filled diamonds) and precipitation (PPT, shaded squares), taken from DWD (1999–2000). Mean monthly precipitation > 100 mm is reduced by 1/10 (dark squares). The DWD station Ebrach is in 3.7 km direct distance to the study site Steinkreuz and was established in 1962, the station Fichtelberg is in 7 km direct distance to the study site Farrenleite. The mean annual  $T_{air}$  is 7.7 °C and 6.1 °C, respectively, the average annual PPT is 808 mm and 1111 mm, respectively.

The **Steinkreuz** stand, in the following referred to as the fenced experimental plot of BITÖK (the forestry unit “Steinkreuz” being much larger), encloses an area of 1.29 ha (Tab. 3.3.1). It is comprised of an overstory reaching 30 to almost 40 m, composed of *F. sylvatica* and *Q. petraea*, the former clearly dominating (Tab. 3.3.2). A few trees of *Carpinus betulus* L. (hornbeam) occur in the sub-canopy, representing < 1 % of the stems and < 0.2 % of the basal area of the plot, and will be discounted in subsequent tables and calculations.

Within the mixed Steinkreuz stand, an additional plot of pure beech was selected in 1999 for comparison with the mixed Steigerwald stands and with the pure beech stand in the Fichtelgebirge (Chap. 3.2). This beech plot, hereafter termed the **Steinkreuz-pure beech plot**, was about 220 m<sup>2</sup> in area (determined by equal distribution of distances between neighbouring trees) and enclosed six live beech trees.

The mixed stand **Großebene** is situated approx. 1.3 km northwest of the stand Steinkreuz on a comparatively level ridge-top near the highest hill-top of the area (Stollberg, 476 m a.s.l.). Within the rather homogeneous forestry unit “Großebene”, a 0.23 ha-plot was mapped. Here, oak dominated the upper canopy and contributed to more than 60 % of the total basal area of the stand, whereas beech dominated the sub-canopy with a large number of small stems. Maximum tree height was < 30 m. All site and stand structural characteristics are summarised below in Tables 3.3.1 and 3.3.2 (Chap. 3.3).

### 3.2. Fichtelgebirge

Further investigations were carried out in the Fichtelgebirge, a densely forested mountain range in NE Bavaria, about 100 km east of the western Steigerwald-escarpment and close to the border of the Czech Republic to the East (Fig. 3.1.1). The C-shaped ridges of the Fichtelgebirge (ca. 700 km<sup>2</sup>) reach more than 1000 m a.s.l. in their south-western part (Schneeberg, 1051 m, and Ochsenkopf, 1023 m) and encircle a lower-lying plateau, open to the East (Selb-Wunsiedel-Plateau, about 600 m a.s.l., ca. 400 km<sup>2</sup>). The beech stand studied was located at the upper slope of the Schneeberg (literally “snow-mountain”). The Fichtelgebirge is built of a large granitic pluton surrounded by metamorphic rock series and is among the highest of several low-elevation mountain ranges confluencing in this area (the Thuringian Forest, the Franconian Forest and the Upper Palatinate Forest are lower, the Ore Mountains, the Bohemian and the Bavarian Forest, further east- and southwards, respectively, are higher), all originating from variscic (palaeozoic) orogenesis (Meynen and Schmithüsen 1953–1962).

The climate of the area is typical for the transition zone from suboceanic to subcontinental, the temperature distribution showing continental, and the precipitation maritime influences (Eiden et al. 1989, Walentowski et al. 2001). Geographic location and topography of the Fichtelgebirge facilitate an influx of cold continental air masses from the east in winter. The mountain range also acts as a barrier for maritime air masses so that especially the western, windward parts of the Fichtelgebirge, similar to the western Steigerwald, receive large amounts of precipitation: the annual precipitation is up to ca. 450 mm higher than at the nearest westward escarpment, the Franconian Jurassic (ca. 600 m a.s.l.), and almost twice as high as the amount of precipitation that the area in the lee of the Franconian Jurassic receives (Meynen and Schmithüsen 1953–1962, BayFORKLIM 1996). This abundant precipitation makes this mountain range a main European watershed and source area of tributaries to the Rhine and the Elbe (North Sea) and the Danube (Black Sea).

The long-term mean monthly air temperature near the study site (DWD German Weather Service-climate station Fichtelberg-Hüttstadel, 659 m a.s.l., 7 km direct distance to the study site; DWD 1999–2000) reaches a maximum of 15.1 °C (interpolated for the elevation of the study site to 13–14 °C, according to BayFORKLIM 1996) in July and a minimum of -3.3 °C (-3 to -4 °C) in January (Fig. 3.1.2b). The mean annual air temperature is 6.1 °C (DWD 1999–2000; 4–5 °C: BayFORKLIM 1996). In contrast to the Steigerwald (see Chap. 3.1.), the higher elevation of the Fichtelgebirge causes a maximum in monthly precipitation in winter (approx. 130 mm in December) with a secondary maximum in summer (June–August, around 100 mm month<sup>-1</sup>) and otherwise fairly constant precipitation with minimum monthly values around 80 mm (Fig. 3.1.2b). The annual precipitation averages ca. 1100 mm (DWD 1999–2000; 1100–1300 mm: BayFORKLIM 1996). The topography is also responsible for the frequent occurrence of fog in the Fichtelgebirge (cf. Tab. 2 in Wresinsky and Klemm 2000).

The **Farrenleite** stand, located at about 950 m a.s.l. on the southern slope of the Schneeberg, was selected for this study as probably the highest mature beech stand of the whole region (see above and Meusel et al. 1965). Beech stands cover most of this slope of the Schneeberg, from about 700 to 950 m a.s.l., and are thought to be autochthonous (Firbas 1952, Firbas and Rochow 1956, Mayer 1998).

Within this stand a plot of about 0.16 ha with a SSW-exposed slope of 12.5° was marked. Established around 1880, the beech trees form a dense stand with a narrow range of stem diameters and a single canopy layer, lacking a shrub layer of re-growth in the understory.

### 3.3. Site characteristics

The following tables summarise information on site and stand structural characteristics. As far as own measurements are involved, the description of methods used is given in the subsequent chapters.

**Table 3.3.1:** Site characteristics: location, geology and soil; compiled from Langusch and Kalbitz 2001, Lischeid 2001, Fleck 2002, and author's measurements.

	Steinkreuz	Großebene	Farrenleite
Coordinates	10°27'38-44" E 49°52'15-19" N	10°26'43-52" E 49°52'41-48" N	11°51'27-34" E 50°02'30-32" N
Region	Steigerwald	Fichtelgebirge	
Mountain	Stollberg (476 m a.s.l.)	Schneeberg (1051 m a.s.l.)	
Elevation [m a.s.l.]	440	460	950
Plot area [ha]	1.29	0.23	0.16
Inclination [°]	5.5	2	12.5
Exposition	SSE	SE	SSW
Bedrock	Middle Keuper (Late Triassic)  Coburger Sandstein (kmC) and Unterer Burgsandstein (kmBu), interbedding of sandstone and clay layers	Middle Keuper (Late Triassic)  Blasensandstein (kmBL) and Coburger Sandstein (kmC), interbedding of sandstone and clay layers	Permo-Carbonian fine- to medium- grained shell granite of the Fichtelgebirge
Soil type (FAO)	Dystric Cambisol	Cambisol, with stony phase	Dystric Cambisol
Soil depth [cm]	50–80	5–40	30–100
Humus thickness [cm]	3	3	5
Soil pH (H <sub>2</sub> O) 0–5 cm	3.7	3.7	4.8
C/N of humus layer	15.2	15.2	17.6

**Table 3.3.2:** Stand structural characteristics of the two mixed beech-oak sites in the Steigerwald, Steinkreuz and Großebeine, and of the small pure beech plot within the Steinkreuz stand (plot area 220 m<sup>2</sup>) and the pure beech stand Farrenleite in the Fichtelgebirge. Only trees with DBH ≥ 7.0 cm included. For Steinkreuz, stand density and DBH-based data are interpolated for spring 1998 from 1996 and 2001 inventories and a subsampling in 1998; Großebeine was measured in spring 1998 and Farrenleite in spring 2000. < 1 % *Carpinus betulus* in the sub-canopy at Steinkreuz not accounted for.

	Steinkreuz	Großebeine	Steinkreuz-pure beech plot	Farrenleite
Overstory species composition	<i>Fagus sylvatica</i> , <i>Quercus petraea</i>	<i>Fagus sylvatica</i> , <i>Quercus petraea</i>	<i>Fagus sylvatica</i>	<i>Fagus sylvatica</i>
Stand age (1998) [yrs]	ca. 140	ca. 120	ca. 140	ca. 120
Density [trees ha <sup>-1</sup> ] (% <i>F. sylvatica</i> )	350.3 (76)	636.6 (67)	279.0 (100)	882.7 (100)
Range of DBH [cm]	<i>F. sylvatica</i> 7.0–68.7 <i>Q. petraea</i> 21.5–50.7	7.3–46.5 25.5–46.1	16.0–65.3	14.0–47.4
Average DBH [cm]	29.1	25.3		
<i>F. sylvatica</i>	26.7	19.4	36.9	26.8
<i>Q. petraea</i>	36.4	37.2		
Basal area A <sub>b</sub> [m <sup>2</sup> ha <sup>-1</sup> ]	29.0	37.9	38.4	52.7
<i>F. sylvatica</i> [%]	69	38		
Sapwood area A <sub>s</sub> [m <sup>2</sup> ha <sup>-1</sup> ]	18.6	17.2	32.1	42.7
<i>F. sylvatica</i> [%]	89	71		
Stand height <sup>b</sup> [m]	32	26	34	20
Max. tree height [m]	<i>F. sylvatica</i> 39 <i>Q. petraea</i> 34	28 30	34	26
Leaf area index LAI <sup>c</sup> [m <sup>2</sup> m <sup>-2</sup> ]	6.7	6.5	6.9	7.2
Ground cover [%]	5–10	<1	5–10	2
Shrub layer composition	few <i>F. sylvatica</i> saplings, <i>Sambucus racemosa</i>	very few <i>F. sylvatica</i> saplings	few <i>F. sylvatica</i> saplings, <i>Sambucus racemosa</i>	no shrub layer
Herb layer composition	tree seedlings, <i>Luzula albida</i> , geophyts, ferns, mosses	tree seedlings, <i>L. albida</i> , geophyts, mosses	tree seedlings, <i>L. albida</i> , geophyts, ferns, mosses	<i>Deschampsia flexuosa</i> , <i>Oxalis acetosella</i> , ferns, mosses, tree seedlings

<sup>a</sup> For *F. sylvatica*: A<sub>s</sub> = 0.666 DBH<sup>1.996</sup> (ST and GR) or A<sub>s</sub> = 0.793 DBH<sup>1.935</sup> (FA); for *Q. petraea*: A<sub>s</sub> = 0.065 DBH<sup>2.264</sup> (ST and GR); see Chap. 5.1.1.

<sup>b</sup> Average of 100 tallest trees per ha.

<sup>c</sup> Average of three years (1998–2000) and three methods (litter collection, optical measurements and allometric relationships from tree harvests); see Chap. 5.1.3.



## 4 Methods

### 4.1. Measurements of xylem sap flow with the thermal dissipation technique

#### 4.1.1. Principles and conversions

The thermal dissipation technique introduced by Granier (1985, 1987a) uses a linear, 20 mm long needle-like heat source that is radially inserted into the xylem of a trunk and supplied with a constant heating current. A temperature difference is measured between an upstream reference and a downstream thermocouple embedded in the heater. The temperature of the heated thermocouple is influenced by the rate of convective heat transport with the moving sap in the xylem conduits away from the heat source. The smaller this temperature difference is, the higher the sap velocity and hence also the convective heat transport. Accordingly, the larger the temperature difference, the slower the sap velocity and convective heat loss. Conductive heat loss is accounted for by using the temperature difference measured under non-transpiring (zero-flow) conditions (usually, but not necessarily at the end of the night, see below) in the calculation of sap flow density: the sap flow index  $K$  (dimension-less) is defined as the difference between the maximum ( $\Delta T_{max}$ ) and the current temperature difference ( $\Delta T_a$ ), divided by the current temperature difference (Granier 1985):

$$K = (\Delta T_{max} - \Delta T_a) \cdot \Delta T_a^{-1} \quad (\text{Eq. 4.1.1})$$

Nocturnal sap flow. During warm, dry nights when the vapour pressure deficit of the air ( $D$ ) was high,  $\Delta T$  regularly did not reach a plateau indicative of the cessation of sap flow (cf. Green et al. 1989). It was observed that  $\Delta T$  during night-time responded closely to changes in  $D$ , which indicates that either the stomata must have been open ("on purpose" or leaking) and/or that cuticular transpiration accounted for this flux. Because of the magnitude of  $\Delta T$ , stomatal opening in response to high  $D$  probably contributed most to this phenomenon (cf. Kavanagh et al. 2007).  $\Delta T$  may also not reach a plateau during nights of zero  $D$  during phases of soil water shortage because of continual refilling of the plant-internal tissues with water during the night (e.g. Daley and Phillips 2006, Kobayashi et al. 2007).

A software program, termed CHANGE and written in Visual Basic by M. Kubota, Institute of Silviculture, University of Shizuoka, Japan, (in cooperation with the Dept. of Plant Ecology, Univ. of Bayreuth) was used to detect  $\Delta T_{max}$  in the raw data after filtering for erroneous logger readings or malfunctioning thermal dissipation probes. The  $\Delta T_{max}$  for a particular day was selected from readings between noon of the previous day and noon of the present day. Nights with high  $D$  were identified from the concurrently recorded meteorological measurements and visual inspection carried out both on the sap flow data and the  $\Delta T_{max}$ -values identified by the software. For occasions when  $D$  was high throughout the night (which was usually reflected in the output from all sap flow sensors) the  $\Delta T_{max}$ -values determined by the software were omitted and excluded from further processing. In the next step of calculating sap flow density  $J_s$ , the software interpolates  $\Delta T_{max}$  for each time step between the two adjacent  $\Delta T_{max}$ -values, irrespective of whether there are 24 h in between these two  $\Delta T_{max}$ -values or several days in case of a warm, dry spell or persistent soil water shortage. If  $\Delta T_{max}$  differs from one day to the next this means that  $\Delta T_{max}$  will change

gradually. The physiological basis for this is that longer-term changes in conductive heat transfer capacity, e.g. reduced heat conductivity of the xylem due to prolonged summer drought and hence reduced wood water content/increased proportion of air in the wood (air being the better insulator or having the lower heat-conducting capacity compared to water), are not expected to happen abruptly. Such longer-term trends can be regularly seen in the raw data of thermal dissipation probes from trees in seasonal climates. Ample precipitation may reverse this pattern and  $\Delta T_{\max}$ -values and the general level of the  $\Delta T$ -signal will decrease rapidly over the course of a day or a night or more gradually over several days.

**Sap flow density.** An empirical calibration is used to convert the sap flow index K into the sap flow density  $J_s$  (the sap flow per unit sapwood area and unit of time; Granier 1985, 1987a):

$$J_s = 118.99 K^{1.231} \quad [\text{g m}^{-2} \text{s}^{-1}] \quad (\text{Eq. 4.1.2})$$

**Sap flux rates.** Absolute sap flux rates  $Q_r$  (in  $\text{g s}^{-1}$ ) are obtained by multiplying sap flow density  $J_s$  with the respective sapwood area  $A_s$ . Calculation of whole-tree sap flux or water use  $Q_t$  was derived from measurements of  $J_s$  in incremental depths of sapwood multiplied by annular sapwood area:

$$Q_t = \sum_{i=1}^{i=n} (J_{s,i} \cdot A_{s,i}) \quad [\text{g} \cdot \text{s}^{-1}] \quad (\text{Eq. 4.1.3})$$

$J_{s,i}$  = sap flow density of annulus  $i$ , in  $\text{g m}^{-2} \text{s}^{-1}$ ,

$A_{s,i}$  = sapwood area of annulus  $i$ , in  $\text{m}^2$ .

**Probing deep sapwood.** Sampling of the large sapwood radius of beech was biased towards the outer sapwood, where highest sap flow densities are usually found and which contribute most to whole tree sap flow (cf. Chap. 2.3.1), and interpolated for the innermost sapwood where sap flow is lowest. This made it possible to combine the monitoring of a large number of trees, in order to cover a wide range of tree sizes and capture the between-tree variability, with a reasonable representation of sap flow within a tree. A maximum of three contiguous annuli of 2 cm width, each corresponding to the radial dimensions of a standard thermal dissipation sensor, were probed in beech, beginning at the cambium-sapwood-boundary (see Fig. 4.1.1). In small suppressed trees only two sensors were necessary to cover the whole sapwood radius, whereas in large dominant trees three sensors did not protrude to the sapwood-ripened wood boundary. Sap flow in sapwood beyond the deepest inserted probe was estimated based on regression functions of the measured relative decrease in  $J_s$  with relative sapwood depth across all trees, assuming zero sap flow at the sapwood-ripened wood boundary, shown in Chapter 5.3 (Fig. 5.3.4c, d) and Chapter 5.4 (Eq. 5.4.1, Eq. 5.4.2). Seasonal averages of  $J_s$  on non-rainy days were used for these regressions. Interpolation was done per 2 cm-wide annuli. If the last remaining (central) annulus

was less than 1 cm wide, e.g. 0.9 cm, it was added to the last but one annulus, increasing its width from 2 cm to 2.9 cm. If the width of the central annulus was  $> 1$  cm, this annulus was treated separately as an annulus with e.g. 1.5 cm radius. In oak, one standard sensor representing a 2 cm-wide annulus was adequate to sample a trees' conducting sapwood.

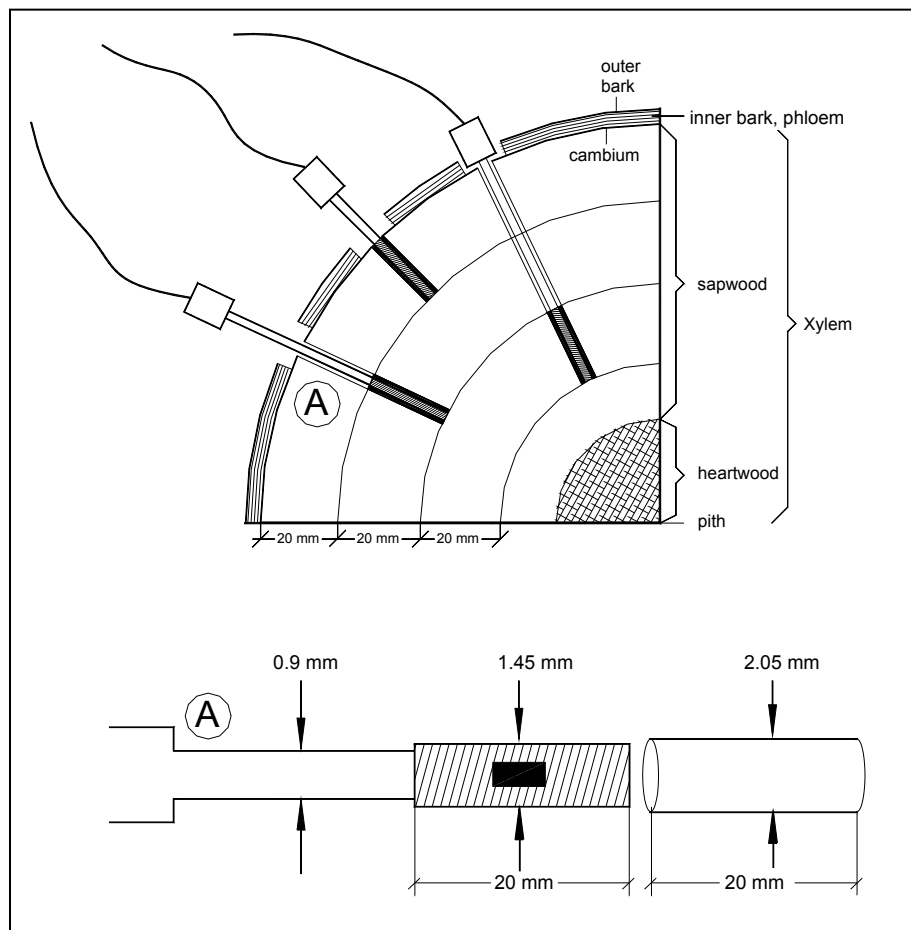


**Figure 4.1.1:** Schematic drawing of the implantation of three thermal dissipation probes (only the heated branch of a complete sensor) in three consecutive sapwood annuli as carried out on beech trees. The tangential distance between probes is not to scale, and the heartwood radius is smaller than would be expected from findings presented in Chapter 5.1.1. Detail "A" gives dimensions of heated probes manufactured in the Dept. of Plant Ecology, Univ. Bayreuth. A copper-constantan thermojunction (dark rectangle) is embedded in a stainless steel hypodermic syringe, 10 mm distant from the tip of the syringe. A teflon-insulated constantan wire, the heater, is coiled around the distal 20 mm of the syringe (hatched area). The probe is inserted into an aluminium tube for implantation into the stem of a tree. For details see text.

Scaling to stand level, canopy transpiration. Trees were selected for sap flow measurements according to diameter classes for each species and according to the contribution of a diameter class to stand basal area and hence sapwood area, i.e. biased towards classes with a large sapwood area (cf. Chap. 2.3.3). Diameter classes corresponded to social classes such as suppressed, intermediate and dominant (Tab. 4.1.1, below). In order to scale up water flux from trees to diameter classes,  $Q_t$  was normalised by its respective sapwood area  $A_{st}$ , averaged over all trees of the class

assessed with thermal dissipation sensors and multiplied by the sapwood area of the class per hectare, using the following equations. Sap flow through the stem can be assumed to be equal to water transpired by the canopy over a 24 h period (Schulze et al. 1985), particularly in species with small stem water storage such as beech (Granier et al. 2000a). Canopy transpiration  $E_c$  was then the sum of water fluxes in all stem diameter classes as described in Granier et al. (1996b):

$$J_{st} = \frac{\sum_{i=1}^{i=n} (J_{si} \cdot A_{si})}{\sum_{i=1}^{i=n} A_{si}} \quad [\text{g} \cdot \text{m}^{-2} \text{ s}^{-1}] \quad (\text{Eq. 4.1.4})$$

$$E_c = \sum_{l=1}^{l=n} \left( \left( \sum_{j=1}^{j=n} J_{stj} \cdot n^{-1} \right) \cdot A_{sc l} \right) \quad [\text{mm} \cdot \text{s}^{-1}] \quad (\text{Eq. 4.1.5})$$

$J_{st}$  = sapwood area-weighted sap flow density of a tree, in  $\text{g m}^{-2} \text{ s}^{-1}$ ,

$J_{si}$  = sap flow density of annulus  $i$ , in  $\text{g m}^{-2} \text{ s}^{-1}$ ,

$A_{si}$  = sapwood area of annulus  $i$ , in  $\text{m}^2$ ,

$E_c$  = canopy transpiration

$J_{stj=n}$  =  $J_{st}$  of  $n$  trees of a DBH-class, in  $\text{g m}^{-2} \text{ s}^{-1}$ ,

$A_{sc l=n}$  = sapwood area of diameter class  $l$  per hectare, in  $\text{m}^2 \text{ ha}^{-1}$ .

Total sap flow or canopy transpiration per day was calculated as the integral of the diurnal course of  $Q_t$  or  $E_c$ .

Canopy conductance. Values of canopy transpiration scaled from sap flow measurements can be used to estimate the total water vapour transfer conductance  $g_t$ , accounting for conductances from the height of the “average” stomata in the tree canopy to the height of measurement of the water vapour pressure deficit of the air  $D$  (Köstner 2001), using the following equation (Köstner et al. 1992):

$$g_t = E_c / D \cdot \rho_w \cdot G_v \cdot T_K \quad [\text{mm s}^{-1}] \quad (\text{Eq. 4.1.6})$$

$E_c$  = canopy transpiration [ $\text{mm s}^{-1}$ ],

$D$  = water vapour pressure deficit of the air [kPa],

$\rho_w$  = density of water (998) [ $\text{kg m}^{-3}$ ],

$G_v$  = gas constant of water vapour (0.462) [ $\text{m}^3 \text{ kPa kg}^{-1} \text{ K}^{-1}$ ],

$T_K$  = air temperature [K].

Total conductance  $g_t$  includes both “average” stomatal ( $g_c$ ) and aerodynamic conductance (leaf boundary layer and eddy diffusive conductance,  $g_a$ ;  $1/g_t = 1/g_c + 1/g_a$ ). Typically,  $g_a$  is large in aerodynamically rough forests (e.g. Jarvis and Steward 1979)

so that  $1/g_a$  becomes very small and  $g_t$  approximates  $g_c$  in such forests and was calculated as:

$$g_c = E_c / D \cdot \rho_w \cdot G_v \cdot T_K \quad [\text{mm s}^{-1}] \quad (\text{Eq. 4.1.7})$$

Half-hourly averages of  $E_c$  (in  $\text{mm s}^{-1}$ ),  $D$  and air temperature were used to compute  $g_c$ , omitting values when  $\text{PFD} < 15 \mu\text{mol m}^{-2} \text{s}^{-1}$  (night-time),  $D < 1.2 \text{ hPa}$  (0.12 kPa), and when  $\text{PPT} \geq 0.2 \text{ mm}$  during the half hour under regard and 2 h prior to it, since after rain the canopy can be expected to be wet. The diurnal maximum  $g_c$  ( $g_{c \max}$ ) of half-hourly values was then determined and used for further analysis.

#### 4.1.2. Probe design

The sap flow sensors used were manufactured by A. Suske, Dept. of Plant Ecology, Univ. of Bayreuth, and by the author, according to the original design by Granier (1985) and consisted of a reference and a heated probe (in the following together referred to as sap flow probe or sensor), constructed from a hypodermic syringe and Teflon-insulated constantan heating wire (0.13 mm diameter) coiled tightly around the tip of the syringe for a radial distance of 20 mm. A T-type copper-constantan-thermocjunction (0.13 mm diameter each) was inserted into the syringe 10 mm away from the tip (Fig. 4.1.1) and connected to that in the reference probe. The original design was modified in that longer hypodermic syringes were used to construct the sensors, reaching desirable depths for the trees under consideration of up to 6 cm xylem depth. As an additional modification, the reference probes were constructed to the same dimensions as in the original design from catheter tube and without coiled heating wire; testing showed no difference in performance compared to the much more costly and time-consuming original construction of the reference.

#### 4.1.3. Field installations

The thermal dissipation sensors were installed on undamaged, long-stemmed trees, on the north-facing side of the trunks to minimise exposure to direct sunlight as has become the standard procedure in most studies of forest water use (Wullschleger and King 2000, Wilson et al. 2001, Wullschleger et al. 2001, Ford et al. 2004b). Sensors were implanted 2 m above ground in order to measure a homogenous water flow and not solely the water drawn from a single main root, but also sufficiently far away from branches to avoid local branch signals, and not in the proximity of surface trunk damage.

The bark was removed down to the cambium with a bark gauge or a 5 mm-diameter drill bit to achieve thermal isolation from bark and phloem. Two fresh holes were drilled per pair of probes using 2.1 or 2.2 mm-drill bits, reaching down 20 mm inwards from the cambium-sapwood boundary and vertically separated about 15 cm from each other. Upon drilling of the holes, colouration, texture and moisture content of the bore chips were carefully inspected, especially in oak, where non-conducting heartwood can be easily determined visually (see Chap. 4.3, below). By doing so it was sought to prevent inserting the gauges into non-conducting heart- or ripewood, which could potentially affect the sap flow estimate as shown by Clearwater et al. (1999). Aluminium tubes, sealed on one end with composite glue and filled with grease to improve thermal contact between probe and aluminium tube, were inserted into the holes. Then the probes were implanted and the four leads from one complete sap

flow sensor with heater and reference were soldered to shielded 4 wire-cables up to 25 m long and differentially connected to the terminal block of a data logger (DL or DL2e, Delta-T Devices Ltd, Cambridge, UK, with LAC-1 analogue input cards in differential mode) in the case of the thermocouple and to a constant current source (built by the electronics workshop at the University of Bayreuth) in the case of the heater. The output of the constant current sources was adjusted so that the heaters were powered with 200 mW (cf. Granier 1985, 1987a). Thermocouple outputs were read every 30 seconds, averaged over 10 minutes and stored.

Power for the sensor set-up, data logger and weather station (see Chap. 4.5) at each site was provided by lead-acid batteries (12 VDC, 100 Ah) which were recharged by an array of 12 V-solar panels (MSX77, Solarex, Frederick, Maryland, USA) and a charge controller (Solarix-Atonic Delta, 20 A maximum loading current, IBC Solar AG, Staffelstein, Germany). Solar panels were mounted on a tripod-like scaffolding made of galvanised tube (1 ½" diameter). The voltage supplied by the batteries was also measured and stored every 10 minutes so that large drops in voltage, potentially influencing the output of the constant current sources and hence the functioning of sap flow gauges, could be detected easily.

The pairs of probes were covered with a roof-like shelter made from 7 mm-thick extruded polystyrene foam mats (Selitron, Selit, Erbes-Büdesheim, Germany; the insulation with 7 mm-thick Selitron equals the insulation with 30 mm of wood, as detailed by the manufacturer). These covers were attached to the trunk using adhesive tape and silicone, in order to reduce the radiative thermal load and to protect the installation from rain, especially important in beech due to significant stemflow, and from wind. The covers were about 50 cm long, at least 15 cm high and of variable width to accommodate all installed sensors.

When a radial sap flow profile was to be measured, a second and third sensor was installed on either side of the first one ("annulus #1", 0–20 mm radial sapwood depth). Sensors were spaced about 5–15 cm in circumferential (horizontal) direction away from sensor #1 and about 5–10 cm in vertical direction above or below it to maximise the distance between the sensors in order to avoid additional heating by conduction and at the same time to minimise the distance between the sensors enabling them to remain on the same side of the trunk. Sensor #2 was always implanted 20–40 mm deep into the sapwood and sensor #3 in 40 mm depth extending 60 mm into the sapwood (see Fig. 4.1.1). Utmost care was taken to precisely drill the holes exactly in this depth to avoid scaling errors associated with positioning of sensors (cf. Nadezhina et al. 2002).

#### 4.1.4. Sample trees

At the Steinkreuz site sap flow was measured during the growing seasons of the years 1998–2000. In 1999 and 2000 six additional trees were equipped that formed a pure patch of beech („pure beech plot“) within the mixed stand Steinkreuz to facilitate comparisons with both the pure beech stand in the Fichtelgebirge and the mixed stands in the Steigerwald. At the second Steigerwald site, Großebene, measurements of sap flow were carried out in 1998 and 1999. At Farrenleite in the Fichtelgebirge, investigations were started in 1998 but radial profiles were only assessed during the vegetation periods of 1999 and 2000, the growing seasons which were evaluated for this study. The same trees were measured in some of the stands over

three years. Sap flow gauges were removed at the end of each vegetation period and re-installed at the beginning of the following in the next year in newly drilled holes. Table 4.1.1 summarises the main characteristics of the sample trees and the sampling scheme regarding the radial profiles of sap flow over the years of the study.

In three smaller oak trees at Großebene, sapwood depth at sensor height was less than 20 mm as revealed on increment cores extracted after the end of the sap flow measurements. For these oaks (E59, E89, E136) a correction according to Clearwater et al. (1999) was carried out, which adjusts the measured temperature differences for the proportion of inactive xylem, assuming the same thermal properties of active xylem (sapwood) and inactive xylem (heartwood) at zero sap flow ( $\Delta T_{\max}$ ):  $\Delta T$  in Equation 4.1.1 is replaced by  $\Delta T_s$ , calculated as

$$\Delta T_s = (\Delta T_a - b \Delta T_{\max}) \cdot a^{-1} \quad (\text{Eq. 4.1.8})$$

with  $a$  the fraction of the probe in contact with sapwood, and  $b = 1 - a$  (Clearwater et al. 1999).

**Table 4.1.1:** Characteristics of trees selected for sap flow measurements and sapwood depth probing protocol during the growing seasons 1998–2000. DBH = stem diameter at 1.3 m height,  $h_t$  = tree height,  $A_{cp}$  = ground-projected crown area,  $A_{lt}$  = leaf area of tree (from allometric relationships, Chap. 4.4.1), DSH = diameter in sensor height,  $A_{st}$  = sapwood area at sensor height (from allometric relationships, Chap. 5.1.1),  $h_s$  = height of sensor installation on the trunk. Annulus #1 denotes 0–20 mm radial sapwood depth, annulus #2 20–40 mm, and #3 40–60 mm depth. In oak, only annulus #1 was probed. The reference season for the tree dimensions is 1999.

Species/Plot	tree	DBH [cm]	$h_t$ [m]	$A_{cp}$ [m <sup>2</sup> ]	$A_{lt}$ [m <sup>2</sup> ]	DSH [cm]	$A_{st}$ [m <sup>2</sup> ]	$h_s$ [m]	Annuli measured: 1998	1999	2000
<b>Steinkreuz-pure beech plot</b>											
Dominant	B4237	66	36	123	563	64	0.272	2	---	1 2 3	1 2 3
	B4213	58	34	64	452	56	0.204	2	---	1 2 3	1 2 3
	B4215	46	30	67	317	46	0.137	2	---	1 2 3	1 2 3
Suppressed	B4234	20	22	38	81	20	0.026	1.6	---	1 2 3	1 2 3
	B4214	19	13	61	74	19	0.023	2	---	1 --	1 --
	B4235	16	16	41	59	16	0.016	1.6	---	1 2 3	1 2 3
<b>Beech Steinkreuz, mixed stand</b>											
Dominant	B4108 <sup>a</sup>	62	32	92	501	60	0.235	2	1 2 3	1 2 3	1 2 3
	B4075	59	36	101	471	57	0.215	2	---	1 --	1 --
	B4133	46	33	52	314	46	0.137	2	---	1 2 3	1 2 3
Intermediate	B4012	39	26	59	235	38	0.093	2	---	1 2 3	1 2 3
	B4018	30	23	66	153	29	0.057	1.6	1 2 -	1 2 3	1 2 3
	B4243	28	26	47	141	27	0.049	2	1 --	1 --	1 --
	B4201	26	24	33	124	25	0.042	2	1 --	1 2 3	1 2 3
	B4322	26	27	33	124	25	0.04	2	---	1 --	1 --
Suppressed	B4050	17	15	40	60	16	0.017	1.4	1 2 -	1 2 -	1 2 -
	B4049	14	17	27	47	14	0.13	2	1 2 -	1 2 -	1 2 -

**Table 4.1.1, continued.**

Species/Plot	tree	DBH [cm]	$h_t$ [m]	$A_{cp}$ [m <sup>2</sup> ]	$A_{lt}$ [m <sup>2</sup> ]	DSH [cm]	$A_{st}$ [m <sup>2</sup> ]	$h_s$ [m]	Annuli measured: 1998	1999	2000
<b>Beech Großebene</b>											
Dominant	B133	40	24	63	253	39	0.098	2	1 2 -	1 2 3	- - -
	B12	39	26	52	241	37	0.092	3	1 2 -	1 2 -	- - -
Intermediate	B107	29	21	59	152	28	0.052	2	- - -	1 2 3	- - -
	B60	28	20	73	140	27	0.047	2	1 2 -	1 2 3	- - -
	B108	26	22	51	127	25	0.042	2	1 2 -	1 2 3	- - -
	B66	23	16	35	99	22	0.031	2	- - -	1 - -	- - -
Suppressed	B110	19	17	48	76	18	0.022	2	1 - -	1 2 3	- - -
	B82	17	20	52	64	17	0.018	2	1 - -	1 2 3	- - -
	B87	13	18	14	43	13	0.011	2	- - -	1 - -	- - -
<b>Beech Farrenleite</b>											
Dominant	x5	35	16	18	198	34	0.072	1.9	- - -	1 2 3	1 2 3
	x8	33	19	16	182	33	0.069	1.8	- - -	1 2 3	1 2 3
	x6	32	18	18	171	32	0.063	1.7	- - -	1 - -	1 2 3
	x4	31	18	18	161	29	0.055	1.8	- - -	1 2 3	1 2 3
Intermediate	x7	24	20	5	109	24	0.037	1.7	- - -	1 2 3	1 2 3
/Suppressed	x9	24	19	5	109	24	0.036	1.7	- - -	1 2 3	1 2 3
	x1	23	20	7	103	24	0.036	1.7	- - -	1 - -	1 2 3
	x2	20	17	7	81	19	0.024	1.8	- - -	1 2 3	1 2 3
	x3	18	15	4	68	18	0.021	1.7	- - -	1 - -	1 2 3
<b>Oak Steinkreuz, mixed stand</b>											
Dominant	E4202	50	31	67	404	49	0.043	2	-	1	1
	E4014	46	29	80	353	45	0.035	2	1	1	1
	E4324	43	30	37	307	41	0.03	2	1	1	1
	E4051	42	31	45	291	40	0.028	2	1	1	1
Intermediate	E4327	39	31	37	257	37	0.023	2	1	1	1
	E4054	38	31	35	252	37	0.023	2	-	1	1
	E4052	37	30	33	238	36	0.021	2	-	1	1
	E4055	36	30	52	228	35	0.02	2	1	1	1
	E4320	33	28	16	196	32	0.016	2	1	1	1
	E4048	30	27	15	167	29	0.014	2	-	1	1
<b>Oak Großebene</b>											
Dominant	E132	46	27	70	349	44	0.035	2	1	1	-
	E68	44	27	49	323	43	0.032	2	-	1	-
	E13	44	25	69	320	40	0.027	3	1	-	-
	E116	43	27	39	309	41	0.029	2	-	1	-
Intermediate	E64	39	25	42	257	37	0.023	2	1	1	-
	E37	38	27	48	247	38	0.025	2	1	1	-
	E86	37	26	53	240	35	0.021	2	-	1	-
Suppressed	E89	31	25	22	178	29	0.014	2	-	1	-
	E59	31	24	33	175	30	0.014	2	1	1	-
	E136	30	25	24	164	29	0.014	2	1	1	-

<sup>a</sup> Beech B4108 is emergent with a stem cross-section not round but lobed.

#### 4.1.5. Accuracy and errors

The resolution of the DL and DL2e data loggers used (with LAC-1 analogue input cards in differential mode) at  $\pm 4$  mV full scale is  $1 \mu\text{V}$ , the full scale error at  $20^\circ\text{C}$  is at most  $\pm 0.07\%$ , typically  $\pm 0.04\%$ , and the differential offset is maximum  $\pm 10 \mu\text{V}$ , typically  $\pm 3 \mu\text{V}$  (Delta-T 1996). The maximum error then is  $11 \mu\text{V}$ , the typical error  $4 \mu\text{V}$  at  $20^\circ\text{C}$  for the range of voltages outputted by thermal dissipation probes. This translates into units of sap flow density ( $J_s$ , in  $\text{g m}^{-2} \text{s}^{-1}$ ) as follows: the limit of detection of sap flow imposed by these data loggers is typically  $0.06 \text{ g m}^{-2} \text{s}^{-1}$  under no-flow conditions, under high-flow conditions the logger resolution equals  $0.09 \text{ g m}^{-2} \text{s}^{-1}$ ,  $0.01 \text{ kg d}^{-1}$  at the tree or  $0.1 \text{ mm d}^{-1}$  at the stand level. The total maximum error of  $J_s$  at  $20^\circ\text{C}$  is less than  $\pm 5\%$ , usually less than  $\pm 4\%$ .

Heat input to the stem additional to the artificial heating of the thermal dissipation probe, such as direct irradiance may cause natural temperature gradients ( $\Delta T_n$ ), violating the assumptions of heat balance and may introduce large errors (e.g. Cabibel and Do 1991, Köstner et al. 1998a, Braun and Schmid 1999, Do and Rocheteau 2002). In the present study precaution against the influence of natural temperature gradients on sap flow measurements was taken by the installation of sensors at the northern side of trunks, by installation in 2 m height above the ground and by careful insulation of the gauges (see above). Vertical natural temperature gradients ( $\Delta T_n$ ) were tracked several times during the growing season for a few days while the heating was turned off. Since all measurements in the present study were carried out in forest stands with a closed canopy, the penetration of direct sunlight into the stand was small in general and  $\Delta T_n$  was negligibly small: the maximum values of  $\Delta T_n$  found were  $0.05 \text{ K cm}^{-1}$  (axial distance) for beech and  $< 0.02 \text{ K cm}^{-1}$  for oak (data not shown).

### 4.2. Tree and stand biometry

Typical parameters used to describe the structure of a stand were measured at all sites and included diameter at breast height, basal area, cross-sectional sapwood area, canopy height, ground-projected crown area, age and leaf area of the trees, and stand density, species composition, basal area and leaf area index of the stands.

The diameter at breast height (DBH), i. e. 1.3 m above ground, was calculated as circumference at breast height, measured with a tape and divided by  $\pi$ . DBH-inventory data for the fenced plot Steinkreuz from spring 1996 and autumn 2001 were provided by P. Gerstberger, Dept. of Plant Ecology, Univ. of Bayreuth. Basal area of a tree,  $A_{bt}$  (in  $\text{m}^2$ ), was calculated from DBH and included bark.  $A_{bt}$  was totalled for the respective trees of a plot and divided by the plot area to give the basal area of the plot,  $A_b$  (in  $\text{m}^2 \text{ ha}^{-1}$ ). Cross-sectional sapwood area ( $A_s$ ) was derived as described in detail in Chapter 4.3.

The ground-projected crown area ( $A_{cp}$ , in  $\text{m}^2$ ) of trees was usually measured in 8 horizontal directions using a compass, crown mirror or clinometer and measuring tape. The octagonal area was calculated as the sum of eight triangles, which was found to represent the projected shape of the crown better than a cylindrical-sectorial shape (cf. Fleck 2002). At Farrenleite,  $A_{cp}$  was measured in four cardinal directions only and adjusted afterwards, based on a linear regression established on beech

from Steinkreuz and Großebene, where  $A_{cp\ 8} = 1.359 * A_{cp\ 4}$  with  $R^2 = 0.9330$ ,  $p < 0.0001$  (data not shown).

The height of the tree top ( $h_t$ , in m) and of the insertion of the lowest living branch on the trunk ( $h_{blc}$ ) was measured with a theodolite (Wild Tachymat, Heerbrugg, Switzerland), a survey laser (Criterion 400 Laser Survey Instrument, Laser Technology, Englewood, Colorado, USA), or a clinometer, measuring tape and compass. Crown length was calculated as  $h_t - h_{blc}$ . Heights and ground-projected crown areas were measured on a subsample of trees in the three plots. Tree positions (x-, y-, z-coordinates) were measured with the same instruments as tree height; data for Steinkreuz were provided by P. Gerstberger, Dept. of Plant Ecology, Univ. of Bayreuth.

The age of several trees at each site was estimated by counting growth rings on increment cores, extracted with a Pressler borer (Mora, Sweden; 5 mm diameter), under a stereo microscope.

#### 4.3. Sapwood area

The radial depth of sapwood in *Quercus petraea*, a ring-porous species with obligatory heartwood formation and darker coloured heartwood (Chap. 2.3.1), was assessed on increment cores extracted from the trees in which sap flow was measured. A 5 mm-diameter Pressler borer (Mora, Sweden) was radially drilled towards the centre of the trunks at positions corresponding to the positions of the sap flow sensors. Since the radius of sapwood is small in ring-porous oak (e.g. Braun 1970, Tyree and Zimmermann 2002), the borer was usually not protruded to the pith of a trunk to minimise the impact on the live trees. Core dimensions such as the radius of the bark, the radius of the sapwood, and total core length, were measured immediately in the field. Additional measurements of bark thickness were made upon installation of sap flow probes with a bark gauge. Growth rings were counted and radial increment per year or per decade determined (to the closest 0.1 mm) with a lens micrometer or callipers, still fresh in the lab under a stereo microscope (up to 100-fold magnification). The sapwood area of a tree  $A_{st}$  (in  $m^2$ ) was calculated as

$$A_{st} = (c_h \cdot 2\pi^{-1} - r_b)^2 \pi - (c_h \cdot 2\pi^{-1} - r_b - r_s)^2 \pi \quad [m^2] \quad (\text{Eq. 4.3.1})$$

where  $c_h$  is circumference at the height of extraction of increment core (in m),  $r_b$  is the radius of the bark and  $r_s$  the radius of the sapwood at the respective height (in m). Supplementary information on sapwood was gathered from trunk disks taken in the same stands but outside the experimental plots. Allometric relationships between stem diameter and sapwood area were established on these data.

The sapwood area of a plot  $A_s$  (in  $m^2 ha^{-1}$ ) was computed from the sum of  $A_{st}$  (using DBH and allometric equations in Table 5.1.1, Chap. 5.1) of all trees in the plot, divided by the plot area  $A_p$  as

$$A_s = \left( \sum_{i=1}^{i=n} A_{st} \right) \cdot A_p \quad [m^2 ha^{-1}] \quad (\text{Eq. 4.3.2})$$

In *Fagus sylvatica* the procedure was essentially the same as for oak, except that the borer was drilled to the centre of the trees or as deep as possible, because the sapwood radius is large in beech (e.g. Braun 1970, Grosser 1977). Furthermore, discolouration, if present at all, is not a reliable criterion to distinguish ripewood from sapwood in this diffuse-porous species. Also the percentage of non-structural carbohydrates on total dry matter shows only a slightly decreasing trend over the whole radius in beech (Hoch et al. 2003) whereas in *Q. petraea* this proportion decreases strongly towards the sapwood-heartwood transition zone (Barbaroux and Breda 2002, Hoch et al. 2003). In some cases the radius of sapwood could be estimated immediately on increment cores from its translucency due to a higher water content compared to the ripewood (cf. Barbour and Whitehead 2003; Grosser 1977, Hillis 1987). Additionally, increment cores were dyed with bromocresol green (Sigma Chemicals, Germany; 0.5 % solution in ethanol; Sandermann et al. 1967, Burrows 1980). This pH-indicator (range from pH 3.8, yellow, to pH 5.4, blue) mostly gave satisfying results, ripewood showing lower pH (green) than sapwood (blue).

On stem disks taken from trees felled in stands adjacent to Steinkreuz and Großebene, using the same indicators as on increment cores, it was found that several beech trees showed eccentric patterns in ripewood. In order to acquire more detailed information on this important scalar, a non-destructive method was sought that would allow the determination of the sapwood area of the trees studied for sap flow without injuring their hydraulic system. Mobile computer tomography meets these prerequisites.

**Computer tomography.** Mobile, or portable computer tomography, as developed by Habermehl et al. at the Centre for Radiology, University of Marburg, Germany, in the 1970s, is an imaging technique that allows the determination of the cross-sectionally varying absorption coefficients for ionising radiation within a thin layer of the trunk of a standing, live tree of up to 70 cm diameter (Habermehl and Ridder 1979, Habermehl 1982a, b, Habermehl et al. 1990, Habermehl and Ridder 1992, 1993). Other CT instruments intended for field use were introduced e.g. by Onoe et al. (1983), Miller (1988) and Davis et al. (1993). Mobile CT so far is the only imaging technique suitable for large, standing trees in the field. It has been mainly employed in tree disease diagnosis (for instance to assess rot in trunks, e.g. Habermehl 1982a) or power pole inspection (e.g. Davis et al. 1993), but has also been successfully used to quantify sapwood area in several species (Wiebe and Habermehl 1994: *Picea abies*, *Larix decidua*, *Quercus robur*; Alsheimer et al. 1998: *Picea abies*; Schäfer et al. 2000: *F. sylvatica*; Schäfer 1997: *Q. petraea*; and more qualitative in *Q. petraea* and *Q. cerris* by Raschi et al. 1995 and Tognetti et al. 1996). Mobile CT has also been utilised to correlate wood properties and sap velocity as measured with the heat pulse technique (Raschi et al. 1995, Tognetti et al. 1996; note that these authors' "wood density" is actually physical density, cf. Chap. 5.1).

The CT-system used in this study was one of three existing MCT-3 (Centre for Radiology, University of Marburg, Germany; Fig. 4.3.1). It records one-dimensional profiles of radiation transmission around the stem by translational and rotational movement of the radiation source ( $^{137}\text{Cs}$ ) and scintillation detectors (each consisting of a lead collimator, 6 mm wide and 18 mm high, a NaJ-crystal and a photomultiplier), mounted parallel to each other on bearing rails (Fig. 4.3.1 right). An elaborate mathematical reconstruction procedure (modified filtered backprojection, Ridder 1979) calculates a distribution matrix of absorption coefficients from the one-dimensional

profiles and allows its two-dimensional visualisation (Ridder 1996). The spatial resolution on the reconstructed CT images depends on the (spatial) scanning interval (which is set by the operator between 4 and 10 mm for small- and large-diameter trees, respectively, to compromise on scanning duration and image resolution). It ranged from 2 mm (stem diameter 17 cm) to 6 mm (stem diameter 66 cm) in this study. The absorption values  $\alpha$  (in  $\text{cm}^{-1}$ ) calculated by the reconstruction software are the physical absorption coefficients multiplied by  $10^3$  (Ridder 1996).

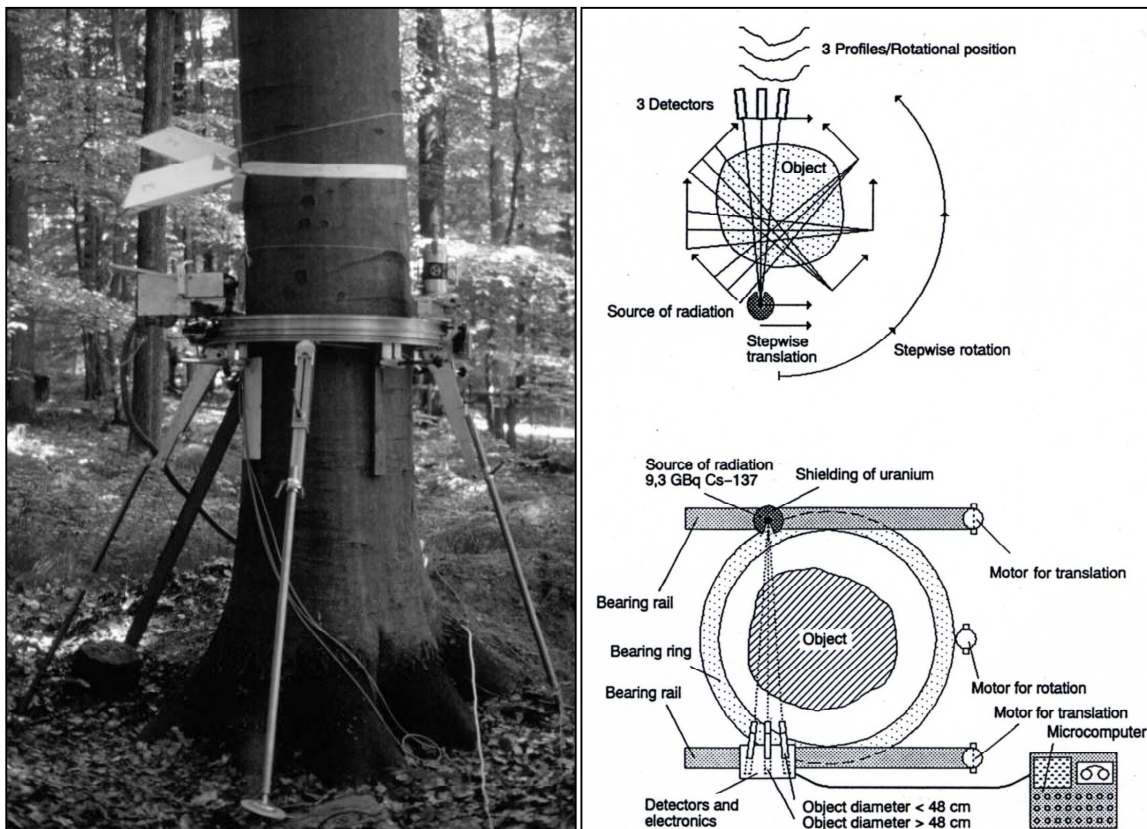


**Figure 4.3.1:** Mobile computer tomograph (MCT-3, Centre for Radiology, University of Marburg, Germany/Dendro-Institut Tharandt, Germany) installed on sap flow beech B4237 in the stand Steinkreuz, May 16, 2000 (**left**). The level of the scan is 1.7 m above the ground at the height of the sap flow sensors (insolation shielding temporarily lifted up, left side of trunk). The source of radiation is seen on the right, the detectors on the left side of the trunk. Schematic drawings (**right**, from Raschi et al. 1995) illustrate the operating principles of the MCT-3.

Measurements with the MCT-3 were carried out between May 15 and 19, 2000, in cooperation with A. Solger, Dendro-Institut Tharandt, Germany. A total of 24 beech trees, covering the whole range of tree diameter classes, were assessed with CT, all nine sap flow trees at Farrenleite, nine sap flow beech trees at Steinkreuz and six (sap flow trees from the previous two years) at Großebene. Only a few of the large beech trees in Steinkreuz were scanned because of the amount of time required: even at low resolution, the tomography of a tree with 66 cm diameter took more than four hours, whereas a scan on a tree with 20 cm diameter was completed in less than 30 minutes at high resolution.

Quantitive use of CT to assess sapwood area. Because of the high quantum energy of the gamma ( $\gamma$ )-radiation emitted by the radionuclide  $^{137}\text{Cs}$  (662 keV) used in the MCT-3 and low atomic numbers of the examined material, absorption is mainly caused by the Compton effect and therefore is proportional to the physical density of the trunk material (Edwards and Jarvis 1983). The density of the material is comprised of the density of the wood itself and of the water within the woody tissues. If CT is intended to be used quantitatively to estimate sapwood area based on the cross-sectional variation of water content in a trunk, these two components of physical density have to be separated (cf. Wiebe 1992, Raschi et al. 1995) as exercised in Chap. 5.1.

The classification of absorption values as sapwood or ripewood was achieved by exemplary calibration against increment cores: immediately after a tomographic scan had been completed, a 5 mm-diameter core was extracted from the wood at the same level on the stem of three beech trees (the number of trees that could be treated in this way was constrained for various reasons). The sapwood-ripenwood boundary was determined visually, the core then divided into 5 mm segments and weighed immediately in the field to the nearest 0.1 mg (draft-shielded electronic balance MC1 AC 210 S, Sartorius, Göttingen, Germany). The volume of the segments was measured according to Archimedes' principle (density of water corrected for temperature) on the same balance after drying ( $80^\circ\text{C}$ , 48 h). The water content ( $W_f$ , in  $\text{g cm}^{-3}$ ) of the segments was computed from fresh mass ( $m_f$ ), dry mass ( $m_d$ ) and dry volume ( $v_d$ ) as

$$W_f = (m_f - m_d) \cdot v_d^{-1} \quad (\text{Eq. 4.3.3}).$$

The wood density ( $\rho_{wd}$ , in  $\text{g cm}^{-3}$ ) was computed as

$$\rho_{wd} = m_d \cdot v_d^{-1} \quad (\text{Eq. 4.3.4}).$$

The relative water content ( $R_w$ , in %) was calculated from the ratio of water content and wood density as

$$R_w = W_f \cdot \rho_{wd}^{-1} \cdot 100 \quad (\text{Eq. 4.3.5}).$$

The respective sapwood area at the beginning of each vegetation period (estimated from circumference measurements using the allometric relationships given in Chap. 5.1.1) was used for calculations of flow rate, stand transpiration etc. for the whole vegetation period.

#### 4.4. Leaf area index of the canopy

Leaves are the active interface of energy, carbon, and water vapour exchange between forest canopies and the atmosphere. The leaf area index (LAI, in  $\text{m}^2 \text{ m}^{-2}$ ), defined by Watson (1947) as the total one-sided area of leaf tissue per unit ground surface area or by Chen and Black (1991, 1992) as half the total green leaf area per unit ground area, is therefore one of the most important physiological characteristics of canopy structure.

Direct, destructive methods such as harvesting trees and the planimetry of their respective leaf area to estimate LAI are very labour-intensive, require many replicates to reduce sampling errors (Chason et al. 1991) and must depend on extrapolation using allometric methods (Chen et al. 1997). More rapid, indirect estimates can be obtained by measuring light transmission through a plant canopy and using Lambert-Beer's law or gap fraction theory (cf. Norman and Campbell 1989, Weiss et al. 2004) to infer the thickness of the absorbing plant layer. The gap fraction is the ratio of the above to the below-canopy radiation. A widely used instrument to estimate LAI based on gap fraction measurements is the Li-Cor LAI-2000 Plant Canopy Analyser (PCA; Li-Cor Inc., Lincoln, Nebraska, USA). A semi-direct, non-destructive method suited to deciduous forests with a single, comparatively short leaf-fall season, is the collection of litter in traps below the canopy.

In the present study, direct, semi-direct and indirect methods were employed to assess the leaf area of trees ( $A_{lt}$ ) and LAI, since all the temporal and spatial levels of resolution mentioned are important in characterising and analysing structure-function relationships for different species and stands over time.

##### 4.4.1. Direct estimates of LAI, allometric relationships

Direct LAI estimates, based on branch harvests and subsequent leaf planimetry, site- and species-specific allometry (e.g. Dixon 1971, Grier and Waring 1974, Waring et al. 1977) and scaling to stand level, were formed in close cooperation with the present study by S. Fleck, Plant Ecology, University of Bayreuth, for four trees at the same investigation sites in 1997 and 1998: one beech and one oak tree at Großebeine and two beech trees at Farrenleite (see Fleck 2002). Harvesting was leaf-cloud-oriented (cf. Fleck 2002) and all the branches of the oak at Großebeine and of the two beech trees at Farrenleite were harvested; of the beech at Großebeine about 40 % of all the branches were harvested. For the purpose of a detailed three-dimensional mechanistic gas exchange model (Fleck 2002), description of structural parameters was very detailed on a sub-tree level, namely on leaf and leaf cloud level, and thus only a few mature trees could be tackled with this strategy. The tree canopies were accessed via a hydraulic lift (Teupen Hylift, Gronau, Germany) whose platform reached 23 m above ground. For a more detailed description of the procedures see Fleck (2002).

Given the limited number of trees considered, more general relationships for beech and oak between the leaf area of a tree ( $A_{lt}$ ) and an easily accessible scalar like DBH or basal area of a tree ( $A_{bt}$ ) were sought. Fleck (2002) and Fleck et al. (2004) approximated the following allometric relationships, for *F. sylvatica* based on harvests by Pellinen (1986), Bartelink (1997) and Fleck (2002), a total of 45 trees:

$$A_{lt} = 0.876 A_{bt}^{0.81} \quad [\text{m}^2], r^2 = 0.89 \text{ (beech)}, \quad (\text{Eq. 4.4.1})$$

for *Q. petraea* using results from Burger (1947, including data from *Q. robur*) and Fleck (2002), totalling 52 trees:

$$A_{lt} = 0.871 A_{bt}^{0.854} \quad [m^2], r^2 = 0.854 \text{ (oak)}, \quad (\text{Eq. 4.4.2})$$

with  $A_{bt}$  in  $cm^2$ .

These data showed a considerable variation among the older trees, which appeared to be stand-specific (Fleck et al. 2004). Leaf area estimated with the above regressions yielded values 10 % (beech) and 27 % (oak) larger than calculated from direct measurements on the trees harvested at Großebene (Fleck 2002). A stand-specific calibration reduced constants in the above equations to 0.77 for beech and to 0.616 for oak (Fleck, pers. comm.):

$$A_{lt} = 0.77 A_{bt}^{0.81} \quad [m^2] \text{ (beech)}, \quad (\text{Eq. 4.4.3})$$

$$A_{lt} = 0.616 A_{bt}^{0.854} \quad [m^2] \text{ (oak)}, \quad (\text{Eq. 4.4.4})$$

with  $A_{bt}$  in  $cm^2$ .

To calculate LAI from these allometric relationships, the equations were applied to all stem diameters of the respective plot, totalled and divided by the plot area (see Fleck 2002). This resulted in values of LAI of 6.4 (Steinkreuz) and 6.3 (Großebene) using the stand-adjusted constants (Fleck et al. 2004). Adjusted LAI at Farrenleite was 8.1 (Fleck 2002).

#### 4.4.2. Semi-direct estimates of LAI, leaf area per unit dry mass

Semi-direct LAI estimates were gained from non-destructive and less labour-intensive litter collections. 10 square-shaped litter traps of  $1 m^2$  or  $0.15 m^2$  surface area were set up on the forest floor at Steinkreuz and Großebene respectively, and three at Farrenleite ( $0.15 m^2$ ). Drainage was facilitated by the use of coarse-meshed material for the bottom of the traps. Litter was collected from the traps weekly or biweekly during autumn. Depending on the amount of foliage, the projected, half-total surface leaf area of the whole sample from a litter trap or of a subsample was measured and scaled up to the whole sample by leaf area per unit of dry mass (or specific leaf area; SLA) after drying the sample and subsample at  $70^\circ C$  to a constant mass. The SLA was determined separately for each trap because of the potentially large spatial variability of SLA due to differences in stand structure (see Bouriaud et al. 2003) and large potential errors of up to 24 % when computing LAI from SLA (Bouriaud et al. 2003). Additionally, the SLA was determined for each sampling date individually because of the known seasonal variability in SLA (Heller and Götsche 1986, Gratani et al. 1987, both in the sun and shade crown), except for Steinkreuz in the year 2000, where an average value from the year 1999 was used ( $198 cm^2 g^{-1}$  and  $138 cm^2 g^{-1}$  for beech and oak respectively). In Großebene, in 1999 the leaf area of all samples was measured and no SLA determined. Projected leaf areas were measured using either a Delta-T Image Analysis System (DIAS; Delta-T Devices Ltd., Cambridge, UK) or a LI-3100 Area Meter (Li-Cor Inc., Lincoln, Nebraska, USA).

#### 4.4.3. Indirect estimates of LAI

Indirect LAI estimates were derived from measurements with the LAI-2000 Plant Canopy Analyser (PCA; Li-Cor Inc., Lincoln, Nebraska, USA). LAI (or more precisely the plant or vegetation area index, PAI or VAI, respectively, see below) is calculated using inverted gap fraction data. The PCA uses fisheye optics to project a hemispheric image of the canopy above the horizontally exposed lenses onto five silicone detectors (photodiodes) arranged in concentric rings. The field of view of those concentric rings is centred around zenith angles of 7°, 23°, 38°, 53°, 68°, numbered 1 to 5, respectively (Li-Cor 1992). The azimuthal field of view is 360°. An optical filter which restricts transmitted radiation to below 490 nm minimises the contribution of light scattered by foliage (Welles 1990, Welles and Norman 1991). The lower limit for radiation measurement is 400 nm (Chen et al. 1997).

Two LAI-2000 Plant Canopy Analyser-units were used in this study. The instruments were used in remote mode, their clocks synchronised and silicone detectors calibrated to each other before any reading was taken at each measurement day. The reference unit was programmed to take readings of the “above canopy” radiation every 15 seconds in nearby forest openings that were large enough not to block more of the horizon than what is detected by the outermost concentric ring of the fisheye optics, since this ring was not going to be used anyway for methodological considerations (see below). The below-canopy measurements were made at 5 m grid points in 50 m x 50 m plots (110 sampling points, marked with wooden posts and tagged lines) in the Steinkreuz and Große Ebene stands, and around the centre of the plot in Farrenleite in 5, 10, 15 and 20 m distance in the four cardinal directions. Readings were taken at 2 m height above the ground in all stands, the sensor head clamped onto a 2 m long wooden stick and levelled from below. This avoided unintended shading of the optics by the operator and standardised the sampling procedure. A view restrictor (Li-Cor 1992) was not used. Since the theory of gap fraction analysis assumes that only skylight is seen by the sensors, measurements were carried out under diffuse light as advised by Welles and Norman (1991), either under overcast sky conditions, or at dawn or dusk. Measurements were repeated several times over the course of the growing seasons and also during winter.

Since all parts of plants (leaves, branches, stems) intercept light on its way through the canopy to the below-canopy sensor, the PCA primarily estimates the plant area index (PAI). PAI was calculated using the Li-Cor software C2000 (Li-Cor 1992), combining the above-canopy and below-canopy light values from the two units based on the time of observation. Readings from the outermost ring (zenith viewing angles 61°–74°) were omitted using only rings 1 to 4 to improve accuracy (Dufrêne and Bréda 1995, Cutini et al. 1998). PCA-readings from sampling points directly beside a tree trunk or directly under low branches were rejected (a total of 12 in Steinkreuz and 2 in Große Ebene) and interpolated from the readings of the surrounding sampling points.

PAI-estimates were afterwards corrected for light interception by woody elements (stems, branches) and for foliage element non-randomness (element clumping) as suggested by Kucharik et al. (1998) to result in LAI. Gap fraction theory assumes random spatial distribution of light intercepting elements (Welles 1990, Welles and Cohen 1996). The non-randomness correction factor for foliage (Kucharik et al. 1998) in closed temperate deciduous oak and maple forest canopies was measured to be close to one (randomness; Kucharik et al. 1999). The LAI of those stands was 4.5

and 6, respectively, and thus comparable to the Steigerwald and Fichtelgebirge sites. Values for the non-randomness correction factor were taken from Fig. 5 in Kucharik et al. (1999) and estimated to be on average 0.91 for oak and 0.96 for beech (sugar maple in their study, assumed to be very similar to beech in its canopy structure) for the zenith angles used in the present data evaluation ( $5^\circ$ – $60^\circ$ , rings 1–4 of PCA). These values have been corroborated by Eriksson et al. (2005). For the mixed species stands under regard here, the non-randomness correction factors for oak and beech were weighted by the species' contribution to stand density. The PAI-estimate calculated by the C2000-software was then divided by this site-adjusted non-randomness correction factor. Then the stem hemi-surface area index (SAI) beneath crowns was estimated by approximating the projected stem area from the height of insertion of the lowest living branch and the stem diameter, and dividing their sum by the plot area (cf. Kucharik et al. 1998). Branch hemi-surface area is mostly masked by foliage in oak and beech canopies during the vegetation period (Dufrêne and Bréda 1995, Kucharik et al. 1999) and was found to amount to only about 6 % of the leaf area of leaf clouds of beech and oak at Großebeine (Fleck et al. 2004) and consequently negligible for corrections. Below-crown SAI was then subtracted from non-randomness corrected PAI to give LAI (Kucharik et al. 1998).

#### 4.5. Meteorological and soil measurements

To quantify atmospheric controls of canopy transpiration, meteorological data were recorded concurrently with sap flow measurements. At Steinkreuz, a climate station located in a large forest gap adjacent to the plot has been operational since the end of 1994. Within a circle of about 25 m in the vicinity of the small meteorological tower, all regrowing trees were periodically removed. Photosynthetical photon flux density (PFD) was measured with a quantum sensor (LI-190SA, Li-Cor Inc., Lincoln, Nebraska, USA), net radiation ( $R_n$ ) with a pyrradiometer (8111, Schenk, Vienna, Austria), both at 5 m height above ground, air temperature ( $T_{air}$ ) and relative humidity (rh) with a humidity-temperature-Probe (HMP45A, Vaisala, Helsinki, Finland) at 2 m height, and wind speed and direction, using a switching anemometer with 3-cup rotor (A100R) and a potentiometric wind vane (W200P, both Vector Instruments, Wind-speed Ltd, Rhyl, UK), installed 5 m above ground. Bulk precipitation (PPT) was measured with an aerodynamic tipping bucket rain gauge (ARG100, Environmental Measurements Ltd, Sunderland, UK, 0.2 mm resolution). All sensors were scanned every 30 seconds and readings averaged or integrated over 10 minutes and stored by a data logger (DL and DL2e with LAC1-cards, Delta-T Devices Ltd, Cambridge, UK). Power was supplied by solar-charged 12 V-lead-acid batteries (see Chap. 4.1.3). For Großebeine, meteorological data from nearby Steinkreuz were taken as representative.

At Farrenleite, a climate station was set up in a small canopy gap some 20 m uphill from the trees instrumented with sap flow gauges. From spring 1999 the same variables as at Steinkreuz were recorded, except for wind speed and direction.  $T_{air}$  and rh were measured with a SKH 1011 (Skye Instruments Ltd, Powys, UK), at about 2 m height like PFD and  $R_n$ . Precipitation was measured only during the growing season, since servicing of the station during winter was hindered by snow. Temperature measurements started in spring 1998. The water vapour pressure deficit of the air (D) was calculated from air temperature and relative humidity for both climate stations using the Magnus formula.

Additional air and soil temperatures were measured inside the three stands with small thermistors (M841/S1/3K, Siemens, Germany) at 2 m and 0.1 m above the ground (both with radiation shields), in the litter layer, and in the mineral soil (-0.1 m, -0.25 m, -0.5 m). Inside the Steinkreuz stand, under the tree canopy, global radiation was measured at 2 m height with a pyranometer (LI-200SA, Li-Cor Inc., Lincoln, Nebraska, USA) from late July 1999 till the end of October 2000.

In order to follow the seasonal change of soil water supply to the vegetation and to identify periods of potential soil water limitation, soil matrix potential  $\Psi_s$  (in MPa) and volumetric soil water content  $\theta$  (in  $m^3 m^{-3}$ ) have been monitored with tensiometers and time domain reflectometry (TDR) probes (resolution  $0.015 m^3 m^{-3}$ ), respectively, (both IMKO GmbH, Ettlingen, Germany) at Steinkreuz since autumn 1994 by the Dept. of Hydrogeology at BITÖK. Tensiometers were installed at 0.2 m, 0.9 m and 2 m soil depth, TDR-probes at 0.2 m, 0.35 m and 0.9 m depth, at five and three different locations inside the fenced plot, respectively, and read out hourly by data loggers. Tensiometers operated down to approx. -0.08 MPa. Data were made available through G. Lischeid, formerly Dept. of Hydrogeology, BITÖK, Univ. of Bayreuth.

Relative extractable water  $\theta_e$  in the soil was calculated as the ratio of actual extractable water to maximum extractable water (Black 1979), the latter term being equal to the difference between maximum and minimum soil water content. The maximum water content, or soil water content at field capacity, was evaluated as the average of the ten highest daily mean values found in winter and early spring after periods of free drainage over the three years under consideration. The minimum water content was estimated from water retention curves established at -1.5 MPa (permanent wilting point) on soil cores from the respective soil horizons at the Steinkreuz site (Langusch and Kalbitz 2001, see Tab. 5.2.1.3).  $\theta_e$  was computed as (Black 1979):

$$\theta_e = (\theta_a - \theta_p)/(\theta_f - \theta_p) \quad (\text{Eq. 4.5.1})$$

where  $\theta_a$ ,  $\theta_p$ , and  $\theta_f$  denote actual soil water content, soil water content at permanent wilting point, and at field capacity, respectively (all in  $m^3 m^{-3}$ ). Minimum  $\theta_e$  is 0 (dry soil), maximum  $\theta_e$  can exceed 1 ( $\theta_e$  at field capacity) after heavy rainfalls as happened occasionally. Only daily mean  $\theta$  was used in calculations, which minimised the transient effect of over-saturating rain. Values of  $\theta_e$  exceeding 1 were excluded. No data were available for approximately 75 days during May–October in 1999 and 2000, for both tensiometers and TDR-probes.

At Großebene, non-automated tensiometers (Oikos, Göttingen, Germany) were installed at the beginning of August 1998 at depths of 0.2 m, 0.35–0.4 m and 0.45–0.65 m. The position of some gauges was changed at the end of March 1999. Values of soil matrix potential  $\Psi_s$  were recorded in irregular intervals (twice a week to monthly) during the vegetation period 1998 and 1999 with a hand-held read-out device (Oikos, Göttingen, Germany). Minimum  $\Psi_s$  measured with this equipment was approx. -0.075 MPa.

At the Farrenleite site in the Fichtelgebirge, volumetric soil water content  $\theta$  was monitored with a FDR (Frequency Domain Reflectometry) probe (ThetaProbe ML2x, Delta-T Devices Ltd, Cambridge, UK) at 0.3 m soil depth and recorded half-hourly. Voltage outputs were converted to values of  $\theta$  afterwards, using the generalised cali-

bration for organic soils provided by the manufacturer (Delta-T 1999). Readings from the year 2000 were erroneous as was found out only later after intense evaluation of the data, probably due to electrical problems in the circuitry. Soil water retention characteristics were not available for this site, so data were evaluated on a relative basis only: Actual soil water content  $\theta_a$  was related to soil water content at field capacity  $\theta_F$ , the latter being measured at the beginning of the growing period (see above; approx.  $0.20 \text{ m}^3 \text{ m}^{-3}$ ).

Daily, monthly and annual averages, amounts and patterns of climatic variables (especially precipitation, air temperature, and radiation) were compared to data from nearby weather stations of the German Weather Service (DWD) or the Bavarian Federal Institute of Forestry (LWF), both for the sites in the Steigerwald and the Fichtelgebirge, for plausibility checks and to compare site-specific results to long-term values available from these institutions only, or to supplement the on-site measurements to fill data gaps.

Statistical calculations were carried out in Microsoft Excel 97, PV-Wave 6.21, SigmaPlot 4.0 and 8.0, and Systat 8.0.

## 5 Results

### 5.1. Structural drivers of canopy transpiration

Structural drivers control canopy transpiration on a mid- to long-term temporal scale and usually do not change markedly within one growing season, except for the leaf area index particularly of deciduous forests, due to leaf phenology and also in case of insect calamites and wind throw.

#### 5.1.1. Sapwood area

The sapwood as the domain of a tree cross-section where water is (potentially) transported from the roots to the leaves must receive special attention when using an experimental sap flow method which relates water flux to sapwood area (see Chap. 4.1). In this study one focus was on radial trends and patterns in sap flow and their anatomical basis. Therefore several characteristics of the wood of *F. sylvatica* associated with sapwood and especially the transition from sapwood to ripewood were studied radially on stem cross-sections of trees, namely wood density, absolute and relative water content.

The wood density ( $\rho_{wd}$ , in  $\text{g cm}^{-3}$ ) in 5 mm-segments of increment cores, taken early in the morning on an overcast day in May 2000, showed no radial trend across the trunks of the sampled beech trees (Fig. 5.1.1.1a), as was also observed on beech by Koltzenburg and Knigge (1987), Klebes et al. (1988) and older works cited there, Lovas (1991), Wiebe (1992), Schäfer (1997), Bouriaud et al. (2004); other studies had found  $\rho_{wd}$  to increase only slightly towards the pith (Trendelenburg and Mayer-Wegelin 1955, Raunecker 1955, both cited in Klebes et al. 1988; Woodcock and Shier 2002 for *F. grandifolia*). This facilitates the use of computer tomography (see Chap. 4.3) in this species to assess sapwood area, making cross-sectional variation in absorption of ionising radiation (cf. Fig. 4.3.1 and 5.1.1.2) mainly dependent on the water content of the trunk.

Wood density  $\rho_{wd}$  ranged from 0.499 to 0.542  $\text{g cm}^{-3}$  for the whole stem radius and from 0.460 to 0.589  $\text{g cm}^{-3}$  (Fig. 5.1.1.1a) for individual 5 mm-core segments. Water content  $W_f$  amounted to 0.257 to 0.315  $\text{g cm}^{-3}$  for the whole stem radius and varied from 0.199 to 0.410  $\text{g cm}^{-3}$  in the segments (Fig. 5.1.1.1b), and relative water content  $R_w$  differed from 51.5 to 58 % (whole stem) and from 37.4 to 73.6 % (segments, Fig. 5.1.1.1c), respectively. These values are well within the range reported in the literature for *F. sylvatica* (e.g. Nepveu 1981, Glavac et al. 1990, Granier et al. 2000a, Wagenführ 2000).

Figure 5.1.1.1b and c show a steady decline of  $W_f$  and  $R_w$  over the outer half of the radial profile. Over the second half of the total radial depth,  $W_f$  and  $R_w$  stay relatively constant, at ca. 0.25  $\text{g cm}^{-3}$  and 50 %, respectively, indicating the transition from sapwood to ripewood. Similar patterns of  $R_w$  in *F. sylvatica* were observed e.g. by Zycha (1948), Trendelenburg and Mayer-Wegelin (1955, cited in Klebes et al. 1988), Nikolov and Enchev (1967, cited in Gartner and Meinzer 2005), Koltzenburg and Knigge (1987), Klebes et al. (1988) and Granier et al. (2000a). Zycha (1948) roughly estimated for beech that at approximately 60 %  $R_w$ , all the water is osmotically and

matrically bound and that a further reduction of  $R_w$  is at the expense of the living cells (rays, wood parenchyma), initiating formation of ripewood (or of discoloured wood).

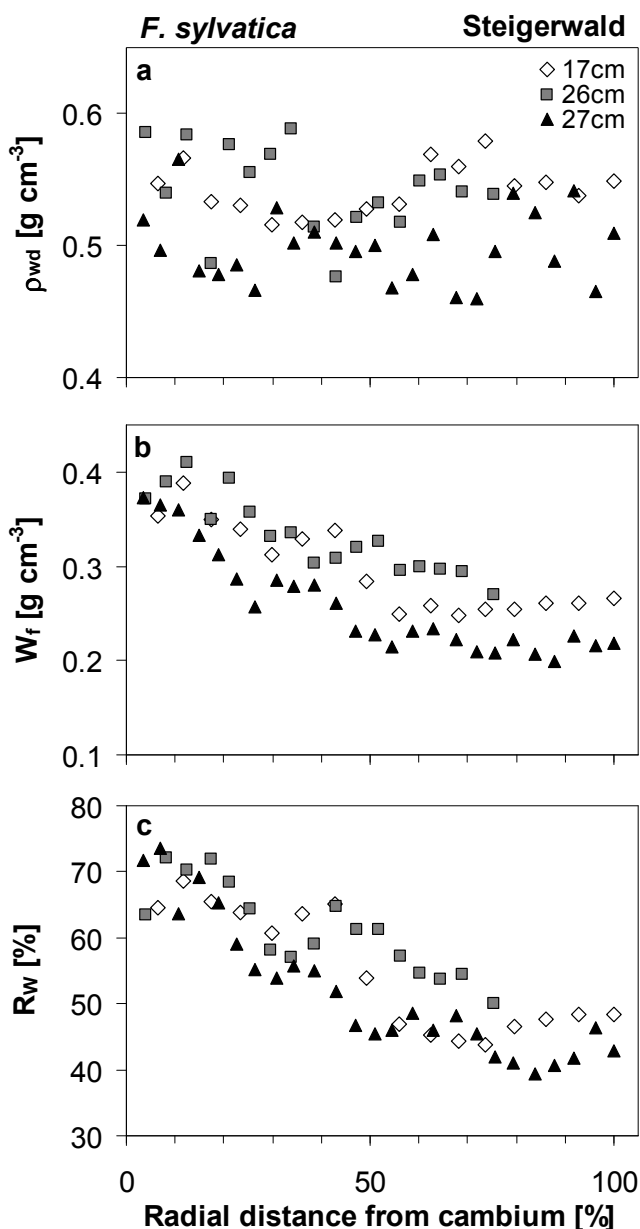


**Figure 5.1.1.1:** Wood properties in relation to the radial distance from the cambium (0 %; pith = 100 %) for three beech trees (open diamonds: B82, 17 cm stem diameter; filled squares: B108, 26 cm; filled triangles: B60, 27 cm):  
**a:** wood density ( $\rho_{wd}$ ), calculated as the dry mass of core segments taken with an increment borer (ca. 5 mm long, core diameter 5 mm) per volume (Archimedes' principle);  
**b:** water content ( $W_f$ ), computed from the difference between fresh and dry mass divided by volume;  
**c:** relative water content ( $R_w$ , ratio of water content and wood density). Cores were extracted at the plot Große Ebene in May 2000, immediately after the tomographic mapping of the tree cross-section at the same height.

Two examples of tomograms taken on beech trees with a portable computer tomograph (MCT3) are given in Figure 5.1.1.2. The concentric pattern of classes of the absorption value  $\alpha$  is obvious here. Values of  $\alpha$  for the xylem range from  $54 \text{ cm}^{-1}$  to  $92 \text{ cm}^{-1}$ , decreasing towards the pith. In comparison, the  $\alpha$  of air is zero (and the MCT3-system is calibrated against absorption in air before each measurement), the  $\alpha$  of pure water is  $84 \text{ cm}^{-1}$  (Raschi et al. 1995), and the  $\alpha$  of air-dried beech wood ranges between  $44 \text{ cm}^{-1}$  and  $60 \text{ cm}^{-1}$  (Lovas 1991).

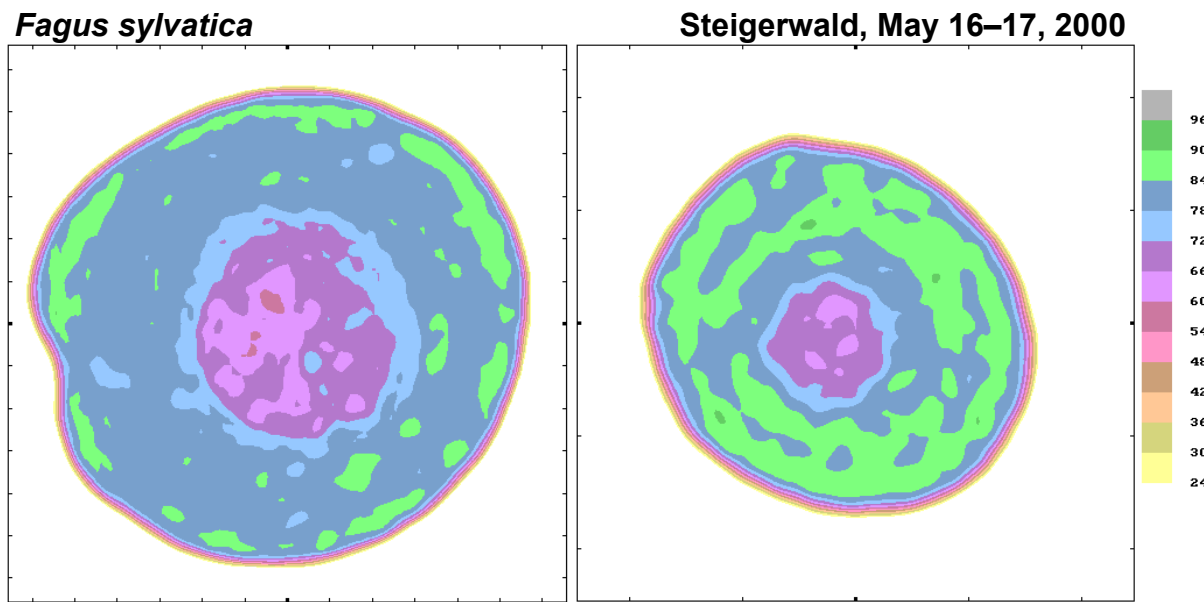


**Figure 5.1.1.2:** Computer tomograms reconstructed from cross-sectional scans on stems acquired with a mobile computer tomograph (MCT-3) on standing live beech trees B4213 (left) and B4050 (right) in the stand Steinkreuz. Diameter at measurement height was 58 cm and 17 cm, respectively. Tick marks on the x and y-axis indicate 5 cm intervals. Different colours depict classes of absorption values  $\alpha$  (far right, in  $\text{cm}^{-1}$ ; see text). The mean squared error is  $1.7 \text{ cm}^{-1}$  for both reconstructed images.

Sapwood-ripenwood boundaries visually estimated on the sectioned cores (Chap. 4.3) and on additional increment cores from tomographed trees (whose wood properties were not analysed) and values of  $W_f$  and  $R_w$  were compared to absorption values  $\alpha$  on the tomographic images (at a spatial resolution of the images of 2.2–2.8 mm, depending on stem diameter, compared to 5 mm core sections). In Figure 5.1.3,  $W_f$  and  $R_w$  obtained from increment core segments (cf. Fig. 5.1.1b, c) are plotted against classes of  $\alpha$ -values. The absorption values  $\alpha$  increased with increasing  $W_f$  and  $R_w$ , and sapwood corresponded to values of  $\alpha$  between  $72 \text{ cm}^{-1}$  and  $90 \text{ cm}^{-1}$ . It was only in two trees (B60 and B82, both Großebe, DBH 27 and 17 cm, respectively) that sapwood corresponded to  $\alpha$ -values between  $60 \text{ cm}^{-1}$  and  $78 \text{ cm}^{-1}$  or  $66 \text{ cm}^{-1}$  and  $84 \text{ cm}^{-1}$ . For those two trees values of  $W_f$  were respectively lower (Fig. 5.1.1.1b) and hence the range of  $\alpha$  had the same absolute values in all trees studied.

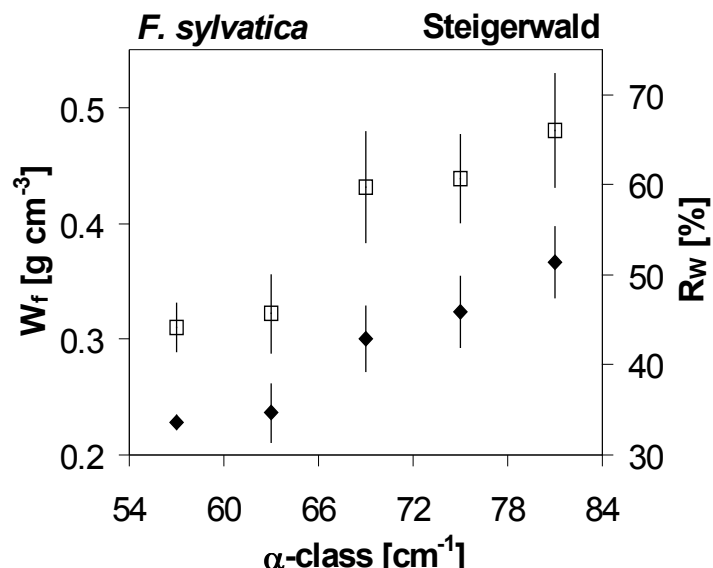


**Figure 5.1.1.3:** Volumetric water content ( $W_f$ , filled diamonds) and relative water content ( $R_w$ , open squares) of 5 mm-sections from increment cores (5 mm diameter) and classes of absorption values  $\alpha$  (upper and lower limit of a class indicated) from three trees,  $\pm 1 \text{ SD}$  (vertical bars). The  $R^2$  for the correlation of  $\alpha$ -class with  $W_f$  is 0.961 with  $p < 0.0001$ ; for the correlation of  $\alpha$ -class with  $R_w$ ,  $R^2$  is 0.906,  $p < 0.05$ . Same cores as in Figure 5.1.1.1.

These findings compared well with the span of absorption values acquired with the MCT-3 for sapwood in beech available in the relevant literature (Lovas 1991, Wiebe 1992, Schäfer et al. 2000). Sapwood area was then estimated from the area of the respective absorption classes (calculated by the reconstruction software) or as described for oak (see Chap. 4.3).

The sapwood area estimated from computer tomograms and computed from increment cores and stem disks in relation to stem diameter is shown in Figure 5.1.1.4a. The results from increment cores taken on oak trees (Chap. 4.3) are given in Figure 5.1.1.4b. Stem diameter and sapwood area  $A_{st}$  were significantly correlated. The variation in sapwood area of beech was explained to 92–99 % by stem diameter, and in oak to 82–92 % (Tab. 5.1.1.1).  $A_{st}$  and stem diameter are auto-correlated, however, since stem diameter is used to convert sapwood radius to sapwood area (Oren et al. 1998). The respective allometric equations are summarised in Table 5.1.1.1.

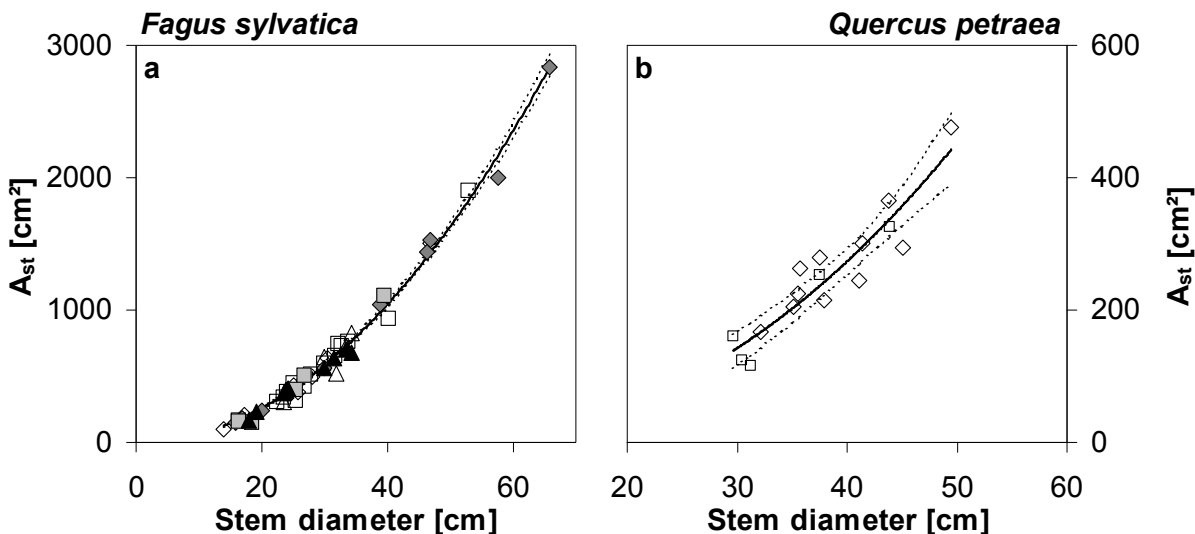


**Figure 5.1.1.4:** Relationships between sapwood area ( $A_{st}$ ) and stem diameter at measurement height (0.7–2.2 m above the ground) for beech (a) and oak (b) from all stands studied, as estimated from increment cores and trunk disks (open symbols) and mobile computer tomography (filled symbols). The diamonds represent data from Steinkreuz, the squares data from GroßeBene, and the triangles data from Farrenleite. The solid line represents a regression over all data, dashed lines indicate 95 %-confidence interval. For regression equations and statistics see Table 5.1.1.1.

The residual plots for the presented regressions (Tab. 5.1.1.1) did not show any bias in the regression models (not shown). The allometric equations were remarkably similar for beech from all three sites. Based on the 95 % confidence intervals of the regressions, there was no significant difference between equations for single stands or the Steigerwald stands combined or all stands combined (data not shown). Therefore, in subsequent calculations of  $A_{st}$  of tree size classes and stands, the combined equation was used for Steinkreuz and GroßeBene ("ST+GR" in Tab. 5.1.1.1) and the specific equation for Farrenleite because of the different diameter range at this site compared to the ones in the Steigerwald. The case was analogous for oak and so the combined equation ("ST+GR") was used.

**Table 5.1.1.1:** Regression equations and statistics for sapwood area  $A_{st}$  (in  $\text{cm}^2$ ) of beech and oak, using stem diameter at breast height (DBH, 1.3 m, in cm), with  $A_{st} = a \text{ DBH}^b$  (see Fig. 5.1.4).  $R^2$ , n, p, SEE, and d denote respectively the coefficient of determination, number of samples, p-value, standard error of the estimate, and range of stem diameters (in cm) for which the equation was established. ST, GR, and FA refer to the stands Steinkreuz, GroßeBene and Farrenleite, respectively.

	a	b	$R^2$	n	p	SEE	d
<b><i>Fagus sylvatica</i></b>							
Steinkreuz	0.763	1.960	0.997	16	<0.0001	61.1	14-66
GroßeBene	0.488	2.082	0.983	20	<0.0001	53.5	16-40
ST+GR	0.666	1.996	0.992	36	<0.0001	57.3	14-66
Farrenleite	0.793	1.935	0.927	16	<0.0001	53.9	18-34
ST+GR+FA	0.629	2.009	0.989	52	<0.0001	55.9	14-66
<b><i>Quercus petraea</i></b>							
Steinkreuz	0.096	2.159	0.818	11	<0.0005	38.4	32-50
GroßeBene	0.041	2.379	0.917	5	<0.05	30.1	30-44
ST+GR	0.065	2.264	0.871	16	<0.0001	34.4	30-50

For beech, the relationship between  $A_{st}$  and the basal area of a tree  $A_{bt}$  was almost constant for the observed range of values, and  $A_{st}$  was between 83.9 % ( $d = 14 \text{ cm}$ ) and 89.4 % ( $d = 66 \text{ cm}$ ) of  $A_{bt}$ , and the sapwood radius ranged from 59.9 % to 59.2 % of the total trunk radius, respectively, based on the regression equations for Steinkreuz + GroßeBene given in Table 5.1.1.1. For Farrenleite,  $A_{st}$  was 83.7–80.3 % of  $A_{bt}$  for the trees investigated ranging 18–34 cm in diameter, and the sapwood radius was 59.6–55.6 % of total radius, respectively, using the Farrenleite-specific equation. Increment cores taken from a sub-sample of sap flow trees ( $n = 7$ ) at the Steigerwald plots showed an average sapwood radius of 8.4 ( $\pm 4.1$ ) cm (range 3.0–16.2 cm) for a total radius of 7.0–23.4 cm. At Farrenleite, sapwood radii between 5.4 cm and 12.2 cm were measured on increment cores, resulting in on average 8.7 ( $\pm 2.5$ ) cm for 7 sap flow trees with 11.8–17.2 cm total radius at the height of core extraction.

In oak, using the regression equation for Steinkreuz + GroßeBene (Tab. 5.1.1.1), the relationship between  $A_{st}$  and  $A_{bt}$  was also nearly linear, and  $A_{st}$  ranged from 20.3 % ( $d = 30 \text{ cm}$ ) to 23.2 % ( $d = 50 \text{ cm}$ ) of  $A_{bt}$ . The sapwood radius in parallel varied between 10.7 % and 12.4 % of total radius. Measured on increment cores from sap flow trees ( $n = 14$ ) the sapwood radius of oaks averaged to 22.8 ( $\pm 8.1$ ) mm over all sampled trees from both stands and varied between 11 mm and 42 mm (total radius 14.8–24.7 cm).

The sapwood area at stand level,  $A_s$ , totalled  $18.6 \text{ m}^2 \text{ ha}^{-1}$  for Steinkreuz (beech:  $16.60 \text{ m}^2 \text{ ha}^{-1}$ , oak:  $1.98 \text{ m}^2 \text{ ha}^{-1}$ ) and  $17.2 \text{ m}^2 \text{ ha}^{-1}$  for GroßeBene (beech:  $12.16 \text{ m}^2 \text{ ha}^{-1}$ , oak:  $5.07 \text{ m}^2 \text{ ha}^{-1}$ ); at Farrenleite  $A_s$  reached  $42.7 \text{ m}^2 \text{ ha}^{-1}$  and at the Steinkreuz-pure beech plot  $32.1 \text{ m}^2 \text{ ha}^{-1}$  (Tab. 3.3.2; referenced to the year 1998). In the mixed stands the percentage contribution of beech to  $A_s$  increased compared to its contribution to stand basal area  $A_b$ , as a consequence of the higher  $A_{st}$  of beech at a given DBH. Thus beech dominated both mixed stands with respect to  $A_s$  (89 % and 71 % of total  $A_s$  at Steinkreuz and GroßeBene, respectively).

The mean number of growth rings in the sapwood of beech was 61.3 ( $\pm 20.1$ ) and ranged from 35 to 92 for the 7 trees counted. Magel et al. (1997) similarly found on beech trees aged 42 to 70 years on average 52 growth rings in sapwood. The mean number of growth rings in the sapwood of oak was 16.5 ( $\pm 3.2$ ) and ranged from 10 to 22 growth rings. In accordance with these findings, Romberger et al. (1993, p 408) state the sapwood of *Q. robur* to constitute an average of 14 growth rings.

The average annual radial stem increment (in 1.3–2 m above ground) for oak from the Steigerwald for the period 1971–1999 was 1.35 ( $\pm 0.48$ ) mm yr<sup>-1</sup> (range 0.66–2.45 mm yr<sup>-1</sup>; range of total radius 14.8–24.7 cm; n = 14 trees). The radial increment for the year 1999 averaged to 1.39 ( $\pm 0.59$ ) mm yr<sup>-1</sup> (range 0.5–2.5 mm, rounded to the nearest 0.5 mm). Results from Lévy et al. (1992) on dominant *Q. petraea* in France calculate to a mean radial increment of 1.5 mm yr<sup>-1</sup>. In mixed high forest stands of *Q. robur* and *Q. petraea*, radial growth revealed an average of 1.75 mm yr<sup>-1</sup> for mature sessile oaks with extremes of 0.89 and 3.18 mm yr<sup>-1</sup> (Lévy et al. 1992). For beech, less data are available, averaging to 1.74 ( $\pm 0.82$ ) mm yr<sup>-1</sup> for the 1971–1999 period for 8 trees from Steinkreuz, varying between 0.73 mm yr<sup>-1</sup> and 3.33 mm yr<sup>-1</sup> in radial growth and from 7.0 cm to 27.5 cm in total radius. The average radial increment for the year 1999 was 1.94 ( $\pm 0.86$ ) mm yr<sup>-1</sup>, extending from 1 to 3 mm. Lang (1999) for instance noted annual radial increments of 3.2–5.0 mm averaged over 20–34 years for beech aged 60–68 years with DBH ranging 42–63 cm and heights of 26–30 m.

### 5.1.2. Stand structure

Of the total density of 350 trees ha<sup>-1</sup> in the Steinkreuz stand, beech held 76 % and was present in all DBH-classes from 7 to 70 cm (Fig. 5.1.2.1, upper panel). Its abundance peaked around DBH-class 20. Oak was present only in classes 25–50, reaching a maximum in class 35. The basal area  $A_b$  of beech was 19.9 m<sup>2</sup> ha<sup>-1</sup> or 69 % of total stand  $A_b$  (29.0 m<sup>2</sup> ha<sup>-1</sup>, Tab. 3.3.2) with the highest values in the DBH-class 60 (Fig. 5.1.2.1, middle panel); for oak,  $A_b$  peaked in the class 45. Beech dominated the total sapwood area of the stand  $A_s$  of 18.6 m<sup>2</sup> ha<sup>-1</sup> (Tab. 3.3.2) by 89 % and was maximum in DBH-class 60 (Fig. 5.1.2.1, lower panel). Beech trees in classes 55 to 70 (14 % of the beech trees or 10 % of beech and oak combined) represented almost 50 % of the total stand's  $A_s$ .

In the Großebene stand, which was only marginally younger but almost twice as dense, 67 % (424 trees ha<sup>-1</sup>) of the trees were beech (Tab. 3.3.2), most of which (> 80 % of all beech trees) were concentrated in the DBH-classes 10 to 25 (Fig. 5.1.2.1). The DBH of beech ranged from 7 to 47 cm. Oak in contrast was absent in the lower DBH-classes, like in Steinkreuz, and the DBH varied between 26 and 46 cm, complementary to the distribution of the abundance of beech across DBH-classes. Oak dominated the  $A_b$  of the stand, with the DBH-classes 40 and 45 holding more than 40 %. The  $A_b$  of Großebene (37.9 m<sup>2</sup> ha<sup>-1</sup>) was 1.3 times that of Steinkreuz, but the  $A_s$  (17.2 m<sup>2</sup> ha<sup>-1</sup>) was slightly lower than that of Steinkreuz, due to the large number of small beech trees and the low fraction of sapwood in the many large oak trees at Großebene. Thus beech contributed > 70 % to the  $A_s$  of this stand (Tab. 3.3.2, Fig 5.1.2.1).

The diameter of beech trees at the sloped stand Farrenleite in the Fichtelgebirge spanned from 14 to 47 cm at a stand density of almost 900 trees ha<sup>-1</sup> (Tab. 3.3.2),

the DBH-classes 25 and 30 being the largest (approx. 60 % of all trees, Fig. 5.1.2.1). The DBH-class 35 contributed most (about 30 %) to  $A_b$  and  $A_s$  of the stand (in total  $52.7 \text{ m}^2 \text{ ha}^{-1}$  and  $42.7 \text{ m}^2 \text{ ha}^{-1}$ , respectively), the former being 1.4 times, the latter 2.5 times higher than that of the stand GroßeBene (Tab. 3.3.2).

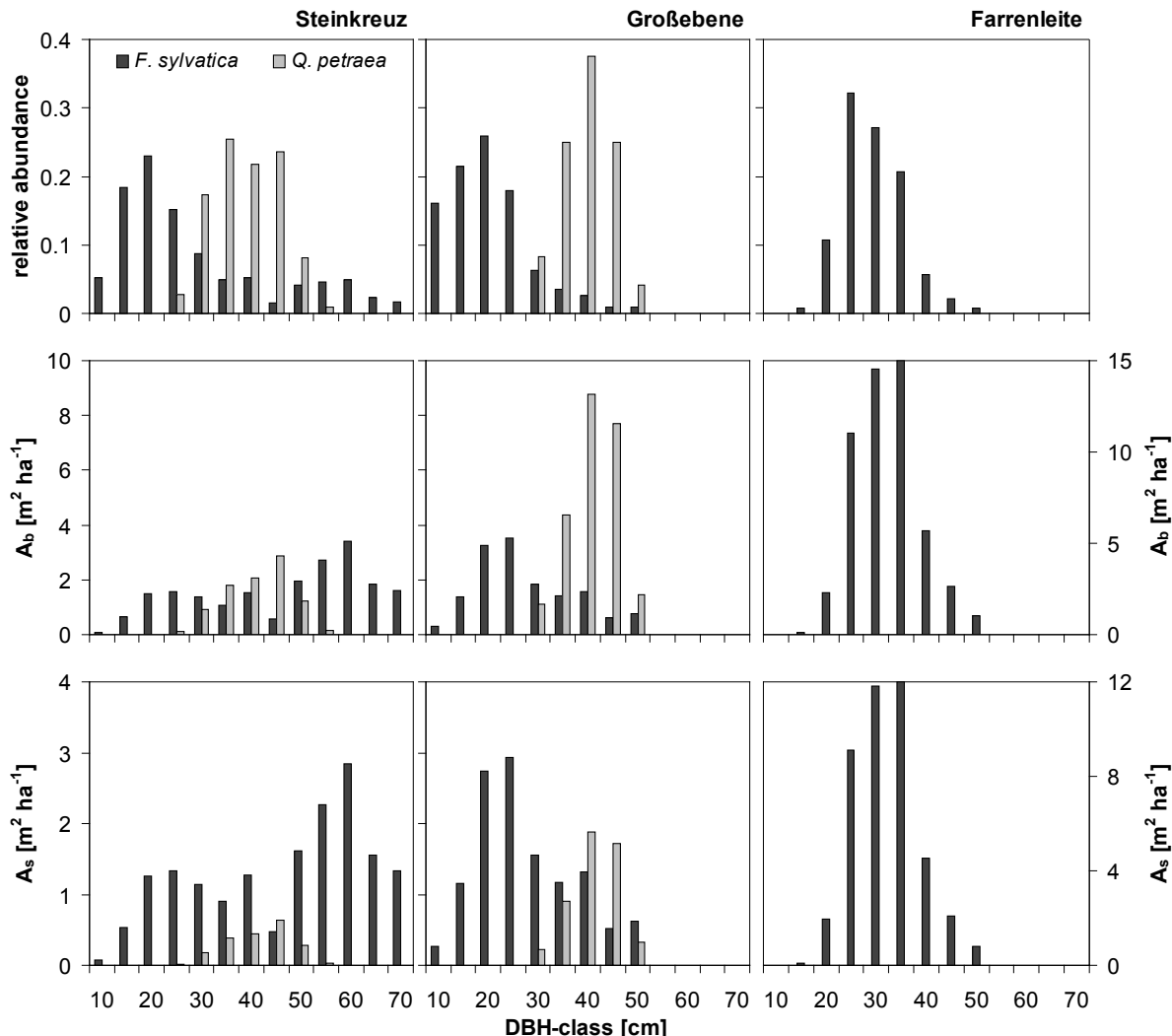


**Figure 5.1.2.1:** Distribution of stand structural characteristics across DBH-classes for the two mixed sites in the Steigerwald, Steinkreuz (**left**) and GroßeBene (**centre**), and for the pure beech stand Farrenleite in the Fichtelgebirge (**right**). Columns are filled for *F. sylvatica* and shaded for *Q. petraea*. DBH is the stem diameter 1.3 m above the ground. The **upper** panel shows the relative abundance of trees, referenced to the total number trees of each species per plot. The **middle** panel represents the basal area ( $A_b$ ), the **lower** panel the sapwood area ( $A_s$ , as calculated from regression equations given in Tab. 5.1.1.1); note the different scales of the y-axes for Farrenleite. DBH-classes are in steps of 5 cm, the numbers indicating the upper limit of a class, e.g. DBH-class "70 cm" includes all trees with a DBH of 65.1–70.0 cm. The DBH-class "10 cm" spans from 7.0–10.0 cm only. For the DBH-class "35 cm" of Farrenleite, the basal area is  $15.3 \text{ m}^2 \text{ ha}^{-1}$  and the sapwood area  $12.3 \text{ m}^2 \text{ ha}^{-1}$ . The data are from an inventory in spring 1998, except at Farrenleite, where the inventory was in spring 2000. The absolute stem densities etc. are given in Table 3.3.2.

The Steinkreuz-pure beech plot within the mixed stand was less dense than both the mixed Steinkreuz stand and the Farrenleite beech stand (Tab. 3.3.2). The  $A_b$  and  $A_s$  of the Steinkreuz-pure beech plot reached 73 % and 75 % of the values of Farrenleite, respectively. The largest and second largest tree of the Steinkreuz-pure beech plot contributed 40 % and 30 % to  $A_b$  and  $A_s$ , respectively (Tab. 3.3.2, Fig. 5.1.2.2).

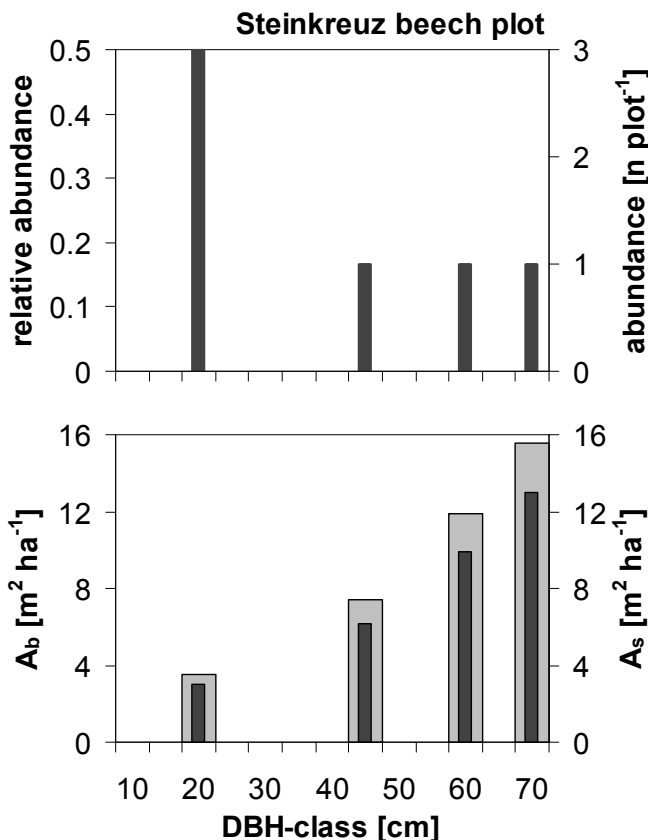


**Figure 5.1.2.2:** Distribution of stand structural characteristics across DBH-classes for a small pure beech plot within the mixed Steinkreuz stand, Steigerwald, for the year 1998. The **upper** graph shows the relative and absolute abundance of beech trees, the **lower** graph the distribution of basal area  $A_b$  (shaded bars) and sapwood area  $A_s$  (filled bars). See also caption to Figure 5.1.2.1.

The height of the Steinkreuz stand (the average height of the 100 strongest trees per hectare, see Chap. 4.2) was 32 m (Tab. 3.3.2). The strongest beech trees at this site reached heights of almost 40 m whereas the highest oaks were about 5 m shorter (Tab. 3.3.2). Oaks in general tended to be less tall than beech trees with the same DBH (Fig. 5.1.2.3 top left), and the trend of tree height to increase with DBH was weaker ( $R^2 = 0.273$ ,  $p < 0.001$ , cf. Tab. A11.3, Appendix) compared to beech. In the latter species, the height of the crown base increased with the DBH, but not as strongly as the total tree height, so that the crown length increased with the DBH as well. In oaks, the height of the crown base did not change with the DBH and the crown length was much shorter than that of beech trees. The ground-projected crown area  $A_{cp}$  of oak was usually also smaller than that of beech with similar DBH (Fig. 5.1.2.3 bottom left) and the beech trees with the largest DBH had by far the largest  $A_{cp}$  of up to  $110 \text{ m}^2$ .

The maximum height of the trees at Großebene was almost 10 m less than at Steinkreuz, and both the oaks and beech were shorter than trees with the same DBH at Steinkreuz (Fig. 5.1.2.3 top middle, see also Fig. A11.3, Appendix). The oaks at Großebene reached a maximum of 30 m and were in general somewhat taller than comparable beech trees, the correlation with the DBH being weak as at Steinkreuz ( $R^2 = 0.193$ ,  $p < 0.005$ , cf. Tab. A11.3, Appendix). The height of the crown base

hardly changed with the DBH in oak, and in beech the increase of the height of the crown base was not as pronounced as at Steinkreuz. Oak crowns were again shorter than those of beech.  $A_{cp}$  was, as at Steinkreuz, much smaller in oak than in beech with the same DBH (Fig. 5.1.2.3 bottom middle), and neither beech nor oak from Steinkreuz and GroßeBene showed significant differences in their respective relationships of  $A_{cp}$  to DBH (cf. caption of Fig. 5.1.2.3 and Fig. A11.3, Appendix).

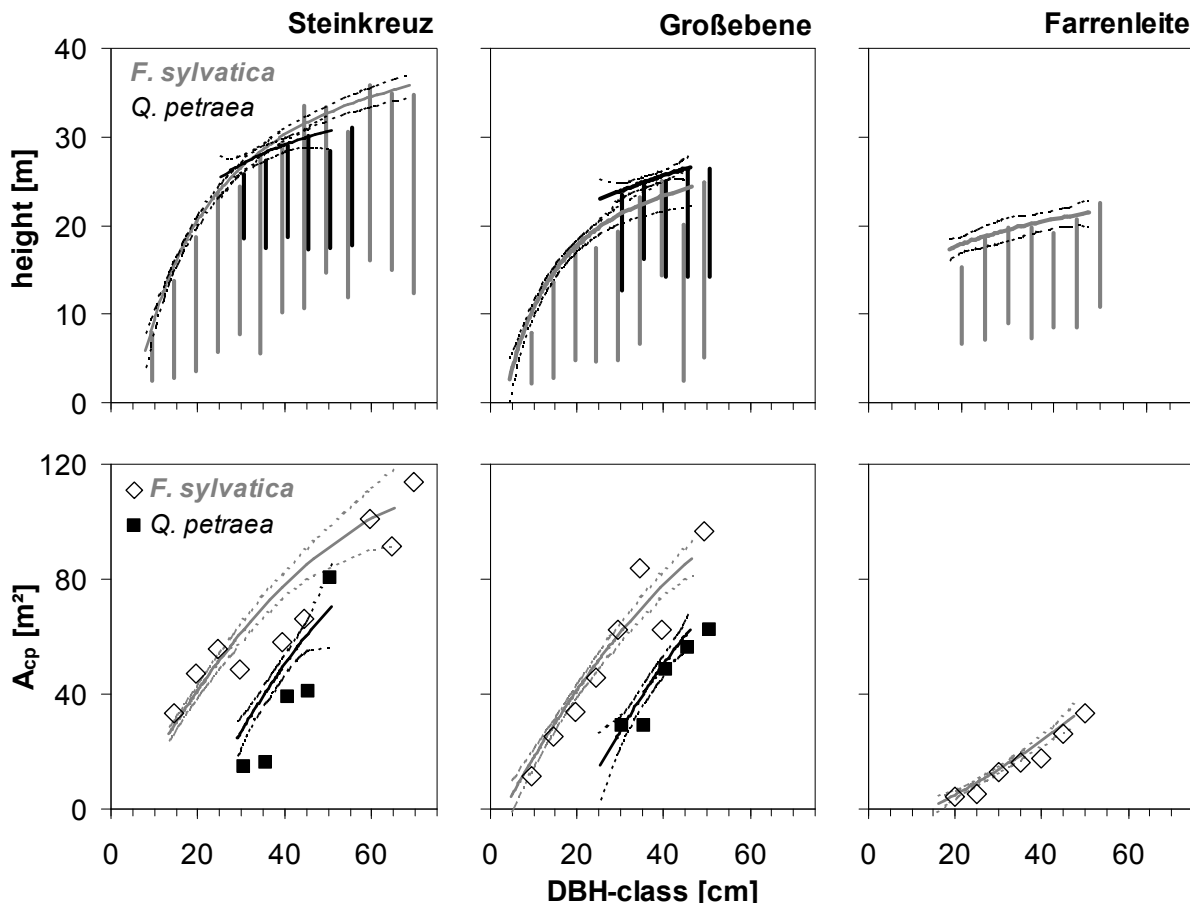


**Figure 5.1.2.3:** Tree height and ground-projected crown area  $A_{cp}$  of DBH-classes in the two mixed sites in the Steigerwald, Steinkreuz (**left**) and GroßeBene (**centre**), and in the pure beech stand Farrenleite in the Fichtelgebirge (**right**). **Upper** panel: vertical bars represent the average crown length of all trees of a DBH-class, a bar's lower end indicating the (average) point of insertion of the lowest living branch on the trunk, its upper end the average tree height. Grey bars are for *F. sylvatica*, dark bars for *Q. petraea*. Curves shown are original (hyperbolic) regression equations based on individual trees of each species, and 95 %-confidence intervals (dashed). **Lower** panel: average ground-projected crown area  $A_{cp}$  of DBH-classes (open diamonds and filled squares) and regression lines and 95 %-confidence intervals from original data. Both beech and oak trees from Steinkreuz and GroßeBene were not significantly different in their relationships of  $A_{cp}$  to DBH, so a combined regression is plotted here for each species. Equations and graphs with original data are shown in Table A11.2 and Figure A11.2 (Appendix).

In the densest stand, Farrenleite, the tree tops and crown lengths of beech were lowest while crown bases were highest of all sites (Fig. 5.1.2.3 top right). The stand height was only 20 m, the maximum height 26 m (Tab. 3.3.2b). The tree height varied

little with DBH, and the respective correlation coefficient was low ( $R^2 = 0.257$ ,  $p < 0.001$ , cf. Tab. A11.3, Appendix). The  $A_{cp}$  was also considerably smaller than for beech trees from the other sites (Fig. 5.2.3 bottom), its correlation with the DBH rather high ( $R^2 = 0.846$ ,  $p < 0.0001$ , cf. Tab. A11.3, Appendix). The stand and maximum height of the Steinkreuz-pure beech plot was 34 m (Tab. 3.3.2) and the  $A_{cp}$  was almost three times that of trees with the same DBH at Farrenleite (cf. Fig. 5.1.2.3 bottom left and right).

Both the large and small trees of the same stand selected for sap flow measurements were of the same age, as revealed by ring count on increment cores. The stands differed very little in ring counts: Farrenleite 108–119 rings, Steinkreuz and Großebene 111–133 rings, in approx. 2 m height of stem, respectively (cf. Tab. 3.3.2, Tab. 4.1).

### 5.1.3. Leaf area index and related variables of tree and stand structure

In order to estimate the leaf area index (LAI) of the stands investigated, direct, semi-direct and indirect methods were employed (Chap. 4.4). The results from the direct measurements of the leaf area of harvested trees (Fleck 2002), which were carried out in close cooperation with the present study, have already been given in Chapter 4.4.1 (Eqs 4.4.1–4). In the following, results from the other methods (litter traps and optical measurements) will be presented and finally all results will be compared.

#### 5.1.3.1. Leaf area per unit dry mass

The results from the measurements of the leaf area per unit of dry mass, or specific leaf area, SLA (the inverse of leaf mass per area, LMA), as obtained from leaf litter collected in traps on the ground under the canopy of the stands are shown in Table 5.1.3.1.

**Table 5.1.3.1:** Leaf area per unit of dry mass (SLA) of leaf litter collected in autumn and winter of the respective years.

SLA [ $\text{cm}^2 \text{ g}^{-1}$ ]		<i>Fagus sylvatica</i>		<i>Quercus petraea</i>	
Stand	Year	average	range	average	range
Steinkreuz	1998	251	240–328	168	161–186
	1999	198	146–309	138	122–169
Großebene	1998	291	285–371	168	148–200
	2000	275	196–366	196	164–218
Farrenleite	1998	200	133–228		

The beech trees had higher average values of leaf litter-SLA than oak during the three years of investigation, and also the range of SLA was larger in beech than in oak in all stands and all years (Tab. 5.1.3.1). The latter fact might reflect the narrower range of the DBH of the oaks, especially the absence of oaks in the understory, and the lack of low shade branches (cf. Chap. 5.1.2). The SLA of leaf litter tended to increase towards the end of the season and was rather variable then (data not shown).

The SLA of green leaves harvested during the summer of 1997 (Farrenleite) and 1998 (Großebene) by S. Fleck, formerly Dept. of Plant Ecology, Univ. of Bayreuth, was on average for two dominant beech trees at Farrenleite  $177 \text{ cm}^2 \text{ g}^{-1}$  ( $n = 772$ ) and  $200 \text{ cm}^2 \text{ g}^{-1}$  ( $n = 105$ ), for a dominant beech at Großebene  $125 \text{ cm}^2 \text{ g}^{-1}$  ( $n = 231$ ) and for a dominant–emergent oak at Großebene  $142 \text{ cm}^2 \text{ g}^{-1}$  ( $n = 552$ ), respectively (Fleck 2002). The range of SLA was  $78\text{--}435 \text{ cm}^2 \text{ g}^{-1}$  for beech and  $74\text{--}1000 \text{ cm}^2 \text{ g}^{-1}$  for oak (Fleck 2002). The large range of values reflects the variability of SLA within a tree crown (sun and shade leaf characteristics). These ranges of the SLA are naturally larger than those of the litter-based SLA because of the different sampling strategy of the former (simultaneous SLA-gradient-sensitive sampling, smaller sample sizes) while the litter-based values represent a thanatocenosis of dead leaves from different positions in the crown (sun vs. shade) of different stages of senescence, necrosis and decomposition.

#### 5.1.3.2. Leaf area index

Estimates of the leaf area index of the tree canopy, LAI, from all methods used (Chap. 4.4) are summarised in Table 5.1.3.2, as are the interannual averages, the averages across different methods and the interannual variation.

Averaged over the observed growing seasons and the three different methods used, the LAI was 6.7 for the stand Steinkreuz, 6.5 for Großebene, 7.2 for Farrenleite and 6.9 for the pure beech plot within the mixed stand Steinkreuz (Tab. 5.1.3.2). Averaging over litter collection and PCA-based estimates only, the LAI for Steinkreuz was 6.8, 6.5 for Großebene, and 6.8 for Farrenleite (Tab. 5.1.3.2); no litter traps had been placed in the pure beech plot of Steinkreuz. Allometric estimates of LAI were 7 % and 13 % smaller than the average of indirect and semi-direct estimates in Steinkreuz and Großebene, respectively (in the year of leaf harvest), 8 % larger for Steinkreuz–pure beech plot and almost 20 % larger in Farrenleite (Tab. 5.1.3.2). At the latter site, however, the harvest had been carried out in the year before the optical measurements and litter collection started. In the two mixed stands the proportion of beech on stand-LAI varied ca. 15–20 % between the direct and semi-direct methods (Tab. 5.1.3.2). Maximum seasonal values of the PCA-based LAI were linearly correlated with litter-based values of LAI ( $R^2 = 0.74$ ,  $p = 0.013$ ,  $n = 7$ ; not shown).

The LAI was reduced at Großebene in 1999 compared to 1998 by 19 % as found by both litter traps and PCA (Tab. 5.1.3.2). At Steinkreuz, LAI was reduced by 9 % based on PCA-estimates but hardly changed based on results from litter collection. In the year 2000, LAI recovered partly and increased by 10 % (litter traps) and 13 % (PCA) at Großebene and rose by 10 % (PCA) at Steinkreuz; litter trap-based estimates at Steinkreuz remained at the same value as the previous years (Tab. 5.1.3.2, Tab. 5.1.3.3, below). Interannual variability was found to be up to 21 % in annual leaf litter production at Steinkreuz from 1996 to 2001 (average biomass of leaf litter  $3847.9 \text{ kg dry mass ha}^{-1} \text{ yr}^{-1}$ , SD  $274.5 \text{ kg ha}^{-1} \text{ yr}^{-1}$ , range  $3655.5\text{--}4314.8 \text{ kg ha}^{-1} \text{ yr}^{-1}$ , P. Gerstberger, Dept. of Plant Ecology, Univ. of Bayreuth, pers. comm.).

At species level, the proportion of beech leaves in the litter collections showed a small increase in Steinkreuz (2 % per year, cf. Tab. 5.1.3.2). The LAI of beech increased by less than 4 % from 1998 to 1999 and less than 1 % from 1999 to 2000 as shown in Table 5.1.3.3. The contribution of oak leaves to stand level-LAI decreased by 10 % from 1998 to 1999 and another 12 % from 1999 to 2000 (Tab. 5.1.3.3), resulting in a total loss of the LAI in oak of 0.24 in two consecutive years.

These opposing trends in the two species balanced out at the stand level. At Großebene, the contribution of beech decreased by 5 % from 1998 to 1999 and did not change in 2000 compared to 1999 (Tab. 5.1.3.2). The absolute LAI of beech decreased by 27 % from 1998 to 1999 and increased by 11 % in the following year. Oak-LAI decreased ca. 9 % from 1998 to 1999 and returned to almost the value of 1998 in the year 2000 (Tab. 5.1.3.3). PCA-based estimates of LAI for the pure beech plot within Steinkreuz decreased only marginally from 1998 to 1999 and increased thereafter in 2000 by less than 4 % (Tab. 5.1.3.2).

**Table 5.1.3.2:** Leaf area index (LAI) of the canopy of the stands investigated and interannual variation (change relative to previous year); average values from litter traps, optical measurements (PCA, LAI-2000 Plant Canopy Analyser; corrected for stem light interception and foliage element non-randomness according to Kucharik et al. 1998, 1999; maximum seasonal values) and from species and site-specific allometric relationships between stem diameter and leaf area (Fleck 2002, Fleck et al. 2004; Chap. 4.4.1). In brackets, percentage contribution of beech to stand LAI where applicable. Means of all the years of investigation and across methods are also given (in brackets 1 standard deviation, SD). No litter traps were set up in the pure beech plot of Steinkreuz ("n.d.").

Method	PCA		litter (% beech)		allometric (% beech)
	LAI	change	LAI	change	LAI
<b>Steinkreuz</b>					
1998	6.92		6.86 (83)		6.4 (66)
1999	6.29	-9.1 %	6.95 (85)	+1.3 %	
2000	6.92	+10 %	6.85 (87)	-1.4 %	
mean (SD)	6.71 (0.30)		6.89 (0.04)		
mean (SD)		6.80 (0.13)			
total mean (SD)			6.67 (0.20)		
<b>Großebene</b>					
1998	7.04		7.42 (54)		6.3 (39)
1999	5.68	-19 %	6.04 (49)	-19 %	
2000	6.40	+13 %	6.61 (49)	+10 %	
mean (SD)	6.37 (0.55)		6.69 (0.57)		
mean (SD)		6.53 (0.23)			
total mean (SD)			6.45 (0.17)		
<b>Farrenleite</b>					
1998	6.70		6.85		8.1 <sup>a</sup>
mean (SD)		6.78 (0.11)			
total mean (SD)			7.22 (0.63)		
<b>Steinkreuz-pure beech plot</b>					
1998	6.61		n.d.		7.17
1999	6.54	-1 %	n.d.		
2000	6.77	+3.5 %	n.d.		
mean (SD)	6.64 (0.1)				
total mean (SD)			6.91 (0.27)		

<sup>a</sup> Harvest carried out in 1997.

**Table 5.1.3.3:** LAI of the individual species and its change from one year to the next (in brackets) as estimated from litter collection in 10 traps per stand for the two mixed beech-oak sites in the Steigerwald.

LAI	Steinkreuz		Großebene	
	<i>F. sylvatica</i>	<i>Q. petraea</i>	<i>F. sylvatica</i>	<i>Q. petraea</i>
1998	5.71	1.15	4.00	3.41
1999	5.92 (+3.7 %)	1.03 (-10 %)	2.94 (-27 %)	3.10 (-9 %)
2000	5.95 (+0.5 %)	0.90 (-12 %)	3.25 (+11 %)	3.37 (+9 %)

At Steinkreuz, the spatial coefficient of variation (CV) for the litter-based estimates of LAI across the traps was 14 % for beech, 28 % for oak and 8 % for both combined in 1998. No CV could be calculated for 1999 and 2000 since litter from all 10 traps in Steinkreuz had been pooled during these years. At Großebene, the spatial CV in litter-derived LAI among the 10 individual litter traps was 14 % for beech, 16 % for oak and 8 % for both combined in 1998, 13 %, 30 % and 15 % in 1999, respectively, and 13 %, 22 % and 12 % in 2000, respectively. At the pure beech stand Farrenleite, CV amounted to 4 % (1998), yet only three traps were set up there. The larger spatial variability in the litter-LAI of oak in both mixed stands compared to beech probably originated from the stand composition, which could be described as a matrix of beech with single to small groups of oak trees mixed in (cf. Tab. 3.3.2a). Yet the effects of differences in the leaf size of beech and oak could also have contributed to the larger CV for oak litter. A methodological limitation in this respect is the use of smaller litter traps with a larger edge effect at Großebene, which may obscure a comparison of the two sites.

PCA-based estimates exhibited values of CV of ca. 10 % in Steinkreuz, 12 % in Großebene, and 3 % in Farrenleite. A direct comparison with coefficients of variation from litter-based LAI-estimates was not appropriate because of the different number of sampling points. But the ranking of coefficients of variation between the stands was similar for both methods: Farrenleite as a monospecific stand showed the lowest CV and Großebene had a slightly higher CV than Steinkreuz.

Figure 5.1.3.1 shows the seasonal change of LAI, as a percentage of maximum seasonal LAI observed with the respective method, during the years 1998–2000 for the three sites. Sampling with the PCA was not as frequent as might have been desirable, but it was not always possible to meet obligatory preconditions (see Chap. 4.4.3). From August 1999 supplemental information on canopy development was derived from continuous below-canopy measurement of global radiation  $R_g$  at Steinkreuz (Fig. 5.1.3.1; see Chap. 4.5), which agreed well with the pattern derived from PCA and litter traps. LAI (PCA) peaked around mid July to mid August in the three consecutive years (Fig. 5.1.3.1). Shedding of leaves always started earlier in beech than oak and first began at Farrenleite in the Fichtelgebirge (for the latter stand data was available only for 1998). Leafing out followed the same pattern, beginning with beech in the Steigerwald, followed by oak, finally at Farrenleite. Beech and oak from the Steigerwald stands did not differ significantly between the two sites regarding

these phenological stages. Litter fall ended somewhat earlier in 1998 and 2000 than in 1999, when considerable litter was found in traps until mid December, whereas not later than the beginning of December during the other years (Fig. 5.1.3.1).

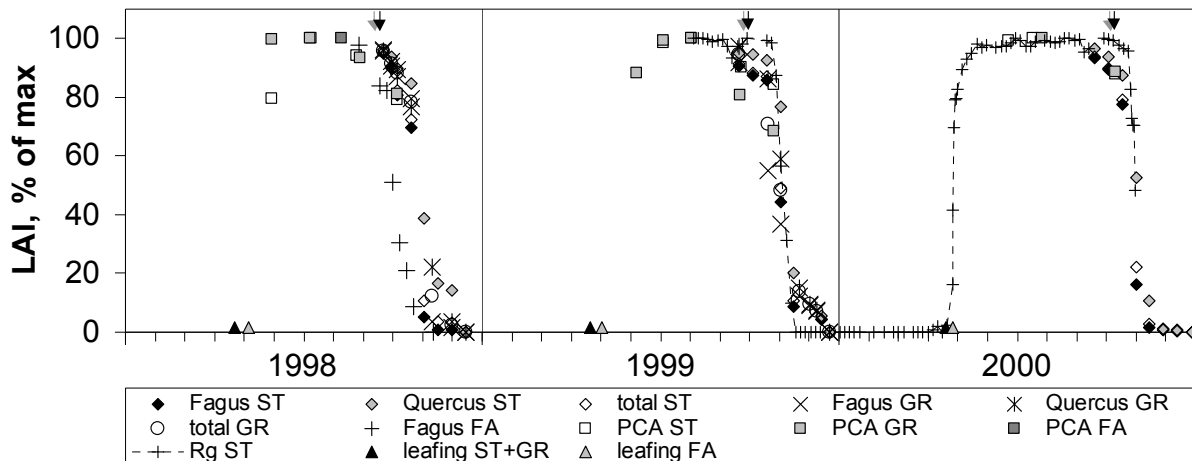


**Figure 5.1.3.1:** Seasonal change of leaf area index (LAI) of the tree canopy during the years 1998–2000 in the three stands studied as estimated from leaf litter collected in traps (“Fagus”, “Quercus”, “total”), and optical measurements (“PCA”, LAI-2000 Plant Canopy Analyser, Li-Cor Inc., Lincoln, Nebraska, USA) and normalised to maximum seasonal LAI observed with the respective method. ST, GR, and GR signify the stands Steinkreuz, Großebeine and Farrenleite, respectively. “R<sub>g</sub> ST” is the inverted transmission of global radiation R<sub>g</sub> as estimated from the comparison of below-canopy measurements inside the stand Steinkreuz with above-canopy measurements (in the nearby forest opening). Extreme values of inverted R<sub>g</sub> during periods of 5 days are shown (the maxima during the vegetation period, minima during winter); measurements started 27.07.1999 and ended 30.10.2000. The beginning of leaf unfolding of *Fagus sylvatica* is indicated (“leafing”, filled and shaded triangles), as well as the approximate beginning of leaf colour change at Steinkreuz/Großebeine (dark arrows) and at Farrenleite (grey arrows). For Farrenleite, litter and PCA-data are available only for the year 1998. In autumn and winter 2000, litter from Großebeine was collected only once after all leaves had fallen (thus not indicated in graph).

### 5.1.3.3. Leaf area-to-sapwood area relationship

The relationship of the leaf area ( $A_{lt}$ ) to the sapwood area ( $A_{st}$ ) of a tree,  $A_{lt}/A_{st}$  (or the inverse of the Huber value, cf. Tyree and Zimmermann 2002), relates the water supplying cross-sectional area in the trunk to the transpiring surface in the canopy. Combining results from Chapters 4.4.1 and 5.1.1, the ratio  $A_{lt}/A_{st}$  for beech and oak trees is shown in Figure 5.1.3.2a.  $A_{lt}$  and  $A_{st}$  were derived from allometric equations (Chap. 4.4.1 and Tab. 5.1.1.1, respectively).  $A_{lt}$  increased with increasing  $A_{st}$  for both species. At the same  $A_{st}$  oak supported a larger leaf area than beech. A unit of sapwood area may therefore have a different quality in beech and oak (e.g. different proportions of conduit cross-sectional area and non-conducting area on total sapwood cross-sectional area in the two species, different distribution of conduit diameter classes), and to a lesser extent also a unit of leaf area.

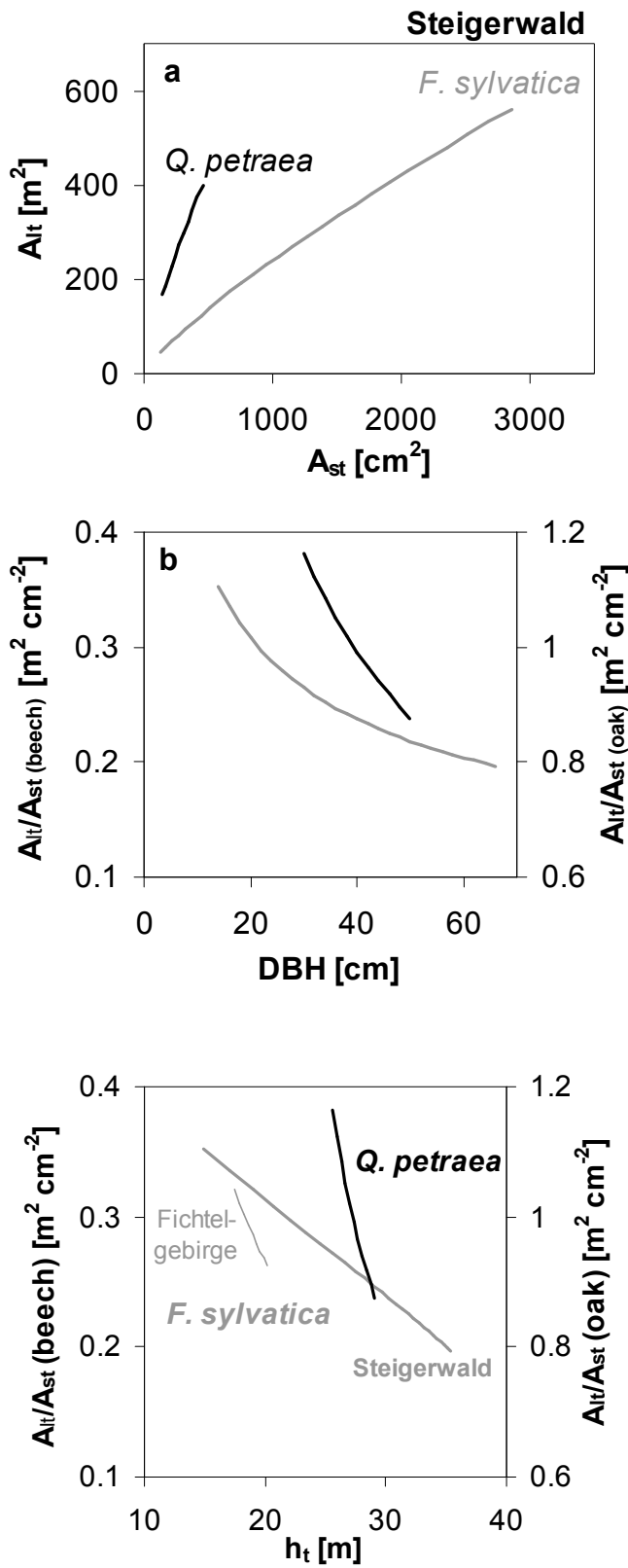


**Figure 5.1.3.2:** Leaf area ( $A_{lt}$ ) to sapwood area ( $A_{st}$ ) relationships (a) for *Fagus sylvatica* (shaded line) and *Quercus petraea* trees (dark), based on allometric equations (see Chap. 4.4.1 and Tab. 5.1.1.1), and ratio of  $A_{lt}$  to  $A_{st}$  versus tree diameter (DBH; b). Graphs are drawn for observed ranges of parameters only. For beech from Farrenleite the graphs are nearly identical to those for beech from the Steigerwald (see text).

**Figure 5.1.3.3:** Ratio of leaf area ( $A_{lt}$ ) to sapwood area ( $A_{st}$ ) for beech (shaded line) and oak trees (dark), as in Figure 5.1.3.2, versus tree height ( $h_t$ , using regression equations given in Tab. A11.2, Appendix). Graphs are drawn for observed ranges of parameters only.

With increasing DBH,  $A_{lt}/A_{st}$  decreased (Fig. 5.1.3.2b). This decrease was steeper for oak. For beech from Farrenleite in the Fichtelgebirge the  $A_{lt}$ -DBH relationship was the same as for the Steigerwald sites (cf. Chap. 4.4.1) and differences in the  $A_{st}$ -DBH relationship were only minor so that the graphs for beech from Farrenleite were virtually identical to the ones shown in Figure 5.1.3.2 for beech from the Steigerwald. The range of DBH was smaller for Farrenleite (18–34 cm, cf. Tab. 5.1.1.1) as can

also be seen in Figure 5.1.3.3 (below). The ratio  $A_{lt}/A_{st}$  declined more strongly with tree height  $h_t$  in beech from Farrenleite than in beech from the Steigerwald, and was even more pronounced in oak (Fig. 5.1.3.3). In taller trees less leaf area was supported by the same sapwood area than in shorter trees (of more or less the same age, see above).

## 5.2. Atmospheric and soil conditions during the investigated years

Atmospheric and soil conditions during the investigated years are detailed in the following, representing the abiotic environmental setting for and short-term drivers of canopy transpiration at the study sites in the Steigerwald (Chap. 5.2.1) and the Fichtelgebirge (Chap. 5.2.2). The following tables show data for the Steigerwald alongside the respective data for the Fichtelgebirge.

### 5.2.1. Steigerwald-sites Steinkreuz and Große Ebene

Meteorological conditions recorded in a large forest gap close to the study site Steinkreuz were considered representative of the nearby site Große Ebene as well (see Chap. 3.1 and Chap. 4.5). Table 5.2.1.1 gives an overview of important variables and characteristics of both the Steigerwald and Fichtelgebirge sites.

**Table 5.2.1.1:** Meteorological variables at the investigation sites in the Steigerwald and the Fichtelgebirge. Data from this study, plus data courtesy of G. Lischeid (Dept. of Hydrogeology, Bayreuth Institute for Terrestrial Ecosystem Research), of the German Weather Service DWD (DWD 1998–2003), and of the Bavarian Forest Institute LWF Bayern (pers. comm.). n.d. = not determined. Long-term averages (1961–1990 for the Fichtelgebirge, 1962–1990 for the Steigerwald) from the nearest DWD-stations were adjusted to the local meteorological stations by means of scaling factors (“adj”; cf. caption of Fig. 5.2.1.1). Precipitation data for Farrenleite were supplemented with monthly data from the DWD-station Fichtelberg-Hüttstadel and adjusted to the site using a scaling factor of 1.18 (cf. caption of Fig. 5.2.1.1) for the whole year of 1998 and for the dormant season in 1999 and 2000.

	Period	Steinkreuz and Große Ebene, Steigerwald	Farrenleite, Fichtelgebirge
Mean annual air temperature [°C]	1998	8.3	5.3
	1999	8.6	6.0
	2000	8.8	6.3
	1998–2000	8.6	5.9
	1961–1990	8.0 (adj to ST)	5.0 (adj to FA)
Mean growing season air temperature (May–October)	1998	13.5	10.3
	1999	14.4	11.5
	2000	13.8	11.4
	1998–2000	13.9	11.1
	1961–1990	14.0 (adj to ST)	10.6 (adj to FA)
Average air temperature of warmest month	1998–2000	16.7 (August)	13.8 (August)
	1961–1990	17.4 (July) (adj to ST)	13.4 (July) (adj to FA)
Mean dormant season air temperature (Nov.–Apr.)	1998	3.3	0.4
	1999	2.4	0.4
	2000	3.3	1.2
	1998–2000	3.0	0.7
	1961–1990	2.0 (adj to ST)	-0.6 (adj to FA)

**Table 5.2.1.1**, continued.

	Period	Steinkreuz and Großebene, Steigerwald	Farrenleite, Fichtelgebirge
Average air temperature of coldest month	1998–2000	0.5 (January)	-1.5 (December)
	1961–1990	-1.6 (January) (adj ST)	-3.9 (January) (adj FA)
Range of mean daily temperatures	1998–2000	-9.8 to 25.0	-12.7 to 24.0
	1998	916	1779
Annual sum of precipitation [mm]	1999	744	1517
	2000	798	1435
	1998–2000	819	1577
Precipitation during growing season [mm]	1961–1990	859 (adj to ST)	1306 (adj to FA)
	1998	586	1191
Annual $R_n$ [ $\text{MJ m}^{-2} \text{yr}^{-1}$ ]	1999	350	676
	2000	483	683
	1998–2000	473	850
Growing season $R_n$ [ $\text{MJ m}^{-2} \text{season}^{-1}$ ]	1961–1990	464 (adj to ST)	631 (adj to FA)
	1998	1781	n.d.
	1999	1701	n.d.
	2000	1814	n.d.
	1998–2000	1765	n.d.
Annual PFD [ $\text{mol m}^{-2} \text{yr}^{-1}$ ]	1998	1432	n.d.
	1999	1381	816
	2000	1479	786
Growing season PFD [ $\text{mol m}^{-2} \text{season}^{-1}$ ]	1998–2000	1431 (1430 <sup>a</sup> )	n.d. (801 <sup>a</sup> )
	1998	5688	n.d.
	1999	6501	n.d.
	2000	6813	n.d.
	1998–2000	6334	n.d.
Fog days <sup>b</sup> per year	1998	4207	n.d.
	1999	4889	3892
	2000	4900	3717
- during growing season	1998–2000	4665 (4895 <sup>a</sup> )	n.d. (3805 <sup>a</sup> )
	1998–2000	40–50 <sup>c</sup>	195
- maximum per month	n.d.		85
	n.d.		22 (October)
	n.d.		7 (June)

<sup>a</sup> average for 1999–2000.<sup>b</sup> defined as visibility below 1000 m for 10 minutes; data from Foken (2003) for Waldstein-Weidenbrunnen, 775 m a.s.l., ca. 12 km direct distance from Farrenleite.<sup>c</sup> long-term average from BayFORKLIM (1996).

Air temperature and phenology. The year 1998 was the coldest at the climate station Steinkreuz (mean annual air temperature  $T_{air}$  8.3 °C, Tab. 5.2.1.1), with 2000 being the warmest year (8.8 °C) and 1999 intermediate (8.6 °C). The average mean  $T_{air}$  of these three years was 0.9 K higher than the long-term average (1962-1990, DWD-station Ebrach, 3.7 km direct distance to Steinkreuz) of 7.7 °C (DWD 1999–2000; see Fig. 3.1.2) or 0.6 K higher than the long-term average of the DWD-station adjusted to the climate station at Steinkreuz (see caption of Fig. 5.2.1.1 and Tab. 5.2.1.1). Average  $T_{air}$  during the growing season (see below) was lowest in 1998 (13.5 °C), highest in 1999 (14.4 °C) and intermediate in 2000 (13.8 °C), and the average of the three years was 0.1 K lower than the site-adjusted long-term average of 14.0 °C (Tab. 5.2.1.1). The number of days per year where  $T_{air}$  was  $\geq 10$  °C reflects the ranking of average  $T_{air}$  during the growing seasons (Tab. 5.2.1.2) and is often used as a proxy for the duration of the growing season. The length of the growing season (defined here as the time span between the beginning of leaf emergence and the beginning of leaf colour change of *F. sylvatica*) as observed in phenological gardens and interpolated region-wide by DWD (DWD 1998-2003) and the order among the three years closely matched these values (Tab. 5.2.1.2). The time of leaf emergence and leaf colouration of beech as published by the DWD (for the regions “Fränkisches Keuper-Lias-Land” and „Thüringisches-Fränkisches Mittelgebirge“) and observations from this study at the sites in the Steigerwald and Fichtelgebirge coincided within a few days (Tab. 5.2.1.2).

In 1998, the first five months of the year were warmer than the site-adjusted long-term average mean monthly values of  $T_{air}$  (Fig. 5.2.1.1a), especially January and February were much warmer (+2.3 K and + 3.6 K, respectively), and monthly deviations of current  $T_{air}$  from long-term  $T_{air}$  added up to +9.3 K. June, August, October and December showed “typical” mean monthly values of  $T_{air}$ , whereas July, September and November were much cooler (deviations of -1.9 K, -1.1 K, -2.8 K, respectively; Fig. 5.2.1.1a). The cool months of July (typically the warmest month, cf. Fig 3.1.2a) and September made this the coldest of all three growing seasons, and together with the cold November the coldest year as well (Tab. 5.2.1.1).

The pattern was similar in 1999 in that the first five months were rather warm again, except for the somewhat cooler than average February. June was cold this year, instead of July as in 1998 (- 1.2 K deviation from long-term  $T_{air}$ , Fig. 5.2.1.1a), as well as November (-1.4 K). September was remarkably warm (+ 3.2 K), which made it, in concert with a somewhat above-normal July, the warmest of the three growing seasons (Tab. 5.2.1.1).

In the year 2000,  $T_{air}$  in late winter and early spring was above normal again (February deviated +3.3 K from the long-term average), particularly in April (+2.6 K, due to a warm last third of the month, Fig 5.2.1.1a, 5.2.1.2). July was outstandingly cold (deviation -3.3 K) which made it the second coldest of the investigated growing seasons (Tab. 5.2.1.1). Yet since September was the only other month with below-average  $T_{air}$ , the whole year was the warmest observed (Fig 5.2.1.1a, Tab. 5.2.1.1).

The highest air temperature during the period 1998-2000 was 36.3 °C (10 minute-average), measured on August 12, 1998, also the day with the highest minimum (19.5 °C; 10 minute-average) and highest average (25.0 °C) air temperature (Fig. 5.2.1.2).

**Table 5.2.1.2:** Phenology. Observations from the present study and data from DWD (1998–2003) are listed. DWD-data are interpolations for a whole region, where the Steigerwald is part of the “Fränkisches Keuper-Lias-Land”, and the Fichtelgebirge part of the “Thüringisches-Fränkisches Mittelgebirge”.

	year	Steinkreuz and Großebene, Steigerwald	Farrenleite, Fichtelgebirge
Duration of growing season <sup>a,b</sup> [d]	1998	166	155
	1999	175	166
	2000	171	161
average	1998–2000	171	160
Leaf emergence [day of year]			
of <i>F. sylvatica</i> <sup>a</sup>	1998–2000	113	118
of <i>Q. robur</i> <sup>a</sup>	1998–2000	119	
Leaf colouring [day of year]			
of <i>F. sylvatica</i> <sup>a</sup>	1998–2000	284	278
of <i>Q. robur</i> <sup>a</sup>	1998–2000	288	
Number of days with mean air temperature $\geq 10^{\circ}\text{C}$	1998	152	102
	1999	171	125
	2000	164	117
Number of days with mean air temperature $\geq 5^{\circ}\text{C}$	1998	250	189
	1999	231	195
	2000	253	205
Beginning of leaf emergence in <i>F. sylvatica</i> [day of year]	1998	113	n.d.
	1999	112	124
	2000	110	117
Beginning of leaf colouring in <i>F. sylvatica</i> [day of year]	1998	273	268
	1999	280	276
	2000	(< 284) <sup>c</sup>	(< 280) <sup>d</sup>
Duration of growing season <sup>b</sup> [d]	1998	160	n. d
	1999	168	152
	2000	(< 174) <sup>c</sup>	(< 163) <sup>d</sup>

<sup>a</sup> data from DWD (1998–2003).

<sup>b</sup> beginning of leaf emergence and leaf colour change of *F. sylvatica*.

<sup>c</sup> no earlier observations available; on day 284 leaf colour change was still at initial stage.

<sup>d</sup> no earlier observations available; on day 280 leaf colour change was already rather advanced.

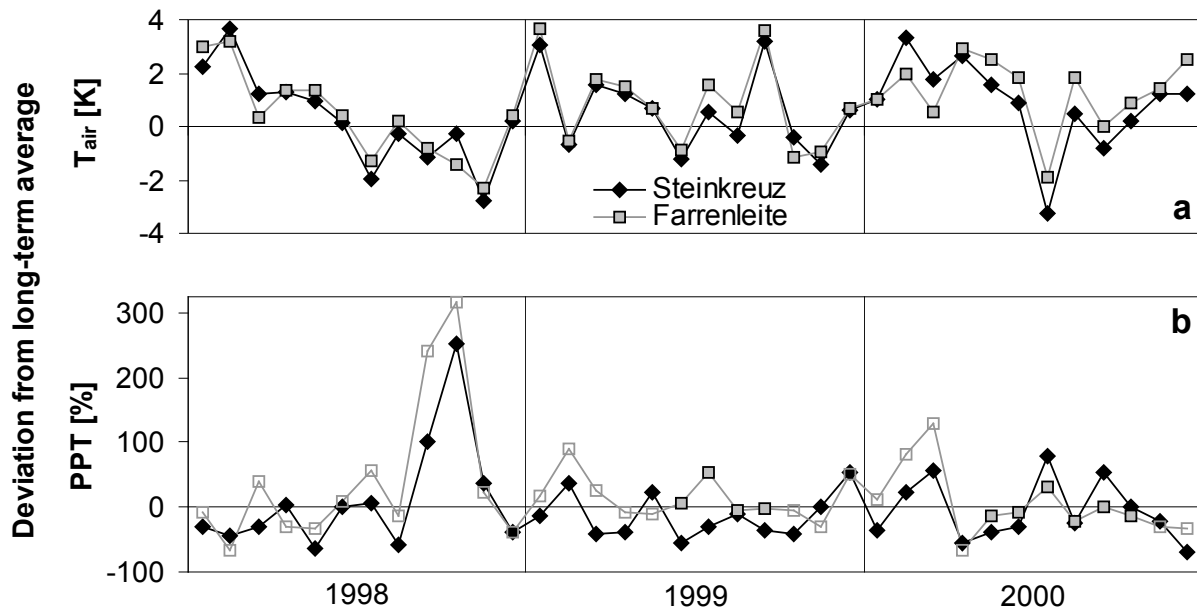


**Figure 5.2.1.1:** Deviation of mean monthly air temperatures ( $T_{air}$ , a) and precipitation (PPT, b) at Steinkreuz, Steigerwald (filled diamonds), and Farrenleite, Fichtelgebirge (shaded squares), for the three years of investigation from the long-term average. Since no long-term observations were available from either investigation site, the respective data from the nearest German weather service (DWD) stations (Ebrach and Fichtelberg-Hüttstадl, cf. caption to Fig. 3.1.2) were multiplied by a scaling factor derived from linear regression between monthly averages of presented and DWD-data (DWD 1999–2000). Regression equations used are for air temperature at Steinkreuz:  $y = 1.0397x$ ;  $R^2 = 0.991$ ,  $p < 0.0001$ ; for air temperature at Farrenleite:  $y = 0.9401x - 0.80$ ;  $R^2 = 0.993$ ,  $p < 0.0001$ ; for precipitation at Steinkreuz:  $y = 1.0625x$ ;  $R^2 = 0.900$ ;  $p < 0.0001$ . For Farrenleite only a few values of monthly precipitation were available so these were used to extract a scaling factor of 1.18. The same factor was derived when using a precipitation gradient of 60–70 mm/100 m, as detailed by Gerstberger et al. (2004) for another mountain in the Fichtelgebirge. Using this factor, deviation from long-term mean precipitation was estimated from DWD-data from the station Fichtelberg for months when the rain gauge at Farrenleite was not operational (open squares).

Precipitation. At Steinkreuz, in the year 1998 the highest annual sum of precipitation (PPT) was observed (916 mm), in 1999 the lowest (744 mm), and in 2000 intermediate amounts (798 mm). The long-term average for the DWD-station Ebrach (1962–1990; DWD 1999–2000) is 808 mm and adjusted to the study site Steinkreuz (see Fig. 5.2.1.1b) amounts to 859 mm (Tab. 5.2.1.1). Thus the average annual PPT of the three years studied was 40 mm below the site-adjusted long-term average. 1998 was also the year with the highest amount of precipitation during the growing season (May–October), namely 586 mm, followed by the year 2000 (483 mm) and 1999 (350 mm). So in 1999, 25 % of the long-term average precipitation (464 mm, site-adjusted) was missing during this period (Tab. 5.2.1.1). The highest daily rate of precipitation of 41 mm was recorded on August 5, 1999 (see Fig. 5.2.1.2).

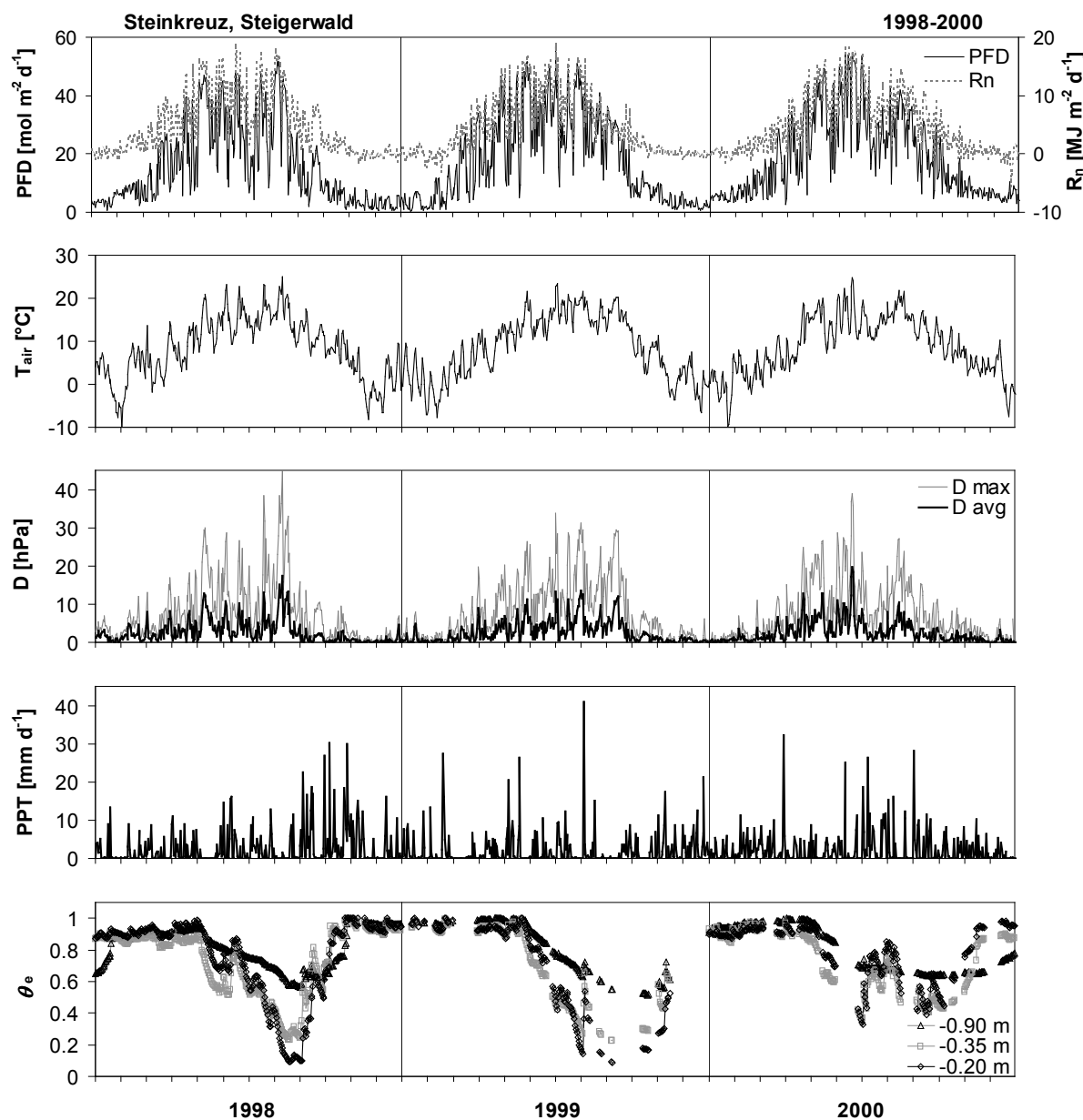


**Figure 5.2.1.2:** Seasonal changes in meteorological variables (photosynthetic photon flux density, PFD; net radiation,  $R_n$ ; air temperature,  $T_{air}$ ; 24 h-average of water vapour pressure deficit,  $D_{avg}$ ; daily maximum D of 10'-values,  $D_{max}$ ; precipitation, PPT) and relative extractable soil water ( $\theta_e$ ) at the site Steinkreuz for the years 1998-2000. Climatic data were measured in 5 m height, above regrowth, in a forest gap. Precipitation was supplemented by data from the German Weather Service (DWD, station Ebrach). Soil water content was measured by TDR-probes in 0.2, 0.35 and 0.9 m soil depth at three below-canopy locations within the experimental plot; frequent data gaps exist in the 1999- and 2000-data sets. For calculation of relative extractable soil water see text. Data courtesy of G. Lischeid, Dept. of Hydrogeology, Bayreuth Institute for Terrestrial Ecosystem Research (BITÖK).

1998 started as a “dry” year with more than 100 mm less precipitation during the first five months than the long-term (site-adjusted) average, and in particular May was dry (29 mm, -64 % deviation from the long-term average, Fig. 5.2.1.1b), with a period of more than two weeks without rain (see also Fig 5.2.1.2). June and July were average

and August (34 mm) lacked 57 % of the long-term precipitation again. Very high amounts of precipitation in September (+100 %) and October (+250%) and to a lesser extent November (+37 %) made this the year with highest annual sum of PPT of the three years investigated. Almost half of the annual sum was precipitated between the beginning of September and mid November (Fig 5.2.1.2).

In 1999, precipitation moderately exceeded long-term average monthly sums in February, May and December by 37 %, 24 %, and 53 %. During the other months precipitation was below average, especially in March and April (around -40 % deviation), June (-55 %, typically the month with most rain, cf. Fig. 3.1.2a), September and October (approx. -40 %, Fig. 5.2.1.1b). As a result this was comparatively the driest of the years studied (Tab. 5.2.1.1).

The year 2000 showed a somewhat more balanced pattern of monthly sums of precipitation in that positive and negative deviations were spread more evenly over the year (Fig. 5.2.1.1b). During April, May and June the site received less than the long-term average precipitation, meanwhile in July and September the amounts were above mean values (78 and 54 %, respectively). Very little precipitation in December then caused the annual sum to drop below the long-term average (Tab. 5.2.1.1).

**Soil moisture.** The amount of soil water available to the vegetation within the mixed Steinkreuz stand was described as relative extractable soil water  $\theta_e$ . The seasonal minima of  $\theta_e$  and associated parameters are given in Table 5.2.1.3 and the seasonal changes of  $\theta_e$  in Figure 5.2.1.2.

**Table 5.2.1.3:** Soil physical characteristics (soil water content at permanent wilting point,  $\theta_P$ , and at field capacity,  $\theta_F$ ) and soil water availability at Steinkreuz during the years studied.  $\theta_{min}$  is minimum observed annual soil water content,  $\theta_{e\ min}$  is minimum annual relative extractable soil water. For further explanations see Chapter 4.5. Values are averages from three sensors per depth. Note that minimum values observed in 1999 may not be the lowest values experienced by the vegetation due to a large data gap for all depths from mid-September to mid-October. Original soil water content-data courtesy of G. Lischeid, Dept. of Hydrogeology, BITÖK. Values for  $\theta_P$ , determined for this site are from Langusch and Kalbitz (2001).

Soil depth	-0.2 m	-0.35 m	-0.9 m
$\theta_P$ [ $m^3\ m^{-3}$ ]	0.068	0.068	0.111
$\theta_F$ [ $m^3\ m^{-3}$ ]	0.246	0.264	0.385
<b>1998</b>			
$\theta_{min}$ [ $m^3\ m^{-3}$ ]	0.084	0.114	0.265
$\theta_{e\ min}$	0.09	0.23	0.56
<b>1999</b>			
$\theta_{min}$ [ $m^3\ m^{-3}$ ]	0.084	0.112	0.252
$\theta_{e\ min}$	0.09	0.23	0.52
<b>2000</b>			
$\theta_{min}$ [ $m^3\ m^{-3}$ ]	0.126	0.140	0.286
$\theta_{e\ min}$	0.33	0.37	0.64

The relative extractable soil water  $\theta_e$  reached values of or near saturation only late in the spring of 1998 (Fig. 5.2.1.2), due to comparatively little precipitation during late winter and early spring (see above and Fig. 5.2.1.1b). The decline in  $\theta_e$  was rather steep then in 0.2 and 0.35 m soil depth from the beginning of May, the time of leafing out, because of little supplementary rain. The decrease of  $\theta_e$  in -0.9 m depth was slower. Frequent rain in late May and in June led to increases in  $\theta_e$  in the upper soil layers, yet infiltration did not reach the deeper horizons (-0.9 m). Rainy spells resulted in increases of  $\theta_e$  around the end of the first third of July and at the end of July (upper two soil levels only). Minimum values of  $\theta_e$  were reached on 21.08.1998 (-0.2 m, -0.35 m) and 02.09.1998 (-0.9 m; Fig 5.2.1.2, Tab. 5.2.1.3). Abundant precipitation in September and October caused  $\theta_e$  to increase rapidly in all measured soil depths.

Rather little precipitation during March and April 1999 may have caused  $\theta_e$  to begin to decrease immediately after the time of leaf emergence, interrupted by intense rains in May. After that,  $\theta_e$  declined more rapidly than in the previous year, particularly at 0.9 m soil depth. Suspended by a rainy spell around mid-July, continuous rains on August 5, 1999 (41.8 mm in 21 hours, visible in increasing  $\theta_e$  down to -0.9 m), and a few rainy days in mid-August, lowest values of  $\theta_e$  were observed on September 8, 1999 (Tab. 5.2.1.3).  $\theta_e$  very probably declined even further, since a long late summer dry spell (daily PPT not exceeding 1.2 mm, beginning in mid-August) lasted until the evening of September 20, 1999, but  $\theta$ -data are lacking from 09.09. until 13.10.1999. Replenishment of soil water stores proceeded much slower than the previous year since October was also lacking typical amounts of rain (Fig. 5.2.1.2, Fig. 5.2.1.1b).

In the year 2000,  $\theta_e$  decreased continuously from the time of leaf unfolding, initially at a somewhat lower rate though than in 1999. Minimum values in the three depths were already reached on July 2, 2000, which was the lowest values for this time of the year during 1998-2000. Precipitation of 77 % above normal afterwards prevented  $\theta_e$  from dropping below the levels reached during the previous two years (cf. Tab. 5.2.1.3). There were only 13 days in July with less than 1 mm of rain and 11 days with more than 5 mm. The upper soil layers repeatedly dried out again in August, September and October, yet soil water supplies from 0.9 m depth remained favourable ( $\theta_e > 0.60$ ). A slow recovery to saturation levels was observed, especially in -0.9 m, during late autumn/early winter (cf. Fig. 5.2.1.1b).

Coefficients of variation (CV) of  $\theta_e$  ranged from 0.01 to 0.17 (i.e. 1 to 17 %) for 0.2 m soil depth, from 0.01 to 0.19 for 0.35 m soil depth and from 0.01 to 0.17 for 0.9 m soil depth. Obviously the three sensors installed per depth cannot represent the spatial heterogeneity of the whole plot. Nonetheless the CV hint at the within-site variability which was highest during phases of soil rewetting and soil dry-down and lowest when  $\theta_e$  reached minimum values (not shown).

Figure 5.2.1.3 shows profiles of seasonal dynamics of the soil water potential  $\Psi_{soil}$  at Steinkreuz. The graphs corroborate the general trends extracted from data of volumetric soil water content  $\theta$  and extend it down to 2 m soil depth. Note that in this data set the same data gap exists as in that of  $\theta_e$ , so corresponding assumptions can be made as above, namely that  $\Psi_{soil}$  probably reached lowest values during the summer of 1999. Changes of  $\Psi_{soil}$  in 2 m soil depth were less pronounced than in the upper layers and commenced only towards the end of the summer.

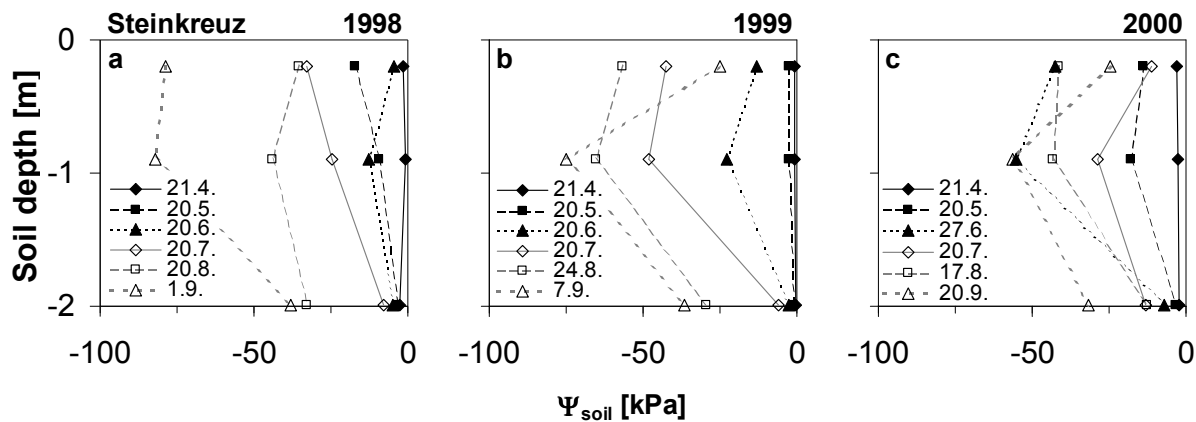


**Figure 5.2.1.3:** Vertical profiles of soil water potential  $\Psi_{\text{soil}}$  at Steinkreuz on different dates in 1998 (a), 1999 (b) and 2000 (c). Data are averages of five soil water potential profiles in the experimental plot. Tensiometers were placed in 0.2 m, 0.9 m and 2.0 m soil depth. Dates were chosen to be in monthly intervals (where possible despite frequent data gaps), except for the last date of each year, which was to show the lowest seasonal  $\Psi_{\text{soil}}$  (in 0.9 m and 2.0 m depth); due to a large data gap from mid-September to mid-October 1999, the shown values for 07.09. are probably not the lowest values for that season (see text). The first date of each year is prior to leaf unfolding. Data courtesy of G. Lischeid, Dept. of Hydrogeology, BITÖK.

**Radiation.** Net radiation  $R_n$  and photosynthetical photon flux density PFD were highest in the year 2000, respectively, both integrated to seasonal (May–October) and to annual levels (Tab. 5.2.1.1). Lowest values were observed for both intervals in 1999 regarding  $R_n$  and in 1998 regarding PFD (Tab. 5.2.1.1).  $R_n$  and PFD closely resembled each other (Fig. 5.2.1.2) over the years. The highest radiation was observed during June and July in 1999 and regarded as typical, whereas in 1998,  $R_n$  and PFD were highest in August, followed by May and June and much lower in July, in accordance with the pattern of  $T_{\text{air}}$  (see also Fig. 5.2.1.1a). In the year 2000, the largest radiation was measured in June, followed by May and August, while for July, values were again the lowest of the four months as in 1998 (Fig. 5.2.1.2).

**Vapour pressure deficit of the air.** As depicted in Figure 5.2.1.2 for the Steigerwald sites, the highest values of vapour pressure deficit of the air  $D$ , the driving force of transpiration, in 1998 were observed during the second half of July and especially August, and maximum daily values of  $D_{\text{avg}}$  (17.5 hPa; 10'-means averaged over 24 hours) and  $D_{\text{max}}$  (46 hPa; 24 hour-maximum of 10'-mean values) were measured on August 11 and August 12, 1998, respectively. During the following year, such high values were not reached again, and the days with higher  $D_{\text{avg}}$  and  $D_{\text{max}}$  were distributed more evenly over the summer, with dry atmospheric conditions long into the warm September (see also Fig. 5.2.1.1a, b). The highest recordings were made on July 3, 1999 with  $D_{\text{max}} = 34$  hPa and on August 2, 1999, with slightly higher  $D_{\text{avg}}$  (13.4 hPa) than on the previous date. In the year 2000, values of high  $D$  were found towards the first half of the growing season, with high evaporative demand already encountered in May and maximum values of  $D_{\text{max}}$  (39 hPa) and  $D_{\text{avg}}$  (19.6 hPa) reached on June 20, 2000 (Fig. 5.2.1.2).

**Differences among the Steigerwald-sites.** Measurements of soil water potential  $\Psi_{\text{soil}}$  carried out at the second Steigerwald-site Großebene in varying intervals are compared with continuous readings from Steinkreuz at similar depths in Figures 5.2.1.4–5 for the vegetation periods of 1998 and 1999, respectively. Apart from the noteworthy spatial variability there may be some indications that at Großebene,  $\Psi_{\text{soil}}$  in deeper soil layers (-0.6 m) stayed higher longer, but towards the end of the vegetation period of 1999 became as negative as at Steinkreuz, given that  $\Psi_{\text{soil}}$  at Steinkreuz was measured in -0.9 m (Fig. 5.2.1.5b).

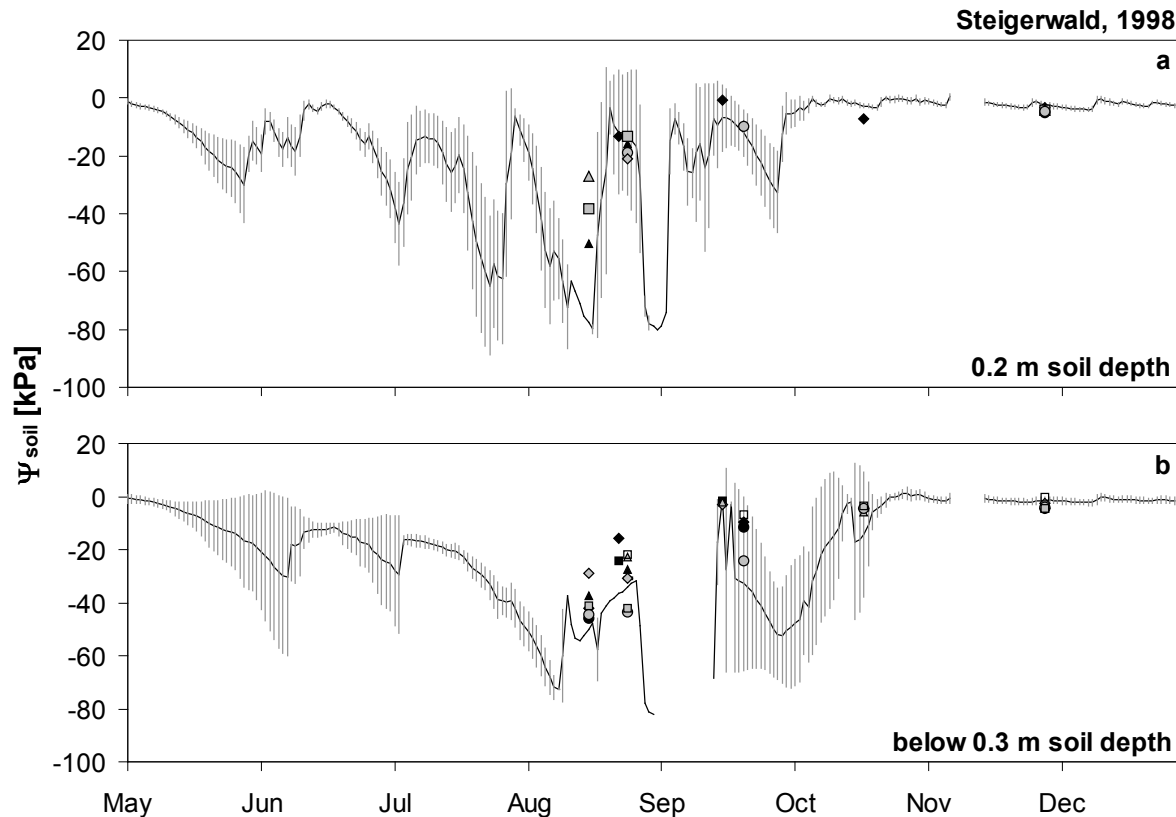


**Figure 5.2.1.4:** Soil water potential  $\Psi_{\text{soil}}$  from May to December 1998 at the sites Steinkreuz and Großebene in 0.2 m soil depth (a; solid line is an average for Steinkreuz,  $n = 5$ , symbols are for Großebene,  $n = 7$ ), and (b) in 0.35 to 0.5 m (symbols, for Großebene) and in 0.9 m soil depth (solid line, for Steinkreuz,  $n = 5$ ). Filled and shaded symbols in b) depict values from tensiometers in 0.35 m ( $n = 5$ ) and in 0.5 m soil depth ( $n = 5$ ) at Großebene, respectively. Bars ( $\pm 1 \text{ SD}$ ) in a and b depict spatial variability within the plot Steinkreuz. Data from Steinkreuz courtesy of G. Lischeid, Dept. of Hydrogeology, BITÖK.

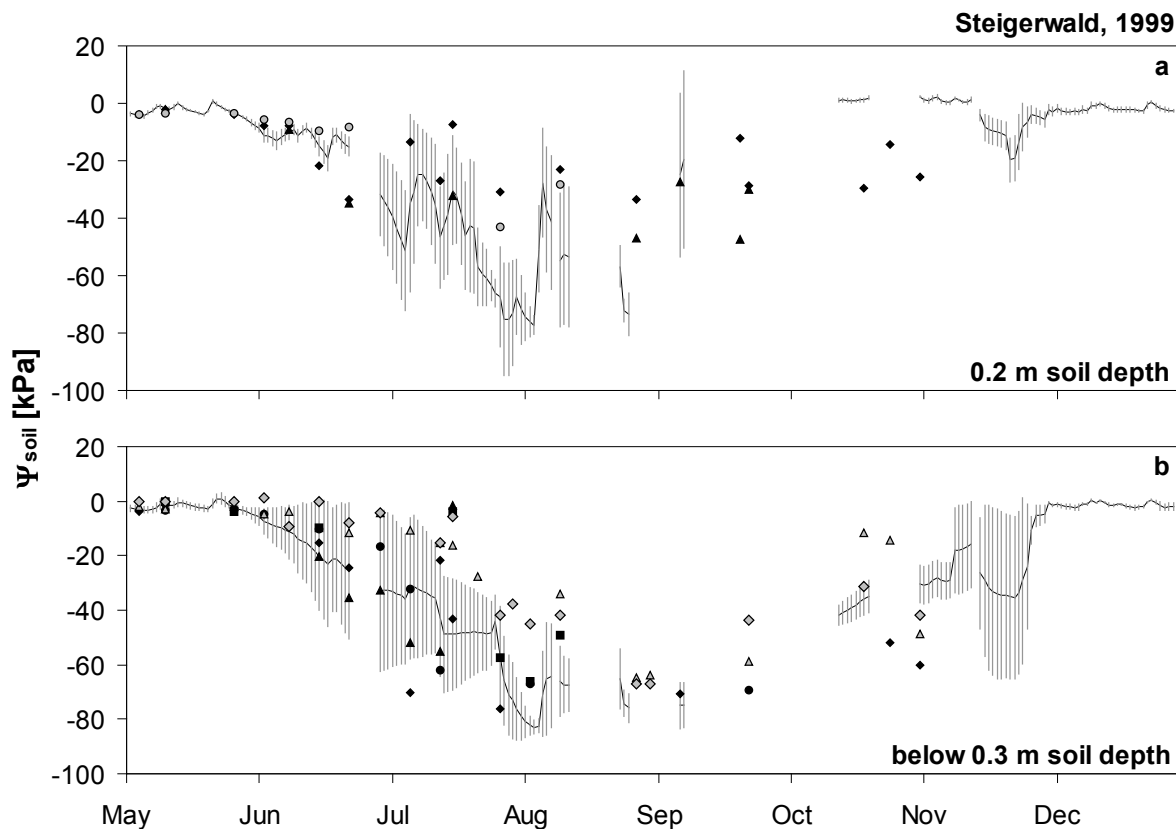


**Figure 5.2.1.5:** Soil water potential  $\Psi_{\text{soil}}$  from May to December 1999 at the sites Steinkreuz and Großebene, in 0.2 m soil depth (a; solid line is average for Steinkreuz,  $n = 5$ , symbols are for Großebene,  $n = 3$ ) and (b) in 0.35 to 0.6 m (symbols, for Großebene) and in 0.9 m soil depth (solid line, for Steinkreuz,  $n = 5$ ). Filled and shaded symbols in b denote water potentials measured in 0.35 m ( $n = 4$ ) and 0.6 m soil depth ( $n = 2$ ) at Großebene, respectively. Bars ( $\pm 1 \text{ SD}$ ) in a and b depict spatial variability within the plot Steinkreuz. Data from Steinkreuz courtesy of G. Lischeid, Dept. of Hydrogeology, BITÖK.

### 5.2.2. Fichtelgebirge-site Farrenleite

Although some measurements were carried out in 1998, the main period of investigation at Farrenleite was 1999-2000. Therefore, most of the following descriptions focus on these two years and are compared with the Steigerwald-sites.

Air Temperature and phenology. The temperatures at the site Farrenleite in the Fichtelgebirge are in general lower during the whole year compared to the sites in the Steigerwald (cf. Fig. 3.1.2; note that the DWD-station Fichtelberg is about 300 m lower than Farrenleite), due to its higher elevation and more eastern location (cold continental air masses in winter, see Chap. 3.2). The mean annual air temperature  $T_{\text{air}}$  at Farrenleite, averaged over the three years of investigation, was 2.7 K lower (5.9 °C) than at Steinkreuz (and 0.4 K higher than the site-adjusted long-term average) and the mean growing season  $T_{\text{air}}$  (May–October) 2.8 K lower compared to Steinkreuz (and again 0.4 K higher than the site-adjusted long-term average, Tab. 5.2.1.1). As at Steinkreuz, 1998 was the coldest, 2000 the warmest year at Farrenleite (Tab. 5.2.1.1). At the latter site, the order was the same for the growing seasons, in contrast to Steinkreuz, where the growing season of 1999 was the warmest (Tab. 5.2.1.1).

Corresponding to the higher location, phenological phases are shifted in the Fichtelgebirge. Leaves at the site Farrenleite emerged about ten days later in spring and changed colour about five days earlier than at the sites in the Steigerwald (the author's own observations 1998–2000; see Tab. 5.2.1.2). The number of days with average  $T_{air} \geq 10^{\circ}\text{C}$  corresponded to the order of average  $T_{air}$  during the growing seasons (Tab. 5.2.1.1), but in contrast to the findings from the Steigerwald did not agree with the absolute duration of the growing season as given by the DWD. However, in contrast to this, dates of leaf emergence and of leaf colour change observed in this study closely matched the dates observed and interpolated by the DWD (1998–2003) for the whole region ("Thüringisches-Fränkisches Mittelgebirge"; Tab. 5.2.1.1).

Deviations from the long-term averages of monthly mean  $T_{air}$  basically followed the same patterns as at Steinkreuz and for many months deviated in almost the same way (Fig. 5.2.1.1a; data in the graph adjusted from German Weather Service-station Fichtelberg at 659 m a.s.l., see figure caption).  $T_{air}$  in February and March was closer to the long-term average (i.e. lower) than at Steinkreuz in 1998 and 2000, October 1998 and 1999 were colder than the long-term average, unlike at Steinkreuz where  $T_{air}$  was normal or almost average, respectively. In contrast to October, the deviation of  $T_{air}$  was slightly higher than at Steinkreuz for all of 1999, particularly in July and August. The same holds true for the growing season of the year 2000, when deviations were always higher (or less negative: July, September) than in the Steigerwald, which continued into the following winter (Fig. 5.2.1.1a). The highest  $T_{air}$  at the site Farrenleite was recorded on 21 June, 2000, with  $28.9^{\circ}\text{C}$  (30 minute-average), also the day with the highest minimum  $T_{air}$  ( $20.1^{\circ}\text{C}$ ; 30 minute-average) and highest average  $T_{air}$  (24.0; Fig. 5.2.2.1, below).

**Precipitation.** The average annual precipitation PPT for 1998–2000 was estimated to be almost two times higher at Farrenleite than at Steinkreuz, namely 819 mm at the latter and approx. 1577 mm at the former site (own data supplemented with data from the DWD, cf. Tab. 5.2.1.1). Precipitation with fog was not accounted for but could be estimated to an additional 9 % of rain as found by Wrzesinsky (2004) for the nearby Waldstein peak (April 2001–March 2002).

During the vegetation period (mean 1998–2000) PPT was more than 1.5 times higher at Farrenleite (850 mm, Steinkreuz 473 mm, cf. Tab. 5.2.1.1). There were slightly more rainy days (precipitation  $> 0.2 \text{ mm d}^{-1}$ ) at Farrenleite in 1999 (two), and considerably more rainy days in 2000 during the growing season (21, data not shown) compared to Steinkreuz. It rained on about 45 % of the days at Steinkreuz in 1999 and 2000 and at Farrenleite in 1999, whereas there was rain on 56 % of the days at Farrenleite in 2000 (data not shown). Rain events were usually more intense (on a daily basis) at Farrenleite, and more than one quarter of all rainy days showed more than 10 mm here, compared to 8–16 % at Steinkreuz (cf. Figs. 5.2.1.2, 5.2.2.1). Fog may have contributed to approx. 8 % of rainy precipitation to the total precipitation during the vegetation period (Wrzesinsky 2004, see "Radiation", below).

The pattern of rainy periods during the vegetation period in general was the same at Farrenleite and Steinkreuz, both being mainly under a maritime influence during the vegetation period and reflecting their location within the same climatic region in summer (cf. Figs. 5.2.1.2, 5.2.2.1). Also, at Farrenleite the patterns of deviation from the long-term average monthly PPT (Fig. 5.2.1.1b) was similar to that of Steinkreuz.

In 1998, the deviation was mostly higher (or less negative) than at Steinkreuz, which was also true for the following winter. Over the course of the growing season of 1999, Farrenleite did not experience substantial below-average PPT as Steinkreuz did (cf. Chap 3.1 and “Soil Moisture”, below). During the growing season of the year 2000, monthly PPT at Farrenleite was somewhat closer to the long-term average than at Steinkreuz, corresponding to the more positive deviations of  $T_{air}$  during that time, July deviated even higher than at Steinkreuz (> 90 % positive deviation, Fig. 5.2.1.1a).

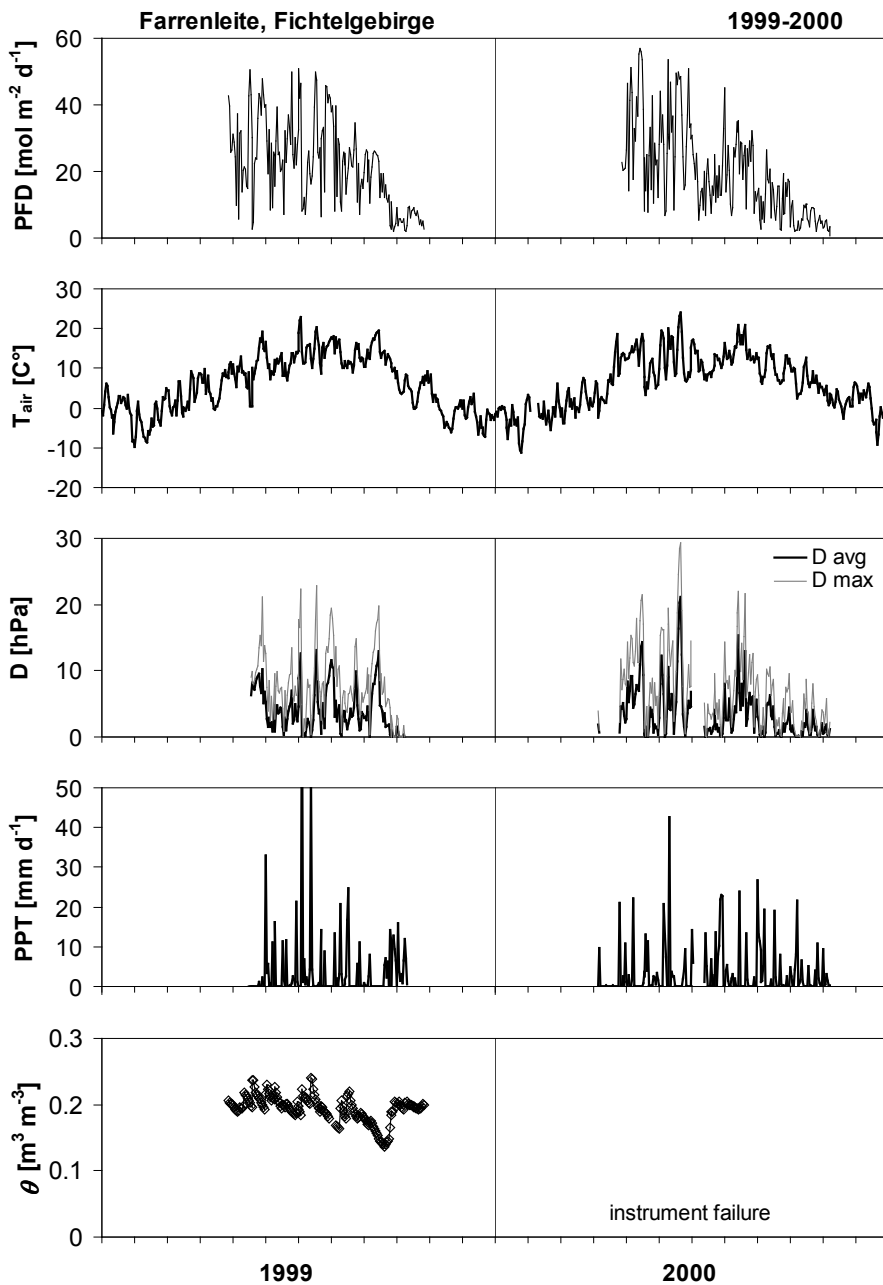


**Figure 5.2.2.1:** Seasonal changes in climatic variables (photosynthetic photon flux density, PFD; air temperature,  $T_{air}$ ; 24 h-average of water vapour pressure deficit,  $D_{avg}$ ; daily maximum D of 10'-values,  $D_{max}$ ; precipitation, PPT) and volumetric soil water content,  $\theta$ , in 0.2 m depth at the site Farrenleite during 1999 and 2000.  $T_{air}$  alone was measured year-round, other variables only during the growing period. Data of  $\theta$  are available for 1999 only. Data of D and PPT missing for July 4-12, 2000. Precipitation amounted to approx. 75 mm on July 6, 1999, and to 55 mm on July 14, 1999.

**Soil moisture.** The wetter site conditions in the Fichtelgebirge are also reflected in soil moisture (Fig. 5.2.2.2; note that expression of  $\theta$  as  $\theta_e$  was not possible for Farrenleite as detailed in Chap. 4.5). At the beginning of the vegetation period in 1999, the volumetric soil water content  $\theta$  in 0.3 m soil depth was so high after the snowmelt that the frequent rain events at that time led to values of  $\theta$  above field capacity ( $\theta_F$ ). Even later in summer  $\theta$  reached saturation. The lowest values of  $\theta$  were recorded towards the end of September 1999 ( $0.14 \text{ m}^3 \text{ m}^{-3}$ ). Thus  $\theta$  decreased by only about 30 % during the vegetation period (minimum  $\theta/\theta_F = 0.68$ , Fig. 5.2.2.2). At Steinkreuz in contrast, the  $\theta$  decreased during the same period more than twice as much, by about 66 % (minimum  $\theta/\theta_F = 0.34$ ), corresponding to an  $\theta_{e \min}$  of 0.09 (Tab. 5.2.1.3, Fig. 5.2.2.2). The  $\theta$  very probably declined even further at Steinkreuz (see chap. 5.2.1, above). Refilling of the soil water reserves was already completed at Farrenleite at the beginning of autumn (Fig. 5.2.2.2) whereas it took much longer at Steinkreuz (cf. Fig. 5.2.1.2). This also allows the assumption that deeper soil layers were also already near saturation at Farrenleite in autumn 1999, while they were not (yet) at Steinkreuz (cf. Fig. 5.2.1.2). When only considering days for which data from both Steinkreuz and Farrenleite were available, the seasonally integrated soil water depletion (calculated from day-to-day changes in  $\theta/\theta_F$ ) reached approximately 120 % of  $\theta/\theta_F$  at Steinkreuz and 70 % of  $\theta/\theta_F$  at Farrenleite, or at Steinkreuz almost 1.8 times the amount at Farrenleite (data not shown). Frequent data gaps in data from Steinkreuz (see Chap. 4.5) hindered a more detailed analysis of differences between the two sites. For the year 2000 no data of  $\theta$  were available for Farrenleite due to instrument failure, but it could be estimated that soil water conditions during the vegetation period should have been even moister than in 1999, due to more frequent rains (though only slightly larger amounts), lower irradiance (-4.5 % PFD, -4 %  $R_n$ ), and longer duration of fog (+14 %, during day-time; see Tab. 5.2.1.1). Even if measured  $\theta$  in 30 cm soil depth had been low enough to potentially cause drought effects in tree water use, additional water reserves in surely root-penetrated soil layers deeper than the assessed upper 30 cm of the soil profile (deeply weathered rock and hence soil depth of up to 100 cm, Tab. 3.3.1) would most likely have prevented such effects.

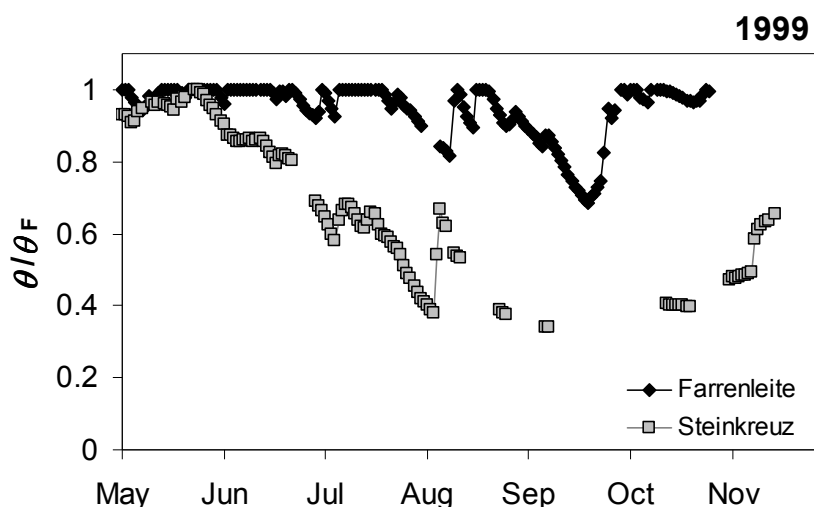


**Figure 5.2.2.2:** Seasonal course of mean daily soil water content  $\theta$  relative to soil water content at field capacity  $\theta_F$  in 0.2 m depth at Farrenleite (Fichtelgebirge, filled diamonds) and Steinkreuz (Steigerwald, shaded squares) in 1999. Data for Steinkreuz are averages of three TDR-probes in the experimental plot, at Farrenleite only one sensor was available. Original data of soil water content from Steinkreuz courtesy of G. Lischeid, Dept. of Hydrogeology, BITÖK.

**Radiation.** Photosynthetical photon flux density (PFD) received by the overstory canopy at Farrenleite (Fig. 5.2.2.1) was on average during the growing season (1999–2000) only 78 % of that at Steinkreuz (cf. Tab. 5.2.1.1). The large number of 80 days with fog (average of growing seasons 1999 and 2000) at the higher elevations of the Fichtelgebirge, measured at 775 m elevation a.s.l. at the nearby (12 km direct distance) Waldstein mountain (Foken 2003, Wrzesinski 2004, Tab. 5.2.1.1) may at least partly explain this difference. The duration of fog was on average (growing seasons 1999 and 2000) 175 hours during day-time (10'-average visibility  $\leq 1000$  m), of which more than 45 % were dense fog (10'-average visibility  $\leq 200$  m; data from BITÖK database). It could be expected that fog was even more frequent at the higher locations of the Fichtelgebirge (Foken 2003) like Farrenleite. The reduction of PFD and  $R_n$  by approx. 5 % at Farrenleite in 2000 (May–October) compared to 1999 coincided with an increase of day-time fog from 164 to 187 hours at Waldstein; the duration of dense day-time fog increased from 68 to 92 hours. In 2000, the growing season-PFD at Farrenleite was only 76 % of that at Steinkreuz, whereas in 1999 it was 80 % (cf. Tab. 5.2.1.1). The differences in  $R_n$  between the two sites were even more pronounced than those in PFD (Tab. 5.2.1.1).

**Vapour pressure deficit of the air.** The vapour pressure deficit of the air, D, observed at Farrenleite (Fig. 5.2.2.1) followed similar patterns as at Steinkreuz (see Chap. 5.2.1, above), and levels of average daily D ( $D_{avg}$ ) were mostly comparable as well, whereas maximum daily D ( $D_{max}$ ) were lower than in the Steigerwald as could be expected from the lower  $T_{air}$  at Farrenleite: In 1998, the maximum seasonal values of  $D_{max}$  (August 12) and  $D_{avg}$  (August 18) was 25 hPa and 14.5 hPa, respectively (data not shown). The following year, highest daily values observed were 23 hPa ( $D_{max}$ ) and 13.2 hPa ( $D_{avg}$ ), both on July 19, 1999. During the year 2000, June 21 was the day with the driest atmospheric conditions with  $D_{max} = 29$  hPa and  $D_{avg} = 21.2$  hPa, also the maximum values for all of 1998–2000 (Fig. 5.2.2.1).

**General trends in the Steigerwald and the Fichtelgebirge.** General trends of climatic change may be seen in mean monthly air temperatures over the three years compared to long-term averages, both in the Steigerwald and Fichtelgebirge (Fig. 5.2.1.1a), namely that winters were warmer, that the warmest month was not July, but August, and perhaps that cold spells occurred at some stage in June or July; but if the latter always occurred in either June or July, then it might not be seen in long-term average monthly temperatures. One might also hypothesise that there was a trend towards less precipitation in winter and/or spring compared to the long-term average at the Steigerwald and the Fichtelgebirge sites (Fig. 5.2.1.1b). Foken (2003) found (non-significant) indications for similar trends for the Fichtelgebirge, particularly decreased precipitation in spring and increased precipitation in July. Significant trends in temperature were observed, namely an increase of the average annual air temperature of  $0.34\text{ K} \cdot (10\text{ a})^{-1}$  or of  $0.5\text{ K} \cdot (10\text{ a})^{-1}$  considering only the winter months (Foken 2003). Average air temperature showed a stronger positive trend in August than in July, coinciding with the trend in precipitation (see above). No trend was detectable in relative humidity (Foken 2003).

### 5.3. Radial within-tree variation of xylem sap flow density $J_s$ (with emphasis on *Fagus sylvatica*)

Radial variability sap flow density in European beech. Raw signals of temperature difference outputted by the thermal dissipation probes were converted to sap flow density  $J_s$ , in  $\text{g H}_2\text{O} \cdot \text{m}^{-2} \text{ sapwood area} \cdot \text{s}^{-1}$ , as detailed in Chapter 4.1.1 (Eq. 4.1.1–2). Recorded 10-minute averages were condensed to half-hourly means (in  $\text{g m}^{-2} \text{ s}^{-1}$ ) and daily integrals of  $J_s$  (in  $\text{kg m}^{-2} \text{ d}^{-1}$ ) for further data analysis and will be presented in the following at these two levels of temporal integration. The total maximum error of  $J_s$  was less than  $\pm 5\%$ , the resolution of  $J_s$  was ca.  $0.1 \text{ g m}^{-2} \text{ s}^{-1}$  as imposed by the data loggers used (cf. Chap. 4.1.5).

In Figure 5.3.1a–c, the diurnal course of sap flow density  $J_s$  in incremental radial depths of sapwood of three beech trees from Steinkreuz, Steigerwald, is shown for a sunny to overcast day (see inset in Fig. 5.3.1a) in late spring after full leaf expansion (June 2, 1999).  $J_s$  was dependent on the depth of probe insertion into the sapwood, and highest values of  $J_s$  were typically measured in the outermost, youngest 2 cm-wide annuli of sapwood, and lowest values in the innermost annuli. In a few trees,  $J_s$  was similar in neighbouring annuli (e.g. Fig. 5.3.1c, 2–4 cm and 4–6 cm), or occasionally a deeper annulus had higher values than a shallower one (data not shown, but see Fig. 5.3.3, below).  $J_s$  of any annulus was in general higher in trees with a larger DBH than in the same annulus of a tree with a smaller DBH (Fig. 5.3.1a–c; see also Fig. 5.3.3, Fig. 5.3.6 and Fig. 5.3.7, below). Sap flow commenced about 3 hours later in the small tree than in the large trees (Fig. 5.3.1a–c), indicating the position of the former in the sub-canopy, shaded during the morning at low sun elevation angles by the neighbouring large trees. (In the large trees sap flow had not ceased completely during the previous night of non-zero vapour pressure deficit of the air D; cf. Chap. 4.1.1.) In the small tree (Fig. 5.3.1a),  $J_s$  in the innermost sapwood annulus lagged behind  $J_s$  in outer sapwood by ca. 2.5 h. Maximum half-hourly averages of  $J_s$  for the outermost 2 cm of sapwood observed on this day were  $33.5 \text{ g m}^{-2} \text{ s}^{-1}$  (Fig. 5.3.1a),  $53.0 \text{ g m}^{-2} \text{ s}^{-1}$  (Fig. 5.3.1b), and  $56.9 \text{ g m}^{-2} \text{ s}^{-1}$  (Fig. 5.3.1c) for beech trees with 16 cm, 58 cm and 66 cm trunk diameter, respectively. Hourly integrals peaked at  $115.9 \text{ kg m}^{-2} \text{ h}^{-1}$ ,  $190.7 \text{ kg m}^{-2} \text{ h}^{-1}$ , and  $204.1 \text{ kg m}^{-2} \text{ h}^{-1}$ , respectively, in the outer annulus that day. Over the 24-hour period shown, the sap flow density totalled  $643.8 \text{ kg m}^{-2} \text{ d}^{-1}$  (0–2 cm),  $456.0 \text{ kg m}^{-2} \text{ d}^{-1}$  (2–4 cm) and  $114.5 \text{ kg m}^{-2} \text{ d}^{-1}$  (4–6 cm) in the smallest of the three trees, to  $1953.4$ ,  $1562.7$  and  $1173.3 \text{ kg m}^{-2} \text{ d}^{-1}$ , respectively, in the 58-cm tree, and to  $2042.5$ ,  $1686.1$ , and  $1762.9 \text{ kg m}^{-2} \text{ d}^{-1}$ , respectively, in the largest tree (see also Fig. 5.3.3a, b, below; for maximum seasonal values of  $J_s$  0–2cm see also Tab. 5.3.1 and Tab. 5.3.2 below).

There was a tight relationship between sap flow density in deeper and in outer sapwood as seen in Figure 5.3.1d–f. The ratio of  $J_s$  in annulus #2 (2–4 cm) and annulus #3 (4–6 cm) to that in annulus #1 (0–2 cm) ( $J_{s \text{ deep}}/J_{s \text{ 0-2cm}}$ , Fig. 5.3.1g–i) was similar during most of the day in the larger trees (Fig. 5.3.1h, i) and changed only during periods when sap flow approached zero, introducing uncertainties in the calculation of the ratio. In smaller trees hysteresis was common, where the ratio  $J_{s \text{ deep}}/J_{s \text{ 0-2cm}}$  was larger in the afternoon and early evening than in the morning at the same magnitude of  $J_{s \text{ 0-2cm}}$  (Fig. 5.3.1g).

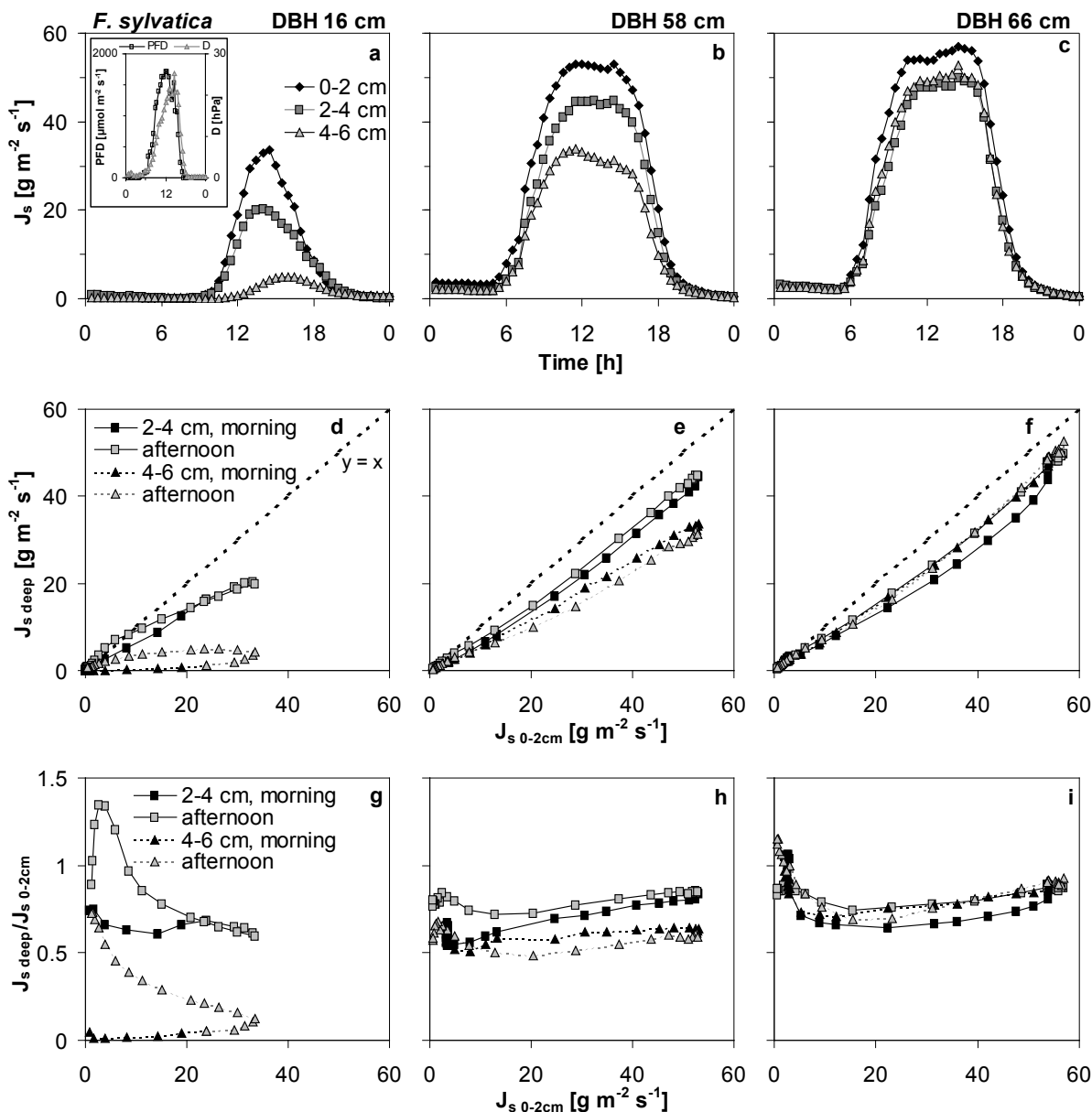


**Figure 5.3.1:** Diurnal course of sap flow density  $J_s$  (in  $\text{g H}_2\text{O} \cdot \text{m}^{-2}$  sapwood area  $\cdot \text{s}^{-1}$ ) in three radial depths of sapwood below the cambium (0–2 cm, 2–4 cm, 4–6 cm) in three beech trees differing in DBH (diameter at 1.3 m height; B4235, smallest studied tree, left; B4213, centre; B4237, largest studied tree, right) on day 153 (June 2) in 1999 (a–c). Values are 10-minute averages condensed to half-hourly averages for clarity. Inset in a: diurnal change of photon flux density, PFD, and vapour pressure deficit of the air, D, as measured in a nearby canopy gap. Between 17.30 and 17.40 precipitation of 0.4 mm was recorded. d–f:  $J_s$  in deeper sapwood (2–4 cm and 4–6 cm) versus  $J_s$  in the outermost sapwood (0–2 cm); same data as in Figs. a–c. Filled symbols denote half-hourly values until 12.00 (morning), shaded symbols after 12.00 (afternoon). g–i: Relationship between the ratio of  $J_{s\text{ deep}}$  to  $J_{s\text{ 0-2cm}}$  (the slope in Figs. d–f) and  $J_{s\text{ 0-2cm}}$ . Filled symbols denote half-hourly values until 12.00 (morning), shaded symbols after 12.00 (afternoon).

Sap flow density  $J_s$  in deeper annuli of sapwood was also correlated with  $J_s$  in the outer annulus of sapwood on the scale of daily values over the course of the season as depicted in Figure 5.3.2 for the same three trees as in Figure 5.3.1 (rainy and very cloudy days were excluded, see figure caption). This relationship between  $J_s$  day in inner (relative to  $J_s$  day in outer) and in outer sapwood was predominantly linear and varied between sensors and trees, as well as the scatter, and the relationship became looser at low values of  $J_s$  day (very low values omitted already, see figure caption), analogous to half-hourly values (see above; Fig. 5.3.1g–i). Seasonal differences are noticeable as well (dark to light shading of symbols in Fig. 5.3.2) and will be detailed later.

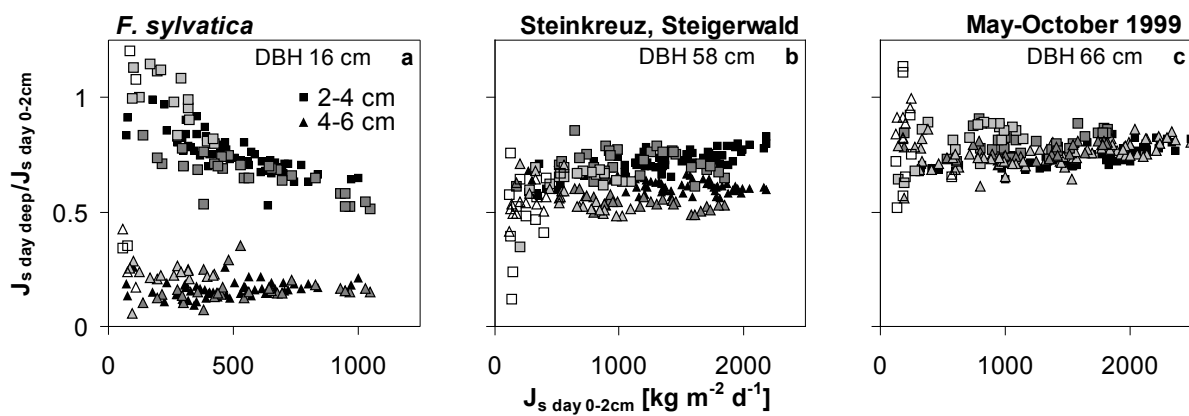


**Figure 5.3.2:** Variation of daily integrated sap flow density in deep sapwood relative to outer sapwood ( $J_s$  day deep/ $J_s$  day 0-2cm) with sap flow density in outer sapwood ( $J_s$  day 0-2cm) over the course of the growing season 1999 for the same three trees from Steinkreuz, Steigerwald, as in Figure 5.3.1. Squares denote data for the middle annulus (2–4 cm) and triangles for the innermost measured annulus (4–6 cm). Filled symbols represent data from May–July, dark shaded from August, light shaded from September and open symbols from October 1999. The lowest 10 % of  $J_s$  day-values (rainy and cloudy days) were omitted, and 58 % (tree 4235, DBH 16 cm, **a**), 67 % (tree 4213, DBH 58 cm, **b**), and 68 % (tree 4237, DBH 66 cm, **c**), of the available data for these sensors for the growing season of 1999 remained.

Figure 5.3.3 shows radial profiles of  $J_s$  from several beech trees in the Steigerwald, integrated for June 2, 1999 ( $J_s$  day; same day as in Fig. 5.3.1). A tendency for  $J_s$  day to decrease with increasing (absolute) sapwood depth could be acknowledged in Figure 5.3.3a, b. Variation of  $J_s$  day among sensors was considerable in each of the three depths (cf. Fig. 5.3.1). When plotted against relative sapwood depth – thus accounting for the differing sapwood dimensions of the more or less even-aged sample trees (Chap. 5.1.2) – a more obvious radial pattern of  $J_s$  day emerged, namely a decrease with (relative) radial depth, either expressed in absolute units of  $J_s$  day (Fig. 5.3.3b) or in units of  $J_s$  day relative to the outermost sapwood annulus ( $J_s$  day deep/ $J_s$  day 0-2cm; Fig. 5.3.3d). Significant linear regressions ( $p < 0.0001$ , see also figure caption) could be fitted to the data, though the correlation coefficient did not exceed 0.42 (best fit, see Fig. 5.3.3b, c) which pointed at still high between-tree and/or between-sensor variability.

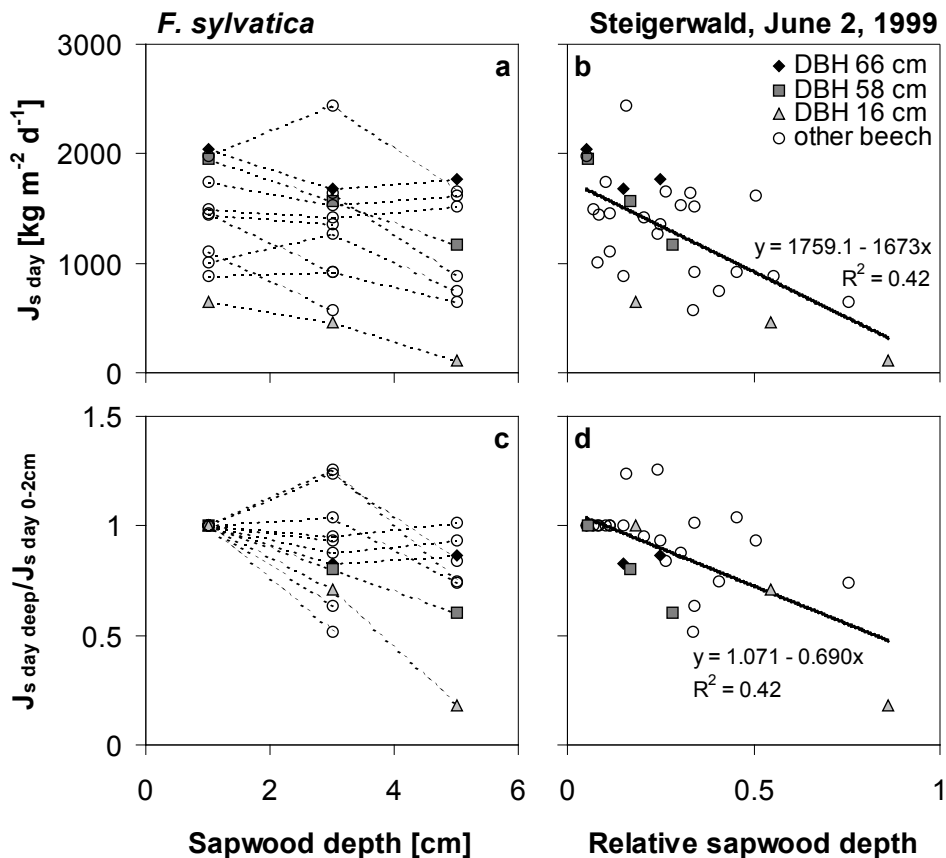


**Figure 5.3.3:** Radial profiles of daily integrated sap flow density,  $J_s$  day, (a, b) and the respective ratio  $J_s$  day deep/ $J_s$  day 0-2cm (c, d) of beech trees on an absolute (a, c) and on a relative scale of sapwood depth (b, d), where "0" denotes the cambium-sapwood-boundary and "1" the sapwood-ripenwood-boundary, on the same day as in Fig. 5.3.1 (June 2, 1999). The radial depth of a thermal dissipation probe is depicted as the centre of the 20 mm-long heater, so that e.g. for the probe in 0–2 cm depth its value is shown at 1 cm sapwood depth. Data shown are from the same trees as in Fig. 5.3.1 (filled and shaded symbols) plus from all other available beech trees at Steinkreuz (both mixed stand and pure beech plot) and Großebene in the Steigerwald (open circles), adding to 32 thermal dissipation probes in 11 trees. Broken lines in a) and c) indicate data from different depths of the same tree, solid lines in b) and d) are linear regression functions (best fit,  $p < 0.0001$ , equations and correlation coefficients also shown; SEE = 406.6 for b, SEE = 0.165 for d).

In Figure 5.3.4 radial profiles are extended to the growing seasons of 1999 and 2000 and all available sites and sap flow sensors. For these graphs, the average  $J_s$  day (Fig. 5.3.4a, b) and the average ratio  $J_s$  day deep/ $J_s$  day 0-2cm (Fig. 5.3.4c, d) of all days except rainy days between the beginning of May and the end of September of each year were calculated. Significant ( $p < 0.0001$ ) and similar radial trends could be established for both years and both expressions of sap flow density (Fig 7.1.4a–d). Linear regression equations yielded the highest correlation coefficients (and lowest  $p$ -values), and relative sapwood depth explained 51 to 64 % (1999 data) and 55 to 66 % (2000 data) of the variability in mean  $J_s$  day or mean  $J_s$  day deep/ $J_s$  day 0-2cm between sensors (see Fig. 5.3.4 for regression equations). Site-specific regressions were statistically not different ( $p = 0.05$ , not shown), but there was a tendency for equations from Farrenleite to have a smaller y-axis intercept and a less negative slope during both

years (not shown). The regressions plotted in Figure 5.3.4 did not improve when normalising  $J_s$  day with the proportion of sapwood area represented by a sensor (area of an annulus relative to the total sapwood area of a tree; not shown).

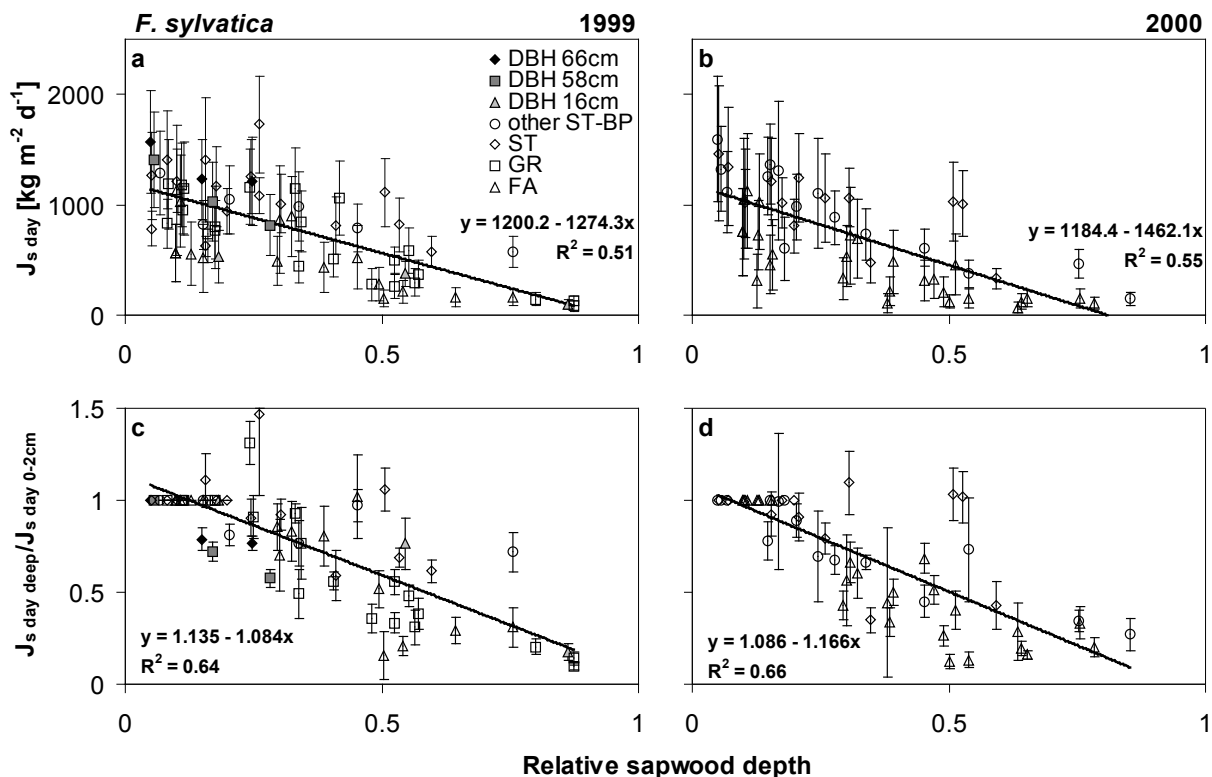


**Figure 5.3.4:** Radial trends of average seasonal daily integrated sap flow density  $J_s$  day (a, b) and the respective ratio  $J_s$  day deep/ $J_s$  day 0-2 cm (c, d) of beech trees on a relative scale of sapwood depth, where "0" denotes the cambium-sapwood-boundary and "1" the sapwood-ripenwood-boundary, during May through September 1999 (left) and 2000 (right). The relative radial depth of a thermal dissipation probe is depicted as the centre of the 2 cm long heater. In a) and c), the three trees from Fig. 5.3.1 from the pure beech plot within Steinkreuz are plotted in corresponding symbols (DBH 66cm, DBH 58cm, DBH 16cm). **ST-BP** is the Steinkreuz-pure beech plot, **ST** is Steinkreuz, **GR** is Großebe, all in the Steigerwald, and **FA** is Farrenleite in the Fichtelgebirge. Vertical bars are  $\pm 1$  standard deviation from the mean. For this analysis only days without rain (< 1 mm between 5 and 19 h) from May to September were selected, totalling 71 days in 1999 and 81 days in 2000. Due to data gaps, the number of available days varied between sensors. The number of sensors shown in the graphs was 70 in 1999 and 56 in 2000, representing 23 and 19 trees, respectively. Lines in a-d are linear regression functions (best fit,  $p < 0.0001$ , equations and correlation coefficients also shown; SEE = 284.1 for regression in a, 290.6 in b, 0.187 in c, and 0.185 in d).

The respective data from 1998 from Steinkreuz (mixed stand) and Großebe were comparable to those from 1999 and 2000 and indicated the same general radial trends (not shown). But because sampling was less intense in 1998, particularly at 4–6 cm sapwood depth, and due to data gaps and initial technical problems, the available data from 1998 did not expand the findings from 1999 and 2000.

In order to generalise the results on radial trends and patterns of sap flow in European beech and to facilitate comparison with trees from other sites and with other species, data from Figures 5.3.4a and b and from Figures 5.3.4c and d, respectively, were combined resulting in the following regression equations:

$$J_s \text{ day annulus (20 mm)} = 1191.5 - 1352.0 \cdot \text{relative sapwood depth}^a \quad (\text{Eq. 5.3.1})$$

$$R^2 = 0.52, \text{ SEE} = 288.0, p < 0.0001.$$

$$J_s \text{ day deep}/J_s \text{ day 0-2cm} = 1.111 - 1.116 \cdot \text{relative sapwood depth}^a \quad (\text{Eq. 5.3.2})$$

$$R^2 = 0.64, \text{ SEE} = 0.189, p < 0.0001.$$

<sup>a</sup> with relative sapwood depth expressed as in Figure 5.3.4 (sapwood-heartwood boundary = 1, cambium-sapwood boundary = 0).

**Sap flow density  $J_s$  and tree diameter.** In Figures 5.3.5 and 5.3.6, seasonally averaged daily integrals of sap flow density ( $J_s \text{ day}$ ) from May till September (excluding rainy days: see figure caption) are graphed against tree diameter for all the sites and all the years of investigation for beech. In trees that were monitored for more than one year, thermal dissipation sap flow gauges were newly installed at the beginning of each growing season and thus may be treated as spatial replicates.

There was a trend of  $J_s$  to increase in beech with tree diameter in all sapwood depths in all stands for all years combined (Fig. 5.3.5a–c) and for each year (regression lines not shown). The regressions against tree diameter (Fig. 5.3.5) explained 57 %, 47 %, and 63 % of the variability in  $J_s$  in annulus #1, #2, and #3, respectively. For the stand Farrenleite in the Fichtelgebirge, this relation was less clear among trees for one sapwood depth (Fig. 5.3.6a–c); within each tree on the other hand, the decreasing radial trend was obvious as shown earlier (Fig. 5.3.4). The high values of  $J_s$  from Farrenleite at a given tree diameter fell well within the range of values from the other stands.

The slope of the regression lines in Figure 5.3.5 became somewhat steeper with increasing sapwood depth, since  $J_s$  decreased more strongly with depth in small trees than in large trees as already seen before (e.g. Fig. 5.3.1).

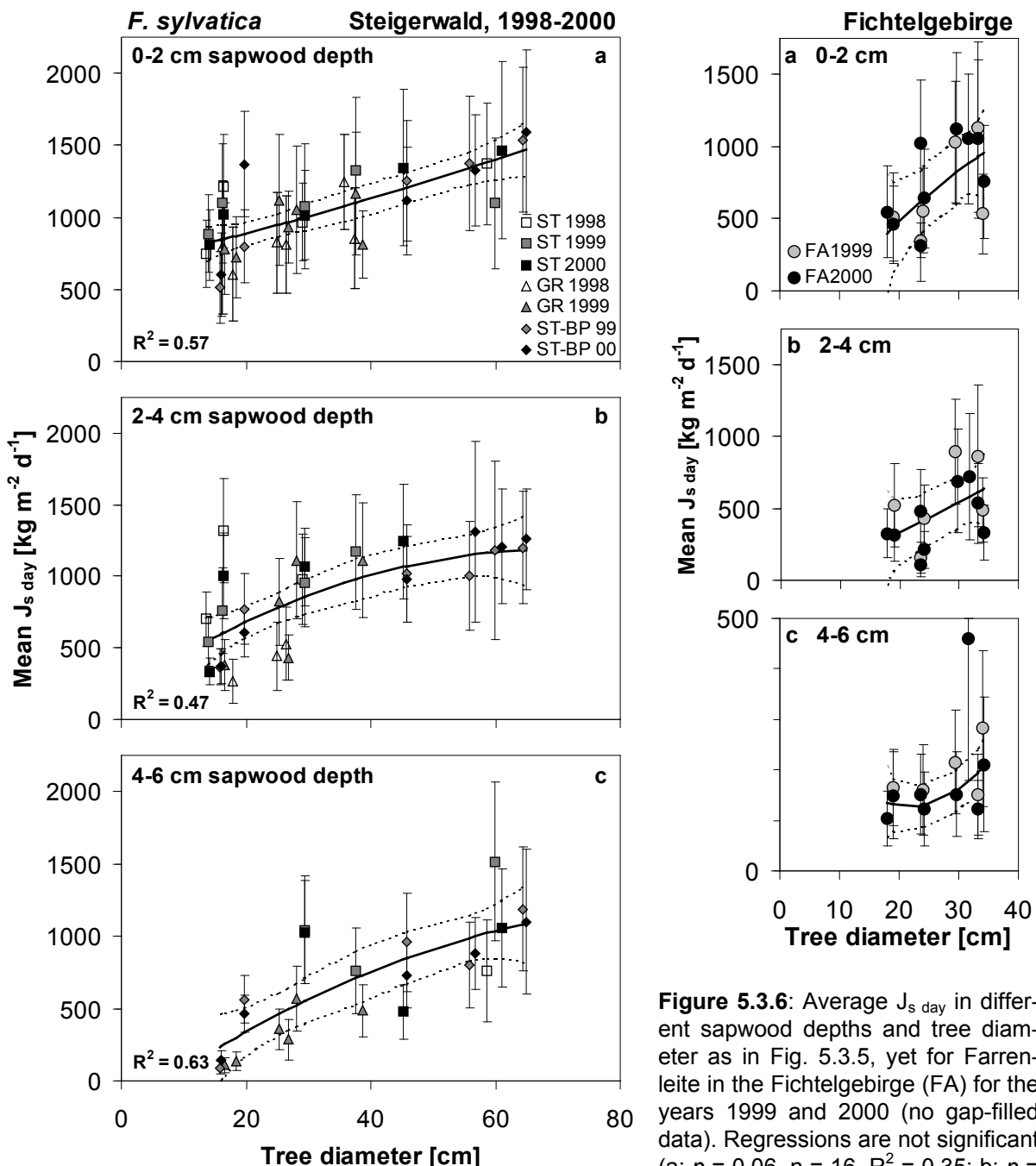


**Figure 5.3.6:** Average  $J_s$  day in different sapwood depths and tree diameter as in Fig. 5.3.5, yet for Farrenleite in the Fichtelgebirge (FA) for the years 1999 and 2000 (no gap-filled data). Regressions are not significant (a:  $p = 0.06$ ,  $n = 16$ ,  $R^2 = 0.35$ ; b:  $p = 0.16$ ,  $n = 15$ ,  $R^2 = 0.26$ ; c:  $p = 0.10$ ,  $n = 14$ ,  $R^2 = 0.34$ ).

**Figure 5.3.5:** Seasonally averaged daily integrals of sap flow density  $J_s$  day in different radial depths of sapwood (a: 0–2 cm; b: 2–4 cm; c: 4–6 cm) and tree diameter (at the height of  $J_s$ -measurement) in beech trees from the Steigerwald. Data from all available trees for the three years studied (1998–2000, no gap-filled data) are shown. Included in this analysis are only days without significant rain (< 5 mm during previous night, < 1 mm during early morning, 0 mm during daytime and <1 mm during late afternoon) from May to September. **ST** stands for Steinkreuz, **GR** for Großebene, **ST-BP** for the Steinkreuz-pure beech plot. Bars are  $\pm 1$  SD. Regression lines (2<sup>nd</sup> order polynomial, statistically significant at  $p < 0.0001$ , dark lines) and 95 %-confidence intervals (broken lines) are shown, including all trees and all years. Regression equations are for a:  $y = 0.0373x^2 + 9.7921x + 678.89$  with  $n = 37$ ; b:  $y = -0.2045x^2 + 28.5021x + 195.19$  with  $n = 34$ ; c:  $y = -0.1695x^2 + 30.9747x - 212.31$  with  $n = 23$ .

Figure 5.3.7 shows seasonally averaged  $J_s$  day for the investigated *Quercus petraea*-trees, where sap flow was recorded in the outermost xylem only, since in this ring-porous species active sapwood is confined to the youngest growth rings (see Chap. 2.3.1 and 4.1.1). No trend of  $J_s$  day with tree diameter was detectable for all years and sites combined. Site- and year-specific analyses revealed no clear correlation either (not shown). Values of  $J_s$  from oak were clearly in the same order of magnitude as those from beech of comparable tree diameter (see also Table 5.3.2, below), but tended to be somewhat smaller. (For GroßeBene, however, a correlation of maximum  $J_s$  day with DBH was observed: see Figure 5.5.1.)

Due to gaps in data sets from different sites, the number of days that contribute to an average seasonal value of  $J_s$  in Figures 5.3.5–7 vary. Therefore, further statistical treatment of the data was not aimed at in this case. When looking at single daily values, the same trends emerged as for the seasonal averages (not shown).

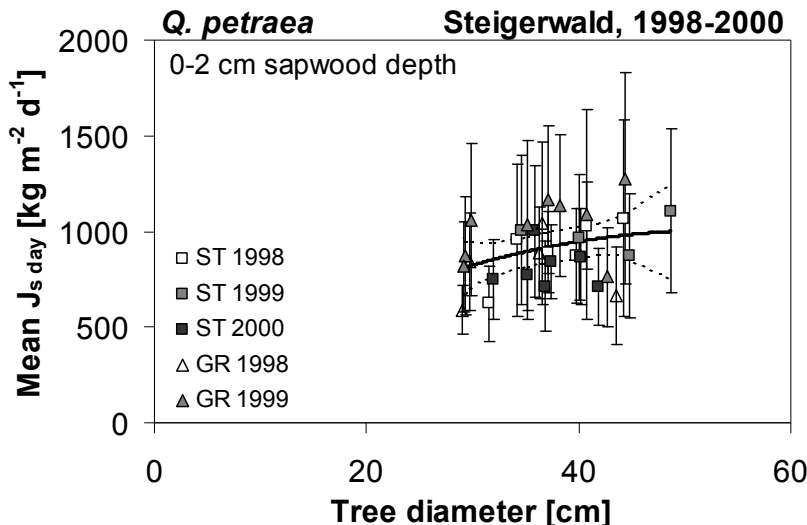


**Figure 5.3.7:** Average  $J_s$  day in outer sapwood (0–2 cm) versus tree diameter as in Figure 5.3.5, yet for oak trees in the Steigerwald (**ST** = Steinkreuz, **GR** = GroßeBene) for the three years studied (no gap-filled data). The regression is not significant ( $p = 0.19$ ,  $n = 31$ ,  $R^2 = 0.11$ ). Bars are  $\pm 1$  SD.

In the following, Table 5.3.1 shows maximum half-hourly and hourly values of  $J_s$  0–2cm,  $J_s$  2–4cm and  $J_s$  4–6cm in beech and oak trees (highest rate, respectively) for the investigated stands, Table 5.3.2 lists average and maximum values of daily integrated  $J_s$  0–2cm and structural characteristics of the respective trees. In Table 5.3.3 the data presented in Figure 5.3.5–7 are summarised. The overall average ratio of radial decline in sap flow density in beech was 1 : 0.75 ( $\pm 0.22$ ) : 0.43 ( $\pm 0.25$ ) (0–2 cm, 2–4 cm, 4–6 cm, respectively) for the investigated trees from all stands and years (Tab. 5.3.3, excluding rainy days).

**Table 5.3.1:** Maximum values of sap flow density in incremental sapwood annuli (0–2 cm, 2–4 cm, 4–6 cm from cambium inwards;  $J_{s\ 0-2cm\ max}$  etc., respectively): half-hourly (expressed per second) and hourly maxima for each stand and species shown. Data from Steinkreuz in this table include the pure beech plot. FA = Farrenleite.

	1999					2000		
	Großebene		Steinkreuz		FA	Steinkreuz		FA
	beech	oak	beech	oak	beech	beech	oak	beech
$J_{s\ 0-2cm\ max}$ [g m <sup>-2</sup> s <sup>-1</sup> ]	65.1	58.7	75.7	55.9	51.0	78.2	40.0	71.6
$J_{s\ 0-2cm\ max}$ [kg m <sup>-2</sup> h <sup>-1</sup> ]	226	207	268	201	181	276	142	236
$J_{s\ 2-4cm\ max}$ [g m <sup>-2</sup> s <sup>-1</sup> ]	54.6		82.9		46.8	72.0		39.7
$J_{s\ 2-4cm\ max}$ [kg m <sup>-2</sup> h <sup>-1</sup> ]	190		294		157	252		142
$J_{s\ 4-6cm\ max}$ [g m <sup>-2</sup> s <sup>-1</sup> ]	30.5		75.0		19.4	52.8		25.1
$J_{s\ 4-6cm\ max}$ [kg m <sup>-2</sup> h <sup>-1</sup> ]	109		264		69	190		90

**Table 5.3.2:** Daily integrated sap flow density  $J_{s\ day}$  in the outermost annulus of sapwood (0–2 cm from cambium inwards) and tree structural characteristics: average and maximum daily sap flow density ( $J_{s\ 0-2cm\ avg}$ ,  $J_{s\ 0-2cm\ max}$ , respectively) for days without rain (< 0.2 mm between 8.30–15.30, < 1 mm between 5.00–8.30 and 15.30–19.00, < 5 mm between 19:00 of previous day–5.00), number of days (without rain) are given; diameter at breast height (1.3 m; DBH), sapwood area ( $A_{s\ 0-2cm}$ ), ground projected crown area ( $A_{cp}$ ), total height ( $h_t$ ) and leaf area ( $A_{lt}$ ) of respective tree. Data for the trees with highest  $J_{s0-2}$  per species and stand are shown (Großebene: beech B108, oak E132; Steinkreuz: beech E4237 (1999), E4108 (2000), oak E4202 (1999), oak E4052 (2000); Farrenleite: beech X8 (1999), X4 (2000)). The data from Steinkreuz in this table include the pure beech plot. FA = Farrenleite.

	1999					2000		
	Großebene		Steinkreuz		FA	Steinkreuz		FA
	beech	oak	beech	oak	beech	beech	oak	beech
$J_{s\ 0-2cm\ avg}$ [kg m <sup>-2</sup> d <sup>-1</sup> ]	1187	1369	1571	1275	1133	1593	1008	1124
± 1 SD	± 404	± 588	± 462	± 320	± 587	± 569	± 344	± 521
number of days	72	74	71	69	81	81	84	74
$J_{s\ 0-2cm\ max}$ [kg m <sup>-2</sup> d <sup>-1</sup> ]	2351	2654	2487	1888	2477	3422	1885	2697
DBH [cm]	26	46	66	50	33	63	37	31
$A_{s\ 0-2cm}$ [cm <sup>2</sup> ]	140	248	384	278	189	361	200	166
$A_{cp}$ [m <sup>2</sup> ]	51.4	70.1	123.2	67.3	16	91.6	32.7	18.5
$A_{lt}$ [m <sup>2</sup> ]	127.1	349.4	562.8	403.8	160.1	572.3	241.7	119.6
$h_t$ [m]	22.0	27	35.5	31.1	19.5	32.2	29.5	18.1

**Table 5.3.3:** Mean (multi-) annual daily integrals of sap flow density  $J_s$  day, averaged over all trees per stand, in different incremental radial depths of sapwood (0–2 cm:  $J_{s\ 0-2cm}$ ; 2–4 cm:  $J_{s\ 2-4cm}$ ; 4–6 cm:  $J_{s\ 4-6cm}$ ), ratio  $J_{s\ deep}/J_{s\ 0-2cm}$  and tree diameter (at height of  $J_s$ -measurement) in beech and oak trees; based on data in Figures 5.3.5, 5.3.6, 5.3.7. Data from all available trees (beech: where radial profile was measured) for the three years studied (1998–2000, no gap-filled data). Included are only days without significant rain (< 5 mm during previous night, < 1 m during early morning, 0 mm during daytime and <1 mm during late afternoon) from May to September. Standard deviation for averages (SD) and number of trees per sapwood depth (n) are indicated. The data from Steinkreuz in this table include the pure beech plot.

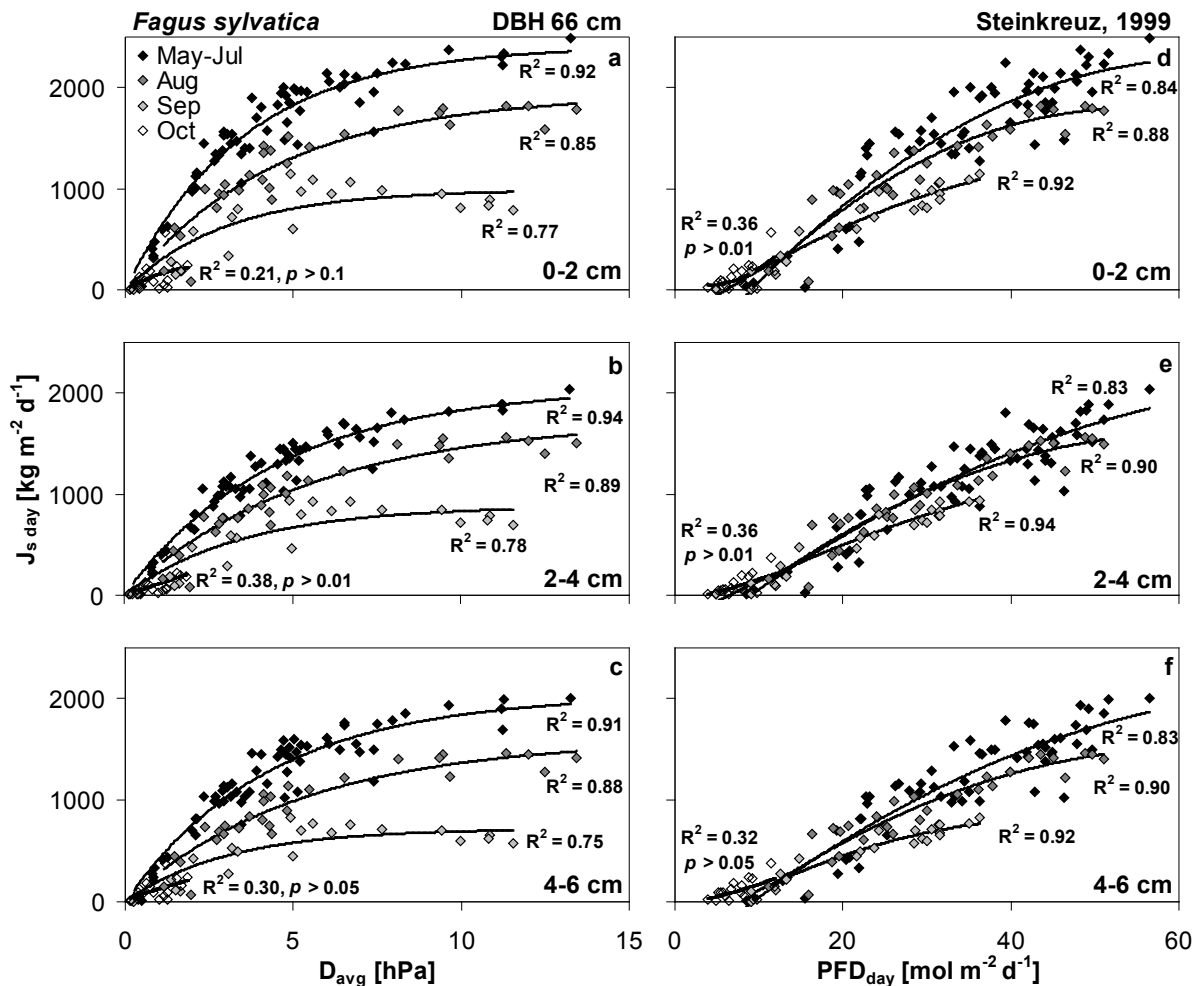
Beech						Oak		
diameter [cm]	$J_{s\ 0-2cm}$ [kg m <sup>-2</sup> d <sup>-1</sup> ]	$J_{s\ 2-4cm}$ [kg m <sup>-2</sup> d <sup>-1</sup> ]	$J_{s2-4}/J_{s0-2}$	$J_{s\ 4-6cm}$ [kg m <sup>-2</sup> d <sup>-1</sup> ]	$J_{s4-6}/J_{s0-2}$	diameter [cm]	$J_{s\ 0-2cm}$ [kg m <sup>-2</sup> d <sup>-1</sup> ]	
<b>Steinkreuz</b>								
Mean	35.2	1121	927	0.82	753	0.61	38.5	885
$\pm 1$ SD	19.3	290	306	0.18	328	0.24	4.7	138
n	24	24	24	24	16	16	17	17
<b>Großebene</b>								
Mean	27.8	946	687	0.72	324	0.35	35.8	865
$\pm 1$ SD	7.5	184	321	0.31	183	0.18	5.7	161
n	10	10	10	10	6	6	14	14
<b>Steinkreuz + Großebene</b>								
Mean	33	1070	856	0.79	636	0.54	37.3	912
$\pm 1$ SD	16.9	273	325	0.23	351	0.25	5.2	168
n	34	34	34	34	22	22	31	31
<b>Farrenleite</b>								
Mean	26.7	730	473	0.65	174	0.27		
$\pm 1$ SD	5.8	322	241	0.16	94	0.12		
n	15	15	15	15	15	15		
<b>All stands</b>								
Mean	31.1	966	739	0.75	449	0.43		
$\pm 1$ SD	14.7	326	348	0.22	358	0.25		
n	49	49	49	49	37	37		

The beech trees from the Steigerwald sites and from the Fichtelgebirge were similar in maximum half-hourly, hourly (Tab. 5.3.1) or daily values (Tab. 5.3.2) of  $J_{s\ 0-2cm\ max}$ , with beech from Steinkreuz, however, usually showing largest rates. Also, beech at Steinkreuz displayed values of  $J_s$  day that were larger than 75 % of  $J_s$  max about twice as often as beech at Farrenleite (data not shown). Peak rates of  $J_{s\ 2-4cm\ max}$  and  $J_{s\ 4-6cm\ max}$  (Tab. 5.3.1) were smaller at Großebene and Farrenleite than at Steinkreuz, beech trees in the former stands being smaller e.g. in diameter. (Trees of similar DBH displayed similar values of  $J_s$  in all annuli though, see Fig. 5.3.5–7.) Differences were also apparent when looking at seasonal mean values (Tab. 5.3.2) or stand-wide average seasonal mean values of daily  $J_s$  (Tab. 5.3.3), since differences in climatic

conditions between the Steigerwald and the Fichtelgebirge and differences in stand structure and the sampling of this structure among Steinkreuz, Großebene and Farrenleite are included as well. Oaks from Steinkreuz and Großebene were found to have virtually the same maximum half-hourly and hourly rates (Tab. 5.3.1), but the average and maximum daily values of  $J_s$  0–2cm were larger at Großebene (Tab. 5.3.2), where oaks were facing less competition with beech. In contrast, mean daily  $J_s$  averaged over all measured oak trees of a stand was larger for Steinkreuz (Tab. 5.3.3), since oak did not occur in the sub-canopy as was the case at Großebene.

**Sap flow density and atmospheric drivers.** The variability of  $J_s$  day over the season was considerable for each sensor, indicated by the standard deviation from the mean (vertical bars) in Figures 5.3.4a and b, Figures 5.3.5 and 5.3.6, especially for sensors implanted in the outer sapwood. Figure 5.3.8 interprets this variability in terms of changes in atmospheric drivers of transpiration (see below). The ratio of  $J_s$  day deep and  $J_s$  day 0–2cm was also variable (Fig. 5.3.4c, d), but less than  $J_s$  day: the average coefficient of variation (CV) of all sensors plotted in Figure 5.3.4 was 19 % (1999) and 24 % (2000) for  $J_s$  day deep/ $J_s$  day 0–2cm, whereas for  $J_s$  day it was 35 % and 44 %, respectively. (Omitting the outer sensors from calculating the average CV of  $J_s$  day over all sensors so that  $n$ , the number of sensors, was equal to those for the ratio, did not alter the average CV; data not shown.)

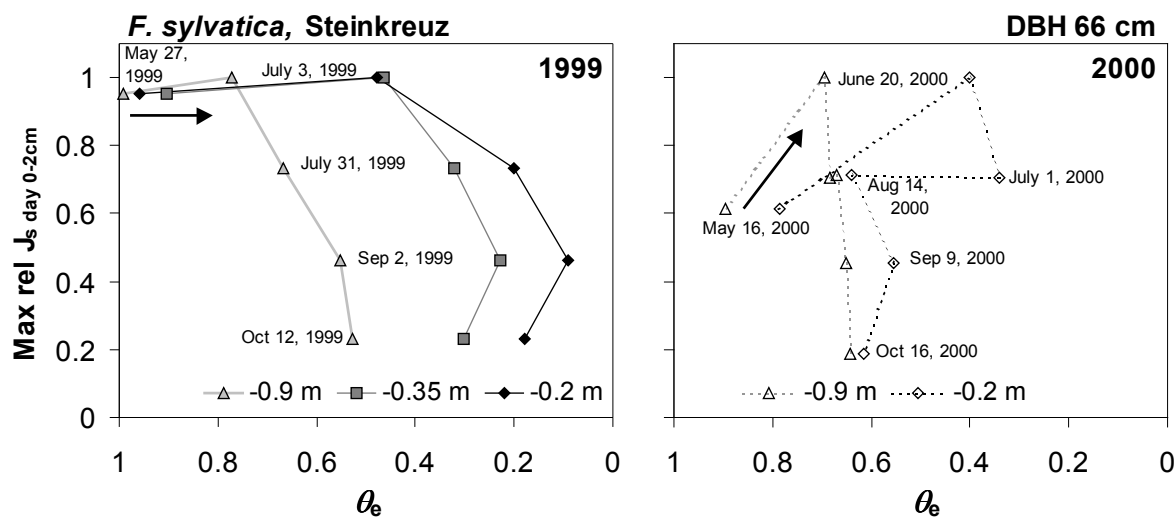
The relationship between  $J_s$  day and the drivers of transpiration and photosynthesis, vapour pressure deficit of the air ( $D_{avg}$ ) and photosynthetic photon flux density ( $PFD_{day}$ ), is exemplified in Figure 5.3.8 for four (contiguous) periods in 1999 (May–July; August; September; October), after the maximum LAI of the stand had been reached. The data shown are from the largest sampled beech tree (DBH 66 cm, B4237), exhibiting the highest observed values of  $J_s$  day (at 0–2 cm depth) which may possibly represent the maximum values of  $J_s$  day to be found under the given site conditions.  $J_s$  day was positively correlated to  $D_{avg}$  and  $PFD_{day}$  in any of the three radial depths studied. Maximum values of  $J_s$  day as well as the initial slope of the relationship with  $D_{avg}$  or  $PFD_{day}$  decreased with the progressing season. These seasonal changes were more pronounced for  $D_{avg}$ . For maximum observed values of  $D_{avg}$  during the respective period,  $J_s$  day was reduced by 22 % and 58 % in 0–2 cm sapwood depth in August and September, respectively, compared to May–July, by 19 % and 55 % in 2–4 cm, and by 24 % and 63 % in 4–6 cm (values calculated from regression models shown in Fig. 5.3.8; for maximum observed  $PFD_{day}$  reductions were for 0–2 cm 18 % in August and 36 % in September compared to May–July, for 2–4 cm 11 % and 25 %, for 4–6 cm 17 % and 41 %). In the cooler and moister growing season of the year 2000, differences in the response of sap flow density to  $D_{avg}$  and  $PFD_{day}$  from month to month were less obvious (Fig. A11.3, Appendix). Response functions changed in a similar manner in the other trees studied at the sites Steinkreuz and Großebene over the growing season and years of investigation (not shown, but see following section). At Farrenleite in contrast, responses of  $J_s$  day to  $D_{avg}$  and  $PFD_{day}$  hardly changed over the course of the season in 1999 and (as well as at the Steigerwald sites) even less so in 2000 (not shown; but see Chap. 5.5).



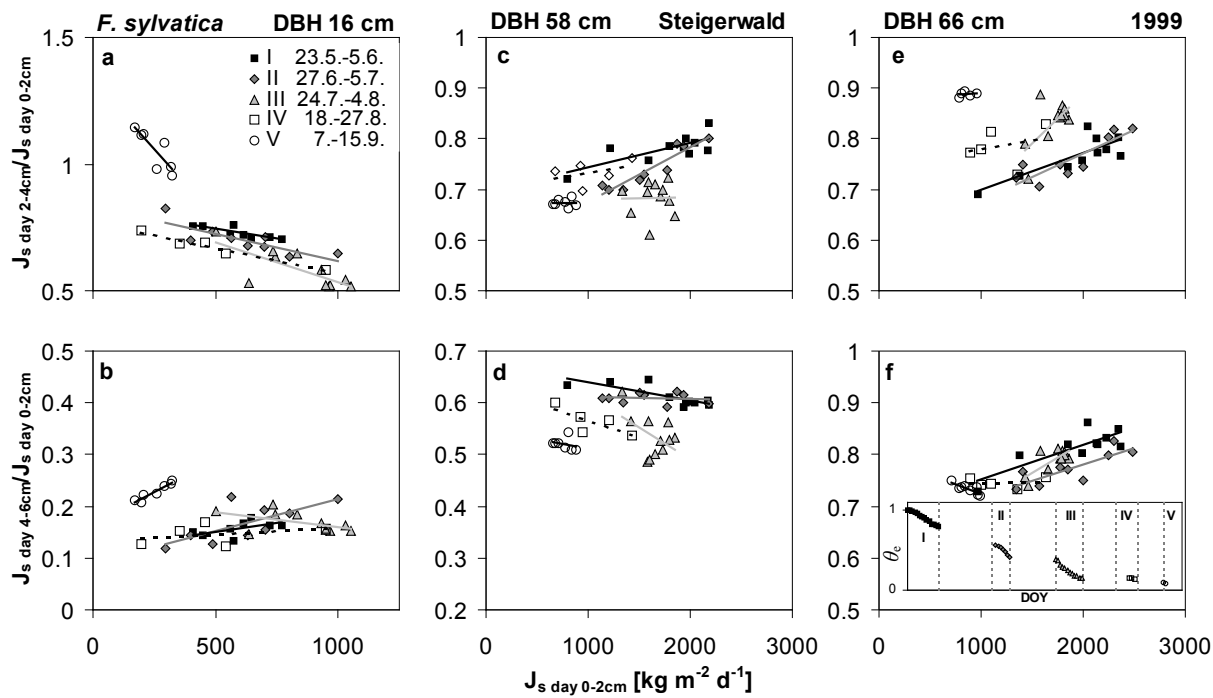
**Figure 5.3.8:** Relationships between atmospheric variables and daily integrated sap flow density ( $J_{s\ day}$ ) in three radial sapwood depths of beech tree B4237 (DBH 66 cm) during four contiguous periods in 1999: relationships with daily average vapour pressure deficit of the air ( $D_{avg}$ ; 24 h-average of 10'-values; **a–c**) and daily integrated photosynthetic photon flux density ( $PFD_{day}$ ; **d–f**) in outer sapwood (0–2 cm; **a, d**), in 2–4 cm depth (**b, e**) and in 4–6 cm depth (**c, f**) for the tree with the highest observed values of  $J_{s\ day}$  (at 0–2 cm depth; largest studied tree). Lines are statistically significant ( $p < 0.0001$ ) non-linear regressions, namely exponential functions for the relationships with  $D_{avg}$  and 2<sup>nd</sup> order polynomial functions for  $PFD_{day}$ , except for data from October where 2<sup>nd</sup> order polynomials gave the best, but not significant correlations for  $D_{avg}$  and  $PFD_{day}$  ( $p > 0.01$ , see Figure). Correlation coefficients are given next to the graphs. (24 h- $D_{avg}$  is related to 10'- $D_{max}$  of the day as follows:  $D_{max} = 4.485 \cdot D_{avg}^{0.77}$ , with  $R^2 = 0.94$ ,  $p < 0.0001$ , SEE = 1.94 and  $n = 187$  days in 1999 under regard here.)

Figure 5.3.8 also hints at the variability of the ratio  $J_{s\ day\ deep}/J_{s\ day\ 0-2cm}$  seen in Figure 5.3.4 c, d, which results from differently large changes of the response to atmospheric drivers of transpiration in different sapwood depths over the season (see also Fig. 5.3.2). This will be further elaborated on in the following section. At the maximum observed values of  $D_{avg}$  for instance, the ratio  $J_{s\ day\ 2-4cm}/J_{s\ day\ 0-2cm}$  for beech B4237 changed from 0.83 in May–July to 0.86 in August and to 0.88 in September, and  $J_{s\ day\ 4-6cm}/J_{s\ day\ 0-2cm}$  changed from 0.83 to 0.81 to 0.73, respectively (calculation based on regression models from Fig. 5.3.8).

**Radial patterns of sap flow density and soil water conditions.** Factors other than  $D_{avg}$  and  $PFD_{day}$  apparently limited  $J_s \text{ day}$  at Steinkreuz from August 1999 onwards till the end of the vegetation period (Fig. 5.3.8, see above). As one of these, the effect of relative extractable soil water  $\theta_e$  on maximum  $J_s \text{ day}$  over the season is shown in Figure 5.3.9 for 1999 and 2000 for a dominant tree (B4237). In 1999, at the end of July (July 31, Fig. 5.3.9),  $\theta_e$  in the upper soil reached values below 0.4 (in -0.2 m soil depth: 0.20, as shown in Fig. 5.3.9; in -0.35 m: 0.32), which is regarded as a threshold of soil water limitation for beech and other species (e.g. Granier et al. 1996b), and maximum  $J_s \text{ day}$  dropped considerably (by more than 25%) compared to the beginning of July under similar favourable atmospheric conditions. Maximum  $J_s \text{ day}$  continued to decrease until the end of the season, when atmospheric conditions were restricting transpiration as well (see Fig. 5.3.8). Lowest values of  $\theta_e$  were 0.09, 0.23 (02.09.99) and 0.53 (12.10.99) in -0.2 m, -0.35 m and -0.9 m, respectively (Fig. 5.3.9, see also Fig. 5.2.1.2 and Chap. 5.2). Beginning replenishment of upper soil water reserves during the first half of October 1999 (which did not reach deeper soil layers yet) had no more effect on maximum observed  $J_s \text{ day}$  over the late period of the growing season. In 2000,  $\theta_e$  may have been potentially limiting only for a short period – earlier than in 1999 – at the end of June–beginning of July when  $\theta_e$  in 20 cm depth dropped below 0.4 (0.34 on July 1, 2000), paralleled by a reduction in  $J_s \text{ day}$  of about 25 %, before frequent and ample precipitation, starting on July 2, 2000 (in combination with low evaporative demand) rewetted the upper soil layers (at least down to -35 cm) and maintained  $\theta_e$  at a high (>0.5) and hardly sap flow-limiting level (see also Fig. 5.2.1.2, Fig. 5.2.1.3). Maximum  $J_s \text{ day}$  did not decrease any further before the middle of August in 2000. From September onwards, values of maximum  $J_s \text{ day}$  did not differ between years though, despite lower  $\theta_e$  in 1999, possibly a sign of beginning leaf senescence. At Farrenleite, where soil water content  $\theta$  ( $\theta_e$  could not be calculated) remained high throughout the vegetation period (cf. Figs. 5.2.2.1, 5.2.2.2), the effects of  $\theta$  on  $J_s \text{ day}$  were not obvious (not shown, see above).



**Figure 5.3.9:** Relationship between maximum monthly  $J_s \text{ day}$  in the outermost sapwood ( $J_s \text{ day}$  0-2cm), relative to the annual maximum  $J_s \text{ day}$  0-2cm of tree B4237 from Steinkreuz, and relative extractable soil water  $\theta_e$  in shallow (-0.2 m; diamonds), intermediate (-0.35 m; squares) and deep soil (-0.9 m; triangles) for days in 1999 (**left**, filled symbols) and in 2000 (**right**, open symbols; data for -0.35 m omitted for clarity). Dates for 1999 are: 27.05., 03.07., 31.07., 2.9., 12.10.1999; and for 2000: 16.05., 20.06., 01.07., 14.08., 09.09., 16.10.2000.



**Figure 5.3.10:** Relationship of daily integrated sap flow density in deep sapwood relative to outer sapwood ( $J_s \text{ day } 2-4\text{cm}/J_s \text{ day } 0-2\text{cm}$ : **upper panel**;  $J_s \text{ day } 4-6\text{cm}/J_s \text{ day } 0-2\text{cm}$ : **lower panel**) and sap flow density in outer sapwood ( $J_s \text{ day } 0-2\text{cm}$ ) for three trees (B4235: **a**, **b**; B4213: **c**, **d**; B4237: **e**, **f**) during five periods of several consecutive days without significant rain (cf. Fig. 5.3.4) in 1999. The periods are: 23.05.-05.06. (I); 27.06.-05.07. (II); 24.07.-04.08. (III); 18.-27.08. (IV); 07.-15.09. (V). Lines are linear regressions for each of the five periods. The scales of x and y-axes vary. **Inset** in **f**: Development of average daily relative extractable soil water  $\theta_e$  in shallow soil (-0.2 m) over the five periods; data gaps exist in periods IV and V. Roman numerals refer to the five periods, the style of the symbols as well.

Seasonal variability of the ratio  $J_s \text{ day deep}/J_s \text{ day } 0-2\text{cm}$ , already pointed at in connection with Figure 5.3.8 (and more general in Figs. 5.3.2 and 5.3.4 c, d) is further elaborated on in Figure 5.3.10. For these graphs, data from the Steigerwald from five short, progressively drier periods in 1999 without significant rainfall (including the days shown in Fig. 5.3.9; see inset in Fig. 5.3.10f) were selected and the daily ratio  $J_s \text{ day deep}/J_s \text{ day } 0-2\text{cm}$  plotted against  $J_s \text{ day } 0-2\text{cm}$  for the same three trees as in Figures 5.3.1–5.3.3. As already seen in Figures 5.3.2 the radial pattern of  $J_s \text{ day}$  ( $J_s \text{ day deep}/J_s \text{ day } 0-2\text{cm}$ ) was variable over time and correlated with  $J_s \text{ day } 0-2\text{cm}$  (Fig. 5.3.10;  $J_s \text{ day } 0-2\text{cm}$  could also be interpreted as a proxy for atmospheric transpirational demand (cf. Fig. 5.3.8), at least under non-limiting soil water conditions, and a as relative proxy under limiting soil water conditions).

In the smallest tree (DBH 16 cm, B4235, Fig. 5.3.10a, b) the ratio  $J_s \text{ day } 2-4\text{cm}/J_s \text{ day } 0-2\text{cm}$  always decreased with increasing  $J_s \text{ day } 0-2\text{cm}$  (Fig. 5.3.10a), i.e. the higher the sap flow density in outer sapwood, the smaller the contribution of inner sapwood, but the opposite was true for  $J_s \text{ day } 4-6\text{cm}/J_s \text{ day } 0-2\text{cm}$  (Fig. 5.3.10b). The ratio increased from period IV (18.–27.08.) to V (07.–15.09.; Fig. 5.3.10a, b), possibly indicating a change in the hydraulic properties of the sapwood of this tree. In the largest tree (DBH 66 cm = tree 4237, Fig. 5.3.10e, f)  $J_s \text{ day deep}/J_s \text{ day } 0-2\text{cm}$  mostly increased with increasing  $J_s \text{ day } 0-2\text{cm}$  and a tendency of both the magnitude and the slope to change may be seen from period II (27.06.–05.07.) to III (24.07.–04.08.), at least for annulus #2 (2–4cm; Fig.

5.3.10e). The relationships were less obvious for the other large tree (DBH 58 cm, B4213, Fig. 5.3.10c, d). As may have been expected, no major changes in these ratios occurred during the summer of the year 2000 (Fig. A11.4).

Since no conclusive pattern emerged from the data of these few trees, in order to trace a more general pattern, if contained in the data, the average ratios  $J_s \text{ day } 2-4\text{cm}/J_s \text{ day } 0-2\text{cm}$  from Figure 5.3.10 for each of the five periods were calculated for all available trees and sensors from the Steigerwald in 1999 and plotted in Figure 5.3.11.

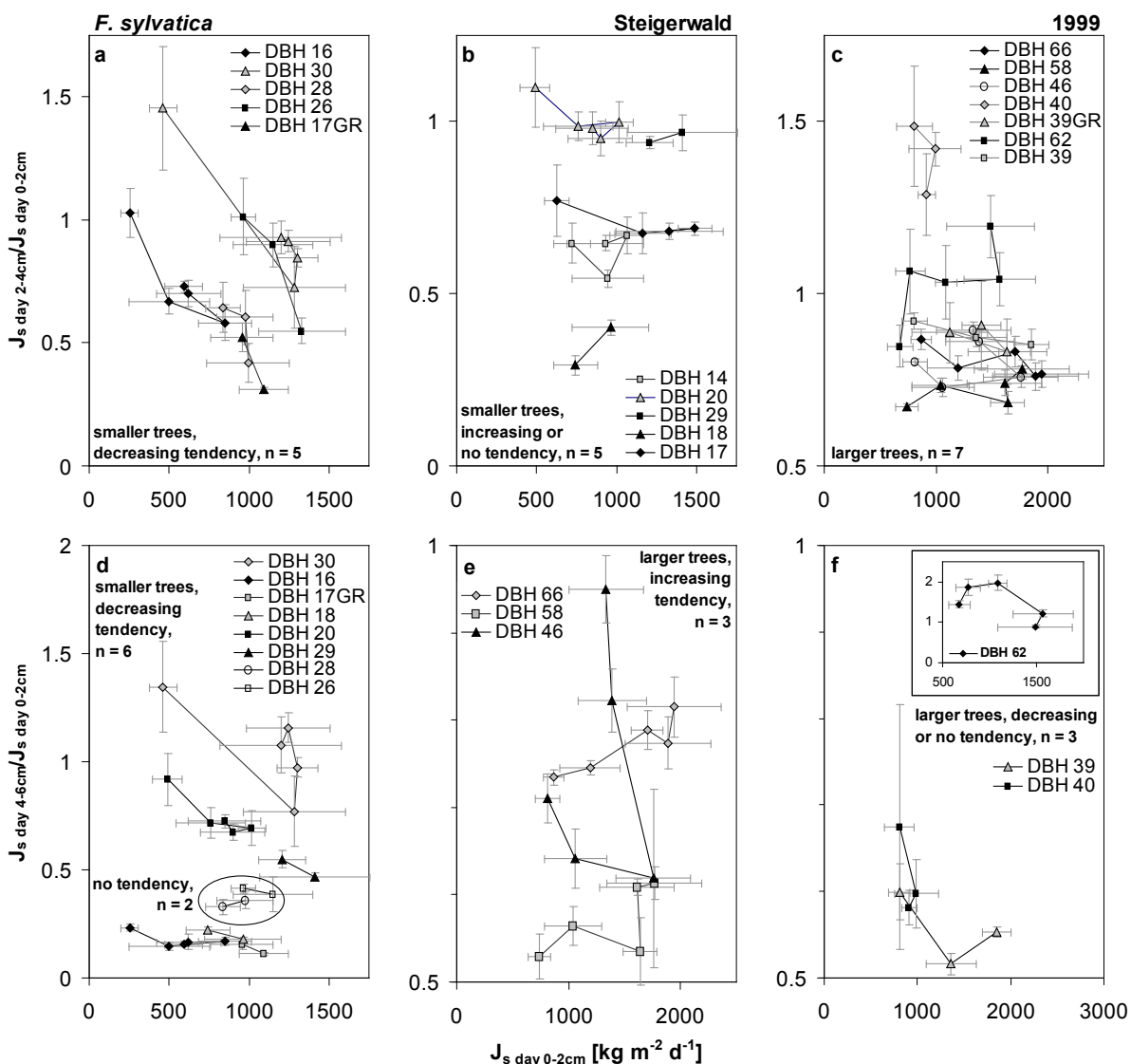


**Figure 5.3.11:** Average ratio of  $J_s \text{ day } 2-4\text{cm}/J_s \text{ day } 0-2\text{cm}$  (a-c) and  $J_s \text{ day } 4-6\text{cm}/J_s \text{ day } 0-2\text{cm}$  (d-f), respectively, for each of the five periods specified in Figure 5.3.10 for all available beech trees studied at the sites in the Steigerwald in 1999 and mean  $J_s \text{ day } 0-2\text{cm}$ . Sensors are grouped according to size (DBH, in cm) and trend. Total number of trees for 2–4 cm was  $n = 17$ , for 4–6 cm  $n = 14$ . Bars are  $\pm 1$  SD from the mean. Lines connect averages from the different periods of the same tree/sensor in calendaric order. Scale of x and y- axes varies.

For 2–4 cm sapwood depth, the average ratio  $J_s \text{ day } 2-4\text{cm}/J_s \text{ day } 0-2\text{cm}$  indicated a decreasing tendency with increasing  $J_s \text{ day } 0-2\text{cm}$  in smaller trees (5 trees; Fig. 5.3.11a), i.e. a decreasing contribution of inner sapwood when sap flow density in outer sapwood increased. Just two small trees showed no or only a vaguely decreasing trend, and one tree showed an increase (Fig. 5.3.11b). In contrast, data from larger trees suggested only weak or divergent tendencies (of 7 trees, 2 showed increasing, 3 weakly decreasing, 2 no trend; Fig. 5.3.11c). The situation was more conclusive for 4–6 cm sapwood depth: in smaller and more suppressed trees a decreasing tendency of  $J_s \text{ day } 4-6\text{cm}$  relative to  $J_s \text{ day } 0-2\text{cm}$  could be observed with increasing  $J_s \text{ day } 0-2\text{cm}$  in 6 out of 8 trees (Fig. 5.3.11d; 2 sensors with no tendency circled), whereas in large trees it increased in three trees (Fig. 5.3.11e), decreased in two trees and one tree displayed no tendency (Fig. 5.3.11f).

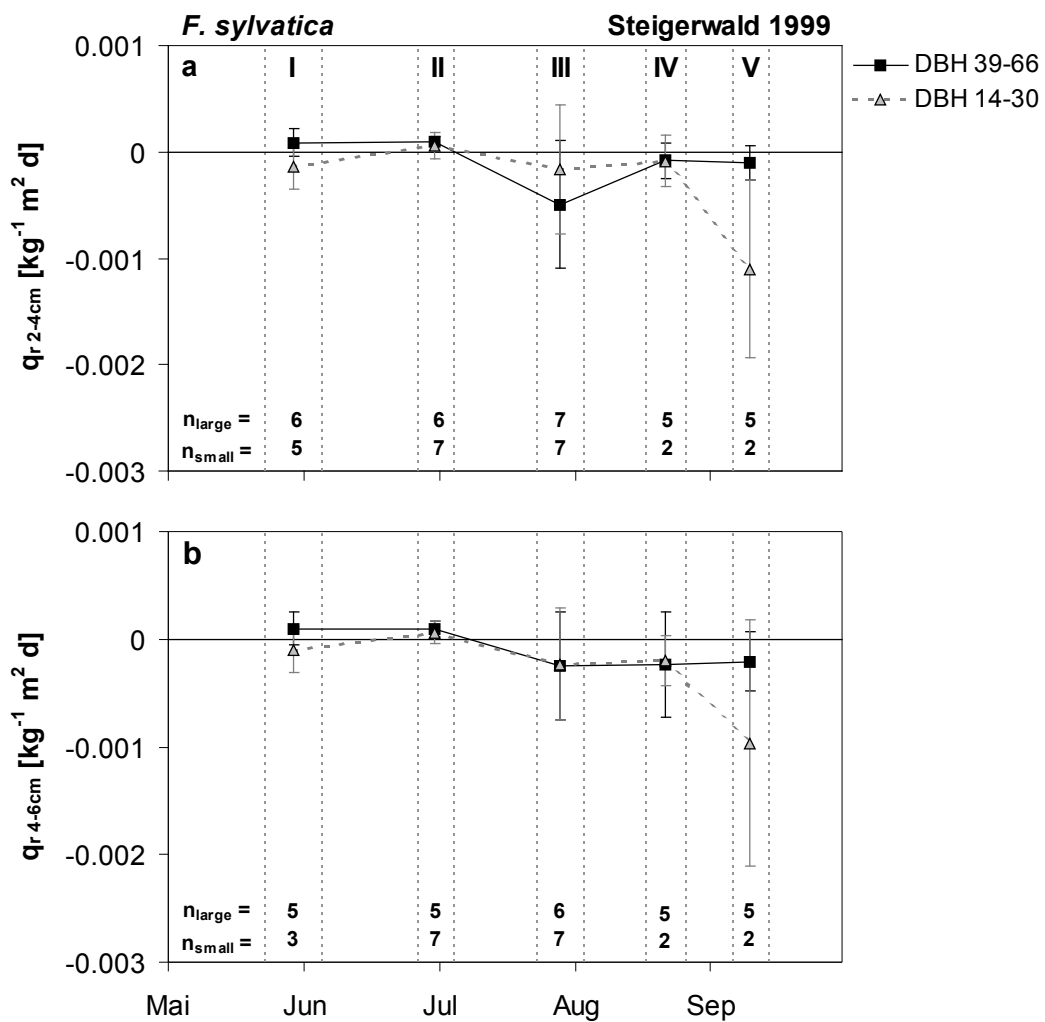


**Figure 5.3.12:** Slope of the relationship between  $J_s \text{ day } 2-4\text{cm}/J_s \text{ day } 0-2\text{cm}$  and  $J_s \text{ day } 0-2\text{cm}$  ( $q_{r \text{ 2-4cm}}$ ; a) and  $J_s \text{ day } 4-6\text{cm}/J_s \text{ day } 0-2\text{cm}$  and  $J_s \text{ day } 0-2\text{cm}$  ( $q_{r \text{ 4-6cm}}$ ; b), respectively, as exemplified in Figure 5.3.10, calculated separately for each of the five periods (I–V) in 1999 from linear regressions and averaged for large (DBH 39–66 cm) and small trees (DBH 14–30 cm). Bars denote  $\pm 1 \text{ SD}$ . Broken vertical lines indicate the five periods selected for this analysis.

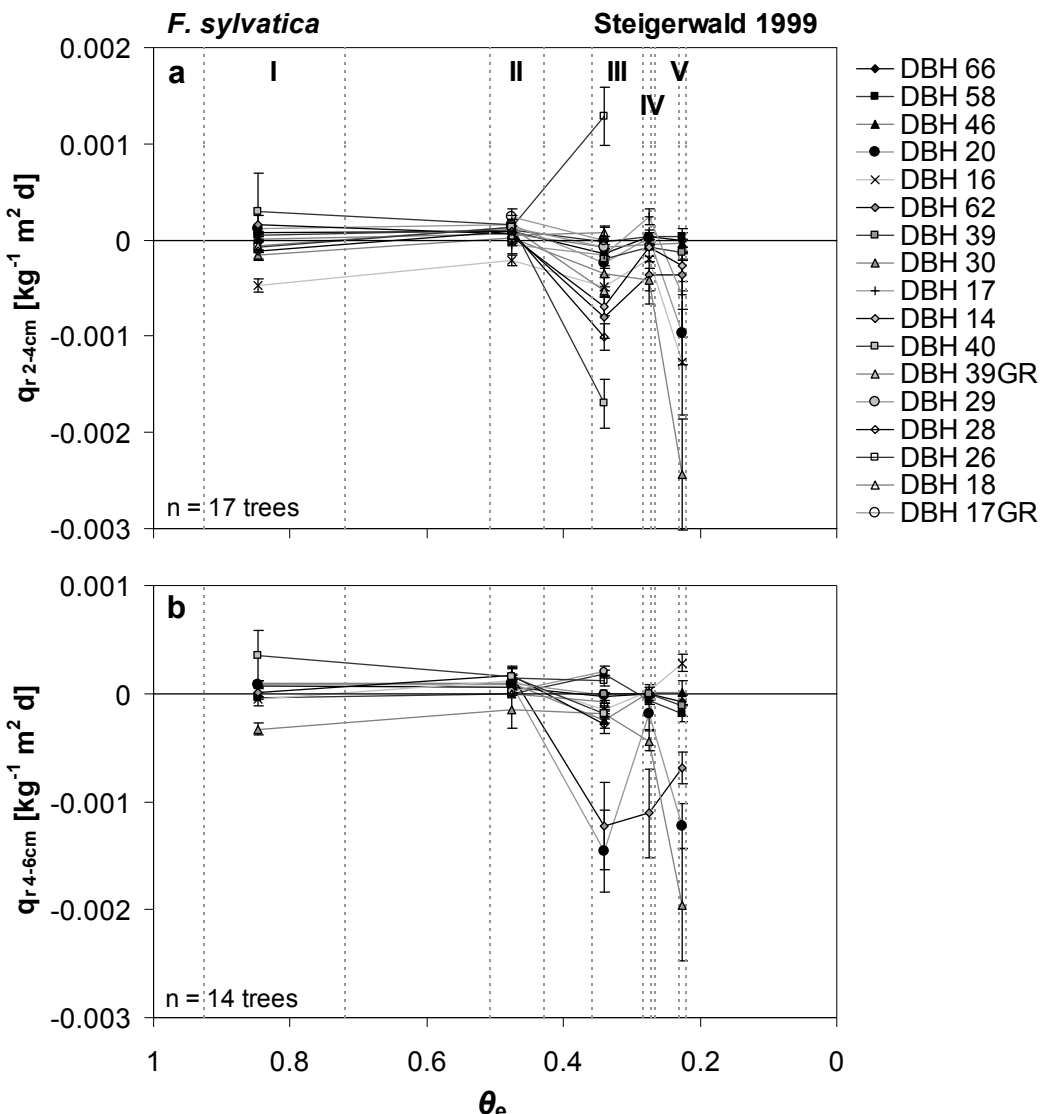


**Figure 5.3.13:** Slope of the relationship between  $J_s$  day 2-4cm/ $J_s$  day 0-2cm and  $J_s$  day 0-2cm ( $q_r$  2-4cm; a) and  $J_s$  day 4-6cm/ $J_s$  day 0-2cm and  $J_s$  day 0-2cm ( $q_r$  4-6cm; b), respectively, as in Fig. 5.3.12, and relative extractable soil water  $\theta_e$  in -0.35 m soil depth for the five selected periods (I–V). Bars denote  $\pm 1$  SE of the slope of linear regression. Broken vertical lines indicate the five periods selected for this analysis (and periods III and IV overlap).  $\theta_e$  decreases from left to right as season progresses. Trees named after their DBH (in cm; GR = GroßeBene).

In a further step of comparison of beech trees from the Steigerwald, the slope of the relationship of  $J_s$  day deep/ $J_s$  day 0-2cm with  $J_s$  day 0-2cm, in the following referred to as  $q_r$  (i.e.  $q_r = (J_s$  day deep/ $J_s$  day 0-2cm)/ $J_s$  day 0-2cm), was calculated from linear regressions such as those shown in Figure 5.3.10 and is plotted in Figure 5.3.12 against time and averaged for large and small trees, respectively, and in Figure 5.3.13 against relative extractable soil water  $\theta_e$  for individual trees. Beginning with mostly positive values of  $q_r$  during period I in large trees, which signify an increasing contribution of deeper sapwood relative to outer sapwood with increasing  $J_s$  day 0-2cm (but not necessarily an absolutely larger  $J_s$  than in outer sapwood), and mainly negative  $q_r$  in small trees,  $q_r$  changed only little and mostly not significantly from period I to II when  $\theta_e$  was still > 0.4. From period II to III in 12 out of 16 trees (2–4 cm; Fig. 5.3.13a) and 9 out of 13 trees (4–6 cm; Fig. 5.3.13b; and “large trees”, Fig. 5.3.12) the sign of  $q_r$  in the

majority of trees changed from positive to negative (or stayed negative), indicative of a decreasing contribution of deeper sapwood relative to outer sapwood with increasing  $J_s$  day 0-2cm. The “sensitivity” of  $J_s$  day deep/ $J_s$  day 0-2cm to changes in  $J_s$  day 0-2cm, i.e. the absolute value of  $q_r$ , increased from period II to III in 13 out of 16 trees (2–4 cm, Fig. 5.3.13a) and 10 out of 13 trees (4–6 cm, Fig. 5.3.13b), in both small and large trees (Fig. 5.3.12). From period III to IV (18.–27.08.) the sign of  $q_r$  remained negative in 6 out of 10 trees (2–4 cm, Fig. 5.3.13a) and 5 out of 8 trees (4–6 cm, Fig. 5.3.13b), but changed to positive in the remaining trees (small and large trees). In most trees the absolute value  $q_r$  decreased from period III to IV (2–4 cm: 7 of 10 trees; 4–6 cm: 6 of 8 trees) to values close to zero. Prior to period IV ample precipitation (15 mm) may have supplied enough water to the shallow soil layers to decrease the “drought stress” for the trees for a few days at the beginning of period IV until the previous stress levels were reached again; values for  $\theta_e$  were available for the last few days of period IV only and therefore may not be representative for the whole period. So the contrasting behaviour of  $q_r$  during period IV may be explained by the less severe soil water depletion at the beginning of that period. From period IV to V (07.-15.09.) the sign of  $q_r$  stayed negative for 6 (5) out of 10 (9) trees (2–4 cm and 4–6 cm, respectively) and turned negative in 3 (1) trees. The absolute values of  $q_r$  became larger again (8 of 10 and 7 of 8 trees for 2–4 cm and 4–6 cm, respectively), particularly in 4 small trees for 2–4 cm (DBH 16, DBH 17, DBH 20, DBH 30) and 2 small trees for 4–6 cm (DBH 20, DBH 30; plus DBH 62). This was less pronounced in large trees (Fig. 5.3.12).

In conclusion, the overall trend of the radial pattern of  $J_s$  day in beech trees from the Steigerwald in 1999 was a decrease in the contribution of the inner sapwood relative to the outermost sapwood annulus (0–2 cm) under increased demand (increasing  $J_s$  day 0-2cm) during seasonally progressing soil water depletion, particularly when  $\theta_e$  declined below 0.4 (in 0.2 m and 0.35 m soil depth). This was manifested in the combination of both negative and large absolute values (i.e. small negative values) of  $q_r$ , especially for periods III and V. Some of the smaller trees responded strongest to the progressing soil drought and radial decrease was more pronounced than in larger trees, yet variation among smaller trees and in general was rather large; introducing a group of “intermediate trees” could not reduce this variability (not shown). Almost all large trees showed a more constant behaviour, with absolute values of  $q_r$  mostly being minor than in small trees ( $q_r$  close to zero). The profile of  $J_s$  across the sapwood radius as a consequence tended to become steeper for a given rate of  $J_s$  0-2cm in small sub-canopy trees as the season of 1999 progressed (larger absolute  $q_r$ ). However, in large trees the sign of  $q_r$  also generally did not turn positive again once  $\theta_e$  had dropped below 0.4. In the year 2000 such seasonal changes in patterns of radial profiles of sap flow density could not be detected (cf. Fig. A11.4).

#### 5.4. Whole-tree water use $Q_t$ of *Fagus sylvatica* and *Quercus petraea*

In order to scale sap flow density  $J_s$  to the whole tree, the values of  $J_{s,i}$  of a 2 cm wide annulus  $i$  were multiplied with the cross-sectional area of the respective annulus  $A_{s,i}$  to reach the sap flux  $Q_i$  of this annulus. All measured  $Q_i$  of a tree were totalled to give the sap flux of the tree  $Q_t$  (Eq. 4.1.3, Chap. 4.1.1). If in beech the deepest inserted thermal dissipation probe did not extend into the innermost sapwood, sap flow density was interpolated as described below. In oak,  $J_s$  was only measured in the outermost 2 cm of sapwood ( $J_{s,0-2cm}$ , one annulus; see Chap 2.2 and 4.1.1) and  $J_{s,0-2cm}$  was multiplied by  $A_{s,0-2cm}$  resulting in the  $Q_t$  for oak.

The linear regression functions for beech shown in Figure 5.3.4c and d were used to scale up sap flow beyond 6 cm sapwood depth (and beyond 2 cm or 4 cm sapwood depth in trees with less than 3 annuli probed) in steps of 2 cm wide annuli where necessary (although the innermost annulus at the sapwood-heartwood boundary may be wider or narrower than 2 cm, see Chap. 4.1.1). The same equations were employed from daily to 10-minute time steps since the relationship between  $J_s$  in deeper and outer sapwood was fairly constant, especially a) for large trees where estimating sap flow beyond 6 cm depth was important (cf. Fig. 5.3.1d-i), b) on high-flow days, and c) during the time of day when  $J_s$  exceeded about  $10 \text{ g m}^{-2} \text{ s}^{-1}$  (cf. Fig. 5.3.1g-i). The magnitude of drought effects examined in Figures 5.3.9–13 on the radial distribution of sap flow density and the radial patterns presented in Figure 5.3.4 were negligibly small on this scale since most of the sap flow was actually measured and did not need to be interpolated. For instance, at seasonally integrated stand level, interpolated (i.e. beyond the measured 0–6 cm sapwood depth) data accounted for 26 % of the total stand estimate of canopy transpiration (total sapwood area) at Steinkreuz or 8 % at GroßeBene in 1999 (see below).

These regressions (Fig. 5.3.4c, d) for the years 1999 and 2000 were not significantly different from each other ( $p = 0.05$ ; not shown), nevertheless year-specific equations were applied to the respective data because of different trees being sampled in the two years. The following equations were used to interpolate  $J_s$  for the innermost sapwood for all sites and trees, derived from Fig. 5.3.4c and d, respectively, by inverting the relative sapwood depth (x-axis) so that the sapwood-heartwood boundary equals zero and the cambium-sapwood boundary equals 1:

in 1999:

$$J_{s,deep}/J_{s,0-2\text{ cm}} = 0.0507 + 1.0842 \cdot \text{relative sapwood depth} \quad (\text{Eq. 5.4.1})$$

in 2000:

$$J_{s,deep}/J_{s,0-2\text{ cm}} = -0.0802 + 1.1664 \cdot \text{relative sapwood depth} \quad (\text{Eq. 5.4.2})$$

For 1998, data quality was very varied, data gaps were rather prominent, and the overall number of sensors limited the upscaling from sensor to tree and especially from tree to stand so that for this work the years 1999 and 2000 were considered in the following only.

In order to arrive at conclusive seasonal sums, data gaps were filled via regression with other sap flow sensors or meteorological parameters, namely vapour pressure deficit (D). If gaps were several days long, filling was done for daily integrals only. In 1999, 24 h-long gapfillings accounted for 20 % (beech, 40 days) and 32 % (oak,

64 days) of the days of the total growing (“sap flow”) season at Steinkreuz in 1999, for 16 % (32 days) at the Steinkreuz-pure beech plot, for 21 % (beech, 41 days) and 24 % (oak, 49 days) at GroßeBene, and 11 % at Farrenleite (16 days). In 2000, at Steinkreuz and the Steinkreuz-pure beech plot, 8 % (15 days) of all days were completely gapfilled, as well as at Farrenleite (12 days).

The maximum error introduced by estimating the total sapwood area of the investigated trees based on the regression equations given in Table 5.1.1.1 was calculated to average  $\pm 16.4\%$  across these trees. Including the error introduced by the data loggers, the total maximum error for the  $Q_t$  of an average tree would be 17.9 % based on a Gaussian error propagation (the additional uncertainty regarding the interpolated portion of  $Q_t$  will be discussed in Chapter 6.3).

In Figure 5.4.1 daily integrated values of sap flux  $Q_{t \text{ day}}$  for beech and oak and the contribution of individual annuli are shown for all sites on a sunny to overcast late spring day (June 2, 1999, cf. Fig. 5.3.1). On this day, scaled sap flux  $Q_t$  of beech ranged from 2.7 kg tree $^{-1}$  d $^{-1}$  (B4049, DBH 16 cm) to 199 kg tree $^{-1}$  d $^{-1}$  (B4237, DBH 66 cm, both trees from Steinkreuz;  $Q_{0-6\text{cm}}$  was 110 kg d $^{-1}$  for B4237), and  $Q_{0-2\text{cm}}$  from 1.9 kg d $^{-1}$  to 43.5 kg d $^{-1}$  (same trees). Sap flux among oak trees was less varied (minimum 18.8 kg tree $^{-1}$  d $^{-1}$ : E132, DBH 46 cm; maximum 37.8 kg tree $^{-1}$  d $^{-1}$ : E4202, DBH 50 cm), as could have been expected given the narrower range of diameters of the species in the two stands (e.g. Fig. 5.2.1) and the smaller variation of sap flow density  $J_s$  between trees (Fig. 5.3.7; see also below). Contribution of the outermost annulus of sapwood (0–2 cm;  $Q_{0-2\text{cm}}$ ) was 21–81 % of total  $Q_t$  and 34–81 % of  $Q_{0-6\text{cm}}$  in the investigated beech trees on this particular day;  $Q_{0-6\text{cm}}$  was 55–100 % of  $Q_t$  for beech, on average 88 %.

Maximum seasonal values of daily integrated sap flux, or water use ( $Q_{t \text{ max}}$ ) of beech and oak trees are plotted in Figures 5.4.2 and 5.4.3 against tree structural scalars.  $Q_{t \text{ max}}$  peaked at values of 435 and 62 kg tree $^{-1}$  d $^{-1}$  for beech and oak in the Steigerwald, respectively, and 100 kg tree $^{-1}$  d $^{-1}$  in the beech stand Farrenleite in the Fichtelgebirge (see also Tab. 5.4.1). The range of  $Q_{t \text{ max}}$  for beech at Steinkreuz was 11–435 kg tree $^{-1}$  d $^{-1}$ , 25–431 for the Steinkreuz-pure beech plot, 12–136 kg tree $^{-1}$  d $^{-1}$  at GroßeBene and 16–100 kg tree $^{-1}$  d $^{-1}$  at Farrenleite, over the two years under consideration here (Fig. 5.4.2). In oak, the range of  $Q_{t \text{ max}}$  was 20–53 kg tree $^{-1}$  d $^{-1}$  at Steinkreuz and 28–62 kg tree $^{-1}$  d $^{-1}$  at GroßeBene (Fig. 5.4.2). Accordingly, the coefficient of variation (CV) of  $Q_{t \text{ max}}$  within stands was considerable for beech, particularly at Steinkreuz (110 %,  $n = 10$ ) and the Steinkreuz-pure beech plot (103 %,  $n = 12$ ), to a lesser extent at GroßeBene (76 %,  $n = 9$ ) and least of all at Farrenleite (54 %,  $n = 13$ ). Among oaks from one stand, the CV was generally much lower (Steinkreuz 28 %,  $n = 11$ ; GroßeBene 26 %,  $n = 9$ ). (When accounting for the sample size ( $CV_r = CV \cdot n^{-0.5}$ ),  $CV_r$  was 35 %, 30 %, 25 % and 15 % for beech of Steinkreuz, Steinkreuz-pure beech plot, GroßeBene and Farrenleite, respectively, and 8 % and 9 % for oak at Steinkreuz and GroßeBene, respectively.)

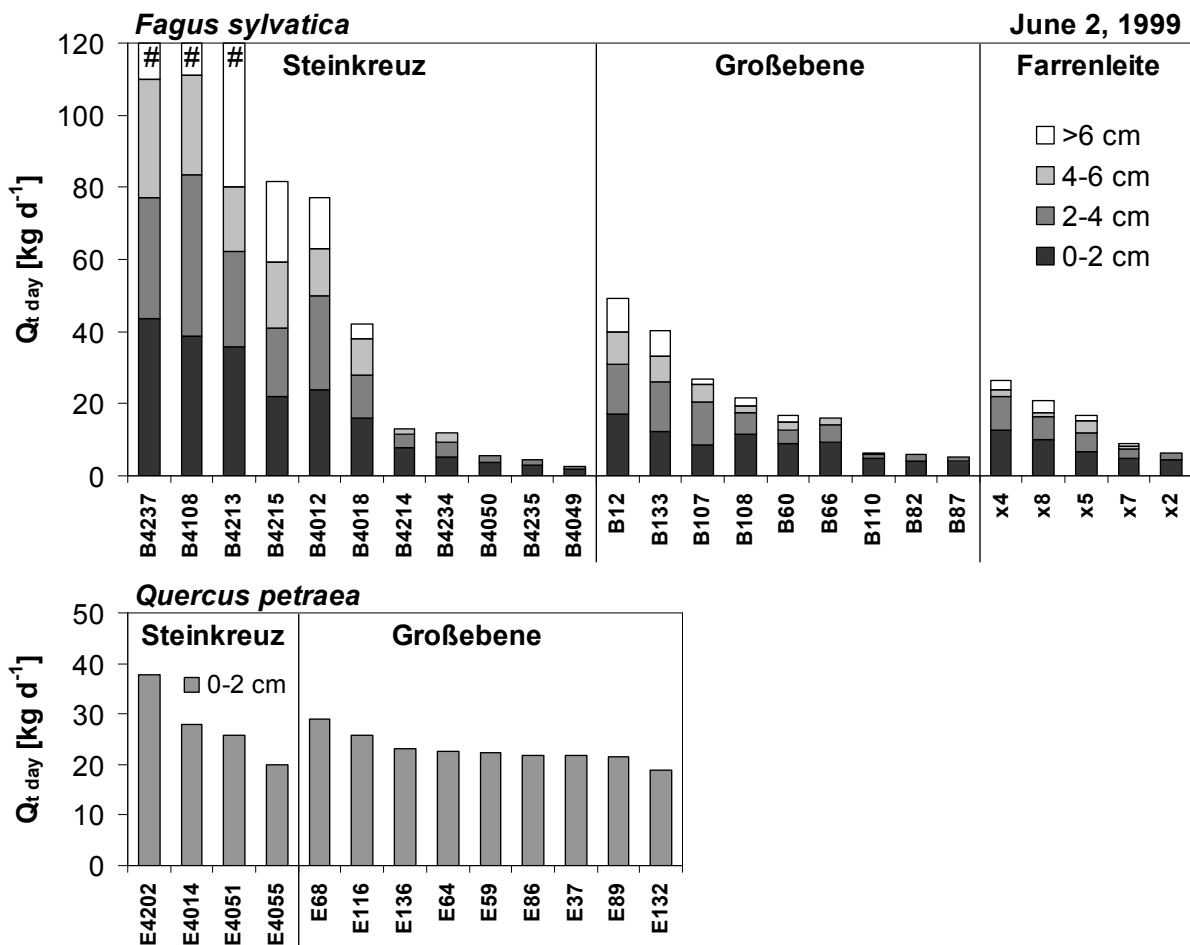


**Figure 5.4.1:** Daily integrated values of tree sap flux  $Q_t$  day for individual annuli (0–2 cm, 2–4 cm, 4–6 cm sapwood depth; measured) and sapwood > 6 cm (interpolated based on Fig. 7.1.4) for beech trees in three stands (**top**) and for oak trees in two stands (**bottom**) on June 2, 1999 (same day as in Fig. 7.1.1). In oak, sap flow was measured in the outermost 2 cm of xylem only due to narrow sapwood of this ring-porous species (see text). Trees are sorted according to total  $Q_t$  for each stand. Totals for the largest trees at Steinkreuz (symbol #) are (from left to right) 199  $\text{kg d}^{-1}$  (beech B4237), 181  $\text{kg d}^{-1}$  (B4108), and 135  $\text{kg d}^{-1}$  (B4213), respectively. For trees B4214 and B66, sap flow in 2–6 cm sapwood depth was also interpolated and not measured, as well as for tree B87 in 2–4 cm and for trees B4050, B4049 and B12 in 4–6 cm sapwood depth.

Half-hourly maxima of  $Q_t$  ( $Q_{t \text{ hh max}}$ , Tab. 5.4.1) reached highest values at Steinkreuz (36.8  $\text{kg h}^{-1}$  and 38.9  $\text{kg h}^{-1}$  in 1999 and 2000, respectively) and much lower values at Großebene (up to 11.2  $\text{kg h}^{-1}$ ) and Farrenleite (6.9  $\text{kg h}^{-1}$  and 6.8  $\text{kg h}^{-1}$  in 1999 and 2000, respectively). The lowest values of  $Q_{t \text{ hh max}}$  at Steinkreuz, namely 1.7  $\text{kg h}^{-1}$  and 1.5  $\text{kg h}^{-1}$ , respectively, were calculated for a suppressed beech (DBH 14 cm). At Großebene minimum  $Q_{t \text{ hh max}}$  was 1.2  $\text{kg h}^{-1}$  (DBH 13 cm) and 2.3  $\text{kg h}^{-1}$  or 1.7  $\text{kg h}^{-1}$  (1999, 2000) at Farrenleite (DBH 20cm). Oaks predictably revealed even lower peak rates of 5.6  $\text{kg h}^{-1}$  and 2.9  $\text{kg h}^{-1}$  at Steinkreuz in 1999 and 2000, respectively, and at Großebene 5.6  $\text{kg h}^{-1}$  (1999; Tab. 5.4.1). Minimum  $Q_{t \text{ hh max}}$  was 3.3  $\text{kg h}^{-1}$  and 1.7  $\text{kg h}^{-1}$  (Steinkreuz 1999, 2000) and 2.4  $\text{kg h}^{-1}$  for oaks with a DBH of 42 cm, 33 cm and 44 cm, respectively.

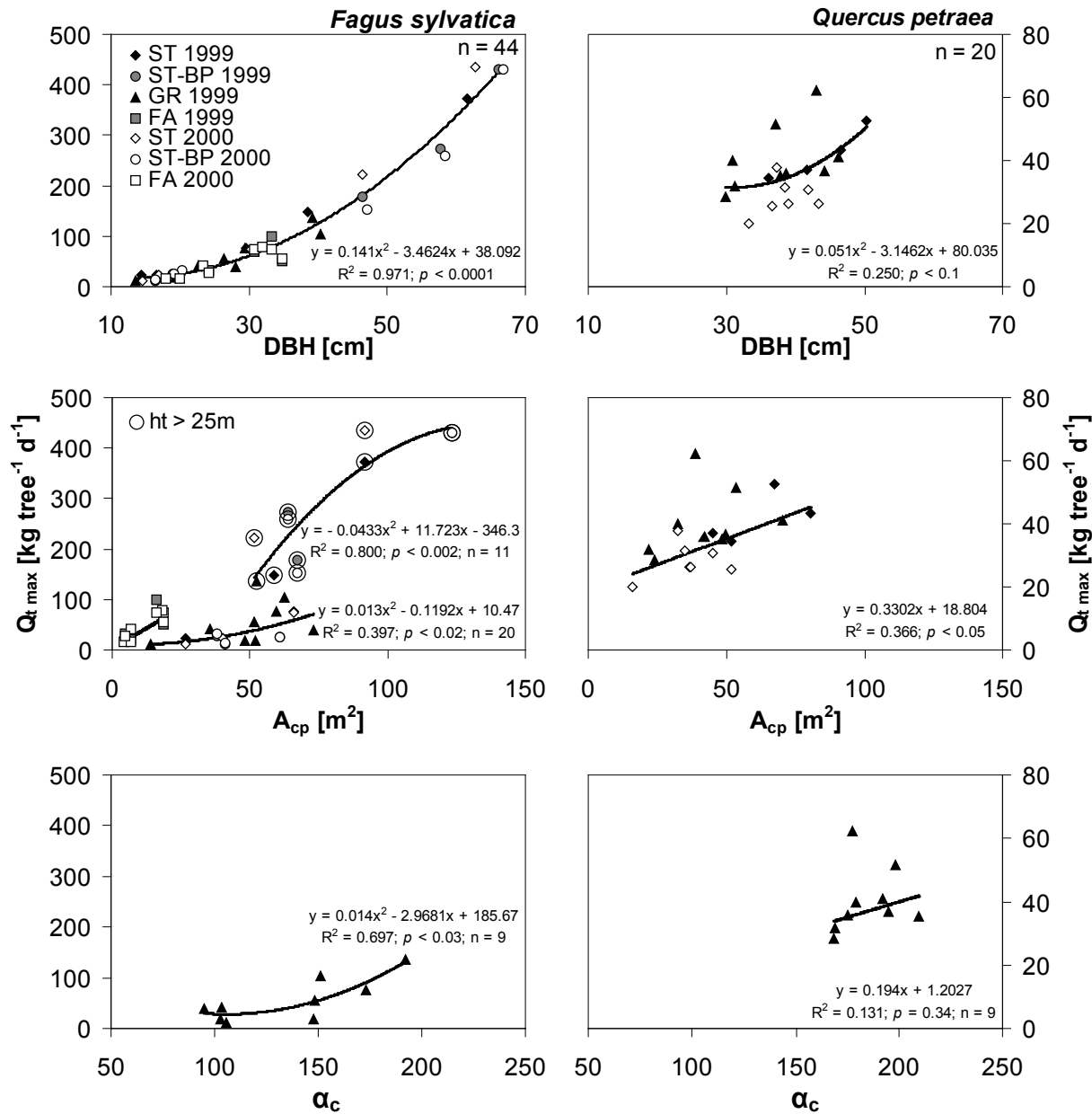


**Figure 5.4.2:** Relationships between tree structural characteristics and seasonal maximum daily tree water use ( $Q_{t \text{ max}}$ ) for *Fagus sylvatica* (left) and *Quercus petraea* (right): diameter at breast height (DBH, **top panel**), ground-projected crown area ( $A_{\text{cp}}$ , **middle**), angle of crown opening ( $\alpha_c$ , **bottom**) for the mixed Steinkreuz stand (ST), Steinkreuz-pure beech plot (ST-BP), Großebene (GR), and Farrenleite (FA) for the years 1999 (filled symbols) and 2000 (open symbols). For regressions of  $Q_{t \text{ max}}$  of beech trees with  $A_{\text{cp}}$ , data were evaluated separately for Farrenleite and for short (tree height  $h_t < 25$  m) and tall trees ( $h_t > 25$  m, circled symbols) at Steinkreuz and Großebene, respectively. The regression equation for Farrenleite is  $y = 3.2414x + 3.1776$ , with  $R^2 = 0.665$ ,  $p < 0.001$ ,  $n = 13$ . Data for  $\alpha_c$  (from S. Fleck, unpublished) are available for Großebene only and represent the average of angles of the centre tree to the competing crowns of neighbouring trees times 2 (i.e.  $180^\circ$  if all trees have the same height), weighted with the length of the border line that the centre tree and its neighbour share in a graph of tree growth space (Voronoi-diagram) based on the Delaunay triangulation method; neighbouring trees with crowns more than 3 m shorter were not regarded as competitors and omitted (S. Fleck, pers. comm.).

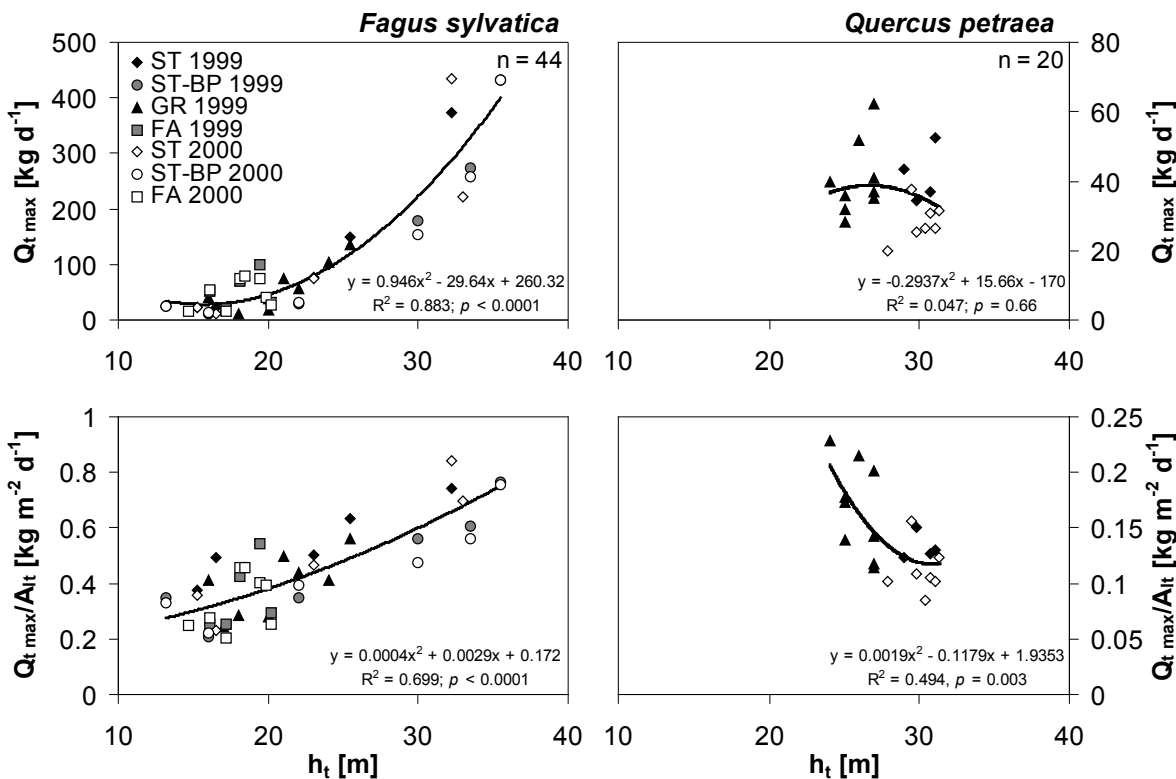


**Figure 5.4.3:** Relationships between total tree height ( $h_t$ ) and seasonal maximum daily tree water use ( $Q_t$  **max**, **top panel**) as well as total tree height and  $Q_t$  **max** per leaf area of trees ( $Q_t$  **max**/ $A_{lt}$ , **bottom**) for *Fagus sylvatica* (left) and *Quercus petraea* (right) for the mixed Steinkreuz stand (ST), Steinkreuz-pure beech plot (ST-BP), Großebeine (GR), and Farrenleite (FA) for the years 1999 (filled symbols) and 2000 (open symbols). Leaf area estimated via allometric equations given in Chap. 4.4.1.

The seasonal sums of  $Q_t$  ( $Q_t$  **sum**) amounted up to  $33.39 \cdot 10^3$  kg season<sup>-1</sup> for the largest measured beech tree (dominant Steinkreuz, 1999; daily average  $Q_t$  **avg** of this tree 162.9 kg d<sup>-1</sup>; Tab. 5.4.1). The highest value observed at Farrenleite was  $4.22 \cdot 10^3$  kg season<sup>-1</sup> (smaller number of sap flow days;  $Q_t$  **avg** of this tree 26.4 kg d<sup>-1</sup>; Tab. 5.4.1). Oak from Großebeine and Steinkreuz differed in  $Q_t$  **sum** ( $3.11 \cdot 10^3$  kg season<sup>-1</sup> vs  $4.55 \cdot 10^3$  kg season<sup>-1</sup>, respectively) mainly because of a different number of sap flow days (larger data gaps for Großebeine, Tab. 5.4.1);  $Q_t$  **avg** was 20.0 kg d<sup>-1</sup> vs 22.2 kg d<sup>-1</sup>, respectively. Rates were rather low for oak in 2000 (cf. Tab. 5.4.1).

For beech, relationships between  $Q_t$  **max** and tree size were similar at all sites and all years, and for all beech trees combined ( $n = 44$ ) high coefficients of determination were observed for regressions with DBH ( $R^2 = 0.971$ ,  $p < 0.0001$ ; Fig. 5.4.2, top panel), tree basal area ( $A_{bt}$ ,  $R^2 = 0.973$ ,  $p < 0.0001$ ), tree leaf area ( $A_{lt}$ ,  $R^2 = 0.973$ ,  $p < 0.0001$ ) and tree sapwood area ( $A_{st}$ ,  $R^2 = 0.977$ ,  $p < 0.0001$ ) (data not shown). That  $Q_t$  **max** and  $A_{st}$  correlate best was to be expected since sap flow was scaled to the whole-tree level using  $A_{st}$ . The ground-projected crown area  $A_{cp}$  of beech correlated best with  $Q_t$  **max** when treating Farrenleite and the two Steigerwald sites separately; Steinkreuz and Großebeine trees behaved similarly. Correlations were further improved when treating tall overstory trees (tree height  $h_t > 25$  m:  $R^2 = 0.800$ ,  $p < 0.002$ ) independently from shorter suppressed trees ( $R^2 = 0.397$ ,  $p < 0.02$ ; Fig. 5.4.2, middle panel). Using crown volume  $V_c$ , calculated as ground-projected crown area times crown length, yielded similar results (beech ST+GR >25 m  $h_t$ :  $R^2 = 0.670$ ,

$p < 0.02$ ; beech ST+GR  $< 25$  m  $h_t$ :  $R^2 = 0.450$ ,  $p = 0.002$ ; Farrenleite:  $R^2 = 0.591$ ,  $p < 0.02$ ; data not shown).

Beech trees at Steinkreuz growing in the pure beech plot – which was a small patch of pure beech within a beech-oak matrix (see Chap. 5.1.2) – did not differ significantly from beech trees of this beech-oak matrix regarding the relationship between  $Q_{t\max}$  and tree structure.

For Großebene, additional data were available from detailed investigations of tree structure in cooperation with S. Fleck (formerly Dept. of Plant Ecology, Univ. Bayreuth), which permitted calculation of the angle of the crown opening ( $\alpha_c$ , Fig. 5.4.2, bottom; data for  $\alpha_c$  from S. Fleck, unpublished).  $\alpha_c$  represents the average of angles of the respective tree's top to the tree tops of competing neighbours times 2 (i.e.  $180^\circ$  if all trees have the same height), weighted with the length of the border line that the respective tree and its neighbour share in a graph of tree growth space (Voronoi-diagram) based on the Delaunay triangulation method; neighbouring trees with crowns more than 3 m shorter were not regarded as competitors and omitted (S. Fleck, pers. comm.). The regression of  $Q_{t\max}$  for all beech trees from Großebene with  $\alpha_c$  yielded a higher coefficient of determination ( $R^2 = 0.697$ ,  $p < 0.03$ ; Fig. 5.4.2, bottom panel) than the regression of  $Q_{t\max}$  with  $A_{cp}$  for Großebene beech trees shorter than 25 m ( $R^2 = 0.284$ ,  $p = 0.43$ ,  $n = 8$ ; not shown).

The  $Q_{t\max}$  of beech also scaled with tree height  $h_t$  ( $R^2 = 0.883$ ,  $p < 0.0001$ ; Fig. 5.4.3, top). Exclusion of data from Farrenleite or of the Steigerwald understory beech trees ( $h_t < 20$  m or  $< 25$  m, respectively), did not improve the regression function ( $R^2 = 0.831$  and  $0.636$ ,  $p < 0.0001$  and  $< 0.02$ , respectively; not shown). For Farrenleite alone,  $h_t$  was not a good predictor of  $Q_{t\max}$  ( $R^2 = 0.241$ ,  $p = 0.25$ ; not shown). Flux rates per leaf area  $Q_{t\max}/A_{lt}$  were positively correlated with  $h_t$  in beech ( $R^2 = 0.699$ ,  $p < 0.0001$ ; Fig. 5.4.3, bottom). Again, for Farrenleite alone there was no clear correlation of  $Q_{t\max}/A_{lt}$  with  $h_t$  ( $R^2 = 0.306$ ,  $p = 0.4$ , not shown).

In oak, correlations between structural scalars and  $Q_{t\max}$  were poorer, if significant at all (Fig. 5.4.2, Fig. 5.4.3), due to large scatter in the data within a stand and between stands. A trend opposite to that in beech may be noticeable for the relationship of  $Q_{t\max}/A_{lt}$  with  $h_t$  ( $R^2 = 0.49$  and  $p = 0.003$ ; Fig. 5.4.3, bottom right), namely a decrease in  $Q_{t\max}/A_{lt}$  with increasing  $h_t$ , when pooling data from Steinkreuz and Großebene. No significant relationships were obtained when treating stands individually (Steinkreuz:  $R^2 = 0.11$ ,  $p = 0.62$ ; Großebene:  $R^2 = 0.38$ ,  $p = 0.24$ ).

**Table 5.4.1:** Sap flux scaled to whole tree-level and tree structural characteristics: seasonal sums of daily integrated sap flux per tree ( $Q_{t \text{ sum}}$ ), average and maximum daily sap flux per tree ( $Q_{t \text{ avg}}$  and  $Q_{t \text{ max}}$ , respectively),  $Q_{t \text{ max}}$  per unit of leaf area ( $Q_{t \text{ max}}/A_{lt}$ ) and maximum half-hourly sap flux per tree ( $Q_{t \text{ hh max}}$ ). Number of days indicated (gapfilled days excluded); diameter at breast height (1.3 m; DBH), sapwood area ( $A_{st}$ ), ground projected crown area ( $A_{cp}$ ), total height ( $h_t$ ) and leaf area ( $A_{lt}$ , allometry) of respective tree. Data for trees with highest  $Q_{t \text{ sum}}$  per species and stand are shown (Großebene: beech B12, oak E86; Steinkreuz: beech B4237, oak E4202 (1999), oak E4052 (2000); Farrenleite (FA): beech x8 (1999), x6 (2000)).

	1999					2000		
	Großebene		Steinkreuz		FA	Steinkreuz		FA
	beech	oak	beech	oak	beech	beech	oak	beech
$Q_{t \text{ sum}}$ [kg season $^{-1}$ ]	7625	3110	33390	4550	4695	30215	2715	4220
$Q_{t \text{ avg}}$ [kg d $^{-1}$ ]	48.9	20.0	162.9	22.2	30.9	152.6	13.7	26.4
number of days	156	156	197	197	151	181	188	160
$Q_{t \text{ max}}$ [kg d $^{-1}$ ]	136	62	431	52	100	435	37	79
$Q_{t \text{ max}}/A_{lt}$ [kg m $^{-2}$ d $^{-1}$ ]	0.56	0.21	0.77	0.13	0.54	0.75	0.16	0.46
$Q_{t \text{ hh max}}$ [kg h $^{-1}$ ]	11.2	3.9 <sup>a</sup>	36.8	5.6	6.9	38.9	2.9	6.8
DBH [cm]	39	37	66	50	33	67	37	32
$A_{st}$ [m $^2$ ]	0.09	0.02	0.27	0.03	0.07	0.28	0.02	0.06
$A_{cp}$ [m $^2$ ]	52.4	53.3	123.2	67.3	16	123.2	32.7	18.3
$A_{lt}$ [m $^2$ ]	240.9	240	562.8	403.8	184.3	572.3	241.7	173.6
$h_t$ [m]	25.5	26	35.5	31.1	19.5	35.5	29.5	18.5

<sup>a</sup> Rate is for tree with highest  $Q_{t \text{ sum}}$ ; absolute maximum  $Q_{t \text{ hh max}}$  was 5.6 kg h $^{-1}$ , for tree E116 with DBH = 43 cm,  $A_{st} = 0.03$  m $^2$ ,  $A_{cp} = 38.8$  m $^2$ ,  $A_{lt} = 309$  m $^2$ ,  $h_t = 27$  m.

### 5.5. Stand water use: Canopy transpiration $E_c$ and canopy conductance $g_c$ of pure and mixed beech forest stands

Scaling from tree to stand was done by normalising  $Q_t$  with the respective sapwood area  $A_{st}$ , resulting in  $J_{st}$  (see Fig. 5.5.1 and Table 5.5.1, below), then averaging  $J_{st}$  of all trees of a size class and finally multiplying by the sapwood area of the size class (Eqs. 4.1.4, 4.1.5, Chap. 4.1.1). Size classes were defined according to stem diameter and canopy position/social status (Tab. A11.5, Appendix, see also Tab. 4.1.1). At Steinkreuz three beech classes were identified, namely suppressed (DBH 7–20 cm), intermediate (DBH 21–50 cm) and dominant trees (DBH 51–70 cm), and two oak classes: intermediate (DBH 21–40 cm) and (co-) dominant (DBH 41–50 cm). For the Steinkreuz-pure beech plot (ST-BP), no size classes were distinguished and scaling up was carried out by totalling the  $Q_t$  of all six trees in the plot and dividing by the plot area. (This also means that no statistics like standard deviation from mean and standard error of the mean etc. were calculated for Steinkreuz-pure beech plot.) At Großebene, beech were classified as suppressed (DBH 7–20 cm), intermediate (DBH 21–30 cm) and (co-) dominant (DBH 31–50 cm), and oak as suppressed (DBH 26–30 cm), intermediate (DBH 31–40 cm) and dominant (DBH 41–50 cm). At Farrenleite, beech trees were grouped into intermediate to suppressed (DBH 14–30 cm) and dominant trees (DBH 31–50 cm).

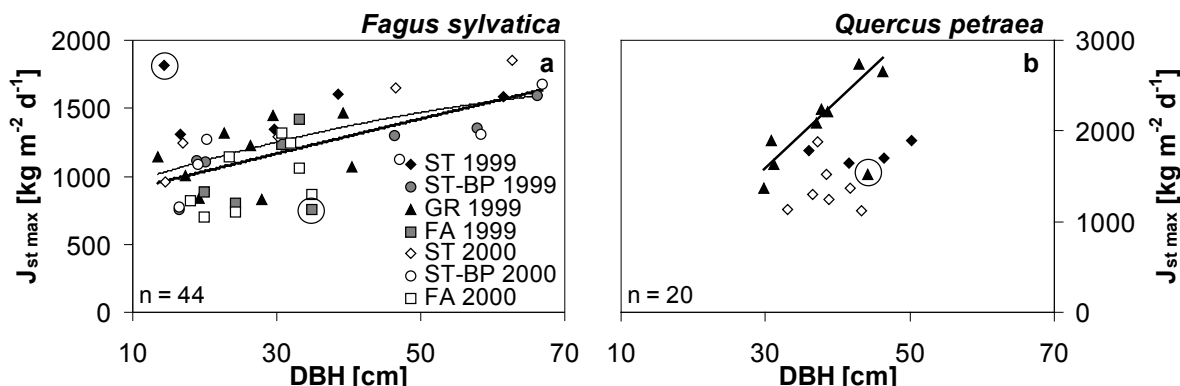


**Figure 5.5.1:** Relationship between sapwood area-weighted whole-tree sap flow density ( $J_{st}$ ) of beech (a) and oak (b) from different stands, and tree diameter (at 1.3 m height, DBH). Shown here are seasonal maxima of daily integrated values of  $J_{st}$  ( $J_{st \max}$ ). For oak,  $J_{st}$  is equal to  $J_{s \ 0-2\text{cm}}$  (see text). Least-square regressions for beech are also plotted, omitting the two circled outliers; a regression for all stands is shown in bold ( $y = -0.006x^2 + 13.26x + 773.9$ ;  $R^2 = 0.470$ ,  $p < 0.0001$ ,  $n = 42$ ), the thin curve is for all stands except Farrenleite ( $y = -0.092x^2 + 18.28x + 786.4$ ;  $R^2 = 0.532$ ,  $p < 0.0001$ ,  $n = 29$ ). For oak, a significant correlation between  $J_{st \max}$  and DBH was found for Großebene only, omitting one circled outlier ( $y = 79.41x - 836.9$ ;  $R^2 = 0.888$ ,  $p = 0.0005$ ,  $n = 8$ ).

Tree water use  $Q_t$  normalised with the respective sapwood area  $A_{st}$ , i.e. sapwood area-weighted total tree sap flow density  $J_{st}$  scaled (non-linearly) with DBH for beech, though  $R^2$  reached only 0.47, or 0.53 when omitting the highly scattered data from Farrenleite (at  $p < 0.0001$ ; Fig 5.5.1a). This justified the use of the aforementioned size classes for beech in the stands Steinkreuz and Großebene. For Farrenleite the situation was less clear, so additionally to the upscaling based on two size classes,

an alternative with just “one” size class (i.e. no size class but an “average tree”) was calculated as well (see below).

For oak,  $J_{st}$  is identical to  $J_{s\ 0-2cm}$  since only the outer 2 cm of sapwood were probed (see Chap 2.2 and 4.1.1) and only the sapwood area of the outer 2 cm-annulus was considered when scaling to tree level; no significant correlation was found when pooling all trees from the two stands (Fig. 5.5.1b), corresponding to the findings for seasonally averaged daily values of  $J_{s\ 0-2cm}$  (see Fig. 5.3.7). Looking at oak trees from Großebebene only though, and omitting one tree that might be regarded as an outlier, a significant ( $p < 0.001$ ) correlation of  $J_{st}$  with DBH could be identified. Thus for oak at Steinkreuz an alternative upscaling variant was computed as well. Table 5.5.1 summarises maximum values of  $J_{st}$  for all stands for the years 1999 and 2000.

**Table 5.5.1:** Sap flow density scaled to whole tree-level  $J_{st}$  (sapwood area-weighted average) and tree structural characteristics: seasonal sums of daily integrated sap flow density per tree ( $J_{st\ sum}$ ), average and maximum daily sap flow density per tree ( $J_{st\ avg}$ ,  $J_{st\ max}$ , respectively) and maximum half-hourly sap flow density per tree ( $J_{st\ hh\ max}$ ). Number of days indicated (gapfilled days excluded); diameter at breast height (1.3 m; DBH), sapwood area ( $A_{st}$ ), ground projected crown area ( $A_{cp}$ ), total height ( $h_t$ ) and leaf area ( $A_{lt}$ , allometry) of respective tree. Data for trees with highest  $J_{st\ sum}$  per species and stand are shown (Großebebene: beech B12, oak E132; Steinkreuz: beech B4012 (1999), B4237 (2000), oak E4202 (1999), oak E4052 (2000); Farrenleite (FA): beech x4 (1999), x6 (2000)).

	1999					2000		
	Großebebene		Steinkreuz		FA	Steinkreuz		FA
	beech	oak	beech	oak	beech	beech	oak	beech
$J_{st\ sum} [10^3 \text{ kg m}^{-2} \text{ season}^{-1}]$	82.6	155.9	128.1	163.5	71.2	117.2	135.6	66.3
$J_{st\ avg} [\text{kg m}^{-2} \text{ d}^{-1}]$	529.4	999.4	625.0	797.5	468.6	592.2	685.1	414.4
number of days	156	156	197	197	152	181	188	160
$J_{st\ max} [\text{kg m}^{-2} \text{ d}^{-1}]$	1468	2653	1602	1887	1232	1673	1884	1248
$J_{st\ hh\ max} [\text{kg m}^{-2} \text{ h}^{-1}]$	121	207	151	201	111	151	142	123
DBH [cm]	39	46	39	50	31	67	37	32
$A_{st} [\text{m}^2]$	0.09	0.02	0.09	0.03	0.06	0.28	0.02	0.06
$A_{cp} [\text{m}^2]$	52.4	70.1	58.7	67.3	18.5	123.2	32.7	18.3
$A_{lt} [\text{m}^2]$	240.9	349.4	234.6	403.8	162.6	572.3	241.7	173.6
$h_t [\text{m}]$	25.5	27.0	25.5	31.1	18.1	35.5	29.5	18.5

Not all sampled trees could be used for upscaling to stand level since some thermal dissipation probes gave noisy readings which could not be filtered out, or produced otherwise unreliable output (see Tab. A11.5, Appendix). Furthermore, some trees were probed in the one year but not in the other, changing the number of trees per

size class. In order to account for these cases, daily estimates of stand water use (canopy transpiration) were adjusted for “missing” trees by means of factors derived from a regression of the “missing tree” with a well-correlated “reference tree” for a year when the “missing tree” was measured and a regression of the “reference tree” in the first year with the “reference tree” in the second year. All available daily values were used for these regressions.

No significant difference in sap flow was found at Steinkreuz between similarly-sized beech trees from the pure beech plot and the ones growing in mixture with oak (see Chap. 5.4, above). This allowed the use of the “mixed” beech trees plus the “pure” beech trees and thus increased the number of sample trees for upscaling and estimating  $E_c$  of the beech component of the mixed stand Steinkreuz (see Tab. A11.5, Appendix).

*Canopy transpiration related to tree size classes and sapwood annuli.* At Steinkreuz in 1999, the size class of intermediate beech trees showed the highest amount of seasonally integrated canopy transpiration  $E_c$  in outermost sapwood (0–2 cm) and in the following two annuli (2–4 cm and 4–6 cm sapwood depth, combined to 2–6 cm) as compared with suppressed and dominant beech trees in the same stand (Fig. 5.5.2, top panel). The dominant trees had the highest sap flow in the innermost sapwood (>6 cm, interpolated) among the three size classes, and within the dominant class innermost sapwood contributed more than any of the outer 2 cm wide annuli separately; all the outer annuli combined (0–6 cm) supplied 59 % of the sap flow in this tree class and the innermost sapwood (> 6 cm, interpolated, see above) 41 % accordingly. Dominant trees were responsible for about 50 % (97 mm season<sup>-1</sup>) of the total  $E_c$  of beech in the stand, the intermediate trees for about 41% and the suppressed trees for ca. 9 %. In 2000, the contribution of dominants was bigger (56 % or 103 mm season<sup>-1</sup>), intermediates contributed less (36 % or 66 mm season<sup>-1</sup>) and the suppressed trees about the same as in 1999 (Fig. 5.5.3). This reduction in the intermediate class was mainly due to a reduction of  $E_c$  in innermost sapwood (> 6 cm: 13 % in 1999, 6 % in 2000), which caused the contribution of outer sapwood to increase in relative terms. In dominant trees,  $E_c$  rose only marginally in all annuli in absolute and relative terms. In the class of suppressed trees, absolute  $E_c$  increased in outermost sapwood (from 8 mm season<sup>-1</sup> to 11 mm season<sup>-1</sup>) and decreased in intermediate sapwood (from 8 mm season<sup>-1</sup> to 4.5 mm season<sup>-1</sup>; innermost sapwood generally contributed only marginally in any year) so  $E_c$  increased relatively much in 0–2 cm (from 50 % to 70 %) from 1999 to 2000.

At Großebene, intermediate beech trees contributed most to total beech  $E_c$ , namely 41 mm season<sup>-1</sup> or 43 %, (dominant beech: 35 %; suppressed beech: 22 %) and  $E_c$  of both outer (0–2 cm) and intermediate sapwood (2–6 cm) was larger in the group of intermediate trees than in suppressed or dominant trees (Fig. 5.5.2, middle panel). The sap flow in innermost sapwood (>6 cm) was largest in the group of dominant beech trees.

At Farrenleite, the dominant trees showed slightly higher values in each of the annuli than the intermediate-suppressed trees and held 56 % (127 mm season<sup>-1</sup>) of total (beech = stand)  $E_c$  in 1999 (Fig 5.5.2, bottom panel). The same was true for 2000, when their contribution was 54 % (111 mm season<sup>-1</sup>; Fig. 5.5.3). The relative importance of outermost sapwood (0–2 cm) increased in both classes compared to 1999 (dominant: 43 % to 50 %; intermediate: 50 % to 59 %).

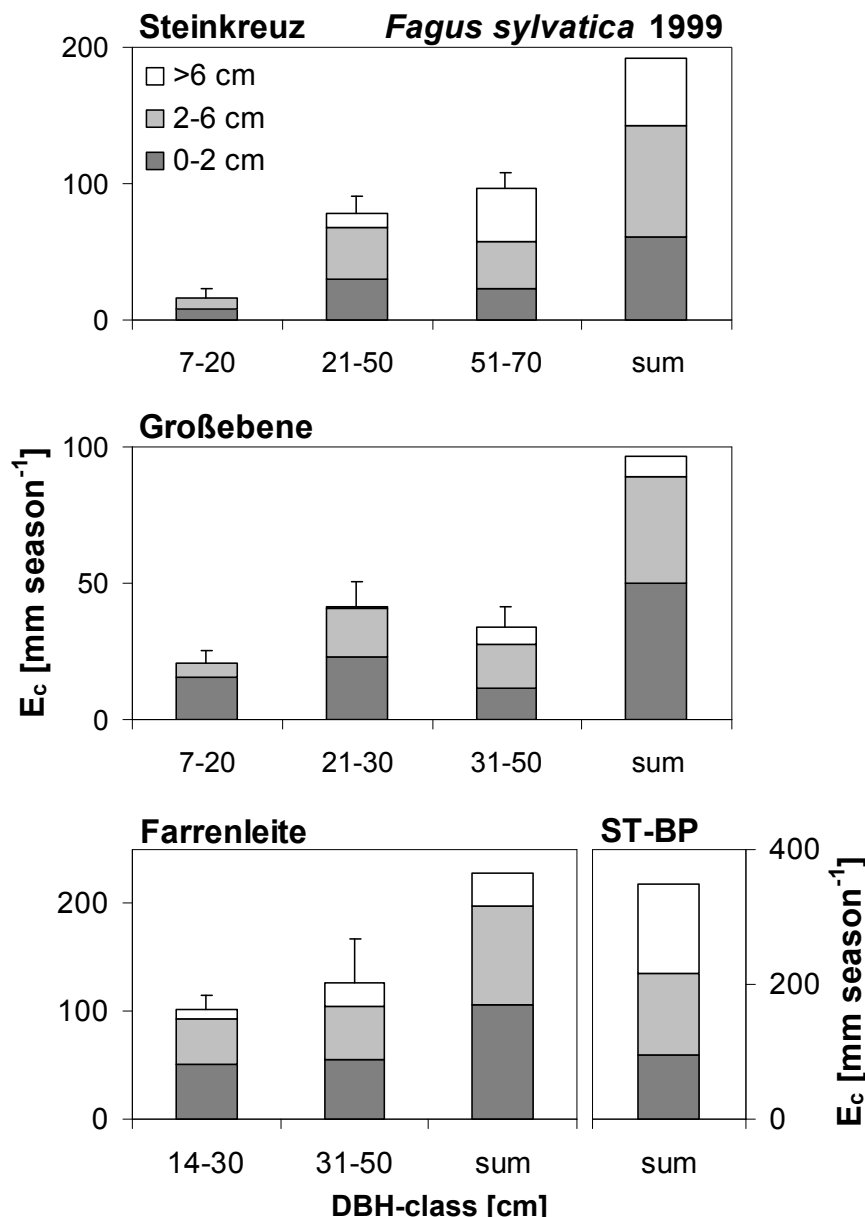


**Figure 5.5.2:** Estimates of canopy transpiration  $E_c$  as scaled from sap flow measurements and summed up for the growing season of 1999 for the beech component of the two mixed beech-oak stands in the Steigerwald (Steinkreuz and Großebene, **top** and **middle** panel, respectively) and for the pure beech in the Fichtelgebirge (Farrenleite) and the Steinkreuz-pure beech plot (ST-BP, **bottom**). Values shown are for size classes (lower and upper limit of DBH of a class is indicated on x-axis) and the contributions of the annuli of the sapwood (0–2 cm sapwood depth, 2–4 cm and 4–6 cm combined, beyond 6 cm depth). The sum of all size classes of a stand is also given. At the Steinkreuz-pure beech plot, scaling to stand level was done differently (see text) so that only the sum is shown. The  $E_c$  for the outermost 6 cm of the sapwood is measured,  $E_c$  for > 6 cm is interpolated based on Figure 7.1.4. In two trees sap flow in 2–6 cm sapwood depth was also interpolated and not measured, as well as for one tree in 2–4 cm and for three trees in 4–6 cm sapwood depth (cf. Fig. 5.4.1). Bars denote +1 SD (cumulated) for the whole size class (scaled to total sapwood area, i.e. all annuli combined).

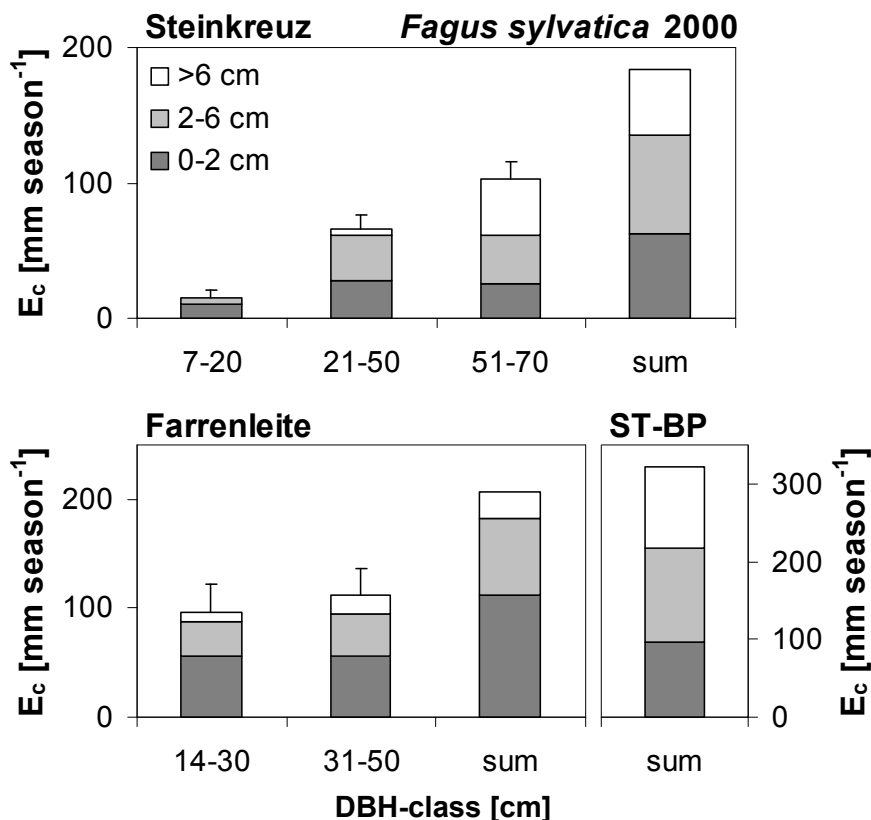


**Figure 5.5.3:** Same as Figure 5.5.2, but for the year 2000, when sap flow measurements at Großebene had been discontinued.

At the stand level, seasonally integrated  $E_c$  of beech in the outermost 2 cm of sapwood accounted for 32 %, 52 %, 46 % and 27 % of the total for beech for the stands Steinkreuz, Großebene, Farrenleite and the Steinkreuz-pure beech plot, respectively, for 1999 (cf. Fig 5.5.2). Sap flow in the outermost 6 cm of sapwood totalled 74 %, 92 %, 86 % and 62 % for the respective stands. In the year 2000,  $E_c$  in 0–2 cm sapwood depth contributed 34 %, 54 % and 30 % to the total for beech at Steinkreuz, Farrenleite and the Steinkreuz-pure beech plot, respectively (cf. Fig. 5.5.3). The outermost 6 cm supplied 75 %, 88 % and 67 % of total beech transpiration respectively, thus slightly increasing its importance from 1999 to 2000. In turn, the relative importance of innermost sapwood (> 6 cm) in total  $E_c$  of beech decreased somewhat from 1999 to 2000 with the decreasing absolute rates.

Figure 5.5.4 shows the total canopy transpiration  $E_c$  of the stands for the 1999 and 2000 growing seasons and the contribution of beech and oak.  $E_c$  ranged from  $166 \text{ mm season}^{-1}$  ( $\pm 11 \text{ mm season}^{-1}$ , i.e.  $\pm 1 \text{ SEM}$ , standard error of the mean; see also Tab. 5.5.2, below) for Großebene to  $349 \text{ mm season}^{-1}$  for the Steinkreuz-pure beech plot in 1999 with intermediate values of  $217 \pm 10 \text{ mm season}^{-1}$  and  $229 \pm 28 \text{ mm season}^{-1}$  for Steinkreuz (mixed stand) and Farrenleite, respectively. The total maximum error, including errors due to estimation of sapwood area and errors introduced by the data loggers, would amount e.g. to 29 % for  $E_c$  in beech from Steinkreuz, to 21 % in oak, and to 36 % for the total Steinkreuz stand for Gaussian error propagation. For Farrenleite, the maximum error calculated in the same way would be 28 % and 37 % for Großebene. Oak contributed only  $25 \pm 1 \text{ mm season}^{-1}$  or 12 % at Steinkreuz and  $69 \pm 7 \text{ mm season}^{-1}$  or 42 % at Großebene. In the year 2000 seasonal sums were generally somewhat lower, with  $321 \text{ mm season}^{-1}$

estimated for the Steinkreuz-pure beech plot (-8 % compared to 1999, Tab. 5.5.2), 207 mm for Farrenleite (-10 %) and 202 mm for Steinkreuz (-7 %). The  $E_c$  of the oak component at Steinkreuz decreased to 18 mm season $^{-1}$  or 9 %, a reduction by 28 % relative to 1999. Hence the beech contribution at Steinkreuz decreased by only 4 %. (Measurements at Großebene were discontinued in 2000.) Interannual differences are further analysed below (Fig. 5.5.17).

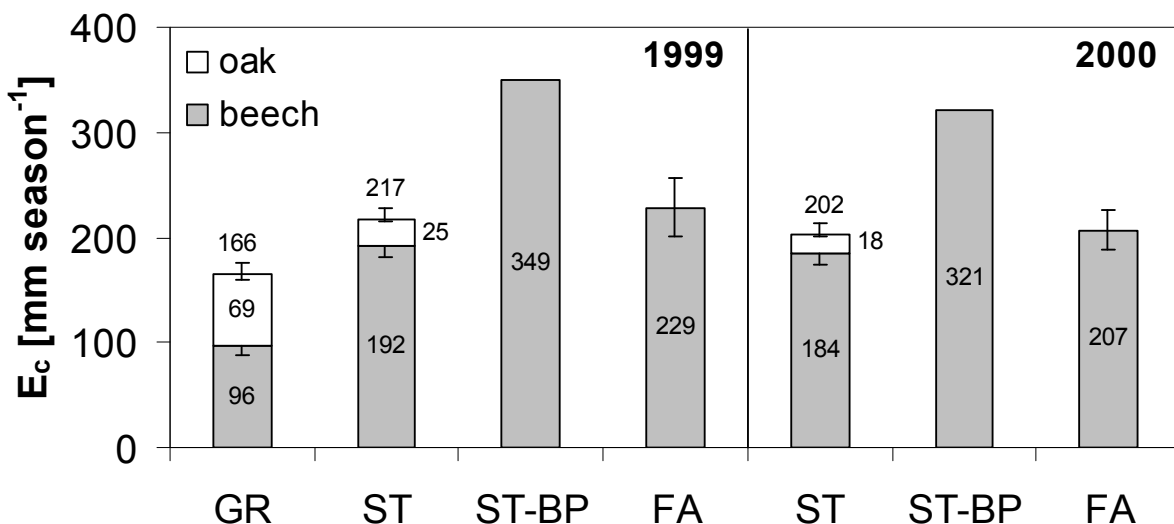


**Figure 5.5.4:** Growing seasonal sums of canopy transpiration  $E_c$ , scaled up from sap flow measurements, for the Steigerwald sites Großebene (GR), Steinkreuz (ST) and Steinkreuz-pure beech plot (ST-BP), and the Fichtelgebirge site Farrenleite (FA) for beech (shaded bars) and oak (open bars) for the years 1999 and 2000. Data for Großebene for 1999 only. Numbers in and above bars indicate beech and oak contribution and stand totals in mm season $^{-1}$ , respectively. Upscaling is based on size classes except for the Steinkreuz-pure beech plot (see text). Bars are cumulated standard errors of means for beech and oak size classes (-1 SEM, respectively) and for stand totals (+1 SEM). Because of a different upscaling approach for Steinkreuz-pure beech plot (see text) no SEM are shown for this plot.

When upscaling transpiration from tree to stand was carried out not based on tree size classes (see above), but derived from an “average tree” (i.e. averaging  $J_{st}$  for all trees of one species of a stand and multiplying this with the total sapwood area of the stand), seasonally integrated stand level estimates were about 6–7 % smaller than the size class-based ones for the mixed stands Steinkreuz and Großebene in 1999 and 2000 (not shown). Differences between both upscaling alternatives were < 5 % for Farrenleite for both years. For the Steinkreuz-pure beech plot, “average tree”-estimates of seasonal  $E_c$  were 9 % smaller in 2000 and 17 % smaller in 1999. The  $E_c$  of oak alone at Steinkreuz did not differ between the two upscaling variants for both years at all, the  $E_c$  of oak at Großebene in contrast differed by ca. 7 %. These results correspond to the sampling strategy which aimed at assessing small, intermediate and large trees at the stands Steinkreuz, Großebene and Farrenleite. So if trees did not differ in their  $J_{st}$  (or if there was no trend in  $J_{st}$  with tree size) then “average tree”-based  $E_c$  and size class-based  $E_c$  should be particularly similar, as was the case for oak at Steinkreuz and beech at Farrenleite. For the Steinkreuz-pure beech plot a larger deviation between the two upscaling approaches was to be expected because trees differed strongly in size (three largest trees holding 90 % of sapwood area) and

proportionally less in  $J_{st}$  (average  $J_{st}$  of three largest trees about 40 % larger than that of the remaining three small trees). When scaling to stand level was done on annulus-basis as in Oren et al. (1998), i.e. averaging  $J_{s,i}$  of annulus  $i$  of a size class (or all trees of the stand = “average tree”), seasonal sums e.g. for Farrenleite in 1999 were 5 % smaller (two size classes) or not different (“average tree”) than when averaging  $J_{st}$  of a size class. Differences were similarly small for the other stands.

***Stand structural controls on canopy transpiration  $E_c$ .*** As well as seasonal sums at stand level (Fig. 5.5.4, Tab. 5.5.2), seasonal maxima of daily canopy transpiration ( $E_{c\max}$ ) were generally slightly higher in the year 1999 than in 2000 (Tab. 5.5.2, below). The daily  $E_c$  reached maximum values of  $4.4 \text{ mm d}^{-1}$  for the Steinkreuz-pure beech plot in 1999, followed by the pure beech stand Farrenleite in the Fichtelgebirge with  $4.25 \text{ mm d}^{-1}$  ( $\pm 0.31 \text{ mm d}^{-1}$ , i.e.  $\pm 1 \text{ SEM}$ ) and the mixed stand Steinkreuz ( $2.72 \pm 0.10 \text{ mm d}^{-1}$ ), with beech alone contributing  $2.44 \pm 0.10 \text{ mm d}^{-1}$  and oak the remaining  $0.30 \pm 0.01 \text{ mm d}^{-1}$  (Fig. 5.5.5 and Tab. 5.5.2, below). For the other mixed stand GroßeBene, a maximum of  $2.28 \pm 0.14 \text{ mm d}^{-1}$  was scaled from sap flow measurements (beech  $1.47 \pm 0.11 \text{ mm d}^{-1}$ , oak  $0.83 \pm 0.12 \text{ mm d}^{-1}$ ). Beech alone at Steinkreuz exceeded its 1999-value with  $2.47 \pm 0.17 \text{ mm d}^{-1}$  slightly, but barely at a statistically significant level.

Relationships between  $E_{c\max}$  and stand density, leaf area index LAI, basal area  $A_b$  and sapwood area  $A_s$  of the stands or stand components were investigated in Figure 5.5.5.  $E_{c\max}$  increased with stand density for the oak component of the mixed stands Steinkreuz and GroßeBene (Fig. 5.5.5a, open symbols) as well as within each mixed stand (oak < beech < stand; additive effect).  $E_{c\max}$  decreased with increasing stand density for the beech components of the mixed stands (shaded symbols) and for the total mixed stands (filled symbols). The pure beech stands (crosses) did not show a clear relationship;  $E_{c\max}$  peaked at maximum stand density (Farrenleite: 883 trees  $\text{ha}^{-1}$ ), but the small pure beech plot had the same  $E_{c\max}$  at about 32 % of the stand density of Farrenleite.  $E_{c\max}$  increased with LAI for the oak component of the mixed Steinkreuz and GroßeBene stands (Fig. 5.5.5b) as well as for the beech component and the total mixed stands. The pure beech stands Farrenleite and Steinkreuz-pure beech plot showed much higher values of  $E_{c\max}$  at slightly higher LAI than the mixed stands. Within GroßeBene, oak had lower  $E_{c\max}$  than beech at comparable or slightly higher LAI. Results for stand basal area  $A_b$  (Fig. 5.5.5c) were similar to those for LAI. The lower  $E_c$  of oak at GroßeBene at higher  $A_b$  compared to beech at GroßeBene or Steinkreuz is remarkable.  $A_b$  obviously has a different quality in beech and oak, pointing to the different proportion of hydroactive xylem on the total cross-sectional area. In agreement with this finding,  $E_{c\max}$  scaled rather well with stand sapwood area  $A_s$  (Fig. 5.5.5d) in that the increase of  $E_{c\max}$  with  $A_s$  was steady up to a maximum value at about  $30 \text{ m}^2 \text{ sapwood area ha}^{-1}$ . A further rise in  $A_s$  did not augment  $E_{c\max}$  any more.  $E_{c\max}$  related to LAI ( $E_{c\max}/\text{LAI}$ , Fig. 5.5.5e) seemed to remain stable over the range of the observed LAI for mixed stands and their components individually and possibly for pure beech stands as well, but the latter varied hardly in their LAI. Beech displayed a higher ratio  $E_{c\max}/\text{LAI}$  than oak, and pure beech stands exhibited higher values than mixed stands or than the beech component of the mixed stands.  $E_{c\max}$  related to  $A_s$  (Fig. 5.5.5f) may be declining with  $A_s$  in pure beech stands and increasing in mixed stands and in their components, but the data presented from four plots are not sufficient to draw general conclusions. Using data from the year 2000 only or adding them to the data presented in Figure 5.5.5 did not change any of the above findings.

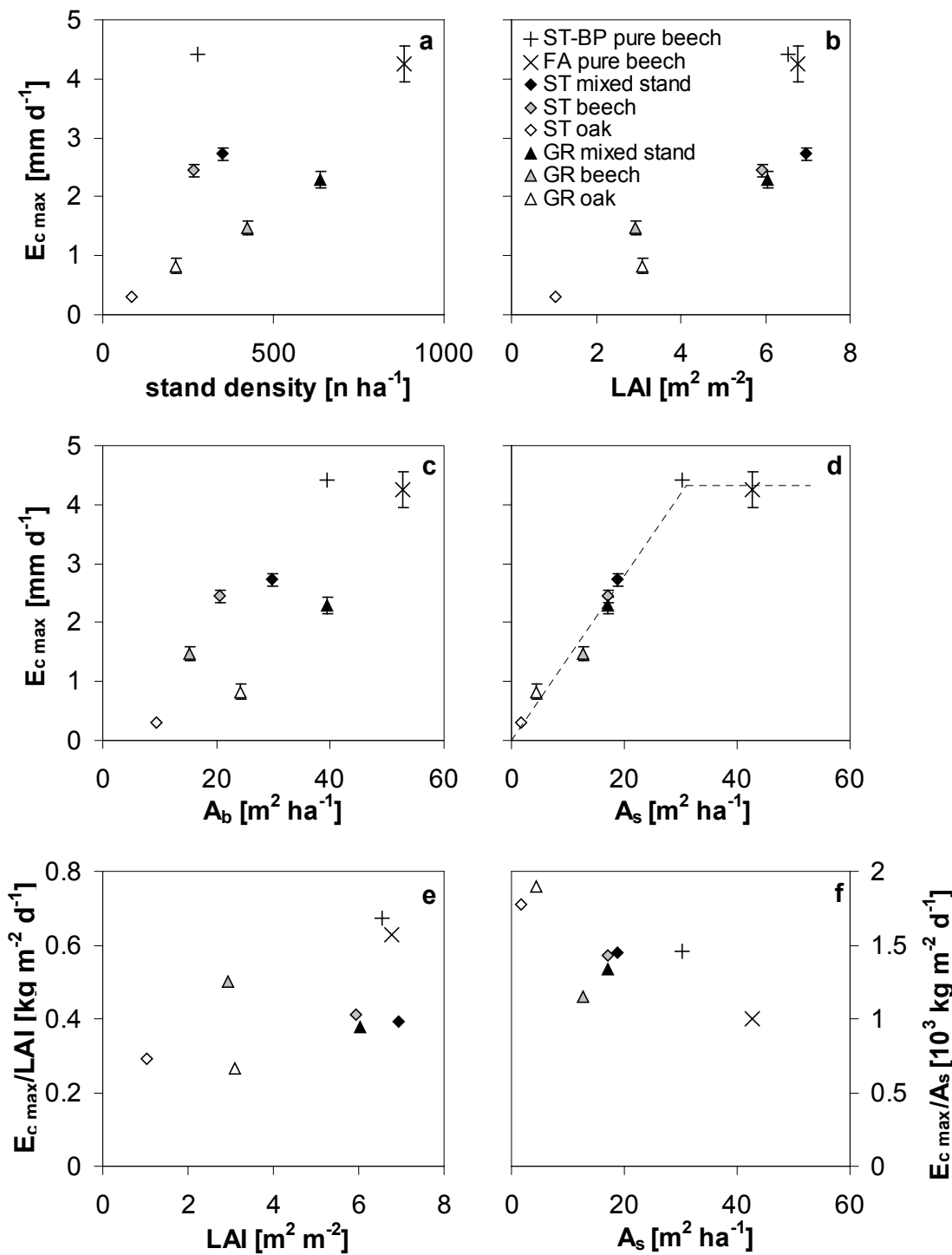


**Figure 5.5.5:** Relationships between seasonal maximum daily integrated canopy transpiration  $E_{c \max}$  and stand density (a), leaf area index LAI (b), basal area  $A_b$  (c) and sapwood area  $A_s$  (d), respectively, and relationships between  $E_{c \max}/\text{LAI}$  and LAI (e) and  $E_{c \max}/A_s$  and  $A_s$  (f), for the investigated stands and for the two species separately (open symbols for oak, shaded for beech, filled for mixed stands, crosses for pure beech stands, respectively). The dashed line is fitted by eye. Bars are  $\pm 1 \text{ SEM}$  and shown where applicable and when larger than the symbol. Data from 1999 are shown; data from 2000 are slightly lower but similar and omitted for clarity of the graphs.

**Table 5.5.2:** Seasonal maximum daily values of canopy transpiration ( $E_{c\ max}$ ), average vapour pressure deficit of the air ( $D_{avg}$ ) and daily integrated photon flux density ( $PFD_{day}$ ) and average air temperature ( $T_{air\ avg}$ ) at the respective day, growing seasonal sums of canopy transpiration ( $E_c$  and standard error of the mean, SEM) , seasonally integrated D ( $D_{int}$ ), seasonally integrated PFD ( $PFD_{int}$ ), number of sap flow days, maximum leaf area index (LAI) and sapwood area of a species ( $A_s$ ) for the investigated stands (GR = GroßeBene, ST-BP = Steinkreuz-pure beech plot) for 1999 and 2000 and changes from 1999 to 2000 (% change). No data for GroßeBene from 2000 available. LAI for Farrenleite is for the year 1998 (average of optical and litter-based estimates, cf. Tab. 5.1.3.2) since no data was available for 1999 and 2000.

	GR beech 1999	GR oak 1999	GR stand 1999	Steinkreuz beech		Steinkreuz oak		Steinkreuz stand		ST-BP stand		Farrenleite stand	
$E_{c\ max}$ [mm d <sup>-1</sup> ]	1.5	0.83	2.3	2.4	2.5	0.29	0.20	2.7	2.6	4.4	4.2	4.3	3.9
% change					1		-30		-4		-5		-9
$D_{avg}$ [hPa]	13.2	4.7	13.2	13.2	10.1	13.2	10.4	13.2	10.1	13.2	17.2	12.5	16.3
% change					-23		-21		-23		30		30
$PFD_{day}$ [mol m <sup>-2</sup> d <sup>-1</sup> ]	56.5	31.8	56.5	56.5	43.8	56.5	38.5	56.5	43.8	56.5	52.0	46.3	49.7
% change					-23		-32		-23		-8		7
$T_{air\ avg}$ [°C]	22.8	14.5	22.2	22.8	22.2	22.8	21.7	22.8	22.2	22.8	22.7	22.9	20.4
% change					-3		-5		-3		-1		-11
$E_c$ [mm season <sup>-1</sup> ]	96	69	166	192	184	25	18	217	202	349	321	229	207
(± 1 SEM)	(± 8)	(± 7)	(± 11)	(± 10)	(± 10)	(± 1)	(± 1)	(± 10)	(± 11)			(± 28)	(± 19)
% change					-4		-28		-7		-8		-9
$D_{int}$ [kPa season <sup>-1</sup> ]	81.5	81.5	81.5	81.5	75.9	81.5	75.9	81.5	75.9	81.5	75.9	58.3	65.3
% change					-7		-7		-7		-7		12
$PFD_{int}$ [mol m <sup>-2</sup> season <sup>-1</sup> ]	5251	5251	5251	5251	5246	5251	5246	5251	5246	5251	5246	3661	3641
% change					-0.1		-0.1		-0.1		-0.1		-1
sap flow days	197	201	205	197	188	201	191	205	198	197	188	152	160
% change					-5		-5		-3		-5		5
LAI	2.9	3.1	6.0	5.9	6.0	1.0	0.9	6.9	6.9	6.5	6.8	6.8	
% change					1		-13		0		1		
$A_s$ [m <sup>2</sup> ha <sup>-1</sup> ]	12.8	4.4	17.2	17.1	17.7	1.69	1.71	18.8	19.4	30.2	30.6	42.7	42.7
% change					4		1		3		1		

Seasonal courses of daily canopy transpiration. In Figure 5.5.6 and Figure 5.5.7 seasonal courses of  $E_c$  are presented for the two mixed oak-beech sites and the two pure beech sites for the years 1999 and 2000, respectively. In 1999 (Fig. 5.5.6), leaf unfolding commenced in beech trees at Steinkreuz and Großebene in the Steigerwald around April 22 (day 112) and about four days later in oaks (cf. Tab. 5.2.1.2). This was simultaneously detectable in the sap flow signal. The last day with significant sap flow was November 4 (day 308) and November 12 (day 316) in 1999 for beech and oak in the Steigerwald, respectively. This resulted in a sap flow-based length of a growing period of 205 days for the whole stand (beech + oak). At Farrenleite, leaf unfolding and sap flow began around May 4 (day 124) in 1999 (Tab. 5.2.1.2), and October 2 (day 275) was already the last day with significant sap flow under beneficial atmospheric conditions in the large study trees, adding to 152 days of sap flow at this site. In smaller trees or in the inner sapwood of larger trees sap flow had already ceased on September 24 (day 267). The highest daily  $E_c$  was found during June and July, peaking on July 3 (Steinkreuz beech and oak, Steinkreuz-pure beech plot, Großebene beech), July 5 (Farrenleite) and July 22 (Großebene oak), respectively (Tab. 5.5.2).

In 2000 (Fig. 5.5.7) leaf-flushing at Steinkreuz began around April 19 (day 110) in sub-canopy beech trees, where sap flow commenced the same day; in dominant overstory beech trees sap flow started on April 21 (day 112). By day 117 all beech trees had started to leaf out and oaks had begun to flush as well. After October 22 and 24 (days 296 and 298) sap flow was marginal in oak and beech, respectively. On October 28 (day 302), some dominant and suppressed beech as well as a few oak trees were bare of leaves. No more sap flow was traceable in the studied trees after November 2 (day 307), bringing the sap flow-based length for beech + oak of the vegetation period to 198 days.

At Farrenleite, leaves started to flush on April 26 in the year 2000 (day 117; Tab. 5.2.1.2), and on April 27 sap flow was detectable in the first tree (x4, largest tree), followed mainly by smaller trees on April 28 (x3) and April 29 (x2, x7, x 5). By May 3 (day 124), all study trees showed significant sap flow. In autumn 2000 sap flow decreased early at Farrenleite. Significant values of  $J_s$  were recorded only until September 30 (day 274) in the majority of trees, while in trees x1 and x4 marginal sap flow was detectable until October 3 (day 277), which was the last day with favourable atmospheric conditions, summing to 160 days of sap flow. Maximum daily  $E_c$  was observed in 2000 in June (Steinkreuz beech: June 10; Steinkreuz-pure beech plot and Farrenleite: June 19) or August (Steinkreuz oak: August 14; Tab. 5.5.2).

Generally, the contribution of oak to total  $E_c$  was lower than that of beech in both mixed stands, even though oak dominated the canopy at Großebene. The relative  $E_c$  of oak increased on rainy days when the canopy was wet and then even exceeded that of beech at Großebene. This may have been caused by faster drying of the more water repellent waxy oak leaves, and after rain sap flow recovered fastest in oaks, followed by dominant overstory beech and was most delayed in suppressed sub-canopy beech. In 1999, the relative  $E_c$  of oak at Großebene exceeded that of beech also towards the end of the season when soil water content was decreasing; at Steinkreuz this was observed only at the time of leaf shedding in beech.

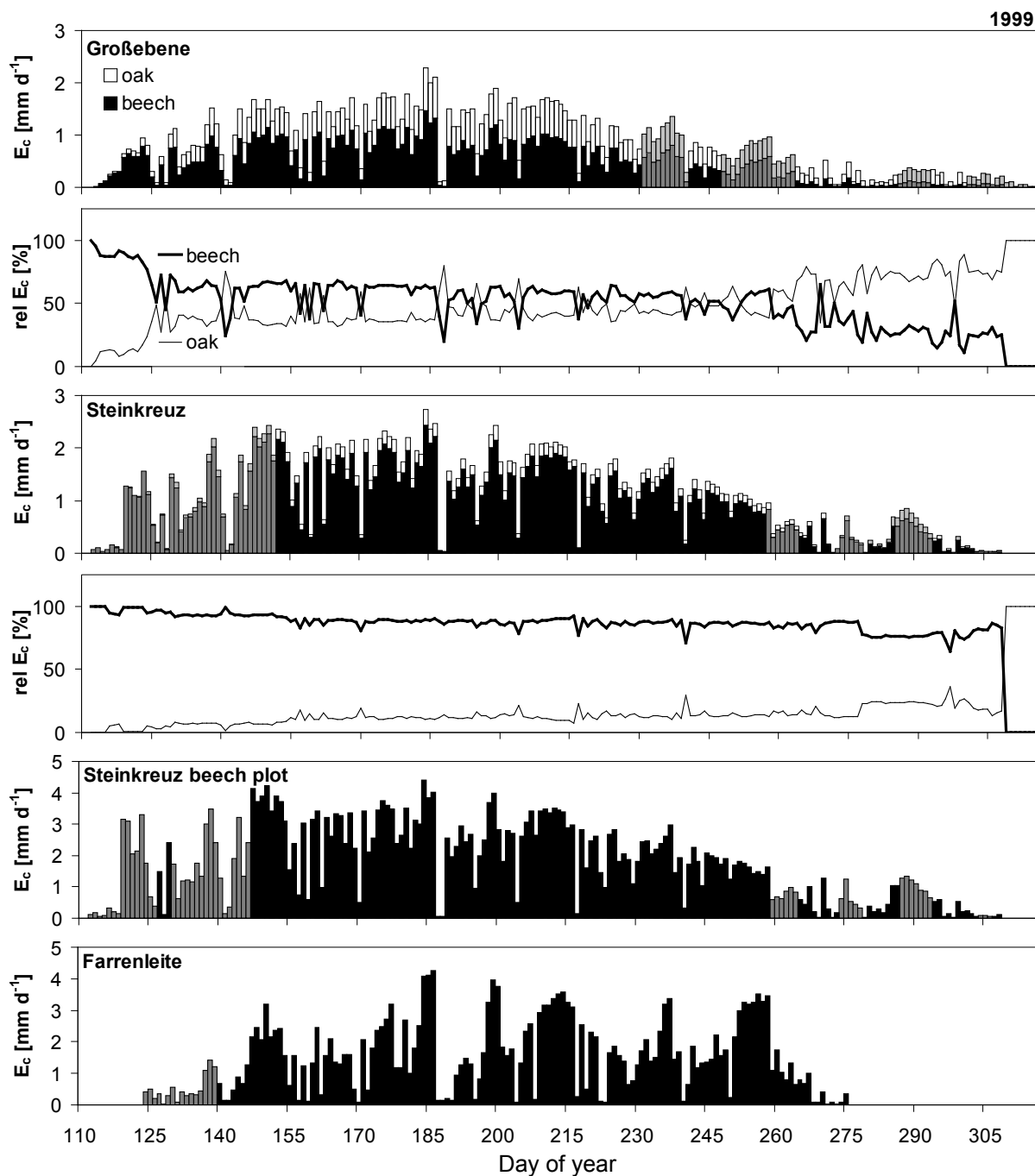


**Figure 5.5.6:** Seasonal course of canopy transpiration  $E_c$  scaled-up from sap flow of oak (open bars) and beech (filled bars) for the four study sites in 1999 and relative  $E_c$  (rel  $E_c$ ) indicating the contribution of oak and beech to total  $E_c$  of the mixed stands. Shaded bars signify gap-filled data that were approximated using relationships with the vapour pressure deficit of the air D and accounting for increasing (or decreasing) leaf area at this phenological stage as observed during the year 2000.

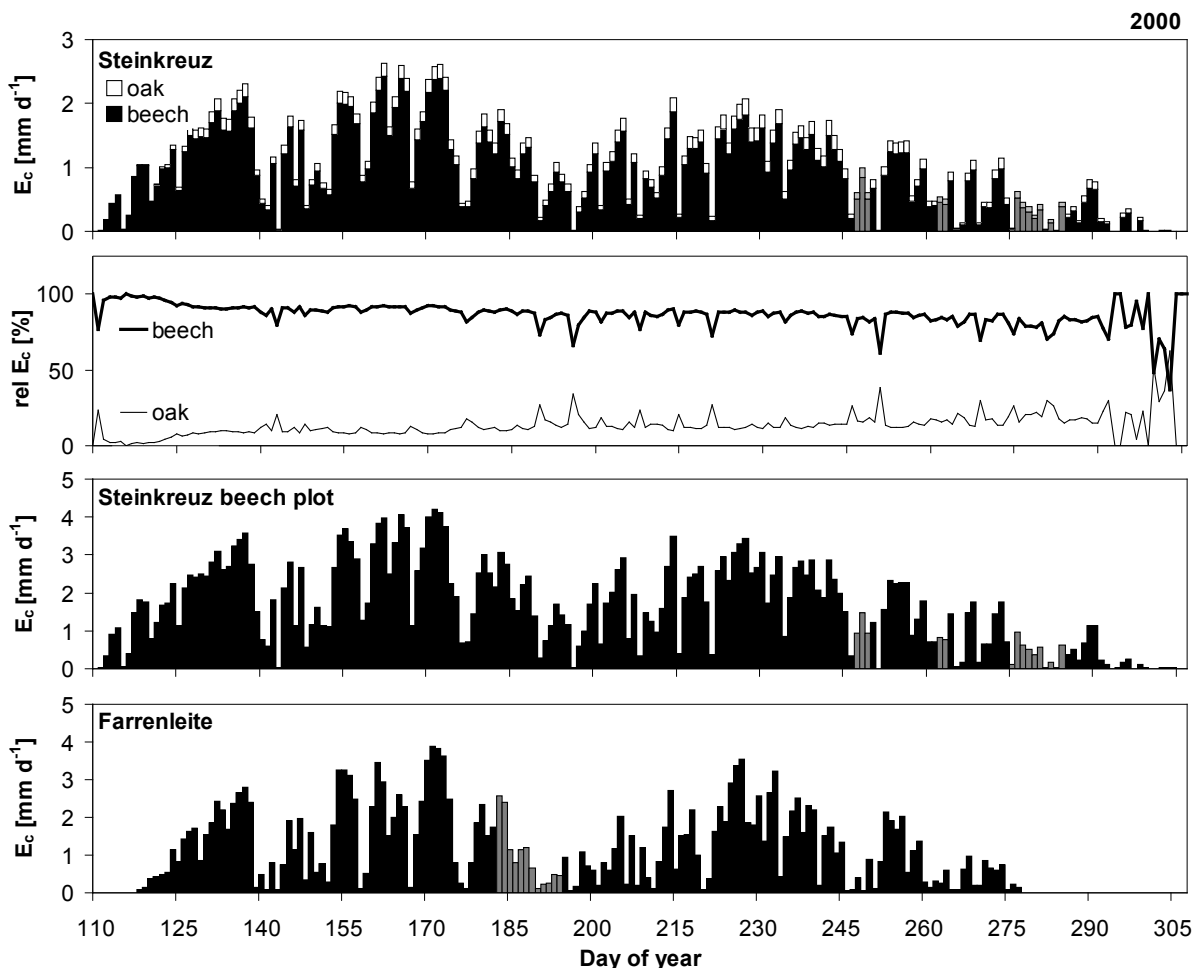


**Figure 5.5.7:** Same as in Figure 5.5.6 for the year 2000, when the mixed Großebeine stand was not monitored any more.

Most of the time, patterns of  $E_c$  were similar among sites, with “low flow-days” (low sap flow on overcast rainy days) and “high flow-days” occurring simultaneously in the Steigerwald and the Fichtelgebirge (Chap. 5.2.2). However, deviations between the Steigerwald and the Fichtelgebirge occurred for instance in late summer when thunderstorms occurred locally (e.g. on September 7, 1999, day 250). Apart from such short-term variation between the two landscapes, quantitative differences in  $E_c$  can be distinguished as well, as depicted in Figure 5.5.8.

Figure 5.5.8 compares the  $E_c$  of the two pure beech sites at the Steigerwald and the Fichtelgebirge during 1999 and 2000. The later and slower leaf development and the earlier leaf shedding are obvious at the higher elevation site Farrenleite, particularly in 1999 (Fig. 5.5.8a, c). The difference between the two sites from approx. day 251 to 266 (8.–23.09.) in 1999 is remarkable, when transpiration was strongly reduced at the Steinkreuz-beech plot ( $E_c$  of Farrenleite reaching > 230 % of  $E_c$  at Steinkreuz, Fig. 5.5.8) due to soil water shortage but not at Farrenleite; at the former, soil water content dropped to about twice as low as at the latter site in 1999 (see Fig. 5.2.2.2, and Figs. 5.5.16, 5.5.17, below). Prior to this, there had been a phase at the end of July/beginning of August 1999 already (day 209–216) when the  $E_c$  of Farrenleite was

as high or higher than the  $E_c$  of the Steinkreuz-beech plot (at high rates) during a dry spell. Integrated over the whole season, soil water depletion at Steinkreuz was about 1.8 times that of Farrenleite (Chap. 5.2). In 2000, when the relative extractable soil water  $\theta_e$  decreased to minimum values of merely about 70 to 80 % of 1999 at Steinkreuz, no pronounced difference was observed between the two sites, and the cumulated difference (Fig. 5.5.8d) increased slower than in 1999. In August 2000 (day 214–244),  $E_c$  at Farrenleite was relatively high compared to  $E_c$  at the Steinkreuz-pure beech plot, possibly due to better atmospheric conditions, in particular the higher vapour pressure deficit of the air (D), see Fig. 5.5.11, below).

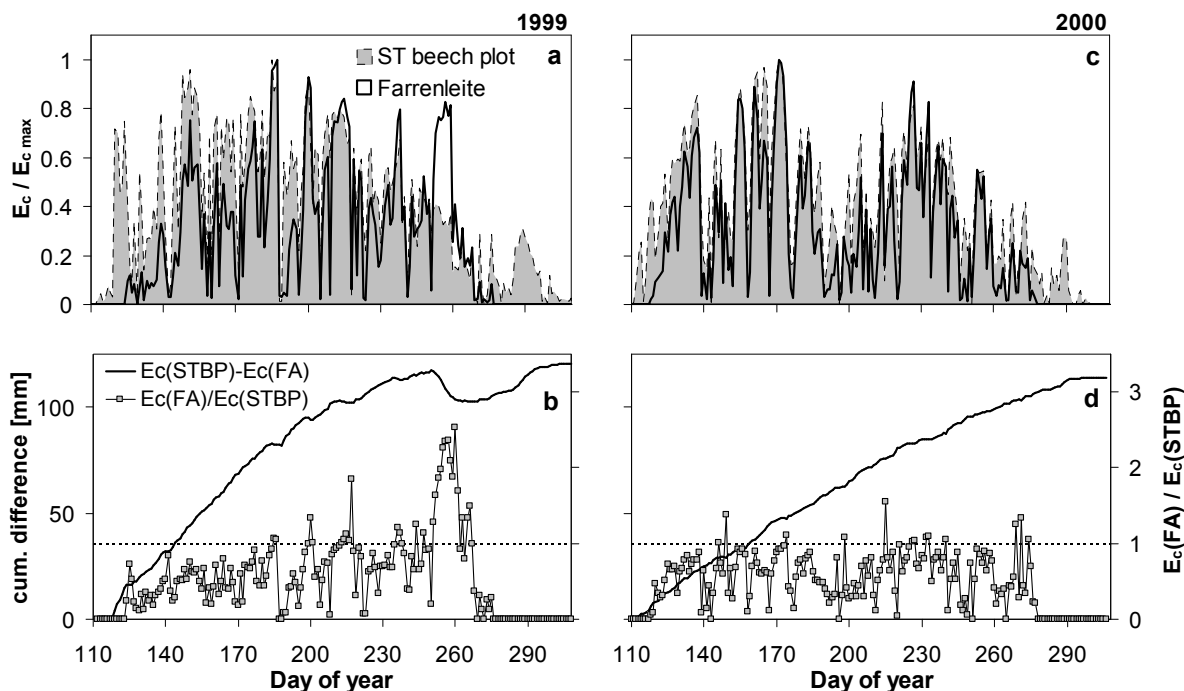


**Figure 5.5.8:** Seasonal course of canopy transpiration  $E_c$  relative to maximum seasonal  $E_c$  ( $E_c/E_{c \text{ max}}$ ) for the two pure beech sites (Steinkreuz-beech plot, broken line, and Farrenleite, bold line, in the Steigerwald and the Fichtelgebirge, respectively) during 1999 (a) and 2000 (c), and the cumulative difference of  $E_c$  between the Steinkreuz-beech plot (STBP) and Farrenleite (FA; bold line) and the ratio of  $E_c$  of Farrenleite to the  $E_c$  of the Steinkreuz-beech plot (thin line with squares) for the same years (b, d). The dashed line in b and d indicates where the ratio  $E_c(\text{FA})/E_c(\text{STBP})$  equals 1; the ratio was calculated only for days where the  $E_c$  of STBP was  $>0.1 \text{ mm d}^{-1}$ .

**Atmospheric controls.** In addition to the structural drivers of  $E_c$  that act on seasonal to annual scales (see above), the most important atmospheric drivers controlling  $E_c$  on shorter temporal scales are vapour pressure deficit of the air (D) and photosynthetical photon flux density (PFD). In Figure 5.5.9, the daily values of  $E_c$  of beech, oak and stand totals are plotted against the daily average D ( $D_{\text{avg}}$ ) for 1999.  $E_c$  followed a saturation curve, at Farrenleite alone this was somewhat less obvious; initial slopes of the relationship were steeper for the Steinkreuz-pure beech plot than for Farrenleite, while the plateau values were higher for Farrenleite. Beech in the mixed Steinkreuz stand displayed a steeper initial increase of  $E_c$  with  $D_{\text{avg}}$  than beech at Große Ebene, meanwhile for oak it was the opposite (for all the three periods shown). In August and September,  $E_c$  was reduced at all sites compared to June–July, except at

Farrenleite, where there was only a change from August to September.  $E_c$  was smaller in April and May, limited by leaf development, and the relationship with  $D_{avg}$  was linear then (not shown). After September, the range of  $D_{avg}$  became very small and so did  $E_c$  (not shown). Values of regression parameters and statistics are summarised in Table A11.6, Appendix.

The relationship of  $E_c$  with daily integrated PFD ( $PFD_{day}$ , Fig. 5.5.10) was more linear – at a larger scatter of data points – and showed less of a saturation than with  $D_{avg}$ , particularly in beech at Steinkreuz and Großebene and even more so at Farrenleite. In autumn, but already beginning in August, the maximum daily sums of PFD were restricted to 60–70 % of the June–July values. Analogously to the relationship of  $E_c$  with  $D_{avg}$ , beech in the mixed Steinkreuz stand exhibited a steeper initial increase of  $E_c$  with  $PFD_{day}$  than beech at Großebene, and the opposite was the case for oak (for all the three periods shown). Taking into account the relatively large scatter, Farrenleite and the Steinkreuz-pure beech plot could be regarded as responding in a similar way to  $PFD_{day}$  as to  $D_{avg}$ : initial slopes of the relationship of  $E_c$  to  $PFD_{day}$  were steeper for the Steinkreuz-pure beech plot than for Farrenleite, except in September, and plateau values were higher for Farrenleite, aside from perhaps June–July.

In the year 2000, very high values of  $D_{avg}$  were recorded in June (Fig. 5.5.11); initial slopes of the regressions of  $E_c$  with  $D_{avg}$  for June–July at Steinkreuz were lower than in 1999, plateau values were similar but were reached at higher values of  $D_{avg}$  (see also Tab. A11.6, Appendix). In August 2000, the situation was reversed in that  $E_c$  reached higher values despite maximum  $D_{avg}$  being lower than in 1999. This pattern continued through September 2000 when  $D_{avg}$  hardly reached 5 hPa. At Farrenleite, initial slopes were similar to 1999 for all three periods, but plateau values were generally lower than in 1999. Compared to the Steinkreuz-pure beech plot, initial slopes at Farrenleite were less steep – as in 1999 –, but  $E_c$  at Farrenleite was lower at the same  $D_{avg}$  than at the Steinkreuz-pure beech plot, unlike in 1999. During the periods of 2000 shown (Fig. 5.5.11), the response of canopy transpiration to  $D_{avg}$  did not change markedly (for the range of  $D_{avg}$  common to all periods), in contrast to 1999 (just at Farrenleite there were no distinct difference between the periods).

As in 1999, the response of  $E_c$  to  $PFD_{day}$  in 2000 (Fig. 5.5.12) was more linear than that of  $E_c$  to  $D_{avg}$ ; at Farrenleite regression curves were somewhat more saturating in 2000 than in 1999. At Steinkreuz, the relationship of  $PFD_{day}$  and  $E_c$  was weaker in initial slope and plateau values than in 1999 for beech in June–July, similar in August and higher in September. For oak the same was found, except that in September 1999 oak revealed a much stronger slope and higher maximum values of  $E_c$  at the same  $PFD_{day}$ . The  $E_c$  of the Steinkreuz-pure beech plot behaved very similar to Farrenleite regarding the response of  $E_c$  to  $PFD_{day}$  in 2000 (all three periods; Fig. 5.5.12). As for  $D_{avg}$ , relationships of  $E_c$  with  $PFD_{day}$  hardly changed from June to September, unlike in 1999.

Coefficients of determination were higher for regressions with  $D_{avg}$  than with  $PFD_{day}$  (average  $R^2$  for all sites, periods and years 0.840 and 0.784, respectively) and higher for beech than for oak (average  $R^2$  for  $D_{avg}$ : 0.857 vs 0.782; for  $PFD_{day}$ : 0.811 vs 0.713, respectively).

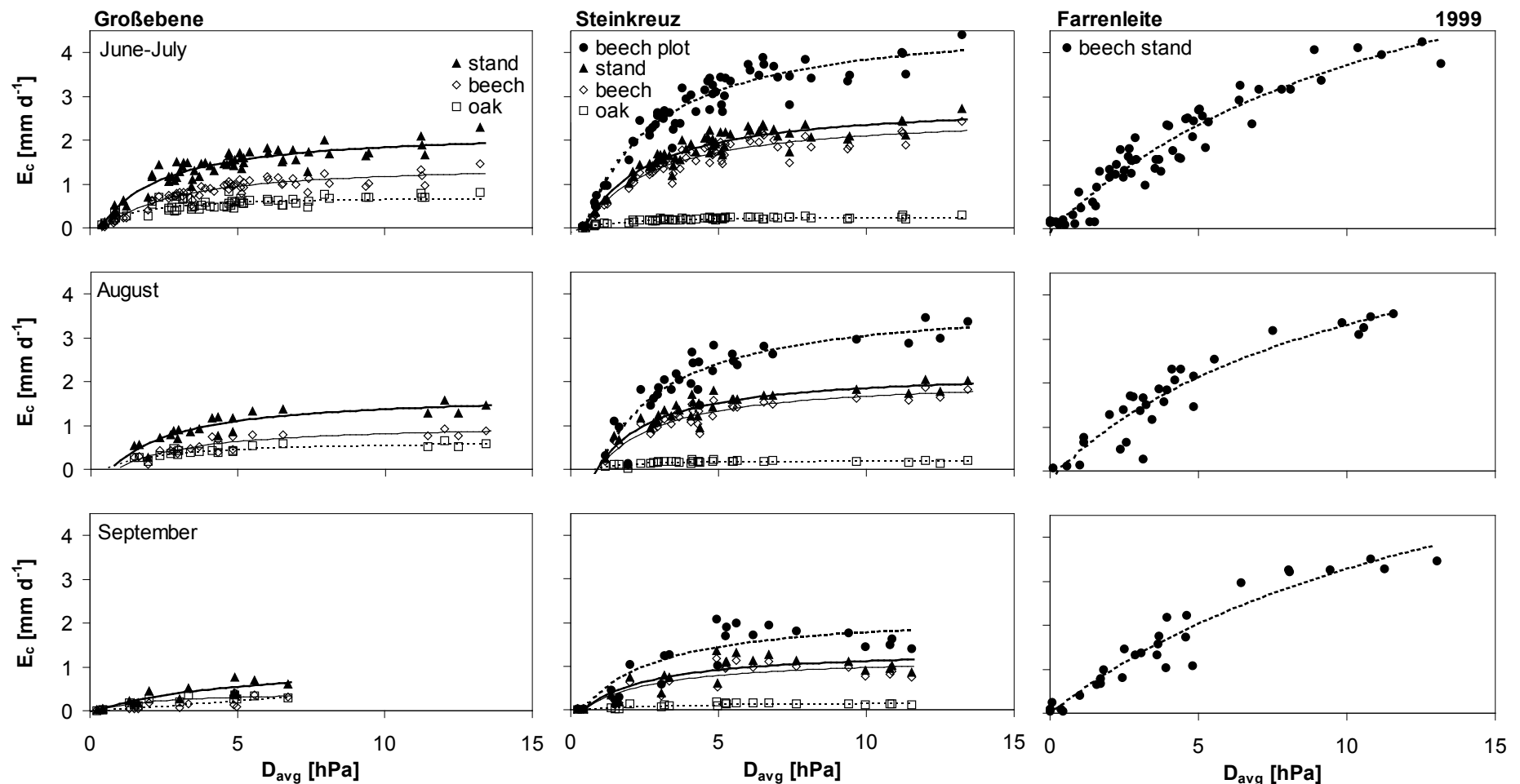


**Figure 5.5.9:** Relationships of daily average vapour pressure deficit of the air ( $D_{\text{avg}}$ ) and daily canopy transpiration ( $E_c$ ) of the study sites for different periods of the growing season of 1999. Values for beech, oak and the total mixed stands are shown.  $D_{\text{avg}}$  is the 24 h-average of 10'-average values of  $D$ . A hyperbolic rectangular model (e.g. Owen et al. 2007) was used for regression analysis ( $E_c = (\alpha \cdot \beta \cdot D_{\text{avg}})/(\alpha \cdot D_{\text{avg}} + \beta) + \gamma$ ), where  $\alpha$  is the initial slope of the response curve,  $\beta$  the plateau parameter and  $\gamma$  the intercept. For parameter values and statistics see Table A11.6, Appendix. Larger data gaps exist at Großebene: 19.–28.08., 5.–20.09.1999, and at Steinkreuz: 15.–21.09., 30.09.1999.

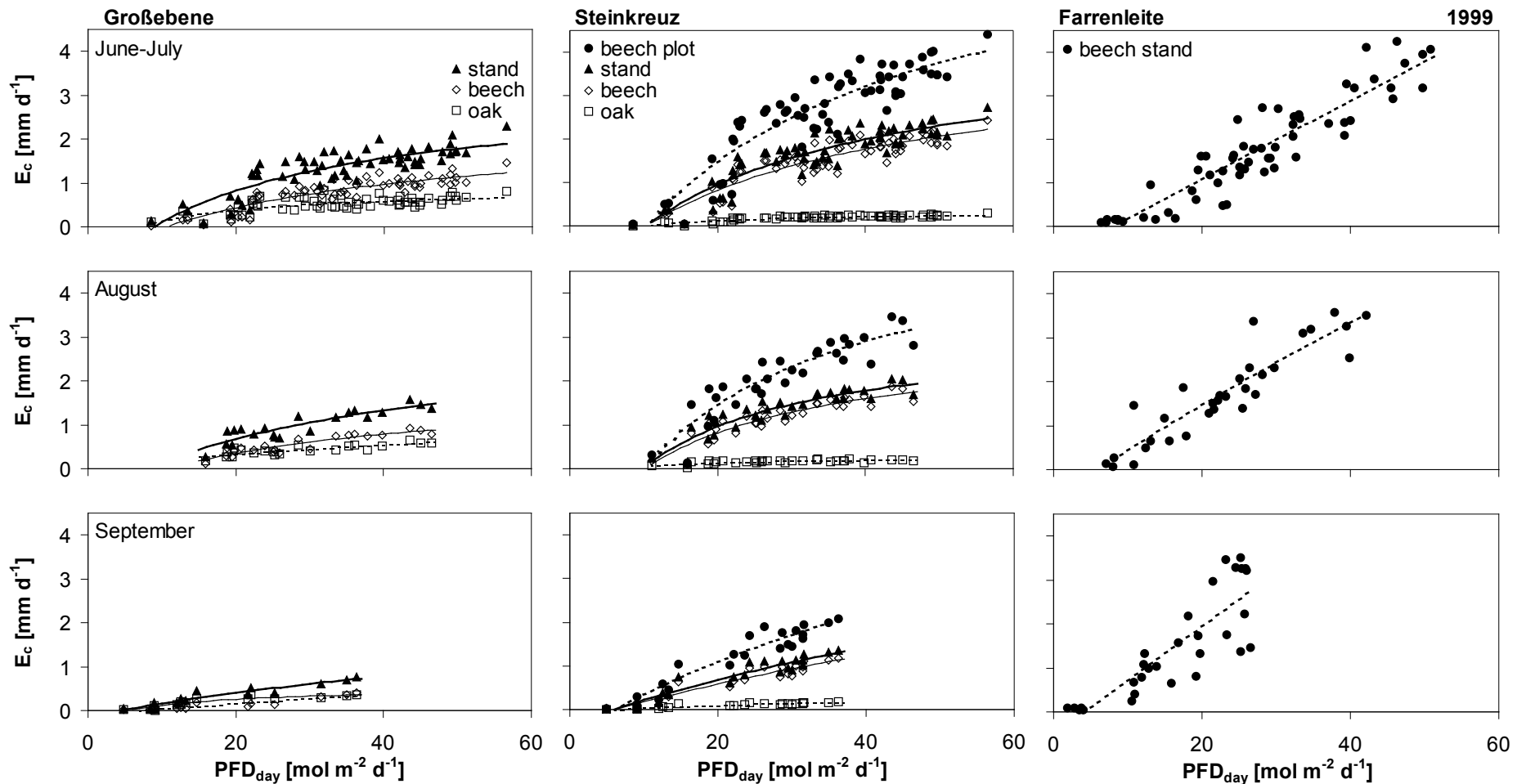


**Figure 5.5.10:** Relationships of daily integrated photosynthetic photon flux density ( $PFD_{day}$ ) and daily canopy transpiration ( $E_c$ ) of the study sites for different periods of the growing season of 1999. Values for beech, oak and total mixed stands are shown.  $PFD_{day}$  is the 24 h-sum of 10' average values of PFD. The same regression model was used as in Figure 5.5.9. Parameter values and statistics given in Table A11.6, Appendix.



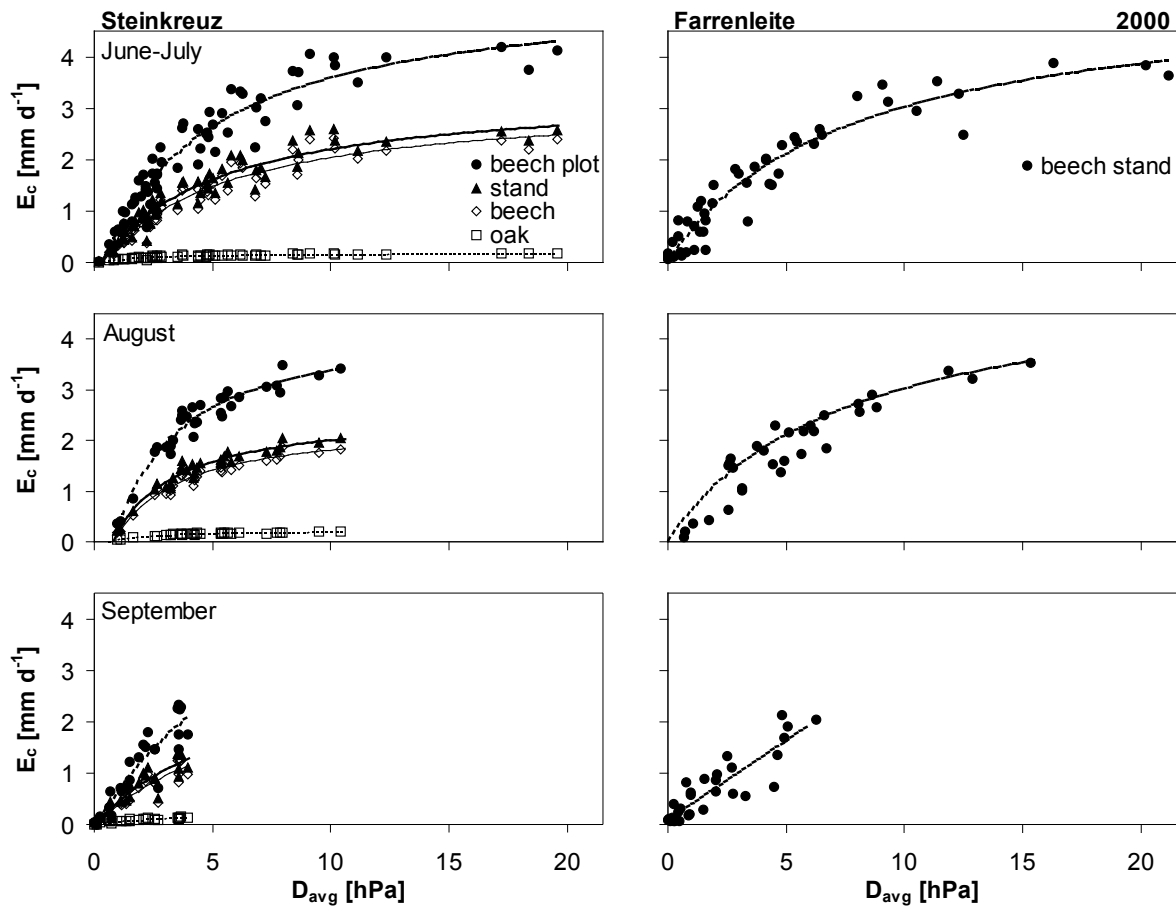


**Figure 5.5.11:** Relationships of daily average vapour pressure deficit of the air ( $D_{avg}$ ) and daily canopy transpiration ( $E_c$ ) of the study sites for the year 2000. See also caption of Figure 5.5.9.

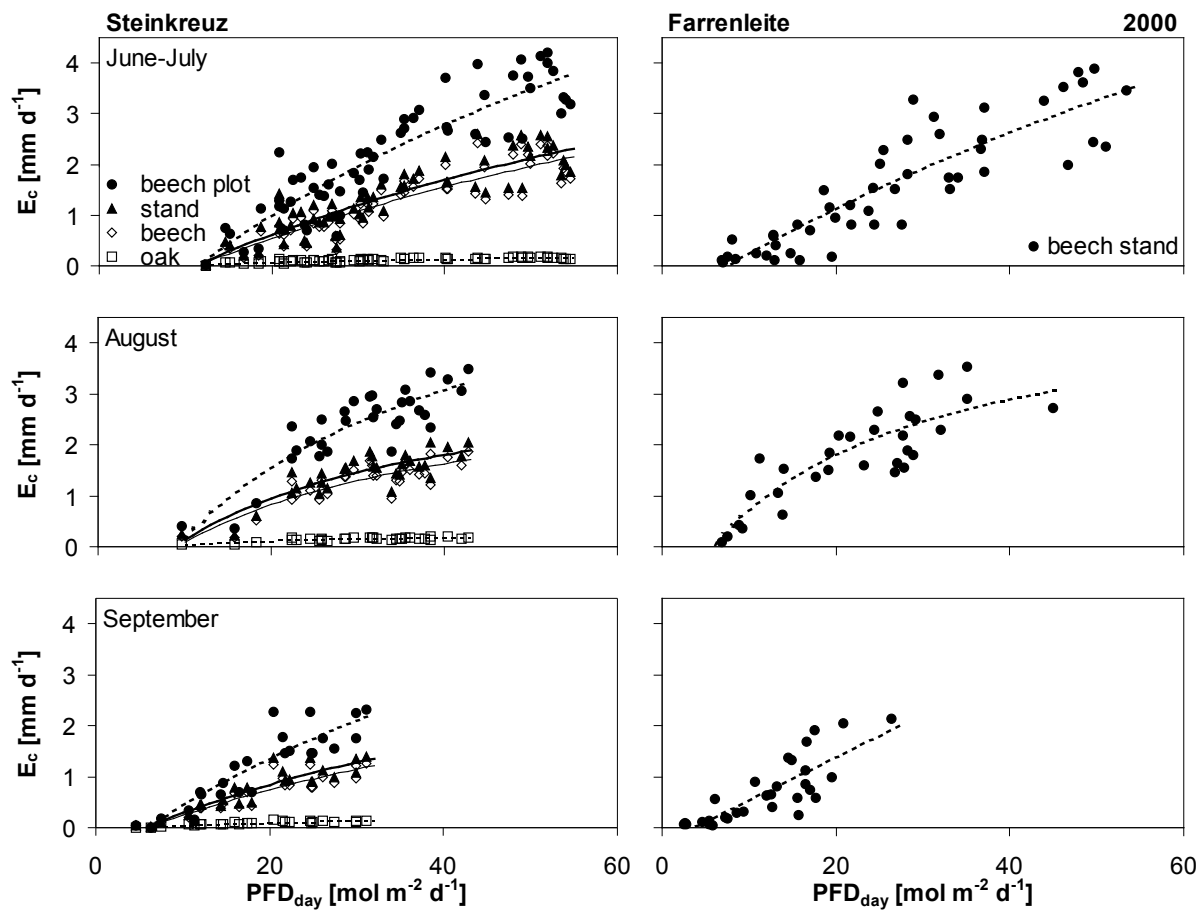


**Figure 5.5.12:** Relationships of daily integrated photosynthetic photon flux density ( $PFD_{day}$ ) and daily canopy transpiration ( $E_c$ ) of the study sites for the year 2000. See also caption of Figure 5.5.10.

As seen in Figure 5.5.10 and 5.5.12,  $E_c$  increased with PFD. Consequently  $E_c$  increased in the same way with net radiation  $R_n$ . When  $R_n$  is expressed in hydrological units ( $\text{mm d}^{-1}$ ) the amount of available net radiation used for transpiration can be estimated as exemplified in Figure 5.5.13. Except for days with intermittent rain or comparatively low D, only about 20–70 % of  $R_n$  was used for transpiration (based on regression equations shown in Fig. 5.5.13 for  $R_n > 1 \text{ mm d}^{-1}$ ). This indicates that available energy generally was not limiting transpiration. The use of  $R_n$  was particularly low at Großebene (20–30%). Ratios were somewhat higher in 2000, indicating better utilisation of radiation for vapourisation of water.

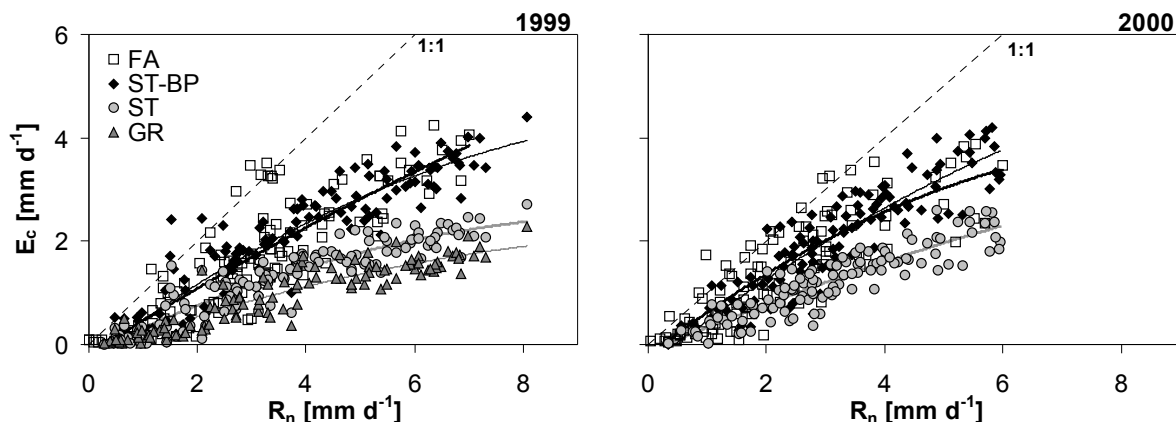


**Figure 5.5.13:** Relationships between daily integrated net radiation ( $R_n$ , daytime values only, expressed in hydrological units, where  $1 \text{ mm d}^{-1} \approx 2.46 \text{ MJ m}^{-2} \text{ d}^{-1}$ , see Köstner 2001) and daily canopy transpiration  $E_c$  for the pure beech sites Farrenleite (FA, open squares), the Steinkreuz-pure beech plot (ST-BP, filled diamonds) and the mixed Steinkreuz (ST, shaded circles) and Großebene stands (GR, dark shaded triangles, 1999 only) for the years 1999 (left) and 2000 (right). Regression equations are as follows ( $p < 0.0001$ ):

1999:

$$\text{ST: } y = -0.024x^2 + 0.508x - 0.163$$

$$R^2 = 0.811$$

$$\text{ST-BP: } y = -0.032x^2 + 0.781x - 0.267$$

$$R^2 = 0.819$$

$$\text{FA: } y = -0.012x^2 + 0.662x - 0.188$$

$$R^2 = 0.732$$

$$\text{GR: } y = -0.015x^2 + 0.379x - 0.152$$

$$R^2 = 0.782$$

2000:

$$\text{ST: } y = -0.014x^2 + 0.492x - 0.146$$

$$R^2 = 0.804$$

$$\text{ST-BP: } y = -0.032x^2 + 0.884x - 0.384$$

$$R^2 = 0.819$$

$$\text{FA: } y = -0.047x^2 + 0.885x - 0.215$$

$$R^2 = 0.761$$

The relationships established in Figures 5.5.9 and 5.5.11 were then further used to investigate seasonal changes in the response of the tree canopy to atmospheric conditions. For Figure 5.5.14 and Figure 5.5.15 the reduction of daily  $E_c$  was calculated as 1 minus the ratio of daily  $E_c$  in August or September to  $E_c$  in June–July as derived from the respective regression equations. In 1999 there was a marked reduction in daily  $E_c$  in August and September as compared to June–July for all plots and species for a given value of  $D_{\text{avg}}$  (Fig. 5.5.14–15). Reductions were smaller in oak than in beech, less distinct at Farrenleite than at the other sites and more pronounced as the season progressed, except for Farrenleite, where August and September differed little. Reduction of  $E_c$  in oak was larger at Steinkreuz than at Großebene in August (0.23 vs 0.14, respectively, looking at values of  $E_c$  at highest observed  $D_{\text{avg}}$ ; Fig.

5.5.14), yet in September  $E_c$  was slightly more reduced in oak at Großebebene than at Steinkreuz (0.48 vs 0.42, respectively). Beech at Großebebene clearly displayed a stronger reduction of  $E_c$  in August (0.30) and particularly in September (0.72) than beech at Steinkreuz (0.20 and 0.54, respectively). At stand level, reduction at Großebebene was larger during both months (0.25 and 0.63) compared to Steinkreuz (0.21 and 0.53). The pure beech plot within Steinkreuz (Fig. 5.5.15) hardly differed from the mixed stand (Fig. 5.5.14). At Farrenleite the reduction was about 10 % in August and September (Fig. 5.5.15).

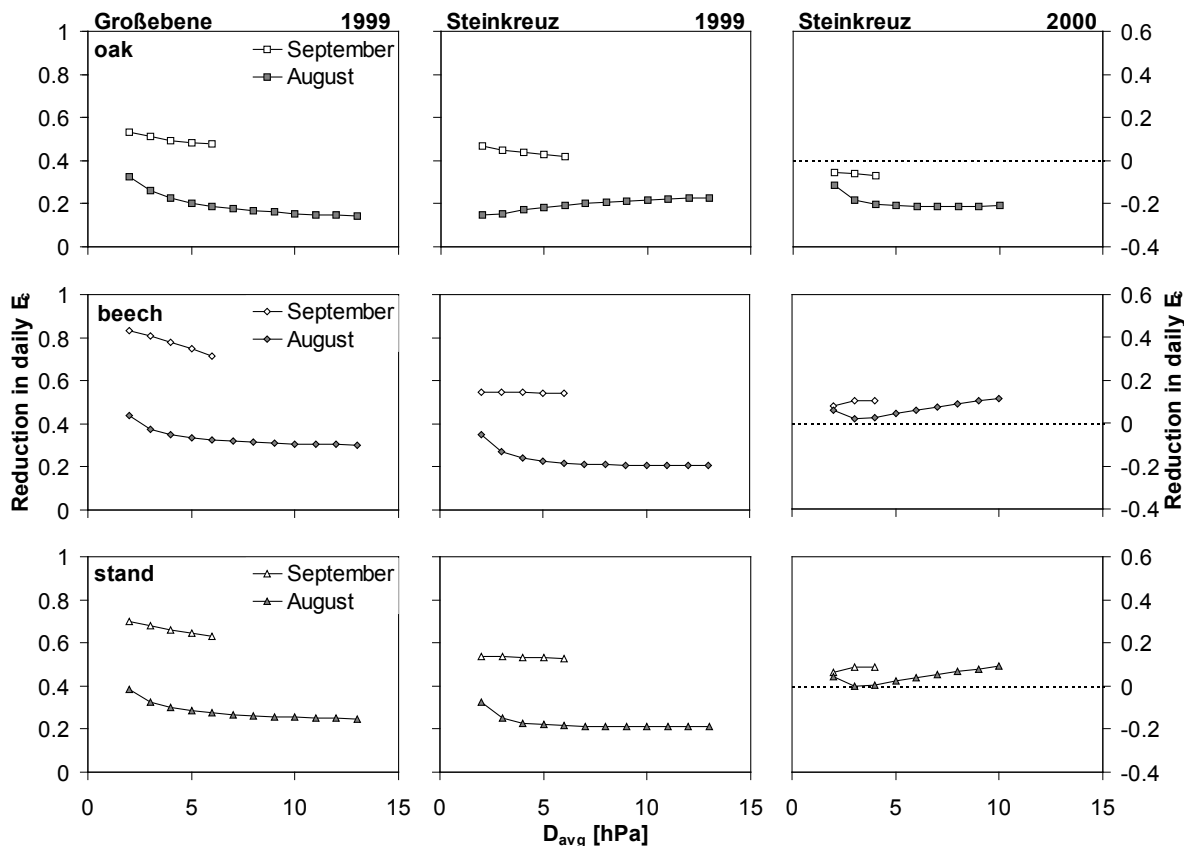


**Figure 5.5.14:** Reduction of daily canopy transpiration  $E_c$  in August (shaded symbols) and September (open symbols), relative to June–July of respective year (i.e. 1 - late season/early season) based on regression equations (Fig. 5.5.9, Fig. 5.5.11 and Tab. A11.6, Appendix) and average daily vapour pressure deficit of the air  $D_{avg}$  for the mixed stands investigated. **Left** panel: Data for Großebebene, 1999; **middle**: Steinkreuz, 1999; **right**: Steinkreuz, 2000. Top row: Data for oak (squares); middle: beech (diamonds); bottom: stand (oak+beech, triangles). Shown here is the range of  $D$  that actually occurred during the respective period of that year. Note the different scale of the y-axis in the right panel; the dotted line there indicates zero reduction in daily  $E_c$ . No measurements were carried out at Großebebene in 2000.

In the year 2000 the maximum  $E_c$  was slightly increased for oak in August compared to June–July at the same  $D_{avg}$  (negative reduction of about 0.21, Fig. 5.5.14 top right); in September, when the range of  $D_{avg}$  was rather small, the reduction was close to that of June–July (-0.07). In beech, the response of  $E_c$  to  $D_{avg}$  was somewhat reduced in August (0.11) and in September as well. The stand in total (beech + oak) behaved in general like its beech component. (In 2000 the warmest and driest phase was in late June, and in July the  $E_c$  of beech responded already like it would in

August, yet the  $E_c$  of oak displayed similar behaviour as in June. July was relatively moist and cold with maximum  $D_{avg}$  only reaching about 50 % of the value of June and with only 2 days of  $D_{avg}$  reaching 25 % of June's maximum (in graphs June and July only shown combined). August was similarly moist and cold with maximum  $D_{avg}$  comparable to July's;  $D_{avg}$  exceeded 25 % of the June maximum on 13 days though.) At the pure beech sites (Fig. 5.5.15 right) changes in the response of  $E_c$  to  $D_{avg}$  relative to June–July of the year 2000 were also only minor (mostly < 0.1).

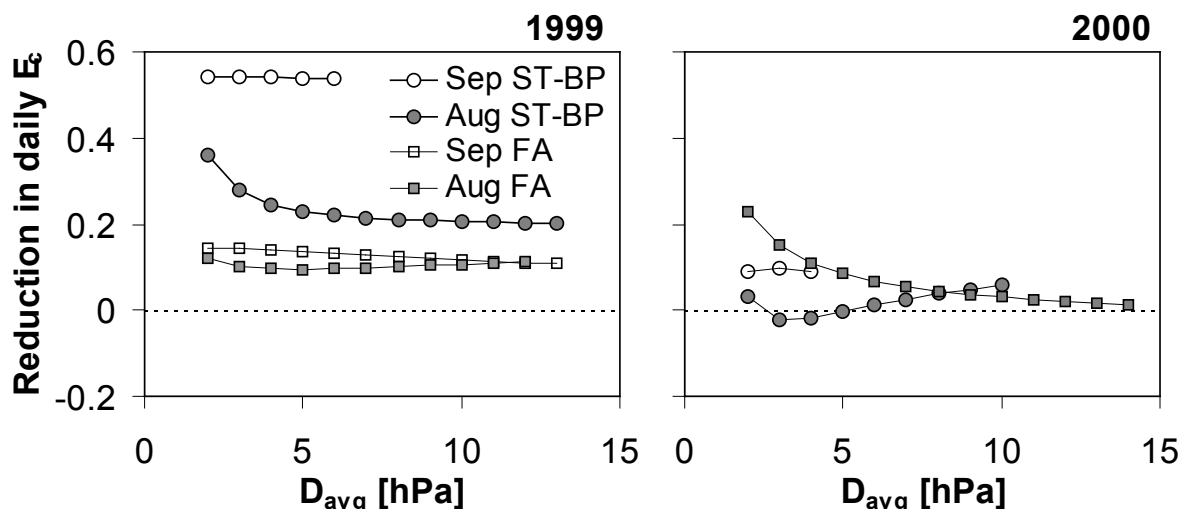


**Figure 5.5.15:** Reduction of daily canopy transpiration  $E_c$  in August (shaded symbols) and September (open symbols), relative to June–July of respective year (i.e. 1 - late season/early season) based on regression equations (Fig. 5.5.9, Fig. 5.5.11 and Tab. A11.6) and average daily vapour pressure deficit of the air  $D_{avg}$  of the Steinkreuz-pure beech plot in the Steigerwald (ST-BP, circles) and Farrenleite in the Fichtelgebirge (FA, squares) for the years 1999 (**left**) and 2000 (**right**). Shown here is the range of  $D$  that actually occurred during the respective period of that year. Because of comparatively large uncertainty of the fitted regression for Farrenleite for September 2000 (Fig. 5.5.11), modelled data from this period have been omitted.

Figure 5.5.16 illustrates the seasonal development of canopy transpiration  $E_c$  and soil water content (as a fraction of water content at field capacity  $\theta/\theta_F$ , at 20 cm soil depth) for selected days with comparable and high PFD<sub>day</sub> and  $D_{avg}$  at the Steinkreuz-pure beech plot and Farrenleite in 1999 and 2000. While at Farrenleite  $E_c$  was ca. 2.2 mm d<sup>-1</sup> at  $\theta/\theta_F$  ranging from 0.98 to 0.83 on selected days during the summer months of 1999, the  $E_c$  of the Steinkreuz-pure beech plot decreased from 2.4 mm d<sup>-1</sup> to 1.7 mm d<sup>-1</sup> when  $\theta/\theta_F$  dropped from 0.64 to 0.34 (equivalent to  $\theta_e$  of 0.5 and 0.09, respectively). The following year, under comparable atmospheric conditions of PFD<sub>day</sub> and  $D_{avg}$ ,  $\theta/\theta_F$  spanned 0.88–0.59 (expressed as  $\theta_e$ : 0.83–0.43, respectively) with  $E_c$  varying between 2.7 and 2.3 mm d<sup>-1</sup>. Thus  $E_c$  decreased only vaguely at this small reduction in soil water availability compared to 1999. (No data from Farrenleite are shown for 2000 due to lack of reliable soil moisture records during that year.)

The year 2000 with its higher  $\theta_e$  could be seen as reference for the drier year 1999, showing a seasonal reduction of canopy transpiration with probably no (large) effect of soil water limitation on the hydraulic capacities in the soil plant atmosphere continuum but solely plant-intrinsic seasonal effects of senescence (e.g. reduced photosynthetic capacity).

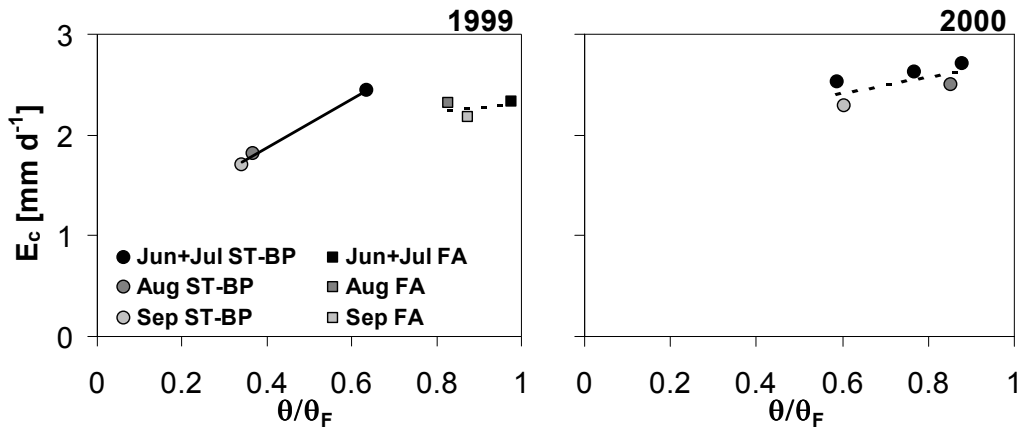


**Figure 5.5.16:** Seasonal development of soil water content in 20 cm depth (as fraction of water content at field capacity  $\theta/\theta_F$ ) and daily canopy transpiration  $E_c$  of the Steinkreuz-pure beech plot in the Steigerwald (**ST-BP**, circles) and Farrenleite in the Fichtelgebirge (**FA**, squares) for the years 1999 (**left**) and 2000 (**right**). For this graph days with similar PFD<sub>day</sub> and D<sub>avg</sub> were selected, not maximum values of  $E_c$ . For 2000 no reliable data of soil moisture were available for the Farrenleite stand. Dates shown for 1999: ST-BP: 12.07., 31.08., 08.09.; FA: 25.07., 08.08., 08.09.; dates for 2000: ST-BP: 27.06., 22.07., 31.07., 05.08., 12.09.

The interannual variability of seasonal sums of canopy transpiration may be explained by differences in atmospheric, phenologic and edaphic conditions and by changes in stand structural characteristics such as LAI. Figure 5.5.17 shows the seasonal sums of  $E_c$  for the years 1999 and 2000 for the two pure beech sites and the mixed oak-beech stand Steinkreuz. Seasonal  $E_c$  decreased from 1999 to 2000 with decreasing D<sub>integr</sub> (the seasonally integrated vapour pressure deficit of the air) for the Steinkreuz plots and stand components, particularly for the Steinkreuz-pure beech plot and oak in the mixed Steinkreuz stand, whereas at Farrenleite D<sub>integr</sub> increased (Fig. 5.5.17a). For both years seasonal  $E_c$  increased with D<sub>integr</sub> from the high elevation site Farrenleite to the low elevation site Steinkreuz-pure beech plot. Seasonally integrated photon flux density (PFD<sub>integr</sub>) hardly changed from 1999 to 2000 at both locations (Fig. 5.5.17b); between the pure beech sites seasonal  $E_c$  increased with PFD<sub>integr</sub>. Seasonal  $E_c$  decreased with a decreasing number of sap flow days (or season length, Fig. 5.5.17c) from 1999 to 2000 at Steinkreuz and it decreased despite increasing season length at Farrenleite. In accordance with D<sub>integr</sub> and PFD<sub>integr</sub>, the seasonal  $E_c$  of pure beech sites increased with the number of sap flow days when moving from high to low elevation. The minimum seasonal soil water content relative to soil water content at field capacity  $\theta/\theta_{F\ min}$  increased from 1999 to 2000 at Steinkreuz, indicative of larger soil water depletion in the first year and suggesting a plentiful water supply in 2000.  $\theta/\theta_{F\ min}$  was lower at Steinkreuz than at Farrenleite (1999), so soil water supply did not limit canopy transpiration at Farrenleite (Fig. 5.5.17d) as already detailed in Figures 5.5.8, 5.5.15–16. Seasonally integrated soil water depletion in 1999, as calculated from cumulated day-to-day changes in  $\theta/\theta_F$ , was 1.8 times higher at Steinkreuz compared to Farrenleite (probably an underestimation of the difference due to large data gaps in the soil water data from Steinkreuz; see also Chap. 5.2); seasonal  $E_c$  was 1.5 times higher at the Steinkreuz-pure beech plot. Soil

water depletion at Steinkreuz in 2000 was 90 % of that in 1999 (likely to be an overestimation, see above). The LAI barely changed from 1999 to 2000 at Steinkreuz (< 5 %, except for the oak component), the LAI of the Steinkreuz-pure beech plot and the mixed Steinkreuz stand was very similar to that of Farrenleite (see Table 5.1.3; LAI at Farrenleite only determined in 1998) so that LAI could neither explain interannual nor between-site variability (Fig. 5.5.17e). An exception may be oak at Steinkreuz, whose LAI was estimated to drop from 1999 to 2000 by more than 10 %, in parallel with the decrease in seasonal  $E_c$  by almost 30 %. Both LAI and seasonal  $E_c$  were about the same for Farrenleite and the mixed Steinkreuz stand. Table 5.5.2 summarises the values and changes in  $E_c$  and its drivers.

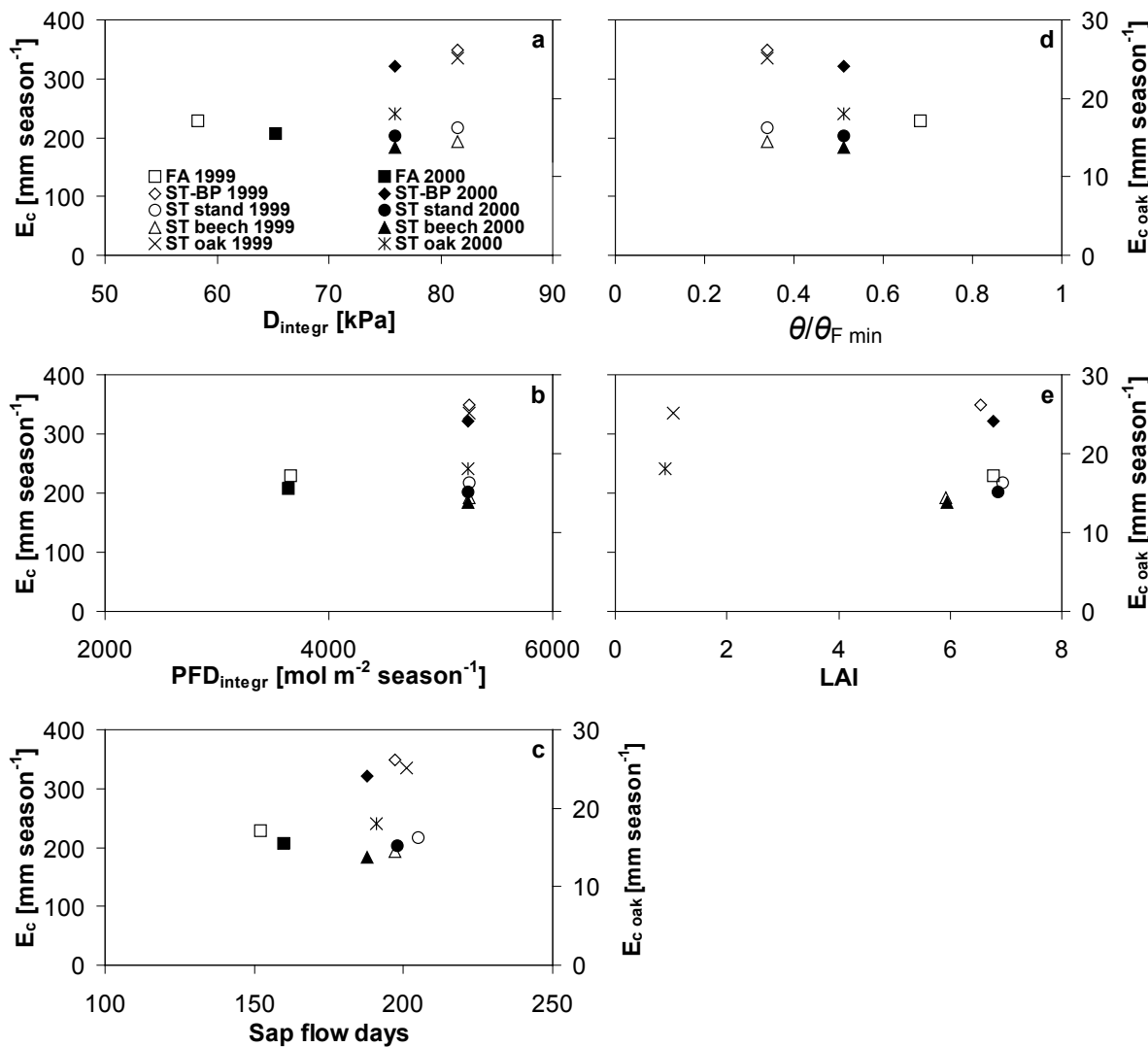


**Figure 5.5.17:** Seasonal sums of canopy transpiration  $E_c$  for the two pure beech sites (Steinkreuz-pure beech plot **ST-BP**, diamonds, and Farrenleite **FA**, squares) and the mixed Steinkreuz stand (**ST**; beech: triangle; oak: cross; total stand: circle) for 1999 (open) and 2000 (filled) and seasonally integrated vapour pressure deficit of the air ( $D_{\text{integr}}$ , **a**), photon flux density ( $PFD_{\text{integr}}$ , **b**), number of sap flow days (**c**), minimum seasonal soil water content relative to soil water content at field capacity ( $\theta/\theta_F \text{ min}$ , **d**; no data for Farrenleite for 2000) and LAI (**e**). Note the different y-axis for the  $E_c$  of oak.

**Canopy conductance.** Canopy conductance  $g_c$  was calculated from canopy transpiration  $E_c$  as described in Chapter 4.1.1 (Eq. 4.1.7) and the respective diurnal maximum canopy conductance ( $g_{c \text{ max}}$ ) is shown in Figure 5.5.18. Time lags between atmospheric conditions and sap flow were less than 30 min, the temporal resolution of the data used to calculate  $g_c$ , as revealed by regression analysis as e.g. in Granier et al. (2000a): time lags of 0.5 h, 1 h, 1.5 h and 2 h were introduced to the data, sap flow lagging behind climatic variables, and regression coefficients were calculated.  $R^2$  was highest for zero time lag (data not shown).

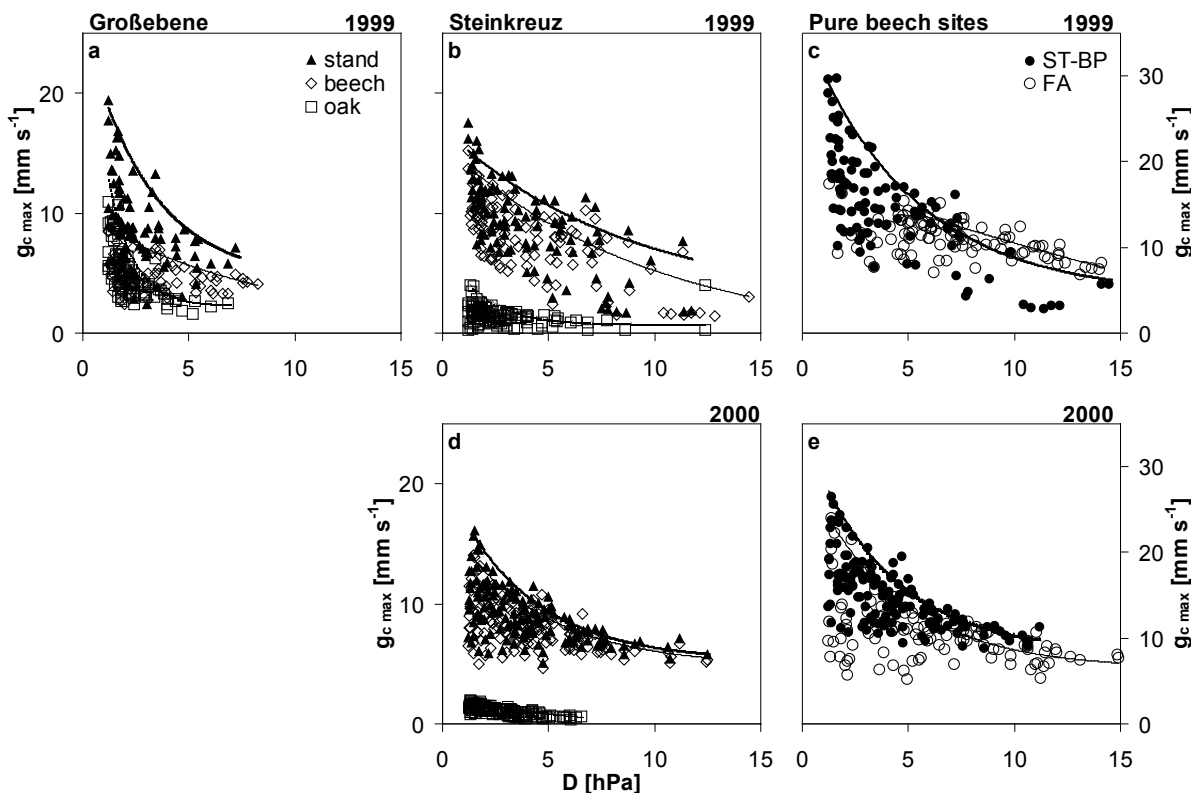


**Figure 5.5.18:** Relationships of vapour pressure deficit of the air (D) with diurnal maximum canopy conductance ( $g_{c \text{ max}}$ ) for the mixed stands Großebene (a, left panel), Steinkreuz (b, d, middle) and the pure beech sites (c, e, right; note different scale of y-axes) the Steinkreuz-pure beech plot (ST-BP) and Farrenleite (FA) for the years 1999 (top) and 2000 (bottom). For determination of  $g_{c \text{ max}}$  only daytime (PFD  $> 15 \mu\text{mol m}^{-2} \text{s}^{-1}$ ) half-hourly values of  $g_c$  were considered when respective D was  $> 1.2 \text{ hPa}$  and when the foliage was assumed to be dry (PPT  $< 0.2 \text{ mm}$  during last 2 h), from June to September. Lines shown are approximations for the maximum values of  $g_{c \text{ max}}$  at a given value of D (capacities under non-limiting conditions). Note different scales of  $g_{c \text{ max}}$  for ST-BP and FA. No gapfilled data estimated via regressions with D were included in this analysis, this being the reason for the missing data points for Großebene in the higher range of D.

Maximum canopy conductance  $g_{c \text{ max}}$  was highest at the Steinkreuz-pure beech plot (maximum 1999:  $29.8 \text{ mm s}^{-1}$ ; 2000:  $26.5 \text{ mm s}^{-1}$ ), followed by Farrenleite (in 2000:  $24.0 \text{ mm s}^{-1}$ ), Großebene ( $19.4 \text{ mm s}^{-1}$ ) and Steinkreuz ( $17.5 \text{ mm s}^{-1}$ ), and was higher in 1999 than in 2000 (except for Farrenleite). The oak component of Steinkreuz had the lowest values of  $g_{c \text{ max}}$  (mean June–Sep. 1999:  $1.47 \pm 0.70 \text{ mm s}^{-1}$ ; average May–Sep. 2000:  $1.09 \pm 0.39 \text{ mm s}^{-1}$ ; for values also see Tab. 5.5.3, below),

corresponding to the lowest values of  $E_c$ . At Steinkreuz,  $g_{c\max}$  of oak was larger in the drier year 1999 than in the wetter year 2000, relative to  $g_{c\max}$  of beech (Tab. 5.5.3).

A similar, non-linear decline of  $g_c$  max with increasing D was found for all stands. The decline was less steep at Steinkreuz (1999) though and almost linear for Farrenleite in 1999. At the latter site, maximum diurnal  $g_c$  was reached at comparatively high values of D most of the time (e.g.,  $g_c$  max was found 3 times more often at  $D > 10$  hPa than at the Steinkreuz-pure beech plot), whereas maximum diurnal values of  $g_c$  at low D were relatively low compared to the Steinkreuz-pure beech plot and occurred rarely. At Farrenleite, the time of the day when  $g_c$  max was reached, was between 11 h and 17 h on 87 % of the days, between 17 h and 20 h on 5 % of the days and between 6.5 h and 11 h on 8 % of the days (not shown). At Steinkreuz in contrast,  $g_c$  max was recorded between 11 h and 17 h only 27 % of the days, between 17 h and 20 h on 29 % of the days and on 44 % of the days between 6.5 h and 11 h. In the year 2000, time of maximum diurnal  $g_c$  at Farrenleite was shifted more towards late afternoon (17–20 h: 15 % of the days) and to a lesser extent also towards earlier morning (6.5–11 h: 11 %). At Steinkreuz  $g_c$  max was encountered more often between 11 h and 17 h (42 % of the days). The air temperature at the time of  $g_c$  max was larger than 14 °C on 87 % of the days at Farrenleite in 1999, and in 2000 on only 67 % of the days. Low temperatures in the mornings and rapid cooling down in late afternoon are suspected to have caused this pattern of  $g_c$  at the high elevation site Farrenleite due to stomatal limitation.

**Table 5.5.3:** Maximum diurnal canopy conductance ( $g_{c \text{ max}}$ , in  $\text{mm s}^{-1}$ ) scaled from sap flow measurements for 1999 (June 1–Sep. 30) and 2000 (May 8–Sep. 30): Maximum (max), mean, standard deviation ( $\pm 1$  SD), number of observations (n, days for which  $g_{c \text{ max}}$  was determined) and maximum  $g_{c \text{ max}}$  per leaf area ( $g_{c \text{ max}}/\text{LAI}$ , in  $\text{kg m}^{-2} \text{s}^{-1}$ ) for the whole stand and the beech and oak component, respectively.

When  $g_{c \max}$  was related to LAI as depicted in Figure 5.5.19 ( $g_c/\text{LAI}$  being a “mean leaf-level conductance”) the pure beech stands still had the highest maximum conductances, but they were more similar to those of the other stands than when comparing “stand-level”  $g_{c \max}$  (cf. Fig. 5.5.18). Oak at Großebene and Steinkreuz (1999) displayed the second highest maximum values, but beech at Großebene had on average higher  $g_{c \max}/\text{LAI}$  than oak and the total mixed Großebene stand, declining less strongly with increasing D than the latter ones (not shown). To a smaller extent this was also true for beech at Steinkreuz. Leaf area-level conductances at Steinkreuz were more similar between beech, oak and the total stand for both years ( $g_c/\text{LAI}$ , Fig. 5.5.19) than the stand level conductances ( $g_{c \max}$ , Fig. 5.5.18). Beech at Großebene showed higher  $g_{c \max}/\text{LAI}$  than beech at Steinkreuz, whereas for oak it was the opposite. Values of  $g_{c \max}$  and  $g_{c \max}/\text{LAI}$  are summarised in Table 5.5.3.

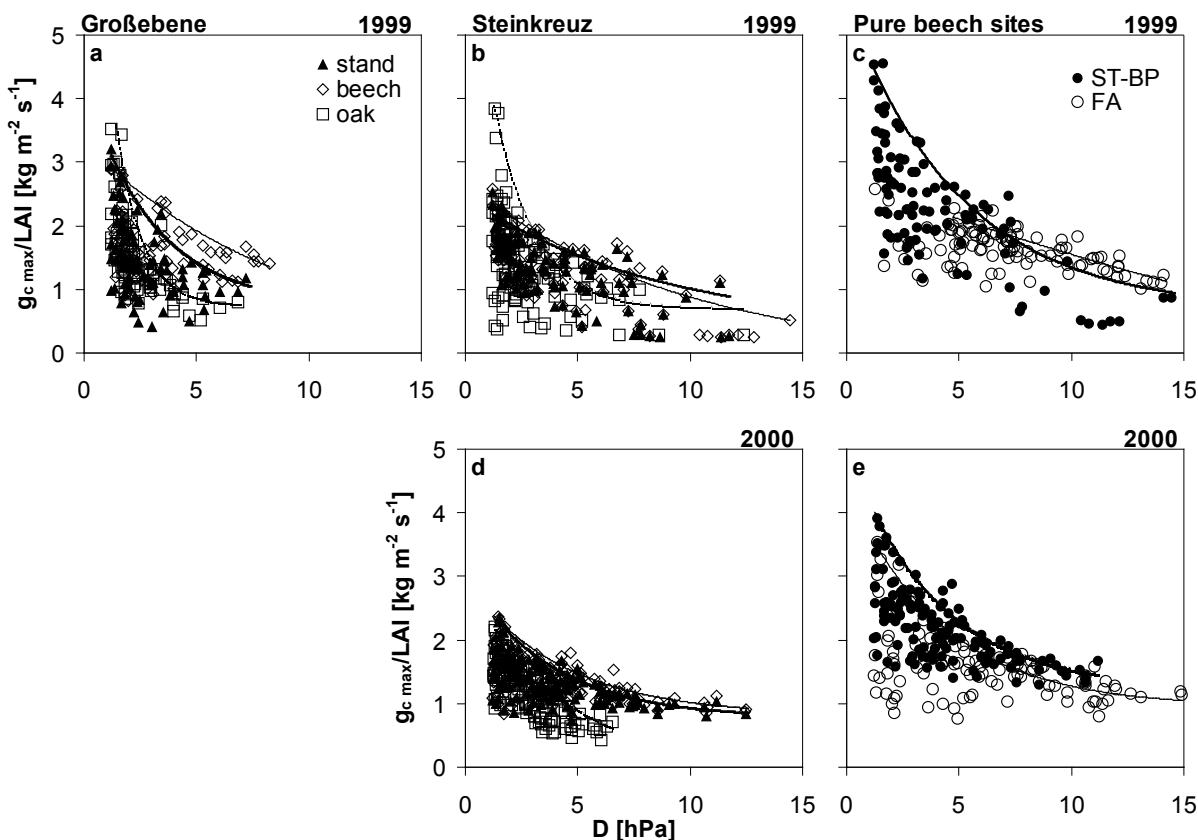


**Figure 5.5.19:** Relationships between vapour pressure deficit of the air (D) and diurnal maximum canopy conductance related to LAI ( $g_{c \max}/\text{LAI}$ ) for the mixed stands Großebene (a, left panel), Steinkreuz (b, d, middle) and the pure beech sites (c, e, right) Steinkreuz-pure beech plot (ST-BP) and Farrenleite (FA) for the years 1999 (top) and 2000 (bottom). See also caption of Fig. 5.5.18. For Farrenleite, data for LAI were available for 1998 only, which were used for both 1999 and 2000.

## 6 Discussion

### 6.1. Structural drivers of canopy transpiration

Sapwood area. The correlation of sapwood area  $A_{st}$  with tree diameter was highly significant in both *Fagus sylvatica* and *Quercus petraea* and similar for trees from all stands studied (Fig. 5.1.1.4, Tab. 5.1.1.1). The  $A_{st}$  of oak was as expected much smaller than  $A_{st}$  in beech at a given tree diameter. Allometric relationships established for beech from other stands in Central Europe compared well to those detailed here and are shown in Figure 6.1.1a for stands of large beech trees and in Figure 6.1.1b for stands of small beech trees:

Equations given by Geßler et al. (2005) and Hölscher et al. (2005) are very similar to the one for Steinkreuz + Großebene, however, the regression of Hölscher et al. (2005) started to deviate considerably from diameters  $\geq 60$  cm (indicating smaller  $A_{st}$  compared to the findings from this study, Fig. 6.1.1a). Hoch et al. (2003) described an average sapwood radius of 10 cm and a ripewood radius of 4.5 cm (their Fig. 4) in beech with a total radius of 15 cm ( $n = 3$  trees) from a mixed-species sub-montane stand in Switzerland. The sapwood area calculated from these data differed  $< 1\%$  from the allometric function for Steinkreuz + Großebene (Fig. 6.1.1a). Schmidt (1954, cited in Huber 1956, p 555f) experimentally found a marked decrease in the axial water permeability of the xylem at approx. 8 cm radial distance from cambium in a beech tree with a total radius of 13 cm, which coincides with the sapwood-ripenwood boundary that the  $A_{st}$ -diameter relationship established in this study would predict at around 60 % radial depth (in ca. 7.8 cm distance from the cambium; not shown). Kolcun (2005) established an allometric equation for small trees from a site comparable to Farrenleite that was very similar to that for Farrenleite (Fig. 6.1.1b). Marc and Robinson (2004) found smaller sapwood radii in three trees at a young but denser montane site in SE-France (Fig. 6.1.1b). Aranda et al. (2005) determined regression functions for European beech and sessile oak growing in a mixed montane stand in Spain. For the beech trees, ranging 2–18 cm in DBH, results were very similar to those from Farrenleite and those published by Kolcun (2005; Fig. 6.1.1b).

The few published allometric relationships between  $A_{st}$  and tree diameter for *Quercus petraea* were established on smaller trees than those studied in the Steigerwald. Therefore, additional ring-porous oak species from temperate habitats were included in a comparison with the regression equation obtained for *Q. petraea* in this study, shown in Figure 6.1.1c–d:

Herbst et al. (2007b) studied large *Q. robur* in an English stand, for which the authors give no range of DBH but indicate that the largest trees were  $> 60$  cm in DBH, and their regression equation yielded smaller values of  $A_{st}$  for large trees than the equation for Steinkreuz + Großebene from this study (Fig. 6.1.1c). The same was true for allometric equations from temperate North American ring-porous oak species (*Q. prinus*, *Q. alba*, *Q. rubra*; Wullschleger et al. 2001; Fig. 6.1.1c). In contrast, regressions detailed by Pataki and Oren (2003) for white oaks (sect. *Lepidobalanus*; Fig. 6.1.1c) and particularly red oaks (sect. *Erythrobalanus*; Fig. 6.1.1d), also from temperate North America, compared very well to that from the Steigerwald. Hoch et al. (2003) noted an average sapwood radius of 6 cm in *Q. petraea* ( $n = 2$ ) growing in a multiple mixed sub-montane forest in Switzerland; the allometric equation presented here would estimate a sapwood radius of about 2 cm (Fig. 6.1.1d). Vincke et al. (2005a) tabulated values of  $A_{st}$  for *Q. robur* from a thinned (reduction of  $A_b$  by 32 % six years before) and an un-thinned control plot from a colline Belgian stand.  $A_{st}$  for trees from the control plot agreed well with the results presented here and the other published values, whereas, as was to be expected, variability among trees from the thinned plot was considerably larger (Fig. 6.1.1d). Wagenführ (2000) listed *Q. robur/Q. petraea* with a 2–5 cm sapwood radius and Lévy et al. (1992) found an average sapwood radius of 29.3 mm in dominant mature *Q. petraea*-trees in central and north-western France (not shown). For trees of *Q. petraea* from a young French stand smaller than those studied in the Steigerwald (average DBH 8.6 cm, maximum 17.5 cm), Bréda et al. (1993a) published an allometric regression resulting in sapwood radii of 1.4–2.1 cm (Fig. 6.1.1d). Aranda et al. (2005) showed a regression for *Q. petraea* (range of DBH 5–19.5 cm) growing in a Spanish montane stand mixed with beech, the results concurring with those of Bréda et al. (1993a; Fig. 6.1.1d).

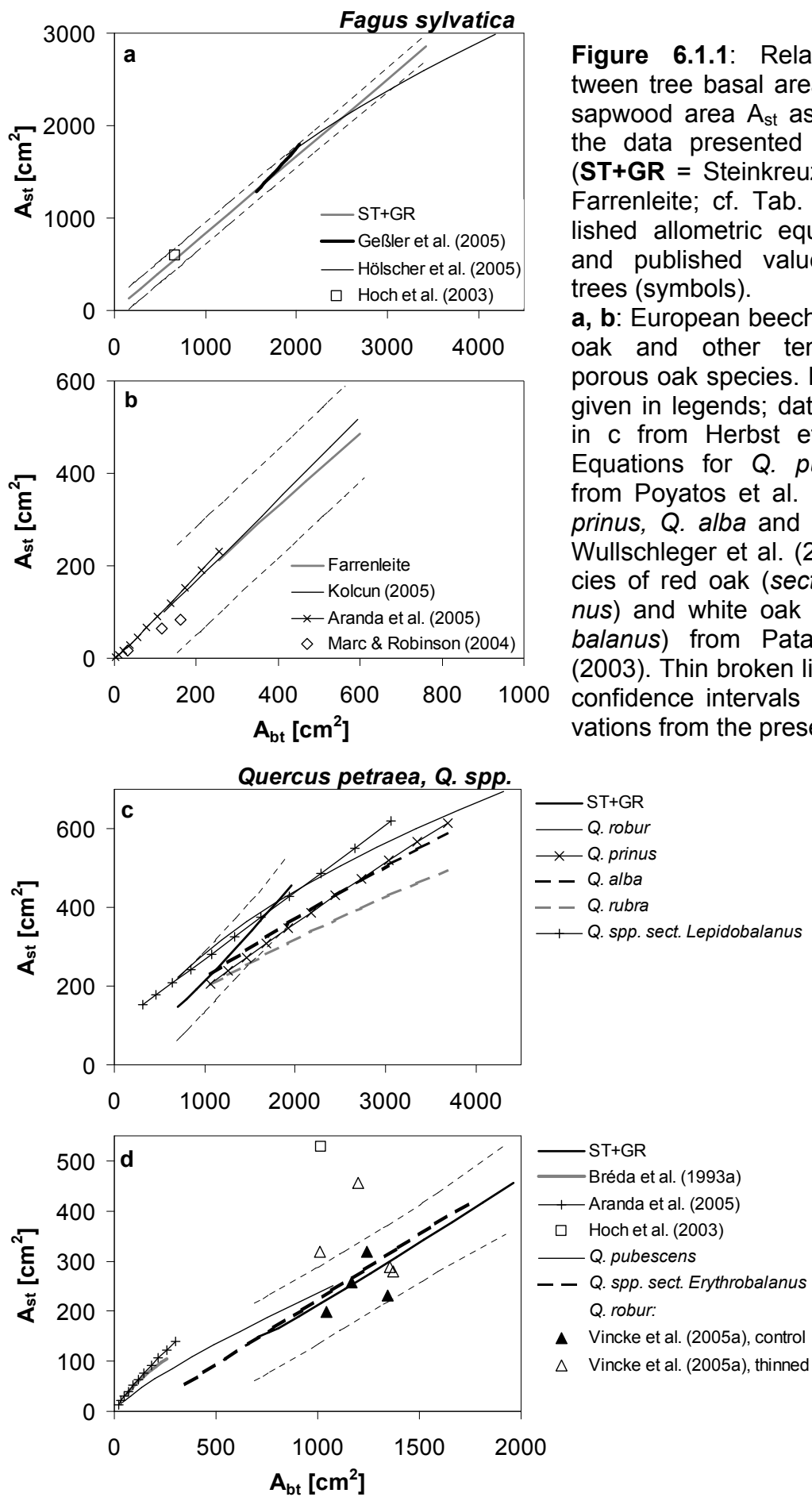


**Figure 6.1.1:** Relationships between tree basal area  $A_{bt}$  and tree sapwood area  $A_{st}$  as derived from the data presented in this study (ST+GR = Steinkreuz+Großebene; Farrenleite; cf. Tab. 5.1.1.1), published allometric equations (lines) and published values for single trees (symbols).

**a, b:** European beech; **c, d:** Sessile oak and other temperate ring-porous oak species. References as given in legends; data for *Q. robur* in c from Herbst et al. (2007b). Equations for *Q. pubescens* are from Poyatos et al. (2005), for *Q. prinus*, *Q. alba* and *Q. rubra* from Wullschleger et al. (2001), for species of red oak (sect. *Erythrobalanus*) and white oak (sect. *Lepidobalanus*) from Pataki and Oren (2003). Thin broken lines are 95 % confidence intervals for the observations from the present study.

A regression equation detailed by Poyatos et al. (2005) for closely related *Q. pubescens* growing in the montane Pyrenees, NE-Spain, estimated lower values of  $A_{st}$  than that of Bréda et al. (1993a, see above) for young *Q. petraea* and slightly higher values of  $A_{st}$  than the equation for *Q. petraea* from the Steigerwald for larger trees presented here; differences were smaller at the upper end of the DBH-range of trees from Poyatos et al. (2005; Fig. 6.1.1d).

Differences in the relationship between sapwood area and tree diameter (or basal area) thus appear to be larger in oak than in beech trees from different stands, but the published data are too few to draw any conclusions from this comparison.

**Leaf area per unit dry mass.** The average values of the leaf area per unit of dry mass (SLA) of leaves from litter collections for beech from Steinkreuz ( $198\text{--}251 \text{ cm}^2 \text{ g}^{-1}$ , Tab. 5.1.3.1) and Farrenleite ( $200 \text{ cm}^2 \text{ g}^{-1}$ ) are mostly within the range of findings from a montane beech forest in central Germany, summarised by Heller and Götsche (1986) as varying interannually from  $167$  to  $222 \text{ cm}^2 \text{ g}^{-1}$  (litter-SLA). The average and maximum values of SLA for beech from Großebene ( $275\text{--}291 \text{ cm}^2 \text{ g}^{-1}$ ) are somewhat higher, possibly reflecting the smaller height of beech compared to oak and thus resulting in the more shaded beech crowns with a larger proportion of shade leaves in beech at Großebene than at Steinkreuz and Farrenleite:

Bouriaud et al. (2003) showed values of SLA of  $150\text{--}320 \text{ cm}^2 \text{ g}^{-1}$  for a dense young beech stand, a finding that could corroborate the above line of argument since there is a high degree of self-shading in dense stands. Further support comes from Bréda (2003) who presented average ranges of SLA for beech-dominated French forests between  $180$  and  $280 \text{ cm}^2 \text{ g}^{-1}$  and of up to  $370 \text{ cm}^2 \text{ g}^{-1}$  for forests where beech was a secondary or understory species. Schipka (2003) showed SLA to range between  $196$  and  $264 \text{ cm}^2 \text{ g}^{-1}$  over three years in four mature central German beech stands, and Leuschner et al. (2006) found values of  $192\text{--}246 \text{ cm}^2 \text{ g}^{-1}$  across 23 beech stands in north central Germany, on average  $217 \text{ cm}^2 \text{ g}^{-1}$ . Jochheim et al. (2007) detailed average annual values of SLA of  $222\text{--}223 \text{ cm}^2 \text{ g}^{-1}$  for three years of investigation in a north-east German mature beech stand and  $135 \text{ cm}^2 \text{ g}^{-1}$  for a dry year (2003) when precipitation from April–June was less than 50 % of the year before (Lütschwager and Remus 2007) and leaves as a consequence showed xeromorphic traits (Jochheim et al. 2007). Bréda et al. (1995a) reported SLA-values for a 43 year-old sessile oak stand of  $150$  and  $130 \text{ cm}^2 \text{ g}^{-1}$  during two consecutive years, comparable to the findings of  $138\text{--}196 \text{ cm}^2 \text{ g}^{-1}$  for oaks from the Steigerwald (Tab. 5.1.3.1).

The average SLA of leaves harvested green from two beech trees at Farrenleite and one beech at Großebene was  $125\text{--}200 \text{ cm}^2 \text{ g}^{-1}$  and  $142 \text{ cm}^2 \text{ g}^{-1}$  for one oak from Großebene (Fleck 2002). These values from the Steigerwald and the Fichtelgebirge fall within the range observed on green leaves of beech ( $85\text{--}410 \text{ cm}^2 \text{ g}^{-1}$ ) and oak trees ( $90\text{--}400 \text{ cm}^2 \text{ g}^{-1}$ ) in other studies across Central Europe:

Bartelink (1997) found an average SLA of  $172 \text{ cm}^2 \text{ g}^{-1}$  for 38 trees differing in social position and ranging in age from 8 to 59 years. At 760 m a.s.l. in the Fichtelgebirge, Niinemets (1995) assessed the SLA as varying from ca.  $170$  to  $330 \text{ cm}^2 \text{ g}^{-1}$  along light gradients within beech canopies. At the same stand Bauer et al. (1997) measured the SLA from the upper third of the crown of beech trees as ranging from ca.  $180$  to  $310 \text{ cm}^2 \text{ g}^{-1}$ . Pellinen (1986) reported SLA for nine 100–115 year-old beech trees from different DBH-classes as spanning from  $137$  to  $333 \text{ cm}^2 \text{ g}^{-1}$  for leaves dried green (between-tree and within-crown variability), on average  $229 \text{ cm}^2 \text{ g}^{-1}$ . Heller and Götsche (1986) showed values of SLA from  $100$  to  $330 \text{ cm}^2 \text{ g}^{-1}$  for a mature beech stand (DBH  $11\text{--}47 \text{ cm}$ ), on average  $200 \text{ cm}^2 \text{ g}^{-1}$ . Gratani et al. (1987) found values of  $87\text{--}366 \text{ cm}^2 \text{ g}^{-1}$  for sun and shade leaves in upper montane beech trees in central Italy, and Hagemeier (1997, 2002) observed  $95\text{--}400 \text{ cm}^2 \text{ g}^{-1}$  in beech trees from several stands in central Germany. Forstreuter (2002) presented average values of  $345 \text{ cm}^2 \text{ g}^{-1}$  and  $111 \text{ cm}^2 \text{ g}^{-1}$  for the shade and sun crown of a 100 year-old beech stand in E-Germany and  $313 \text{ cm}^2 \text{ g}^{-1}$  and  $85 \text{ cm}^2 \text{ g}^{-1}$ , respectively, for a 120 year-old beech stand in N-Italy. Prskawetz and Lexer (2000) tabulated values in the range  $175\text{--}411 \text{ cm}^2 \text{ g}^{-1}$  for dense young beech stands in Austria. Le Dantec et

al. (2000) averaged the SLA of leaves from the top of the canopy of a total of 23 beech and oak stands in Fontainebleau, France, to  $104 \text{ cm}^2 \text{ g}^{-1}$  for beech and  $133 \text{ cm}^2 \text{ g}^{-1}$  for oak (*Q. robur*, *Q. petraea*). Hoch et al. (2003) gave values for the SLA of leaves from the upper part of the crowns of 100 year-old *F. sylvatica* and *Q. petraea* in Switzerland, at 500 m a.s.l., of  $98 \text{ cm}^2 \text{ g}^{-1}$  and  $87 \text{ cm}^2 \text{ g}^{-1}$ , respectively. Eriksson et al. (2005) published values of  $103 \text{ cm}^2 \text{ g}^{-1}$  for sun leaves and  $309 \text{ cm}^2 \text{ g}^{-1}$  for shade leaves of beech from southern Sweden, and of 96 and  $155 \text{ cm}^2 \text{ g}^{-1}$ , respectively, for oak (not detailed whether *Q. petraea* or *Q. robur*), obtained on a small number of freshly dried leaves collected at the end of the growing season. In young Danish beech and oak stands Ladefoged (1963) measured  $120\text{--}270 \text{ cm}^2 \text{ g}^{-1}$  in 10 beech and  $118\text{--}143 \text{ cm}^2 \text{ g}^{-1}$  in 9 sessile oak trees. Burger (1947) reported a range of  $230\text{--}400 \text{ cm}^2 \text{ g}^{-1}$  for several oak trees from Switzerland.

**Leaf area index.** The variability in LAI derived from the different methods employed in this study (Tab. 5.3.1.2) was 7–13 % for the Steigerwald sites and 20 % at the site in the Fichtelgebirge, where the harvest had been carried out in the year before the commencement of the other measurements. For the Steigerwald sites these differences between the methods were comparatively small, and they may relate to the different spatial and temporal resolution of these techniques. Direct harvesting can be done down to e.g. branch level resolution and integrated to tree and stand level using allometric relationships between leaf area and branch or stem diameter. Single tree-leaf area and stand level-LAI can hence be calculated. Because harvesting is so laborious, seasonal and even inter-annual dynamics can hardly be followed (Chason et al. 1991). Semi-direct estimates based on litter collection are most suitable to derive an LAI to the resolution of a species. Because of the seasonality of leaf-fall, only inter-annual variation can be assessed (Chason et al. 1991). Indirect optical methods (e.g. Li-Cor LAI2000 Plant Canopy Analyser, PCA), on the other hand, integrate over a large field of view and are most commonly used to estimate stand level-LAI. The contribution of different species to stand level-LAI cannot be determined with the standard optical methodology in mixed stands. Since measurements with a PCA are executed rapidly (the time requirement for measuring a stand is less than half a day), intra-annual variation and the seasonality of leaf development can be followed. Indirect estimates are usually compared to direct estimates of LAI, the latter regarded as most accurate (e.g. Gower and Norman 1991, Dufrêne and Bréda 1995). But (semi-) direct methods do not necessarily provide accurate and unbiased LAI estimates (Burton et al. 1991, Bouriaud et al. 2003, Eriksson et al. 2005).

Regarding the accuracy of the direct estimates of LAI via allometric relationships at tree level (see Chap. 4.4.1), the following points should be considered: Fleck (2002) and Fleck et al. (2004) found a large scatter in the allometric relationships of DBH with leaf area  $A_{lt}$  for beech and oak across several stands (cf. Chap. 4.4.1). Relating  $A_{lt}$  to sapwood area  $A_{st}$  instead of basal area or DBH could be expected to have resulted in stronger correlations (see e.g. Rogers and Hinckley 1979, Meadows and Hodges 2002). On the other hand, the relationship between DBH and  $A_{lt}$  can be expected to differ between stands, as stand density will affect crown form and size (Burger 1950). Results on beech stands e.g. from Bartelink (1997) support this view, since he found relationships between  $A_{lt}$  and  $A_{bt}$  or  $A_{st}$  to differ significantly between stands, but these differences disappeared when crown dimensions, especially the height of the crown base, were used as covariates (Bartelink 1997). In addition, the ratio of  $A_{lt}$  to  $A_{st}$  was found to be larger in fast-growing than in slow-growing conifer stands (Binkley and Reid 1984, Espinosa Bancalari et al. 1987). The use of published ratios of  $A_{lt}$  to  $A_{st}$  has been cautioned for these reasons (Espinosa Bancalari et al. 1987). In contrast, Le Dantec et al. (2000) found the average  $A_{lt}$  of 33 pure and

mixed beech and oak stands to be correlated with the average DBH of a stand, based on optical measurements. Since leaf harvesting at the Großebene and Farrenleite stands was not aimed at providing statistically sturdy allometric relationships at stand canopy level, but at a detailed 3D-description of individual tree canopies and their leaf clouds (cf. Fleck 2002, Fleck et al. 2004), estimates of stand level-LAI based on these direct measurements and connected allometrics should be taken as additional information rather than as a reference for the other methods. This may especially be true for the comparatively dense and short Farrenleite stand.

A general tendency towards underestimating LAI by the PCA and other optical methods when compared to direct methods has emerged from a considerable number of studies on coniferous (review by Gower et al. 1999) and deciduous forests (e.g. Chason et al. 1991, Dufrêne and Bréda 1995, Cutini et al. 1998, Planchais and Pontailler 1999, Prskawetz and Lexer 2000, Mussche et al. 2001, Gaydarova 2003, Wang et al. 2004). Yet direct and indirect estimates of LAI correlate linearly and highly significantly as observed in this study (Chap. 5.1.3.2) and in published reports (e.g. Chason et al. 1991, Fassnacht et al. 1994, Cutini et al. 1998, Gower et al. 1999, Prskawetz and Lexer 2000, Mussche et al. 2001). Also, the PCA is able to capture temporal and spatial variations of LAI and differences in the structure of deciduous stands (Chason et al. 1991, Cutini et al. 1998, Mussche et al. 2001). The similar spatial coefficients of variation noted in the present study for litter-based and PCA-based LAI may indicate the same, as well as the seasonal development of LAI shown in Figure 5.1.3.1.

The underestimation in LAI when using the PCA usually decreases considerably when only the inner four of the five concentric rings (1–4) of the PCA-optics (Chap. 4.4.3) are used for calculations as was done in the study presented here, e.g. from 26.5 % to at least 11.5 % in a study by Cutini et al. (1998) or from 23 % to 5 % in a report by Prskawetz and Lexer (2000). Explanations for the systematic underestimation of the PCA are summarised in the following:

Chen and Black (1991) stated that errors in PCA-based measurements result from enhanced diffuse radiance due to the scattering of blue light by the foliage and estimated the error to be especially high (10–30 %) at lower elevation angles ( $68^\circ$ , ring 5 of the PCA; on average over all rings 4 % error). This could at least in part explain the reported underestimation of the PCA compared to direct methods, and also why omitting the outer ring (ring 5) of the PCA results in improved estimates (Dufrêne and Bréda 1995, Strachan and McCaughey 1996, Cutini et al. 1998, Leblanc and Chen 2001, but see Planchais and Pontailler 1999). Gower et al. (1999) summarised that direct and indirect estimates of LAI, corrected for foliage clumping (non-randomness) and light interception by woody tissue, compared to within 25–30 % for a wide range of agricultural and forest canopies. They caution, however, that gap fraction-based (i.e. optical) estimates of LAI plateau around 5–6, which they attribute to the saturation of gap fraction as LAI reaches 5–6. Jones et al. (2003) state that all methods measuring below-canopy radiation (as well as remotely sensed above-canopy radiation-based methods) become less and less accurate as LAI increases above 4–5; remotely sensed vegetation indices may even saturate in forests with  $\text{LAI} > 3–5$  (Burrows et al. 2002). In accord with these authors, Cutini et al. (1998) also found a better correlation between direct and indirect estimates for leaf area indices  $< 5$ .

Another source of underestimation of LAI by indirect optical methods can originate from the non-random spatial distribution of foliage elements (the clumping of foliage; and also from the clumping of woody components: Deblonde et al. 1994), violating the assumptions of the PCA-method (Chason et al. 1991, Gower et al. 1999, Mussche et al. 2001). Kucharik et al. (1999) reported that closed-canopy deciduous forest stands of oak and sugar maple exhibited a nearly random spatial distribution of foliage at any angle of view, thus hardly undermining the assumptions of gap fraction theory, in contrast to conifer forests, where corrections of considerable magnitude have to be carried out (e.g. Chen

et al. 1997, Kucharik et al. 1998, 1999). Mussche et al. (2001) attributed the underestimation of LAI by the LAI-2000 PCA in a mixed beech-oak (*Q. robur*) forest to non-random foliage distribution.

Additionally, direct methods, using planimetry on flat leaves, will give a half-total surface leaf area index, whereas the indirect optical methods will result in projected leaf area index, which can be substantially lower than half-sided LAI depending on the zenith angle of measuring optics and leaf inclination angles (Chen and Black 1992, Leuschner 1994, Gower et al. 1999).

Kucharik et al. (1998) showed that indirect estimates of LAI adjusted for non-random foliage distribution and light-intercepting branch area can approximate direct estimates of LAI to within 5 %, based on measurements in a boreal aspen forest with a direct LAI of 3.3. In the present study indirectly estimated LAI, using only rings 1–4 of the PCA and procedures as in Kucharik et al. (1998, 1999; see Chap. 4.4.3), also were mainly within 5 % of semi-direct litter-based estimates with just one exception of a 9 % difference (Steinkreuz 1999, see Tab. 5.1.3.1).

The LAI was 6.7 for the Steinkreuz stand, 6.5 for Großebene, 7.2 for Farrenleite and 6.9 for the pure beech plot within the mixed stand at Steinkreuz, averaged over the monitored growing seasons and methods (Tab. 5.1.3.2). Published values for the LAI of pure stands of *Fagus sylvatica* range from 2.5–10.2, on average 6.4 ( $\pm$  1.76, n = 104 European stands; based on stand averages if data for more than one year was available) as summarised from 37 references (not shown). For mixed beech-oak (*Quercus petraea*, *Q. robur*) stands (plus mixed stands of either beech or oak with other broadleaved deciduous species), the range was 1.9–7.5, the average 5.4 ( $\pm$  1.13, n = 33 European stands; 22 references included). Hence the results presented here are close to the average values reported in the related literature.

The range of variability in the LAI at stand level, the temporal coefficient of variation (-19 % to +13 % between the years 1998 and 2000, Tab. 5.1.3.2, Tab. 5.1.3.3), compares well with the interannual variability observed in other temperate pure beech ( $\pm$  1–33 %) and mixed beech-oak stands ( $\pm$  8–19 %):

Cutini et al. (1998) reported interannual variations in two young beech stands in Italy of 7–21 % over three years (both litter traps and PCA); the variability of LAI estimates was higher for the PCA than for the litter. Granier et al. (2000a) and Wang et al. (2004) showed litter-derived LAI to vary between 1 % and 31 % over five years in a 30 year-old beech forest in France; an optical estimate of LAI changed from one year to the next by 8 %. Modelling results using above- and below-canopy measurements of global radiation suggested a range of changes from 5 to 23 % (Wang et al. 2004). Ehrhardt (1988) provided LAI estimates for a mature beech forest in central Germany (Göttinger Wald), varying by up to 20 %. In a 120 year-old beech forest in the montane Solling, central Germany, LAI differed by ca. 10 % from year to year (Heller and Götsche 1986, calculated from their Tab. 15 and Fig. 52, p. 118). Schipka (2003) presented data from four central German mature beech stands, including those studied by Ehrhardt (1988, above) and Heller and Götsche (1986, above), showing variabilities of up to 8 % between consecutive years. Jochheim et al. (2007) detailed litter-based LAI estimates for a 117 year-old north-east German beech forest varying 2–33 % from year to year. Le Dantec et al. (2000) compared the interannual variation of the LAI at 34 beech, oak, and mixed oak-beech stands of different structure in temperate France. Among those stands the ones comparable to Steinkreuz, Großebene and Farrenleite varied as follows: the LAI of the beech stands differed interannually 1–14 %, that of the oak stands 2–16 %, and in oak-beech stands 8–17 % (Le Dantec et al. 2000). Leuschner et al. (2001a) observed, in a mature mixed oak-beech forest in NW Germany, a variability of LAI (litter) over five years (estimated from their Fig. 3) which amounted to 10–19 % for the whole stand, to 11–29 % for beech alone (which held 69 % of the total LAI), and to 6–27 % for oak. Hanson et al. (2003a, b) reported the litter-based LAI to vary by 23 % during a 7-year period in an upland mixed oak forest in Tennessee, USA. Bréda and Granier (1996) observed a variation of the litter-derived LAI of 7–18 % over a 5-year period in a young French oak stand.

The reduction of LAI in 1999 compared to the previous year, observed in both litter and optical estimates for Großebene (-19 %) and in optical estimates for Steinkreuz (-9 %, Tab. 5.1.3.2, Tab. 5.1.3.3) may be viewed in connection with the masting of beech and especially oak in 1998 in both Steigerwald stands: carbohydrates might have been allocated to seed production in 1998 at the cost of leaf primordia for the year 1999 (cf. Makowka et al. 1991, Burton et al. 1991). Also, less radiation received during the vegetation period 1998 compared to the previous year (approx. 10 % less net radiation, data courtesy of G. Lischeid, Dept. of Hydrogeology, Univ. of Bayreuth, not shown) may have contributed to the reduction of LAI (cf. Roloff 1986). No insect calamities (especially the defoliation of oak by caterpillars of *Tortrix viridana*) were observed during 1998–2000 at any of the sites. In 1995 and 1996, in contrast, the defoliation of oak was considerable (Schäfer 1997; some oaks being completely defoliated), and a carry-over effect may be responsible for keeping LAI low at least in the year immediately after defoliation by this insect as observed by Kruijt (1989) in a young oak stand. It seems unlikely, however, that such a calamity on its own would reduce the LAI for more than one or two years. Bréda and Granier (1996) discussed a decrease of the LAI from one year to the next in an oak stand as the consequence of a critically deep spring frost just after leaf unfolding, and of drought. The frost damage did not lead to a decrease of LAI in the same year but was thought to have depleted the stored reserves so persistently that LAI was reduced during the following two years, which were both dry. Late frosts, i.e. after leaf unfolding, were not observed during the years 1998–2000 at Steinkreuz, however.

Le Dantec et al. (2000) and Hogg (1999) interpreted their findings of reduced LAI in terms of a decreased carbon balance having been caused by drought in the previous year (the year of bud formation), which was observed only in stands with an  $LAI > 5.5$  (Le Dantec et al. 2000). Drought may also affect the LAI through reduced leaf water potentials during leaf emergence as a direct consequence of low soil water content at the time or as an indirect result of drought-induced cavitation during the previous year (Tyree et al. 1994). However, Leuschner et al. (2001a) could not detect any effects of drought on the LAI of beech or oak in a mixed stand in NW-Germany under moderate drought stress. Jochheim et al. (2007) in contrast found LAI to have decreased from 6.4 and 6.3 in the two previous years to 4.5 in an extremely dry year (2003; see e.g. Ciais et al. 2005) when precipitation was already very low during the early part of the growing season and evaporative demand very high (Lütschwager and Remus 2007); leaves showed xeromorphic traits as a consequence. In the year following the drought LAI recovered to 6.0 (Jochheim et al. 2007). Since the year 1998 was not extremely dry (Chap. 5.2.1, below) the reduction of the LAI at the Steigerwald sites in 1999 may be more likely to have been caused by the masting of the trees (see above). In the following year, the LAI increased again by ca. 10 % in both mixed Steigerwald stands (Tab. 5.1.3.2, Tab. 5.1.3.3).

## 6.2. Xylem sap flow density $J_s$

### 6.2.1. Radial patterns of sap flow density $J_s$ in *Fagus sylvatica*

Using thermal dissipation probes of 20 mm radial heater length, patterns of sap flow density  $J_s$  assessed in up to three incremental depths in the sapwood of beech (0–2 cm pith-wards from the cambium-xylem boundary, annulus #1; annulus #2: 2–4 cm; annulus #3: 4–6 cm) showed a radial trend of decreasing sap flow density  $J_s$  with increasing sapwood depth (Fig. 5.3.1a–c, Fig. 5.3.3).  $J_s$  typically peaked in the outermost annulus, or in a few trees in the second annulus, as also observed in other studies on European beech (Köstner et al. 1998a, Lang 1999, Granier et al. 2000a, Granier et al. 2003 (including data from Steinkreuz from the study presented here), Schäfer et al. 2000, Patzner 2004, Geßler et al. 2005, Hölscher et al. 2005, Lüttschwager and Remus 2007) and other diffuse-porous tree species (e.g. Kubota et al. 2005a, b: *F. crenata*).

The maximum half-hourly values of  $J_s$  in annulus #1 ( $J_{s\ 0-2cm}$ ) reached 65–78 g m<sup>-2</sup> s<sup>-1</sup> in beech of the stands studied and maximum hourly rates of up to 181–276 kg m<sup>-2</sup> h<sup>-1</sup> (Tab. 5.3.1). These rates are comparable to the published values for beech, which range from 30–140 g m<sup>-2</sup> s<sup>-1</sup> and 110–250 kg m<sup>-2</sup> h<sup>-1</sup>:

Granier et al. (2000a) detailed maximum half-hourly rates of  $J_{s\ 0-2cm}$  of ca. 110 g m<sup>-2</sup> s<sup>-1</sup> for dominant trees (DBH 10–21 cm) from a young dense north-east French beech forest. Kolcun (2005) observed maximum half-hourly rates of around 110 g m<sup>-2</sup> s<sup>-1</sup> for a dense sub-montane beech stand in south-eastern Germany. Geßler et al. (2005) gave ca. 30 g m<sup>-2</sup> s<sup>-1</sup> as the mean maximum value for June (6 beech trees, DBH 44–51 cm, southern Germany). Geßler et al. (2001) reported an average ( $n = 7–9$ ) maximum half-hourly  $J_{s\ 0-2cm}$  of approx. 40 g m<sup>-2</sup> s<sup>-1</sup> (SD ca.  $\pm 20$  g m<sup>-2</sup> s<sup>-1</sup>) for mature beech trees from two stands in SW Germany. Steppe et al. (2002) calculated a mean maximum 10'-value of 86 g m<sup>-2</sup> s<sup>-1</sup> (0–3 cm sapwood depth) for four similar days in August for a dominant beech (DBH 61 cm,  $h_t = 27$  m, 75 yrs) in lowland Belgium. Leuzinger et al. (2005) detailed maximum rates of 80–140 g m<sup>-2</sup> s<sup>-1</sup> for beech in a Swiss mixed sub-montane stand. Hölscher et al. (2005) showed values of  $J_s$  for *F. sylvatica* from a mature pure stand in Central Germany of about 50 g m<sup>-2</sup> s<sup>-1</sup>, but it is not clear whether this is for outer sapwood (i.e.  $J_{s\ 0-2cm}$ ), or averaged over the whole sapwood radius (i.e.  $J_{st}$ ). In the former case their value would be a bit lower than the maximum values in similar sized trees from this study, in the latter case their value would be corresponding to 180 kg m<sup>-2</sup> h<sup>-1</sup> and would be slightly higher than findings from this study (maximum  $J_{st\ hh\ max}$  151 kg m<sup>-2</sup> h<sup>-1</sup>, Tab. 5.5.1). Lüttschwager and Remus (2007) exemplified half-hourly values of  $J_{s\ 0-2cm}$  of up to 110 kg m<sup>-2</sup> h<sup>-1</sup> measured on beech (DBH 24–68 cm) in a pure stand in NE-Germany. Aranda et al. (2005) presented midday maxima of  $J_{s\ 0-2cm}$  of around 200 kg m<sup>-2</sup> h<sup>-1</sup> for smaller *F. sylvatica* (DBH 10–17 cm), growing in a closed mixed forest with *Q. petraea* in sub-Mediterranean Spain at the southern limit of the species' distributions, less than the larger beech at Steinkreuz, Großebene and Farrenleite (see above and Tab. 5.3.1). Lang (1999) listed a maximum  $J_{s\ 0-2cm}$  of about 200 kg m<sup>-2</sup> h<sup>-1</sup> for four beech trees from a stand in south-western Germany. Patzner (2004) only depicted very little data of hourly  $J_s$  (presumably in 0–2 cm depth), maximum values reaching about 250 kg m<sup>-2</sup> h<sup>-1</sup> (northern site of stem; values from southern side around 350 kg m<sup>-2</sup> h<sup>-1</sup>) in a beech tree growing in a beech-spruce forest in southern Germany. Schäfer (1997) showed maximum midday values of  $J_{s\ 0-2cm}$  of round 220 kg m<sup>-2</sup> h<sup>-1</sup> for beech from Steinkreuz in the Steigerwald (same stand as in this study, but different trees and year).

Within the same tree,  $J_s$  in different depths was correlated on levels of half-hourly to daily values (Fig. 5.3.1d–i, Fig. 5.3.2). Furthermore, the daily integrated  $J_s$  ( $J_{s\ day}$ ) increased with tree diameter in all measured sapwood depths in beech at the Steinkreuz and Großebene stands (Fig. 5.3.5). At the Farrenleite stand the increase of  $J_{s\ day}$  with tree diameter was less pronounced (Fig. 5.3.6). This may be due to the different stand structure of Farrenleite, namely the larger stand density compared to the Steigerwald sites, resulting in high (intra-specific) competition and small radial

stem increments. Also, the stand's location on a steeper slope compared to the more level stands in the Steigerwald could have resulted in more carbon investment in height growth than in radial growth in order to counterbalance depressions in the slope in competition with neighbouring trees for light. Thus in such a stand, and particularly in comparison with stands on less steep slopes, DBH may not be the best predictor for  $J_s$  (see also Chap. 6.3, below).

Both seasonal average and maximum daily values of  $J_{s\ day}$  increased with an increase in the sapwood area of the annulus  $A_{si}$  or with the sapwood area of the whole tree  $A_{st}$  (not shown; the sapwood area-weighted maximum seasonal  $J_{st\ day}$  was also positively correlated with DBH: Fig. 5.5.1a). Granier et al. (2000a) correspondingly reported an increase in  $J_s$  with an increase in basal area or circumference for *F. sylvatica*. Hölscher et al. (2005) in contrast found a linear decrease of  $J_s$  with DBH in the same species, though the range of DBH of the mere five trees they studied was much smaller (mean DBH 65 cm  $\pm$  7 cm SD: Hölscher et al. 2005). Lütschwager and Remus (2007) could not detect any trends in seasonally averaged  $J_{s\ day}$  in 0–22 mm sapwood depth with DBH in 10–12 beech trees, ranging 24–68 cm in DBH, over three seasons (altogether 22 trees), and variability in  $J_s$  was large among trees. In 22–44 mm depth no trend was discernible either (5–7 trees per season, 12 trees in total). These authors reasoned that the relatively high values of  $J_s$  in small trees perhaps originated from thinning in the past, causing higher light interception in formerly shaded trees or increased leaf area–sapwood area ratios ( $A_{lf}/A_{st}$ ). Hence  $J_s$  increased with DBH when taking into account the effects of thinning (Lütschwager and Remus 2007). An increase of  $J_s$  with DBH was also observed in other angiosperm tree species, e.g. by Kelliher et al. (1992) for southern hemispheric temperate *Nothofagus fusca* and *N. menziesii*, by Granier et al. (1996c) in several tropical rainforest species, by Hölscher et al. (2005) for temperate *Acer pseudoplatanus*, *Tilia cordata* and *Carpinus betulus*. In temperate ring-porous *Fraxinus excelsior* in contrast, Hölscher et al. (2005) found a decrease of  $J_s$  with DBH, like Meinzer et al. (2001) and Meinzer (2003) in 31 tropical species. (However, the number of sampled trees per species was mostly only one (14 species) and at most three (five species), four (two species) and five individuals (two species) in the reports by Meinzer et al. (2001) and Meinzer (2003)). Phillips et al. (1999) and Ewers et al. (2002) found no trend in species of a Panamanian moist tropical forest and in several species of temperate North American forest types. In the present study,  $J_s$  was not generally correlated with DBH in *Q. petraea* (Fig. 5.3.7, Fig. 5.5.1b), except for the Großebene stand when considering the seasonal maxima of  $J_{s\ day}$  there (Fig. 5.5.1b).

The correlation of radial variability of  $J_s$  in beech with depth observed in the present study (see above) was further increased when using relative instead of absolute sapwood depth (Fig. 5.3.3, Fig. 5.3.4), also shown by Granier et al. (2003), Kubota et al. (2005b) and Lütschwager and Remus (2007). In concert with this, Kubota et al. (2005b) demonstrated that also the count of growth rings from the cambium was a good predictor of  $J_s$ .

The seasonal mean  $J_{s\ day}$  of beech (averaged across all trees of a stand and over two to three growing seasons) in outermost sapwood (0–2 cm) spanned 1121 ( $\pm$  290, 1 SD) kg m<sup>-2</sup> d<sup>-1</sup> (Steinkreuz) to 730 ( $\pm$  322) kg m<sup>-2</sup> d<sup>-1</sup> (Farrenleite). In 2–4 cm depth it ranged from 927 ( $\pm$  306) kg m<sup>-2</sup> d<sup>-1</sup> to 473 ( $\pm$  241) kg m<sup>-2</sup> d<sup>-1</sup>, respectively, and in 4–6 cm from 753 ( $\pm$  328) kg m<sup>-2</sup> d<sup>-1</sup> to 174 ( $\pm$  94) kg m<sup>-2</sup> d<sup>-1</sup>, respectively (Tab. 5.3.3). Lang (1999) found similar seasonal averages ( $n = 140$  d) for four beech trees (DBH

42–63 cm) of approx. 995 ( $\pm 175$ ) kg m<sup>-2</sup> d<sup>-1</sup> in 0–2 cm sapwood depth, of 790 ( $\pm 210$ ) kg m<sup>-2</sup> d<sup>-1</sup> in 2–4 cm, of 575 ( $\pm 340$ ) kg m<sup>-2</sup> d<sup>-1</sup> in 4–6 cm and of 455 ( $\pm 200$ ) kg m<sup>-2</sup> d<sup>-1</sup> in 6–8 cm depth (averages and SD calculated from his Table 12). Lütschwager and Remus (2007) reported for *F. sylvatica* for 0–22 mm sapwood depth averages from 10–12 trees to amount to a comparable 961–1107 kg m<sup>-2</sup> d<sup>-1</sup> for three seasons ( $\pm 206$ –346 kg m<sup>-2</sup> d<sup>-1</sup>) and for 22–44 mm depth to 764–779 ( $\pm 419$ –208) kg m<sup>-2</sup> d<sup>-1</sup>, (5–7 trees). Hölscher et al. (2005) observed a mean of 1520 kg m<sup>-2</sup> d<sup>-1</sup> for five beech trees during a three-week period in July with ample soil moisture.

Using all the available data of  $J_s$  day to calculate a seasonal average  $J_s$  day (excluding rainy days with low flow rates and thus high uncertainties) for each sapwood annulus for each tree, a relationship emerged when plotted against relative sapwood depth (Fig. 5.3.4) which could be satisfactorily described with a linear regression function (highest correlation coefficient and lowest  $p$ -value). This relationship did not differ significantly between sites and years. Based on Equation 5.3.2 (using both data from 1999 and 2000),  $J_s$  in 25 % relative sapwood depth from cambium decreased to 83 % of  $J_s$  0–2cm, in the middle of the sapwood to ca. 55 % and in 75 % relative depth to ca. 27 % of  $J_s$  0–2cm. In absolute radial dimensions of sapwood the decline from annulus #1 (0–2 cm) to annuli #2 (2–4 cm) and #3 (4–6 cm) was 1 : 0.75 ( $\pm 0.22$ ) : 0.43 ( $\pm 0.25$ ), respectively, for the pooled trees from all stands and years (Tab. 5.3.3). The stand-specific (averaged) patterns of the radial decline of  $J_s$  relative to  $J_s$  in outer sapwood were steeper for the denser stands with smaller trees (Farrenleite 1: 0.65 : 0.27; GroßeBene 1 : 0.72 : 0.35) and gentler for Steinkreuz with its large number of strong trees (1: 0.82 : 0.61; Tab. 5.3.3). This is largely in concert with findings from other reports on the same species:

Lang (1999) showed a similar radial profile of average daily  $J_s$  measured on 4 trees (DBH 42–63 cm, ca. 60 yrs) in a colline SW German beech stand where  $J_s$  2–4cm was 69 %,  $J_s$  4–6cm 59 % and  $J_s$  6–8cm 44 % of  $J_s$  0–2cm, respectively; based on the given exponential decay function the proportions in these depths from outer to inner sapwood were 1 : 0.73 : 0.56 : 0.46.  $J_s$  reported by Patzner (2004) averaged over a total of 93 days in three years for two beech trees (DBH not specified, between 14 cm and 37 cm) from a 60 year-old colline–sub-montane mixed beech-spruce stand in southern Bavaria, declined to 70 % of  $J_s$  0–2cm in 2–4 cm and to 50 % of  $J_s$  0–2cm in 4–6 cm sapwood depth. In a (mixed deciduous) beech forest in eastern Denmark, L. Dalsgaard (pers. comm. 2003) assessed the radial variability of  $J_s$  in 0–2cm, 2–4 cm and 4–6 cm sapwood depth in four co-dominant beech trees (DBH 35–42 cm) and found a similar decrease of 1 : 0.82 : 0.49 averaged over a period of 8 days in July.

Lütschwager and Remus (2007) measured  $J_s$  in 5–7 beech trees (DBH 19–60 cm, on average 47 cm) in several sapwood depths over three growing seasons in a mature beech stand in NE-Germany. Based on the average seasonal values reported in their Table 3,  $J_s$  day in 2.2–4.4 cm depth calculated to 61–76 % of  $J_s$  day in 0–2.2 cm during three growing seasons, on average 67 %, which compares well with results from this study. During one year,  $J_s$  was measured in one tree in 6 contiguous depths down to 13.2 cm and in another tree in four increments down to 8.8 cm (Lütschwager and Remus 2007). Averaged over 64 days in 2004 and the two trees (calculated from values in their Tab. 5) the radial pattern was 1 : 1.10 : 0.25: 0.34: 0.22 : 0.32 from 0–13.2 cm. They used a combined model, consisting of an exponentially increasing part for the outermost xylem and a decay function for inner xylem, to describe the radial pattern observed on these two trees. Sapwood and ripewood were not distinguished and the maximum measured xylem depth was 40 % of the total radius. The decrease estimated from the regression model was much steeper than in this study: in a radial xylem depth of 10 % of the total radius (from cambium to pith)  $J_s$  with 85 % of maximum  $J_s$  was comparable to results from this study (92 %, assuming the sapwood area–DBH relationship from the Steigerwald holds for their stand in NE-Germany as well), while in 20 % relative depth  $J_s$  decreased to 30 % of  $J_s$  max (74 %), in 30 % depth to 17 % of  $J_s$  max (55 %) and in 40 % depth to 13 % of  $J_s$  max (37 %). There might be, however, considerable uncertainty in the data underlying the regression model presented by Lütschwager and Remus (2007), given the small number (or absence) of replicates for deep sapwood positions and the increased likelihood of errors caused by heat transfer along the shaft of a thermal

dissipation probe implanted deep inside the trunk (see also remarks below; no information about the installation procedure were detailed by the authors).

Geßler et al. (2005) described rather qualitatively a more gentle decrease of  $J_s$  with increasing radial depth (down to 14 cm) in two beech trees (DBH 51 cm each).  $J_s$  only started to decrease at a distance of 6–8 cm from the cambium. Unfortunately only few data are shown and no daily sums of  $J_s$  in different depths are detailed, merely an average diurnal pattern measured over a period of two months. These authors employed long thermal dissipation probes with 7 thermocouples in line in equal distances of 2 cm, beginning at 1 cm distance from the tip of the probe, and with a heating wire coiled around the whole length of the probe (14 cm). This gives rise to the concern that the radial gradient of  $J_s$  may have been smoothed by heat transfer through the metallic shaft of the needle from sapwood regions with lower sap flow to regions of higher sap flow (Jiménez et al. 2000). This limits the conclusions that can be drawn from the work of Geßler et al. (2005).

Measurements of radial variation of  $J_s$  carried out in the same stand as in the present study (Steinkreuz) in a previous year (1996: Schäfer 1997, Schäfer et al. 2000) on a smaller number of beech trees (5, DBH 13–59 cm) but down to 10 cm sapwood depth ( $n \leq 3$  probes per depth in inner sapwood, in total 9 probes in deep sapwood) revealed a steeper radial decline than in the study presented here. Based on their plotted regression function,  $J_s$  declined to merely ca. 22 % of  $J_{s\ 0-2cm}$  in 2–4 cm sapwood depth, then declined only marginally deeper in the sapwood, to ca. 20 % of  $J_{s\ 0-2cm}$  in 8–10 cm depth (Schäfer et al. 2000). A different sensor design was used in the study by Schäfer (1997) and Schäfer et al. (2000) which may have facilitated heat transfer from the heated zone in inner sapwood to the outer sapwood and to the atmosphere outside the tree trunk, due to a thicker shaft of the heater (the heating zone having the standard diameter and length). This in turn may have damped the temperature difference signal and thus resulted in the calculation of too low a diurnal amplitude of  $J_s$  deep compared to  $J_{s\ 0-2cm}$ . Köstner et al. (1998a) also presented a steeper radial profile of  $J_s$  for beech, using part of the data of Schäfer (1997) from the Steigerwald plus data from one mature French beech tree (Amance forest, Nancy, DBH not detailed), for one summer day, where  $J_{s\ 2-4cm}$  was about 50 % and  $J_{s\ 4-6cm}$  approx. 25 % of  $J_{s\ 0-2cm}$ . Hölscher et al. (2005) detailed a radial profile of  $J_s$  measured on five adult beech trees (DBH  $65 \pm 7$  cm) in a colline old-growth forest in central Germany, which they described with an exponential decay function. The relative decline of  $J_s$  was 1 : 0.36 : 0.23 : 0.17 for the four investigated sapwood depths. In their study, radial profiles were assessed in only one tree at a time and only for five days. Granier et al. (2000a) observed an exponential radial decline in  $J_s$  similar to that of Köstner et al. (1998a) or Hölscher et al. (2005) but in three trees from a young beech stand (30 a).  $J_s$  in 2–4 cm depth was ca. 42 % of  $J_{s\ 0-2cm}$  and in 4–6 cm depth ca. 24 % of  $J_{s\ 0-2cm}$ . This agrees with the observation that the radial decline of  $J_s$  was steeper in smaller trees (cf. Fig. 5.3.5–6, and above).

In *Fagus crenata* (Japanese beech; closely related to *F. sylvatica*: Wilmanns 1989, Peters 1997) Kubota et al. (2005b) employed exponential decay functions to describe the radial patterns of  $J_s$  at three Japanese sites differing, among other characteristics, in elevation (550–1500 m a.s.l.). Showing values of  $J_{s\ day}$  comparable to those in European beech from the study presented,  $J_{s\ 2-4cm}$  accordingly was 60–72 % of  $J_{s\ 0-2cm}$  and  $J_{s\ 4-6cm}$  36–52 % of  $J_{s\ 0-2cm}$  in *F. crenata* (Kubota et al. 2005b). A Weibull-function was applied by Kubota et al. (2005a) to describe the radial pattern of  $J_s$  in *F. crenata* and to interpolate the decline of  $J_s$  beyond probed sapwood. The Weibull-function was individually fitted to the data from each tree using three coefficients, which varied between trees (Kubota et al. 2005a). No general pattern was extracted that could be used to predict the radial distribution of  $J_s$  in other trees. This points to a general constraint of such mathematically elaborate functions, namely that the apparent “precision” in the description of the radial pattern requires a larger number of coefficients (Ford et al. 2004a, Kubota et al. 2005a). This may result in a lower generality of such functions compared e.g. to the linear function used in this study and/or they may require a larger number of radial measurement depths to parameterise such a function (cf. Poyatos et al. 2007). Obviously, less regular radial patterns of  $J_s$  than observed on *F. sylvatica* in this study at the given spatial resolution might require a larger number of measurements in greater sapwood depth in order to be detected at all.

Thus the range of  $J_s$  in 2–4 cm sapwood depth for beech trees and stands comparable to the ones studied here, regarding the DBH and the sampling protocol, was rather narrow, namely 0.65–0.82 relative to  $J_{s\ 0-2cm}$ . In 4–6 cm sapwood depth  $J_s$  reached values from 0.27 to 0.61 of  $J_{s\ 0-2cm}$ . Correspondingly, published basal area–sapwood area relationships for *F. sylvatica* were similar to the ones from the stands

in the Steigerwald and the Fichtelgebirge (Fig. 6.1.1, Chap. 6.1), which, taken together, may indicate a common functional anatomy of beech sapwood under the conditions prevailing in Central Europe. Interestingly, mature *F. crenata* from submontane to montane and upper montane sites in Japan seemed very similar to *F. sylvatica* with regard to the radial decline of  $J_s$ . This may underline the close relatedness of the two species. Expressing sapwood depth in relative terms, as exemplified in Figure 5.3.4, would perhaps explain part of the variation between the published radial trends of  $J_s$  from different, particularly young stands. The lack of an even basic description of measured trees, however, often limits the closer analysis of published data. Nevertheless the compiled data and that presented here point to a general pattern of radial decline in  $J_s$  in beech across the Central European stands studied so far.

This is further substantiated when comparing the two landscapes and elevations studied here: the maximum rates of  $J_s$  0–2cm were similar for beech from the Steigerwald and the Fichtelgebirge, for temporal scales ranging from half-hourly to daily values (Tab. 5.3.1, Tab. 5.3.2): this indicates that the same general controls are operating at the two elevations, despite climatic gradients and large stand structural differences (see also Chap. 5.5 and discussion in Chap. 6.4.2). Such similar behaviour of  $J_s$  has also been observed along a larger altitudinal gradient in Japanese *F. crenata*, spanning almost 1000 m in elevation (550–1500m; Kubota et al. 2005b). High values of daily  $J_s$  0–2cm, however, were about twice as frequent at Steinkreuz as at Farrenleite. Also,  $J_s$  differed in deeper sapwood (when comparing the largest trees from each site, Tab. 5.3.1), given the smaller dimensions of beech trees at Farrenleite in the Fichtelgebirge. Trees of similar DBH were comparable in  $J_s$  also in deeper sapwood (Fig. 5.3.5–7). Mean seasonal values were considerably smaller at the high elevation site (Tab. 5.3.2, Tab. 5.3.3) due to a shorter growing season and lower temperatures, radiation and vapour pressure deficit of the air D (Tab. 5.2.1.1).

### 6.2.2. Sap flow density $J_s$ in *Quercus petraea*

In sessile oak, one standard thermal dissipation probe was sufficient to cover the whole (or in some cases at least the most significant part of the) sapwood depth of the mature trees sampled at the study sites (Tab. 4.1.1) in order to scale up sap flow density  $J_s$  to tree and stand level. Radial patterns of axial sap flow in ring-porous oaks exist at spatial resolutions higher than that of the thermal dissipation sensors used in this study, and are already well documented in the literature (see Chap. 2.3). If the fine-scale (< 20 mm) radial pattern of  $J_s$  in *Q. petraea* changed over the course of the season with progressing soil water depletion and if as a consequence wide parts of the xylem became dysfunctional due to cavitation, then additional errors due to imperfect integration of sap flow across the 20 mm-long standard thermal dissipation probe could arise (cf. Clearwater et al. 1999, Kučera and Tatarinov 2003, Tatarinov et al. 2005, Herbst et al. 2007b).

The sap flow density in 0–2 cm sapwood depth ( $J_s$  0–2cm) showed no significant trend with tree diameter for the mature oak trees studied here (Fig. 5.3.7); the narrow range of stem diameters (30–50 cm) compared to beech (14–66 cm, cf. Tab. 4.1.1) may have obscured a pattern if existent at all. Accordingly, Bréda et al. (1993a, b) noted no significant differences between codominant and dominant trees, but identified lower values of  $J_s$  in suppressed *Q. petraea* and *Q. robur*. Vertessy et al. (1995) also found no systematic relationship between stem diameter and mean daily  $J_s$  in

*Eucalyptus regnans*, and neither did Phillips et al. (2003b) within even-aged stands of deciduous ring-porous *Quercus garryana*. When comparing stands though, Phillips et al. (2003a, b) recorded higher  $J_s$  in oaks from an old stand than in oaks from a younger stand. Recently, Herbst et al. (2007b) reported that the  $J_s$  of *Q. robur* in a mixed English forest was positively related to DBH, but that tree-to-tree variability was high, as in the present study.

Values of  $J_{s\ 0-2cm}$  for oak were of the same order of magnitude as values of  $J_{s\ 0-2cm}$  for beech, though somewhat smaller than those of beech, reaching maximum half-hourly values of up to  $56\text{ g m}^{-2}\text{ s}^{-1}$  and  $59\text{ g m}^{-2}\text{ s}^{-1}$  or maximum hourly values of up to  $201\text{ kg m}^{-2}\text{ h}^{-1}$  and  $207\text{ kg m}^{-2}\text{ h}^{-1}$  at Steinkreuz and Großebene, respectively (beech:  $78\text{ g m}^{-2}\text{ s}^{-1}$  and  $276\text{ kg m}^{-2}\text{ h}^{-1}$ , respectively; Tab. 5.3.1 and Chap. 6.2.1). In other comparisons of ring- and diffuse-porous tree species, Oren and Pataki (2001), Wullschleger et al. (2001) and Pataki and Oren (2003) also found smaller  $J_{s\ 0-2cm}$  in ring-porous (mostly *Quercus* species) than in diffuse-porous tree species. The rates of  $J_{s\ 0-2cm}$  for *Q. petraea* from the present study are in the range of values reported in the literature, which reach  $30-100\ (-300)\text{ g m}^{-2}\text{ s}^{-1}$  and  $200-350\text{ kg m}^{-2}\text{ h}^{-1}$  in *Q. petraea* or *Q. robur* and  $30-70\text{ g m}^{-2}\text{ s}^{-1}$  or  $90-430\text{ kg m}^{-2}\text{ h}^{-1}$  in North American deciduous oak species:

Aranda et al. (2005) reported very similar rates of midday maxima for  $J_{s\ 0-2cm}$  of around  $200\text{ kg m}^{-2}\text{ h}^{-1}$  for smaller *Q. petraea* (DBH 12–16 cm) in a mountain region in Spain. Bréda et al. (1993a) observed somewhat higher maximum values of up to  $280\text{ kg m}^{-2}\text{ h}^{-1}$  in trees of the same species in a young (32 a) dense ( $3644\text{ trees ha}^{-1}$ ,  $A_b\ 25\text{ m}^2\text{ ha}^{-1}$ ) French stand and Vincke et al. (2005a) of up to  $350\text{ kg m}^{-2}\text{ h}^{-1}$  in a thinned ( $107\text{ trees ha}^{-1}$ ,  $A_b\ 14\text{ m}^2\text{ ha}^{-1}$ ) and up to  $250\text{ kg m}^{-2}\text{ h}^{-1}$  in an un-thinned ( $175\text{ trees ha}^{-1}$ ,  $A_b\ 20\text{ m}^2\text{ ha}^{-1}$ ) colline Belgian stand (105 a) of *Q. robur*. Leuzinger et al. (2005) detailed a maximum of  $30-90\text{ g m}^{-2}\text{ s}^{-1}$  for sessile oak in a mixed sub-montane forest in Switzerland. Rates of  $J_s$  reported by Herbst et al. (2007b) for *Q. robur* from a mixed forest in the UK are exceptionally high, reaching up to  $300\text{ g m}^{-2}\text{ s}^{-1}$ , but mostly up to  $100\text{ g m}^{-2}\text{ s}^{-1}$ ; these authors used 30 mm-long probes and corrected for inactive heartwood according to Clearwater et al. (1999), the average fraction of the probes in contact with sapwood being only 0.7, which may introduce additional uncertainty to the data. In other ring-porous oak species, Phillips et al. (1996) measured up to  $90\text{ kg m}^{-2}\text{ h}^{-1}$  in *Q. alba* (sampled late in the growing season), Pataki et al. (1998) found maximum values of  $210\text{ kg m}^{-2}\text{ h}^{-1}$  in *Q. phellos*, and Wullschleger et al. (2001) listed  $160\text{ kg m}^{-2}\text{ h}^{-1}$  for *Q. alba*,  $170\text{ kg m}^{-2}\text{ h}^{-1}$  for *Q. prinus* and  $200\text{ kg m}^{-2}\text{ h}^{-1}$  for *Q. rubra*. Spicer and Holbrook (2005) depicted maxima of ca.  $30\text{ g m}^{-2}\text{ s}^{-1}$  for *Q. rubra*. All these investigators used 20 mm-thermal dissipation probes to measure  $J_s$ . Poyatos et al. (2007) for sub-Mediterranean deciduous *Q. pubescens* described a maximum rate of  $J_s$  in 3 mm sapwood depth of  $69\text{ g m}^{-2}\text{ s}^{-1}$  and of  $36\text{ g m}^{-2}\text{ s}^{-1}$  in 11 mm depth using heat field deformation-sensors and similar values with 10 mm-long thermal dissipation probes. Asbjørnsen et al. (2007) for deciduous *Q. macrocarpa* growing in a denser woodland and in a more open (thinned) woodland ("savanna") in the Midwestern U.S., showed maximum average ( $n = 2$  or 3 trees) hourly values of  $J_s$  of  $180\text{ kg m}^{-2}\text{ h}^{-1}$  and  $430\text{ kg m}^{-2}\text{ h}^{-1}$ , respectively, and  $J_{s\ day}$  averaged to  $2070\ (\pm 500)\text{ kg m}^{-2}\text{ d}^{-1}$  and  $3590\ (\pm 2770)\text{ kg m}^{-2}\text{ d}^{-1}$ , respectively (32 days between June 23 and September 15). These authors used 30 mm long thermal dissipation probes and corrected for the proportion of the probes that was located in the heartwood, according to Clearwater et al. (1999). However, because this proportion was about 50 % (sapwood depth 12.4–18.6 mm, Asbjørnsen et al. 2007), the uncertainty in the corrected values of  $J_s$  would still have to be considered substantial. Rates from their (Asbjørnsen et al. 2007) denser stand with  $A_b = 38.3\text{ m}^2\text{ ha}^{-1}$  similar to Steinkreuz and Großebene are comparable to those of oak from the Steigerwald, regarding the hourly maximum (see above and Tab. 5.3.1) and by and large also with respect to average daily values ( $1369 \pm 588\text{ kg m}^{-2}\text{ d}^{-1}$ , Tab. 5.3.2). Poyatos et al. (2005) mentioned  $J_{s\ day}$  in *Q. pubescens* as similarly reaching up to  $1200\text{ kg m}^{-2}\text{ d}^{-1}$  in 0–1 cm sapwood depth. In *Q. prinus*, Wullschleger et al. (2001) recorded maxima of  $2520\text{ kg m}^{-2}\text{ d}^{-1}$  (average of nine trees, DBH 37–69 cm, mean DBH 48 cm), in *Q. rubra*  $1910\text{ kg m}^{-2}\text{ d}^{-1}$  (DBH 42 cm) and in *Q. alba*  $1790\text{ kg m}^{-2}\text{ d}^{-1}$  (DBH 53 cm). Values for *Q. alba*, *Q. velutina* and *Q. falcata* shown by Oren and Pataki (2001) (average DBH 38–45 cm) are slightly lower than those for *Q. alba* from Wullschleger et al. (2001) while rates of  $J_{s\ day}$  given by Pataki and Oren (2003) for *Q. alba* and *Q. rubra* are considerably smaller (ca.  $500\text{ kg m}^{-2}\text{ d}^{-1}$ , DBH 18–46 cm).

### 6.2.3. General radial pattern of $J_s$

The general radial patterns in the (axial) sap flow of European beech – a decrease of  $J_s$  with increasing distance from cambium – as shown in Chapter 5.3 and discussed above are indicative of the variation in hydraulic conductivity  $K_h$  and may be explained by general variation in wood anatomical parameters due to tree growth and ageing (e.g. Gartner and Meinzer 2005, Chap. 2.3). Superimposed on these general anatomical trends are changes in wood properties caused by environmental factors (e.g. Bouriaud et al. 2004, Skomarkova et al. 2006) which in turn may be modulated by competition (Piutti and Cescatti 1997). The points discussed in the following are basically also valid for *Q. petraea* (cf. Cermák et al. 1992, Granier et al. 1994, Poyatos et al. 2007), only on different spatial scales since the sapwood radius of this ring-porous species is smaller than that of diffuse-porous *F. sylvatica*.

In this study, no significant radial trend in wood density  $\rho_{wd}$  was observed on 5 mm long segments of increment cores taken from three beech trees (Fig. 5.1.1a), as found in the majority of reports on this species in the literature (see Chap. 5.1.1). Similarly Lang (1999), in concert with the findings of Sass and Eckstein (1995) and Bouriaud et al. (2004; see Chap. 2.3), observed no tendency of vessel density ( $\text{mm}^{-2}$ ) in the earlywood of beech over the outermost 20–34 growth rings of trees aged 60–68 years, and only a weak tendency of percentage vessel lumen area (conductive area) of the earlywood to decrease from the youngest to older growth rings. Based on the theoretical treatise of Roderick and Berry (2001), Barbour and Whitehead (2003) postulated that wood density and xylem sap velocity should not correlate in angiosperms while a relationship was observed in gymnosperms – at least from hydric sites – due to the fact that angiosperms generally have a few large, velocity-determining vessels embedded in a matrix of smaller tracheids.

Water content  $W_f$  (in  $\text{g cm}^{-3}$ ) and relative water content  $R_w$  (%) measured on the same increment core segments as  $\rho_{wd}$  decreased steadily with increasing radial depth from bark approximately halfway through to the pith and remained rather constant in innermost xylem (Fig. 5.1.1b, c). The depth where  $W_f$  and  $R_w$  did not decline any further indicated the transition from moister sapwood to drier ripewood. These observations are consistent with published patterns of  $W_f$  and  $R_w$  for beech (see Chap. 5.1.1). Corresponding with changes in  $W_f$  and  $R_w$ , absorption values  $\alpha$  (in  $\text{cm}^{-1}$ ), measured with a mobile computer tomograph (Chap. 4.3) on the same trees prior to core extraction, changed as well (Fig. 5.1.3).

Direct measurements of radial variation of  $K_h$  on trunks are destructive and calculation of theoretical  $K_h$  requires more detailed anatomical information, both approaches being beyond the scope of this study. Lang (1999) observed a barely significant radial decline of theoretical specific conductivity  $K_s$  in the earlywood of European beech, in contrast to a prominent radial decrease in  $J_s$ . This could be due to the fact that Lang (1999) measured vessel lumen areas only of part of the earlywood of a growth ring or due to the presence of embolisms or tyloses not accounted for on the microscopic sections prepared by Lang (1999). Differences between theoretical and actual  $K_s$  may also arise from other additional resistances to flow along the path not accounted for in theoretical  $K_s$  (see Chap. 2.3). In *Pinus ponderosa*, Domec et al. (2005) measured lower (maximum)  $K_s$  in inner than in outer sapwood, but the decrease in  $K_s$  was lower than the typical radial decline of  $J_s$  in this species (not measured concurrently in their study). Thus they considered that  $J_s$  and  $K_s$  may not be linearly (but non-linearly) correlated, supported by the findings of James et al.

(2003), Domec et al. (2006) and Meinzer et al. (2006). This tendency of  $J_s$  to saturate with increasing  $K_s$  indicated that factors other than  $K_s$  began to limit maximum  $J_s$  (James et al. 2003). The latter authors considered the most likely explanation to be that for a certain water potential gradient between leaf and soil (the driving force for  $J_s$ ), regions of sapwood with higher  $K_s$  would experience smaller axial tension gradients, and this in turn would diminish the response of  $J_s$  to increasing  $K_s$  (James et al. 2003). Meinzer et al. (2006) concluded from results for temperate conifers comparable to the findings of James et al. (2003) for tropical tree species that the similarity of the relationship between theoretical  $K_s$  and measured  $J_s$  implies a comparable stomatal regulation of xylem tension gradients among co-occurring species to produce similar rates of  $J_s$  at a particular value of  $K_s$ . Clearly, more specific experiments are desirable to elucidate general patterns and differences in the relationships of  $J_s$  and  $K_s$ , between species and anatomical-systematical groups of plants.

Radial trends in  $J_s$  may also be brought about by patterns in the hydraulic connectivity of certain parts of the sapwood radius with specific regions in the crown. A sap flow gauge in other words could merely be sensing the supply to one particular branch. Waring and Roberts (1979) stated for *Pinus sylvestris* that "the older, inner sapwood possibly supplies water mainly to the older lower branches which generally have less foliage and are less well irradiated than limbs higher in the crown", a view also taken by Nadezhina et al. (2002) for the same species. As well, Dye et al. (1991) suggested from measurements on *P. patula* that inner xylem originally supplied branches and leaves that are now shed and therefore inner xylem would not be as well-connected or functional as outer sapwood. And similarly, Jiménez et al. (2000) concluded that sap flow in the inner xylem layers is connected with the lower, deeper parts of crowns and outer xylem connected to the well-illuminated upper canopy of broad-leaved tree species (*Laurus azorica* and *Persea indica*). Nadezhina et al. (2007) attributed different radial patterns in the trunks of *Pinus sylvestris* growing in shallow and deep soil to different rooting and water extraction patterns, with deep sinker roots, which they propose are connected to the inner xylem, contributing more to sap flow than sinker roots on the shallow soil.

Studies of patterns of vascular sectoriality to date have mostly been carried out on branches, shrubs and small trees or saplings (e.g. Waisel et al. 1972, Orians et al. 2004, Zanne et al. 2006), which are easier to handle experimentally. But the results from such studies cannot be assumed to be directly transferable to axial long-distance transport in tall stems of large adult (forest) trees as studied in the present work. This is first of all because wood anatomy changes from juvenile to adult wood (see Chap. 2.3). Secondly, patterns of tangential and radial spreading of vessels along the stem axis as retrieved from dye injections have to be interpreted with caution since pressure gradients and hence flow directions are altered upon applying dye at atmospheric pressure and because dyes do not necessarily behave like xylem sap (Cermák et al. 1992, Tyree and Zimmermann 2002, p 32, p 44, pp 255–257). And thirdly, the probability of contact between conduits increases with an increasing axial length of the pathway, as detailed below:

Vité (1958) pointed out the significance of the spiral grain of xylem for water transport in conifers. He stated that spiral grain is a physiological necessity which enables the distribution of different water demands of different parts of the canopy across the whole water-conducting stem cross-sectional area. Braun (1959) showed for a deciduous broad-leaved tree species (*Populus sect. Aigeiros*) that vessels are connected within growth rings and across growth rings (growth ring bridges), forming a radial and tangential network of vessels. Tangential spreading of vessels was also shown for *Fraxinus*

*excelsior* (Burggraaf 1972) and *F. lanuginosa* (Kitin et al. 2004). Bosshard and Kučera (1973) quantified the network of vessels in a mature *Fagus sylvatica*, where they found an average radial spread of vessels of  $218 \mu\text{m} \cdot 10 \text{ mm}^{-1}$  (maximum  $420 \mu\text{m} \cdot 10 \text{ mm}^{-1}$ ) and an almost twice as large average tangential spread of  $402 \mu\text{m} \cdot 10 \text{ mm}^{-1}$  (maximum  $594 \mu\text{m} \cdot 10 \text{ mm}^{-1}$ ). One vessel was on average in contact with 5.6 (range 3–8) vessels over a length of 10 mm, and the contact length ranged from 0.1 mm to 1.9 mm, with lengths between 0.1 mm and 0.2 mm being the most frequent class (22 %; Bosshard and Kučera 1973).

The distance between the height of installation of the thermal dissipation probes and the height of the lowest living branch was  $\geq 7 \text{ m}$  (but about 3.9 m in two suppressed trees) for beech from Steinkreuz,  $\geq 6 \text{ m}$  for Großebeine, and  $\geq 7 \text{ m}$  for Farrenleite,  $\geq 13 \text{ m}$  for oak from Steinkreuz and  $\geq 12 \text{ m}$  for oak from Großebeine (Fig. 5.2.3). Using the findings from Bosshard and Kučera (1973, see above), the tangential spread for an axial distance of 7 m would be on average 28.1 cm, at most 41.6 cm. The calculation of a radial spread over 7 m axial distance is not reasonable because a vessel cannot leave its growth ring. Still, the meandering of vessels within a growth ring in combination with the existence of growth ring bridges allows the distribution of water across and between growth rings:

Kučera (1975) noted frequent vessel-to-ray contacts in beech, demonstrating that ray parenchyma is part of the hydraulic system of trees, particularly in the radial movement of water (Braun 1984, Hirose et al. 2005) and in water storage (Meinzer 2002). In *Quercus robur* and *Fraxinus excelsior* a smaller radial tissue displacement was observed than in beech (Bosshard et al. 1978, 1982), which was in part counterbalanced by vessel contacts across growth ring borders, and tangential spread was similar in magnitude to radial spread (Bosshard 1976, Bosshard et al. 1982). *Q. robur* exhibited a pronounced vessel-to-ray network to compensate for more isolated vessels (with less vessel-to-vessel contacts) than in diffuse-porous *F. sylvatica* (Bosshard et al. 1978, 1982). Bosshard et al. (1982) hypothesised that in the wood of beech the tangential spreading of vessels has a similar function for the water transport as the ring of large vessels in ring-porous species (and the radial cell wall pores in earlywood tracheids of conifers). And Bosshard (1976) stressed that growth-ring boundaries are not functional boundaries, but imposed on the tree by external factors.

A sectorial connection of a certain root with a certain part of sapwood as observed in orchard-grown apple (Cabibel 1994), cherry (Cabibel and Isberie 1997) and mango trees (Lu et al. 2000), may introduce a circumferential (azimuthal) variation of  $J_s$  on top of the radial variation since the sap flow gauges need to be spaced out from neighbouring gauges for thermal isolation. But the circumferential variation of sap flow is much less pronounced in tall, long-stemmed trees growing in closed stands (e.g. Schulze et al. 1985, Granier 1987b). Azimuthal variation has also been attributed to soil texture (Cermák et al. 1995, Cienciala et al. 1999, Oliveras and Llorens 2001). The same general considerations as for the stem–leaf connectivity regarding tangential spreading (see above) apply here. Nevertheless, by installing thermal dissipation probes between 1.3 m and 2 m above the ground it was sought to circumvent this additional source of uncertainty in the present study, as well as by installing probes in a fashion that allowed minimising the tangential distance between them (cf. Chap. 4.1.3). Thus for the large forest trees studied here it seems that patterns in the hydraulic connectivity of roots or branches to the trunk would only have a minor influence on the observed radial patterns of  $J_s$ . This is also the reason why it seemed statistically appropriate to confine the sampling of sap flow to one side of the trunk which was not randomly chosen but decided to be in the thermally least noisy northern exposition on the stems (cf. Wullschleger and King 2000, Wilson et al. 2001, Ford et al. 2004b). This sampling strategy then allowed a larger number of individual trees to be monitored with the limited resources of such a study and balanced the aims of the investigation at the different spatial levels (within-tree, tree and stand level).

#### 6.2.4. Effects of soil conditions, and seasonal trends in general, on radial patterns of $J_s$ in *Fagus sylvatica*

During periods of a relatively constant LAI in deciduous forests, soil water availability controls the potential canopy conductance, while PFD and D control the actual diurnal patterns of conductance (Körner 1994). Thus differences in the response of  $J_s$  day to atmospheric drivers of transpiration over the course of the season at the Steigerwald sites (Fig. 5.3.8), as also observed in *F. sylvatica* by Aranda et al. (2005) and Hölscher et al. (2005), could be due to changes in relative extractable soil water  $\theta_e$  as exemplified in Figure 5.3.9 (see also Chap. 6.4, below). European beech has been shown to rather tightly control stomatal water loss by reducing stomatal conductance under conditions of decreasing (more negative) leaf water potentials brought about by soil water shortage (e.g. Hacke and Sauter 1995, Tognetti et al. 1995, Backes 1996, Herbst et al. 1999, Aranda et al. 2000, Lemoine et al. 2002, Gallé and Feller 2007).

The vegetation period of 1999 was rather xeric, but dry spells were interrupted by rain events that supplied water to the upper soil layers (see Chap. 5.2.1, Fig. 5.2.1.1, Fig. 5.2.1.2) which beech was able to respond to immediately (cf. changes from period III to IV, most likely to be explained by precipitation immediately prior to period IV, Figs. 5.3.12, 5.3.13). When  $\theta_e$  dropped below 0.4 in 20 cm and 35 cm soil depth (in -90 cm  $\theta_e$  remained  $> 0.53$  during the whole season), the maximum observed  $J_s$  day 0-2cm decreased considerably ( $> 25\%$ , Fig. 5.3.8).  $\theta_e = 0.4$  has been found to be a threshold for the onset of soil water deficit and corresponding stomatal regulation of water flux by stomatal closure (Granier et al. 1999) in several tree species under various soil types (Black 1979, Dunin and Aston 1984, Granier 1987a, Granier and Loustau 1994, Wilson and Baldocchi 2000, Bernier et al. 2002, Pataki and Oren 2003, Rambal et al. 2003, Poyatos et al. 2005), including sessile oak (Bréda et al. 1993a, Bréda and Granier 1996, Granier et al. 2000b) and European beech (Granier et al. 1999, 2000b, 2002, 2007, Bréda et al. 2006).

The analysis of five short, progressively drier periods, each in itself decreasing in  $\theta_e$ , revealed changes in  $q_r$ , i.e. the slope of the relationship of  $J_s$  day deep/ $J_s$  day 0-2cm with  $J_s$  day 0-2cm (Figs. 5.3.12, 5.3.13). The sign of  $q_r$  turned from positive to negative for most large trees when  $\theta_e$  fell below 0.4 (after period II) whereas it had been negative already during period I (and prior) for most small trees; a negative  $q_r$  denotes the decrease of  $J_s$  day in deeper sapwood relative to outer sapwood with increasing  $J_s$  day 0-2cm. Concurrently with this, the absolute magnitude of  $q_r$  increased in small trees while it remained stable in large trees. This in small trees signifies, in combination with a negative  $q_r$ , a marked reduction of the contribution of deeper sapwood with increasing demand (indicated by increasing  $J_s$  day 0-2cm). Thus, in summary, the “capacitive” or “demand-driven” radial pattern of  $J_s$  day became steeper in small beech trees as the season progressed, with deeper sapwood contributing less and less. In large trees in contrast, the capacity of deeper sapwood remained relatively unchanged after the initial change in the sign of  $q_r$  when  $\theta_e$  declined below 0.4. Under more beneficial soil water conditions (period I–III), the contribution of deeper sapwood increased with demand (i.e. increasing  $J_s$  day 0-2cm) in large trees as signified by a large absolute value of  $q_r$  (Figs. 5.3.10c, e, f, 5.3.12–5.3.13); the large variability within the groups of small and large trees, however, demands a cautious interpretation of these findings and limits any generalisations.

Support for this view comes from Lütschwager and Remus (2007) who measured the radial variability of  $J_s$  in five beech trees during the extremely dry summer of 2003 (e.g. Ciais et al. 2005, Rebetez et al. 2005) and observed a less steep radial decline (at greatly reduced average monthly  $J_s$ ) compared to the spring of 2003 or compared to the summer months of the years 2002 and 2004, indicating a relative increase of the contribution of  $J_s$  in deeper sapwood. The trees studied by Lütschwager and Remus (2007) were predominantly large compared to trees from the Steigerwald, and volumetric soil water content  $\theta$  did not reach extremely low values though, so it was more of an atmospheric drought only at their study site. Furthermore, Kubota et al. (2005a) found in two out of three *F. crenata* trees that the peak of  $J_s$  day moved further inside the sapwood under drought, which may be interpreted as an increase in the relative contribution of  $J_s$  in deeper sapwood to total  $J_{st}$  as well. Becker (1996) described a decrease or even complete cessation of sap flow in deeper sapwood during a dry period compared to a wet period in Bornean dipterocarps; sap flow in outer sapwood was depressed as well. Schiller et al. (2003) similarly showed a reduction of the sapwood radius active in sap flow by approx. 50 % (from 48 mm to 24 mm) in (diffuse-porous) east Mediterranean *Quercus calliprinos*. In conifers the few reports on the effect of drought on radial patterns of  $J_s$  are less conclusive: Nadezhina et al. (2002) noted that the proportion of sap flow in outer sapwood decreased during a dry spell in one *Pinus sylvestris* while it did not change in deeper layers of sapwood, also observed in some (but not all studied) *P. taeda* studied by Ford et al. (2004b). In contrast, Phillips et al. (1996) and Schäfer et al. (2002) reported a larger decrease of  $J_s$  in inner than in outer sapwood under conditions of decreasing soil water availability in *P. taeda*.

One may hypothesise that the inner sapwood of large beech trees is a more dynamic component of water transport compared to that in small trees in that the contribution of  $J_s$  in inner sapwood of large trees can increase with increasing  $J_s$  in outer sapwood (with increasing "demand") as indicated by a positive  $q_r$ , but only up to a threshold ( $\theta_e = 0.4$ ) from which point on the hydraulic properties of the respective part of the sapwood become limiting (negative  $q_r$ , absolute value of  $q_r$  similar). In small sub-canopy beech trees deeper sapwood may be hydraulically close to its maximum capacity at low atmospheric demand already so that critically low  $\theta_e$  only reduces the contribution of deeper sapwood further. One may even speculate that in intermediate beech trees annulus #2 (2–4 cm) behaves like that of large trees, while annulus #3 (4–6 cm) shows reduced hydraulic capacities like that of small trees (Fig. 5.3.10c, d). Granier et al. (2000a), similarly to these findings on large trees, noted a tendency of the proportion of  $J_s$  in deeper sapwood to increase with increasing tree transpiration in a young dense beech stand. And similarly Phillips et al. (2003b) noted a slight but significant increase of the ratio of inner to outer  $J_s$  with the magnitude of  $J_s$  in *Quercus garryana*.

Inner and thus older sapwood, more specifically the conduits in older sapwood, have a higher resistance to sap flow than younger (outer) conduits. The youngest and hydraulically most effective (wider, more conductive) vessels on the other hand are also the first to cavitate, thus increasing resistance to flow in these conduits and making other portions of sapwood more "viable" for flow (see Chap. 2.3.). Therefore deeper sapwood would particularly be used in axial sap flow under more negative plant water potentials. Older xylem conduits have at the same time been shown to be more vulnerable to embolism as a result of increased permeability of inter-vessel pit membranes to air than young ones (Sperry et al. 1991), which in a number of angio-

sperm tree species could be attributed to repeated cycles of cavitation and refilling, thus causing so-called cavitation fatigue (Hacke et al. 2001, Stiller and Sperry 2002). Older conduits may therefore fail after some time of persistent drought stress. On the other hand embolism reversal on temporal scales from hours to season is being observed in more and more species (e.g. Tyree and Zimmermann 2002, Clearwater and Goldstein 2005). Only a few studies so far looked at embolism repair in beech, and no general conclusions can be drawn from those: Hacke and Sauter (1995) observed no recovery from embolism in twigs during the course of a growing season, while (small) positive pressures at the bottom of the trunk were found at the end of winter, possibly refilling vessels embolised during freeze-thaw-events in winter (Hacke and Sauter 1996, Lemoine et al. 1999, Cochard et al. 2001).

A general trend of decreasing wood water content  $W_f$  with the progressing season has been shown in many tree species, including conifers (e.g. Whitehead and Jarvis 1981, Irvine and Grace 1997, Cermák and Nadezhdina 1998, Cinnirella et al. 2002) and both ring- and diffuse-porous tree species, growing in seasonal climates (e.g. Sauter 1966 (cited in Hacke and Sauter 1995), Brough et al. 1986, Constantz and Murphy 1990, Borchert 1994a, b, Wullschleger et al. 1996, Pausch et al. 2000) and also in beech (Glavac et al. 1990, Lovas 1994). Glavac et al. (1990) for instance observed large contiguous areas of dry wood in inner sapwood on stem disks of beech during a dry summer, while outer growth rings remained water-filled. Longer-term changes in the level of maximum nocturnal temperature difference  $\Delta T_{max}$  measured with the thermal dissipation sap flow probes in the present study seem to reflect similar behaviour in *Fagus sylvatica* and *Quercus petraea* (namely the increase of  $\Delta T_{max}$ , very likely due to drier and therefore thermally better insulated wood – cf. Kučera et al. 1977 –, reversible by ample precipitation; not shown). Values of  $W_f$  have also been found to be higher in wet years and lower in dry years (Wullschleger et al. 1996, Pausch et al. 2000). Additionally, changes in  $W_f$  have been observed during the course of the day (Brough et al. 1986, Constantz and Murphy 1990, Holbrook 1992, Sparks et al. 2001); computer tomograms recorded about 30 minutes after each other on a beech tree at Großebeine (Fig. A11.1b, Appendix) may also point to an intra-day variation of  $W_f$ . Edwards and Jarvis (1982) linked measurements of sapwood water content  $R_w$  and sapwood hydraulic conductivity  $K_h$  in conifers and reported a drop of >80 % in  $K_h$  when  $R_w$  decreased from 98 % to 90 % (see also Waring and Running 1978). In concert with these trends, hydraulic conductance  $k_h$ , the sap flow rate per unit pressure drop as calculated from measurements of leaf water potentials and sap flow, has been shown to decrease over the course of the growing period in several species, including European beech (Hacke and Sauter 1995, Magnani and Borghetti 1995, Backes 1996, Lang 1999, Aranda et al. 2005).

**Tree size effects.** The small suppressed beech trees in the stands studied are of a similar age as the large dominant trees, i.e. the growth rings of the small-diameter trees are much narrower than those of the large trees (cf. Chap. 5.1.1). Therefore, at the same absolute radial sapwood depth, specific conductance  $K_s$  may be lower in the small, slow-growing beech trees than in the large, fast-growing beech trees and the water potentials required to activate the same sapwood annulus may have to be more negative in small than in large trees. If this were the case, then the inner sapwood of the small beech trees could not be switched into the axial pathway of water flow as easily as in large trees, and small trees would be less flexible and dynamic in the use of the relatively wide sapwood depth than large ones. Indications for such a difference between small and large trees were presented in this study (Chap. 5.3,

Fig. 5.3.10–5.3.13, see above). This line of argumentation is supported by the findings of Ewers and Oren (2000) who indicated that  $J_s$  decreased more pronouncedly with radial depth in fast-growing than in slow-growing *P. taeda* in a young plantation subjected to different levels of fertilisation. Smaller hydraulic conductivities were also measured in suppressed trees compared to dominant trees (e.g. Sellin 1993, Shelburne and Hedden 1996, Reid et al. 2003), in slow-growing compared to faster growing stands of *P. banksiana* (Pothier et al. 1989a, b) and in slow-growing compared to fast-growing branches of *Populus tremuloides* (Sperry et al. 1991).

Apart from possibly lower  $K_s$  in the deep sapwood of small trees compared to large trees as discussed above, differences in rooting patterns may need to be considered as well; Köstler et al. (1968), however, reported that the social position of a beech tree does not seem to influence its rooting depth. Within the stands studied here, soil depth varied considerably (Tab. 3.3.1), and limited soil (water) reserves may be one cause of different growth rates among even-aged neighbouring trees. This would result in variation in  $J_s$  among trees under limiting soil water conditions which might be reached earlier for smaller sub-canopy trees with less available soil water. Hence a dynamic relative increase in  $J_s$  in deeper sapwood would not be possible. The between-tree variation of sap flow will be further analysed below.

To conclude the discussion on sap flow density, results from published studies and from this author's own measurements are indicative of seasonal changes in the functionality of sapwood in (axial) water transport brought about by an increasing number of embolised vessels caused by decreasing plant water potentials (Sperry et al. 1988, Glavac et al. 1990, Hatton et al. 1995, Hacke and Sauter 1995). Generally though, studies of the hydraulic architecture and structure-function relationships of sapwood water transport are still largely incoherent, despite the proliferation of reports on allometric scaling (e.g. West et al. 1999, Enquist 2003, Zianis and Mencuccini 2003, McCulloh et al. 2004, Meinzer et al. 2005, Coomes 2006, Mäkelä and Valentine 2006, Pretzsch 2006, Westoby and Wright 2006, Mencuccini et al. 2007). Recent methodological developments such as microcasting (e.g. André 2005) in combination with mighty optical tools and powerful computer software for 3D-reconstruction have renewed the interest in functional wood anatomy (e.g. Kitin et al. 2004). Also, high-resolution X-ray computed tomography (HRCT) seems a promising tool for the study of the wood anatomy of dry specimen (e.g. Stuppy et al. 2003). Nuclear magnetic resonance (NMR) imaging (MRI) on the other hand offers non-destructive views on *in-situ* transport processes with high spatial and temporal resolution, enabling the quantification of water movement in the xylem (e.g. van As et al. 1980, Köckenberger et al. 1997; Windt et al. 2006, van As 2007). MRI also provides a method to study the process of cavitation and embolism repair in intact plants and to understand the factors influencing the maintenance of water transport capacity in xylem (Holbrook et al. 2001, Clearwater and Clark 2003, Schneider et al. 2003, Scheenen et al. 2007). These technologies, in combination with ecophysiological methods hold the promise of more integrated views on this matter emerging soon (cf. Gartner and Meinzer 2005). Particularly the study of relationships in large trees clearly deserves more effort to quantitatively increase our knowledge.

### 6.3. Whole-tree water use $Q_t$

#### 6.3.1. $Q_t$ of European beech

Water use scaled up from measurements of sap flow density to whole-tree level sap flux,  $Q_t$ , was positively correlated with DBH in *Fagus sylvatica* across all sites. The seasonal maximum daily whole-tree water use  $Q_{t\ max}$  of beech (Fig. 5.4.2, Tab. 5.4.1) reached up to  $435 \text{ kg d}^{-1}$  for a dominant tree at Steinkreuz (DBH 63 cm), while the lowest  $Q_{t\ max}$  at the same site was up to 40-fold smaller ( $11 \text{ kg d}^{-1}$  in a suppressed tree, DBH 14 cm). The maximum half-hourly values of  $Q_t$  ( $Q_{t\ hh\ max}$ ) peaked at  $38.9 \text{ kg h}^{-1}$  for the same dominant tree (Tab. 5.4.1) whereas the lowest maximum half-hourly rate was  $1.5 \text{ kg h}^{-1}$  (suppressed tree). At Großebene and at Farrenleite, lower peak values were attained, namely a  $Q_{t\ max}$  of  $136 \text{ kg d}^{-1}$  and  $100 \text{ kg d}^{-1}$ , respectively, and a  $Q_{t\ hh\ max}$  of  $11.2 \text{ kg h}^{-1}$  and  $6.9 \text{ kg h}^{-1}$ , respectively.

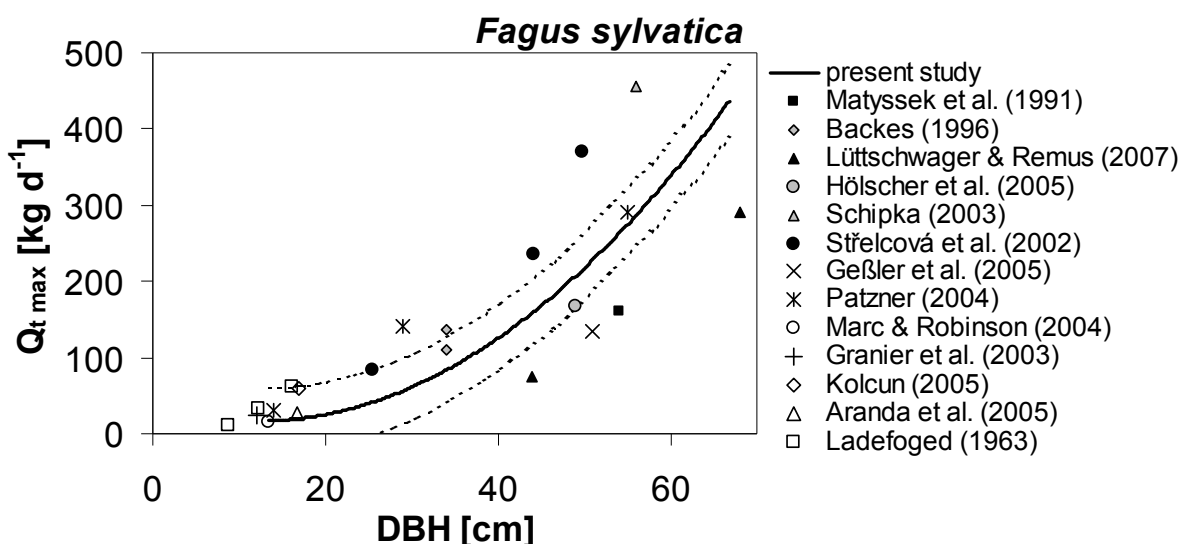


**Figure 6.3.1.1:** Published maximum daily rates of whole-tree sap flux of forest-grown European beech,  $Q_{t\ max}$  (symbols), and regression equation established for measurements of  $Q_{t\ max}$  with DBH from the present study (thick line; cf. Fig. 5.4.2, top left). Thin broken lines are 95 %-confidence intervals for the author's observations. References given in legend. The regression equation is  $y = 0.141x^2 - 3.4624x + 38.092$ ;  $R^2 = 0.971$ ,  $p < 0.0001$ ,  $n = 44$  trees.

Figure 6.3.1.1 compares results from the present study, summarised in the regression equation given in Figure 5.4.2a, with those published in the literature:

Matyssek et al. (1991, see also Cermák et al. 1993) reported a maximum  $Q_t$  of  $161 \text{ kg d}^{-1}$  and  $20.5 \text{ kg h}^{-1}$  for a beech (DBH 54 cm,  $h_t = 35 \text{ m}$ ,  $A_{cp} = 22 \text{ m}^2$ , 115 a) in a colline–sub-montane mixed Swiss stand during August as estimated with the trunk sector heat balance method. Employing the same method, Backes (1996) gave maxima of  $110 \text{ kg d}^{-1}$  and  $137 \text{ kg d}^{-1}$  for two beech trees in two years (one tree per season; DBH both 34 cm,  $h_t = 27 \text{ m}$ , 100 a) in lowland NW Germany. For the same site, Coners and Leuschner (2005) detailed a maximum hourly rate for August of approx.  $12 \text{ kg h}^{-1}$ . In a study by Schipka (2003) a maximum daily rate of  $457 \text{ kg d}^{-1}$  for a beech with a DBH of 56 cm and  $h_t = 35 \text{ m}$ , aged 120 a (trunk sector heat balance) from a colline–sub-montane Central German location was given. The maximum hourly  $Q_t$  was about  $70 \text{ kg h}^{-1}$  (Schipka 2003). Střelcová et al. (2002) estimated rather high rates of  $Q_{t\ max}$  in three beech trees of a montane stand in Slovakia, namely 83–

$371 \text{ kg d}^{-1}$  (DBH 26–50 cm; trunk sector heat balance). In the same trees hourly rates of up to nearly  $35 \text{ kg h}^{-1}$  were shown (Střelcová et al. 2006; not necessarily highest overall values, only hourly rate from one day plotted). Using the same method as in the present study, Lütschwager and Remus (2007) presented rates of up to approx.  $290 \text{ kg d}^{-1}$  for a beech with DBH 68 cm and  $h_t = 32.6 \text{ m}$  and of up to  $75 \text{ kg d}^{-1}$  for a smaller beech (DBH 44 cm,  $h_t = 31.6 \text{ m}$ ) from a pure stand in lowland NE-Germany at the beginning of June, employing 6 thermal dissipation probes down to 13 cm sapwood depth (4 in the smaller tree, down to 8.8 cm). Hölscher et al. (2005) noted a maximum  $Q_t$  for July–August of  $168 \text{ kg d}^{-1}$  (DBH 49 cm; 4 consecutive depths, 0–8 cm) for a beech in a Central German stand, and Geßler et al. (2005) detailed a 4 day-average (June) of  $135 \text{ kg d}^{-1}$  for six beech trees from a southern German stand (DBH 51 cm, modified thermal dissipation probe, with 7 thermocouples in row, 0–14 cm). Patzner (2004) showed  $Q_t$  of about  $200\text{--}290 \text{ kg d}^{-1}$  as the maximum of average beech water use in dominant beech trees in a colline (DBH 37 cm) and a montane stand (DBH 44–61 cm), in both stands mixed with *Picea abies*;  $J_s$  was assessed with the thermal dissipation method down to 6 cm sapwood depth in a few trees and interpolated for innermost sapwood. For intermediate trees she described maximum rates of  $100\text{--}140 \text{ kg d}^{-1}$  (DBH 19–38 cm) and  $20\text{--}30 \text{ kg d}^{-1}$  for suppressed trees (DBH 13–22 cm) from the two sites (Patzner 2004). Since these rates were extracted from figures and since the upscaling procedure could not be reconstructed, these data from Patzner (2004) remain qualitative. Kolcun (2005) studied beech in a sub-montane S-German stand and measured maximum  $Q_t$  of  $60\text{--}141 \text{ kg d}^{-1}$  for a range of DBH of 17–72 cm. Thermal dissipation probes were installed in 0–4 cm sapwood depth only and hence  $141 \text{ kg d}^{-1}$  for the large beech with DBH 72 cm is very likely to be an underestimation and therefore not shown in Figure 6.3.1.1. For comparison, on a day where  $Q_t$  was  $431 \text{ kg d}^{-1}$  for the largest measured tree in this study (DBH 65 cm),  $Q_{0\text{--}4 \text{ cm}}$  was  $169 \text{ kg d}^{-1}$ . Granier et al. (2003) depicted maximum daily rates from  $2\text{--}25 \text{ kg d}^{-1}$  during bright summer days and maximum hourly rates (Granier et al. 2000a) for a sunny late spring day ranging  $0.3\text{--}2.3 \text{ kg h}^{-1}$  for young beech trees with DBH 4–12 cm, comparable to this author's own findings on small trees (see above). Aranda et al. (2005) published maximum rates of  $26.7 \text{ kg d}^{-1}$  for a dominant beech (DBH 17 cm) growing in a dense sub-Mediterranean (montane) stand. Marc and Robinson (2004) found up to  $15.6 \text{ kg d}^{-1}$  averaged over a period of two weeks in July for a tree (DBH 13.4 cm,  $h_t = 7.6 \text{ m}$ ) in a dense young stand, using the deuterium tracing method. With a modified heat pulse technique, Ladefoged (1963) estimated maximum  $Q_t$  to vary between  $10.3 \text{ kg d}^{-1}$  and  $61.5 \text{ kg d}^{-1}$  in 10 beech trees (DBH 9–16 cm) from three dense Danish stands (ca. 30 years old); maximum hourly rates reached  $1.1\text{--}7.4 \text{ kg h}^{-1}$ .

Lang (1999) measured  $Q_t$  in four consecutive radial depths (0–8 cm) with thermal dissipation probes in four beech trees in a colline mixed beech-oak forest (SW-Germany) and found seasonal average  $Q_t$  ( $Q_{t \text{ avg}}$ ) of up to  $182 \text{ kg d}^{-1}$  (DBH 58 cm). This rate is very similar to  $Q_{t \text{ avg}}$  from Steinkreuz for a comparable tree, which was scaled to  $163 \text{ kg d}^{-1}$  (Tab. 5.4.1); forest trees studied by Lang (1999) were actually growing very close to the edge of a narrow stretch of forest, which may indicate a higher resource availability at his site (cf. Herbst et al. 2007b). Lang (1999) also tabulated values of sapwood area-weighted total tree sap flow density  $J_{st}$ , which averaged over the growing season to  $847\text{--}1487 \text{ kg}^{-2} \text{ d}^{-1}$  for trees with DBH 42–63 cm, whereas in the present study, a maximum of  $625 \text{ kg m}^{-2} \text{ d}^{-1}$  was attained (Tab. 5.5.1), averaged over a larger number of days though (197 d compared to 144 d in Lang 1999). Patzner (2004) presented seasonally averaged values of  $Q_t$  ( $Q_{t \text{ avg}}$ ), ranging from  $83\text{--}102 \text{ kg d}^{-1}$  for dominant beech (DBH 38–72 cm) over three growing seasons and from two sites (see above), from  $36\text{--}51 \text{ kg d}^{-1}$  for intermediate beech (DBH 19–38 cm) and from  $5\text{--}29 \text{ kg d}^{-1}$  for suppressed beech (DBH < 19 cm). Since rates from Patzner (2004) are averaged over a whole size class, they should be expected to be smaller than values from the present study given above; on the other hand Patzner averaged over 124 days only. Seasonal averages given by Střelcová et al. (2002) were  $18 \text{ kg d}^{-1}$ ,  $64 \text{ kg d}^{-1}$  and  $79 \text{ kg d}^{-1}$  for a suppressed and two dominant beech trees from a montane (850 m a.s.l.) site in central Slovakia, respectively.

Thus published and values presented here for small and suppressed beech trees concur, while for dominant forest-grown beech trees maximum daily rates of  $Q_t > 300 \text{ kg d}^{-1}$  only seem to have been shown to date by Střelcová et al. (2002) and Schipka (2003; he also showed the highest hourly rate of  $Q_t$  so far:  $70 \text{ kg h}^{-1}$ , see above). However, Schipka (2003) noted that the trunk sector heat balance method may have overestimated the real sap flux due to a so-called phloem effect (the inserted electrodes were not insulated from the phloem and attempts to correct for this failed, see discussion in Schipka 2003, pp 103–106). On the other the inserted electrodes reached only 5.6 cm deep into the sapwood (Schipka 2003), while total sapwood

depth of the presented tree (DBH 56 cm) would be estimated to be around 16 cm with the allometric equation in Table 5.1.1.1. Therefore some doubt about the quality of these results remains. Given that Střelcová et al. (2002) used the trunk sector heat balance method as well, the same limitations may apply. In the present study, values of  $Q_t > 400 \text{ kg d}^{-1}$  were observed on four days in 1999 and on five days in 2000 for tree B4237 and on one day in 2000 for tree B4108. At least 54 % of  $Q_t$  were measured ( $Q_{0-6\text{cm}}$ ) on these days or, correspondingly, at most 46 % of  $Q_t$  were estimated from the regression equations (Eqs. 5.4.1, 5.4.2). Considering values of seasonal average  $Q_t$  ( $Q_{t\ avg}$ ), a much higher rate than for the forest-grown beech trees from the present study was reported by Lang (1999) for a solitary beech (DBH 62 cm,  $h_t$  15 m, 53 yrs), namely  $311 \text{ kg d}^{-1}$  ( $n = 144$  d; compared to  $163 \text{ kg d}^{-1}$  in this study, see above), assessed with four thermal dissipation probes down to 8 cm sapwood depth.

Most values from the literature for large, dominant beech trees fall below the regression line, which may be explained by the short duration of these experiments (few days to few weeks: Matyssek et al. 1991, Geßler et al. 2005, Lütschwager and Remus 2007) or possibly by inadequate sampling of the deep sapwood of beech (no details on the depth of inserted electrodes given by Matyssek et al. 1991 or Cermák et al. 1993). The rates presented by Backes (1996), Marc and Robinson (2004) and Hölscher et al. (2005) are well within the range of values observed in this study. Values estimated from Patzner (2004, see above) are rather qualitative, but mostly comparable as well. Therefore, in conclusion, the high maximum rates of  $Q_t > 400 \text{ kg d}^{-1}$  seem all the more reasonable. Nevertheless, some uncertainty concerning the interpolation of sap flow from the three measured sapwood depths to the total cross-sectional sapwood area of a tree may remain, despite the rather similar patterns of radial decline observed in other studies on *F. sylvatica* discussed in Chapter 6.2.1.

Highly significant ( $p < 0.0001$ ) non-linear relationships were found not only for  $Q_{t\ max}$  of beech with DBH (see above), but also with basal area  $A_{bt}$ , leaf area  $A_{lt}$  and sapwood area  $A_{st}$  ( $R^2 > 0.97$ ), the highest correlation coefficient (0.977) obtained for the latter, as may be expected given the sapwood area was used to scale up  $J_s$  to  $Q_t$ . The high correlation coefficients thus should not be over-interpreted since DBH,  $A_{bt}$  and  $A_{st}$  are auto-correlated and so in turn are auto-correlated with  $Q_t$  (Oren et al. 1998). Increasing  $Q_t$  with increasing tree diameter, sapwood area or leaf area was also observed e.g. by Granier et al. (2000a) and Marc and Robinson (2004) in younger beech stands, or by Ladefoged (1963), Střelcová et al. (2002, 2004), Schipka et al. (2005) and Patzner (2004, mentioned but not shown) in mature (mixed) beech stands and by Köstner et al. (1992) in *Nothofagus* species. In other angiosperm tree species this positive correlation was demonstrated by Dawson (1996) and Raulier et al. (2002) for *Acer saccharum*, by Schaeffer et al. (2000) for *Populus fremontii*, by Wullschleger et al. (2000) – to some extent – in *A. rubrum*, by Santiago et al. (2000) in *Metrosideros polymorpha* (Myrtaceae), by Calder et al. 1992 for *Eucalyptus tereticornis* and *E. camaldulensis*, by Hunt and Beadle (1998) for *E. nitens* and *Acacia dealbata* and by Hatton and Wu (1995) and Vertessy et al. (1995, 1997) in stands of *E. regnans* as summarised in the report of Wullschleger et al. (1998). Raulier et al. (2002) studied two stands of *A. saccharum* that were similar in age and  $A_b$  but differed in diameter and height distribution, stand density and LAI. As in the present study, the two stands did not differ in their relationship of  $Q_t$  with DBH.

Regression analysis of  $Q_{t\ max}$  and ground-projected crown area  $A_{cp}$  yielded the highest correlation coefficients when taking into account the stand structure, separating

tall overstory from lower suppressed sub-canopy trees and treating the much denser Fichtelgebirge-site differently from the Steigerwald sites (see also below). The angle of crown opening  $\alpha_c$  (Fig. 5.4.2, bottom), a measure of competition and of how much light a tree canopy may attain, proved to be a fairly good estimator of  $Q_{t \max}$  (even though higher correlation coefficients were obtained with other scalars), but  $\alpha_c$  was only available for Großebene.

The  $Q_{t \max}$  of the pooled beech trees also scaled positively with tree height  $h_t$  (Fig. 5.4.3 top left). Relating  $Q_{t \max}$  to the leaf area of a tree ( $Q_{t \max}/A_{lt}$ ) reduced the difference between short and tall trees (range  $0.2\text{--}0.8 \text{ kg m}^{-2} \text{ d}^{-1}$  compared to  $11\text{--}435 \text{ kg d}^{-1}$  for  $Q_{t \max}$ , see above), but  $Q_{t \max}/A_{lt}$  still increased with  $h_t$  (Fig. 5.4.3 bottom left). This indicates a high transpirational capacity of beech leaves even in large crowns. However, given that short and tall trees were growing in the same stands, small trees of the sub-canopy were limited by light as confirmed by clear differences in stable isotope signals measured along the canopy profile of a dominant and suppressed tree beech at Steinkreuz (Dawson et al., unpublished, cited in Köstner et al. 2004, see also Skomarkova et al. 2006). Leaves of the sub-canopy trees are more shade-adapted, transpiring less water (per unit leaf area) and requiring less sapwood area for the water supply, whereas a larger sapwood area is maintained in taller overstory trees for water transport which transpire more (Köstner et al. 2004). Accordingly, the ratio of leaf area to sapwood area,  $A_{lt}/A_{st}$ , declined considerably with tree height (Fig. 5.1.3.3) as reported for most species studied so far (McDowell et al. 2002), including *F. sylvatica* (Bartelink 1997, Schäfer et al. 2000).

Backes (1996) reported values of  $Q_{t \max}/A_{lt}$  of 0.59 and  $0.99 \text{ kg m}^{-2} \text{ d}^{-1}$  for two beech trees comparable in size to the large Steigerwald beech trees, using the trunk sector heat balance method to measure sap flow in a mixed oak-beech stand in north-western Germany. Yet the differences between these two trees could not be explained with the structural information given; the trees had been measures in different years. Rates of  $Q_{t \max}/A_{lt}$  reported by Ladefoged (1963), measured with a modified heat pulse method, range between  $0.55 \text{ kg m}^{-2} \text{ d}^{-1}$  and  $1.4 \text{ kg m}^{-2} \text{ d}^{-1}$  for trees from young, dense (unthinned) beech stands in Denmark; the large variation of  $Q_{t \max}/A_{lt}$  at a narrow range of  $h_t$  made no trends of  $Q_{t \max}/A_{lt}$  with  $h_t$  discernible. Maximum values of  $Q_{t \max}/A_{lt}$  for beech from the present study ranged from  $0.46 \text{ kg m}^{-2} \text{ d}^{-1}$  (Farrenleite) to  $0.77 \text{ kg m}^{-2} \text{ d}^{-1}$  (Steinkreuz; Fig. 5.4.3, Tab. 5.4.1).

Looking at the stand Farrenleite on its own, however, no significant correlation was found for either  $Q_{t \max}$  or  $Q_{t \max}/A_{lt}$  with  $h_t$ . The structure of this stand was rather different from that of the Steigerwald sites, due to a larger tree density (2.5 times more trees than Steinkreuz and ca. 1.4 times more trees than Großebene, Tab. 5.5.2, Tab. 3.3.2) and especially due to a larger inclination ( $12.5^\circ$  compared to  $5.5^\circ$  and  $2^\circ$ , respectively, Tab. 3.3.1).  $A_{cp}$  was more strongly correlated with DBH than  $h_t$  with DBH at Farrenleite (Fig. 5.1.2.3, Chap. 5.1.2), which may point on the one hand to a possibly strong influence of the large inclination of the site on the height growth (trees growing in a depression on a slope have to compensate for this disadvantageous micro-site by enhanced height growth or else they will be suppressed). Or, on the other hand this could indicate an enforced height growth as a means to escape horizontal competition in a dense stand, or both. In any of these cases, less carbon would be available for radial tree increment, obscuring relationships with DBH. The smallest trees of the stand may have lost the competition for light and are confined to the lower strata of the stand with narrow crown projections: the two distinct groups of

beech at Farrenleite that emerged when  $Q_{t \max}$  was plotted against  $A_{cp}$  (Fig. 5.4.2) may support this view. The crown bases of beech at Farrenleite were rather high compared to the Steigerwald sites (Fig. 5.1.2.3), presumably because of the dense competing canopies and the dark shade they cast. The absence of a shrub layer (Tab. 3.3.2b) could also be indicative of this.

In general, beech from Farrenleite was comparable to beech from Steinkreuz or Großebene regarding the relationships of  $Q_{t \max}$  and DBH (Fig. 5.4.2),  $Q_{t \max}$  and  $A_{bt}$ ,  $Q_{t \max}$  and  $A_{lt}$ , and  $Q_{t \max}$  and  $A_{st}$  (not shown), despite the mentioned constraints.

### 6.3.2. $Q_t$ of sessile oak

The whole-tree transpiration  $Q_t$  of *Quercus petraea* peaked at daily rates of  $52 \text{ kg d}^{-1}$  ( $Q_{t \max}$ ) at Steinkreuz and  $62 \text{ kg d}^{-1}$  at Großebene (Fig. 5.4.2, Tab. 5.4.1) and at half-hourly rates of  $5.6 \text{ kg h}^{-1}$  (Tab. 5.4.1). Thus at the tree level, values for oak were much smaller than for beech (cf. Tab. 5.4.1). In contrast to beech,  $Q_{t \max}$  of the oak trees was hardly correlated to structural scalars at all (Fig. 5.4.2, Fig. 5.4.3), due to large scatter in the data within a stand and between stands. The lack of a significant increase of average seasonal  $J_s$  with stem diameter (Fig. 5.3.7) mentioned earlier (Chap. 6.2.2) points in the same direction. When looking at maximum seasonal  $J_s$  on the other hand, a correlation with DBH was discernible at least for Großebene (Fig. 5.5.1b); on the whole-tree level though (Fig. 5.4.2, Fig. 5.4.3) this was not apparent any more. In contrast to these observations, Herbst et al. (2007b) noted  $J_s$  (and hence  $Q_t$ ) in forest-grown *Q. robur* in the UK to be positively related with DBH, and putatively with leaf area as well. Schiller et al. (2007) also found an increase of average  $Q_t$  with trunk circumference in open-grown East-Mediterranean *Q. aegilops* L. ssp. *Ithaburensis* (DBH 20–43 cm). The data from Ladefoged (1963) reveal an increase of  $Q_{t \max}$  with increasing DBH or leaf area for young trees of *Q. petraea* (25 year-old, DBH 8–12 cm,  $n = 5$ ) from dense Danish stands. For trees from recently thinned stands (25–40 year-old, DBH 13–17 cm, 4 trees), however, the relationship was shifted to markedly higher values of  $Q_{t \max}$  (Ladefoged 1963).

The few published values of  $Q_{t \max}$  for *Q. petraea* range from  $10 \text{ kg d}^{-1}$  to  $360 \text{ kg d}^{-1}$  for trees spanning 8–54 cm in DBH and up to  $400 \text{ kg d}^{-1}$  for a large *Q. robur*, as compiled in Figure 6.3.2.1:

Backes (1996) found rates of  $Q_{t \max}$  of  $175 \text{ kg d}^{-1}$  and  $360 \text{ kg d}^{-1}$  for *Q. petraea* with a DBH of 51 cm and 54 cm and  $h_t$  of 26 m and 25 m, respectively, measured in different years; trees were about 190 years old and growing in a mixed beech-oak stand in lowland NW Germany. The trunk sector heat balance method was employed here and also by Coners and Leuschner (2005) at the same site, who reported a maximum hourly rate of  $17 \text{ kg h}^{-1}$  in early August for a sessile oak probably similar in size to the ones studied by Backes (1996). The same sap flow technique was used by Cermák et al. (1980, 1982), who showed maximum hourly rates of  $28 \text{ kg h}^{-1}$  for a *Q. robur* x *petraea* (DBH 38 cm,  $h_t = 17$  m, > 100 years old) from lowland Southern Moravia, Czech Republic (Cermák et al. 1980) and of  $40 \text{ kg h}^{-1}$  and  $400 \text{ kg d}^{-1}$  for a mature (emergent?) *Q. robur* (> 100 yrs) from the same area with  $h_t = 33$  m (Cermák et al. 1982); DBH was estimated from their Figure 2 and Table 1 as 44 cm. On oaks smaller than those assessed in the present study, but by means of the thermal dissipation technique as well, Bréda et al. (1993b) recorded  $11.5 \text{ kg d}^{-1}$  (10 d-average) for *Q. petraea* with DBH 17 cm (Bréda et al. 1993a) from a dense (3640 trees  $\text{ha}^{-1}$ ) French stand. Aranda et al. (2005) detailed a maximum of  $19 \text{ kg d}^{-1}$  for *Q. petraea* with a DBH of 16 cm from a dense (3900 trees  $\text{ha}^{-1}$ ) sub-Mediterranean (1400 m a.s.l.) stand. For 25 year-old sessile oaks from a dense (1740 stems  $\text{ha}^{-1}$ ) Danish stand Ladefoged (1963) estimated a maximum  $Q_t$  of  $0.9\text{--}4.4 \text{ kg h}^{-1}$  and  $10\text{--}45 \text{ kg d}^{-1}$  (DBH 8–12 cm). In the deciduous ring-porous *Q. garryana* from the NW U.S., Phillips et al. (2003a) measured a maximum hourly rate of  $1.8 \text{ kg h}^{-1}$  and  $7.2 \text{ kg h}^{-1}$  and a maximum daily water use of  $20 \text{ kg d}^{-1}$  and  $50 \text{ kg d}^{-1}$ , averaged over

three trees with a mean DBH of 23 cm and 55 cm, a  $h_t$  of 10 m and 25 m and aged 40 years and 250 years, respectively. Wullschleger et al. (2001) showed maximum rates of  $84 \text{ kg d}^{-1}$  for *Q. prinus* (estimated from a maximum average  $J_s \text{ day}$  of nine trees and average  $A_{st}$  in their Tab. 1; DBH 37–69 cm,  $h_t$  23–31 m), of  $71 \text{ kg d}^{-1}$  for *Q. alba* (DBH 53 cm,  $h_t$  = 31 m), and of  $46 \text{ kg d}^{-1}$  for *Q. rubra* (DBH 42 cm,  $h_t$  = 31 m), all growing in a mixed deciduous forest in Tennessee, U.S.

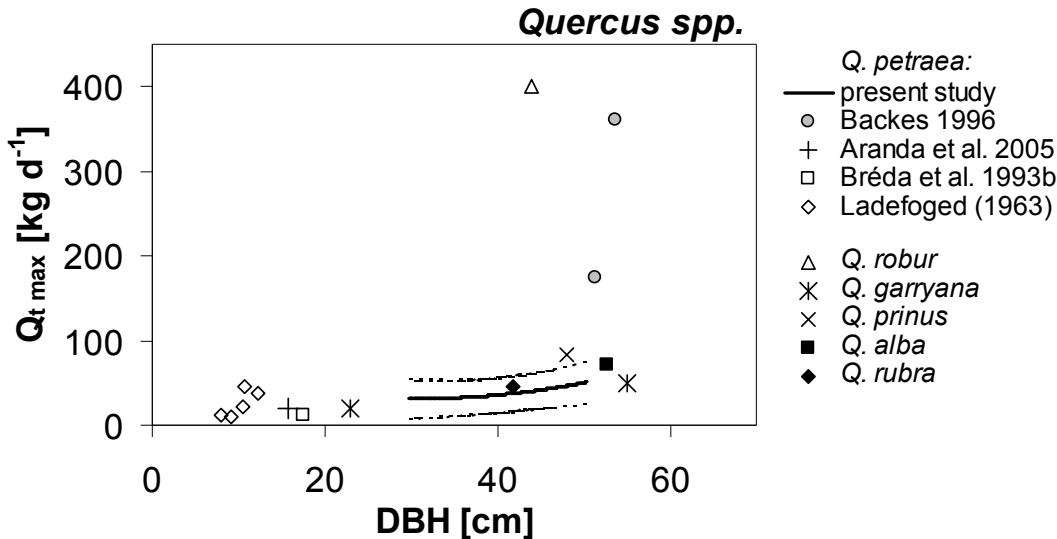


**Figure 6.3.2.1:** Published maximum daily rates of whole-tree sap flux of forest-grown sessile oak and other oak species,  $Q_t \text{ max}$  (symbols), and measurements from this study of  $Q_t \text{ max}$  of sessile oak (thick line: regression equation shown in Fig. 5.4.2, top right, is given for clarity, even though non-significant) versus DBH. Thin broken lines are 95 % confidence intervals for these observations. The equation for the shown regression is  $y = 0.051x^2 - 3.1462x + 80.035$ ;  $R^2 = 0.250$ ,  $p = 0.086$ ,  $n = 20$  trees. References are: for *Q. robur*: Cermák et al. (1982), for *Q. garryana*: Phillips et al. (2003a), for *Q. prinus*, *Q. alba* and *Q. rubra*: Wullschleger et al. (2001).

The rates of  $Q_t \text{ max}$  for three oak trees comparable in DBH to the oaks at Steinkreuz and Großebene are higher than the rates from the present study (Fig. 6.3.2.1). These values, given by Cermák et al. (1982) and Backes (1996), were retrieved from measurements with the trunk sector heat balance method which has recently been suspected to overestimate fluxes due to a “phloem effect” (Schipka 2003, see Chap. 6.3.1). Hourly rates recorded with this method (Cermák et al. 1980, 1982, Coners and Leuschner 2005) were higher than the ones reported here, too (see above). The rate for the one tree shown by Cermák et al. (1982) seems somewhat qualitative, and the structural characterisation of the studied tree is rather scant. The large variability of  $Q_t \text{ max}$  between two trees with similar DBH documented by Backes (1996) was only partly explained by different leaf area (Backes 1996). This finding points to the earlier mentioned observation that DBH (and the other assessed tree structural characteristics) may not be a good scalar for tree water use in oak (see also below). Values of  $Q_t \text{ max}$  observed in smaller (but dominant) oaks (Ladefoged 1963, Bréda et al. 1993b, 1995a, Aranda et al. 2005) were similar to those from the smallest oaks from the Steigerwald (Fig. 6.3.2.1). Interestingly, *Q. garryana* from interior Oregon (Phillips et al. 2003a) and *Q. alba*, *Q. rubra* and *Q. prinus* from eastern Tennessee (Wullschleger et al. 2001) displayed rates similar to those from European sessile oaks of comparable DBH (Fig. 6.3.2.1).

Higher rates of  $Q_{t \max}$  than for oak and beech have been observed in trees larger than those studied here in moist tropical or mesic temperate forests (up to 1180 kg d<sup>-1</sup>, see most recent review by Wullschleger et al. 1998; Schaeffer et al. 2000 showed a rate of 500 kg d<sup>-1</sup> for a *Populus fremontii* with a DBH of ca. 70 cm, and James et al. 2001 reported ca. 750 kg d<sup>-1</sup> for an *Anacardium excelsum* with a diameter of 98 cm at a height of 3.1 m above the ground, the sapwood radius was 35 cm and  $h_t$  38 m).

Maximum sap flux per tree related to leaf area,  $Q_{t \max}/A_{lt}$ , was correlated with tree height  $h_t$  in the oaks studied ( $R^2 = 0.49$ ,  $p < 0.005$ , all trees from both stands; Fig. 5.4.3, bottom right). However, in contrast to beech (Chap. 6.3.1),  $Q_{t \max}/A_{lt}$  decreased with increasing  $h_t$ .  $Q_{t \max}/A_{lt}$  was much smaller than in beech and for oak ranged from 0.13 kg m<sup>-2</sup> d<sup>-1</sup> (Steinkreuz) to 0.21 kg m<sup>-2</sup> d<sup>-1</sup> (Großebene): at the same DBH, beech and oak had similar leaf areas ( $A_{lt}$ ; see also Le Dantec et al. 2000), increasing slightly stronger with DBH in oak than in beech (cf. Fig. 5.1.3.2b). Because of the smaller sapwood area ( $A_{st}$ ) of ring-porous oak, which also increased less strongly with increasing DBH than in beech (Fig. 5.1.1.4),  $A_{lt}/A_{st}$  was much larger in oak than in beech, declining in both species with DBH (somewhat stronger in oak; Fig. 5.1.3.2b). For a given DBH  $Q_{t \max}$  of oak was much smaller than that of beech (Fig. 5.4.2); however, when  $Q_{t \max}$  was normalised with  $A_{st}$  ( $Q_{t \max}/A_{st} = J_{st \max}$ ; Fig. 5.5.1) it was larger in oak, increasing stronger with DBH than in beech (particularly for Großebene). Because of the larger  $A_{lt}/A_{st}$  of oak,  $Q_{t \max}/A_{lt}$  was smaller in oak than in beech for a certain DBH (and even more so for a particular  $h_t$  (Fig. 5.4.3), since  $h_t$  increased more strongly with DBH in beech, Fig. 5.1.2.3). In other words, with increasing  $h_t$  or DBH,  $Q_{t \max}$  increased less than  $A_{lt}$ . This points at higher leaf area densities (leaf area per crown volume, cf. Fig. 5.1.2.3) and increased self-shading in oak with increasing DBH,  $h_t$  and  $A_{lt}$  (cf. Leuschner 1994, Fleck 2002, Hagemeier 2002). Moreover, oaks were also shaded by neighbouring, often taller beech trees (at least at Steinkreuz) which in addition cast a deeper shade than oaks. In contrast to the lower  $Q_{t \max}/A_{lt}$  of oak at the whole-tree level observed here, leaf-level measurements of transpiration yielded higher transpiration rates in sessile oak than in European beech when comparing sun leaves (Aranda et al. 2000, 2005, Leuschner et al. 2001a, Fleck 2002, Fleck et al. 2004).

Vertessy et al. (1995) also observed a decrease of  $Q_t/A_{lt}$  with increasing DBH (and hence  $h_t$ ) in an Australian stand of *Eucalyptus regnans*, data from Ladefoged (1963) on *Q. petraea* remain inconclusive, perhaps due to small differences of the trees in  $h_t$  and a high stand density.

However, the scatter in the correlation of  $Q_{t \max}/A_{lt}$  and  $h_t$  was large, and in general oak from Großebene and Steinkreuz may not compare as well as e.g. beech from these two sites. This is probably due to the fact that the oaks from Steinkreuz presented in Figure 5.4.3 were taller than the oaks from Großebene, but oaks from Steinkreuz were less tall than the competing beech trees. There was no statistically significant relationship of  $Q_{t \max}/A_{lt}$  with  $h_t$  among oaks from one stand. A simple scalar like tree height may not capture this competitive structural environment of a tree adequately, but the more elaborate parameter “angle of crown opening  $\alpha_c$ ” (Fig. 5.4.2, bottom right) could not describe it better either. Therefore other explanations for the lack of correlation and or the large scatter in the data were sought (see below).

Two oak trees comparable in size to the Steigerwald oaks (but older, > 180 years) studied with the trunk sector heat balance method in a mixed oak-beech stand in NW Germany reached maximum values of  $Q_{t \max}/A_{lt}$  of 0.98 and  $1.47 \text{ kg m}^{-2} \text{ d}^{-1}$  (Backes 1996). Highest values of  $Q_{t \max}/A_{lt}$  from the present study ranged from  $0.13 \text{ kg m}^{-2} \text{ d}^{-1}$  (Steinkreuz) to  $0.21 \text{ kg m}^{-2} \text{ d}^{-1}$  (Großebene) for oak. The comparatively low  $Q_{t \max}/A_{lt}$  of oak in the Steigerwald may be attributable to strong competition with beech and to periodical defoliation by the caterpillars of *Tortrix viridana* L. (Horstmann et al. 1984; last calamity at Steinkreuz in 1995 and 1996; Schäfer 1997, Fleck 2002; see also Carlisle et al. 1966, Kruijt 1989, Bréda et al. 1995a, Vincke et al. 2005a). The combination of severe insect defoliation in at least two consecutive years with climatic extremes, such as severe summer drought and/or strong winter frost, is thought to be the most significant complex of factors in the incidence of oak decline generally observed in Germany (Thomas et al. 2002). An increased nitrogen content of leaves, as also observed at the Steigerwald sites (Köstner et al. 2004), in connection with drought stress was found to reduce foliar concentrations of allelochemicals in *Q. robur*, thereby probably making these trees more susceptible to insect defoliation (Thomas et al. 2002). (Infestation with *Phytophthora* species as one potential cause of the oak decline syndrome in Central Europe (e.g. Jung et al. 2000, Thomas et al. 2002, Camy et al. 2003) may be another source of between-tree variability.) Therefore growth of oak in the stands studied may be irregular and sapwood may have a different quality depending on the severity of the defoliation and its consequences on radial growth and conduit characteristics (cf. Thomas et al. 2006). Mainly latewood formation seems to be negatively affected by defoliation (Rubtsov 1996, Blank 1997), and Gieger and Thomas (2002) observed in saplings of *Q. petraea* that had been artificially defoliated a reduction in latewood growth and decreased hydraulic conductance. Reduced vigour and large interannual variation in radial growth caused in part by insect defoliation has also been observed by Hogg et al. (2005) in Canadian *Populus tremuloides*. If insect calamities had caused marked irregularities in the sapwood as indicated by rather inhomogeneous stem cross-sections of oak on computer tomographic images taken in 1996 (Köstner et al. 2004), and if sap flow thus was confined to only the very youngest annual growth rings, leaving the older sapwood hydro-passive, then the standard 20 mm-thermal dissipation probes may have been too long to accurately represent  $J_s$  (Green and Clothier 1988, Clearwater et al. 1999, cf. Köstner et al. 2004).

A source of error that potentially could have contributed to the oaks' low values of  $Q_{t \max}/A_{lt}$  and of  $Q_t$  in general is the small sapwood area of sessile oak. The sapwood depth of the trees studied was about 20 mm; a small misplacement of a thermal dissipation probe into the heartwood therefore cannot be ruled out completely, despite the most careful installation. This would result in an underestimation of  $J_s$  (Clearwater et al. 1999). But given the number of oak trees sampled over the years (20, e.g. Fig. 5.4.2, Table A11.5, Appendix) this error should not be able to completely mask the true order of magnitudes; it could, however, be a reason for the large scatter in the data for oak observed in Figures 5.4.2 and 5.4.3. Sap flow measured in *Q. petraea* with various methods (thermal dissipation, trunk sector heat balance and heat pulse velocity, see Chap. 2) nevertheless agreed well in an earlier study (Granier et al. 1994, 1996b). Besides, the original calibration of the thermal dissipation probes was done on *Q. pedunculata* EHRH. (= *Q. robur* L.; Granier 1985, Köstner et al. 1998a) and recently successfully validated by Herbst et al. (2007b). Backes (1996, see above) on the other hand monitored just two oak trees and variation of  $Q_{t \max}/A_{lt}$  between these two was also considerable.

Phillips et al. (2003b) studied Oregon white oak, *Q. garryana*, and observed values of  $Q_t \text{ max}/A_{lt}$  of about  $0.45 \text{ kg m}^{-2} \text{ d}^{-1}$  for short trees ( $h_t = 10 \text{ m}$ , DBH 23 cm, 40 a) and about  $0.2 \text{ kg m}^{-2} \text{ d}^{-1}$  for tall trees ( $h_t = 25 \text{ m}$ , DBH 56 cm, 250 a), growing in two even-aged groves. The rates for the tall trees are comparable to those for sessile oak from Großebeine (which reached the uppermost part of the tree canopy), and  $Q_t \text{ max}/A_{lt}$  declined with  $h_t$  in the present study as well (see above).

Based on the results presented and the considerations outlined above and despite some uncertainty regarding methods, it may be speculated that in oak the large variability in relationships (or even the absence of significant correlations) of  $Q_t$  and structural scalars such as DBH,  $\alpha_c$ ,  $h_t$  (Fig. 5.4.2–3) may be caused by one of the following factors or by a combination of several or all of them: defoliation by phytophagous insects (and perhaps infestation with *Phytophthora* species) and hence reduced radial growth, irregular sapwood and reduced vigour, low shade tolerance (see also Chap. 6.4.3) and inferior competitiveness compared to beech, brought about by a number of traits and differences (see Chap. 6.4.3).

Speculatively, the basic differences between ring-porous and diffuse-porous wood anatomy perhaps could also contribute to the lack of a significant correlation between the tree size and the magnitude of  $Q_t$  in sessile oak: according to Braun (1970), the histological organisation of beech is more basic than that of oak. In beech, the wood consists of micro-porous vessels embedded in a matrix of tracheids. Tracheids serve both the mechanical support and water conduction. In contrast, the wood of oak is more elaborately differentiated into water conducting vessels and tracheids and supporting fibres (Braun 1970). Thus in beech more or less the whole sapwood area participates in axial water transport, whereas in oak just a portion of it does. Consequently, the relationship between “bulk” sapwood area and water flux will be comparatively loose in oak (cf. Roderick and Berry 2001, Barbour and Whitehead 2003, Barbour et al. 2005), irrespective of whether the thermal dissipation technique adequately assesses sap flow in oak or not (see above). Hence smaller-scale anatomical parameters might better explain the variation in sap flow among oak trees, as recently shown for sapwood density in *Dacrydium cupressinum* in an Australian old-growth rainforest (Barbour et al. 2005). Also, due to the wide range of conduit diameters within a growth ring and the very high hydraulic conductance of the large earlywood vessels in oak, the hydraulic variability is condensed within one or a few annual rings in oak whereas it is spread out over a very wide sapwood radius in beech.

One could finally hypothesise that oak was more “flexible” in its tree-level suite of structure-function relationships, in its hydraulic architecture and allometry compared to beech, forced by beech’s superior competitiveness (cf. Osada et al. 2004). Beech in contrast could realise one optimal structure-functional design.

Such hypotheses, provoked by the loose relationships of tree water use and tree structural scalars in oak, call for further studies that systematically assess tree structure and function in transpiration, and beech as well is understudied in this regard. For instance, the methodology to determine LAI is a field of ongoing research and development, receiving input from global change and remote sensing sciences out of the need to validate remotely sensed estimates of LAI, used as drivers in regional to global models e.g. of the carbon cycle, with ground-based estimates of LAI. The wide availability and affordability of digital photography is currently advancing optical ways

to measure and model LAI and related characteristics of plant canopies (e.g. Zhang et al. 2005, Leblanc et al. 2005, Chen et al. 2006, Cescatti 2007, Chapman 2007). These joint efforts may result in technology and protocols facilitating the retrieval of more robust indirect estimates of LAI in the near future. Portable LIDAR (Light Detection And Ranging)-technology is commercially available now to rapidly assess forest structure at a satisfying spatial resolution (e.g. Lefsky et al. 2002, Parker et al. 2004), thus also supplying valuable structural information to interpret forest function from tree to plot to stand and landscape level more easily. This, together with an adequate sampling of sap flow in trees (e.g. Kumagai 2005a, b), should help to quantitatively advance our understanding of structure–function relationships at these spatial levels in the near future.

#### 6.4. Canopy transpiration $E_c$ and canopy conductance $g_c$

Sap flow in the outermost annulus of the sapwood (0–2 cm) of beech contributed between 27 % (Steinkreuz-pure beech plot) and 54 % (Farrenleite) to stand level seasonal canopy transpiration  $E_c$ ; sap flow in 0–6 cm sapwood depth supplied 62 % (Steinkreuz-pure beech plot) to 92 % (Großebene) of all the water transpired by the beech component of the tree canopy at stand level (Fig. 5.5.2–3). The portion of interpolated sap flow (beyond 6 cm sapwood depth) was thus at least 8 % of  $E_c$  (oak-rich stand Großebene), at most ca. 40 % (Steinkreuz-pure beech plot with large trees dominating the distribution of sapwood area) and ca. 26 % and 12 % for Steinkreuz (mixed) and Farrenleite, respectively. Confidence in this interpolation is based first of all on similar radial patterns of the decline in  $J_s$  in beech trees from several other studies as examined in Chapter 6.2.1. Furthermore, values of  $Q_{t \max}$  also compared well to those from published reports on Central European beech, discussed in Chapter 6.3.1.

The proportion of sap flow in outer or inner sapwood in relation to total  $E_c$  in the different stands thus mirrored the frequency of beech in small, intermediate and dominant size classes in these stands: A larger number of small trees (e.g. Farrenleite, see Fig. 5.1.2.1) resulted in a higher percentage of sap flow in 0–2 cm sapwood depth compared to a stand with a lot of large trees (e.g. Steinkreuz-pure beech plot). Similarly, the marked differences of  $Q_t$  in beech trees from different size classes (Fig. 5.4.2, Tab. 5.4.1, Fig. 6.3.1.1) were reflected in the contribution of the size classes to stand level  $E_c$ , depending on the relative proportion of  $A_s$  of a class on total stand level  $A_s$  (cf. Köstner et al. 1992). Figure 5.5.2 and Figure 5.5.3 show that the rates of the class of dominant beech trees were higher than those of the class of intermediate and suppressed trees at all stands. And this is despite the larger frequency of smaller trees but because of the larger sapwood area of the class of dominant beech trees (Fig. 5.1.2.1) plus the higher sap flow densities in larger trees (Fig. 5.3.5–6, Fig. 5.5.1); similar findings were presented e.g. by Köstner et al. (1992) for a *Nothofagus* forest where a few emergent trees dominated  $E_c$  as well.

Stand level estimates of  $E_c$  reached 166–217 mm season<sup>-1</sup> for the mixed beech-oak stands and 207–349 mm season<sup>-1</sup> for the pure beech plots (Fig. 5.5.4, Tab. 5.5.2, Tab. 6.4.1.1, below). This is within the range of seasonal rates reported in the literature, based on various methods, which range at 149–454 mm season<sup>-1</sup> for mixed beech and mixed oak stands (mostly but not necessarily beech-oak mixtures; mixtures with conifers disregarded), at 164–443 mm season<sup>-1</sup> for beech stands and at 224–365 mm season<sup>-1</sup> for oak (*Q. petraea*, *Q. robur*) stands (see Chap. 6.4.4, Fig. 6.4.4.1-2, and Tab. A11.8, Appendix). The maximum total error of  $E_c$  at the stand level, estimated based on a Gaussian error propagation, ranged around 30 % which is not surprising given the large variability in sap flow among the trees of the heterogeneous stands investigated. Köstner (1999) detailed a maximum error of 18–23 % for a 140 year-old montane spruce stand that was more uniform regarding the tree canopy layer than the stands studied here. An alternative way to determine errors in this context are Monte Carlo simulations (Hatton et al. 1995, Oren et al. 1998, Wullschleger and King 2000, Kumagai et al. 2005a).

Seasonal maximum daily rates of canopy transpiration  $E_{c \max}$  were 2.3–2.7 mm d<sup>-1</sup> for the mixed stands and 3.9–4.4 mm d<sup>-1</sup> for the pure beech plots (Fig. 5.5.5–7, Tab. 5.5.2). Rates published in the literature span 1.6–5 mm d<sup>-1</sup> for pure oak stands and

1.1–8.6 mm d<sup>-1</sup> for pure beech stands (Tab. A11.7, Appendix, and Fig. 6.4.1.1, below); apart from an earlier estimate from Steinkreuz (for the year 1996) of approx. 2.6 mm d<sup>-1</sup> (Köstner 2001), no published values of  $E_c$  max for mixed beech-oak stands were available, only for one declining mixed oak-maple-ash stand in Belgium, where  $E_c$  max ranged from 0.9 to 1.3 mm d<sup>-1</sup> (Vincke et al. 2005a). For both beech and the oak species considered, the highest values of  $E_c$  max were reported for lowland and colline stands, whereas at higher elevation sites only low values of  $E_c$  max were found (Fig. 6.y.b, below). This is not surprising given the lapse rate and consequently decreasing D with increasing elevation (e.g. Körner et al. 1989). The studied small pure beech plot at Steinkreuz at intermediate elevation displayed values of  $E_c$  max clearly smaller than the highest rates of  $E_c$  max observed in other beech stands at similar elevations due to reasons discussed below (Chap. 6.4.4), whereas the montane pure beech stand Farrenleite reached high  $E_c$  max that may well fall onto a line of declining maximum  $E_c$  max with increasing altitude (Fig. 6.y.b).

Daily sums of  $E_c$  were generally non-linearly related to D and saturated at higher D (Fig. 5.5.9, Fig. 5.5.11, Tab. A11.6, Appendix). This was the case at all sites and for both beech and oak of the two mixed stands and has been shown many times (for instance for beech e.g. by Herbst 1995, Granier et al. 2000a, Köstner 2001, for sessile oak by Bréda et al. 1993a). Only  $E_c$  at Farrenleite showed less of a saturation than, for instance, the Steinkreuz-pure beech plot, which will be discussed in more detail below (Chap. 6.4.2). The relationship of daily  $E_c$  with PFD was more linear, and in general not as tight as the relationship with D (Fig. 5.5.10, Fig. 5.5.12, Tab. A11.6; see also Chap. 6.4.3). These response functions changed species- and site-specifically during the season, particularly in 1999 as a consequence of depleted soil water reserves. The high elevation site Farrenleite was least affected, oak at Großebene and Steinkreuz more so, and beech at Steinkreuz and especially at Großebene were impacted the most (Fig. 5.5.14–16, see also Chap. 6.4.2, 6.4.3).

The results for the maximum diurnal canopy conductance  $g_c$  max are similar to those for  $E_c$  max when comparing the different stands, because D was similar at these stands (cf. Tab. 5.5.2, Tab. 5.5.3, Fig. 5.5.18). The  $g_c$  max was highest for the pure beech stands (ca. 24–30 mm s<sup>-1</sup>), followed by the oak-rich mixed stand at Großebene (19.4 mm s<sup>-1</sup>) and the beech-rich mixed Steinkreuz stand (17.5 mm s<sup>-1</sup>, Tab. 5.5.3). Oaks showed the lowest values (10.9 mm s<sup>-1</sup> at Großebene, 2–4 mm mm s<sup>-1</sup> at Steinkreuz), consistent with their low values of  $E_c$  under the same meteorological conditions.

The highest values of  $g_c$  max for the pure beech stands at a reference D of 10 hPa (8.6–10.5 mm s<sup>-1</sup>) compared well to published data (8–14 mm s<sup>-1</sup>: Herbst 1995, Magnani et al. 1998, Granier et al. 2000a, 2003). Values of  $g_c$  max for the oaks of the mixed stands, however, reached only 2.3 mm s<sup>-1</sup> (Großebene) and 0.2–0.7 mm s<sup>-1</sup> (Steinkreuz) at a D of 10 hPa, whereas for a pure French oak stand  $g_c$  max ranged at 10–14 mm s<sup>-1</sup> (Bréda et al. 1993a, Granier et al. 2000b), similar to the pure beech stands. Thus  $g_c$  max of the mixed stands at the reference D was lower (5.3 mm s<sup>-1</sup> for Großebene, 6.4–7.0 mm s<sup>-1</sup> for Steinkreuz) than that of pure beech stands. In a temperate North American stand composed of diffuse-porous *Acer rubrum* and ring-porous *Quercus alba*, Oren and Pataki (2001) calculated canopy conductances for individual trees scaled from sap flow measurements and observed lower values of canopy conductance (at a reference D of 10 hPa) in the more drought-tolerant *Q. alba* than in less drought-tolerant *A. rubrum*. From a comparison with two other

studies on mesic and more xeric sites they concluded that ring-porous species tended to show lower single-tree canopy conductances and a lower stomatal sensitivity to D than diffuse-porous species (Oren and Pataki 2001), the latter indicating a higher drought tolerance. Furthermore they suggested that stands with a high proportion of ring-porous species similar to those studied should exhibit lower values of  $g_c \max$ , while stands with a high proportion of diffuse-porous species in contrast should reveal higher rates of  $g_c \max$  (Oren and Pataki 2001). Data presented here seem to point in a similar direction. The response functions of  $g_c \max$  and D shown in Figure 5.5.18 were comparable to those published e.g. by Bréda et al. (1993a), Herbst (1995), Magnani et al. (1998) and Granier et al. (2000a, b, 2003).

Regarding the general comparability of the sites studied in the Steigerwald and the Fichtelgebirge, the following arguments may be put forward, since obviously not only the assessed meteorological variables differ between the stands in the Steigerwald and the Fichtelgebirge, but also the soil characteristics (cf. Tab. 3.3.1): Leuschner et al. (2004b) showed that the fine root (< 2 mm root diameter) morphology of beech from stands with very different soil and climate characteristics differed very little. Even though the root system structure and probably fine root mortality may be affected in acidic infertile soils, higher root tip densities are hypothesised to compensate for this (Leuschner et al. 2004b). Yet the soil at the Steinkreuz stand is not considered infertile by Langusch and Kalbitz (2001), the large rooting depth counterbalancing the low basic cation contents in the B-horizon caused by rather low soil pH (pH (CaCl<sub>2</sub>) 3.2 in the A<sub>h</sub>-horizon, 3.8 in the B<sub>v</sub>-horizon, Langusch and Kalbitz 2001). A comparison of the sites Steinkreuz and Farrenleite should therefore not suffer from major differences in soil or root characteristics. At Großebene the soil depth was considerably smaller (up to 40 cm) than at Steinkreuz (up to 80 cm), while soil pH and C/N-ratio were similar (Tab. 3.3.1). The smaller tree height at Großebene (26 m compared to 32 m at Steinkreuz, Tab. 3.3.2) at approximately the same stand age may reflect the contrasting soil depths. Differences in tree height, however, could also originate from the different slopes of the stands (Tab. 3.3.1, see also Chap. 6.3.1).

#### 6.4.1. Structural controls on $E_c$ and $g_c$

In Table 6.4.1.1 the results of seasonally integrated  $E_c$  from this study are summarised, together with stand structural characteristics. From this it can be clearly drawn that beech dominated stand level  $E_c$  in the mixed stand Steinkreuz: beech held 69 % of the total basal area  $A_b$ , 76 % of the stems per hectare, 87 % of the leaf area index LAI, 91 % of the sapwood area  $A_s$  and 88–91 % of  $E_c$ . Even in the oak-rich Großebene stand, beech controlled  $E_c$ , contributing 58 % of  $E_c$ , 39 % of the total  $A_b$ , 67 % of the stand density, 48 % of the LAI and 74 % of  $A_s$ . Thus the proportion of a species on  $A_s$  approximated its contribution to  $E_c$  better than the proportion of  $A_b$  or stand density. The contribution of a species to the stand level LAI served this purpose equally well. In a study conducted in a multi-species broadleaved hardwood forest in the eastern US, containing both diffuse- and ring-porous species as well,  $J_{st}$  of ring-porous oaks was similar or even smaller than that of diffuse-porous species, and Wullschleger et al. (2001) concluded likewise that  $E_c$  was dominated by the species with the largest sapwood area and not by the species with the largest basal area or the largest number of stems. Similarly Oren and Pataki (2001) inferred from their results on a mixed deciduous stand also in the eastern US (with rates of  $J_s$  similar for both ring- and diffuse-porous species) that stands with a high proportion of

ring-porous species will have a lower maximum  $E_c$  and  $g_c$  than stands with a high proportion of diffuse-porous species.

In the mixed stands studied,  $E_c/A_s$  was larger for oak than for beech, particularly for Großebeine (Tab. 6.4.1.1). This was caused, at Großebeine, by the abundant small beech trees with small values of  $Q_{t \max}/A_{st} = J_{st}$  (Fig. 5.5.1) and the absence of large beech, in combination with many large oaks with large  $Q_{t \max}/A_{st}$ . At Steinkreuz, the many small beech with small  $Q_{t \max}/A_{st}$  outweighed the large beech trees with mostly smaller  $Q_{t \max}/A_{st}$  than that of the present oaks. In agreement with this, the lowest rates of  $E_c/A_s$  were observed for the densest, high-elevation stand Farrenleite in the Fichtelgebirge, where additionally the shorter growing season (Tab. 6.4.1.1) and generally less beneficial atmospheric conditions played a role, discussed in Chapter 6.4.2, below. Canopy transpiration related to total leaf area,  $E_c/LAI$ , conversely was larger in beech than in oak in the mixed stands, as a consequence of the larger  $A_{lt}/A_{st}$  of oak (Fig. 5.1.3.2b, see also Chap. 6.3.2, above) and the specific contribution of different size classes of a species to  $A_s$ . At Farrenleite,  $E_c/LAI$  was similar to that of the beech component of Steinkreuz. The highest  $E_c/LAI$  was calculated for the Steinkreuz-pure beech plot.

**Table 6.4.1.1:** Growing seasonal sums of canopy transpiration ( $E_c$ ) for 1999 and 2000, length of the growing season (number of sap flow days) and stand structural characteristics and percent contribution of a species to totals of the mixed stands. GR = Großebene, ST-BP = Steinkreuz-pure beech plot.  $A_s$  = sapwood area, LAI = leaf area index (derived from litter collection, at Farrenleite only available in 1998, at ST-BP based on optical measurements, cf. Tab. 5.1.3.2),  $A_b$  = basal area, of a species or the whole stand, respectively.

	GR beech 1999	GR oak 1999	GR stand 1999	Steinkreuz beech 1999	Steinkreuz oak 2000	Steinkreuz oak 1999	Steinkreuz stand 1999	Steinkreuz stand 2000	ST-BP stand 1999	ST-BP stand 2000	Farrenleite stand 1999	Farrenleite stand 2000	
E <sub>c</sub> [mm season <sup>-1</sup> ] (% of total stand)	96 (58)	69 (42)	166	192 (88)	184 (91)	25 (12)	18 (9)	217	202	349	321	229	207
sap flow days	197	201	205	197	188	201	191	205	198	197	188	152	160
A <sub>s</sub> [m <sup>2</sup> ha <sup>-1</sup> ] (% of total stand)	12.8 (74)	4.4 (26)	17.2	17.1 (91)	17.7 (91)	1.69 (9)	1.71 (9)	18.8	19.4	30.2	30.6	42.7	42.7
E <sub>c</sub> /A <sub>s</sub> [kg m <sup>-2</sup> season <sup>-1</sup> ]	7.5	15.7	9.7	11.2	10.4	14.8	10.5	11.5	10.4	11.6	10.5	5.4	4.8
LAI (% of total stand)	2.9 (48)	3.1 (52)	6.0	5.9 (86)	6.0 (87)	1.0 (14)	0.9 (13)	6.9	6.9	6.5	6.8	6.8	
E <sub>c</sub> /LAI [kg m <sup>-2</sup> season <sup>-1</sup> ]	33.1	22.3	27.7	32.5	30.7	25.0	20.0	31.4	29.3	53.7	47.2	33.7	30.4
LAI/A <sub>s</sub> [10 <sup>4</sup> m <sup>2</sup> m <sup>-2</sup> ]	0.227	0.705	0.349	0.345	0.339	0.592	0.526	0.367	0.356	0.215	0.222	0.159	
Stand density [trees ha <sup>-1</sup> ] (% of total stand)	424 (67)	212 (33)	637	265 (76)	265 (76)	85 (24)	85 (24)	350	350	279	279	883	883

Figure 6.4.1.1 shows these and published values for  $E_c \text{ max}/\text{LAI}$  for *F. sylvatica* and several species of the genus *Quercus* (to supplement the few data on *Q. petraea*). By using  $E_c \text{ max}$  when examining structural controls it was sought to circumvent differences in atmospheric conditions and growing season length which would dominate differences among seasonal totals of  $E_c$  from different regions (see above). Nonetheless during a particular year of study, atmospheric or soil conditions may have been limiting (cf. Tab. 5.5.2), causing scatter in the relationships. For instance, in a young French beech stand (Granier et al. 2000a),  $E_c \text{ max}/\text{LAI}$  was  $0.67 \text{ kg m}^{-2} \text{ d}^{-1}$  and  $0.52 \text{ kg m}^{-2} \text{ d}^{-1}$  in two consecutive years, in a young oak stand, average daily transpiration varied between  $0.4 \text{ kg m}^{-2} \text{ d}^{-1}$  and  $0.5 \text{ kg m}^{-2} \text{ d}^{-1}$  over five years (Bréda and Granier 1996). For the pure beech plot at Steinkreuz from the present study the range was  $0.63\text{--}0.57 \text{ kg m}^{-2} \text{ d}^{-1}$  and for Farrenleite  $0.67\text{--}0.62 \text{ kg m}^{-2} \text{ d}^{-1}$ , for the oaks of the mixed stands  $0.22\text{--}0.29 \text{ kg m}^{-2} \text{ d}^{-1}$  and for the mixed stands  $0.38\text{--}0.39 \text{ kg m}^{-2} \text{ d}^{-1}$ , for the growing seasons 1999–2000, respectively (Fig. 6.4.1.1). Uncertainties in the determination of both  $E_c$  (see Chap. 6.4) and LAI (Chap. 6.1) certainly add to the variation in the data. Yet despite the scatter (range  $0.52\text{--}1.32 \text{ kg m}^{-2} \text{ d}^{-1}$ ),  $E_c \text{ max}/\text{LAI}$  for (pure) beech stands remained comparatively stable over a wide range of LAI (1.5–9.0), with an average value of  $0.80 (\pm 0.21) \text{ kg m}^{-2} \text{ d}^{-1}$  ( $n = 24$ , median  $0.75 \text{ kg m}^{-2} \text{ d}^{-1}$ , including Farrenleite and Steinkreuz-pure beech plot and multiple years from sites where available).

Very few data are available for pure oak stands: in a young French sessile oak stand (Bréda et al. 1993a),  $E_c \text{ max}/\text{LAI}$  was the same as that of the Steinkreuz-pure beech plot (Fig. 6.4.1.1). At much lower LAI, a sub-Mediterranean stand of *Q. pubescens* revealed  $E_c \text{ max}/\text{LAI}$  similar to *Q. petraea* (at large year-to-year variability). Thus these oak stands were at the lower end of the range of the beech stands ( $0.66 \text{ kg m}^{-2} \text{ d}^{-1}$ ). Values provided by Vincke et al. (2005a) for the oak component of a declining mixed stand of *Q. robur* calculated to rates of  $E_c \text{ max}/\text{LAI}$  lower than the ones from the two aforementioned pure oak stands and more similar to those of the mixed Steigerwald stands. Data from the mixed (ring- and diffuse-porous) deciduous forest in the eastern US studied by Oren and Pataki (2001), Wullschleger et al. (2001) and Pataki and Oren (2003) were similar to those of the mixed Steigerwald stands, over a range of LAI from 3.3 to 6.2 (Fig. 6.4.1.1).

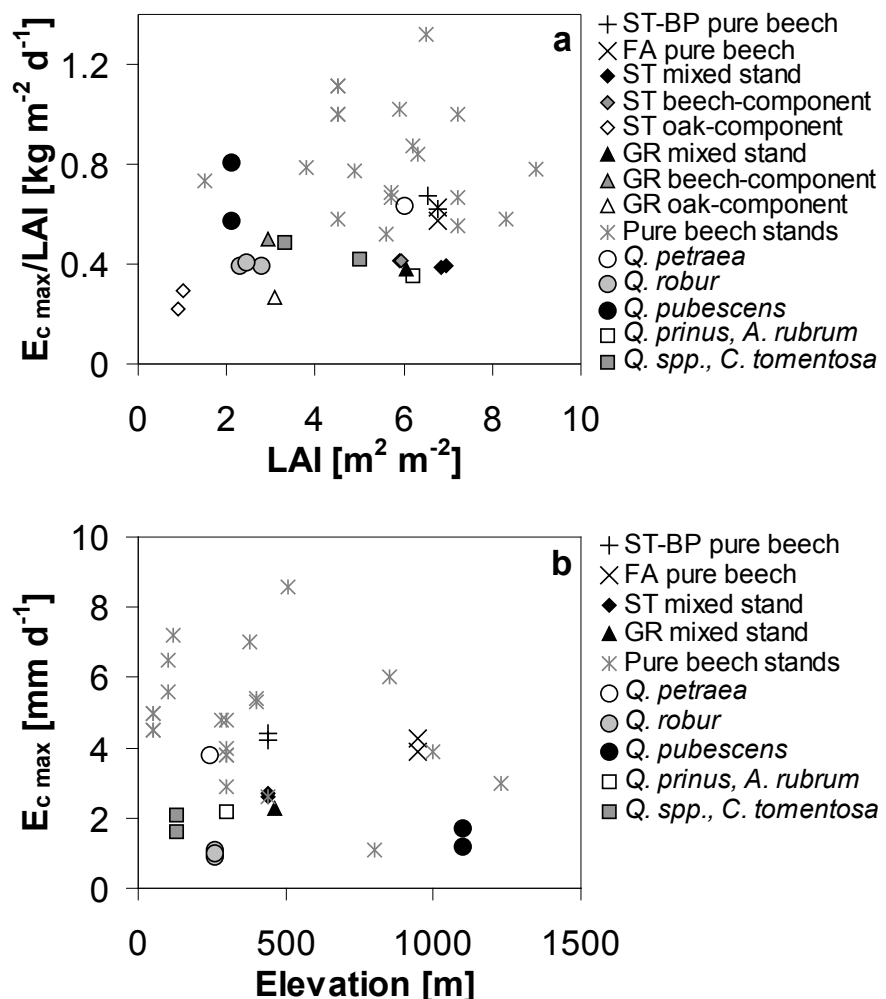


**Figure 6.4.1.1a:** Maximum daily canopy transpiration of closed stands related to LAI ( $E_c \text{ max/LAI}$ ) and LAI from the literature for beech (double-crosses), oak (circles) and mixed oak stands (squares) and from the present study (see legend). FA is Farrenleite, ST-BP pure beech plot within the mixed stand Steinkreuz, ST Steinkreuz and GR Großebene. The open circle is a young pure *Quercus petraea*-stand (Bréda et al. 1993a), shaded circles a (declining) mixed stand of *Q. robur* (*Acer pseudoplatanus*, *Fraxinus excelsior* admixed, only oak component shown here; Vincke et al. 2005a) and filled circles a *Q. pubescens*-stand (Poyatos et al. 2007); the open square denotes a *Q. prinus* / *Acer rubrum* / *Nyssa sylvatica* / *Q. alba*-stand (Wullschleger et al. 2001), shaded squares are two stands of *Quercus* species / *Carya tomentosa* and other admixed species (Oren and Pataki 2001, Pataki and Oren 2003). Other references and data are given in Table A.11.7, Appendix. Data from all available years for each location are shown. **Figure 6.4.1.1b:**  $E_c \text{ max}$  and site elevation above sea level for the same sites as in a.

From this comparison of the results presented here and published results it would seem that pure stands of beech differ noticeably from mixed stands of beech and/or oak with respect to  $E_c \text{ max/LAI}$  (Fig. 6.4.1.1): namely that beech maintains high  $E_c \text{ max/LAI}$  even at high LAI in pure stands, whereas in mixed stands of beech and/or oak  $E_c \text{ max/LAI}$  is lower. This supports the view that beech is very effective in crown space capture, in minimising self-shading and in the adaptation of leaves to the specific light

environment, not only at the tree level (Niinemets 1995, Leuschner 2001, Fleck 2002, Hagemeier 2002, Hansen et al. 2002, Köstner et al. 2004; see also Chap. 6.3.2), but also at canopy or stand level (see also Chap. 6.4.3). Consequently, the LAI is a key structural factor in explaining between-stand variation of transpiration in beech, as also reported by Granier et al. (2003, 2007) or e.g. by Bréda and Granier (1996) Granier et al. (2000b) and Santiago et al. (2000) for a range of tree species from contrasting climates (see also Running and Coughlan 1988). While in the data set compiled here  $E_c$  of pure beech stands still increased at  $LAI > 6$  (cf. Fig. 6.4.1.1), Granier et al. (2000b) had suggested that (standardised)  $g_c$  (and hence  $E_c$ ) saturates at an LAI of 6, based on several species from boreal, temperate and tropical stands. However, their data set contained only beech stands with an LAI of up to 6 (4.5–5.7,  $n = 3$ ) and thus did not represent the high shade tolerance of beech. Included were, on the other hand, stands of shade tolerant *Abies bornmulleriana* and semi-shade tolerant *Picea abies* with  $LAI > 8$ , which indeed displayed higher  $E_c$  than stands with an LAI of around 6 (cf. Granier et al. 2000b). This may be taken as yet another indication of the significance of shade tolerance and minimised self-shading in the relationship between  $E_c$  and LAI. For oak on the contrary, it would seem plausible for  $E_c$  to saturate at relatively lower LAI (e.g. around 5–6, cf. Bréda and Granier 1996, Granier and Bréda 1996, Granier et al. 2000b), since self-shading will become increasingly limiting (Granier and Bréda 1996, Granier et al. 2000b, Leuschner 2001, Fleck 2002, Hagemeier 2002). Data from more oak stands would be imperative, however, to elucidate this issue. The positive effect of the reduced shading of oak was shown in a thinned sessile oak plot where average daily  $E_c/LAI$  increased by ca. 15–40 % during two years compared to an unthinned plot within the same stand (Bréda and Granier 1996).

It may be speculatively concluded from the above that it does matter for the general relationship of  $E_c$  of a species with LAI whether the species is more shade tolerant like *F. sylvatica* or less shade tolerant like *Q. petraea* (increasing  $E_c$  even at high LAI in the former species, in contrast to earlier saturation of  $E_c$  with increasing LAI in the latter), at least at high values of LAI. The conclusion of Granier et al. (2000b) that LAI was more important than the species in determining  $g_c$  (or  $E_c$ ) at stand level, would then only be valid for the lower range of LAI of forest stands (e.g. 2–6, cf. Granier et al. 2000b, see above). However, there may be some indications that oaks operate on a lower  $E_c \text{ max}/\text{LAI}$  altogether (Fig. 5.5.5b, e, Fig. 6.4.1.1). Whether this species falls within the (rather wide) species-independent relationship of  $E_c$  and LAI drawn by Granier et al. (2000b) or whether it follows one of its own has to remain open to speculation until adequate data are available for *Q. petraea*.

The higher self-shading and lower shade tolerance of oak in turn should also limit the LAI of oak stands to values lower than those of beech stands, as emerged from the literature survey presented in Chapter 6.1: the LAI of 104 pure stands of *F. sylvatica* was 2.5–10.2, on average 6.4 ( $\pm 1.76$ ), for 29 pure stands of oak (*Q. petraea*, *Q. robur*) the LAI ranged from 0.5 to 6.5, on average 3.8 ( $\pm 1.74$ ). In an earlier overview Röhrlig (1991) had noted similar differences in the LAI of these species (*F. sylvatica*: 5.0–6.6, *Q. petraea*, *Q. robur*: 4.6–5.7, Röhrlig 1991, p 167f). The LAI of mixed stands of beech and oak accordingly ranged in between these two end points (1.9–7.5, mean  $5.4 \pm 1.13$ ,  $n = 33$  stands, cf. Chap. 6.1).

$E_{c\ max}$  also increased with sapwood area  $A_s$ , for the oak component of the mixed stands at the lower range of  $A_s$ , for the beech components and the total mixed stands at the middle range of  $A_s$  and up to the pure beech stands where  $E_{c\ max}$  then did not increase any further beyond the  $A_s$  of  $32\ m^{-2}\ ha^{-1}$  (Steinkreuz-pure beech plot; Fig. 5.5.5d). Via a higher LAI/ $A_s$  of oak compared to beech (Tab. 6.4.1.1; corresponding to higher  $A_{lt}/A_{st}$  at the tree level, Fig. 5.1.3.2), the lower  $E_{c\ max}/LAI$  in oak, discussed above, is linked to a higher  $E_{c\ max}/A_s$  as shown in Figure 5.5.5f: the oak component of Steinkreuz and Großebene reached values for  $E_{c\ max}/A_s$  of  $1.8\text{--}1.9 \cdot 10^3\ kg\ m^{-2}\ d^{-1}$ , at the lowest values of  $A_s$  ( $1.7\text{--}4.4\ m^{-2}\ ha^{-1}$ ; see also above for  $E_{c\ season}/A_s$ ), while values for pure beech, total mixed stands and the beech component of mixed stands ranged between  $1.0\text{--}1.5 \cdot 10^3\ kg\ m^{-2}\ d^{-1}$ , for  $A_s$  spanning  $12.8\text{--}42.7\ m^{-2}\ ha^{-1}$ . The lowest value of  $E_{c\ max}/A_s$  was recorded, as for seasonal  $E_c/A_s$ , at the densest stand Farrenleite, which also had the least LAI per  $A_s$  (Tab. 6.4.1.1). This is because the stand is composed of many small trees with little  $A_{lt}$  and  $A_{st}$ .

The range of  $E_{c\ max}/A_s$  as shown in Figure 5.5.5f, for an  $A_s$  of  $1.7\text{--}32\ m^{-2}\ ha^{-1}$  (the “linear” part of the  $E_{c\ max}$  vs  $A_s$  relationship, see above), was smaller than the range of  $E_{c\ max}/LAI$  (Fig. 5.5.5e; variation by a factor of 1.65 for the former and of 2.48 for the latter ratio). Therefore, it could perhaps be concluded for the stands studied here that  $E_{c\ max}$  was better predicted by  $A_s$  than by LAI. On the other hand  $E_{c\ max}/A_s$  saturated at high  $A_s$  while this did not seem to be the case for  $E_{c\ max}/LAI$ , at least for beech. However, these speculations cannot be further substantiated because  $A_s$  is rarely detailed in publications, and data on oak and mixed beech-oak stands is largely lacking or missing in the literature.

Maximum diurnal canopy conductance related to LAI ( $g_{c\ max}/LAI$ ) was highest at the Steinkreuz-pure beech plot ( $3.9\text{--}4.6\ kg\ m^{-2}\ s^{-1}$  for the two years considered) and at Farrenleite ( $2.6\text{--}3.6\ kg\ m^{-2}\ s^{-1}$ ), followed by the oaks from the mixed stands (Steinkreuz  $2.2\text{--}3.9\ kg\ m^{-2}\ s^{-1}$ , Großebene  $3.5\ kg\ m^{-2}\ s^{-1}$ ; Fig. 5.5.19, Tab. 5.5.3). In general, normalising  $g_{c\ max}$  with LAI reduced the differences between stands and their composing species observed for  $g_{c\ max}$  (see Chap. 6.4.). This is in concert with the usually higher stomatal conductance (and leaf level transpiration, cf. Chap. 6.3.2) of oak compared to beech as observed in studies of gas exchange on sun leaves (e.g. Aranda et al. 2000, 2005, Leuschner et al. 2001a, Fleck 2002, Valladares et al. 2002, Fleck et al. 2004), when taking into account the dampening effect of shade leaves at whole-canopy level as presented here. Still, even during the more xeric year 1999 the  $g_{c\ max}/LAI$  of Steinkreuz-pure beech plot was higher than that of Großebene (both total stand or oak component only). Published values of  $g_{c\ max}/LAI$ , referenced to a D of 10 hPa, range at ca.  $1.8\text{--}2.4\ kg\ m^{-2}\ s^{-1}$  for beech stands (Herbst 1995, Magnani et al. 1998, Granier et al. 2000a) and at  $1.4\text{--}1.8\ kg\ m^{-2}\ s^{-1}$  for a sessile oak stand (Granier and Bréda 1996), which compare to values of  $1.3\text{--}1.6\ kg\ m^{-2}\ s^{-1}$  for the pure beech stands, to  $0.9\text{--}1.0\ kg\ m^{-2}\ s^{-1}$  for the mixed stands, to  $0.9\text{--}1.1\ kg\ m^{-2}\ s^{-1}$  for the beech component of the mixed stands and to  $0.7\text{--}1.0\ kg\ m^{-2}\ s^{-1}$  for the oak components (at 10 hPa) from the present study. Thus  $g_{c\ max}/LAI$  at a reference D of 10 hPa seems to be smaller in mixed beech-oak stands than in pure beech or oak stands. However, data from the two mixed stands studied here and the oak stand studied by Granier and Bréda (1996) need support from further investigations to draw conclusions.

#### 6.4.2. Comparison of beech in the Steigerwald and the Fichtelgebirge

The  $E_{c\ max}$  reached similar values at the high elevation site Farrenleite (950 m a.s.l.: 4.3 mm d<sup>-1</sup> in 1999, 3.9 mm d<sup>-1</sup> in 2000) and at the lower elevation site Steinkreuz-pure beech plot (440 m a.s.l.: 4.4 mm d<sup>-1</sup> in 1999 and 4.2 mm d<sup>-1</sup> in 2000; Fig. 5.5.5–7, Tab. 5.5.2). The lower rates of  $J_{st}$  and  $Q_t$  (Tab. 5.4.1, Fig. 5.4.2, Tab. 5.5.1, Fig. 5.5.1) in the smaller trees at Farrenleite were compensated by the large stand density (3.2 times larger stand density at Farrenleite), and sapwood area (1.4 times larger). Interestingly though,  $E_{c\ max}$  did not increase any further with increasing  $A_s$  from the Steinkreuz-pure beech plot (30.2 m<sup>2</sup> ha<sup>-1</sup>) to Farrenleite (42.7 m<sup>2</sup> ha<sup>-1</sup>, Fig. 5.5.5d, see also Chap. 6.4.1, above). Atmospheric conditions can almost certainly be ruled out as factors limiting  $E_{c\ max}$  at Farrenleite (Fig. 5.5.9), and the soil water supply should have been even less likely to control transpiration (e.g. Fig. 5.5.14, Fig. 5.5.15, Fig. 5.5.16). Instead, stand structure may be controlling maximum daily canopy transpiration here: water use per tree  $Q_t$  showed a strong non-linear increase with DBH (Fig. 5.4.2), the consequence of the exponential increase of sapwood area with DBH (Fig. 5.1.1.4) plus the radial decline of sap flow density  $J_s$  with sapwood depth (Fig. 5.3.4), which was found to be steeper for small trees on an absolute scale of radial sapwood depth than for large trees (Fig. 5.3.3). Thus  $E_c$  of a stand composed of many small beech trees will be smaller than that of a stand with the same  $A_s$  but fewer and larger trees (cf. Vertessy et al. 1995). In this respect  $A_s$  at Farrenleite had a different quality than that of the Steinkreuz-pure beech plot as can be derived from Figure 5.5.5f,  $E_{c\ max}/A_s$  of Farrenleite being only 68 % of that of the Steinkreuz-pure beech plot. At the same time, LAI was very similar for Farrenleite and the Steinkreuz-pure beech plot and therefore may have also resulted in similar rates of  $E_{c\ max}$ . This is supported by the finding that  $E_{c\ max}/LAI$  is rather constant over a wide range of LAI (see above). Correspondingly, Granier et al. (2000a) found daily rates of  $E_c$  in a young colline (300 m a.s.l.) and a mature montane stand (1000 m a.s.l.) with similar LAI to compare well. These two sites were also comparable in their  $E_{c\ max}$  to the stands Farrenleite and the Steinkreuz-pure beech plot (Fig. 6.4.1.1, b).

The seasonal sums of canopy transpiration  $E_c$  at Farrenleite and the Steinkreuz-pure beech plot differed significantly, the  $E_c$  of the latter being 1.5 times larger than that of Farrenleite for 1999 and 2000 (Fig. 5.5.4, Tab. 5.5.2, Tab. 6.4.1.1). This was on the one hand due to the shorter growing season (= duration of sap flow; e.g. Fig. 5.5.17c), lower air temperature (e.g. Tab. 5.2.1.1), larger number of rain and fog days (Chap. 5.2.2, Tab. 5.2.1.1), lower radiation (e.g. Tab. 5.2.1.1) and the lower vapour pressure deficit of the air at the higher elevation site Farrenleite (Fig. 5.2.1.2, Fig. 5.2.2.1, Fig. 5.5.17a). On the other hand, the response of  $E_c$  to atmospheric drivers also differed among these sites: the initial increase of  $E_c$  with increasing D and PFD was steeper and saturation was reached at lower D and PFD in the Steinkreuz-pure beech plot compared to Farrenleite (if reached at all at Farrenleite). The observation that beech at the montane site Farrenleite reached rates of  $E_c$  comparable to those at the colline–sub-montane Steinkreuz-pure beech plot signifies the high potential of beech transpiration at Farrenleite and limitations other than physiological ones (see above). A study conducted in a montane beech stand in the Pol'ana mountains of central Slovakia (Střelcová et al. 2002, 2004, 2006) points in the same direction: High maximum rates of  $Q_t$  of dominant trees (up to 371 kg d<sup>-1</sup>) contrasted with low season-long averages (79 kg d<sup>-1</sup>, see Chap. 6.3) compared to similar trees from the Steigerwald, indicating atmospheric conditions to limit transpiration on a considerable number of days (also implied by a 5 % contribution of fog to total growing season pre-

cipitation: Střelcová et al. 2006). And also results from Granier et al. (2000a) demonstrate the effects of higher altitude, which resulted in a lower seasonal  $E_c$  at a montane beech stand compared to a colline site while the maximum daily  $E_c$  was similar at both sites (see above).

Lower air temperatures at Farrenleite could be the cause of the difference in initial slope and in the value of saturating D (see below). This was the case during the year 2000 (Fig. 5.5.11–12) and during June–July 1999 (Fig. 5.5.9–10, top panel). In August and September 1999 the initial slope and the maximum values of the response functions of  $E_c$  with D (and PFD) for the Steinkreuz-pure beech plot decreased. The correlation between  $E_c$  and PFD was not higher at Farrenleite than at the Steinkreuz-pure beech plot. In contrast, solar radiation mostly controlled the transpiration of an oak woodland in the humid, hazy Midwest of the US (Asbjørnsen et al. 2007).

Using the established response functions of  $E_c$  with D mentioned above, it could be estimated for the comparatively dry year of 1999 that the reductions in daily  $E_c$  reached about 20 % in August and about 50 % in September at the Steinkreuz-pure beech plot, relative to June–July, but only around 10 % at Farrenleite (Fig. 5.5.15). This reduction of  $E_c$  in the Steigerwald was paralleled by considerable reductions in relative extractable soil water  $\theta_e$ , while at Farrenleite soil water content remained higher (Fig. 5.2.1.2, Fig. 5.2.2.2, Fig. 5.5.16). Also, the water storage capacity across the total soil profile is likely to have been much higher at Farrenleite (cf. Chap. 5.2.2). It can be concluded that stomatal regulation, induced by a decrease of  $\theta_e$  below the critical threshold of 0.4, caused the reduction of  $E_c$  at the Steinkreuz-pure beech plot, as has been observed in beech in several studies (e.g. Granier et al. 1999, 2000b, 2002, 2007, cf. Chap. 6.2.4). Beech is known to tightly control stomatal conductance to prevent plant water potential dropping below critically low (more negative) values in order to reduce the risk of cavitation (e.g. Hacke and Sauter 1995, Tognetti et al. 1995, Backes 1996, Herbst et al. 1999, Aranda et al. 2000, Lemoine et al. 2002).

In the year 2000 reductions in  $E_c$  for the same periods as in 1999 was merely around 5–10 % for both sites (Fig. 5.5.15), which may be attributable to the “normal” senescing of the foliage. Cloudy and wet spells during summers were usually more pronounced at Farrenleite (Fig. 5.5.6–7, Fig. 5.5.8a, c) than at Steinkreuz, as also indicated by the number of rainy days, particularly for the year 2000 (Chap. 5.2.2), or fog days (Tab. 5.2.1.1) and the lower seasonal integrals of D and PFD (Fig. 5.5.17a, b). Thus in 1999 the late summer drought reduced the difference in seasonal  $E_c$  between Farrenleite and the Steinkreuz-pure beech plot (Fig. 5.5.8) but did not outweigh lower D (and PFD) and shorter growing season (Fig. 5.5.17). In 2000 the rather wet summer reduced totals of  $E_c$  at both stands below values of 1999 – for the Steinkreuz-pure beech plot likely through lower D (Fig. 5.5.11, Fig. 5.5.17a) – yet at Farrenleite even higher values of D on several days in July and September but especially in August (Fig. 5.5.11), resulting in higher seasonally integrated D (Fig. 5.5.17a), could not counterbalance the large number of rain and fog days (see above).

In a dendroecological study, Dittmar and Elling (1999) investigated radial growth of beech from several Bavarian stands from different elevations, including Steinkreuz in the Steigerwald and Farrenleite in the Fichtelgebirge. At colline to sub-montane sites precipitation (or its lack) during the growing season limited growth, while at montane

sites temperature and radiation were limiting, lending support to the above explanations. Dittmar et al. (2003) extended their investigations to Central Europe and pointed to the widely acknowledged increased growth rate in beech since about the 1950s in connection with atmospheric nitrogen deposition (see also e.g. Pretzsch 1999) at lower elevations and to growth depressions after 1975 at higher elevations which they attributed to the changed ecological fitness of trees due to increased tropospheric ozone concentrations.

As mentioned above (Chap. 6.4), the ranking of maximum canopy conductance  $g_c \text{ max}$  followed that of  $E_c \text{ max}$ . Given the similar LAI of Farrenleite and the Steinkreuz-pure beech plot, the latter site had both the highest values of  $g_c \text{ max}$  and of  $g_c \text{ max}/\text{LAI}$  (Fig. 5.5.18–19, Tab. 5.5.3). Interestingly, at Farrenleite, values of  $g_c \text{ max}$  at low D were mostly much lower than those from the Steinkreuz-pure beech plot at the same D, especially during the year 1999. The time when the diurnal maximum of  $g_c$  was reached was shifted in general to later hours of the day at Farrenleite compared to Steinkreuz. This was probably brought about by more rapid cooling of the air in the afternoon and particularly slower warming of the air in the morning at the more exposed, higher elevated site Farrenleite (temperature effect, see above). Granier et al. (2000a) correspondingly have shown that canopy conductance of beech was reduced at air temperatures below 17 °C (see also Cochard et al. 2000). This temperature sensitivity, together with lower values of D in the morning at Farrenleite, may also explain why beech at Farrenleite did not reach values of  $g_c \text{ max}$  (Fig. 5.5.18) or  $g_c \text{ max}/\text{LAI}$  (Fig. 5.5.19) as high as those of beech at the Steinkreuz-pure beech plot: assuming that  $T_{\text{air}}$  drops to lower values at night at Farrenleite than at Steinkreuz (as was the case most of the time; not shown) and that D drops to zero at both sites (not every night, more frequently at Farrenleite though) then the same D will be reached later at Farrenleite than at Steinkreuz. For reasons not known

In conclusion, no indications of a different physiological potential of beech at the high and the low elevation site were found, as reflected in similar  $E_c \text{ max}$ , but actual canopy transpiration and canopy conductance of beech at Farrenleite often remained below their capacity, limited on a daily basis by atmospheric conditions (D,  $T_{\text{air}}$ ) and seasonally by the short foliated period (driven by lower  $T_{\text{air}}$  as well).

#### 6.4.3. Comparison of beech and oak in mixed stands in the Steigerwald

The canopy transpiration  $E_c$  of beech and oak and their contribution to total  $E_c$  of the stands studied here followed the same general pattern as dictated by the meteorological conditions, apart from the later onset of sap flux in oak (about 4–5 days after beech) and its later termination (8 days in 1999, no difference in 2000 at very low D towards leaf shedding; Tab. 5.5.2) when beech or oak contributed solely to  $E_c$ , respectively (Fig. 5.5.6–7). Differences in contribution to total  $E_c$  of the stands were also visible on rainy days when the oak canopy at Steinkreuz and GroßeBene seemed to dry faster than that of beech (Fig. 5.5.6–7), facilitating an earlier commencement of gas exchange in oak leaves (even though the effect on  $E_c$  of oak was only marginal).

$E_c$  revealed a higher correlation with  $D_{avg}$  ( $R^2 = 0.840$ ) than with PFD<sub>day</sub> ( $R^2 = 0.784$ ; average for all stands and periods, respectively), and a stronger correlation for beech than for oak (average  $R^2$  for  $D_{avg}$ : 0.857 vs 0.782; for PFD<sub>day</sub>: 0.811 vs 0.713, respectively; Fig. 5.5.9–12, Tab. A11.6, Appendix). The water vapour pressure deficit of the air, D, has been reported previously to be the main driver of  $E_c$  in beech (Köstner 2001, Granier et al. 2003, 2007) and other temperate tree species (e.g. Köstner 2001, Ewers et al. 2002, Pataki and Oren 2003, Tang et al. 2006). In both shade tolerant and intolerant tree species of an eastern North American oak-hickory forest, a high correlation of water use with D was observed by Pataki and Oren (2003), while they only noticed a high correlation with radiation in a shade intolerant species. Wullschleger et al. (2001) found daily radiation to mainly determine the seasonal pattern and daily magnitude of  $J_s$  in *Q. prinus*, a white oak (sect. *Lepidobalanus*) intermediate in shade tolerance. No such differences in the response to D and PFD were observed in the present study between *Fagus sylvatica* and *Quercus petraea*, the former being a typical shade tolerant tree species and the latter a more shade intolerant species (see Chap. 6.3.2 and below). (*Q. petraea* in fact has been regarded (qualitatively) as more similar to beech concerning shade tolerance and (height) growth than *Q. robur* (Ellenberg 1996, Leuschner 1998). In unison with this perspective, Petit et al. (2004), compiling results from various fields of research, reviewed *Q. robur* as the more pioneering and *Q. petraea* as the more late successional of the two species. For comparisons between *Q. robur* and *Q. petraea* see also e.g. Cochard et al. (1992), Lévy et al. (1992), Tyree and Cochard (1996), Bréda et al. (1993b, 1995b), Epron and Dreyer (1993), Thomas and Gausling (2000), Ponton et al. (2001, 2002), Gieger and Thomas (2002, 2005), Thomas et al. (2002, 2006).)

The most striking difference in the partitioning of total  $E_c$  among beech and oak as seen in Figures 5.5.6–7, however, emerged with progressing soil water depletion during August and September in 1999 at GroßeBene, when oak began to dominate total  $E_c$  (Fig. 5.5.6–7, see also Fig. 5.2.1.2–3, Fig. 5.2.1.5). At Steinkreuz this trend was weaker, and the season-long difference in the percentage of beech on total  $E_c$  was only 3 % between the dry year 1999 and the wet year 2000 (88 % in the former year, 91 % in the latter, Tab. 6.4.1.1; no measurements at GroßeBene in 2000). These differences were demonstrated in Figure 5.5.9–12 to be functional changes in the response of  $E_c$  to atmospheric drivers: For a given D or PFD, lower rates of  $E_c$  were attained in August and September 1999 compared to June–July (and lower absolute maxima) and also the initial slope of the response curve of  $E_c$  to D (and PFD) was reduced. In oak from both stands these decreases were less strong than for

beech (see also Tab. A11.6, Appendix), which indicates a larger drought tolerance in oak than in beech.

Summarised in Figure 5.5.14, the reduction in the response of  $E_c$  to D (relative to June–July) in oak at Steinkreuz compared to oak at Großebene was considerably larger in August (0.23 vs 0.14) and slightly lower in September (0.42 vs 0.48). In beech at Großebene, reductions were much larger than in oak (August: 0.30 = 2 times larger reduction; September: 0.72 = 1.5 times larger reduction). At Steinkreuz, beech responded with approx. 20 % reduction in  $E_c$  at a given D in August compared to June–July and about 54 % in September. Thus at Steinkreuz, the decline in  $E_c$  was similar for beech and oak in August (only slightly smaller in beech) but almost 1.3 times larger in beech than in oak in September. These reductions were linked in Figure 5.5.16 to the depletion of soil water reserves (see also Fig. 5.3.9, Fig. 5.2.1.1, Fig. 5.2.1.3, Fig. 5.2.1.5). In the year 2000 only a short period of moderate soil water depletion was observed earlier in the summer than in 1999 (cf. Fig. 5.3.9), and soil water was not limiting  $E_c$  (e.g. Fig. 5.5.14, right panel, Fig. 5.5.16), as may also be followed from the larger use of available energy ( $R_n$ ) for vapourisation in 2000 compared to 1999 (Fig. 5.5.13). As another indication of the larger drought tolerance of oak, the maximum canopy conductance,  $g_{c \max}$ , of oak at Steinkreuz in 1999 was higher than in 2000, relative to the  $g_{c \max}$  of less drought-tolerant beech (cf. Tab. 5.5.3). Also, in 1999 the maximum observed  $g_{c \max}$  per unit leaf area ( $g_{c \max}/LAI$ ) was higher in the oak component of both mixed stands than in beech and higher at Großebene than at Steinkreuz (total stands), reflecting the higher stomatal conductance  $g_s$  of oak observed in studies of leaf gas exchange (cf. Chap. 6.4.1). In the more mesic year 2000 the highest values of  $g_{c \max}/LAI$  were nearly identical in both species (Tab. 5.5.3).

Several studies similarly demonstrated reductions of transpiration in beech at tree or canopy level caused by drought: Granier et al. (2007) for instance studied the effect of the extreme drought during the summer of 2003 across Europe. In a young beech stand in France (Hesse forest) for example,  $E_c$  was reduced from around  $4 \text{ mm d}^{-1}$  to  $< 3 \text{ mm d}^{-1}$  when  $\theta_e$  declined below 0.4;  $\theta_e$  reached a minimum  $< 0.1$ . PAI decreased by about 1 due to the premature leaf fall of green leaves (probably due to embolised petioles; Granier et al. 2007). Hölscher et al. (2005) found a reduction of  $J_s \text{ day } 0\text{--}2 \text{ cm}$  of about 39 % in beech during a dry period compared to pre-drought values. The magnitude of the drought was described on a relative scale only though and could not be compared to findings from the present study. Matyssek et al. (1991, see also Cermák et al. 1993) and Granier et al. (2000a) also noted a decreased (but not quantified) transpiration of beech under limited soil water supply. The radial growth of beech stems was also shown to react very sensitively to soil water shortage (Gutiérrez 1988, Jump et al. 2006).

Aranda et al. (2005) showed stronger reductions of  $J_s$  in *F. sylvatica* than in *Q. petraea* with seasonally progressing soil water depletion in a mixed stand of both species near their southern limit of distribution in Europe. The same authors also observed more pronounced stomatal closure in response to high D in beech than in oak (see also Aranda et al. 2000) and a much more reduced specific hydraulic conductance  $k_s$  in beech (-56 %) than in oak (-34 %) during the course of a dry summer; absolute values of  $k_s$  were mostly larger in oak throughout the summer (Aranda et al. 2005). Bréda et al. (1993a) in a rain exclusion experiment under more extreme soil drought than Aranda et al. (2005) showed a reduction of  $k_s$  in sessile oak of around

50 % relative to pre-stress values, yet stomatal conductance of oak was still considerable. Leuzinger et al. (2005) in a sub-montane mixed stand found a reduction of daily maximum  $J_s$  of about 40 % in beech but only of around 15 % in sessile oak under atmospheric and soil drought. Stomatal conductance was also more reduced in beech than in oak and resumed to pre-drought values in oak after the drought ceased in September, but not in beech (Leuzinger et al. 2005). Stem radial growth was reduced in all studies species, but least of all in *Q. petraea* (Leuzinger et al. 2005). Keel et al. (2007) for the same site reported reductions of stomatal conductance of only 6 % for oak in 2003 (extreme drought) compared to 2001, and of > 50 % in beech. Similar leaf-level observations on European beech and sessile oak (*Q. petraea* ssp. *medwediewii* = *Q. dalechampii*) were also made by Raftoyannis and Radoglou (2002) during an extreme drought at a montane site in Greece.

Backes and Leuschner (2000) concluded from their comparative study of beech and sessile oak in a mixed stand in north-western Germany that beech is a drought-sensitive species conservative in water use (and therefore also limited in carbon assimilation capacity). In moderately dry summers sensitive stomatal regulation was sufficient to prevent critical reductions in leaf water potential. Under severe drought conditions, however, this fine stomatal control seemed insufficient to avoid marked reductions in predawn leaf water potential, photosynthetic capacity, radial stem growth and fine root biomass in *F. sylvatica* (Backes and Leuschner 2000). Based on their findings and those of other investigators, Backes and Leuschner (2000) summarised that *Q. petraea*, in contrast to *F. sylvatica*, displayed traits of a drought stress tolerator, namely higher tissue elasticity during severe drought, a potential for osmotic adjustment at leaf level, low vulnerability to cavitation, a photosynthetic apparatus rather insensitive to dehydration and turgor reduction and a relatively drought-tolerant fine root system. Furthermore Backes and Leuschner (2000) indicated that in *F. sylvatica* and *Q. petraea* "the capacity to tolerate and cast shade seems to be positively correlated with the sensitivity to drought". Thus there would be a trade-off between shade production and drought resistance, since leaves of the shade canopy are effective in radiation absorption, but lack morphological adaptations to resist drought (Backes and Leuschner 2000). Hein and Dhôte (2006) pointed out in their evaluation of the radial growth in 30 long-term permanent oak-beech plots in northern France that the basal area increment of oak decreased with an increasing admixture of beech, corroborating the competitive superiority of beech under mesic conditions. On more xeric sites in central France on the other hand oak dominated over beech (Goreaud 2000, cited in Hein and Dhôte 2006). Twig abscission (cladoprosis, more common in *Q. robur* than in *Q. petraea* though: Roloff and Klugmann 1998), may be a mechanism by which oak can adjust its leaf area as a consequence of repeated drought (Rust and Roloff 2004, Rust et al. 2004).

With respect to drought, stem growth and fine root mortality and fine root production proved to be sensitive indicators in beech (Leuschner et al. 2001a), and these authors found reductions in radial stem growth in beech but not in oak during a dry year. Also, in oak no increased fine root mortality could be detected, indicative of fine roots apparently being less sensitive to soil water shortage, whereas in beech fine root mortality was significant (Leuschner et al. 2001a). Remarkably though, beech obviously compensated for this loss of fine root biomass by stimulated fine root growth during a comparatively mild drought, which in turn may have reduced radial stem growth (see above; Leuschner et al. 2001a). Mainiero and Kazda (2006) on the other hand noted a relative conservative fine root investment pattern of beech that

did not respond to severe soil drought, which indicated the limited vigour of beech under repeated, strong soil drought. In a literature survey of 16 Central European beech stands Leuschner and Hertel (2003) found a highly significant positive correlation of fine root biomass and annual precipitation. And beech appeared to be the species most sensitive to reduced soil water availability, as revealed by an analysis of more than 100 temperate forest stands, including *Fagus*, *Quercus*, *Picea*, *Pinus* species and other species (Leuschner and Hertel 2003). Constituents of the (putatively) higher resistivity of oak fine roots to soil drought could be the larger number of peridermal cell layers, the larger periderm thickness and the twice as large amount of suberin compared to fine roots of beech as observed by Leuschner et al. (2003, 2004a).

Leuschner et al. (2001b) investigated in detail the competition between beech and oak at root level at a study site in lowland NW Germany, where forest patches of pure (> 95 % of stems) beech and pure oak and mixed beech-oak co-occurred. In mixed plots where beech and oak held similar stem densities and leaf areas, the fine root (< 2 mm) biomass, number of root tips and of ectomycorrhiza was 3–5 times larger in beech than in oak. Oak roots grew slower than beech roots. These authors ascribed the rather small fine root biomass of oak to its competitive replacement by beech roots as suggested from the comparison with oak growing in a pure oak patch (Leuschner et al. 2001b). The fine root systems of the two species completely intermingled in the nitrogen-rich organic topsoil of that site. The beech fine root biomass increased with distance from the stem, in oak it did not. The authors suggested that the cause of this was a higher nutrient content further away from the beech stem and that hence beech was more successful at colonising such patches than oak. Oak in contrast displayed a much higher coarse root (< 5 mm) biomass and deeper rooting than beech (Leuschner et al. 2001b). These findings agree with the general rooting patterns: *F. sylvatica* is known for intensive, more shallow rooting whereas sessile (and pedunculate) oak roots only extensively colonise the soil but are capable of penetrating clay layers and skeleton-rich, stony soils, and root deeper than beech (Köstler et al. 1968, Polomski and Kuhn 1998). Because of these traits oak is fostered by the regional forestry administration on sites with near-surface clay layers as present in the Heldburg layers of the Lower Burgsandstein in the Steigerwald (Sperber and Regehr 1983, Oberforstdirektion Oberfranken 1999). On such sites hornbeam (*Carpinus betulus*), European silver fir (*Abies alba*) and Scots pine (*Pinus sylvestris*), all known to root deeply as well (Köstler et al. 1968), are also promoted by the forestry administration (Oberforstdirektion Oberfranken 1999). Schmid (2002) observed that the fine root biomass of beech was larger in mixed stands with spruce than in pure beech stands, another indication of beech as a superior below-ground competitor. Thus beech seems to be the more successful below-ground competitor as well, as long as soil water supply does not become a limiting factor.

Against the background of the competitive superiority of beech under mesic and moderate drought conditions and the higher drought tolerance of oak under more severe and prolonged drought conditions, as summarised above, the differentially reduced response of  $E_c$  of both beech and oak to D at Steinkreuz and Großebene during progression drought (see above) could be explained as follows. At Steinkreuz, beech dominates the canopy and probably also the soil; oak is under strong competition from beech. Consequently the relative reduction of  $E_c$  in oak was large compared to that of oak at Großebene in August. The larger drought tolerance of oak, however, kept the reduction of  $E_c$  in oak comparable to that in beech in August. In September,

under deteriorated conditions of soil water supply, beech reduced its water use more strongly than oak, but  $E_c$  in oak also declined compared to August.

At Großebe in contrast, oak dominates the upper canopy. Here the soil is not as deep as at Steinkreuz, and clay bands in the Heldburg layers of the Lower Burgsandstein are found near the surface (cf. Tab. 3.3.1). Oak is very likely to have penetrated these layers (see above) and accessed deeper water resources whereas beech is not. At Steinkreuz these clay layers are mostly found deeper in the soil than at Großebe (cf. Tab. 3.3.1). Thus at Großebe the dominating oaks may be assumed to first use the soil water stored in the upper layers where beech competes with oak, but given the earlier stomatal regulation (i.e. stomata closure) of beech (see above), oak may continue to exploit more water from the upper soil layers and deteriorate the situation for beech, while probably also having access to water from deeper soil layers. Under certain circumstances the hydraulic redistribution (Caldwell et al. 1998, Ryel et al. 2002) of water from moister deep to drier shallow soil layers may reduce this advantage for oak though. Nevertheless in August  $E_c$  in oak was only reduced half as much as  $E_c$  in beech (beech being mostly confined to intermediate canopy positions), and was also slightly less reduced than  $E_c$  in beech at Steinkreuz (due to the larger drought tolerance of oak). In September the reduction of  $E_c$  of oak in response to D reached values slightly lower than at Steinkreuz; the reduction in the inferior beech again was much more drastic. It may be argued that soil water reserves were smaller than at Steinkreuz due to smaller soil depth at Großebe and that the store in the soil layers below the clay pan may be rather limited, too, given the stand's rather level location on a ridge. On the other hand, the available water may have been depleted earlier at Großebe because of the unrestricted use by oak, whereas at Steinkreuz in this sense beech may have saved water for oak due to the reduction of stomatal conductance in beech at soil water potentials which leave the stomatal conductance of oak largely unchanged (see above). Lower values of  $g_{c \max}/LAI$  in beech than in oak may relate to this.

Years with severe drought, that lead to reduced growth rates in beech and to none or only to a lesser extent in oak have however occurred too seldom in the past at the investigated site Steinkreuz to reduce the competitive superiority of beech. The frequency of such critical drought events, however, may increase in the near future (e.g. Schär et al. 2004, Davi et al. 2006). Additionally, oak has to cope with periodical defoliation by caterpillars of *Tortrix viridana* (see Chap. 6.3.2). As a consequence, beech at Steinkreuz clearly has outcompeted oak and at the current stage of competitive advantage and the crown dominance of beech (the tallest beech trees are up to 5 m higher than tallest oaks, cf. Tab. 3.3.2, Fig. 5.1.2.3), drought periods very likely will not be sufficient to re-establish an equal competition state between the two species. Forest management practice in this part of the Steigerwald originally aimed at growing oak in competition with beech to foster the development of long branchless, commercially valuable trunks. In this stand though oak probably was not protected enough from the superior beech and will remain confined to the lower strata of the upper canopy without human intervention.

Lemée (1987) investigated the stand dynamics in an unmanaged temperate old-growth forest at Fontainebleau, France, that had been dominated by sessile oak up to the end of the Middle Ages, but at the time of the investigation was dominated by beech. Beech was able to successfully regenerate under oak crowns and the mortality rate of seedlings and saplings was lower than that of sessile oak. Only once

during a period of 150 years were oak seedlings and saplings able to conquer forest gaps (Lemée 1987) and stem numbers of oak decreased from 124 in the year 1903 to 47 in 1992 (Lemée et al. 1992). So as the mortality rate of fertile oak trees greatly exceeded the rate of recruitment, even though oak is longer-lived than beech, the species declined rapidly in abundance (Lemée 1987). In the same forest reserve Koop and Hilgen (1987) found oak trees which had survived competition with beech only in less competitive stands.

White oak (*Q. alba*) in the eastern US seems to be undergoing similar dramatic decreases in its contribution to forest cover (Abrams 2003) as *Q. petraea* and *Q. robur* in the forest of Fontainebleau (see above) and as can be concluded from findings of Leuschner et al. (2001a) and this study. Abrams (2003) summarised that an altered disturbance regime – in fact reduced low-intensity disturbance –, including fire suppression, have prevented the successful seedling recruitment of *Q. alba* and thus more shade tolerant, late-successional species like *Q. rubra* and *F. grandifolia* currently dominate temperate forests in the eastern US. It emerged from the studies in Europe (see above) that oak, under favourable soil conditions, is outcompeted by beech in the long run if historical levels of disturbance (fire, storms, felling, livestock browsing) are not met any more.

Overall, oak appeared less competitive, possibly due to changed boundary conditions such as increased atmospheric nitrogen deposition, than suggested by earlier qualitative assumptions, which have been questioned and adapted in recent years as recapitulated below:

Hofmann (1968) used Ellenberg's (1963, 1996) climate index (= mean temperature of the warmest month / annual sum of precipitation \*1000) to differentiate potential habitats or ranges of forest types in Lower Franconia and adjacent regions. In his study, Hofmann (1968) classified the northern and central Steigerwald as a beech-dominated sub-region of an oak-beech-hornbeam-area (climate index = 21–25). The site of the present study is located in the central Steigerwald in this sense. The average temperature in July at Ebrach is 16.7 °C, the average annual precipitation 808 mm (1962–1990; DWD 1999), resulting in a climate index of 21. Areas with a climate index between 20 and 15 are classified as beech-(oak)-areas (Hofmann 1968), where beech is naturally dominant, accompanied by oak, the latter perhaps (Hofmann 1968) or probably (Weiß 1985) being over-represented due to human activities. Ellenberg (1996) stated that in the whole area where the climate index is between 21 and 30 and where beech is naturally dominating, it was easy to foster oak abundance by more frequent logging of beech. The local forestry administration also considers the abundance of oak to be a result of early economic interest in this species (Oberforstdirektion Oberfranken 1999). Regions more dominated by oak are related to climate indices between 26 and 30, like the southern Steigerwald and the low-lying plateau west of the Steigerwald (Hofmann 1968, Ellenberg 1996). Ellenberg (1996) suggested that 600 mm annual precipitation and a mean temperature of the warmest month of 18–20 °C (i.e. climate index > 30) are critical xeric limits of beech survival.

In contrast, Freist-Dorr (1992a,b) found a higher competitive strength of beech in experimental mixed beech-oak stands in north-western Bavaria, areas with high climate indices of around 26–28. And Felbermeier (1993, 1994) concluded from a model exercise, using a large number of inventory data of the forestry administration from all over Bavaria, that beech is most productive in the dry-warm areas of Bavaria with (long-term mean) annual precipitation as low as 475 mm, such as the Franconian "Gäulandschaft" west of the Steigerwald, and that the growth potential of beech on such sites had been underestimated previously. No significant correlation between tree height and climate index was observed (Felbermeier 1993). Palynological findings (Huntley et al. 1989) support a beech optimum in climates warmer than that (currently) found in Bavaria. The present maximum pollen density of *F. sylvatica* is found in southeastern Europe (Huntley and Birks 1983) which coincides with a mean January temperature of -1 °C and mean July temperature of 18 °C (Huntley et al. 1989). Peters (1992) held that beech could potentially dominate in future Central Europe under increased temperatures if humidity also increases, as concluded from findings from closely related *Fagus*-species in warm and

humid Florida, Mexico and China. And Peters (1997) listed 470 mm of average annual precipitation as the lower boundary of current *F. sylvatica*-distribution.

Nüßlein (1995) reported on mixed stands of *Fagus sylvatica*-*Acer pseudoplatanus*, *F. sylvatica*-*A. platanoides* and *F. sylvatica*-*Fraxinus excelsior* in northernmost Bavaria, where beech outgrew the other hardwoods at the age of ca. 65 years, after initially higher growth rates of these other hardwoods. He attributed this to the higher shade tolerance of beech and its tolerance to trees growing towards it, and with a large crown growth plasticity and a high potential for space occupation (Nüßlein 1995). Roloff (1986) in turn explained the high plasticity of the beech crown and beech's potential to capture canopy space by its many modes of reiteration and especially its ability to produce short shoots under less favourable and long shoots under more favourable conditions. Oak may achieve only a moderate crown plasticity compared to beech by means of lammas shoot production and cladoprosis (Roloff and Klugmann 1998). Leuschner (1994, 2001) also analysed the crown occupation strategy of beech and compared it to that of oak. He could show that the costs for crown space occupation regarding leaf dry matter and leaf nitrogen were lower in European beech than in sessile oak (Leuschner 2001, p 557f) and that beech is able to produce a deeper shade than oak at lower investments of magnesium, nitrogen and carbon (Leuschner 2001, p. 558ff; see also Hagemeier 2002). And this is mainly because the shade canopy of beech has horizontally oriented leaves organised in a so-called monolayer (Leuschner 2001, p 559) with lower leaf mass per area (LMA) or higher SLA than oak (Leuschner 1994, pp 97, 200, 324; Hagemeier 2002). Similarly, Pretzsch (2006) concluded from detailed allometric analyses of forest inventory data from monospecific stands that beech invests relatively little in biomass compared to oak and Norway spruce, but that the invested biomass is used more efficiently to occupy additional canopy space than by the other species. A certain diameter increment was coupled in beech with rather low biomass increase yet with the highest increase in growing space of the studied species. The opposite was found for oak, which achieved little lateral growing space extension despite a relatively high biomass investment (Pretzsch 2006). Stickan et al. (1991) traced the very wide ecological amplitude of *F. sylvatica* (Ellenberg 1996) to the capability of differentiating sun and shade leaves within one year, as was shown by Eschrich et al. (1989).

Leuschner (1997, 1998) summarised the underestimation of beech's ecological amplitude, based on published and his own phytosociological, soil chemical and root distribution data (see also Leuschner 1993, Büttner and Leuschner 1994, Coners et al. 1998, Leuschner et al. 2001b and above). He gave examples of beech stands in the central German arid zone („Mitteldeutsches Trockengebiet“) where, under favourable soil conditions, annual precipitation is 450–480 mm (Leuschner 1998), and he narrowed down the limits of beech survival in Central Europe to edaphically caused drought (Leuschner 1997, 1998), as Firbas (1949, p 243) had already implied. This underlines the fact that bulk precipitation is only a proxy for plant available soil water and actual measurements of plant available water could yield a more precise picture of the limits of beech. Firbas (1949: pp 243–244, p 357; 1952: pp 99, 236) based on his own and older works, already indicated a possibly underestimated potential of beech in drier areas of its distributional range before the beginning of major human influence on land cover, but he was lacking more detailed information, especially on annual precipitation. He (Firbas 1949, p 244) even questioned the climatic limitation of beech in Central Europe altogether and cited Zeidler (1939, in Firbas 1949, p 243) for explaining that in the dry zone of Lower Franconia (= Franconian “Gäulandschaft”, west of the Steigerwald, see above), beech-rich forests were once thriving on soils that were later converted into fields. Firbas (1949, p 243) cited another older work where beech was reported to thrive in an area with less than 500 mm precipitation in western Poland. Bonn (2000) studied radial growth in mixed stands of beech and oak (*Q. robur*, *Q. petraea*) under a range of climatic and soil conditions in central Germany and found a larger sensitivity of growth to environmental influences in beech compared to oak: beech responded to drought with a larger reduction in radial growth than oak, but under beneficial conditions with a larger radial growth than oak. And beech was superior to oak in growth at all investigated sites in the long term, including dry sites with climate indices > 30 (Bonn 2000). Similarly, in a dendroecological study of beech across Europe, Dittmar et al. (2003) observed a high growth potential and rather constant growth rates even on sites where growth was primarily limited by water availability; they also found a fast recovery of growth in the year after depressed growth, due to severe drought stress combined with masting, supporting the view of a rather large resistance of beech to (moderate) drought stress.

The Bavarian forestry administration also acknowledged the accumulating information on the superior competitiveness of beech in its latest map of the regional natural forest composition (based on the current habitat potential ("gegenwärtiges Standortpotential"); Walentoskwi et al. 2001). They stressed that growing conditions for beech have improved due to the continuous melioration of soils after over-exploitation in the past, reduction of deer browsing, and the atmospheric nitrogen fertilisation of the soils (Walentowski et al. 2001, Kölling and Walentowski 2001). If oak is to be sustained beside beech on sites such as Steinkreuz, repeated thinning of beech in the vicinity of oak is required (cf. Göpfert 1950, Sperber and Regehr 1983, Spiecker 1983, Pretzsch 2003).

Geßler et al. (2007) emphasised in their review of the potential risks for European beech in a changing climate that an increase of the frequency of drought could negatively affect growth and the competitive ability of adult beech trees. They emphasise a possibly reduced regeneration of beech seedlings under conditions of prolonged drought, enhanced by other understory species competing for water and nitrogen (Geßler et al. 2007). On the other hand Gallé and Feller (2007) showed that, despite the complete reduction of net photosynthesis and stomatal conductance during severe drought stress, young saplings of beech completely restored their photosynthetic capacity after re-watering, because of physiological and morphological adjustments, as these authors presumed. Thomas (2000) similarly observed a fast recovery of beech saplings upon cessation of drought stress. In the present study indications of a fast recovery of adult beech after (moderate) drought may be seen in the change of the sign of  $q_r$  (the contribution of  $J_s$  deep relative to  $J_s$  0–2 cm with increasing  $J_s$  0–2 cm, Fig. 5.3.12–13; see also Chap. 6.2.4): prior to soil water shortage (relative extractable soil water  $\theta_e > 0.4$ )  $q_r$  had been positive in large trees, then with progressing soil water depletion ( $\theta_e < 0.4$ )  $q_r$  turned negative, but after some intermittent rain changed to positive again for a short period before turning negative once more when  $\theta_e$  decreased again. On the basis of annual patterns of radial growth of mature beech, Dittmar et al. (2003) also observed the return to normal rates of increment the year after a severe growth reduction.

It is not possible in the field to examine the effect of (ideally) gradually changing stand structure on  $E_c$  without concomitantly varying environmental drivers in even a small number of stands (cf. Köstner et al. 2004). Hence comprehensive gas exchange models that incorporate the 3D-stand structure and microclimate are indispensable as analytical tools to further investigate structure-function relationships, based on empirical results such as those presented in this study and as e.g. shown in a preliminary modelling exercise by Köstner et al. (2004) for the mixed Steigerwald stands.

#### 6.4.4. Variation of $E_c$ of beech and oak across Central Europe

**Beech stands.** The range of  $E_c$  for beech forest stands in Central Europe is rather wide, spanning 164–443 mm season<sup>-1</sup> (Fig. 6.4.4.1, Tab. A.11.8), on average 283 mm season<sup>-1</sup> ( $\pm 64.7$  mm season<sup>-1</sup>,  $n = 75$ ) across 30 sites (including Farrenleite and the Steinkreuz-pure beech plot from this study), from lowland (50 m a.s.l.) to montane habitats (1165 m a.s.l.). Considering only one value of  $E_c$  per stand (i.e. averages where data for more than one growing season was available), the mean over all sites amounts to a slightly lower 277 mm season<sup>-1</sup> ( $\pm 58.1$  mm season<sup>-1</sup>, median = 267 mm season<sup>-1</sup>,  $n = 30$ ).

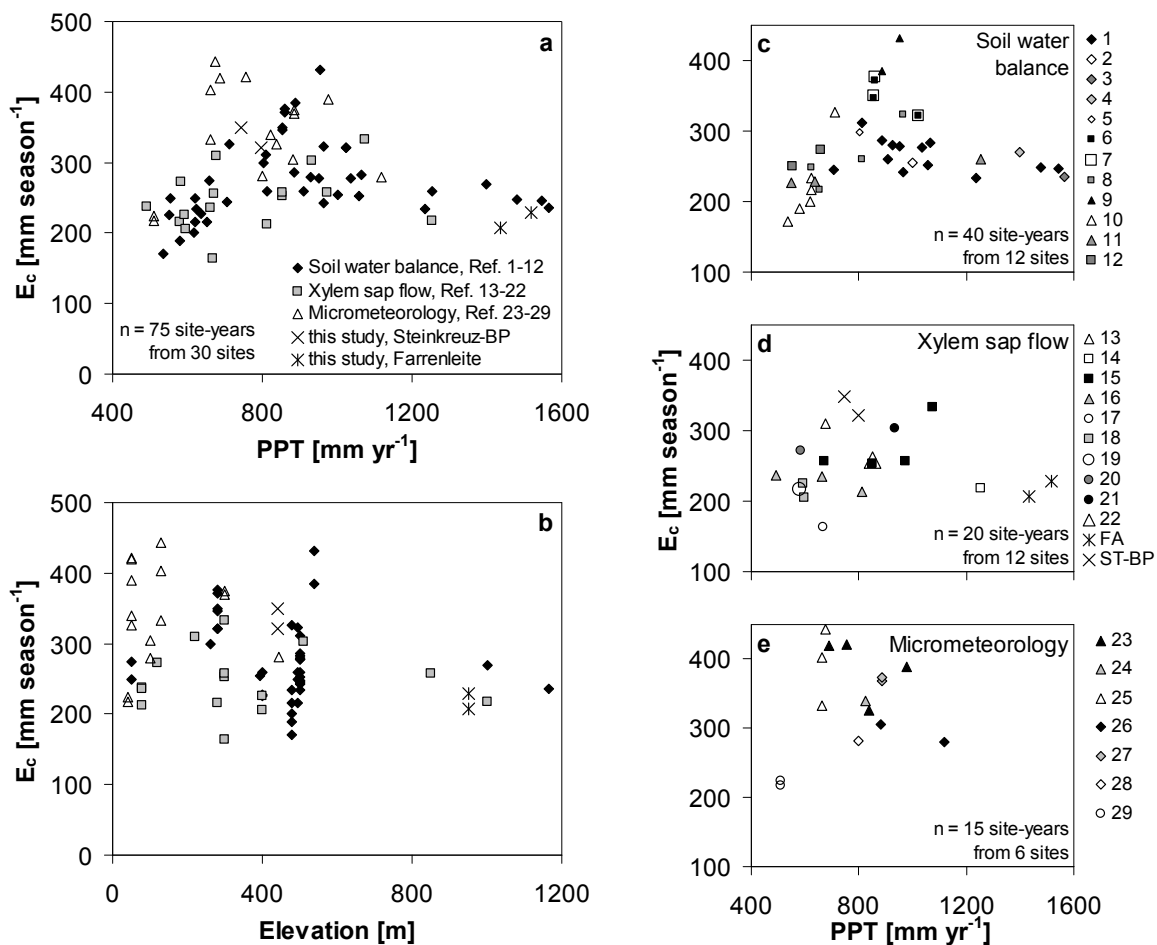


**Figure 6.4.4.1:** Seasonal rates of canopy transpiration  $E_c$  in closed stands and annual rates of precipitation PPT (a) and site elevation (a.s.l., b) for 30 pure forest stands of *Fagus sylvatica* from lowland to montane Central European forest stands (references 1–29, below; FA is Farrenleite in the Fichtelgebirge, ST-BP is the Steinkreuz-pure beech plot in the Steigerwald, both from this study). Estimates based on measurements of soil water balance (c), xylem sap flow (d), micrometeorological parameters (e), plus varying degrees of modelling. If several methods have been used, the presumably dominating one is indicated. Some studies reported values of evapotranspiration rather than  $E_c$  of the tree layer, and annual instead of seasonal rates. For a few sites, only long-term average annual PPT was available. Five stands were  $\leq 80$  yr-old, of which only one  $< 50$  yr-old (30 yr-old, Hesse in France: Granier et al. 2000a, 2003). Data from all available years from a site are included. Table A.11.8 summarises the information from the studies shown here. References are:

1 = Benecke (1984), Salihi (1984); 2 = Cheusson (2004); 3, 4 = Heil (1996); 5 = Brechtel and Balázs (1988); 6, 7 = Ernstberger (1985); 8 = Fleck (1986); 9 = Rothe (1997); 10 = Tuzinsky (1987); 11 = Gerke (1987); 12 = Müller (2001), Bolte et al. (2001); 13 = Lang (1999); 14 = Granier et al. (2000a); 15 = Granier et al. (2000a, 2003); 16 = Jochheim et al. (2007); 17 = Koch (2002, in Schipka 2003); 18 = Schipka (2003), Schipka et al. (2005); 19–21 = Schipka et al. (2005); 22 = Střelcová et al. (2002, 2006); 23 = Herbst et al. (1999); 24 = Herbst and Hörmann (1998); 25 = Roberts and Rosier (1994); 26 = Roberts and Rosier (2005a), Roberts et al. (2005); 27–29 = Owen et al. (2007).

The data set presented in Figure 6.4.4.1 contains stand level estimates derived from xylem sap flow, micrometeorological and soil water balance methods (*sensu lato*, including catchment water balance and local soil water balance) and modelling approaches in connection with one of the aforementioned methods. Several of the studies of soil water balance did not distinguish between tree and herb/shrub layer transpiration, between transpiration and evapotranspiration (ET) or included the non-foliated period (“annual” instead of “growing seasonal” rates). This was also the case for most micrometeorological studies. Since all listed sites were closed beech forest stands, the contribution of the understory could be negligible. ET during winter may reach 4–5 % of growing season ET (Gerke 1987), 4–8 % (Benecke and van der Ploeg 1978, Benecke 1984), 6–10 % (Salihi 1984) or even 16–17 % (Heil 1996). This may at least in part explain the relatively high values of  $E_c$  gained from these methods. In general the use of different methods with different levels of spatial and temporal integration can be expected to introduce additional variation. Apart from these methodological issues, the large variability seen in Figure 6.4.4.1 is also due to differences in edaphic site conditions, in meteorological conditions (including altitudinal trends), in phenology and in stand structure. Since additional information provided in the literature together with the estimates of  $E_c$  (e.g. meteorological, structural variables) varied widely in quality and quantity, a meticulous analysis of this data set is not intended here.

The highest  $E_c$  observed at a given annual precipitation (PPT) increased with PPT up to about 650–950 mm yr<sup>-1</sup> where  $E_c$  reached maxima > 400 mm season<sup>-1</sup> (Fig. 6.4.4.1.a). At even higher PPT the values of  $E_c$  decreased. This pattern was evident in data based on any of the three methodologies distinguished. In a recent review, Schipka et al. (2005) similarly observed a “hump-backed” shape of the precipitation-transpiration relationship; their assessment was based on just 25 observations from 7 colline to sub-montane stands, which are included in Figure 6.4.4.1a. Schipka et al. (2005) hypothesised that  $E_c$  would be limited if PPT was < 700 mm yr<sup>-1</sup> due to eventual soil water shortage in summer and if PPT was > 1000 mm yr<sup>-1</sup> due to presumably more abundant cloud cover and hence reduced incident solar radiation and/or lower vapour pressure of the air (D), plus more frequent and longer duration of leaf wetness. Support for this interpretation comes from Dittmar and Elling (1999) and Dittmar et al. (2003) who found radial growth of beech across Central Europe to decrease with decreasing precipitation and higher temperatures at lower altitudes (330–600 m a.s.l.) and to increase with temperature and radiation at higher altitudes (750–1350 m a.s.l.). Thus plotting  $E_c$  vs elevation revealed a negative trend of the highest rates of  $E_c$  with elevation (Fig. 6.4.4.1.b), because concurrently with altitude, the length of the foliated period,  $T_{air}$ , D, PPT and – often – PFD decrease (cf. Chap. 5.2). Dittmar and Elling (1999) and Dittmar et al. (2003) stressed that at the higher elevation sites studied, including the Farrenleite stand in the Fichtelgebirge, temperatures and radiation were limiting growth most of the years, and that late frosts (beech being very sensitive to late frosts, e.g. Ellenberg 1996) and cold, moist conditions were responsible for narrow growth rings. (Data from Rothe (1997, reference 9 in Fig. 6.4.4.1.c; soil water balance + model) deviated somewhat from this, likely caused by the combination of both annual integration and inclusion of soil ET, see above.) The scatter of  $E_c$  at a given elevation (and at a given PPT) hints at the large influence of atmospheric, phenological, edaphic and structural factors and their interannual variability.

In longer-term studies the encountered interannual variability of  $E_c$ , expressed in the coefficient of variation (CV), spanned 5.8–24.7 % (on average 10.1 %, n = 15, including two-year studies). When expressed as maximum deviation from the minimum estimate of  $E_c$ , the interannual variability reached 8.7–91 % (average 25 %). The annual precipitation showed a CV of 0.2–47 % (average 14.7 %; maximum deviation from the minimum PPT: 0.3–128 %, average 40 %). In comparison, the CV of LAI ranged between 2 % and 17 % (1–33 % from year to year), available at the four sites out of the 17 sites for which two or more years of data for  $E_c$  were available (including the Steinkreuz-pure beech plot and Farrenleite; Chap. 6.1). Based on the larger range of PPT (and of its CV) compared to  $E_c$ , the transpiration of beech could be described as a fairly conservative process (cf. Roberts 1983, 2007), or more specifically, as a process under rather tight ecophysiological control, concluded also by Schipka et al. (2005). Roberts' (1983) hypothesis that forest transpiration in Central Europe was generally similar irrespective of species, however, has been demonstrated to fall too short (Köstner 2001), which can also be acknowledged from Figure 6.4.4.1.

Precipitation in Figure 6.4.4.1a, c–e is only used as a proxy for atmospheric conditions and soil water supply, because the majority of studies lack other relevant environmental data. Scrutinising relationships of  $E_c$  with its drivers and constrictors, both atmospheric and structural, as done for the stands investigated in this study (e.g. Fig. 5.5.5, Fig. 5.5.17), would be necessary next steps to extract general functions for the transpiration of beech across European regions.

***Mixed stands of beech and oak.*** The canopy transpiration estimated for mixed forest stands of European beech and oak (*Q. petraea/Q. robur*; not necessary beech-oak mixtures) ranges from 149 mm season<sup>-1</sup> to 331 mm season<sup>-1</sup> across 16 observations from 8 sites, including Steinkreuz and Großebene from this study (Fig. 6.4.4.2a, b). The average  $E_c$  over all site-years was 233 ( $\pm 56.3$ ) mm season<sup>-1</sup>. The mean of all site-specific averages was 227 ( $\pm 55.9$ ) mm season<sup>-1</sup>, spanning 156–310 mm season<sup>-1</sup> (n = 8 sites); site elevation was 95–520 m a.s.l. At most sites, beech was dominant in the species distribution, only the stand studied by Vincke et al. (2005a, b) was oak-dominated.

Cermák et al. (2001) reported on stand level estimates of  $E_c$  for a Czech floodplain forest dominated by *Q. robur* (75 % of A<sub>b</sub>) with admixed *Fraxinus excelsior* (17 %) and *Tilia cordata* (7 %) under the variable influence of groundwater.  $E_c$  ranged from 210–454 mm season<sup>-1</sup> (average 300  $\pm$  98.9 mm season<sup>-1</sup>), measured during eight years between 1972 and 1996. However, apart from the hydrological management that dramatically changed over the years (prevention of regular flooding after the first year, with a later reintroduction of flooding), the sampling differed considerably from year to year (number of trees, number of species). It is not clear how and to what extent sap flux in *F. excelsior* and *T. cordata* was represented in stand level  $E_c$ . Including these data would result in a mean site-specific average  $E_c$  of 235 ( $\pm 57.6$ ) mm season<sup>-1</sup>.

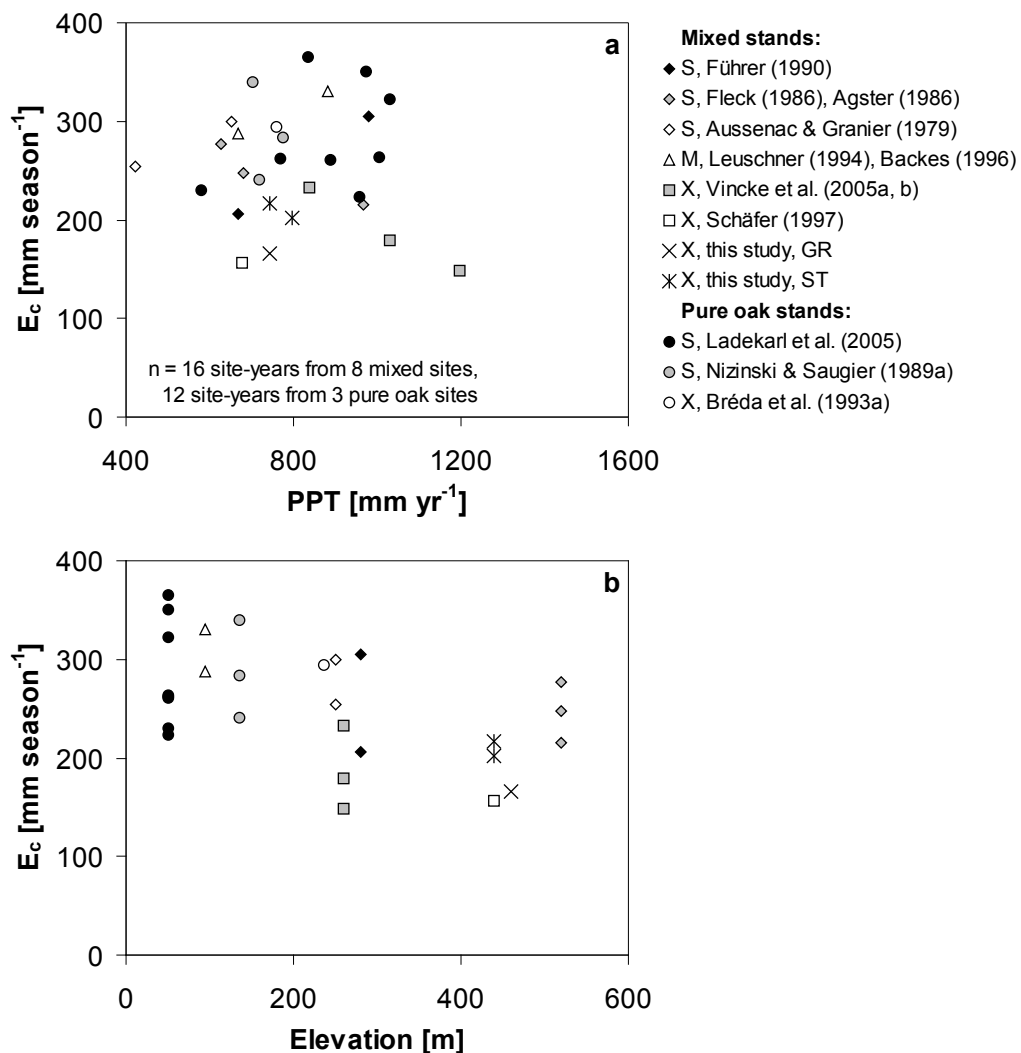


**Figure 6.4.4.2** Seasonal rates of canopy transpiration  $E_c$  of closed stands and annual rates of precipitation PPT (a) and site elevation (a.s.l., b) for 8 mixed forest stands of *Fagus sylvatica* and/or *Quercus* and for 3 pure oak stands from lowland to colline/sub-montane Central European forest stands. ST = Steinkreuz, GR = Groß-ebene both from this study. Estimates predominantly based on measurements of soil water balance (S), xylem sap flow (X), micrometeorological parameters (M), plus varying degrees of modelling. See also the caption of Figure 6.4.4.1. The seasonal estimate by Bréda et al. (1993a) is for 127 days only, lacking probably about 40 days of the growing period; precipitation is the long-term mean here. Data from all available years from a site are included.

Included in Figure 6.4.4.2 are also three Central European pure oak stands, reaching 224–365 mm season $^{-1}$  (mean  $287 \pm 48.1$  mm season $^{-1}$ , n = 12 observations). Rates of  $E_c$  from the Steigerwald mixed stands (this study and Schäfer 1997) were among the smallest. During the season monitored by Schäfer (1997) oaks were partially defoliated by caterpillars. Data from four other pure oak sites (250–434 mm season $^{-1}$ ), for which no precipitation data were available, increased the average (considering site averages only) to 307 ( $\pm 24.8$ ) mm season $^{-1}$  (n = 7 sites). The range of  $E_c$  for mixed beech/oak stands and pure oak stands is somewhat smaller than for beech stands, and so is the range of PPT and elevations. In some stands the interannual

variability of  $E_c$  is larger than that of PPT; speculation thereupon, however, that oak was less “conservative” in controlling  $E_c$  is lacking a substantial experimental foundation.

The assessment of interannual variability of the magnitude of processes such as  $E_c$ , net ecosystem exchange of CO<sub>2</sub> (NEE) or gross primary productivity (GPP) requires long-term studies, which increase the range of observed climate conditions and extremes as outlined by Ma et al. (2007). Multi-year data sets allow the singling out and quantifying of the contributions of environmental and structural drivers, of biotic responses to the environmental forcing (including lag or carry-over effects due to singular or repeated drought, defoliation, storm break etc. or combinations of such disturbances and subsequent recovery) or of (forest) succession, with the help of models as analytical tools (e.g. Baldocchi and Meyers 1998, Barford et al. 2001, Wilson et al. 2001, Baldocchi et al. 2002, Richardson et al. 2007). For instance, the interannual variability in NEE at a temperate deciduous forest site was attributed to a combination of factors including the occurrence of a summer drought, the extent of summer cloudiness and the absence or presence of winter snow, whereas for a boreal deciduous site it corresponded to variations in LAI and summer drought, as summarised by Ma et al. (2007). More longer-term studies would also be needed to assess the importance of LAI (cf. Bréda and Granier 1996) and  $A_s$ , as the main structural drivers, and of environmental drivers in the interannual variability of  $E_c$ .

An increasing number of studies on stand water use report meteorological conditions and at least some structural properties of the stands, but still a considerable number of works being published at present give scarce information particularly on stand structure, so that the restrictions limiting the generalisation of such results as stressed by Peck and Mayer (1996), continue to be valid (cf. Owen et al. 2007). The existing and currently still expanding networks of tower sites that use micrometeorological eddy covariance methods to measure the exchanges of CO<sub>2</sub>, water vapour, and energy between terrestrial ecosystems and the atmosphere across a wide range of vegetation and land use types on all continents (organised under the umbrella of “FLUXNET”, see FLUXNET 2007) hold the promise of overcoming such limitations (cf. Tenhunen et al. 1998, but see Owen et al. 2007). Recent examinations of latent heat flux at such sites that consider structural idiosyncrasies within the tower footprints suggest that careful analyses may in the future provide potentials for reliable generalisations on vegetation water use (Falge and Foken, unpublished). Additionally, the need for accompanying ecophysiological measurements (e.g. sap flow, understory evapotranspiration) and ancillary data (such as LAI and basal area distribution, collected following a common protocol) to help the biological interpretation of fluxes and as a prerequisite for successful inter-site comparison is widely acknowledged (Baldocchi 2003). Examples of such integrating efforts across ecosystem types and continents have been published e.g. by Falge et al. (2002a, b), Law et al. (2002), Luyssaert et al. (2007) and Owen et al. (2007). Regarding water use in European beech, a first tentative synthesis was limited to few sites and years of data (Granier et al. 2003).

## 7 Conclusions

### 7.1. Review of hypotheses

This study has used xylem sap flow methodology concurrently on the largest number of beech (*Fagus* species) trees over a whole growing season that is documented in the literature. In the year 1998, 12 trees were monitored in two plots (Steinkreuz, Große Ebene), in the year 2000 25 trees in three plots (Steinkreuz, Steinkreuz-pure beech plot, Farrenleite) and in 1999 34 trees (all four plots). Adding the oak trees monitored, the total number of trees assessed was 24 in 1998, 35 in 2000 and 53 in 1999. The overall number of measuring points (i.e. one depth in one tree or one sap flow sensor per growing season, excluding sensors which had to be replaced during the course of a season) was 167 in beech and 41 in oak, adding to a total of 208 "sensor-seasons". Malfunction of sensors and loss of data due to power failure reduced the number of measuring points actually evaluated. Data from 142 measuring points assessed in beech trees over the three years were evaluated for the radial profiles of  $J_s$ , thus the average number of probes per tree (in different radial depths) was 2.9 for 49 evaluated "tree-seasons". For the upscaling from tree to stand, data from 25 beech trees were used in 1999 (four plots) and 19 in the year 2000 (three plots), for oak, data from 13 trees were included in 1999 and 7 in the year 2000.

The following general conclusions can be drawn with regard to the hypotheses formulated in Chapter 2.4:

Hypothesis: The axial xylem sap flow density  $J_s$  of beech declines radially towards the sapwood-ripenwood boundary.

Axial xylem sap flow density  $J_s$ , measured in 0–2 cm ( $J_{s\ 0-2cm}$ ), 2–4 cm ( $J_{s\ 2-4cm}$ ) and 4–6 cm ( $J_{s\ 4-6cm}$ ) sapwood depth radially inside from the cambium, declined with depth in *Fagus sylvatica* growing in mixed stands in the Steigerwald (Steinkreuz, Große Ebene), in a pure beech stand in the Fichtelgebirge (Farrenleite) and in a plot of pure beech inside a mixed stand in the Steigerwald (Steinkreuz-pure beech plot; Fig. 5.3.1, Fig. 5.3.4).  $J_s$  was highest in outer, youngest sapwood and smallest in inner, older sapwood, on half-hourly to seasonal scales (Fig. 5.3.1–6). The radial decrease of  $J_s$  across the 6 cm assessed was steeper in small trees with a narrow sapwood radius than in larger trees with a wider sapwood radius.

Hypothesis: A relationship between tree diameter and  $J_s$  exists in beech and oak.

In beech,  $J_s$  in any sapwood depth increased with DBH (diameter at breast height; Fig. 5.3.5–6). At the denser stand Farrenleite in the Fichtelgebirge, higher competition may be responsible for a less tight relationship between  $J_s$  and tree dimensions (Fig. 5.3.6). In *Quercus petraea* no significant correlation of  $J_s$  with DBH could be observed in seasonally averaged daily  $J_s$  (Fig. 5.3.7; rainy days not considered). Maximum daily  $J_s$  in contrast was correlated with DBH in oaks at Große Ebene (Fig. 5.5.1).  $J_{s\ 0-2cm}$  at a given DBH was of the same order of magnitude in beech and oak (Fig. 5.3.5–7).

Hypothesis: A general relationship of the decrease of  $J_s$  with radial sapwood depth can be described for trees of different size when normalising both the probed sapwood radius with total sapwood radius and  $J_s$  with  $J_s$  0-2cm.

The sapwood area of a tree ( $A_{st}$ ) was correlated with DBH in both species studied, and trees from the different stands showed similar  $A_{st}$ -DBH relationships (Fig. 5.1.1.4, Tab. 5.1.1.1). Thus, when the depth of sap flow sensor insertion in the sapwood was normalised with total sapwood radius from the cambium to the sapwood-ripenwood boundary in order to account for the different diameters of the probed beech trees, then the radial decrease of  $J_s$ , expressed in relative terms as  $J_s$  2-4cm/ $J_s$  0-2cm and  $J_s$  4-6cm/ $J_s$  0-2cm, respectively, could be described by a linear regression function for all beech trees of various sizes from all sites (Fig. 5.3.4c, d).

Plots of  $J_s$  2-4cm/ $J_s$  0-2cm and  $J_s$  4-6cm/ $J_s$  0-2cm, averaged over longer periods of time, versus relative sapwood depth as presented in Figure 5.3.4 seem promising as a way to generalise radial patterns of  $J_s$  in beech of different size and from different (closed) stands. Support for this view comes from a comparison of published radial trends in beech with those presented in this study (Chap. 6.2.1). This comparison was done on an absolute scale of sapwood depth, however, since total sapwood depth was not detailed in these publications. Nevertheless trees with similar DBH revealed comparable patterns of radial decline of  $J_s$ . Such a convergence of behaviour seems all the more likely given the similarity of sapwood area–basal area relationships across several European beech stands (Chap. 6.1, Fig. A11).

Hypothesis: Beech trees growing at higher elevation are comparable to trees from lower elevations in their capacity of  $J_s$  (similar maximum  $J_s$ ).

Maximum daily  $J_s$  0-2cm in beech trees at the dense, high-elevation site Farrenleite was comparable to that of beech from the pure beech plot at low elevation (Tab. 5.3.1–2), pointing at a similar capacity of water transport in beech at different elevations. This capacity, however, was put to use on fewer days (only ca. half as often) at Farrenleite than at Steinkreuz (Chap. 5.3).

Hypothesis: Large overstory beech trees, due to their large sapwood area, differ from smaller sub-canopy trees in their ability to respond to increased transpirational water demand in the crown (increasing proportion of  $J_s$  in deeper sapwood).

Dominant beech trees with a large sapwood area seemed to be able to respond more dynamically to increased water demand in the canopy (as expressed in increasing  $J_s$  0-2cm) in that  $J_s$  deep could increase relative to  $J_s$  0-2cm with increasing  $J_s$  0-2cm, especially when relative extractable soil water  $\theta_e$  (in 0.20 m and 0.35 m soil depth) was  $> 0.4$ . In contrast, in smaller trees  $J_s$  deep decreased relative to  $J_s$  0-2cm with increasing  $J_s$  0-2cm, even under high soil water availability (Fig. 5.3.12). Thus, the deep sapwood, particularly that of large dominant trees, appears to be a flexible component of the hydro-system of beech that can be activated when needed.

Hypothesis: The radial pattern of  $J_s$  changes seasonally with progressive soil water deficit in that the water conducting radius decreases.

During progressive soil drought as experienced at the sites in the Steigerwald in one of the years of the study, indications for changes in the functionality of the hydraulic system of beech trees were found: when  $\theta_e$  dropped below 0.4 in 0.20 m and 0.35 m soil depth, the contribution of  $J_{s\ 2-4cm}$  and  $J_{s\ 4-6cm}$  relative to  $J_{s\ 0-2cm}$  decreased with increasing transpirational demand (expressed by increasing  $J_{s\ 0-2cm}$ ), most pronounced in suppressed, but also noticeably in dominant trees (Fig. 5.3.10–13).

Hypothesis: Whole tree water use  $Q_t$  is related to scalars of tree size, in both beech and oak, and across stands.

The seasonal maximum daily whole-tree water use  $Q_{t\ max}$  of beech from all sites scaled positively (non-linearly) with DBH (and related scalars,  $R^2 = 0.70–0.97$ ; Fig. 5.4.2–3), since both  $J_s$  and sapwood area  $A_{st}$  were positively correlated with DBH.  $Q_{t\ max}$  ranged between 11 kg d<sup>-1</sup> and 435 kg d<sup>-1</sup> for beech trees with a DBH of 14–63 cm in the stand with the widest range of stem diameters. Values of  $Q_{t\ max}$  for beech compiled from the literature generally followed the same relationship of  $Q_{t\ max}$  with DBH as established for the stands in the Steigerwald and the Fichtelgebirge (Fig. 6.3.1.1).

$Q_{t\ max}$  of oak trees from the mixed Steigerwald stands was lower than that of beech trees with the same DBH, reaching 20–62 kg d<sup>-1</sup> for trees with a DBH of 29–49 cm. The correlation of  $Q_{t\ max}$  with DBH and other scalars was weak in the oaks studied (Fig. 5.4.2–3) and also in the few other relevant reports (Fig. 6.3.2.1). Possible reasons for the unexplained between-tree variation in oak include, apart from methodological uncertainties, irregular radial growth and sapwood anatomy, reduced vigour due to defoliation by insects (and infestation with *Phytophthora* species?), low shade tolerance and in general its inferior competitiveness in mixed stands with beech.

Hypothesis: Whole tree water per unit leaf area  $Q_t/A_{lt}$  decreases with increasing tree height, in both beech and oak.

Maximum tree water use per unit leaf area  $Q_{t\ max}/A_{lt}$  increased in beech with tree height  $h_t$  (Fig. 5.4.3), indicating a high capacity for transpiration in beech even in large crowns, contrary to expectations. Shade-adapted sub-canopy trees transpired less per unit leaf area and required less sapwood area while large overstory trees transpired more water and maintained a larger sapwood area as evident from the considerable decline of the leaf area–sapwood area relationship ( $A_{lt}/A_{st}$ ) with  $h_t$  (Fig. 5.1.3.3).

In oak much smaller values of  $Q_{t\ max}/A_{lt}$  and an opposite trend with increasing  $h_t$  was found (Fig. 5.4.3). This points to a less shade-adapted lower crown and to increased self-shading with increasing leaf area in oak, in part due to a higher leaf area density of oak compared to beech caused by shorter crowns and smaller ground-projected crown area  $A_{cp}$  at the same  $A_{lt}$  (Fig. 5.1.2.3, Fig. 5.1.3.2). Reduced vigour and irregular sapwood may be sources of the higher unexplained between-tree variation in the relationship of  $Q_{t\ max}/A_{lt}$  and  $h_t$  compared to beech.

Hypothesis: Beech trees of similar size from higher and lower elevation reach similar values of  $Q_t$ .

Beech trees with comparable DBH achieved similar rates of  $Q_{t\ max}$  at both the high and low elevation sites (Fig. 5.4.2–3). Hence transpirational capacity was comparable for similarly sized beech trees from the two elevations, not only at the level of sap flow density (see above), but also at the whole-tree level of sap flux  $Q_t$ . For beech at the high-elevation site Farrenleite, however, no significant correlation of  $Q_{t\ max}$  with tree height  $h_t$  was found, perhaps due to stronger (intra-specific) competition (dense stand) and the stand being on a steeper slope compared to the low-elevation site Steinkreuz.

Hypothesis: Because of the inferior ability to occupy crown space, the higher self-shading and smaller shade tolerance of oak compared to beech, canopy transpiration  $E_c$  in mixed stands of oak and beech is smaller than  $E_c$  in pure beech stands.

At comparable leaf area index LAI or basal area  $A_b$ , the mixed stands in the Steigerwald had considerably lower maximum daily and lower seasonal rates of canopy transpiration  $E_c$  (Großebene 2.3 mm d<sup>-1</sup> and 166 mm season<sup>-1</sup>, Steinkreuz 2.6–2.7 mm d<sup>-1</sup> and 202–217 mm season<sup>-1</sup>, respectively) than the pure beech plot in the Steigerwald (4.2–4.4 mm d<sup>-1</sup> and 321–349 mm season<sup>-1</sup>, Fig. 5.5.4–8, Tab. 5.5.2–3, Tab. 6.4.1.1).

Hypothesis: The contribution of beech and oak to stand level  $E_c$  in mixed stands can be assessed via contributions of stand structural characteristics of these species to stand level totals; relationships of maximum daily  $E_c$  and scalars, such as leaf area index or basal area, exist.

Beech dominated  $E_c$  in both mixed stands, and  $A_s$  described this dominance better than  $A_b$  because of the different  $A_s$ – $A_b$  relationships of beech and oak (Fig. 5.1.1.4, Fig. 6.1.1): at Steinkreuz, beech contributed ca. 90 % to stand level seasonal  $E_c$  and 91 % to stand level  $A_s$ , but only 69 % to  $A_b$ ; at Großebene 58 %, 74 % and 39 %, respectively (Tab. 6.4.1.1). The contribution of a species to total LAI also reflected the proportions on  $E_c$ : beech held ca. 87 % of the LAI at Steinkreuz and 48 % at Großebene. Thus, the higher the contribution of beech to  $A_s$  or the LAI of a stand, the higher the  $E_c$ . Conversely, a larger proportion of oak on stand level  $A_s$  resulted in a smaller stand level  $E_c$  (Tab. 6.4.1.1, Fig. 5.5.5).

The seasonal maximum daily canopy transpiration  $E_{c\ max}$  increased with LAI for the mixed stands, for beech from the mixed stands and for oak from the mixed stands (Fig. 5.5.5b, see also Tab. 6.4.1.1 for seasonal values). In the two pure beech plots LAI and  $E_{c\ max}$  were very similar. Thus it emerged that LAI had a different quality in the pure beech stands and when mixed with oak.  $E_{c\ max}$  per unit leaf area,  $E_{c\ max}/LAI$ , was highest in the two beech stands (0.63–0.67 kg m<sup>-2</sup> d<sup>-1</sup>), intermediate for the mixed stands (0.39–0.40 kg m<sup>-2</sup> d<sup>-1</sup>) and for beech in the mixed stands (0.41–0.50 kg m<sup>-2</sup> d<sup>-1</sup>), and lowest in oak from the mixed stands (0.27–0.29 kg m<sup>-2</sup> d<sup>-1</sup>; Fig. 5.5.5e). For each of these four stand types or stand components,  $E_{c\ max}/LAI$  seemed

rather constant with increasing LAI, however, only two samples per type were available.

Data compiled from the literature also suggest a large  $E_c \text{ max/LAI}$  for pure beech stands, on average  $0.80 \text{ kg m}^{-2} \text{ d}^{-1}$ , for a wide range of LAI (1.5–9.0; Fig. 6.4.1.1), while for the few pure oak and mixed beech/oak stands studied values of  $E_c \text{ max/LAI}$  were lower. These findings are indicative of beech having a successful strategy to occupy crown space, of little self-shading and of leaves well-adapted to the particular light environment deep inside the beech crown, also at the whole-canopy level (cf. Fig 5.4.3 for  $Q_{t \text{ max}}/A_{lt}$ ). For oak the results point to a higher degree of self-shading.

$E_c \text{ max}$  increased with  $A_s$  similarly for the total mixed stands and for beech and oak in the mixed stands. At the highest values of  $A_s$ , observed in the pure beech plots,  $E_c \text{ max}$  saturated (Fig. 5.5.5d). In a range of  $A_s$  of  $10\text{--}30 \text{ m}^2 \text{ ha}^{-1}$ ,  $E_c \text{ max}$  seemed proportional to  $A_s$  in beech and  $E_c \text{ max}/A_s$  was  $1.1\text{--}1.5 \cdot 10^3 \text{ kg m}^{-2} \text{ d}^{-1}$  (Fig. 5.5.5f). At the highest value of  $A_s$ , at Farrenleite,  $E_c \text{ max}/A_s$  decreased. For the oaks in the two (mixed) stands studied  $A_s$  spanned only  $1.7\text{--}4.4 \text{ m}^2 \text{ ha}^{-1}$ , and  $E_c \text{ max}/A_s$  averaged to  $1.8 \cdot 10^3 \text{ kg m}^{-2} \text{ d}^{-1}$  (Fig. 5.5.5f). Thus  $E_c \text{ max}/A_s$  was larger in oak than in beech (and also  $E_c \text{ season}/A_s$ ; Tab. 6.4.1.1). Comparisons of  $E_c \text{ max}$  with basal area ( $A_b$ ) or stand density were less conclusive.

Hypothesis: Maximum daily  $E_c$  is similar at low and high elevation sites under similar atmospheric conditions.

Maximum daily  $E_c$  ( $E_c \text{ max}$ ) reached similar values in both pure beech plots:  $4.4 \text{ mm d}^{-1}$  at Steinkreuz,  $4.3 \text{ mm d}^{-1}$  at Farrenleite in 1999 and  $4.2 \text{ mm d}^{-1}$  and  $3.9 \text{ mm d}^{-1}$  in 2000, respectively (Fig. 5.5.5, Tab. 5.5.2). This indicates a similar physiological capacity of beech at lower and higher elevations in stands with similar LAI (6.5–6.8).

Hypothesis: Seasonal canopy transpiration of beech stands is lower at higher elevation due to lower air temperatures, lower D and a shorter growing season than at lower elevation.

The seasonal sum of canopy transpiration  $E_c$  was higher at the low-elevation pure beech plot (Steinkreuz-pure beech plot; on average  $335 \text{ mm season}^{-1}$ ) than at the high-elevation stand (Farrenleite;  $218 \text{ mm season}^{-1}$ , respectively; Fig. 5.5.4, Tab. 5.5.2, Tab. 6.4.1.1). A shorter growing season, lower vapour pressure deficit of the air D, lower air temperatures, more rain and fog days limited  $E_c$  at the high elevation site, resulting in the differences between the two stands at seasonal time scales (Fig. 5.5.17, Tab. 6.4.1.1).

Hypothesis: Critically low soil water supply reduces  $E_c$  more strongly in beech than in the more drought-tolerant oak, and is more frequently limiting  $E_c$  at lower elevation than at higher elevation.

Soil water shortage occurred at the Steigerwald sites during August and September 1999 (Fig. 5.2.1.2–3, Fig. 5.2.1.5, Fig. 5.5.16);  $\theta_e$  decreased to 0.23 in 0.35 m soil depth and  $E_c$  was reduced as a consequence.  $E_c$  of the beech component of the mixed stands was more reduced (reduction in the response of  $E_c$  to D of 54–72 % in September relative to June–July) than  $E_c$  of the oak component (reductions of 42–48 %; Fig. 5.5.14).  $E_c$  of the beech component at Großebene was more reduced (30 % in August, 72 % in September) than  $E_c$  of the beech at Steinkreuz (20 % and 54 %, respectively) and may relate to the different canopy positions of beech in these stands, which are also likely to be reflected in the root distributions.

For oak the opposite was true: at Steinkreuz, where oak was under strong competition from beech, the reduction in the response of  $E_c$  to D was larger during the early phase of the drought (August: 23 %) than at Großebene (14 %) where oak dominated the canopy. At Steinkreuz the reduction of oak was perhaps even slightly larger than that of beech (23 % compared to 20 %), likely due to the dominance of beech also below-ground in this stand. During advanced soil drought in September, differences between oak from the two stands decreased (at Steinkreuz 42% reduction, at Großebene 48 %), possibly because the superior drought tolerance of oak overruled the structural dominance of beech at Steinkreuz in combination with a probably larger rooting depth of oak. The slightly larger reduction of oak at Großebene compared to Steinkreuz in September could be an effect of larger soil water depletion by the many large oaks which did not reduce their stomatal conductance in response to increasing soil water potentials to the extent that beech probably did. So, speculatively, at Steinkreuz the oaks may have used the water that the beech trees had saved.

The high elevation pure beech stand Farrenleite in the Fichtelgebirge was not affected by soil water depletion (Fig. 5.2.2.1–2), due to more frequent rain, lower average D, more fog days and somewhat larger soil depth (Tab. 5.2.1.1, Chap. 5.2), and daily  $E_c$  was up to 2.3 times larger than  $E_c$  of the Steinkreuz-pure beech plot in the Steigerwald in the first half of September 1999 (Fig. 5.5.8, Fig. 5.5.15–16).

Hypothesis: The canopy conductance of mixed stands of beech and oak is only slightly higher or as high as in pure beech stands because of the larger dominance of beech in canopy space capture.

At Großebene, maximum diurnal canopy conductance  $g_{c \max}$  of oak was larger than  $g_{c \max}$  of beech.  $g_{c \max}$  of the total stand Großebene, however, was smaller than that of the Steinkreuz-pure beech plot (maximum  $19.4 \text{ mm s}^{-1}$  compared to  $30 \text{ mm s}^{-1}$ , respectively; Tab. 5.5.3). The  $g_{c \max}$  of oak was higher at Großebene, where oak contributed more to LAI and  $A_s$ , than at Steinkreuz and the  $g_{c \max}$  of beech was much higher at Steinkreuz than that of oak. For the total stand Steinkreuz  $g_{c \max}$  was smaller than at Großebene ( $17.5 \text{ mm s}^{-1}$ ). In the drier year 1999 the  $g_{c \max}$  of oak at Steinkreuz was larger than in the wetter year 2000, relative to beech. The  $g_{c \max}$  of the pure beech plots compared well in the year 2000 ( $24 \text{ mm s}^{-1}$  and  $26.5 \text{ mm s}^{-1}$  at

Farrenleite and the Steinkreuz-pure beech plot, respectively), in 1999 they differed markedly ( $17.5 \text{ mm s}^{-1}$  compared to  $30 \text{ mm s}^{-1}$ , respectively).

$g_{c \max}$  decreased with D in all stands and in the mixed stands in both species (Fig. 5.5.18).  $g_{c \max}$  of Farrenleite was similar to  $g_{c \max}$  of the Steinkreuz-pure beech plot, but lower at low D, particularly in the year 1999. It seemed likely that air temperature was limiting  $g_c$  at Farrenleite at times when D was also low (in the mornings), reflecting the higher altitude of the site.

When  $g_{c \max}$  was expressed in units of leaf area as  $g_{c \max}/\text{LAI}$ , differences between the pure and mixed plots in the Steigerwald became smaller, and  $g_{c \max}/\text{LAI}$  of oak was larger than that of beech in both mixed stands in 1999 but still smaller than that of Steinkreuz-pure beech plot (Fig. 5.5.19, Tab. 5.5.3). The higher values of  $g_{c \max}/\text{LAI}$  observed in oak at the mixed stands may relate to the higher drought tolerance indicated in the presented data (cf. Fig. 5.5.14).

## 7.2. Future perspectives

The determination of radial patterns in sap flow density  $J_s$  in tree species with large sapwood area is essential for defensible estimates of whole-tree water use  $Q_t$ . Furthermore, changes in the radial distribution of sap flux with progressing drought advocate the continuous monitoring of  $J_s$  for representative seasonal sums of  $J_s$  and  $Q_t$ , or at least under various conditions of soil water supply and atmospheric demand.

For *Fagus sylvatica* radial patterns of  $J_s$  for trees from different closed stands, averaged over longer periods (weeks to months), seem to follow a general relationship; at least there are indications that regressions of  $J_s$  relative to  $J_s$  in outer sapwood and radial sapwood depth relative to total sapwood depth may be suitable as a way to transfer radial patterns of  $J_s$  from one stand to another. The similar sapwood area–basal area relationships and a rather small scatter in the comparison of  $Q_t$  and stem diameter in beech trees from stands across Central Europe reinforce such expectations. The extensive study of the radial patterns of  $J_s$  in a large number of beech trees presented here provides the framework for such a generalisation, which now would have to be applied to and tested on independent data sets.

In *Quercus petraea* and other ring-porous species, some ambiguity about the capability of the thermal dissipation sensors used here to represent sap flow correctly remains, despite the successful calibration and validation of these sensors in closely related *Q. robur*. More studies on oak are needed to determine whether a common functionality between scalars of tree size and sap flow exists as proposed for beech. Recurring insect calamities and the generally reduced vigour of oak in the region in addition to the strong competitive pressure from beech were considered the most plausible reasons for the lack of a significant correlation of sap flow with scalars of tree size at the mixed stands in the Steigerwald. Fundamental differences in the histology and hence hydraulic functionality between oak and beech were also considered. Further comparisons of estimates of  $Q_t$  in beech (and in oak) from different sites and their respective scalars of tree structure might well result in a suite of relationships that would reduce the observed variation of tree water use.

At the stand level, relationships of  $E_{c\max}$  and LAI or  $E_{c\max}$  and  $A_s$  show considerable potential to yield general envelopes of structure-function interrelationships, as demonstrated for  $E_{c\max}$  and LAI. The high canopy transpiration per unit of leaf area of beech, indicative of optimal spatial arrangement and light utilisation of its leaves, emerged as a prominent feature of this species' dominance at the canopy level compared to oak and supports a higher competitive capacity of beech over oak also at less mesic sites under the current conditions. The co-existence of beech and oak in mixed stands in the future will depend on whether the frequency and intensity of summer droughts increases locally enough so that oak gains competitive advantage over beech. Under moderately increased drought conditions, however, beech is likely to remain superior. This speculation disregards co-occurring changes of the biotic (e.g. altered pathogen activity) and abiotic environment (e.g. an increasing number of freeze-thaw cycles and late frost events). Nevertheless, mixed forest stands, especially of beech and oak, may be more resilient to climatic change, distributing the risk of extreme events among two contrasting species.

Structure-function relationships in forest water use deserve further study on all spatial levels addressed here and particularly in mixed stands of economically and ecologically important beech and oak. This study showed that systematic relationships between structure and function exist and quantified several of these on the within-tree, the tree and the stand level and thus provides a framework for further refinement and generalisation of such “transfer functions”. The scope of subsequent ecophysiological investigations and modelling exercises could be extended to include aspects of growth and productivity in relation to stand structure, especially species contribution, including the effects of changing growing conditions on the competition between beech and oak.

## 8 Summary

The overall goal of this study was to quantify and analyse the function of forest stands, regarding the transpiration of the tree canopy and its short-term control by environmental drivers and its long-term control by structural characteristics. Such functional relationships were sought in a regional examination of beech stands distributed across Upper Franconia, Northern Bavaria, where European beech (*Fagus sylvatica* L.) and sessile oak (*Quercus petraea* (MATT.) LIEBL.) occur together in the colline–submontane stands of the Steigerwald and where at higher elevation in the Fichtelgebirge pure beech stands are found.

Canopy transpiration was estimated from measurements of xylem sap flow with the thermal dissipation method. The radial distribution of sap flow in beech was assessed in three incremental sapwood depths down to 6 cm and scaled to the whole-tree level based on these measurements, using a linear regression function for the relative decrease of sap flow density with relative sapwood depth. In oak, the narrow sapwood could be assessed with one sap flow sensor. Scaling up to stand level in beech and oak was based on the sapwood area of tree size classes. Structural characteristics considered to have potential influences on sap flow included stem diameter, tree height, stand density, basal area, sapwood area and leaf area index.

Two mixed stands with different proportions of beech and oak were selected in the Steigerwald (440–460 m a.s.l.) and additionally a pure beech plot within one of these mixed stands and a pure beech stand in the Fichtelgebirge (950 m a.s.l.) for study. All stands had a closed canopy and were 120–140 years old. Field measurements were carried out over three years, and in total 71 tree-seasons of sap flow data were collected in beech and 41 in oak.

The axial xylem sap flow density,  $J_s$ , declined radially from outer to inner sapwood in *F. sylvatica*. This decrease of  $J_s$  was stronger in small trees with a restricted sapwood than in larger trees with wide sapwood.  $J_s$  in any sapwood depth increased with stem diameter. In *Q. petraea* a significant correlation of  $J_s$  with stem diameter was only observed in a stand where oak dominated over beech regarding tree size.  $J_s$  in the outer sapwood was of the same order of magnitude in beech and oak at a given stem diameter. When the depth of sap flow sensor insertion in the sapwood was related to the total sapwood radius, the radial decrease of  $J_s$ , normalised with  $J_s$  in outer sapwood, could be described by a linear regression function for all beech trees of various sizes from all sites. During progressive soil drought, when the relative extractable soil water content dropped below 0.4 in 0.35 m soil depth, the contribution of deeper sapwood relative to  $J_s$  in outer sapwood decreased, most pronounced in suppressed but also in intermediate and dominant beech trees.

The seasonal maximum daily whole-tree water use,  $Q_{t \max}$ , of beech from all sites scaled positively and non-linearly with stem diameter and related scalars. The  $Q_{t \max}$  ranged between 11 kg d<sup>-1</sup> and 435 kg d<sup>-1</sup> for beech trees with a stem diameter of 14 cm and 63 cm, respectively. The  $Q_{t \max}$  in oaks was lower than in beech trees with the same stem diameter, and maxima of 20–62 kg d<sup>-1</sup> for oaks with a stem diameter of 29–49 cm were found. The correlation of  $Q_{t \max}$  with stem diameter and other scalars was weak in the oaks studied. The maximum tree water use per unit leaf area,  $Q_{t \max}/A_{lt}$ , increased with tree height in beech. In oak much smaller values of  $Q_{t \max}/A_{lt}$  and an opposite trend with increasing tree height was found.

At comparable leaf area index, LAI, or basal area, maximum daily and seasonal rates of stand-level canopy transpiration  $E_c$  for the mixed stands in the Steigerwald were 2.3–2.7 mm d<sup>-1</sup> and 166–217 mm season<sup>-1</sup>, while the highest rates, observed in the pure beech plot in the Steigerwald, reached up to 4.4 mm d<sup>-1</sup> and 349 mm season<sup>-1</sup>. Among the mixed stands,  $E_c$  increased with a higher contribution of beech to stand level LAI or sapwood area,  $A_s$ . Maximum daily canopy transpiration,  $E_{c\ max}$ , increased with increasing LAI, and  $E_{c\ max}$  per unit leaf area,  $E_{c\ max}/LAI$ , was highest in the two pure beech stands, intermediate in the mixed stands and in beech from the mixed stands, and smallest in oak from the mixed stands.  $E_{c\ max}$  also increased with  $A_s$ . But at the highest values of  $A_s$  observed in the pure beech plots,  $E_{c\ max}$  was saturated. Higher values of  $E_{c\ max}/A_s$  were found in oak than in beech. Progressive soil drought reduced  $E_c$  in the beech component of the mixed stands more than in the oak component, compared to the same vapour pressure deficit of the air under more favourable soil water conditions. Differences in the reduction of  $E_c$  in beech and oak from the two mixed stands may relate to the different canopy positions of the two species in these stands, which are also likely to be reflected in the root distributions. The pattern of the highest values of maximum diurnal canopy conductance,  $g_{c\ max}$ , among the sites and species studied reflected that of  $E_{c\ max}$ . When  $g_{c\ max}$  was expressed in units of leaf area as  $g_{c\ max}/LAI$ , values for oak were higher than those for beech in the mixed stands during a dry year, which may relate to the supposedly higher drought tolerance and stomatal conductance of oak compared to beech well documented in the literature.

Beech and oak differed regarding relationships of structure and transpiration on all spatial levels studied. These findings are indicative of differences in the hydraulic architecture of the two species and stress the more successful strategy of beech to optimise leaf area distribution and better adapt to specific light environments inside the crown as compared to oak. The data presented also point to a high capacity for transpiration in beech even in stands with high LAI.

Beech trees with comparable stem diameter achieved similar rates of  $J_s$  and  $Q_{t\ max}$  at both the high elevation site in the Fichtelgebirge and the low elevation site in the Steigerwald. Also at the stand level, the pure beech stand at higher elevation compared well with the lower elevation pure beech plot of similar LAI regarding the seasonal maximum daily  $E_c$  of up to 4.3 mm d<sup>-1</sup>. The seasonal sums of  $E_c$  were at most 229 mm season<sup>-1</sup> at the cooler and moister high elevation stand. This stand was not affected by soil water depletion, and daily  $E_c$  was up to 2.3 times larger than in the pure beech plot in the Steigerwald during summer drought conditions.

The dominance of beech over oak regarding water use observed in the mixed stands studied supports a higher competitive capacity of beech over oak also at less mesic, more xeric sites under the current conditions. In this study, it could be shown that systematic relationships between structure and function exist in beech forests, observed on the within-tree, the tree and the stand level. These findings provide a framework for further generalisations of structure-function relationships especially in systematic investigations of beech stands across Central Europe. Functional relationships were less clear in oaks than in beech and deserve particular attention in future studies.

## 9 Zusammenfassung

Ziel der vorliegenden Untersuchung war, die Funktion von Waldbeständen hinsichtlich ihrer Kronendachtranspiration und deren kurzfristigen Kontrolle durch Umweltbedingungen und ihrer langfristigen Kontrolle durch Struktureigenschaften zu quantifizieren und zu analysieren. Diese funktionalen Zusammenhänge wurden regional an Buchenbeständen in Oberfranken, Nordbayern, untersucht, wo die Rotbuche (*Fagus sylvatica* L.) zusammen mit der Traubeneiche (*Quercus petraea* (MATT.) LIEBL.) in kollin bis submontanen Beständen des Steigerwaldes vorkommt und wo in den montanen Lagen des Fichtelgebirges reine Buchenwälder stocken.

Die Kronendachtranspiration wurde anhand von Messungen des Xylemsaftflusses geschätzt. Die radiale Verteilung des Saftflusses im Splintholz von Buchen wurde in drei Stufen bis in 6 cm Tiefe gemessen. Basierend auf diesen Messungen wurde mittels einer linearen Regressionsfunktion der relativen Abnahme der Saftflussdichte mit relativer Splintholztiefe auf die Baumebene skaliert. Der Saftfluss im schmalen Splintholz der Eichen konnte mit einem Sensor erfasst werden. Die Hochrechnung auf Bestandesebene erfolgte aufgrund der Splintfläche von Baumgrößenklassen. Strukturgrößen, die als potentiell einflussreich auf den Saftfluss erachtet wurden, waren Stammdurchmesser, Baumhöhe, Bestandesdichte, Grundfläche, Splintfläche und Blattflächenindex.

Zwei Mischbestände mit unterschiedlichen Anteilen von Buche und Eiche wurden im Steigerwald ausgewählt (440–460 m NN) sowie eine zusätzliche Messfläche mit reiner Buche in einem dieser Mischbestände, außerdem ein Buchenreinbestand im Fichtelgebirge (950 m NN). Alle Bestände waren geschlossen und 120–140jährig. Die Freilandmessungen wurde über drei Vegetationsperioden hinweg durchgeführt und insgesamt 71 Baum-Jahre an Saftflussdaten an Buchen sowie 41 an Eichen erhoben.

Die axiale Xylemsaftflussdichte  $J_s$  nahm in *F. sylvatica* radial vom äußeren zum inneren Splintholz ab. Diese Abnahme war in kleinen Buchen mit schmalem Splint größer als in großen Buchen mit breitem Splint.  $J_s$  stieg in jeder Splintholztiefe mit dem Stammdurchmesser an. Eine signifikante Korrelation von  $J_s$  mit dem Stammdurchmesser wurde in *Q. petraea* nur in einem Bestand beobachtet, in dem Eichen bezüglich der Baumgröße dominierten.  $J_s$  im äußeren Splintholz lag bei beiden Arten für einen gegebenen Stammdurchmesser in der gleichen Größenordnung. Wenn die Position eines Saftfluss-Sensors im Splintholz relativ zum Gesamtsplintradius angegeben wurde, zeigte sich ein linearer Zusammenhang zur radialen Abnahme von  $J_s$  relativ zu  $J_s$  im äußeren Splintholz, und zwar für alle Buchen unterschiedlicher Größe aus allen Beständen. Wenn mit fortschreitender sommerlicher Bodenaustrocknung der relative extrahierbare Bodenwassergehalt in 0.35 m Tiefe unter 0.40 fiel, nahm  $J_s$  im inneren Splintholz relativ zu  $J_s$  im äußeren Splintholz ab, am deutlichsten in unterdrückten, aber auch in intermediären und dominanten Buchen.

Die Maxima des täglichen Wasserverbrauches,  $Q_{t \max}$ , aller untersuchten Buchen waren positiv und nicht-linear mit dem Stammdurchmesser und verwandten Skalaren korreliert.  $Q_{t \max}$  variierte zwischen 11 kg d<sup>-1</sup> und 435 kg d<sup>-1</sup> für Buchen mit einem Stammdurchmesser von 14 cm und 63 cm.  $Q_{t \max}$  war in Eichen kleiner als in Buchen und erreichte 20–62 kg d<sup>-1</sup> für Bäume mit einem Stammdurchmesser von 29–49 cm. Bei den Eichen war die Korrelation von  $Q_{t \max}$  mit dem Stammdurchmesser und

anderen Skalaren gering. Der maximale Wasserverbrauch pro Einheit Blattfläche,  $Q_{t \max}/A_{lt}$ , nahm in Buchen mit der Baumhöhe zu. Die Werte von  $Q_{t \max}/A_{lt}$  waren in Eichen niedriger und folgten einem entgegengesetzten Trend.

Bei vergleichbaren Blattflächenindices oder Bestandesgrundflächen lagen die täglichen Maxima der Kronendachtranspiration auf Bestandesebene sowie die saisonalen Summen in den Mischbeständen bei 2.3–2.7 mm d<sup>-1</sup> bzw. 166–217 mm Saison<sup>-1</sup>, während die höchsten Raten mit 4.4 mm d<sup>-1</sup> und 349 mm Saison<sup>-1</sup> für die reine Buchenfläche im Steigerwald errechnet wurde. Die Kronendachtranspiration  $E_c$  stieg in den Mischbeständen mit zunehmendem Anteil von Buchen am Bestandes-LAI oder an der Bestandessplintholzfläche  $A_s$  an. Die maximale tägliche Kronendachtranspiration  $E_{c \ max}$  nahm mit steigendem LAI zu;  $E_{c \ max}$  pro Einheit Blattfläche,  $E_{c \ max}/LAI$ , war in den Reinbeständen am höchsten, in den Mischbeständen und dem Buchenanteil der Mischbestände intermediär und im Eichenanteil der Mischbestände am niedrigsten.  $E_{c \ max}$  stieg auch mit  $A_s$  an, sättigte aber in den Buchenreinbeständen bei den höchsten Werten von  $A_s$ . Für Eichen wurden höhere Werte für  $E_{c \ max}/A_s$  beobachtet als für Buchen. Bei fortschreitender Bodenaustrocknung wurde  $E_c$  des Buchenanteils der Mischbestände stärker reduziert als  $E_c$  des Eichenanteils, im Vergleich zu  $E_c$  bei gleichem Wasserdampfsättigungsdefizit der Luft unter günstigen Bodenwasserbedingungen. Die Unterschiede zwischen Buchen und Eichen in der Reduktion von  $E_c$  könnten mit ihren verschiedenen Kronenpositionen zusammenhängen, welche sich wahrscheinlich auch in der Wurzelverteilung widerspiegeln. Die Reihenfolge der höchsten Werte der maximalen diurnalen Kronendachleitfähigkeit  $g_{c \ max}$  zwischen den untersuchten Beständen glich der der maximalen täglichen Kronendachtranspiration. Die Kronendachleitfähigkeit pro Einheit Blattfläche  $g_{c \ max}/LAI$  war in einem Jahr mit trockenerem Sommer für die Eichenanteile der Mischbestände höher als für die Buchenanteile, was in Zusammenhang mit der bekannt höheren Trockentoleranz und höheren stomatären Leitfähigkeit von Eiche im Vergleich zu Buchen stehen könnte.

Buche und Eiche unterschieden sich hinsichtlich ihrer Struktur-Funktions-Beziehungen auf allen drei untersuchten räumlichen Ebenen. Diese Resultate deuten auf Unterschiede in der hydraulischen Architektur beider Arten hin und unterstreichen die Bedeutung der erfolgreicheren Strategie der Rotbuche bei der Optimierung der Blattflächenverteilung und der Anpassung an das spezifische Lichtklima im Kroneninnenraum im Vergleich zur Traubeneiche. Die vorgestellten Daten weisen auch auf eine hohe Transpirationsleistung der Buche, sogar in Beständen mit hohem LAI, hin.

Im höher gelegenen Bestand im Fichtelgebirge erreichten Buchen mit vergleichbarem Stammdurchmesser ähnliche Werte für  $J_s$  und  $Q_{t \ max}$  wie im tiefer gelegenen Steigerwald. Beide Bestände waren bei ähnlichen LAI auch auf der Bestandesebene bezüglich  $E_{c \ max}$ , mit bis zu 4.3 mm d<sup>-1</sup> im Fichtelgebirge, vergleichbar. Der höher gelegene Bestand erreichte über die gesamte Vegetationsperiode gesehen jedoch nur 229 mm Saison<sup>-1</sup>. Dieser Buchenbestand war nicht von Bodenwasserknappheit betroffen, und die tägliche Kronendachtranspiration erreichte während der Sommertrockenheit bis zu 2.3-fach höhere Werte als im Buchenreinbestand im Steigerwald.

Die Dominanz der Buche über die Eiche bezüglich des Wasserverbrauchs, wie er in den untersuchten Beständen beobachtet wurde, unterstreicht die höhere Konkurrenzkraft der Buche unter den gegenwärtigen Wuchsbedingungen, auch auf weniger mesischen, mehr xerischen Standorten. In der vorliegenden Studie konnte gezeigt

werden, dass systematische Beziehungen zwischen Struktur und Funktion in Buchenwäldern existieren, und zwar auf der stamminternen, der Baum- und der Bestandesebene. Diese Ergebnisse liefern die Grundlage für die weitere Generalisierung von Struktur-Funktionsbeziehungen, insbesondere in systematischen Untersuchungen von Buchenbeständen in Mitteleuropa. Die funktionalen Zusammenhänge in Eichen waren weniger deutlich als in Buchen und verdienen in zukünftigen Studien besondere Aufmerksamkeit.

## 10 References

- Abrams MD (2003) Where has all the white oak gone? BioScience 53, 927-939.
- Agster G (1986a) Wasser- und Grundwasserhaushalt der Einzugsgebiete des Schönbuchs in Abhängigkeit von Waldbestand und Untergrund. In: Einsele G (ed) Das landschaftsökologische Forschungsprojekt Schönbuch. Wasser- und Stoffhaushalt, bio-, geo- und forstwirtschaftliche Studien in Südwestdeutschland. VCH Weinheim, Germany, pp 85-112.
- Alsheimer M (1997) Xylemflußmessungen zur Charakterisierung raum-zeitlicher Heterogenitäten in der Transpiration montaner Fichtenbestände (*Picea abies* (L.) Karst.). Bayreuther Forum Ökologie 49, 143 pp.
- Alsheimer M, Köstner B, Falge E, Tenhunen JD (1998) Temporal and spatial variation in transpiration of Norway spruce stands within a forested catchment of the Fichtelgebirge, Germany. Ann Sci For 55, 103-123.
- André J-P (2005) Vascular organization of angiosperms: a new vision. Science Publishers, Inc., Enfield, USA, 140 pp.
- Anfodillo T, Sigalotti GB, Tomasi M, Semenzato P, Valentini R (1993) Applications of a thermal imaging technique in the study of the ascent of sap in woody species. Plant Cell Environ 16, 997-1001.
- Aranda I, Gil L, Pardos J (1996) Seasonal water relations of three broadleaved species (*Fagus sylvatica* L., *Quercus petraea* (Mattuschka) Liebl. and *Quercus pyrenaica* Willd.) in a mixed stand in the centre of the Iberian Peninsula. For Ecol Manage 84, 219-229.
- Aranda I, Gil L, Pardos JA (2000) Water relations and gas exchange in *Fagus sylvatica* L. and *Quercus petraea* (Mattuschka) Liebl. in a mixed stand at their southern limit of distribution in Europe. Trees 14, 344-352.
- Aranda I, Gil L, Pardos JA (2005) Seasonal changes in apparent hydraulic conductance and their implications for water use of European beech (*Fagus sylvatica* L.) and sessile oak [*Quercus petraea* (Matt.) Liebl] in South Europe. Plant Ecol 179, 155-167.
- Asbjornsen H, Tomer MD, Gomez-Cardenas M, Brudvig LA, Greenan CM, Schilling K (2007) Tree and stand transpiration in a Midwestern bur oak savanna after elm encroachment and restoration thinning. For Ecol Manage 247, 209-219.
- Aussenac G, Granier A (1979) Etude bioclimatique d'une futaie feuillue (*Fagus sylvatica* L. et *Quercus sessiliflora* Salisb.) de l'Est de la France. II. Etude de l'humidité du sol et de l'évapotranspiration réelle. Ann Sci For 36, 265-280.
- Backes K (1996) Der Wasserhaushalt vier verschiedener Baumarten der Heide-Wald-Sukzession. PhD thesis, University of Göttingen, Cuvillier Verlag Göttingen, Germany, pp 134.
- Backes K, Leuschner C (2000) Leaf water relations of competitive *Fagus sylvatica* and *Quercus petraea* trees during 4 years differing in soil drought. Can J For Res 30, 335-346.
- Baldocchi DD (2003) Assessing the eddy covariance technique for evaluating carbon dioxide exchange rates of ecosystems: past, present and future. Global Change Biol 9, 479-492.
- Baldocchi DD, Amthor JS (2001) Canopy photosynthesis: history, measurements, and models. In: Roy J, Saugier B, Mooney HA (eds) Terrestrial global productivity. Academic Press, San Diego, USA, pp 9-31.
- Baldocchi DD, Hicks BB, Meyers TP (1988) Measuring biosphere-atmosphere exchanges of biologically related gases with micrometeorological methods. Ecology 69, 1331-1340.
- Baldocchi DD, Meyers TP (1998) On using eco-physiological, micrometeorological and biogeochemical theory to evaluate carbon dioxide, water vapour and trace gas fluxes over vegetation: a perspective. Agric For Meteorol 90, 1-25.
- Baldocchi DD, Wilson KB, Gu L (2002) How the environment, canopy structure and canopy physiological functioning influence carbon, water and energy fluxes of a temperate broad-leaved deciduous forest - an assessment with the biophysical model CANOAK. Tree Physiol 22, 1065-1077.
- Bamber RK, Fukazawa K (1985) Sapwood and heartwood: a review. Forestry Abstracts 46, 567-580.
- Barbaroux C, Bréda N (2002) Contrasting distribution and seasonal dynamics of carbohydrate reserves in stem wood of adult ring-porous sessile oak and diffuse-porous beech trees. Tree Physiol 22, 1201-1210.

- Barbour MM, Hunt JE, Walcroft AS, Rogers GND, McSeveny TM, Whitehead D (2005) Components of ecosystem evaporation in a temperate coniferous rainforest, with canopy transpiration scaled using sapwood density. *New Phytol* 165, 549-558.
- Barbour MM, Whitehead D (2003) A demonstration of the theoretical prediction that sap velocity is related to wood density in the conifer *Dacrydium cupressinum*. *New Phytol* 158, 477-488.
- Barford CC, Wofsy SC, Goulden ML, Munger JW, Pyle EH, Urbanski SP, Hutyra L, Saleska SR, Fitzjarrald D, Moore K (2001) Factors controlling long- and short-term sequestration of atmospheric CO<sub>2</sub> in a mid-latitude forest. *Science* 294, 1688-1691.
- Bartelink HH (1997) Allometric relationships for biomass and leaf area of beech (*Fagus sylvatica* L.). *Ann Sci For* 54, 39-50.
- Bauer G, Schulze E-D, Mund M (1997) Nutrient contents and concentrations in relation to growth of *Picea abies* and *Fagus sylvatica* along a European transect. *Tree Physiol* 17, 777-786.
- Bayerische Staatsforstverwaltung (2002) Zahlen und Fakten Wald und Holz. Munich, Germany, 25 pp.
- BayFORKLIM (1996) Klimaatlas von Bayern. Bayerischer Klimaforschungsverbund, Munich, Germany.
- Becker P (1996) Sap flow in Bornean heath and dipterocarp forest trees during wet and dry periods. *Tree Physiol* 16, 295-299.
- Benecke P (1984) Der Wasserumsatz eines Buchen- und eines Fichtenwaldökosystems im Hochsolling. Schriften aus der Forstlichen Fakultät der Universität Göttingen und der Niedersächsischen Forstlichen Versuchsanstalt, Vol. 77, J. D. Sauerländer's Verlag, Frankfurt (Main), pp 159.
- Benecke P, van der Ploog RR (1978) Quantifizierung des Wasserumsatzes am Beispiel eines Buchen- und eines Fichtenaltbestandes im Solling. *Forstarchiv* 49, 26-32.
- Berbigier P, Bonnefond JM, Loustau D, Ferreira MI, David JS, Pereira JS (1996) Transpiration of a 64-year-old maritime pine stand in Portugal. 2. Evapotranspiration and canopy stomatal conductance measured by an eddy covariance technique. *Oecologia* 107, 43-52.
- Bernier PY, Bréda N, Granier A, Raulier F, Mathieu F (2002) Validation of a canopy gas exchange model and derivation of a soil water modifier for transpiration for sugar maple (*Acer saccharum* Marsh.) using sap flow density measurements. *For Ecol Manage* 163, 185-196.
- Beyschlag W, Ryel RJ, Caldwell MM (1995) Photosynthesis of vascular plants: assessing canopy photosynthesis by means of simulation models. In: Schulze E-D, Caldwell MM (eds) *Ecophysiology of Photosynthesis*. Springer Study Edition, Berlin, Germany, pp 409-430.
- Binkley D, Reid P (1984) Long-term responses of stem growth and leaf area to thinning and fertilization in a Douglas-fir plantation. *Can J For Res* 14, 656-660.
- Black TA (1979) Evapotranspiration from Douglas fir stands exposed to soil water deficits. *Water Resources Res* 15, 164-170.
- Blank R (1997) Ringporigkeit des Holzes und häufige Entlaubung durch Insekten als spezifische Risikofaktoren der Eichen. *Forst und Holz* 52, 235-242.
- BMVEL (2001a) Gesamtwaldbericht der Bundesregierung. Bundesministerium für Verbraucherschutz, Ernährung und Landwirtschaft, Bonn, Germany, 141 pp.
- BMVEL (2001b) Die biologische Vielfalt des Waldes. Bundesministerium für Verbraucherschutz, Ernährung und Landwirtschaft, Bonn, Germany.
- BMVEL (2003) Waldzustandsbericht 2003. Bundesministerium für Verbraucherschutz, Ernährung und Landwirtschaft, Berlin, Germany, 55 pp.
- Bohn U, Gollub G, Hettwer C, Neuhäuslová Z, Schlüter H, Weber H (2003) Karte der natürlichen Vegetation Europas / Map of the natural vegetation of Europe. Maßstab / Scale 1 : 2 500 000. Erläuterungstext / Explanatory text. Bundesamt für Naturschutz, Bonn, Germany, 655 pp.
- Bolte A, Leßner C, Müller J, Kallweit R (2001) Zur Rolle der Bodenvegetation im Stoff- und Wasserhaushalt von Kiefernökosystemen – Level II-Untersuchungen in Brandenburg. *Beiträge für Forstwirtschaft und Landschaftsökologie* 35, 26-29.
- Bonn S (2000) Konkurrenzdynamik in Buchen/Eichen-Mischbeständen und zu erwartende Modifikationen durch Klimaveränderungen (Competition dynamics in mixed beech-oak stands and its modifications expected due to climate changes). *Allg Forst Jagd Ztg* 171, 81-88.
- Booker RE (1984) Dye-flow apparatus to measure the variation in axial xylem permeability over a stem cross-section. *Plant Cell Environ* 7, 623-628.

- Booker RE, Kininmonth JA (1978) Variation in longitudinal permeability of green radiata pine wood. New Zealand J For Sci 8, 295-308.
- Borchert R (1994a) Soil and stem water storage determine phenology and distribution of tropical dry forest trees. Ecology 75, 1437-1449.
- Borchert R (1994b) Electric resistance as a measure of tree water status during seasonal drought in a tropical dry forest in Costa Rica. Tree Physiol 14, 299-312.
- Bork H-R, Dalchow C, Faust B, Piorr H-P, Toussaint V, Werner A (2001) Future development of landscapes in marginal agrarian regions of Central Europe: long-term effects of land use on the water balance. In: Tenhunen JD, Lenz R, Hantschel R (eds) Ecosystem approaches to landscape management in Central Europe. Ecol Stud 147, Springer-Verlag, Berlin, Germany, pp 571-581.
- Bosshard HH (1976) Jahrringe und Jahrringbrücken. Schweiz Z Forstwesen 127, 675-693.
- Bosshard HH, Kučera L (1973) Die dreidimensionale Strukturanalyse des Holzes 1. Mitteilung: Die Vernetzung des Gefäßsystems in *Fagus sylvatica* L. Holz Roh Werkst 31, 437-445.
- Bosshard HH, Kučera L, Stocker U (1978) Gewebe-Verknüpfungen in *Quercus robur* L. Schweizerische Zeitschrift für Forstwesen 129, 219-242.
- Bosshard HH, Kučera LJ, Stocker U (1982) Das Gefäß-System im präjuvenilen Holz von *Fraxinus excelsior* L. Vierteljahresschr Naturforsch Ges Zürich 127, 29-48.
- Bouriaud O, Bréda N, Le Moguédec G, Nepveu G (2004) Modelling variability of wood density in beech as affected by ring age, radial growth and climate. Trees 18, 264-276.
- Bouriaud O, Soudani K, Bréda N (2003) Leaf area index from litter collection: impact of specific leaf area variability within a beech stand. Can J Remote Sens 29, 371-380.
- Bovard BD, Curtis PS, Vogel CS, Su H-B, Schmid HP (2005) Environmental controls on sap flow in a northern hardwood forest. Tree Physiol 25, 31-38.
- Braun HJ (1959) Die Vernetzung der Gefäße bei *Populus*. Z f Botanik 47, 421-434.
- Braun HJ (1970) Funktionelle Histologie der sekundären Sproßachse. 1. Das Holz. Handbuch der Pflanzenanatomie/Encyclopedia of plant anatomy, Vol. 9,1. Borntraeger, Berlin, Germany, 190 pp.
- Braun HJ (1984) The significance of the accessory tissues of the hydrosystem for osmotic water shifting as the second principle of water ascent, with some thoughts concerning the evolution of trees. IAWA Bull 5, 275-294.
- Braun P, Schmid J (1999) Sap flow measurements in grapevines (*Vitis vinifera* L.) 2. Granier measurements. Plant Soil 215, 47-55.
- Brechtel HM, Balazs A (1988) Wieviel Wasser kommt aus dem Bramwald? AFZ 43, 397-400.
- Bréda N, Cochard H, Dreyer E, Granier A (1993a) Water transfer in a mature oak stand (*Quercus petraea*): seasonal evolution and effects of a severe drought. Can J For Res 23, 1136-1143.
- Bréda N, Cochard H, Dreyer E, Granier A (1993b) Field comparison of transpiration, stomatal conductance and vulnerability to cavitation of *Quercus petraea* and *Quercus robur* under water stress. Ann Sci For 50, 571-582.
- Bréda N, Granier A (1996) Intra- and interannual variations of transpiration, leaf area index and radial growth of a sessile oak stand (*Quercus petraea*). Ann Sci For 53, 521-536.
- Bréda N, Granier A, Aussenac G (1995a) Effects of thinning on soil and tree water relations, transpiration and growth in an oak forest (*Quercus petraea* (Matt.) Liebl.). Tree Physiol 15, 295-306.
- Bréda N, Granier A, Barataud F, Moyne C (1995b) Soil water dynamics in an oak stand: soil moisture, water potentials and root water uptake. Plant Soil 172, 17-27.
- Bréda N, Roland Huc R, André Granier A, Dreyer E (2006) Temperate forest trees and stands under severe drought: a review of ecophysiological responses, adaptation processes and long-term consequences. Ann For Sci 63, 625-644.
- Bréda NJJ (2003) Ground-based measurements of leaf area index: a review of methods, instruments and current controversies. J Exp Bot 54, 2403-2417.
- Brooks RJ, Meinzer FC, Coulombe R, Gregg J (2002) Hydraulic redistribution of soil water during summer drought in two contrasting Pacific Northwest coniferous forests. Tree Physiol 22, 1107-1117.
- Brough DW, Jones HG, Grace J (1986) Diurnal changes in water content of the stems of apple trees as influenced by irrigation. Plant Cell Environ 9, 1-7.
- Buchmüller KS (1986) Jahrringcharakteristik und Gefäßlängen in *Fagus sylvatica* L. Vierteljahresschr Naturforsch Ges Zürich 131, 161-182.

- Büttner V, Leuschner C (1994) Spatial and temporal patterns of fine root abundance in a mixed oak-beech forest. *For Ecol Manage* 70, 11-21.
- Burger H (1947) Die Eiche. *Mitt Schweiz Anst Forstl Versuchswes* 25, 211-279.
- Burger H (1950) Holz, Blattmenge und Zuwachs. X: Die Buche. *Mitt Schweiz Anst Forstl Versuchswes* 26, 419-468.
- Burggraaf PD (1972) Some observations on the course of the vessels in the wood of *Fraxinus excelsior* L. *Acta Botanica Néerlandica* 21, 32-47.
- Burrows LE (1980) Differentiating sapwood, heartwood and pathological wood in live mountain beech. New Zealand Forest Service, Forest Research Institute, Protection Forestry Report 172.
- Burrows SN, Gower ST, Clayton MK, Mackay DS, Ahl DE, Norman JM, Diak G (2002) Application of geostatistics to characterize leaf area index (LAI) from flux tower to landscape scales using a cyclic sampling design. *Ecosystems* 5, 667-679.
- Burton AJ, Pregitzer KS, Reed DD (1991) Leaf area and foliar biomass relationships in northern hardwood forests located along an 800 km acid deposition gradient. *For Sci* 37, 1041-1059.
- Cabibel B (1994) Continuity of water transfer in soil-plant system: The case of fruit trees. *Agronomie* 14, 503-514.
- Cabibel B, Do F (1991) Mesures thermiques des flux de sève dans les troncs et les racines et fonctionnement hydrique des arbres. I. Analyse théoretique des erreurs sur la mesure des flux et validation des mesures en présence de gradients thermiques extérieurs. *Agronomie* 11, 669-678.
- Cabibel B, Isberie C (1997) Sap flow and water consumptive use in cherry trees irrigated or not irrigated under trickle irrigation. *Agronomie* 17, 97-112 1997.
- Calder IR, Swaminath MH, Kariyappa GS, Srinivasulu NV, Srinivasa Murty KV, Mumtaz J (1992) Deuterium tracing for the estimation of transpiration from trees Part 3. Measurements of transpiration from *Eucalyptus* plantation, India. *J Hydrol* 130, 37-48.
- Caldwell MM, Dawson TE, Richards JH (1998) Hydraulic lift: consequences of water efflux from the roots of plants. *Oecologia* 113, 151-161.
- Camy C, Delatour C, Marçais B (2003) Relationships between soil factors, *Quercus robur* health, *Collybia fusipes* root infection and *Phytophthora* presence. *Ann For Sci* 60, 419-426.
- Cannell MGR (1982) World forest biomass and primary production data. Academic Press, London, 391 pp.
- Carlisle A, Brown AHF, White EJ (1966) Litterfall, leaf production and the effects of defoliation by *Tortrix viridana* in a sessile oak (*Quercus petraea*) woodland. *J Ecol* 54, 65-85.
- Catovsky S, Holbrook NM, Bazzaz FA (2002) Coupling whole-tree transpiration and canopy photosynthesis in coniferous and broad-leaved tree species. *Can J For Res* 32, 295-309.
- Cermák J, Cienciala E, Kučera J, Hällgren J-E, (1992) Radial velocity profiles of water flow in trunks of Norway spruce and oak and the response of spruce to severing. *Tree Physiol* 10, 367-380.
- Cermák J, Cienciala E, Kučera J, Lindroth A, Bednárová (1995) Individual variation of sap-flow rate in large pine and spruce trees and stand transpiration: a pilot study at the central NOPEX site. *J Hydrol*, 17-27.
- Cermák J, Deml M; Penka M (1973) A new method of sap flow rate determination in trees. *Biol Plant* 15, 171-178.
- Cermák J, Huzulák J, Penka M (1980) Water potential and sap flow rate in adult trees with moist and dry soil as used for the assessment of root system depth. *Biol Plant* 22, 34-41.
- Cermák J, Kucera J, Prax A, Bednarova E, Tatarinov F, Nadyezhdin V (2001) Long-term course of transpiration in a floodplain forest in southern Moravia associated with changes of underground water table. *Ekologia-Bratislava* 20, 92-115 Suppl 1.
- Cermák J, Matyssek R, Kučera J (1993) Rapid response of large, drought-stressed beech trees to irrigation. *Tree Physiol* 12, 281-290.
- Cermák J, Nadezhina N (1998) Sapwood as the scaling parameter – defining according to xylem water content or radial pattern of sap flow? *Ann Sci For* 55, 509-521.
- Cermák J, Úlehla J, Kučera J, Penka M (1982) Sapflow rate and transpiration dynamics in full-grown oak (*Quercus robur* L.) in floodplain forest exposed to seasonal floods as related to potential evapotranspiration and tree dimensions. *Biol Plant* 24, 446-460.
- Cescatti A (1997) Modelling the radiative transfer in discontinuous canopies of asymmetric crowns. I. Model structure and algorithms. *Ecol Mod* 101, 263-274.

- Cescatti A (2007) Indirect estimates of canopy gap fraction based on the linear conversion of hemispherical photographs: Methodology and comparison with standard thresholding techniques. Agric For Meteorol 143, 1-12.
- Chapman L (2007) Potential applications of near infra-red hemispherical imagery in forest environments. Agric For Meteorol 143, 151-156.
- Chason JW, Baldocchi DD, Huston MA (1991) A comparison of direct and indirect methods for estimating forest canopy leaf area. Agric For Meteorol 57, 107-128.
- Chen JM, Black TA (1991) Measuring leaf area index of plant canopies with branch architecture. Agric For Meteorol 57, 1-12.
- Chen JM, Black TA (1992) Defining leaf area index for non-flat leaves. Plant Cell Environ 15, 421-429.
- Chen JM, Govind A, Sonnentag O, Zhang Y, Barr A, Amiro B (2006) Leaf area index measurements at Fluxnet-Canada forest sites. Agric For Meteorol 140, 257-268.
- Chen JM, Rich PM, Gower ST, Norman JM, Plummer S (1997) Leaf area index of boreal forests: theory, techniques, and measurements. J Geophys Res 102 (D24), 29429-29443.
- Cheussum L (2004) Hydrological pattern in a mixed forest of northern Germany. Ber Forschungszentrum Waldökosysteme A187, 172 pp.
- Choat B, Jansen S, Zwieniecki MA, Smets E, Holbrook NM (2004) Changes in pit membrane porosity due to deflection and stretching: the role of vested pits. J Exp Bot 55, 1569-1575.
- Choat B, Lahr EC, Melcher PJ, Zwieniecki MA, Holbrook NM (2005) The spatial pattern of air seeding thresholds in mature sugar maple trees. Plant Cell Environ 28, 1082-1089.
- Ciais P, Reichstein M, Viovy N, Granier A, Ogée J, Allard V, Aubinet M, Buchmann N, Bernhofer C, Carrara A, Chevallier F, De Noblet N, Friend AD, Friedlingstein P, Grünwald T, Heinesch B, Kersten P, Knohl A, Krinner G, Loustau D, Manca G, Matteucci G, Miglietta F, Ourcival JM, Papale D, Pilegaard K, Rambal S, Seufert G, Soussana JF, Sanz MJ, Schulze E-D, Vesala T, Valentini R (2005) Europe-wide reduction in primary productivity caused by the heat and drought in 2003. Nature 437, 529-533.
- Cienciala E, Kučera J, Lindroth A (1999) Long-term measurements of stand water uptake in Swedish boreal forest. Agric For Meteorol 98-99, 547-554.
- Cienciala E, Kučera J, Ryan MG, Lindroth A (1998) Water flux in boreal forest during two hydrologically contrasting years; species specific regulation of canopy conductance and transpiration. Ann Sci For 55, 47-61.
- Cinnirella S, Magnani F, Saracino A, Borghetti M (2002) Response of a mature *Pinus laricio* plantation to a three-year restriction of water supply: structural and functional acclimation to drought. Tree Physiol 22, 21-30.
- Clearwater MJ, Clark CJ (2003) In vivo magnetic resonance imaging of xylem vessel contents in woody lianas. Plant Cell Environ 26, 1205-1214.
- Clearwater MJ, Goldstein G (2005) Embolism repair and long distance water transport. In: Holbrook NM, Zwieniecki MA (eds) Vascular transport in plants. Elsevier Academic Press, Amsterdam, pp 375-399.
- Clearwater MJ, Meinzer FC, Andrade JL, Goldstein G, Holbrook NM (1999) Potential errors in measurement of nonuniform sap flow using heat dissipation probes. Tree Physiol 19, 681-687.
- Cochard H, Bréda N, Granier A, Ausselac G (1992) Vulnerability to air embolism of three European oak species (*Quercus petraea* (Matt) Liebl, *Q. pubescens* Willd, *Q. robur* L). Ann Sci For 49, 225-233.
- Cochard H, Lemoine D, Améglio T, Granier A (2001) Mechanisms of xylem recovery from winter embolism in *Fagus sylvatica*. Tree Physiol 21, 27-33.
- Cochard H, Tyree MT (1990) Xylem dysfunction in *Quercus*: Vessel sizes, tyloses, cavitation and seasonal changes in embolism. Tree Physiol 6, 393-407.
- Committee on Nomenclature, International Association of Wood Anatomists (1964) Multilingual glossary of terms used in wood anatomy, second revision. Mitt Schweiz Anst Forst Versuchsw 40, 186 pp.
- Comstock GL (1965) Longitudinal permeability of green eastern hemlock. For Prod J 15, 441-449.
- Coners H, Hertel D, Leuschner C (1998) Horizontal- und Vertikalstruktur der Grob- und Feinwurzelsystems von konkurrierenden Buchen und Eichen in einem Mischbestand. Verh Ges Ökol 28, 435-440.

- Coners H, Leuschner C (2005) In situ measurement of fine root water absorption in three temperate tree species-Temporal variability and control by soil and atmospheric factors. *Basic Appl Ecol* 6, 395-405.
- Constantz J, Murphy F (1990) Monitoring moisture storage in trees using time domain reflectometry. *J Hydrol* 119, 31-42.
- Coomes DA (2006) Challenges to the generality of WBE theory. *Trends Ecol Evol* 21, 593-596.
- Crombie DS, Hipkins MF, Milburn JA (1985) Maximum sustainable xylem sap tension in *Rhododendron* and other species. *Planta* 163, 27-33.
- Cruiziat P, Cochard H, Améglio T (2002) Hydraulic architecture of trees: main concepts and results. *Ann For Sci* 59, 723-752.
- Cutini A, Matteucci G, Scarascia Mugnozza G (1998) Estimation of leaf area index with the Li-Cor 2000 in a deciduous forest. *For Ecol Manage* 105, 55-65.
- Daley MJ, Phillips NG (2006) Interspecific variation in nighttime transpiration and stomatal conductance in a mixed New England deciduous forest. *Tree Physiol* 26, 411-419.
- Davi H, Dufrene E, Francois C, Le Maire G, Loustau D, Bosc A, Rambal S, Granier A, Moors E (2006) Sensitivity of water and carbon fluxes to climate changes from 1960 to 2100 in European forest ecosystems. *Agric For Meteorol* 141, 35-56.
- Davi H, Dufrene E, Granier A, Le Dantec V, Barbaroux C, Francois C, Breda N (2005) Modelling carbon and water cycles in a beech forest: Part II: Validation of the main processes from organ to stand scale. *Ecol Mod* 185, 387-405.
- David TS, Ferreira MI, David JS, Pereira JS (1997) Transpiration from a mature *Eucalyptus globulus* plantation in Portugal during a spring-summer period of progressively higher water deficit. *Oecologia* 110, 153-159.
- Davis J, Davies R, Wells P, Benci N (1993) A field transportable computerized-tomography scanner for the nondestructive testing of wooden power poles. *Mater Eval* 51, 332.
- Dawson TE (1996) Determining water use by trees and forests from isotopic, energy balance and transpiration analyses: the roles of tree size and hydraulic lift. *Tree Physiol* 16, 263-272.
- Deblonde G, Penner M, Royer A (1994) Measuring leaf area index with the Li-Cor LAI 2000 in pine stands. *Ecology* 75, 1507-1511.
- Delta-T (1996) Delta-T DL2e logger user manual, version 2.02. Delta-T Devices Ltd., Burwell, Cambridge, UK.
- Delzon S, Loustau D (2005) Age-related decline in stand water use: sap flow and transpiration in a pine forest chronosequence. *Agric For Meteorol* 129, 105-119.
- Dittmar C, Elling W (1999) Jahrringbreite von Fichte und Buche in Abhängigkeit von Witterung und Höhenlage (Radial growth of Norway spruce and European beech in relation to weather and altitude). *Forstw Cbl* 118, 251-270.
- Dittmar C, Zech W, Elling W (2003) Growth variations of Common beech (*Fagus sylvatica* L.) under different climatic and environmental conditions in Europe - a dendroecological study. *For Ecol Manage* 173, 63-78.
- Dixon AFG (1971) The role of aphids in wood formation. I. The effect of the sycamore aphid, *Drepanosiphum platanoides* (Schr.) (Aphidae), on the growth of sycamore, *Acer pseudoplatanus* (L.). *J Appl Ecol* 8, 165-179.
- Do F, Rocheteau A (2002) Influence of natural temperature gradients on measurements of xylem sap flow with thermal dissipation probes. 1. Field observations and possible remedies. *Tree Physiol* 22, 641-648.
- Domec J-C, Gartner BL (2001) Cavitation and water storage capacity in bole xylem segments of mature and young Douglas-fir trees. *Trees* 15, 204-214.
- Domec J-C, Gartner BL (2003) Relationship between growth rates and xylem hydraulic characteristics in young, mature and old-growth ponderosa pine trees. *Plant Cell Environ* 26, 471-483.
- Domec J-C, Meinzer FC, Gartner BL, Woodruff D (2006) Transpiration-induced axial and radial tension gradients in trunks of Douglas-fir trees. *Tree Physiol* 26, 275-284.
- Domec J-C, Pruyn ML, Gartner BL (2005) Axial and radial profiles in conductivities, water storage and native embolism in trunks of young and old-growth ponderosa pine trees. *Plant Cell Environ* 28, 1103-1113.

- Dufrêne E, Bréda N (1995) Estimation of deciduous forest leaf area index using direct and indirect methods. *Oecologia* 104, 156-162.
- Dunin FX, Aston AR (1984) The development and proving of models of large scale evapotranspiration: an Australian study. In: Sharma ML (ed) *Evapotranspiration from plant communities*. Elsevier, Amsterdam, pp 305-323.
- Dunn GW, Connor DJ (1993) An analysis of sapflow in mountain ash (*Eucalyptus regnans*) forests of different ages. *Tree Physiol* 13, 321-336.
- DWD Deutscher Wetterdienst (1998–2003) *Deutsches Meteorologisches Jahrbuch 1995–2000*. Deutscher Wetterdienst, Offenbach, Germany.
- DWD Deutscher Wetterdienst (1999) *Deutsches Meteorologisches Jahrbuch 1996*. Deutscher Wetterdienst, Offenbach, Germany.
- DWD Deutscher Wetterdienst (1999–2000) *Witterungsreport 1999–2000*. Deutscher Wetterdienst, Offenbach, Germany.
- Dye PJ, Olbrich BW, Poulter AG (1991) The influence of growth rings in *Pinus patula* on heat pulse velocity and sap flow measurements. *J Exp Bot* 42, 867-870.
- Edwards WRN, Booker RE (1984) Radial variation in the axial conductivity of *Populus* and its significance in heat pulse velocity measurements. *J Exp Bot* 35, 551-561.
- Edwards WRN, Jarvis PG (1982) Relations between water content, potential and permeability in stems of conifers. *Plant Cell Environ* 5, 271-277.
- Edwards WRN, Jarvis PG (1983) A method for measuring radial differences in water content of intact tree stems by attenuation of gamma radiation. *Plant Cell Environ* 6, 255-260.
- Ehman JL, Schmid HP, Grimmond CSB, Randolph JC, Hanson PJ, Wayson CA, Cropley FD (2002) An initial intercomparison of micrometeorological and ecological inventory estimates of carbon exchange in a mid-latitude deciduous forest. *Global Change Biol* 8, 575-589.
- Ehrhardt O (1988) Der Strahlungshaushalt eines Buchenwaldes und dessen Abwandlung während der verschiedenen phänologischen Entwicklungsphasen. Ber Forschungszentrum Waldökosysteme A45, 172 pp.
- Ellenberg H (1963) *Vegetation Mitteleuropas mit den Alpen*. Ulmer, Stuttgart, Germany, 1<sup>st</sup> edition, 943 pp.
- Ellenberg H (1996) *Vegetation Mitteleuropas mit den Alpen*. Ulmer, Stuttgart, Germany, 5<sup>th</sup> edition, 1096 pp.
- Ellmore GS, Ewers FW (1985) Hydraulic conductivity in trunk xylem of *Ulmus americana*. *IAWA Bull* ns 6, 303-307.
- Ellmore GS, Ewers FW (1986) Fluid flow in the outermost xylem increment of a ring-porous tree, *Ulmus americana*. *Am J Bot* 73, 1771-1774.
- Ellsworth DS, Reich PB (1993) Canopy structure and vertical patterns of photosynthesis and related leaf traits in a deciduous forest. *Oecologia* 96, 169-178.
- Enquist BJ (2003) Cope's Rule and the evolution of long-distance transport in vascular plants: allometric scaling, biomass partitioning and optimization. *Plant Cell Environ* 26, 151-161.
- Epron D, Dreyer E (1993) Long-term effects of drought on photosynthesis of adult oak trees [*Quercus petraea* (Matt.) Liebl. and *Quercus robur* L.] in a natural stand. *New Phytol* 125, 381-389.
- Eriksson H, Eklundh L, Hall K, Lindroth A (2005) Estimating LAI in deciduous forest stands. *Agric For Meteorol* 129, 27-37.
- Ernstberger H (1985) Aktuelle Evapotranspiration eines bewaldeten Einzugsgebietes in Mittelhessen. Symposium Wald und Wasser, Grafenau, Germany, Vol 1, 103-116.
- Eschrich W, Burchardt R, Essiamah S (1989) The induction of sun and shade leaves of the European beech (*Fagus sylvatica* L.): anatomical studies. *Trees* 3, 1-10.
- Espinosa Bancalari MA, Perry DA, Marshall JD (1987) Leaf area-sapwood area relationships in adjacent young Douglas-fir stands with different early growth rates. *Can J For Res* 17, 174-180.
- Ewers BE, Mackay DS, Gower ST, Ahl DE, Burrows SN, Samanta SS (2002) Tree species effects on stand transpiration in northern Wisconsin. *Water Resources Res* 38, 1103.
- Ewers BE, Oren R (2000) Analyses of assumptions and errors in the calculation of stomatal conductance from sap flux measurements. *Tree Physiol* 20, 579-589.
- Falge E, Baldocchi D, Tenhunen J, Aubinet M, Bakwin P, Berbigier P, Bernhofer C, Burba G, Clement R, Davis KJ, Elbers JA, Goldstein AH, Grelle A, Granier A, Guomundsson J, Hollinger D, Kowalski AS,

- Katul G, Law BE, Malhi Y, Meyers T, Monson RK, Munger JW, Oechel W, Paw KT, Pilegaard K, Rannik U, Rebmann C, Suyker A, Valentini R, Wilson K, Wofsy S (2002a) Seasonality of ecosystem respiration and gross primary production as derived from FLUXNET measurements. *Agric For Meteorol* 113, 53-74.
- Falge E, Ryel RJ, Alsheimer M, Tenhunen JD (1997) Effects of stand structure and physiology on forest gas exchange: a simulation study for Norway spruce. *Trees* 11, 436-448.
- Falge E, Tenhunen J, Baldocchi D, Aubinet M, Bakwin P, Berbigier P, Bernhofer C, Bonnefond JM, Burba G, Clement R, Davis KJ, Elbers JA, Falk M, Goldstein AH, Grelle A, Granier A, Grunwald T, Gudmundsson J, Hollinger D, Janssens IA, Keronen P, Kowalski AS, Katul G, Law BE, Malhi Y, Meyers T, Monson RK, Moors E, Munger JW, Oechel W, U KTP, Pilegaard K, Rannik U, Rebmann C, Suyker A, Thorgeirsson H, Tirone G, Turnipseed A, Wilson K, Wofsy S (2002b) Phase and amplitude of ecosystem carbon release and uptake potentials as derived from FLUXNET measurements. *Agric For Meteorol* 113, 75-95.
- Falge E, Tenhunen JD, Ryel R, Alsheimer M, Köstner B (2000) Modelling age- and density-related gas exchange of *Picea abies* canopies in the Fichtelgebirge, Germany. *Ann Sci For* 57, 229-243.
- Fassnacht KS, Gower ST, Norman JM, McMurtie RE (1994) A comparison of optical and direct methods for estimating foliage surface area index in forests. *Agric For Meteorol* 71, 183-207.
- Felbermeier B (1993) Einfluß von Klimaänderungen auf die Areale von Baumarten – Methodenstudie und regionale Abschätzung für die Rotbuche (*Fagus sylvatica* L.) in Bayern. *Forstliche Forschungsberichte München* 134, 214 pp.
- Felbermeier B (1994) Arealveränderungen der Buche infolge von Klimaänderungen. *AFZ* 49, 222-224.
- Fiora A, Cescatti A (2006) Diurnal and seasonal variability in radial distribution of sap flux density: implications for estimating stand transpiration. *Tree Physiol* 26, 1217-1225.
- Firbas F (1949) Spät- und nacheiszeitliche Waldgeschichte Mitteleuropas nördlich der Alpen. I. Allgemeine Waldgeschichte. Gustav Fischer Verlag, Jena, Germany, 480 pp.
- Firbas F (1952) Spät- und nacheiszeitliche Waldgeschichte Mitteleuropas nördlich der Alpen. II. Waldgeschichte der einzelnen Landschaften. Gustav Fischer Verlag, Jena, Germany, 256 pp.
- Firbas F, Rochow v M (1956) Zur Geschichte der Moore und Wälder im Fichtelgebirge. *Forstw Cbl* 75, 367-380.
- Fleck S (2002) Integrated analysis of relationships between 3D-structure, leaf photosynthesis, and branch transpiration of mature *Fagus sylvatica* and *Quercus petraea* trees in a mixed forest stand. *Bayreuther Forum Ökologie* 97, 183 pp.
- Fleck S, Schmidt M, Köstner B, Faltin W, Tenhunen JD (2004) Impacts of canopy internal gradients on carbon and water exchange of beech and oak trees. In: Matzner E (ed) Biogeochemistry of forested catchments in a changing environment. A German case study. *Ecol Stud* 172, Springer-Verlag, Berlin, Germany, pp 99-126.
- Fleck W (1986) Bodenwasserbilanz, Streuverdunstung und Wasserverbrauch von Buche und Fichte auf Standorten und in Einzugsgebieten des Schönbuchs. In: Einsele G (ed) Das landschaftsökologische Forschungsprojekt Schönbuch. Wasser- und Stoffhaushalt, bio-, geo- und forstwirtschaftliche Studien in Südwestdeutschland. VCH Weinheim, Germany, 133-160.
- FLUXNET (2007) <http://www.fluxnet.ornl.gov/fluxnet/index.cfm>
- Foken T (2003) Lufthygienisch-bioklimatische Kennzeichnung des oberen Egertales. *Bayreuther Forum Ökologie* 100, 69 pp.
- Ford CR, Goranson CE, Mitchell RJ, Will RE, Teskey RO (2004b) Diurnal and seasonal variability in the radial distribution of sap flow: predicting total stem flow in *Pinus taeda* trees. *Tree Physiol* 24, 951-960.
- Ford CR, McGuire MA, Mitchell RJ, Teskey RO (2004a) Assessing variation in the radial profile of sap flux density in *Pinus* species and its effect on daily water use. *Tree Physiol* 24, 241-249.
- Forstamt Weißenstadt (2002) <http://www.forst.bayern.de/docs/foa-weissenstadt.html>
- Forstreuter M (2002) Auswirkungen globaler Klimaänderungen auf das Wachstum und den Gaswechsel ( $\text{CO}_2/\text{H}_2\text{O}$ ) von Rotbuchenbeständen (*Fagus sylvatica*). *Landschaftsentwicklung und Umweltforschung (Schriftenreihe der Fakultät Architektur Umwelt Gesellschaft, Technical University of Berlin)* 119, 317 pp.
- Freist-Dorr M (1992a) Struktur und Wachstum süddeutscher Traubeneichen-Buchen-Mischbestände. Darstellung am Beispiel langfristig beobachteter Versuchsflächen. *Forstliche Forschungsberichte München* 124, 221 pp.

Freist-Dorr M (1992b) Das Einzelbaumwachstum in langfristig beobachteten Mischbestandsversuchen, dargestellt am Beispiel der Eichen-Buchen-Versuchsfläche Waldbrunn 105. Forstw Cbl 111, 106-116.

Führer H-W (1990) Einflüsse des Waldes und waldbaulicher Maßnahmen auf Höhe, zeitliche Verteilung und Qualität des Abflusses aus kleinen Einzugsgebieten. Forstliche Forschungsberichte München 106, 326 pp.

Gallé A, Feller U (2007) Changes of photosynthetic traits in beech saplings (*Fagus sylvatica*) under severe drought stress and during recovery. Physiol Plant 131, 412-421.

Gartner BL, Meinzer FC (2005) Structure-function relationships in sapwood water transport and storage. In: Holbrook NM, Zwieniecki MA (eds) Vascular transport in plants. Elsevier Academic Press, Amsterdam, pp 307-331.

Gascó A, Nardini A, Gortan E, Salleo S (2006) Ion-mediated increase in the hydraulic conductivity of Laurel stems: role of pits and consequences for the impact of cavitation on water transport. Plant Cell Environ 29, 1946-1955.

Gascó A, Salleo S, Gortan E, Nardini A (2007) Seasonal changes in the ion-mediated increase of xylem hydraulic conductivity in stems of three evergreens: any functional role? Physiol Plant 129, 597-606.

Gasson P (1985) Automatic measurement of vessel lumen area and diameter with particular reference to pedunculate oak and common beech. IAWA Bull ns 6, 219-237.

Gasson P (1987) Some implications of anatomical variations in the wood of pedunculate oak (*Quercus robur* L.), including comparison with common beech (*Fagus sylvatica* L.). IAWA Bull ns 8, 149-166.

Gaydarova PN (2003) Deciduous forest communities in the Black Sea coastal Strandzha region: temporal and spatial characteristics of leaf area index and density. Trees 17, 237-243.

Gerke H (1987) Untersuchungen zum Wasserhaushalt eines Kalkbuchenwald-Ökosystems und zur Wasserbewegung in flachgründigen Böden und im durchwurzelten Kalkgestein als Grundlage zur Modellentwicklung. Ber Forschungszentrum Waldökosysteme/Waldsterben A27, 189 pp.

Gerstberger P (ed) (2001) Waldökosystemforschung in Nordbayern: Die BITÖK-Untersuchungsflächen im Fichtelgebirge und Steigerwald. Bayreuther Forum Ökologie 90, 194 pp.

Geßler A, Keitel C, Kreuzwieser J, Matyssek R, Seiler W, Rennenberg H (2007) Potential risks for European beech (*Fagus sylvatica* L.) in a changing climate. Trees 21, 1-11.

Geßler A, Rienks M, Dopatka T, Rennenberg H (2005) Radial variation of sap flow in the sap-wood of beech trees (*Fagus sylvatica* L.). Phyton 45, 257-266.

Geßler A, Schrempp S, Matzarakis A, Mayer H, Rennenberg H, Adams MA (2001) Radiation modifies the effect of water availability on the carbon isotope composition of beech (*Fagus sylvatica*). New Phytol 150, 653-664.

Gholz HL (1982) Environmental limits on above-ground net primary production, leaf-area, and biomass in vegetation zones of the Pacific Northwest. Ecology 63, 469-481.

Gieger T, Thomas FM (2002) Effects of defoliation and drought stress on biomass partitioning and water relations of *Quercus robur* and *Quercus petraea*. Basic Appl Ecol 3, 171-181.

Gieger T, Thomas FM (2005) Differential response of two Central-European oak species to single and combined stress factors. Trees 19, 607-618.

Glavac V, Koenies H, Ebbin U (1990) Auswirkung sommerlicher Trockenheit auf die Splintholz-Wassergehalte im Stammkörper der Buche (*Fagus sylvatica* L.). Holz Roh Werkst 48, 437-441.

Göpfert F (1950) Bestockung- und Betriebsziele im unterfränkischen Steigerwald. Printed in AFZ 35, 431-434, 1980.

Goulden ML, Field CB (1994) Three methods for monitoring the gas exchange of individual tree canopies: ventilated-chamber, sap-flow and Penman-Monteith measurements on evergreen oaks. Funct Ecol 8, 125-135.

Gower ST, Kucharik CJ, Norman JM (1999) Direct and indirect estimation of leaf area index,  $f_{APAR}$ , and net primary production of terrestrial ecosystems. Remote Sens Environ 70, 29-51.

Gower ST, Norman JM (1991) Rapid estimation of leaf area index in conifer and broad-leaf plantations. Ecology 72, 1896-1900.

Granier A (1985) Une nouvelle méthode pour la mesure du flux de sève brute dans le tronc des arbres. Ann Sci For 42, 193-200.

- Granier A (1987a) Evaluation of transpiration in a Douglas-fir stand by means of sap flow measurements. *Tree Physiol* 3, 309-320.
- Granier A (1987b) Mesure du flux de sève brute dans le tronc du Douglas par une nouvelle méthode thermique. *Ann Sci For* 44, 1-14.
- Granier A, Anfodillo T, Sabatti M, Cochard H, Dreyer E, Tomasi M, Valentini R, Bréda N (1994) Axial and radial water flow in the trunks of oak trees: a quantitative and qualitative analysis. *Tree Physiol* 14, 1383-1396.
- Granier A, Aubinet M, Epron D, Falge E, Gudmundsson J, Jensen NO, Köstner B, Matteucci G, Pilegaard K, Schmidt M, Tenhunen J (2003) Deciduous forests: carbon and water fluxes, balances and ecophysiological determinants. In: Valentini R (ed) *Fluxes of carbon, water and energy of European forests*. Ecol Stud 163, Springer-Verlag, Berlin, Germany, pp 55-70.
- Granier A, Aubinet M, Epron D, Falge E, Gudmundsson J, Jensen NO, Köstner B, Matteucci G, Pilegaard K, Schmidt M, Tenhunen J (2003) Deciduous forests: carbon and water fluxes, balances and ecophysiological determinants. In: Valentini R (ed) *Fluxes of carbon, water and energy of European forests*. Ecol Stud 163, Springer-Verlag, Berlin, Germany, 55-70.
- Granier A, Biron P, Bréda N, Pontailler J-Y, Saugier B (1996b) Transpiration of trees and forest stands: short and long-term monitoring using sapflow methods. *Global Change Biol* 2, 265-274.
- Granier A, Biron P, Köstner B, Gay LW, Najjar G (1996a) Comparisons of xylem sap flow and water vapour flux at the stand level and derivation of canopy conductance for Scots pine. *Theor Appl Climatol* 53, 115-122.
- Granier A, Biron P, Lemoine D (2000a) Water balance, transpiration and canopy conductance in two beech stands. *Agric For Meteorol* 100, 291-308.
- Granier A, Bobay V, Gash JHC, Gelpe J, Saugier B, Shuttleworth WJ (1990) Vapour flux density and transpiration rate comparisons in a stand of Maritime pine (*Pinus pinaster* Ait.) in Les Landes forest. *Agric For Meteorol* 51, 309-319.
- Granier A, Bréda N (1996) Modelling canopy conductance and stand transpiration of an oak forest from sap flow measurements. *Ann Sci For* 53, 537-546.
- Granier A, Bréda N, Biron P, Villette S (1999) A lumped water balance model to evaluate duration and intensity of drought constraints in forest stands. *Ecol Mod* 116, 269-283.
- Granier A, Huc R, Barigah ST (1996c) Transpiration of natural rain forest and its dependence on climatic factors. *Agric For Meteorol* 78, 19-29.
- Granier A, Loustau D (1994) Measuring and modelling the transpiration of a maritime pine canopy from sap-flow data. *Agric For Meteorol* 71, 61-81.
- Granier A, Loustau D, Bréda N (2000b) A generic model of forest canopy conductance dependent on climate, soil water availability and leaf area index. *Ann For Sci* 57, 755-765.
- Granier A, Pilegaard K, Jensen NO (2002) Similar net ecosystem exchange of beech stands located in France and Denmark. *Agric For Meteorol* 114, 75-82.
- Granier A, Reichstein M, Bréda N, Janssens IA, Falge E, Ciais P, Grünwald T, Aubinet M, Berbigier P, Bernhofer C, Buchmann N, Facini O, Grassi G, Heinesch B, Ilvesniemi H, Kersten P, Knoblauch A, Köstner B, Lagergren F, Lindroth A, Longdoz B, Loustau D, Mateus J, Montagnani L, Nys C, Moors E, Papale D, Peiffer M, Pilegaard K, Pita G, Pumpanen J, Rambal S, Rebmann C, Rodrigues A, Seufert G, Tenhunen J, Vesala T, Wang Q (2007) Evidence for soil water control on carbon and water dynamics in European forests during the extremely dry year: 2003. *Agric For Meteorol* 143, 123-145.
- Gratani L, Fida C, Fiorentino E (1987) Ecophysiological features in leaves of a beech ecosystem during the growing period. *Bull Soc R Bot Belg* 120, 81-88.
- Green SR, Clothier BE (1988) Water use by kiwifruit vines and apple trees by the heat-pulse technique. *J Exp Bot* 39, 115-123.
- Green SR, McNaughton KG, Clothier BE (1989) Observations of night-time water use in kiwifruit vines and apple trees. *Agric For Meteorol* 48, 251-261.
- Greenidge KNH (1952) An approach to the study of vessel length in hardwood species. *Am J Bot* 39, 570-574.
- Grier CC, Running SW (1977) Leaf area of mature Northwestern coniferous forests: relation to site water balance. *Ecology* 58, 893-899.
- Grier CC, Waring RH (1974) Conifer foliage mass related to sapwood area. *For Sci* 20, 205-206.
- Grosser D (1977) Die Hölzer Mitteleuropas. Springer-Verlag, Berlin, Germany, 208 pp.

- Gutiérrez E (1988) Dendroecological study of *Fagus sylvatica* L. in the Montseny mountains (Spain). Acta Oecol/Oecol Plant 9, 301-309.
- Habermehl A (1982a) A new non-destructive method for determining internal wood condition and decay in living trees. 1. Principles, method and apparatus. Arboricultural Journal 6, 1-8.
- Habermehl A (1982b) A new non-destructive method for determining internal wood condition and decay in living trees. 2. Results and further developments. Arboricultural Journal 6, 121-130.
- Habermehl A, Hüttermann A, Lovas G, Ridder H-W (1990) Computer-Tomographie an Bäumen. Biologie in unserer Zeit 20, 193-200.
- Habermehl A, Ridder H-W (1979) Zerstörungsfreies Verfahren und Gerät zum Nachweis von Stammfäulen am stehenden Stamm. AFZ 34, 754-759.
- Habermehl A, Ridder H-W (1992) Computerized-tomography applied to studies on wood of living trees. Holz Roh Werkst 50, 465-474.
- Habermehl A, Ridder H-W (1993) Anwendung der mobilen Computer-Tomographie zur zerstörungsfreien Untersuchung des Holzkörpers von stehenden Bäumen (Application of computed-tomography for non-destroying investigations on wood of living trees - forestry studies). Holz Roh Werkst 51, 1-6.
- Hacke U, Sauter JJ (1995) Vulnerability of xylem to embolism in relation to leaf water potential and stomatal conductance in *Fagus sylvatica* f. *purpurea* and *Populus balsamifera*. J Exp Bot 46, 1177-1183.
- Hacke U, Sauter JJ (1996) Xylem dysfunction during winter and recovery of hydraulic conductivity in diffuse-porous and ring-porous trees. Oecologia 105, 435-439.
- Hacke UG, Stiller V, Sperry JS, Pittermann J, McCulloh KA (2001) Cavitation fatigue. Embolism and refilling cycles can weaken the cavitation resistance of xylem. Plant Physiol 125, 779-786.
- Hagemeier M (1997) Kronenstruktur und Schattenwurf verschiedener Pionier- und Schlusswald-Baumarten. Diploma thesis, University of Göttingen, Germany, 83 pp.
- Hagemeier M (2002) Funktionale Kronenarchitektur mitteleuropäischer Baumarten am Beispiel von Hängebirke, Waldkiefer, Traubeneiche, Hainbuche, Winterlinde und Rotbuche. Dissertationes Botanicae 361, Verlag J. Cramer, Berlin, 154 pp.
- Hansen U, Fiedler B, Rank B (2002) Variation of pigment composition and antioxidative systems along the canopy light gradient in a mixed beech/oak forest: a comparative study on deciduous tree species differing in shade tolerance. Trees 16, 354-364.
- Hanson PJ, Huston MA, Todd DE (2003a) Walker Branch throughfall displacement experiment. In: Hanson PJ, Wullschleger SD (eds) North American temperate deciduous forest responses to changing precipitation regimes. Ecol Stud 166. Springer-Verlag, New York, USA, pp 8-31.
- Hanson PJ, Todd DE, Joslin JD (2003b) Canopy production. In: Hanson PJ, Wullschleger SD (eds) North American temperate deciduous forest responses to changing precipitation regimes. Ecol Stud 166. Springer-Verlag, New York, USA, pp 303-315.
- Hatton TJ, Catchpole EA, Vertessy RA (1990) Integration of sapflow velocity to estimate plant water use. Tree Physiol 6, 201-209.
- Hatton TJ, Moore SJ, Reece PH (1995) Estimating stand transpiration in a *Eucalyptus populnea* woodland with the heat pulse method: Measurement errors and sampling strategies. Tree Physiol 15, 219-227.
- Hatton TJ, Wu H-I (1995) Scaling theory to extrapolate individual tree water use to stand water use. Hydrol Process 9, 527-540.
- Heil K (1996) Wasserhaushalt und Stoffumsatz in Fichten- (*Picea abies* (L.) Karst.) und Buchenökosystemen (*Fagus sylvatica* L.) der höheren Lagen des Bayerischen Waldes. PhD thesis, University of Munich, Germany, 395 pp.
- Hein S, Dhôte J-F (2006) Effect of species composition, stand density and site index on the basal area increment of oak trees (*Quercus* sp.) in mixed stands with beech (*Fagus sylvatica* L.) in northern France. Ann For Sci 63, 457-467.
- Helinska-Raczkowska L (1994) Variation of vessel lumen diameter in radial direction as an indication of the juvenile wood growth in oak (*Quercus petraea* Liebl). Ann For Sci 51: 283-290.
- Heller H, Götsche D (1986) Biomasse-Messungen an Buche und Fichte. In: Ellenberg H, Mayer R, Schauermann J (eds) Ökosystemforschung - Ergebnisse des Sollingprojekts 1966-1986. Ulmer, Stuttgart, Germany, pp 109-127.

- Herbst M (1995) Stomatal behaviour in a beech canopy: an analysis of Bowen ration measurements compared with porometer data. *Plant Cell Environ* 18, 1010-1018.
- Herbst M, Eschenbach C, Kappen L (1999) Water use in neighbouring stands of beech (*Fagus sylvatica* L.) and black alder (*Alnus glutinosa* (L.) Gaertn.) *Ann For Sci* 56, 107-120.
- Herbst M, Hörmann G (1998) Predicting effects of temperature increase on the water balance of beech forest - an application of the "Kausha" model. *Clim Change* 40, 683-698.
- Herbst M, Roberts JM, Rosier PTW, Gowing DJ (2007a) Seasonal and interannual variability of canopy transpiration of a hedgerow in southern England. *Tree Physiol* 27, 321-333.
- Herbst M, Roberts JM, Rosier PTW, Taylor ME, Gowing DJ (2007b) Edge effects and forest water use: A field study in a mixed deciduous woodland. *For Ecol Manage* 250, 176-186.
- Hillis WE (1987) Heartwood and tree exsudates. Springer-Verlag, Berlin, Germany. 268 pp.
- Hoch G, Richter A, Körner C (2003) Non-structural carbon compounds in temperate forest trees. *Plant Cell Environ* 26, 1067-1081.
- Hölscher D, Koch O, Korn S, Leuschner C (2005) Sap flux of five co-occurring tree species in a temperate broad-leaved forest during seasonal soil drought. *Trees* 19, 628-637.
- Hofmann W (1968) Vitalität der Rotbuche und Klima in Mainfranken. *Feddes Repert* 78, 135-137.
- Hogg EH (1999) Simulation of interannual responses of trembling aspen stands to climatic variation and insect defoliation in western Canada. *Ecol Mod* 114, 175-193.
- Hogg EH, Black TA, den Hartog G, Neumann HH, Zimmermann R, Hurdle PA, Blanken PD, Nesic Z, Yang PC, Staebler RM, McDonald KC, Oren R (1997) A comparison of sap flow and eddy fluxes of water vapor from a boreal deciduous forest. *J Geophys Res* 102, D24, 28929-28937.
- Hogg EH, Brandt JP, Kochtubajda B (2005) Factors affecting interannual variation in growth of western Canadian aspen forests during 1951-2000. *Can J For Res* 35, 610-622.
- Holbrook NM (1992) Frequency and time-domain dielectric measurements of stem water content in the arborescent palm, *Sabal palmetto*. *J Exp Bot* 43, 111-119.
- Holbrook NM, Ahrens ET, Burns MJ, Zwieniecki MA (2001) In vivo observation of cavitation and embolism repair using Magnetic Resonance Imaging. *Plant Physiol* 126, 27-31.
- Horstmann K (1984) Untersuchungen zum Massenwechsel des Eichenwicklers, *Tortrix viridana* L. (Lepidoptera, Tortricidae), in Unterfranken. *Z angew Entomol* 98, 73-95.
- Huber B (1935) Die physiologische Bedeutung der Ring- und Zerstreutporigkeit. *Ber Dtsch Bot Ges* 53, 711-719.
- Huber B (1956) Die Gefäßleitung. In: Ruhland W (ed) *Handbuch der Pflanzenphysiologie*, Springer-Verlag, Berlin, Germany, vol 3, pp 541-582.
- Hunt MA, Beadle CL (1998) Whole-tree transpiration and water-use partitioning between *Eucalyptus nitens* and *Acacia dealbata* weeds in a short-rotation plantation in northeastern Tasmania. *Tree Physiol* 18, 557-563.
- Huntley B, Bartlein PJ, Prentice IC (1989) Climatic control of the distribution and abundance of beech (*Fagus* L.) in Europe and North America. *J Biogeogr* 16, 551-560.
- Irvine J, Grace J (1997) Non-destructive measurements of stem water content by time domain reflectometry using short probes. *J Exp Bot* 48, 813-818.
- James SA, Clearwater MJ, Meinzer FC, Goldstein G (2002) Heat dissipation sensors of variable length for the measurement of sap flow in trees with deep sapwood. *Tree Physiol* 22, 277-283.
- James SA, Meinzer FC, Goldstein G, Woodruff D, Jones T, Restom T, Mejia M, Clearwater M, Campanello P (2003) Axial and radial water transport and internal water storage in tropical forest canopy trees. *Oecologia* 134, 37-45.
- Jansen S, Sano Y, Choat B, Rabaey D, Lens F, Dute RR (2007) Pit membranes in tracheary elements of Rosaceae and related families: new records of tori and pseudotori. *Am J Bot* 94, 503-514.
- Jiménez MS, Nadezhina N, Cermák J, Morales D (2000) Radial variation in sap flow in five laurel forest tree species in Tenerife, Canary Islands. *Tree Physiol* 20, 1149-1156.
- Jochheim H, Einert P, Ende H-P, Kallweit R, Lüttschwager D, Schindler U (2007) Wasser- und Stoffhaushalt eines Buchen-Altbestandes im Nordostdeutschen Tiefland – Ergebnisse einer 4jährigen Messperiode (Water and element budget of a mature beech stand in the northeastern German lowlands – results of a 4 years' measurement period). *Archiv Forstwesen Landschaftsökologie* 41, 1-14.
- Jones HG, Archer N, Rotenberg E, Casa R (2003) Radiation measurement for plant ecophysiology. *J Exp Bot* 54, 879-889.

- Jones HG, Sutherland RA (1991) Stomatal control of xylem embolism. *Plant Cell Environ* 14, 607-612.
- Jump AS, Hunt JM, Peñuelas J (2006) Rapid climate change-related growth decline at the southern range edge of *Fagus sylvatica*. *Global Change Biol* 12, 2163-2174.
- Jung T, Blaschke H, Oßwald W (2000) Involvement of soilborne *Phytophthora* species in Central European oak decline and the effect of site factors on the disease. *Plant Pathol* 49, 706-718.
- Kavanagh KL, Pangle R, Schotzko AD (2007) Nocturnal transpiration causing disequilibrium between soil and stem predawn water potential in mixed conifer forests of Idaho. *Tree Physiol* 27, 621-629.
- Keel SG, Pepin S, Leuzinger S, Körner C (2007) Stomatal conductance in mature deciduous forest trees exposed to elevated CO<sub>2</sub>. *Trees* 21, 151-159.
- Kelliher FM, Köstner BMM, Hollinger DY, Byers JN, Hunt JE, McSeveny TM, Meserth R, Weir PL, Schulze E-D (1992) Evaporation, xylem sap flow, and tree transpiration in a New Zealand broad-leaved forest. *Agric For Meteorol* 62, 53-73.
- Kelty MJ (1992) Comparative productivity of monocultures and mixed-species stands. In: Kelty MJ, Larson BC, Oliver CD (eds) (1992) Ecology and silviculture of mixed-species forests. Kluwer Academic Publishers, Dordrecht, The Netherlands, pp 125-141.
- Kelty MJ, Larson BC, Oliver CD (eds) (1992) Ecology and silviculture of mixed-species forests. Kluwer Academic Publishers, Dordrecht, The Netherlands, 287 pp.
- Kitin PB, Fujii T, Abe H, Funada R (2004) Anatomy of the vessel network within and between tree rings of *Fraxinus lanuginosa* (Oleaceae). *Am J Bot* 91, 779-788.
- Klebes J, Mahler G, Höwecke B (1988) Holzkundliche Untersuchungen an Buchen mit neuartigen Waldschäden. *Mitt Forst Vers- Forschungsanstalt Baden-Württemberg* 141, 65 pp.
- Kobayashi N, Hiyama T, Fukushima Y, Lopez ML, Hirano T, Fujinuma Y (2007), Nighttime transpiration observed over a larch forest in Hokkaido, Japan. *Water Resour Res* 43, W03407, doi:10.1029/2006WR005556.
- Köckenberger W, Pope JM, Xia Y, Jeffrey KR, Komor E, Callaghan PT (1997) A non-invasive measurement of phloem and xylem water flow in castor bean seedlings by nuclear magnetic resonance microimaging. *Planta* 201, 53-63.
- Kölling C, Walentowski H (2001) Die Legende zur Karte – Erläuterungen und Hinweise. LWF aktuell 31, 9-13. Bayerische Landesanstalt für Wald und Forstwirtschaft, Freising, Germany.
- König A, Mössmer R, Bäumler A (1995) Waldbauliche Dokumentation der flächigen Sturmschäden des Frühjahrs 1990 in Bayern und meteorologische Situation zur Schadenszeit. Berichte aus der Bayerischen Landesanstalt für Wald und Forstwirtschaft 2, Freising, Germany.
- Körner C (1994) Leaf diffusive conductances in the major vegetation types of the globe. In: Schulze E-D, Caldwell MM (eds) Ecophysiology of photosynthesis. *Ecol Stud* 100, Springer-Verlag, Berlin, pp 463-490.
- Körner C (1999) Alpine plant life. Functional ecology of high mountain ecosystems. Springer-Verlag, Berlin, Germany, 337 pp.
- Körner C, Wieser G, Cernusca A (1989) Der Wasserhaushalt waldfreier Gebiete in den Österreichischen Alpen zwischen 600 und 2.600 m Höhe. In: Cernusca A (ed) Struktur und Funktion von Graslandökosystemen im Nationalpark Hohe Tauern. Veröffentlichungen des österreichischen MaB-Programms Band 13. Österr Akad Wiss and Wagner, Innsbruck, 13, 119-153.
- Köstler JN, Brückner E, Bibelriether H (1968) Die Wurzeln der Waldbäume. Parey, Hamburg, Germany, 284 pp.
- Köstner B (1999) Die Transpiration von Wäldern – Quantifizierung als Xylemsaftfluss und Faktoren-abhängigkeit von Teilflüssen. Habilitation thesis, University of Bayreuth, Germany, 283 pp.
- Köstner B (2001) Evaporation and transpiration from forests in Central Europe – relevance of patch-level studies for spatial scaling. *Meteorol Atmos Phys* 76, 69-82.
- Köstner B, Biron P, Siegwolf R, Granier A (1996) Estimates of water vapor flux and canopy conductance of Scots pine at the tree level utilizing different xylem sap flow methods. *Theor Appl Climatol* 53, 105-113.
- Köstner B, Falge EM, Alsheimer M, Geyer R, Tenhunen JD (1998b) Estimating tree canopy water use via xylem sapflow in an old Norway spruce forest and a comparison with simulation-based canopy transpiration estimates. *Ann Sci For* 55, 125-139.
- Köstner B, Granier A, Cermák J (1998a) Sapflow measurements in forest stands: methods and uncertainties. *Ann Sci For* 55, 13-27.

- Köstner B, Schmidt M, Falge E, Fleck S, Tenhunen JD (2004) Atmospheric and structural controls on carbon and water relations in mixed-forest stands of beech and oak. In: Matzner E (ed) Biogeochemistry of forested catchments in a changing environment. A German case study. *Ecol Stud* 172, Springer-Verlag, Berlin, pp 69-98.
- Köstner B, Tenhunen JD, Alsheimer M, Wedler M, Scharfenberg H-J, Zimmermann R, Falge E, Joss U (2001) Controls on evapotranspiration in a spruce forest catchment in the Fichtelgebirge. In: Tenhunen JD, Lenz R, Hantschel R (eds) Ecosystem approaches to landscape management in Central Europe. *Ecol Stud* 147, Springer-Verlag, Berlin, Germany, pp 378-415.
- Köstner BMM, Schulze E-D, Kelliher FM, Hollinger DY, Byers JN, Hunt JE, McSeveny TM, Meserth R, Weir PL (1992) Transpiration and canopy conductance in a pristine broad-leaved forest of *Nothofagus*: an analysis of xylem sap flow and eddy correlation measurements. *Oecologia* 91, 350-359.
- Kolcun O (2005) Water use of forests along elevation gradients in the Berchtesgaden National Park. PhD thesis, University of Bayreuth, Germany, 203 pp.
- Koltzenburg C, Knigge W (1987) Holzeigenschaften von Buchen aus immissionsgeschädigten Beständen. *Holz Roh Werkst* 45, 81-87.
- Koop H, Hilgen P (1987) Forest dynamics and regeneration mosaic shifts in unexploited beech (*Fagus sylvatica*) stands at Fontainebleau (France). *For Ecol Manage* 20, 135-150.
- Kozlowski TT, Winget CH (1963) Patterns of water movement in forest trees. *Bot Gaz* 124, 301-311.
- Krauss KW, Young PJ, Chambers JL, Doyle TW, Twilley RR (2007) Sap flow characteristics of neotropical mangroves in flooded and drained soils. *Tree Physiol* 27, 775-783.
- Krüger S, Mößmer R (1993) Ergebnisse der Bundeswaldinventur für Bayern. *AFZ* 48, 1198-1201.
- Krüger S, Mößmer R, Bäumler A (1994) Der Wald in Bayern. Ergebnisse der Bundeswaldinventur 1986-1990. Berichte aus der LWF 1, 91 pp, Bayerische Landesanstalt für Wald und Forstwirtschaft, Freising, Germany.
- Kruijt B (1989) Estimating canopy structure of an oak forest at several scales. *Forestry* 62, 269-284.
- Kubota M, Tenhunen J, Zimmermann R, Schmidt M, Adiku S, Kakubari Y (2005b) Influences of environmental factors on the radial profile of sap flux density in *Fagus crenata* growing at different elevations in the Naeba Mountains, Japan. *Tree Physiol* 25, 537-548.
- Kubota M, Tenhunen J, Zimmermann R, Schmidt M, Kakubari Y (2005a) Influence of environmental conditions on radial patterns of sap flux density of a 70-year *Fagus crenata* trees in the Naeba Mountains, Japan. *Ann For Sci* 62, 289-296.
- Kučera J, Cermák J, Penka M (1977) Improved thermal method of continual recording the transpiration flow rate dynamics. *Biol Plant* 19, 413-420.
- Kučera J, Tatarinov F (2003) Physical background of thermal methods of tree sap flow measurement. *Geophys Research Abstracts* 5, 886.
- Kučera L (1975) Die dreidimensionale Strukturanalyse des Holzes. 2. Das Gefäß/Strahl-Netz bei der Buche (*Fagus sylvatica* L.). *Holz Roh Werkst* 33, 276-282.
- Kucharik CJ, Norman JM, Gower ST (1998) Measurements of branch area and adjusting leaf area index indirect measurements. *Agric For Meteorol* 91, 69-88.
- Kucharik CJ, Norman JM, Gower ST (1999) Characterization of radiation regimes in nonrandom forest canopies: theory, measurements, and a simplified modeling approach. *Tree Physiol* 19, 695-706.
- Kumagai T, Aoki S, Nagasawa H, Mabuchi T, Kubota K, Inoue S, Utsumi Y, and Otsuki K (2005a) Effects of tree-to-tree and radial variations on sap flow estimates of transpiration in Japanese cedar. *Agric For Meteorol* 135, 110-116.
- Kumagai T, Nagasawa H, Mabuchi T, Ohsaki S, Kubota K, Kogi K, Utsumi Y, Koga S, Otsuki K (2005b) Sources of error in estimating stand transpiration using allometric relationships between stem diameter and sapwood area for *Cryptomeria japonica* and *Chamaecyparis obtusa*. *For Ecol Manage* 206, 191-195.
- Ladefoged K (1952) The periodicity of wood formation. *Dan Biol Skr* 7, 1-98.
- Ladefoged K (1963) Transpiration of forest trees in closed stands. *Physiol Plant* 16, 378-414.
- Ladekarl UL, Rasmussen KR, Christensen S, Jense KH, Hansen B (2005) Groundwater recharge and evapotranspiration for two natural ecosystems covered with oak and heather. *J Hydrol* 300, 76-99.
- Lang S (1999) Ökophysiologische und anatomische Untersuchungen zum Saftfluss in verschiedenen Splintholzbereichen von *Fagus sylvatica* L. PhD thesis, University of Karlsruhe, Germany, 184 pp.

- Langusch J, Kalbitz K (2001) Bodenkundliche Charakterisierung der Intensiv-Messfläche Steinkreuz. Bayreuther Forum Ökologie 90, 159-167.
- Larson BC (1992) Pathways of development in mixed-species stands. In: Kelty MJ, Larson BC, Oliver CD (eds) Ecology and silviculture of mixed-species forests. Kluwer Academic Publishers, Dordrecht, The Netherlands, pp 3-10.
- Lassoie JP, Scott DRM, Fritschen LJ (1977) Transpiration studies in Douglas-fir using the heat pulse technique. For Sci 23, 377-390.
- Law BE, Falge E, Gu L, Baldocchi DD, Bakwin P, Berbigier P, Davis K, Dolman AJ, Falk M, Fuentes JD, Goldstein A, Granier A, Grelle A, Hollinger D, Janssens IA, Jarvis P, Jensen NO, Katul G, Mahli Y, Matteucci G, Meyers T, Monson R, Munger W, Oechel W, Olson R, Pilegaard K, Paw U KT, Thorgeirsson H, Valentini R, Verma S, Vesala T, Wilson K, Wofsy S (2002) Environmental controls over carbon dioxide and water vapor exchange of terrestrial vegetation. Agric For Meteorol 113, 97-120.
- Law BE, Goldstein AH, Anthoni PM, Unsworth MH, Panek JA, Bauer MR, Fracheboud JM, Hultman N (2001) Carbon dioxide and water vapor exchange by young and old ponderosa pine ecosystems during a dry summer. Tree Physiol 21, 299-308.
- Le Dantec V, Dufrêne E, Saugier B (2000) Interannual and spatial variation in maximum leaf area index of temperate deciduous stands. For Ecol Manage 134, 71-81.
- Leblanc SG, Chen JM (2001) A practical scheme for correcting multiple scattering effects on optical LAI measurements. Agric For Meteorol 110, 125-139.
- Leblanc SG, Chen JM, Fernandes R, Deering DW, Conley A (2005) Methodology comparison for canopy structure parameters extraction from digital hemispherical photography in boreal forests. Agric For Meteorol 129, 187-207.
- Lebourgeois F, Cousseau G, Ducos Y (2004) Climate-tree-growth relationships of *Quercus petraea* Mill. stand in the Forest of Bercé ("Futaie des Clos", Sarthe, France). Ann For Sci 61, 361-372.
- Lefsky MA, Cohen WB, Parker GG, Harding DJ (2002) Lidar Remote Sensing for Ecosystem Studies. Bioscience 52, 19-30.
- Lemée G (1987) Les populations de chênes (*Quercus petraea*) des réserves biologiques de la Tillae et du Gros Fouteau en forêt de Fontainebleau: structure, démographie et évolution. Rev Ecol 42, 329-356.
- Lemée G, Faillie A, Pontailler JY, Roger JM (1992) Hurricanes and regeneration in a natural beech forest. In: Teller A, Mathy P, Jeffers JNR (eds) Responses of forest ecosystems to environmental changes. Elsevier Science Publishers, London, UK, pp 987-988.
- Lemoine D, Cochard H, Granier A (2002) Within crown variation in hydraulic architecture in beech (*Fagus sylvatica* L): evidence for stomatal control of xylem embolism. Ann Sci For 59, 19-27.
- Lemoine D, Granier A, Cochard H (1999) Mechanism of freeze-induced embolism in *Fagus sylvatica* L. Trees 13, 206-210.
- Leuschner C (1993) Patterns of soil water depletion under coexisting oak and beech trees in a mixed stand. Phytocoenologia 23, 19-33.
- Leuschner C (1994) Walddynamik in der Lüneburger Heide: Ursachen, Mechanismen und die Rolle der Ressourcen. Habilitation thesis, University of Göttingen, Germany, 368 pp.
- Leuschner C (1997) Das Konzept der potentiellen natürlichen Vegetation (PNV): Schwachstellen und Entwicklungsperspektiven. Flora 192, 379-391.
- Leuschner C (1998) Mechanismen der Konkurrenzüberlegenheit der Rotbuche. Ber Reinh-Tüxen-Ges 10, 5-18.
- Leuschner C (2001) Changes in forest ecosystem function with succession in the Lüneburger Heide. In: Tenhunen JD, Lenz R, Hantschel R (eds) Ecosystem approaches to landscape management in Central Europe. Ecol Stud 147, Springer-Verlag, Berlin, Germany, pp 517-568.
- Leuschner C, Backes K, Hertel D, Schipka F, Schmitt U, Terborg O, Runge M (2001a) Drought responses at leaf, stem and fine root levels of competitive *Fagus sylvatica* L. and *Quercus petraea* (Matt) Liebl. trees in dry and wet years. For Ecol Manage 149, 33-46.
- Leuschner C, Coners H, Icke R (2004a) In situ measurement of water absorption by fine roots of three temperate trees: species differences and differential activity of superficial and deep roots. Tree Physiol 24, 1359-1367.

- Leuschner C, Coners H, Icke R, Hartmann K, Effinger ND, Schreiber L (2003) Chemical composition of the periderm in relation to in situ water absorption rates of oak, beech and spruce fine roots. *Ann For Sci* 60, 763-772.
- Leuschner C, Hertel D (2003) Fine root biomass of temperate forests in relation to soil acidity and fertility, climate, age and species. *Prog Bot* 64, 405-438.
- Leuschner C, Hertel D, Coners H, Büttner V (2001b) Root competition between beech and oak: a hypothesis. *Oecologia* 126, 276-284.
- Leuschner C, Hertel D, Schmid I, Koch O, Muhs A, Hölscher D (2004b) Stand fine root biomass and fine root morphology in old-growth beech forests as a function of precipitation and soil fertility. *Plant Soil* 258, 43-56.
- Leuschner C, Voß S, Foetzki A, Clases Y (2006) Variation in leaf area index and stand leaf mass of European beech across gradients of soil acidity and precipitation. *Plant Ecol* 186, 247-258.
- Leuzinger S, Zotz G, Asshoff R, Körner C (2005) Responses of deciduous forest trees to severe drought in Central Europe. *Tree Physiol* 25, 641-650.
- Lévy G, Becker M, Duhamel D (1992) A comparison of the ecology of pedunculate and sessile oaks: radial growth in the centre and northwest of France. *For Ecol Manage* 55, 51-63.
- Li-Cor (1992) LAI-2000 plant canopy analyzer operating manual. Li-Cor Inc., Lincoln, USA.
- Lischeid G (2001) Geologie des Einzugsgebietes Steinkreuz. Bayreuther Forum Ökologie 90, 127-131.
- López-Portillo J, Ewers FW, Angeles G (2005) Sap salinity effects on xylem conductivity in two mangrove species. *Plant Cell Environ* 28, 1285-1292.
- Lovas G (1991) Computertomographische Untersuchungen an stehenden Bäumen. Ber Forschungszentrum Waldökosysteme A70, 90 pp.
- Lovas G (1994) CT-Untersuchungen zum Nachweis der jahreszeitlichen Wassergehaltsänderungen in Bäumen. In: Habermehl A (ed) Die Computer-Tomographie als diagnostische Methode bei der Untersuchung von Bäumen. Baum-Zeitung Verlag, Minden, Germany, pp 38-44.
- Lu P, Biron P, Bréda N, Granier A (1995) Water relations of adult Norway spruce (*Picea abies* (L.) Karst.) under soil drought in the Vosges mountains: water potential, stomatal conductance and transpiration. *Ann Sci For* 52, 117-129.
- Lu P, Müller WJ, Chacko EK (2000) Spatial variations in xylem sap flux density in the trunk of orchard-grown, mature mango trees under changing soil water conditions. *Tree Physiol* 20, 683-692.
- Lu P, Urban L, Zhao P (2004) Granier's thermal dissipation probe (TDP) method for measuring sap flow in trees: Theory and practice. *Acta Bot Sinica* 46, 631-646.
- Lütschwager D, Remus R (2007) Radial distribution of sap flux density in trunks of a mature beech stand. *Ann For Sci* 64, 431-438.
- Lundblad M, Lagergren F, Lindroth A (2001) Evaluation of heat balance and heat dissipation methods for sapflow measurements in pine and spruce. *Ann For Sci* 58, 625-638.
- Luyssaert S, Inglima I, Jung M, Richardson AD, Reichstein M, Papale D, Piao SL, Schulze E-D, Wingate L, Matteucci G, Aragao L, Aubinet M, Beer C, Bernhofer C, Black KG, Bonal D, Bonnefond J-M, Chambers J, Ciais P, Cook B, Davis KJ, Dolman AJ, Gielen B, Goulden M, Grace J, Granier A, Grelle A, Griffis T, Grünwald T, Guidolotti G, Hanson PJ, Harding R, Hollinger DY, Hutyra LR, Kolari P, Kruijt B, Kutsch W, Lagergren F, Laurila T, Law BE, Le Maire G, Lindroth A, Loustau D, Malhi Y, Mateus J, Migliavacca M, Misson L, Montagnani L, Moncrieff J, Moors E, Munger JW, Nikinmaa E, Ollinger SV, Pita G, Rebmann C, Roupsard O, Saigusa N, Sanz MJ, Seufert G, Sierra C, Smith M-L, Tang J, Valentini R, Vesala T, Janssens IA (2007) CO<sub>2</sub> balance of boreal, temperate, and tropical forests derived from a global database. *Global Change Biol* doi:10.1111/j.1365-2486.2007.01439.x
- Ma S, Baldocchi DD, Xu L, Hehn T (2007) Inter-annual variability in carbon dioxide exchange of an oak/grass savanna and open grassland in California. *Agric For Meteorol* 147, 157-171.
- Mäkelä A, Valentine HT (2006) Crown ratio influences allometric scaling in trees. *Ecology* 87, 2967-2972.
- Magel E, Hillinger C, Höll W, Ziegler H (1997) Biochemistry and physiology of heartwood formation: role of reserve substances. In: Rennenberg H, Eschrich W, Ziegler H (eds) *Trees – contributions to modern tree physiology*. Backhuys Publishers, Leiden, The Netherlands, pp 477-506.
- Magnani F, Borghetti M (1995) Interpretation of seasonal changes of xylem embolism and plant hydraulic resistance in *Fagus sylvatica*. *Plant Cell Environ* 18, 689-696.

- Magnani F, Leonardi S, Tognetti R, Grace J, Borghetti M (1998) Modelling the surface conductance of a broad-leaf canopy: effects of partial decoupling from the atmosphere. *Plant Cell Environ* 21, 867-879.
- Mainiero R, Kazda M (2006) Depth-related fine root dynamics of *Fagus sylvatica* during exceptional drought. *For Ecol Manage* 237, 135-142.
- Makowka I, Stickan W, Worbes M (1991) Jahrringbreitenmessung an Buchen (*Fagus sylvatica* L.) im Solling; Analyse des Klimaeinflusses auf den jährlichen Holzzuwachs. Ber Forschungszentrum Waldökosysteme B18, 83-159.
- Marc V, Robinson M (2004) Application of the deuterium tracing method for the estimation of tree sap flow and stand transpiration of a beech forest (*Fagus sylvatica* L.) in a mountainous Mediterranean region. *J Hydrol* 285, 248-259.
- Mark WR, Crews DL (1973) Heat-pulse velocity and bordered pit condition in living Engelmann spruce and lodgepole pine trees. *For Sci* 19, 291-296.
- Martin TA, Brown KJ, Cermák J, Ceulemans R, Kučera J, Meinzer FC, Rombold JS, Sprugel DG, Hinckley TM (1997) Crown conductance and tree and stand transpiration in a second-growth *Abies amabilis* forest. *Can J For Res* 27, 797-808.
- Matyssek R, Cermák J, Kučera J (1991) Ursacheneingrenzung eines lokalen Buchensterbens mit einer Messmethode der Kronendachtranspiration. *Schweiz Z Forstwes* 142, 809-828.
- Matzner E (ed) (2004) Biogeochemistry of forested catchments in a changing environment. A German case study. *Ecol Stud* 172, Springer-Verlag, Berlin, Germany, 520 pp.
- Matzner E, Köstner B (eds) (2001) Grundlagen zur nachhaltigen Entwicklung von Ökosystemen bei veränderter Umwelt. BITÖK Forschungsbericht 1998-2000. Bayreuther Forum Ökologie 84, 382 pp.
- Mayer K-H (1998) Die Forstgeschichte des Fichtelgebirges. *Forstliche Forschungsberichte München* 167, 297 pp.
- McCulloh KA, Sperry JS, Adler FR (2004) Murray's law and the hydraulic vs mechanical functioning of wood. *Funct Ecol* 18, 931-938.
- McCulloh KA, Winter K, Meinzer FC, Garcia M, Aranda J, Lachenbruch B (2007) A comparison of daily water use estimates derived from constant-heat sap-flow probe values and gravimetric measurements in pot-grown saplings. *Tree Physiol* 27, 1355-1360.
- McDowell N, Barnard H, Bond BJ, Hinckley T, Hubbard RM, Ishii H, Köstner B, Magnani F, Marshall JD, Meinzer FC, Phillips N, Ryan MG, Whitehead D (2002) The relationship between tree height and leaf area:sapwood area ratio. *Oecologia* 132, 12-20.
- Meadows JS, Hodges JD (2002) Sapwood area as an estimator of leaf area and foliar weight in cherrybark oak and green ash. *For Sci* 48, 69-76.
- Meinzer FC (2002) Co-ordination of vapour and liquid phase water transport properties in plants. *Plant Cell Environ* 25, 265-274.
- Meinzer FC (2003) Functional convergence in plant responses to the environment. *Oecologia* 134, 1-11.
- Meinzer FC, Bond BJ, Warren JM, Woodruff DR (2005) Does water transport scale universally with tree size? *Funct Ecol* 19, 558-565.
- Meinzer FC, Brooks JR, Domec J-C, Gartner BL, Warren JM, Woodruff DR, Bible K, Shaw DC (2006) Dynamics of water transport and storage in conifers studied with deuterium and heat tracing techniques. *Plant Cell Environ* 29, 105-114.
- Meinzer FC, Clearwater MJ, Goldstein G (2001) Water transport in trees: current perspectives, new insights and some controversies. *Env Exp Bot* 45, 239-262.
- Mencuccini M, Hölttä T, Petit G, Magnani F (2007) Sanio's laws revisited. Size-dependent changes in the xylem architecture of trees. *Ecol Lett* 10, 1084-1093.
- Meusel H, Jäger E, Weinert E (1965) Vergleichende Chorologie der zentraleuropäischen Flora. Gustav Fischer Verlag, Jena, Germany. 583 + 258 pp.
- Meynen E, Schmithüsen J (eds) (1953-1962) Handbuch der naturräumlichen Gliederung Deutschlands. Bundesanstalt für Landeskunde und Raumforschung, Bad Godesberg, Germany, 1339 pp.
- Miller DR, Vavrina CA, Christensen TW (1980) Measurement of sap flow and transpiration in ring-porous oaks using the heat pulse velocity technique. *For Sci* 26, 485-494.
- Miller WH (1988) Design and implementation of a portable computerized axial tomography system for field use. *Nucl Instrum Methods A*, 270, 590-597.

- Moore GW, Bond BJ, Jones JA, Phillips N, Meinzer FC (2004) Structural and compositional controls on transpiration in 40- and 450-year-old riparian forests in western Oregon, USA. *Tree Physiol* 24, 481-491.
- Mussche S, Samson R, Nachtergale L, De Schrijver A, Lemeur R, Lust N (2001) A comparison of optical and direct methods for monitoring the seasonal dynamics of leaf area index in deciduous forests. *Silva Fenn* 35, 373-384.
- Nadezhina N, Cermák J (2000) Responses of sap flow rate along tree stem and coarse root radii to changes of water supply. In: Stokes A (ed) *The supporting roots of trees and woody plants: Form, function and physiology*. Kluwer Academic Publishers, Dordrecht, Netherlands, pp 227-238.
- Nadezhina N, Cermák J, Ceulemans R (2002) Radial patterns of sap flow in woody stems of dominant and understory species: scaling errors associated with positioning of sensors. *Tree Physiol* 22, 907-918.
- Nadezhina N, Cermák J, Meiresonne L, Ceulemans R (2007) Transpiration of Scots pine in Flanders growing on soil with irregular substratum. *For Ecol Manage* 243, 1-9.
- Nepveu G (1981) Propriétés du bois de hêtre. In: Teissier du Cros et al. (eds) *Le hêtre*. INRA, Paris, France, pp 377-409.
- Niinemets Ü (1995) Distribution of foliar carbon and nitrogen across the canopy of *Fagus sylvatica*: adaptation to a vertical light gradient. *Acta Oecol* 16, 525-541.
- Niinemets Ü, Kull O, Tenhunen JD (2004) Within-canopy variation in the rate of development of photosynthetic capacity is proportional to integrated quantum flux density in temperate deciduous trees. *Plant Cell Environ* 27, 293-313.
- Nizinski J, Saugier B (1989) Dynamique de l'eau dans une chênaie (*Quercus petraea* (Matt.) Liebl.) en forêt de Fontainebleau. *Ann Sci For* 46, 173-186.
- Norman JM, Campbell GS (1989) Canopy structure. In: Percy RW, Ehleringer J, Mooney HA, Rundel PW (eds) *Plant physiological ecology: field methods and instrumentation*. Chapman and Hall, New York, USA, pp 301-325.
- Nüßlein S (1995) Struktur und Wachstumsdynamik jüngerer Buchen-Edellaubholz-Mischbestände in Nordbayern. *Forstliche Forschungsberichte München* 151, 295 pp.
- Oberforstdirektion Oberfranken (1999) *Forstwirtschaftsplan für das Forstamt Ebrach*.
- Oliver CD (1992) Similarities of stand structures and stand development processes throughout the world – some evidence and applications to silviculture through adaptive management. In: Kelty MJ, Larson BC, Oliver CD (eds) *Ecology and silviculture of mixed-species forests*. Kluwer Academic Publishers, Dordrecht, The Netherlands, pp 11-26.
- Oliver CD, Larson BC (1990) *Forest stand dynamics*. Mc Graw-Hill, New York, USA, 467 pp.
- Oliveras I, Llorens P (2001) Medium-term sap flux monitoring in a Scots pine stand: analysis of the operability of the heat dissipation method for hydrological purposes. *Tree Physiol* 21, 473-480.
- Onoe M, Tsao JW, Yamada H, Nakamura H, Kogure J, Kawamura H, Yoshimatsu M (1983) Computed tomography for measuring the annual rings of a live tree. *Proc IEEE* 71, 907-908.
- Oren R, Pataki DE (2001) Transpiration in response to variation in microclimate and soil moisture in southeastern deciduous forests. *Oecologia* 127, 549-559.
- Oren R, Phillips N, Ewers BE, Pataki DE, Megonigal JP (1999) Sap-flux-scaled transpiration responses to light, vapor pressure deficit, and leaf area reduction in a flooded *Taxodium distichum* forest. *Tree Physiol* 19, 337-347.
- Oren R, Phillips N, Katul G, Ewers BE, Pataki DE (1998) Scaling xylem sap flux and soil water balance and calculating variance: a method for partitioning water flux in forests. *Ann Sci For* 55, 191-216.
- Orians CM, Vuuren van MMI, Harris NL, Babst BA, Ellmore GS (2004) Differential sectoriality in long-distance transport in temperate tree species: evidence from dye flow, <sup>15</sup>N transport, and vessel element pitting. *Trees* 18, 501-509.
- Osada N, Tateno R, Hyodo F, Takeda H (2004) Changes in crown architecture with tree height in two deciduous tree species: developmental constraints or plastic response to the competition for light? *For Ecol Manage* 188, 337-347.
- Owen KE, Tenhunen J, Reichstein M, Wang Q, Falge E, Geyer R, Xiao X, Stoy P, Ammann C, Arain A, Aubinet M, Aurela M, Bernhofer C, Chojnicki BH, Granier A, Gruenwald T, Hadley J, Heinesch B, Hollinger D, Knohl A, Kutsch W, Lohila A, Meyers T, Moors E, Moureaux C, Pilegaard K, Saigusa N, Verma S, Vesala T, Vogel C (2007) Linking flux network measurements to continental scale

- simulations: ecosystem carbon dioxide exchange capacity under non-water-stressed conditions. *Global Change Biol* 13, 734-760.
- Parker GG, Harding DJ, Berger ML (2004) A portable LIDAR system for rapid determination of forest canopy structure. *J Appl Ecol* 41, 755-767.
- Pataki DE, Oren R (2003) Species differences in stomatal control of water loss at the canopy scale in a mature bottomland deciduous forest. *Adv Water Resour* 26, 1267-1278.
- Pataki DE, Oren R, Katul G, Sigmon J (1998) Canopy conductance of *Pinus taeda*, *Liquidambar styraciflua* and *Quercus phellos* under varying atmospheric and soil water conditions. *Tree Physiol* 18, 307-315.
- Pataki DE, Oren R, Smith WK (2000) Sap flux of co-occurring species in a western subalpine forest during seasonal soil drought. *Ecology* 81, 2557-2566.
- Patzner KM (2004) Die Transpiration von Waldbäumen als Grundlage der Validierung und Modellierung der Bestandestranspiration in einem Wassereinzugsgebiet des Flusses 'Ammer'. PhD thesis, Technical University of Munich, Germany, 172 pp.
- Pausch RC, Grote EE, Dawson TE (2000) Estimating water use by sugar maple trees: considerations when using heat-pulse methods in trees with deep functional sapwood. *Tree Physiol* 20, 217-227.
- Peck A, Mayer H (1996) Einfluß von Bestandesparametern auf die Verdunstung von Wäldern (Influence of stand parameters on evapotranspiration in forests). *Forstw Cbl* 115, 1-9.
- Pellinen P (1986) Biomasseuntersuchungen im Kalkbuchenwald. PhD thesis, University of Göttingen, Germany, 145 pp.
- Peters R (1992) Can beech adapt to climatical change? In: Teller A, Mathy P, Jeffers JNR (eds) *Responses of forest ecosystems to environmental changes*. Elsevier Science Publishers, London, UK, pp 639-640.
- Peters R (1997) Beech forests. *Geobotany* 24, Kluwer Academic Publishers, Dordrecht, The Netherlands, 169 pp.
- Petit RJ, Bodénès C, Ducousoo A, Roussel G, Kremer A (2004) Hybridization as a mechanism of invasion in oaks. *New Phytol* 161, 151-164.
- Phillips N, Bond BJ, McDowell NG, Ryan MG (2002) Canopy and hydraulic conductance in young, mature and old Douglas-fir trees. *Tree Physiol* 22, 205-211.
- Phillips N, Bond BJ, McDowell NG, Ryan MG, Schauer A (2003b) Leaf area compounds height-related hydraulic costs of water transport in Oregon White Oak trees. *Funct Ecol* 17, 832-840.
- Phillips N, Oren R, Zimmermann R (1996) Radial patterns of xylem sap flow in non-, diffuse- and ring-porous tree species. *Plant Cell Environ* 19, 983-990.
- Phillips N, Oren R, Zimmermann R, Wright SJ (1999) Temporal patterns of water flux in trees and lianas in a Panamanian moist forest. *Trees* 14, 116-123.
- Phillips NG, Ryan MG, Bond BJ, McDowell NG, Hinckley TM, Cermák J (2003a) Reliance on stored water increases with tree size in three species in the Pacific Northwest. *Tree Physiol* 23, 237-245.
- Piutti E, Cescatti A (1997) A quantitative analysis of the interactions between climatic response and intraspecific competition in European beech. *Can J For Res* 27, 277-284.
- Planchais I, Pontailler JY (1999) Validity of leaf areas and angles estimated in a beech forest from analysis of gap frequencies, using hemispherical photographs and a plant canopy analyzer. *Ann Sci For* 56, 1-10.
- Polomski J, Kuhn N (1998) *Wurzelsysteme*. Haupt, Bern, Switzerland, 290 pp.
- Ponton S, Dupouey J-L, Bréda N, Dreyer E (2002) Comparison of water-use efficiency of seedlings from two sympatric oak species: genotype x environment interactions. *Tree Physiol* 22, 413-422.
- Ponton S, Dupouey J-L, Bréda N, Feuillat F, Bodénès C, Dreyer E (2001) Carbon isotope discrimination and wood anatomy variations in mixed stands of *Quercus robur* and *Quercus petraea*. *Plant Cell Environ* 24, 861-868.
- Pothier D, Margolis HA, Poliquin J, Waring RH (1989b) Relation between the permeability and the anatomy of jack pine sapwood with stand development. *Can J For Res* 19, 1564-1570.
- Pothier D, Margolis HA, Waring RH (1989a) Patterns of change of saturated sapwood permeability and sapwood conductance with stand development. *Can J For Res* 19, 432-439.
- Poyatos R, Cermák J, Llorens P (2007) Variation in the radial patterns of sap flux density in pubescent oak (*Quercus pubescens*) and its implications for tree and stand transpiration measurements. *Tree Physiol* 27, 537-548.

- Poyatos R, Llorens P, Gallart F (2005) Transpiration of montane *Pinus sylvestris* L. and *Quercus pubescens* Willd. forest stands measured with sap flow sensors in NE Spain. *Hydrol Earth Syst Sci* 9, 493-505.
- Pretzsch H (1999) Waldwachstum im Wandel. *Forstw Cbl* 118, 228-250.
- Pretzsch H (2003) Diversität und Produktivität von Wäldern (Diversity and productivity of forests). *Allg Forst Jagd Ztg* 174, 88-98.
- Pretzsch H (2006) Species-specific allometric scaling under self-thinning: evidence from long-term plots in forest stands. *Oecologia* 146, 572-583.
- Prskawetz M, Lexer MJ (2000) Evaluierung des LAI-2000 zur Ermittlung des Blattflächenindex in Buchenjungbeständen. *Allg Forst Jagd Ztg* 171, 185-191.
- Raftoyannis Y, Radoglou K (2002) Physiological responses of beech and sessile oak in a natural mixed stand during a dry summer. *Ann Bot* 89, 723-730.
- Rambal S, Ourcival J-M, Joffre R, Mouillot F, Nouvellon Y, Reichstein M, Rocheteau A (2003) Drought controls over conductance and assimilation of a Mediterranean evergreen ecosystem: scaling from leaf to canopy. *Global Change Biol* 9, 1813-1824.
- Raschi A, Tognetti R, Ridder H-W, Beres C (1995) Water in the stems of sessile oak (*Quercus petraea*) assessed by computer tomography with concurrent measurements of sap velocity and ultrasound emission. *Plant Cell Environ* 18, 545-554.
- Raulier F, Bernier PY, Ung C-H, Boutin R (2002) Structural differences and functional similarities between two sugar maple (*Acer saccharum*) stands. *Tree Physiol* 22, 1147-1156.
- Rebetez M, Mayer H, Dupont O, Schindler D, Gartner K, Kropp JP, Menzel A (2006) Heat and drought 2003 in Europe: a climate synthesis. *Ann For Sci* 63, 569-577.
- Reid DEB, Silins U, Lieffers VJ (2003) Stem sapwood permeability in relation to crown dominance and site quality in self-thinning fire-origin lodgepole pine stands. *Tree Physiol* 23, 833-840.
- Reif A (1989) The Vegetation of the Fichtelgebirge: Origin, site conditions, and present status. In: Schulze E-D et al. (eds) Forest decline and air pollution. *Ecol Stud* 77, Springer-Verlag, Berlin, Germany, pp 8-22.
- Richardson AD, Hollinger DY, Aber JD, Ollinger SV, Braswell BH (2007) Environmental variation is directly responsible for short- but not long-term variation in forest-atmosphere carbon exchange. *Global Change Biol* 13, 788-803.
- Ridder H-W (1979) Ein neuer Algorithmus zur gefilterten Rückprojektion in der Computer-Tomographie. *Medizinische Physik* 13, 379-384.
- Ridder H-W (1996) Beschreibung der PC-Software zur Computer-Tomographie. Radiologie-Zentrum, University of Marburg, Germany.
- Roberts J (1977) The use of tree-cutting techniques in the study of water relations of mature *Pinus sylvestris* L. *J Exp Bot* 28, 751-767.
- Roberts J (1983) Forest transpiration: a conservative hydrological process? *J Hydrol* 66, 133-141.
- Roberts J (2007) The role of plant physiology in hydrology: looking backwards and forwards. *Hydrol Earth Syst Sci* 11, 256-269.
- Roberts J, Rosier P (2005a) The impact of broadleaved woodland on water resources in lowland UK: I. Soil water changes below beech woodland and grass on chalk sites in Hampshire. *Hydrol Earth Syst Sci* 9, 596-606.
- Roberts J, Rosier P (2005b) The impact of broadleaved woodland on water resources in lowland UK: III. The results from Black Wood and Bridgets Farm compared with those from other woodland and grassland sites. *Hydrol Earth Syst Sci* 9, 614-620.
- Roberts J, Rosier P, Smith DM (2005) The impact of broadleaved woodland on water resources in lowland UK: II. Evaporation estimates from sensible heat flux measurements over beech woodland and grass on chalk sites in Hampshire. *Hydrol Earth Syst Sci* 9, 607-613.
- Roberts J, Rosier PTW (1994) Comparative estimates of transpiration of ash and beech forest at a chalk site in southern Britain. *J Hydrol* 162, 229-245.
- Roberts S, Vertessy R, Grayson R (2001) Transpiration from *Eucalyptus sieberi* (L. Johnson) forests of different age. *For Ecol Manage* 143, 153-161.
- Roderick ML, Berry SL (2001) Linking wood density with tree growth and environment: a theoretical analysis based on the motion of water. *New Phytol* 149, 473-485.

- Röhrig E (1991) Biomass and productivity. In: Röhrig E, Ulrich B (eds) Ecosystems of the world. Vol. 7, Temperate deciduous forests. Elsevier, Amsterdam, The Netherlands, pp 165-174.
- Röhrig E (1991) Seasonality. In: Röhrig E, Ulrich B (eds) Ecosystems of the world. Vol. 7, Temperate deciduous forests. Elsevier, Amsterdam, The Netherlands, pp 25-33.
- Rogers R, Hinckley TM (1979) Foliage weight and area related to current sapwood area in oak. *For Sci* 25, 298-303.
- Roloff A (1986) Morphologie der Kronenentwicklung von *Fagus sylvatica* L. (Rotbuche) unter besonderer Berücksichtigung möglicherweise neuartiger Veränderungen. *Ber Forschungszentrum Waldökosysteme/Waldsterben* 18, 177 pp.
- Roloff A, Klugmann K (1998) Ursachen und Dynamik von Eichen-Zweigabsprüngen. *AFZ/Der Wald* 24, 202-207.
- Romberger JA, Hejnowicz Z, Hill JF (1993) Plant structure: Function and development. A treatise on anatomy and vegetative development, with special reference to woody plants. Springer-Verlag, Berlin, Germany, 524 pp.
- Rothe A (1997) Einfluss des Baumartenanteils auf Durchwurzelung, Wasserhaushalt, Stoffhaushalt und Zuwachsleistung eines Fichten-Buchen-Mischbestandes am Standort Höglwald. *Forstliche Forschungsberichte München* 163, 174 pp.
- Rothe A, Kreutzer K (1998) Wechselwirkungen zwischen Fichte und Buche im Mischbestand. *AFZ* 53, 784-787.
- Roupsard O, Ferhi A, Granier A, Pallo F, Depommier D, Mallet B, Joly HI, Dreyer E (1999) Reverse phenology and dry-season water uptake by *Faidherbia albida* (Del.) A. Chev. in an agroforestry parkland of Sudanese west Africa. *Funct Ecol* 13, 460-472.
- Rubtsov VV (1996) Influence of repeated defoliations by insects on wood increment in common oak (*Quercus robur* L.). *Ann Sci For* 53, 407-412.
- Running SW, Coughlan JC (1988) A general model of forest ecosystem processes for regional applications. I. Hydrological balance, canopy gas exchange, and primary production processes. *Ecol Mod* 42, 125-154.
- Rust S (1999) Hydraulische Architektur und Wasserhaushalt von Kiefer (*Pinus sylvestris* L.) mit begleitenden Untersuchungen an Fichte (*Picea abies* (L.) Karst.), Buche (*Fagus sylvatica* L.) und Balsampappelklonen. *Cottbuser Schriften zu Bodenschutz und Rekultivierung* 3, 107 pp.
- Rust S, Roloff A (2004) Acclimation of crown structure to drought in *Quercus robur* L. – intra- and inter-annual variation of abscission and traits of shed twigs. *Basic Appl Ecol* 5, 283-291.
- Rust S, Solger A, Roloff A (2004) Bottlenecks to water transport in *Quercus robur* L.: the abscission zone and its physiological consequences. *Basic Appl Ecol* 5, 293-299.
- Ryan MG (2002) Canopy processes research. *Tree Physiol* 22, 1035-1043.
- Ryel RJ, Caldwell MM, Yoder CK, Or D, Leffler AJ (2002) Hydraulic redistribution in a stand of *Artemisia tridentata*: evaluation of benefits to transpiration assessed with a simulation model. *Oecologia* 130, 173-184.
- Salihi OOA (1984) Potentielle Verdunstung eines Buchen- und eines Fichtenwaldes auf der Basis von Daten des Deutschen Wetterdienstes als Parameter der aktuellen Evapotranspiration. PhD thesis, University of Göttingen, Germany, 107 pp.
- Sandermann W, Hausen B, Simatupang M (1967) Orientierende Versuche zur Differenzierung von Splint und Kern sowie zum Sichtbarmachen der Übergangszone von Fichte und anderen Nadelhölzern. *Das Papier*. 21, 349-354.
- Santiago LS, Goldstein G, Meinzer FC, Fownes JH, Mueller-Dombois D (2000) Transpiration and forest structure in relation to soil waterlogging in a Hawaiian montane cloud forest. *Tree Physiol* 20, 673-681.
- Sass U, Eckstein D (1995) The variability of vessel size in beech (*Fagus sylvatica* L.) and its ecophysiological interpretation. *Trees* 9, 247-252.
- Saugier B, Granier A, Pontailler JY, Dufrêne E, Baldocchi DD (1997) Transpiration of a boreal pine forest measured by branch bag, sap flow and micrometeorological methods. *Tree Physiol* 17, 511-519.
- Savenije HHG (2004) The importance of interception and why we should delete the term evapotranspiration from our vocabulary. *Hydrol Process* 18, 1507-1511.

- Schäfer KVR (1997) Wassernutzung von *Fagus sylvatica* L. und *Quercus petraea* (MATT.) LIEBL. im Wassereinzugsgebiet Steinkreuz im Steigerwald, Bayern. Diploma thesis, University of Bayreuth, Germany, 128 pp.
- Schäfer KVR, Oren R, Lai C-T, Katul GG (2002) Hydrologic balance in an intact temperate forest ecosystem under ambient and elevated atmospheric CO<sub>2</sub> concentration. Global Change Biology 8, 895-911.
- Schäfer KVR, Oren R, Tenhunen JD (2000) The effect of tree height on crown level stomatal conductance. Plant Cell Environ 23, 365-375.
- Schaeffer SM, Williams DG, Goodrich DC (2000) Transpiration of cottonwood/willow forest estimated from sap flux. Agric For Meteorol 105, 257-270.
- Schär C, Vidale PL, Lüthi D, Frei C, Häberli C, Liniger MA, Appenzeller C (2004) The role of increasing temperature variability in European summer heatwaves. Nature 427, 332-336.
- Scheenen TWJ, Vergeldt FJ, Heemskerk AM, van As H (2007) Intact plant magnetic resonance imaging to study dynamics in long-distance sap flow and flow-conducting surface area. Plant Physiol 144, 1157-1165.
- Schiller G, Cohen S, Ungar ED, Moshe Y, Herr N (2007) Estimating water use of sclerophyllous species under East-Mediterranean climate: III. Tabor oak forest sap flow distribution and transpiration. For Ecol Manage 238, 147-155.
- Schiller G, Unger ED, Moshe Y, Cohen S, Cohen Y (2003) Estimating water use by sclerophyllous species under east Mediterranean climate: II. The transpiration of *Quercus calliprinos* Webb. in response to silvicultural treatments. For Ecol Manage 179, 483-495.
- Schipka F (2003) Blattwasserzustand und Wasserumsatz von vier Buchenwäldern entlang eines Niederschlagsgradienten in Mitteldeutschland. PhD thesis, University of Göttingen, Germany, 155 pp.
- Schipka F, Heimann J, Leuschner C (2005) Regional variation in canopy transpiration of Central European beech forests. Oecologia 143, 260-270.
- Schmid I (2002) The influence of soil type and interspecific competition on the fine root system of Norway spruce and European beech. Basic Appl Ecol 3, 339-346.
- Schneider H, Manz B, Westhoff M, Mimietz S, Szimtenings M, Neuberger T, Faber C, Krohne G, Haase A, Volke F, Zimmermann U (2003) The impact of lipid distribution, composition and mobility on xylem water refilling of the resurrection plant *Myrothamnus flabellifolia*. New Phytol 159, 487-505.
- Schulze E-D (1970) Der CO<sub>2</sub>-Gaswechsel der Buche (*Fagus sylvatica* L.) in Abhängigkeit von den Klimafaktoren im Freiland. Flora 159, 177-232.
- Schulze E-D, Cermák J, Matyssek R, Penka M, Zimmermann R, Vasícek F, Gries W, Kučera J (1985) Canopy transpiration and water fluxes in the xylem of the trunk of *Larix* and *Picea* trees – a comparison of xylem flow, porometer and cuvette measurements. Oecologia 66, 475-483.
- Sellin A (1993) Resistance to water flow in xylem of *Picea abies* (L.) Karst. trees grown under contrasting light conditions. Trees 7, 220-226.
- Shelburne VB, Hedden RL (1996) Effect of stem height, dominance class, and site quality on sapwood permeability in loblolly pine (*Pinus taeda* L.). For Ecol Manage 83, 163-169.
- Shuttleworth WJ (1989) Micrometeorology of temperate and tropical forests. Phil Trans R Soc London B 324, 299-334.
- Skomarkova MV, Vaganov EA, Mund M, Knöhl A, Linke P, Boerner A, Schulze E-D (2006) Inter-annual and seasonal variability of radial growth, wood density and carbon isotope ratios in tree rings of beech (*Fagus sylvatica*) growing in Germany and Italy. Trees 20, 571-586.
- Smaltschinski T (1990) Mischbestände in der Bundesrepublik Deutschland. Forstarchiv 61, 137-140.
- Smith DM, Allen SJ (1996) Measurement of sap flow in plant stems. J Exp Bot 47, 1833-1844.
- Sparks JP, Campbell GS, Black RA (2001) Water content, hydraulic conductivity and ice formation in winter stems of *Pinus contorta*: a TDR case study. Oecologia 127, 468-475.
- Sperber G (1983) Zehn Jahre naturgemäße Waldwirtschaft im Bayerischen Forstamt Ebrach. Forstarchiv 54, 90-97.
- Sperber G, Regehr A (1983) Vorratspflege in Unterfranken am Beispiel des Steigerwaldes. AFZ 38, 1020-1025.
- Sperry JS, Donnelly JR, Tyree MT (1988b) Seasonal occurrence of xylem embolism in sugar maple (*Acer saccharum*) Am J Bot 75, 1212-1218.

- Sperry JS, Hacke UG, Pittermann J (2006) Size and function in conifer tracheids and angiosperm vessels. Am J Bot 93, 1490-1500.
- Sperry JS, Hacke UG, Wheeler JK (2005) Comparative analysis of end wall resistivity in xylem conduits. Plant Cell Environ 28, 456-465.
- Sperry JS, Perry AH, Sullivan JEM (1991) Pit membrane degradation and air-embolism formation in ageing xylem vessels of *Populus tremuloides* Michx. J Exp Bot 42, 1399-1406.
- Sperry JS, Sullivan JEM (1992) Xylem embolism in response to freeze-thaw cycles and water stress in ring-porous, diffuse-porous, and conifer species. Plant Physiol 100, 605-613.
- Spicer R, Gartner BL (2001) The effects of cambial age and position within the stem on specific conductivity in Douglas-fir (*Pseudotsuga menziesii*) sapwood. Trees 15, 222-229.
- Spicer R, Holbrook NM (2005) Within-stem oxygen concentration and sap flow in four temperate tree species: does long-lived xylem parenchyma experience hypoxia? Plant Cell Environ 28, 192-201.
- Spiecker H (1983) Durchforstungsansätze bei Eichen unter besonderer Berücksichtigung des Dickenwachstums (Thinning intensity in oak stands with special regard to diameter growth). Allg Forst Jagd Ztg 154, 21-36.
- Steppe K, Lemeur R, Samson R (2002) Sap flow dynamics of a beech tree during the solar eclipse of 11 August 1999. Agric For Meteorol 112, 139-149.
- Stickan W, Schulte M, Kakubari Y, Niederstadt F, Schenk J, Runge M (1991) Ökophysiologische und biometrische Untersuchungen in einem Buchenbestand (*Fagus sylvatica* L.) des Sollings als ein Beitrag zur Waldschadensforschung. Berichte des Forschungszentrums Waldökosysteme B 18, pp 1-81.
- Stiller V, Sperry JS (2002) Cavitation fatigue and its reversal in sunflower (*Helianthus annuus* L.). J Exp Bot 53, 1155-1161.
- Strachan IB, McCaughey JH (1996) Spatial and vertical leaf area index of a deciduous forest resolved using the LAI-2000 plant canopy analyzer. For Sci 42, 176-181.
- Stratton L, Goldstein G, Meinzer FC (2000) Stem water storage capacity and efficiency of water transport: their functional significance in a Hawaiian dry forest. Plant Cell Environ 23, 99-106.
- Střelcová K, Matejka F, Kučera J (2004) Beech stand transpiration assessment - two methodical approaches. Ekologia-Bratislava 23, 147-162 Suppl 2.
- Střelcová K, Matejka F, Mindáš J (2002) Estimation of beech transpiration in relation to their social status in forest stand. J For Sci 48, 130-140.
- Střelcová K, Mindáš J, Škvarenina J (2006) Influence of tree transpiration on mass water balance of mixed mountain forests of the West Carpathians. Biologia 61, Suppl 19, S305-S310.
- Stuppy WH, Maisano JA, Colbert MW, Rudall PJ, Rowe TB (2003) Three-dimensional analysis of plant structure using high-resolution X-ray computed tomography. Trends Plant Sci 8, 2-6.
- Swanson RH (1967) Seasonal course of transpiration of lodgepole pine and Engelmann spruce. In: Sopper WE, Lull HW (eds) Proc Int Symp Forest Hydrology, Pergamon Press, Oxford, pp 417-432.
- Swanson RH (1974) A thermal flowmeter for estimating the rate of xylem sap ascent in trees. In: Dowdell RB (ed) Flow – its measurement and control in science and industry. Instrument Society of America, Pittsburghs, USA, pp 647-652.
- Swanson RH (1994) Significant historical developments in thermal methods for measuring sap flow in trees. Agric For Meteorol 72, 113-132.
- Swenson NG, Enquist BJ (2007) Ecological and evolutionary determinants of a key plant functional trait: wood density and its community-wide variation across latitude and elevation. Am J Bot 94, 451-459.
- Tang JW, Bolstad PV, Ewers BE, Desai AR, Davis KJ, Carey EV (2006) Sap flux-upscaled canopy transpiration, stomatal conductance, and water use efficiency in an old growth forest in the Great Lakes region of the United States. J Geophys Res 111, G02009.
- Tatarinov FA, Kučera J, Cienciala E (2005) The analysis of physical background of tree sap flow measurement based on thermal methods. Meas Sci Technol 16, 1157-1169.
- Tenhunen JD, Falge E, Ryel R, Manderscheid B, Peters K, Ostendorf B, Joss U, Lischeid G (2001) A flux model hierarchy for spruce forest ecosystems. In: Tenhunen JD, Lenz R, Hantschel R (eds) Ecosystem approaches to landscape management in Central Europe. Ecol Stud 147, Springer-Verlag, Berlin, Germany, pp 417-462.
- Tenhunen JD, Valentini R, Köstner B, Zimmermann R, Granier A (1998) Variation in forest gas exchange at landscape to continental scales. Ann Sci For 55, 1-11.

- Thomas FM (2000) Growth and water relations of four deciduous tree species (*Fagus sylvatica* L., *Quercus petraea* Matt. L., *Q. pubescens* Willd., *Sorbus aria* L. Cr.) occurring at Central-European tree-line sites on shallow calcareous soils: physiological reactions of seedlings to severe drought. Flora 195: 104–115.
- Thomas FM, Bartels C, Gieger T (2006) Alterations in vessel size in twigs of *Quercus robur* and *Q. petraea* upon defoliation and consequences for water transport under drought. IAWA J 27, 395–407.
- Thomas FM, Blank R, Hartmann G (2002) Abiotic and biotic factors and their interactions as causes of oak decline in Central Europe. For Path 32, 277–307.
- Thomas FM, Gausling T (2000) Morphological and physiological responses of oak seedlings (*Quercus petraea* and *Q. robur*) to moderate drought. Ann For Sci 57, 325–333.
- Thomasius H (1992) Prinzipien eines ökologisch orientierten Waldbaus. Forstw Cbl 111, 141–155.
- Thorburn PJ, Hatton TJ, Walker GR (1993) Combining measurements of transpiration and stable isotopes of water to determine ground water discharge from forests. J Hydrol 150, 563–587.
- Tognetti R, Johnson JD, Michelozzi M (1995) The response of European beech (*Fagus sylvatica* L.) seedlings from two Italian populations to drought and recovery. Trees 9, 348–354.
- Tognetti R, Raschi A, Beres C, Fenyvesi A, Ridder H-W (1996) Comparison of sap flow, cavitation and water status of *Quercus petraea* and *Quercus cerris* trees with special reference to computer tomography. Plant Cell Environ 19, 928–938.
- Türk W (1983) Entwurf einer Karte der Potentiellen Natürlichen Vegetation von Oberfranken. Tüxenia 13, 33–55.
- Tuzinsky L (1987) Water balance in forest ecosystems of the Small Carpathians (Czechoslovakia). Ekológia (CSSR) 6, 23–39.
- Tyree MT, Cochard H (1996) Summer and winter embolism in oak: impact on water relations. Ann Sci For 53, 173–180.
- Tyree MT, Kolb KJ, Rood SB, Patiño S (1994) Vulnerability to drought-induced cavitation of riparian cottonwoods in Alberta: a possible factor in the decline of the ecosystem? Tree Physiol 14, 455–466.
- Tyree MT, Sperry JS (1989) Vulnerability of xylem to cavitation and embolism. Annu Rev Plant Phys Mol Bio 40, 19–38.
- Tyree MT; Zimmermann MH (2002) Xylem structure and the ascent of sap. Springer-Verlag, Berlin, Germany, 2<sup>nd</sup> edition, 283 pp.
- UBA (2003) Naturnahe Waldwirtschaft. Umweltbundesamt, Berlin, Germany.
- Valentini R (2003) Fluxes of carbon, water and energy of European forests. Ecol Stud 163, Springer-Verlag, Berlin, Germany, 270 pp.
- Valladares F, Chico J, Aranda I, Balaguer L, Dizengremel P, Manrique E, Dreyer E (2002) The greater seedling high-light tolerance of *Quercus robur* over *Fagus sylvatica* is linked to a greater physiological plasticity. Trees 16, 395–403.
- van As H (2007) Intact plant MRI for the study of cell water relations, membrane permeability, cell-to-cell and long distance water transport. J Exp Bot 58, 743–756.
- van As H, van Vliet WPA, Schaafsma TJ (1980) [<sup>1</sup>H] spin-echo nuclear magnetic resonance in plant tissue. Biophys J 32, 1043–1050.
- Vertessy RA, Benyon RG, O'Sullivan SK, Gribben PR (1995) Relationships between stem diameter, sapwood area, leaf area and transpiration in a young mountain ash forest. Tree Physiol 15, 559–567.
- Vertessy RA, Hatton TJ, Reece P, O'Sullivan SK, Benyon RG (1997) Estimating stand water use of large mountain ash trees and validation of the sap flow measurement technique. Tree Physiol 17, 747–756.
- Vertessy RA, Watson FGR, O'Sullivan SK (2001) Factors determining relations between stand age and catchment water balance in mountain ash forests. For Ecol Manage 143, 13–26.
- Vincke C, Bréda N, Granier A, Devillez F (2005a) Evapotranspiration of a declining *Quercus robur* (L.) stand from 1999 to 2001. I. Trees and forest floor daily transpiration. Ann For Sci 62, 503–512.
- Vincke C, Bréda N, Granier A, Devillez F (2005b) Evapotranspiration of a declining *Quercus robur* (L.) stand from 1999 to 2001. II. Daily actual evapotranspiration and soil water reserve. Ann For Sci 62, 615–623.
- Vité JP (1958) Über die transpirationsphysiologische Bedeutung des Drehwuchses bei Nadelbäumen. Forstw Cbl 77, 193–256.

- Vollenweider P, Dustin I, Hofer R-M, Vittoz P, Hainard P (1994) A study on the cambial zone and conductive phloem of common beech (*Fagus sylvatica* L.) using an image analysis method. I. Influence of tree age on the structure. *Trees* 9, 106-112.
- Wagenführ R (2000) Holzatlas. Fachbuchverlag Leipzig, Munich, Germany, 707 pp.
- Waisel Y, Lipschitz N, Kuller Z (1972) Patterns of water movement in trees and shrubs. *Ecology* 53, 520-523.
- Walentowski H, Gulder H-J, Kölling C, Ewald J, Türk W (2001) Die regionale natürliche Waldzusammensetzung Bayerns. LWF-Berichte 32, 99 pp. Bayerische Landesanstalt für Wald und Forstwirtschaft, Freising, Germany.
- Walter H, Breckle S-W (1994) Spezielle Ökologie der Gemäßigten und Arktischen Zonen Euro-Nordasiens. Gustav Fischer Verlag, Stuttgart, Germany, 2<sup>nd</sup> edition, 726 pp.
- Walter H, Lieth H (1960–1967) Klimadiagramm-Weltatlas. Gustav Fischer Verlag, Jena, Germany.
- Wang Q, Tenhunen J, Granier A, Reichstein M, Bouriaud O, Nguyen D, Bréda N (2004) Long-term variations in leaf area index and light extinction in a *Fagus sylvatica* stand as estimated from global radiation profiles. *Theor Appl Climatol* 79, 225-238.
- Wang YP, Jarvis PG (1990a) Description and validation of an array model – MAESTRO. *Agric For Meteorol* 51, 257-280.
- Wang YP, Jarvis PG (1990b) Influence of crown structural properties on PAR absorption, photosynthesis, and transpiration in Sitka spruce: application of a model (MAESTRO). *Tree Physiol* 7, 297-316.
- Waring RH, Gholz HL, Grier CC, Plummer ML (1977) Evaluating stem conducting tissue as an estimator of leaf area in four woody angiosperms. *Can J Bot* 55, 1474-1477.
- Waring RH, Roberts JM (1979) Estimating water flux through stems of Scots pine with tritiated water and phosphorous-32. *J Exp Bot* 30, 459-471.
- Waring RH, Running SW (1978) Sapwood water storage: its contribution to transpiration and effect upon water conductance through the stems of old-growth Douglas-fir. *Plant Cell Environ* 1, 131-140.
- Watson DJ (1947) Comparative physiological studies in the growth of field crops. I. Variation in net assimilation rate and leaf area between species and varieties, and within and between years. *Ann Bot* 11, 41-76.
- Weiss M, Baret F, Smith GJ, Jonckheere I, Coppin P (2004) Review of methods for in situ leaf area index (LAI) determination: Part II. Estimation of LAI, errors and sampling. *Agric For Meteorol* 121, 37-53.
- Welles J, Cohen S (1996) Canopy structure measurement by gap fraction analysis using commercial instrumentation. *J Exp Bot* 47, 1335-1342.
- Welles JM (1990) Some indirect methods of estimating canopy structure. *Remote Sens Rev* 5, 31-43.
- Welles JM, Norman JM (1991) Instrument for indirect measurement of canopy architecture. *Agron J* 83, 818-825.
- Welß W (1985) Waldgesellschaften im nördlichen Steigerwald. *Dissertationes Botanicae* 83, Verlag J. Cramer, Vaduz, 174 pp.
- West GB, Brown JH, Enquist BJ (1999) A general model for the structure and allometry of plant vascular systems. *Nature* 400, 664-667.
- Westoby M, Wright IJ (2006) Land-plant ecology on the basis of functional traits. *Trends Ecol Evol* 21, 261-268.
- Wheeler JK, Sperry JS, Hacke UG, Hoang N (2005) Inter-vessel pitting and cavitation in woody Rosaceae and other vesseled plants: a basis for a safety versus efficiency trade-off in xylem transport. *Plant Cell Environ* 28, 800-812.
- Whitehead D, Jarvis PG (1981) Coniferous forests and plantations. In: Kozlowski TT (ed) Water deficits and plant growth. Vol. VI Woody plant communities. Academic Press, New York, USA, pp49-152.
- Wiebe S (1992) Untersuchungen zur Wundentwicklung und Wundbehandlung an Bäumen unter besonderer Berücksichtigung der Holzfeuchte. PhD thesis, University of Munich, Germany, 131 pp.
- Wiebe S, Habermehl A (1994) Feuchtigkeitsänderungen im Bereich von Wunden. In: Habermehl A (ed) Die Computer-Tomographie als diagnostische Methode bei der Untersuchung von Bäumen. Baum-Zeitung Verlag, Minden, Germany, pp 60-72.
- Wilmanns O (1989) Die Buchen und ihre Lebensräume. *Ber Reinh-Tüxen-Ges* 1, 49-72.

- Wilson KB, Baldocchi DD (2000) Seasonal and interannual variability of energy fluxes over a broadleaved temperate deciduous forest in North America. *Agric For Meteorol* 100, 1-18.
- Wilson KB, Hanson PJ, Mulholland PJ, Baldocchi DD, Wullschleger SD (2001) A comparison of methods for determining forest evapotranspiration and its components: sap-flow, soil water budget, eddy covariance and catchment water balance. *Agric For Meteorol* 106, 153-168.
- Windt CW, Vergeldt FJ, de Jager PA, van As H (2006) MRI of long-distance water transport: a comparison of the phloem and xylem flow characteristics and dynamics in poplar, castor bean, tomato and tobacco. *Plant Cell Environ* 29, 1715-1729.
- Woodcock DW, Shier AD (2002) Wood specific gravity and its radial variations: the many ways to make a tree. *Trees* 16, 437-443.
- Wrzesinsky T, Klemm O (2000) Summertime fog chemistry at a mountainous site in central Europe. *Atmos Environ* 34, 1487-1496.
- Wullschleger SD, Hanson PJ, Todd DE (1996) Measuring stem water content in four deciduous hardwoods with a time-domain reflectometer. *Tree Physiol* 16, 809-815.
- Wullschleger SD, Hanson PJ, Todd DE (2001) Transpiration from a multi-species deciduous forest as estimated by xylem sap flow techniques. *For Ecol Manage* 143, 205-213.
- Wullschleger SD, King AW (2000) Radial variation in sap velocity as a function of stem diameter and sapwood thickness in yellow-poplar trees. *Tree Physiol* 20, 511-518.
- Wullschleger SD, Meinzer FC, Vertessy RA (1998) A review of whole-plant water use studies in trees. *Tree Physiol* 18, 499-512.
- Wullschleger SD, Wilson KB, Hanson PJ (2000) Environmental control of whole-plant transpiration, canopy conductance and estimates of the decoupling coefficient for large red maple trees. *Agric For Meteorol* 104, 157-168.
- Zang D, Beadle CL, White DA (1996) Variation of sapflow velocity in *Eucalyptus globulus* with position in sapwood and use of a correction coefficient. *Tree Physiol* 16, 697-703.
- Zanne AE, Sweeney K, Sharma M, Orians CM (2006) Patterns and consequences of differential vascular sectoriality in 18 temperate tree and shrub species. *Funct Ecology* (2006) 20, 200-206.
- Zhang Y, Chen JM, Miller JR (2005) Determining digital hemispherical photograph exposure for leaf area index estimation. *Agric For Meteorol* 133, 166-181.
- Zianis D, Mencuccini M (2003) Aboveground biomass relationships for beech (*Fagus moesiaca* Cz.) trees in Vermio Mountain, Northern Greece, and generalised equations for *Fagus* sp. *Ann For Sci* 60, 439-448.
- Zimmermann MH, Jeje AA (1981) Vessel-length distribution in stems of some American woody plants. *Can J Bot* 59, 1882-1892.
- Zimmermann MH, Potter D (1982) Vessel-length distribution in branches, stems, and roots of *Acer rubrum* L. *IAWA Bull* ns 3, 103-109.
- Zimmermann R, Schulze E-D, Wirth C, Schulze E-E, McDonald KC, Vygodskaya NN, Ziegler W (2000) Canopy transpiration in a chronosequence of Central Siberian pine forests. *Global Change Biol* 6, 25-37.
- Zobel BJ, van Buijtenen JP (1989) Wood variation: its causes and control. Springer-Verlag, Berlin, Germany, 363 pp.
- Zycha H (1948) Über die Kernbildung und verwandte Vorgänge im Holz der Rotbuche. *Forstw Cbl* 67, 80-109.

## 11 Appendix

### 11.1 Computer tomograms (Chapter 5.1.1)

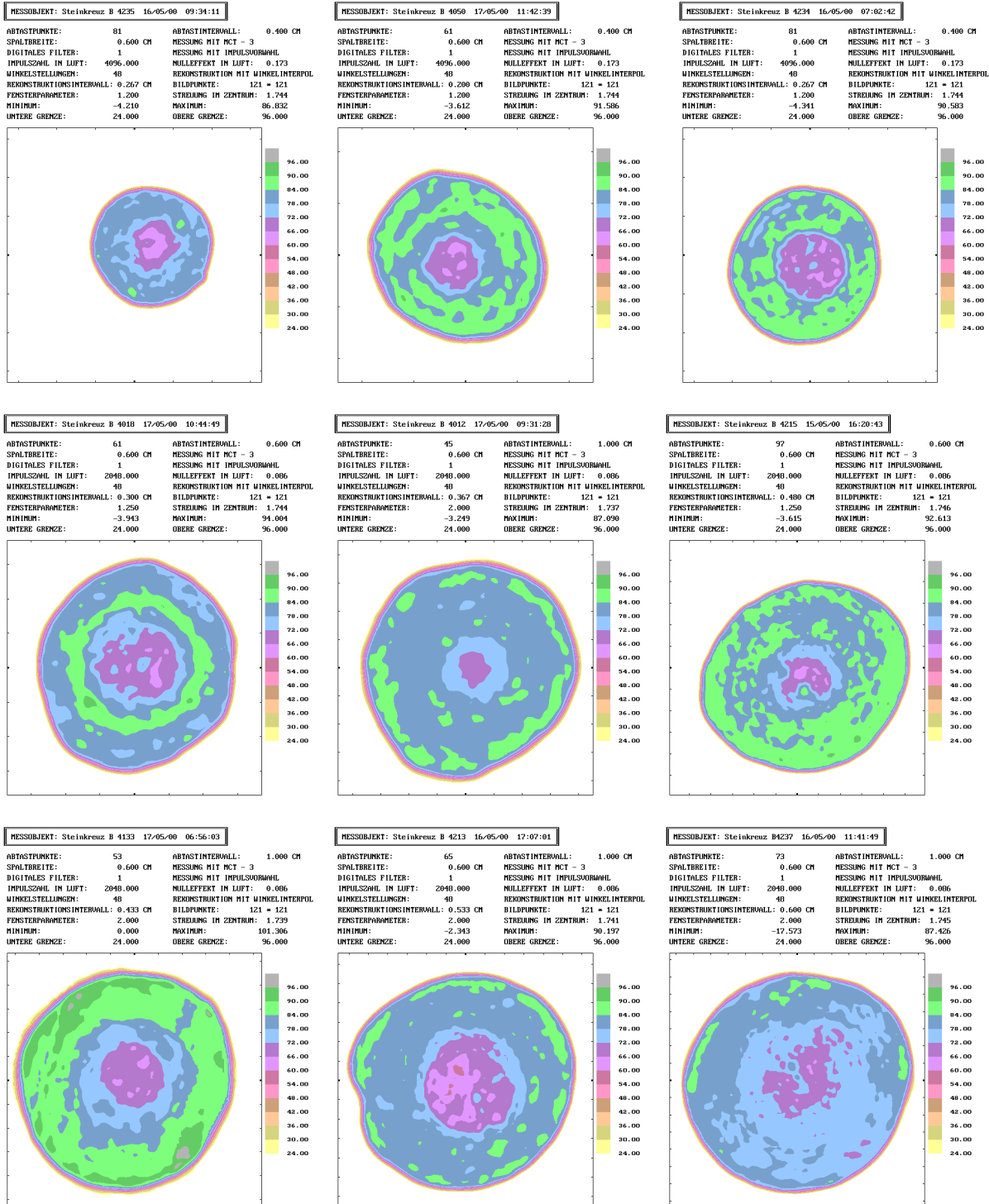


**Figure A11.1:** Computer tomograms reconstructed from cross-sectional scans on standing live *Fagus sylvatica* trees, performed with a mobile computer tomograph (see Chap. 5.1.1), a: at Steinkreuz in the Steigerwald, May 15–17, 2000. Tick marks on x and y axes indicate 5 cm intervals, different colours depict classes of absorption values  $\alpha$ . Site, tree number, date and scanning details given above each tomogram. The image at the top left is always for the smallest tree, that at the bottom right for the largest tree.

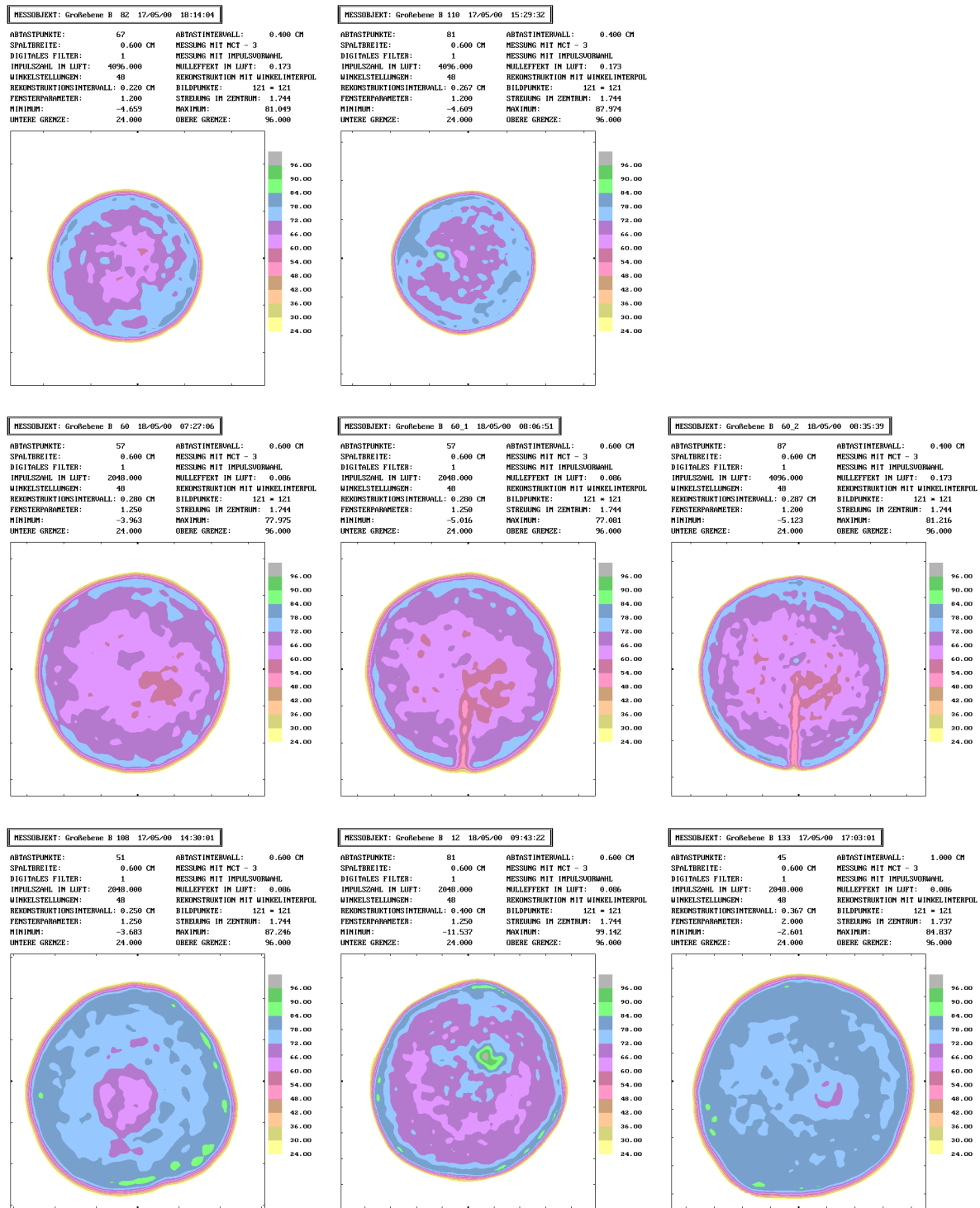


**Figure A11.1, continued, b:** Großebene, Steigerwald, May 17–18, 2000. On tree B60, the CT-scan was repeated after extracting an increment core with a Pressler borer (5 mm diameter) in the plane of the CT-scan, leaving the MCT-3 in place, about 30 minutes after the first scan. A third scan with higher spatial resolution (scanning interval then 0.4 cm instead of 0.6 cm in previous two scans) was carried out another 30 minutes later (middle panel, left to right).

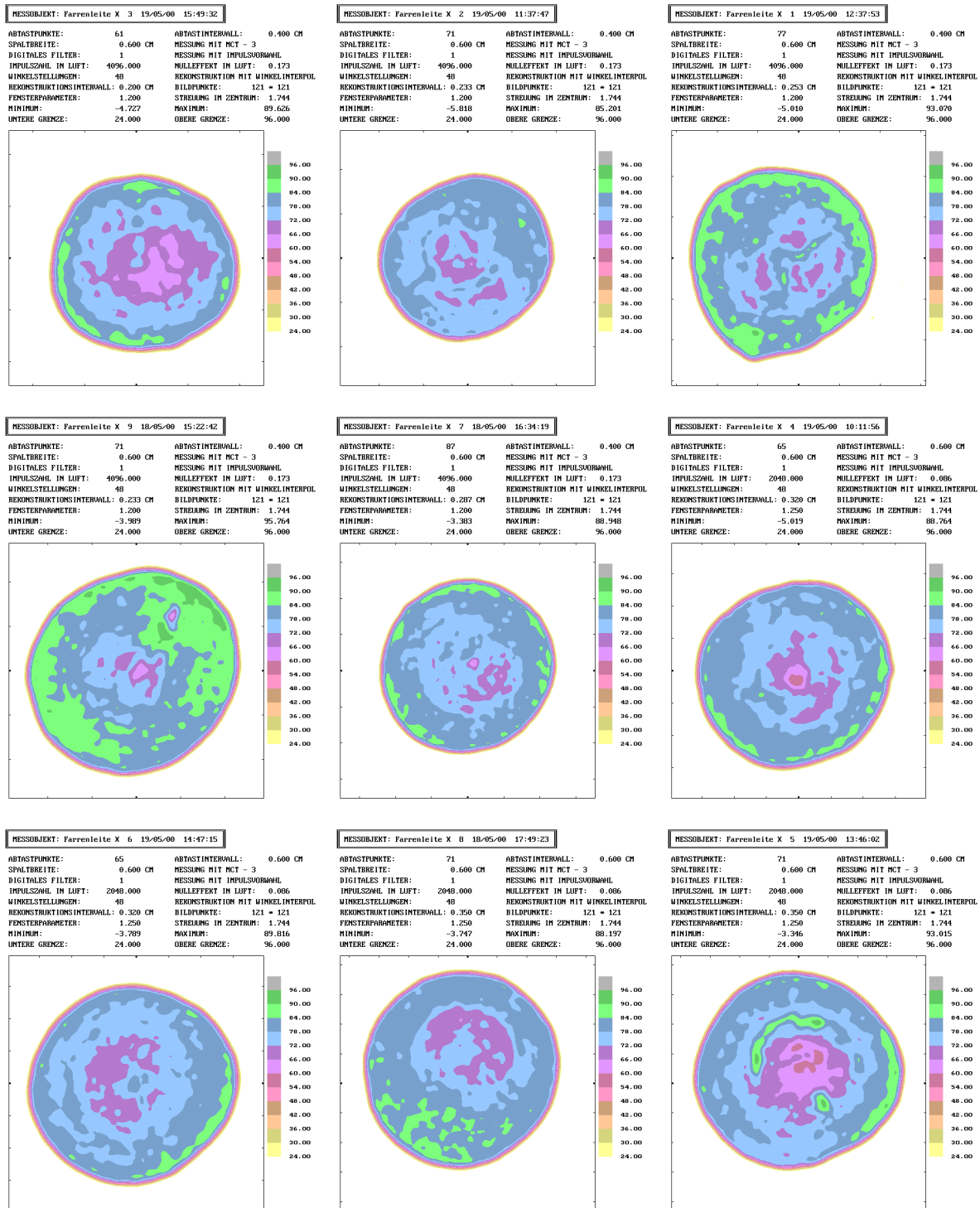
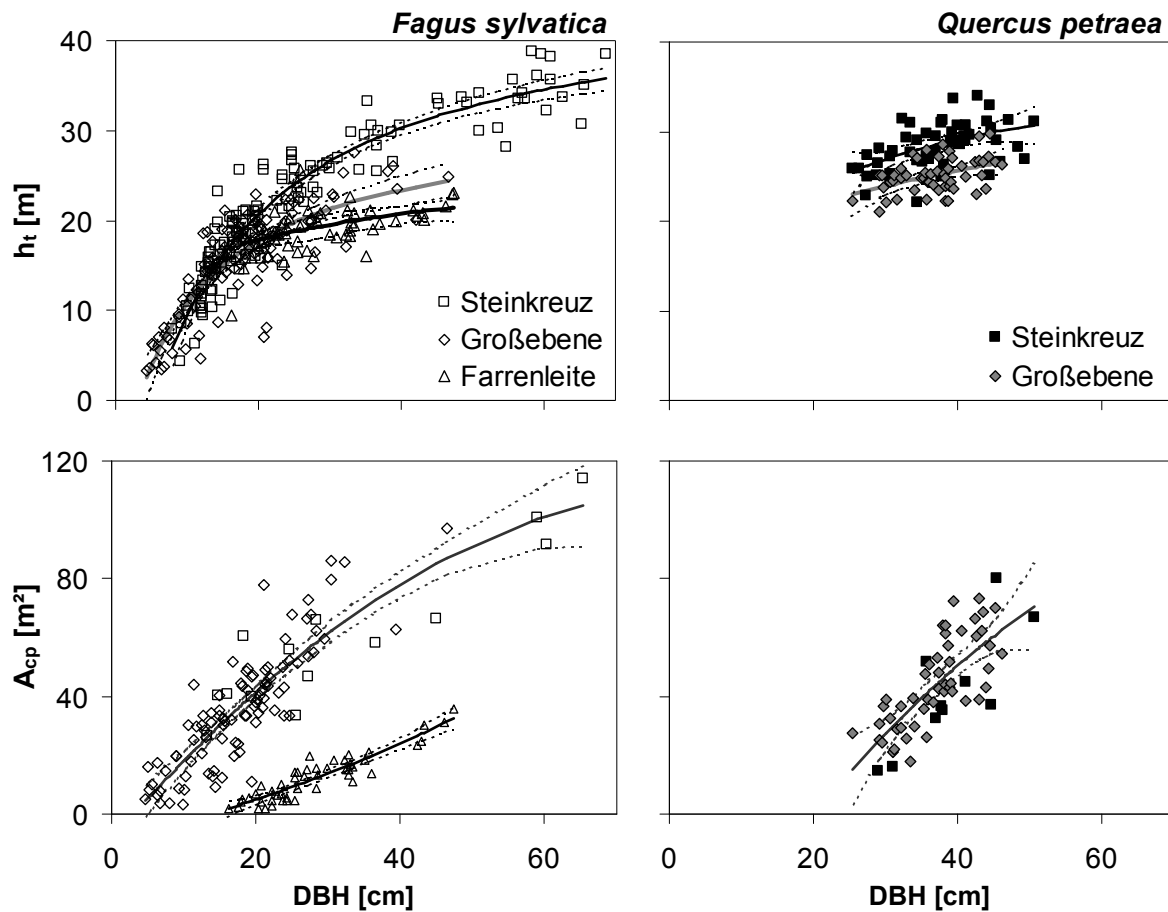


Figure A11.1, continued, c: Farrenleite, Steigerwald, May 18–19, 2000.

## 11.2. Allometric relationships (Chapter 5.1.2)



**Figure A11.2:** Tree height  $h_t$  and ground-projected crown area  $A_{cp}$  of all assessed beech (left) and oak trees (right) at the two mixed sites in the Steigerwald, Steinkreuz and GroßeBene, and of beech trees in the pure Farrenleite stand in the Fichtelgebirge. **Upper** panel: Height of tree top above the ground, respective (hyperbolic) regression lines and 95 %-confidence intervals (dotted). **Lower** panel:  $A_{cp}$  of all measured trees, regression lines and 95 %-confidence intervals. Both beech and oak trees from Steinkreuz and GroßeBene were not significantly different in their relationship between  $A_{cp}$  and DBH, so a combined regression was used for each species. Equations are given in Table A11.2.

**Table A11.2:** Allometric relationships and statistics for tree height and ground-projected crown area, using stem diameter at breast height (DBH, 1.3 m, in cm).  $R^2$ , n, p, and SEE denote respectively the coefficient of determination, number of samples, p-value, standard error of the estimate. ST+GR is combined a regression for Steinkreuz and Großebene (cf. Chap. 5.1.2).

	a	b	c	$R^2$	n	p	SEE	
<b>Tree height <math>h_t</math> vs DBH</b>		$h_t = a + b \cdot DBH \cdot (c+DBH)^{-1}$						
<i>F. sylvatica</i>								
Steinkreuz	-19.9	65.7	12.4	0.898	133	<0.0001	2.62	
Großebene	-9.9	41.8	10.2	0.725	111	<0.0001	3.01	
Farrenleite	11.3	16.8	30.8	0.257	51	0.0008	1.97	
<i>Q. petraea</i>								
Steinkreuz	2.8	36.3	15.2	0.273	52	0.0004	2.26	
Großebene	15.3	27	63.8	0.193	53	0.0047	1.76	
<b>Ground-projected crown area <math>A_{cp}</math> vs DBH</b>		$A_{cp} = a + b \cdot DBH + c \cdot DBH^2$						
<i>F. sylvatica</i>								
ST+GR	-8.7	2.8	-0.017	0.776	108	<0.0001	10.8	
Farrenleite	-8.3	0.5	0.007	0.846	48	<0.0001	3.26	
<i>Q. petraea</i>								
ST+GR	-69.9	3.9	-0.023	0.559	59	<0.0001	10.79	

### 11.3. Atmospheric drivers and daily sap flow density (Chapter 5.3)

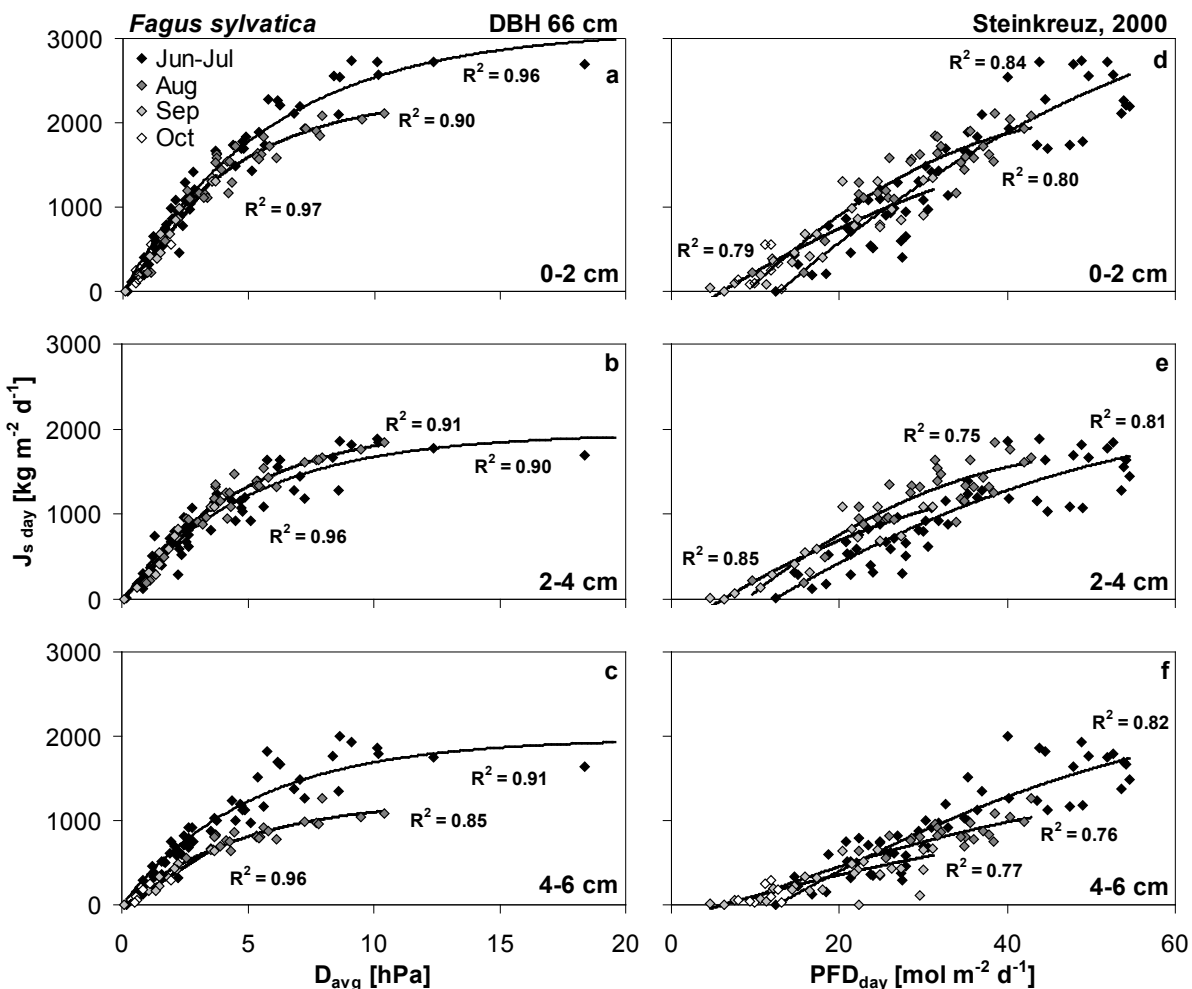


**Figure A11.3:** Same as Figure 5.3.8, but for the year 2000. Relationships between atmospheric variables and daily integrated sap flow density ( $J_s$  day) in three radial sapwood depths of beech tree B4237 (DBH 66 cm) during four contiguous periods in the year 2000: relationships with daily average vapour pressure deficit of the air ( $D_{avg}$ ; 24 h-average of 10'-values; **a–c**) and daily integrated photosynthetic photon flux density ( $PFD_{day}$ ; **d–f**) in outer sapwood (0–2 cm; **a, d**), in 2–4 cm depth (**b, e**) and in 4–6 cm depth (**c, f**) for the tree with the highest observed values of  $J_s$  0–2 cm day (the largest studied tree). Lines are statistically significant ( $p < 0.0001$ ) non-linear regressions, namely exponential functions for the relationships with  $D_{avg}$  and 2<sup>nd</sup> order polynomial functions for  $PFD_{day}$ ; no regressions were calculated for October due to few data and very low rates of  $J_s$  day. Correlation coefficients are given next to the graphs.

### 11.4. Seasonal change of $J_s$ deep/ $J_s$ 0-2cm (Chapter 5.3)

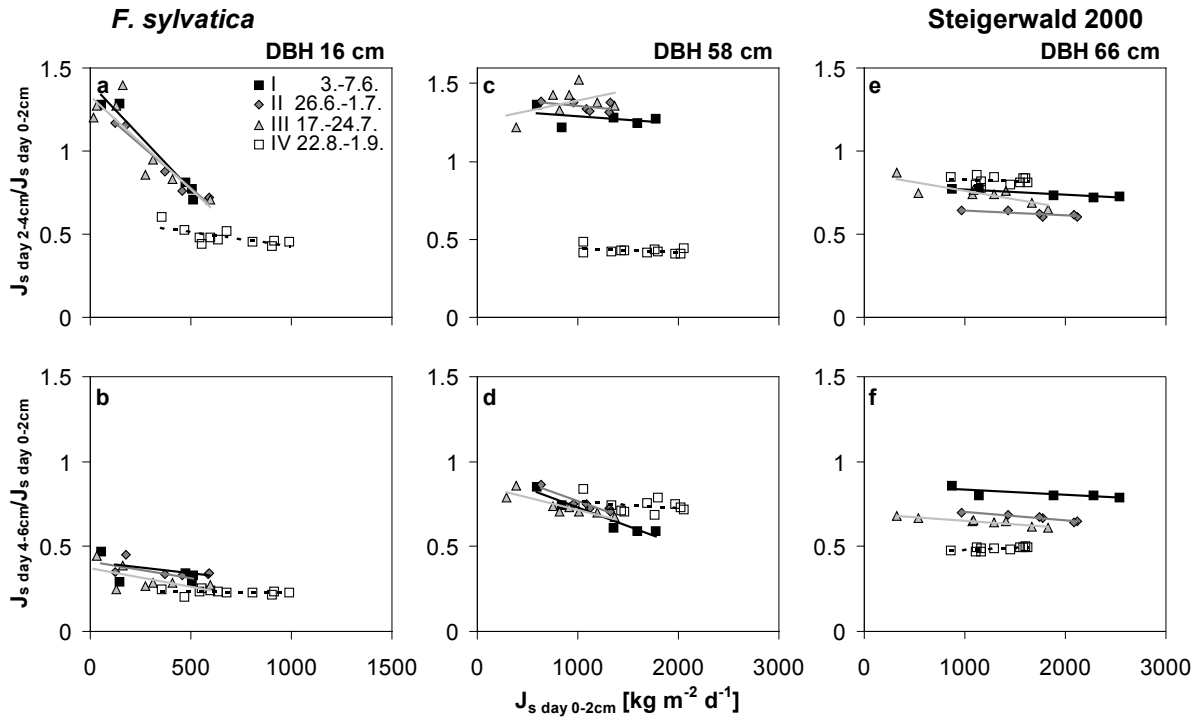


**Figure A11.4:** Same as Figure 5.3.10, but for the year 2000. Relationship of daily integrated sap flow density in deep sapwood relative to outer sapwood ( $J_s$  day 2-4cm/ $J_s$  day 0-2cm: **upper panel**;  $J_s$  day 4-6cm/ $J_s$  day 0-2cm: **lower panel**) and sap flow density in outer sapwood ( $J_s$  day 0-2cm) for three trees (B4235: a, b; B4213: c, d; B4237: e, f) during four periods of several consecutive days without significant rain (cf. Fig. 5.3.4) in 2000. The periods are: 3.-07.06. (I); 26.06.-1.07. (II); 17.07.-24.07. (III); 22.08.-1.09. (IV). Lines are linear regressions for each of the five periods. The scale of x-axes varies.

### 11.5. Size classes of beech and oak for upscaling (Chapter 5.5)

**Table A11.5:** Size classes for upscaling of sap flow from tree to stand;  
m = measured, r = not measured but estimated via regression (see Chap. 5.4).

Stand	Species	Size class	Range of DBH [cm]	Tree	1999	2000
Steinkreuz	beech	dominant	51–70	4213 <sup>a</sup>	m	m
				4108	m	m
				4237 <sup>a</sup>	m	m
		intermediate	21–50	4018	m	m
				4133	r	m
				4215 <sup>a</sup>	m	m
				4012	m	r
		suppressed	7–20	4049	m	m
				4050	m	m
				4234 <sup>a</sup>	m	m
				4235 <sup>a</sup>	m	m
				4214 <sup>a</sup>	m	m
	oak	(co-) dominant	41–50	4051	m	m
				4014	m	r
				4202	m	r
				4324	r	m
		intermediate	21–40	4055	m	m
				4320	r	m
				4052	r	m
				4054	r	m
				4327	r	m
Großebene	beech	(co-) dominant	31–50	12	m	-
				133	m	-
		intermediate	21–30	60	m	-
				107	m	-
				108	m	-
				66	m	-
		suppressed	7–21	82	m	-
				87	m	-
				110	m	-
		oak	dominant	68	m	-
				116	m	-
				132	m	-
		intermediate	31–40	37	m	-
				64	m	-
				86	m	-
		suppressed	26–30	59	m	-
				89	m	-
				136	m	-
Farrenleite	beech	dominant	31–50	X4	m	m
				X5	m	m
				X6	r	m
				X8	m	m
		intermediate/ suppressed	14–30	X1	r	m
				X2	m	m
				X3	r	m
				X7	m	m

<sup>a</sup> trees also part of the Steinkreuz-pure beech plot

### 11.6. Relationships of $E_c$ and atmospheric drivers (Chapter 5.5)

**Table A11.6:** Parameters and statistics of the regression analysis of daily  $E_c$  and daily average vapour pressure deficit of the air ( $D_{avg}$ ) or daily integrated photon flux density ( $PFD_{day}$ ), using a rectangular hyperbolic model in the form of:

$E_c = (\alpha\beta \cdot \text{variable})/(\alpha \cdot \text{variable} + \beta) + \gamma$ , where the variable is either  $D_{avg}$  or  $PFD_{day}$  (Figs. 5.5.9–12).  $\alpha$  is the initial slope of the response curve,  $\beta$  the plateau parameter,  $\gamma$  the intercept. SEE is the standard error of the estimate. Levels of significance: \*\*\*\* is  $p < 0.0001$ , \*\*\* is  $p < 0.001$ , \*\* is  $p < 0.01$ , \* is  $p < 0.05$ , n.s. is  $p \geq 0.05$ .

month	n	$\alpha$	$\beta$	$\gamma$	$R^2$	SEE	$p$
<b>D<sub>avg</sub> 1999</b>							
<b>Großebene <i>F. sylvatica</i></b>							
June-July	61	0.9135	***	1.8602	****	-0.3744	**
August	21	0.7722	n.s.	1.5197	**	-0.4589	n.s.
September	14	0.0487	***	73929	n.s.	-0.0046	n.s.
<b>Großebene <i>Q. petraea</i></b>							
June-July	61	0.8804	n.s.	0.9198	****	-0.1688	n.s.
August	21	0.5753	n.s.	0.8851	*	-0.2057	n.s.
September	14	0.2911	n.s.	0.499	****	-0.066	n.s.
<b>Großebene stand</b>							
June-July	61	1.5269	***	2.7087	****	-0.4598	*
August	21	1.3151	n.s.	2.391	**	-0.6509	n.s.
September	14	0.2269	n.s.	1.2128	x	-0.0377	n.s.
<b>Steinkreuz <i>F. sylvatica</i></b>							
June-July	61	1.755	****	3.2841	****	-0.6648	**
August	31	2.4573	n.s.	3.4448	***	-1.3551	n.s.
September	22	0.7045	n.s.	1.4785	****	-0.2538	n.s.
<b>Steinkreuz <i>Q. petraea</i></b>							
June-July	61	0.3828	**	0.3955	****	-0.1095	**
August	31	92623	n.s.	123.654	n.s.	-123.443	n.s.
September	22	0.1365	n.s.	0.2202	****	-0.0416	n.s.
<b>Steinkreuz stand</b>							
June-July	61	2.0536	****	3.6548	****	-0.752	*
August	31	3.6216	n.s.	4.0705	**	-1.807	n.s.
September	22	0.8352	n.s.	1.6966	****	-0.2939	n.s.
<b>Steinkreuz-pure beech plot</b>							
June-July	61	2.9358	****	5.9613	****	-1.1228	***
August	31	3.6051	n.s.	6.0069	****	-2.1058	n.s.
September	22	1.2508	n.s.	2.7266	****	-0.4637	n.s.

**Table A11.6**, continued.

month	n	$\alpha$	$\beta$	$\gamma$	$R^2$	SEE	p
<b>Farrenleite stand</b>							
June-July	61	0.6666	****	8.7446	****	-0.0697	n.s.
August	31	0.6686	***	7.3051	****	-0.173	n.s.
September	32	0.5363	****	8.5713	****	-0.0215	n.s.
<b>D<sub>avg</sub> 2000</b>							
<b>Steinkreuz <i>F. sylvatica</i></b>							
June-July	61	0.6824	****	3.391	****	-0.2243	n.s.
August	31	1.6103	**	3.2979	****	-0.9271	**
September	25	0.4475	*	3.4024	n.s.	-0.0196	n.s.
<b>Steinkreuz <i>Q. petraea</i></b>							
June-July	61	0.1034	***	0.2016	****	-0.0083	n.s.
August	31	0.2992	n.s.	0.342	****	-0.1129	n.s.
September	25	0.0809	**	0.2176	****	0.006	n.s.
<b>Steinkreuz stand</b>							
June-July	61	0.7523	****	3.5664	****	-0.217	n.s.
August	31	1.8469	**	3.6171	****	-1.0209	**
September	25	0.5196	**	3.4766	x	-0.012	n.s.
<b>Steinkreuz-pure beech plot</b>							
June-July	61	1.2984	****	5.8047	****	-0.4281	*
August	31	3.175	**	6.1996	****	-1.813	**
September	25	0.8158	*	6.3946	n.s.	-0.054	n.s.
<b>Farrenleite stand</b>							
June-July	49	0.6705	****	5.327	****	0.0532	n.s.
August	31	0.709	***	5.855	****	-0.2764	n.s.
September	33	0.3081	****	66935	n.s.	0.082	n.s.
<b>PFD<sub>day</sub> 1999</b>							
<b>Großebene <i>F. sylvatica</i></b>							
June-July	61	0.1038	n.s.	3.1262	****	-0.8112	*
August	21	0.0913	n.s.	2.5633	****	-0.7197	n.s.
September	14	0.0117	****	87994	n.s.	-0.0753	*
<b>Großebene <i>Q. petraea</i></b>							
June-July	61	0.1586	n.s.	1.5475	*	-0.6494	n.s.
August	21	0.0161	n.s.	2.0984	n.s.	0.0501	n.s.
September	14	0.0751	n.s.	0.8179	****	-0.273	n.s.
<b>Großebene stand</b>							
June-July	61	0.1991	n.s.	4.3938	****	-1.2637	n.s.
August	21	0.106	n.s.	3.8743	*	-0.6956	n.s.
September	14	0.0324	n.s.	3.1246	n.s.	-0.1364	n.s.
<b>Steinkreuz <i>F. sylvatica</i></b>							
June-July	61	0.2037	*	5.5584	****	-1.532	*
August	31	0.2987	n.s.	4.8653	****	-1.8641	n.s.
September	22	0.0506	*	6.4008	n.s.	-0.2891	n.s.

**Table A11.6**, continued.

Month	n	$\alpha$	$\beta$	$\gamma$	$R^2$	SEE	p
<b>Großebene stand</b>							
June-July	61	0.1991	n.s.	4.3938 ****	-1.2637	n.s.	0.7268
August	21	0.106	n.s.	3.8743 *	-0.6956	n.s.	0.8152
September	14	0.0324	n.s.	3.1246 n.s.	-0.1364	n.s.	0.8969
<b>Steinkreuz <i>F. sylvatica</i></b>							
June-July	61	0.2037	*	5.5584 ****	-1.532	*	0.8241
August	31	0.2987	n.s.	4.8653 ****	-1.8641	n.s.	0.8521
September	22	0.0506	*	6.4008 n.s.	-0.2891	n.s.	0.9042
<b>Steinkreuz <i>Q. petraea</i></b>							
June-July	61	0.0692	n.s.	0.6992 ***	-0.3369	n.s.	0.7689
August	31	0.709	n.s.	1.3003 n.s.	-1.0507	n.s.	0.5133
September	22	0.0141	n.s.	0.4341 **	-0.0698	n.s.	0.8721
<b>Steinkreuz stand</b>							
June-July	61	0.2489	n.s.	6.1348 ****	-1.8021	*	0.8272
August	31	0.4059	n.s.	5.4687 ***	-2.3076	n.s.	0.8392
September	22	0.0624	*	6.1123 n.s.	-0.3502	n.s.	0.9021
<b>Steinkreuz-pure beech plot</b>							
June-July	61	0.3468	*	10.1498 ****	-2.6572	*	0.8289
August	31	0.4239	n.s.	8.6665 ****	-2.8436	n.s.	0.8432
September	22	0.108	*	8.342 n.s.	-0.6275	n.s.	0.9115
<b>Farrenleite stand</b>							
June-July	61	0.0906	****	65833 n.s.	-0.7505	**	0.8599
August	31	0.1134	*	33.8148 n.s.	-0.6714	n.s.	0.8366
September	32	0.123	****	107493 n.s.	-0.5259	*	0.7314
<b>PFD<sub>day</sub> 2000</b>							
<b>Steinkreuz <i>F. sylvatica</i></b>							
June-July	61	0.0827	n.s.	8.8568 **	-0.8542	n.s.	0.7894
August	31	0.1826	n.s.	4.6883 ****	-1.2274	n.s.	0.7531
September	25	0.0714	n.s.	5.4725 n.s.	-0.393	n.s.	0.8311
<b>Steinkreuz <i>Q. petraea</i></b>							
June-July	61	0.027	n.s.	0.4091 ****	-0.1569	n.s.	0.7554
August	31	0.1697	n.s.	0.6921 n.s.	-0.4524	n.s.	0.6131
September	25	0.0195	n.s.	0.3321 ****	-0.076	n.s.	0.8642
<b>Steinkreuz stand</b>							
June-July	61	0.0933	n.s.	8.7822 *	-0.9235	n.s.	0.7917
August	31	0.2246	n.s.	5.0465 ****	-1.4288	n.s.	0.7466
September	25	0.0855	n.s.	5.3556 n.s.	-0.4528	n.s.	0.8358

**Table A11.6**, continued.

Month	n	$\alpha$	$\beta$	$\gamma$	$R^2$	SEE	p	
<b>Steinkreuz-pure beech plot</b>								
June-July	61	0.1596	n.s.	14.1041 *	-1.6243	n.s.	0.8072	0.5011 <0.0001
August	31	0.3161	n.s.	8.9423 ****	-2.1738	n.s.	0.7736	0.3801 <0.0001
September	25	0.1282	n.s.	10.591 n.s.	-0.7267	n.s.	0.8204	0.3272 <0.0001
<b>Farrenleite stand</b>								
June-July	49	0.1073	*	16.4443 n.s.	-0.7876	n.s.	0.784	0.557 <0.0001
August	31	0.3196	n.s.	6.5424 ****	-1.4435	n.s.	0.7275	0.4925 <0.0001
September	33	0.0844	****	71448 n.s.	-0.3234 *		0.6751	0.3623 <0.0001

### 11.7. Maximum daily $E_c$ of beech and oak stands (Chapter 6.4.1)

**Table A.11.7:** Maximum rates of daily tree canopy transpiration ( $E_{c \max}$ , in  $\text{mm d}^{-1}$ ), respective leaf area index (LAI, in  $\text{m}^2 \text{ m}^{-2}$ ) and ratio of both ( $E_{c \max}/\text{LAI}$ , in  $\text{kg m}^{-2} \text{ d}^{-1}$ ) and elevation (a.s.l., in m) for stands of beech and oak and mixed stands.  $E_{c \max}$  estimated (Est) from measurements of xylem sap flow using the thermal dissipation method (TD), trunk sector heat balance (TB), heat pulse velocity (HV), or heat field deformation method (HD), or from micrometeorological measurements (M). Included are only studies that list the LAI as well as rates of  $E_{c \max}$ . See Figure 6.4.1.1.

Stand, location	a.s.l.	Year	$E_{c \max}$	LAI	$E_{c \max}/\text{LAI}$	Est	Reference
<b><i>Fagus sylvatica</i></b>							
Fichtelgebirge, SE Germany	950	1999	4.3	6.8	0.63	TD	this study, Farrenleite
	950	2000	3.9	6.8	0.57	TD	this study, Farrenleite
Steigerwald, SE Germany	440	1999	4.4	6.5	0.67	TD	this study, ST-BP
	440	2000	4.2	6.8	0.62	TD	this study, ST-BP
Steigerwald, SE Germany	440	1999	2.4	5.9	0.41	TD	this study, Steinkreuz beech
	440	2000	2.5	6.0	0.41	TD	this study, Steinkreuz beech
Steigerwald, SE Germany	460	1999	1.5	2.9	0.50	TD	this study, Großebene beech
Ziegelroda, C Germany	280	1996	4.8	8.3	0.58	TB	Schipka (2003)
Göttinger Wald, C Germany	400	1995	5.4	6.2	0.87	TB	Schipka (2003)
	400	1996	5.3	6.3	0.84	TB	Schipka (2003)
Lüneburger Heide, N Germany	120	1996	7.2	7.2	1.00	TB	Schipka (2003)
Solling, C Germany	510	1996	8.6	6.5	1.32	TB	Schipka (2003)
Pol'ana Mts, C Slovakia	850	1996	6.0 <sup>a</sup>	5.9	1.02	TB	Střelcová et al. (2006)
Hainich, C Germany	300	2001	3.8	4.9	0.78	TD	Koch (2002, in Schipka 2003)
Aubure, E France	1000	1995	3.9	5.7	0.68	TD	Granier et al. (2000a)
Hesse, E France	300	1996	3.8	5.7	0.67	TD	Granier et al. (2000a)
	300	1997	2.9	5.6	0.52	TD	Granier et al. (2000a)
	300	2002	4.8	7.2	0.67	TD	Granier et al. (2007)
	300	2003	4.0	7.2	0.56	TD	Granier et al. (2007)
Schachtenau, SE Germany	800	1991	1.1	1.5	0.73	TB	Köstner (2001)
Hohe Warte, SE Germany	380	1992	7.0	9	0.78	TB	Köstner (2001)
Steigerwald, SE Germany	440	1996	2.6	4.5	0.58	TD	Köstner (2001)
Abetone, N Italy	1230	?	3.0	3.8	0.79	HV	Magnani et al. (1998)
Bornhöved, N Germany	50	1992	5.0	4.5	1.11	M	Herbst et al. (1999)
	50	1993	4.5	4.5	1.00	M	Herbst et al. (1999)
	50	1994	4.5	4.5	1.00	M	Herbst et al. (1999)
	50	1995	5.0	4.5	1.11	M	Herbst et al. (1999)

**Table A11.7**, continued.

<b>Stand, location</b>	<b>a.s.l.</b>	<b>Year</b>	<b><math>E_{c\ max}</math></b>	<b>LAI</b>	<b><math>E_{c\ max}/LAI</math></b>	<b>Est</b>	<b>Reference</b>
<b><i>Quercus petraea</i> and other <i>Quercus</i> species</b>							
Steigerwald, SE Germany	440	1999	0.3	1.0	0.29	TD	this study, Steinkreuz oak
	440	2000	0.2	0.9	0.22	TD	this study, Steinkreuz oak
Steigerwald, SE Germany	460	1999	0.8	3.1	0.27	TD	this study, Große Ebene oak
Champenoux, E France	240	1990	3.8	6	0.63	TD	Bréda et al. (1993a)
Chimay, SW Belgium	260	1999	1.1	2.8	0.39	TD	Vincke et al. (2005a)
<i>Q. robur</i> <sup>b</sup>	260	2000	0.9	2.3	0.39	TD	Vincke et al. (2005a)
	260	2001	1.0	2.5	0.41	TD	Vincke et al. (2005a)
Vallcebre, E Spain	1100	2003	1.2	2.1	0.57	HD,	Poyatos et al. (2007)
<i>Q. pubescens</i>	1100	2004	1.7	2.1	0.81	TD	Poyatos et al. (2007)
<b>Mixed stands</b>							
Steigerwald, SE Germany	440	1999	2.7	7.0	0.39	TD	this study, Steinkreuz
	440	2000	2.6	6.9	0.38	TD	this study, Steinkreuz
Steigerwald, SE Germany	460	1999	2.3	6.0	0.38	TD	this study, Große Ebene
Walker Branch, E USA <sup>c</sup>	300	1996	2.2	6.2	0.35	TD,HV	Wullschleger et al. (2001)
Duke Forest, E USA <sup>d</sup>	130	1997	1.6	3.3	0.48	TD	Pataki and Oren (2003)
Duke Forest, E USA <sup>e</sup>	130	1993	2.1	5.0	0.42	TD	Oren and Pataki (2001)

<sup>a</sup> Stand-level estimate based on only three trees.

<sup>b</sup> Only oak considered.

<sup>c</sup> *Q. prinus*, *Acer rubrum*.

<sup>d</sup> Bottomland forest, *Quercus* species, *Carya tomentosa*.

<sup>e</sup> Upland forest, *Quercus* species, *Carya tomentosa*.

### 11.8. Seasonal sums of $E_c$ (Chapter 6.4.4)

**Table A11.8:** Seasonal rates of canopy transpiration ( $E_c$ , in mm season $^{-1}$ ) in closed Central European beech, oak and mixed beech or mixed oak stands at various elevations (a.s.l., in m), average annual air temperature (T, in °C) and annual rates of precipitation (PPT, in mm yr $^{-1}$ ). Estimates (Est) based on soil water balance (S), xylem sap flow (TD = thermal dissipation method, TB = trunk sector heat balance method) or micrometeorological measurements (M), plus varying degrees of modelling; the dominant method is indicated. See Figures 6.4.4.1–2.

Stand, location	a.s.l.	Year	T	PPT	$E_c$	Est	Reference
<b><i>Fagus sylvatica</i></b>							
Solling, C Germany	500	1969	6.3	1064	283	S	Benecke (1984)
	500	1970	6.0	1479	248	S	Benecke (1984)
	500	1971	6.9	810	311	S	Benecke (1984)
	500	1972	6.2	910	260	S	Benecke (1984)
	500	1973	6.6	1037	277	S	Benecke (1984)
	500	1974	7.1	1236	234	S	Benecke (1984)
	500	1975	7.6	884	286	S	Benecke (1984)
	500	1976	6.5 <sup>a</sup>	706	245 <sup>b</sup>	S	Salihi (1984)
	500	1977	6.5 <sup>a</sup>	928	280 <sup>b</sup>	S	Salihi (1984)
	500	1978	6.5 <sup>a</sup>	963	242 <sup>b</sup>	S	Salihi (1984)
	500	1979	6.5 <sup>a</sup>	952	278 <sup>b</sup>	S	Salihi (1984)
	500	1980	6.5 <sup>a</sup>	1058	252 <sup>b</sup>	S	Salihi (1984)
	500	1981	6.5 <sup>a</sup>	1545	246 <sup>b</sup>	S	Salihi (1984)
	395	2001	7.0	1000	255	S	Cheussom (2004)
Bayerischer Wald, SE Germany	1165	1989	4.0	1565	235	S	Heil (1996)
Bramwald, C Germany	260	1931-1960	7.8	803	299	S	Brechtl and Balázs (1988)
Krofdorf, C Germany	280	1981	8.0 <sup>a</sup>	1023	321	S	Ernstberger (1985)
	280	1982	8.0 <sup>a</sup>	855	346	S	Ernstberger (1985)
	280	1983	8.0 <sup>a</sup>	860	371	S	Ernstberger (1985)
	280	1981	8.0 <sup>a</sup>	1023	321	S	Ernstberger (1985)
	280	1982	8.0 <sup>a</sup>	855	350	S	Ernstberger (1985)
	280	1983	8.0 <sup>a</sup>	860	376	S	Ernstberger (1985)
Schönbuch, SW Germany	495	1979	7.1	622	249	S	Fleck (1986)
	495	1980	7.3	812	260	S	Fleck (1986)
	495	1981	7.2	653	216	S	Fleck (1986)
	495	1982	7.6	963	323	S	Fleck (1986)
Höglwald, S Germany	540	1994-1995	9.4	954	431 <sup>b</sup>	S	Rothe (1997)
	540	1984-1995	7.9	888	385 <sup>b</sup>	S	Rothe (1997)
Small Carpathians, W Slovakia	480	1978	9.3 <sup>a</sup>	625	234 <sup>b</sup>	S	Tuzinsky (1987)
	480	1979	9.3 <sup>a</sup>	713	327 <sup>b</sup>	S	Tuzinsky (1987)
	480	1981	9.3 <sup>a</sup>	534	171 <sup>b</sup>	S	Tuzinsky (1987)
	480	1982	9.3 <sup>a</sup>	622	217 <sup>b</sup>	S	Tuzinsky (1987)
	480	1983	9.3 <sup>a</sup>	579	189 <sup>b</sup>	S	Tuzinsky (1987)
	480	1984	9.3 <sup>a</sup>	617	201 <sup>b</sup>	S	Tuzinsky (1987)

**Table A11.8**, continued.

<b>Stand, location</b>	<b>a.s.l.</b>	<b>Year</b>	<b>T</b>	<b>PPT</b>	<b>E<sub>c</sub></b>	<b>Est Reference</b>
Göttinger Wald, C Germany	400	1981	7.9 <sup>a</sup>	1252	260	S Gerke (1987)
	400	1982	7.9 <sup>a</sup>	550	226	S Gerke (1987)
	400	1983	7.9 <sup>a</sup>	635	228	S Gerke (1987)
Eberswalde, NE Germany	50	1997?		659	274	S Müller (2001),
	50	1998		554	250	S Bolte et al. (2001)
Pfinzgau, SW Germany	220	1998	10.3	677	310	TD Lang (1999)
Aubure, E France	1000	1995	6.0	1255	218	TD Granier et al. (2000a)
Hesse, E France	300	1996	9.0 <sup>a</sup>	672	256	TD Granier et al. (2000a)
	300	1997	9.0 <sup>a</sup>	853	253	TD Granier et al. (2000a)
	300	1998	9.0 <sup>a</sup>	974	257	TD Granier et al. (2003)
	300	1999	9.0 <sup>a</sup>	1073	333	TD Granier et al. (2003)
Beerensbusch, NE Germany	78	2002	8.0 <sup>a</sup>	813	213	TD Jochheim et al. (2007)
	78	2003	8.0 <sup>a</sup>	492	237	TD Jochheim et al. (2007)
	78	2004	8.0 <sup>a</sup>	661	235	TD Jochheim et al. (2007)
Hainich, C Germany	300	2001?	7.5	669	164	TD Koch (2002, in Schipka 2003)
Ziegelroda, C Germany	280	1996	6.9	581	216	TB Schipka et al. (2005)
Göttinger Wald, C Germany	400	1995	7.8	595	205	TB Schipka (2003),
	400	1996	5.8	593	225	TB Schipka et al. (2005)
Lüneburger Heide, N Germany	120	1996	6.9	584	272	TB Schipka et al. (2005)
Solling, C Germany	510	1996	5.3	933	303	TB Schipka et al. (2005)
Pol'ana Mts, C Slovakia	850	1996	5.8 <sup>a</sup>	853 <sup>a</sup>	258	TB Střelcová et al. (2002, 2006)
Bornhöved, N Germany	50	1992	9.6	756	421	M Herbst et al. (1999)
	50	1993	7.8	838	326	M Herbst et al. (1999)
	50	1994	8.6	977	389	M Herbst et al. (1999)
	50	1995	8.0	687	419	M Herbst et al. (1999)
	50	1961-1990	8.7	823	340	M Herbst and Hörmann (1998)
	130	1989	-	675	443	M Roberts and Rosier (1994)
Winchester, S UK	130	1990	-	661	403	M Roberts and Rosier (1994)
	130	1991	-	662	333	M Roberts and Rosier (1994)
	100	1999	-	881	305	M Roberts and Rosier (2005a),
Black Wood, S UK	100	2000	-	1119	280	M Roberts et al. (2005)
	300	2001	9.2 <sup>a</sup>	885 <sup>a</sup>	369 <sup>c</sup>	M Owen et al. (2007)
Hainich, C Germany	300	2002	9.2 <sup>a</sup>	885 <sup>a</sup>	374 <sup>c</sup>	M Owen et al. (2007)
	445	2002	7.0 <sup>a</sup>	800 <sup>a</sup>	281 <sup>c</sup>	M Owen et al. (2007)
Sorø, Denmark	40	2001	8.1 <sup>a</sup>	510 <sup>a</sup>	224 <sup>c</sup>	M Owen et al. (2007)
	40	2002	8.1 <sup>a</sup>	510 <sup>a</sup>	218 <sup>c</sup>	M Owen et al. (2007)
Fichtelgebirge, SE Germany	950	1999	6.0	1517	229	TD this study
	950	2000	6.3	1435	207	TD this study
Steigerwald, SE Germany	440	1999	8.6	744	349	TD this study
	440	2000	8.8	798	321	TD this study

**Table A11.8**, continued.

Stand, location	a.s.l.	Year	T	PPT	E <sub>c</sub>	Est	Reference
<b>Mixed beech and oak stands</b>							
Krofdorf, C Germany <sup>d</sup>	280	1982-1986	8.0 <sup>a</sup>	667	206	S	Führer (1990)
	280	1982-1986	8.0 <sup>a</sup>	979	305	S	Führer (1990)
Schönbuch, SW Germany <sup>d</sup>	520	1980	7.3	680	247	S	Fleck (1986), Agster (1986)
	520	1981	7.2	628	277	S	Fleck (1986), Agster (1986)
	520	1982	7.6	966	215	S	Fleck (1986), Agster (1986)
Amance, E France <sup>d</sup>	250	1976	-	421	254	S	Aussenac and Granier (1979)
	250	1977	-	651	300	S	Aussenac and Granier (1979)
Lüneburger Heide, N Germany	95	1991	7.6	669	288	M	Leuschner (1994),
	95	1992	7.7	883	331	M	Backes (1996)
Chimay, SW Belgium <sup>e</sup>	260	1999	8.4 <sup>a</sup>	837	233	TD	Vincke et al. (2005a, b)
	260	2000	8.4 <sup>a</sup>	1197	149	TD	Vincke et al. (2005a, b)
	260	2001	8.4 <sup>a</sup>	1031	179	TD	Vincke et al. (2005a, b)
Steigerwald, SE Germany <sup>d</sup>	440	1996	6.0	676	156	TD	Schäfer (1997)
Horni les, S Czech Republic <sup>f</sup>	160	1972	9.0 <sup>a</sup>	329	210	TB	Cermák et al. (2001)
	160	1973	9.0 <sup>a</sup>	263	385	TB	Cermák et al. (2001)
	160	1974	9.0 <sup>a</sup>	457	207	TB	Cermák et al. (2001)
	160	1978	9.0 <sup>a</sup>	296	454	TB	Cermák et al. (2001)
	160	1979	9.0 <sup>a</sup>	388	387	TB	Cermák et al. (2001)
	160	1982	9.0 <sup>a</sup>	493	230	TB	Cermák et al. (2001)
	160	1988	9.0 <sup>a</sup>	369	210	TB	Cermák et al. (2001)
	160	1996	9.0 <sup>a</sup>	454	314	TB	Cermák et al. (2001)
Steigerwald, SE Germany <sup>d</sup>	440	1999	8.6	744	217	TD	this study, Steinkreuz
	440	2000	8.8	798	202	TD	this study, Steinkreuz
Steigerwald, SE Germany <sup>g</sup>	460	1999	8.6	744	166	TD	this study, Großebene
<b><i>Quercus</i> species</b>							
Hald Ege, NW Denmark <sup>h</sup>	50	1992	7.9 <sup>a</sup>	888	261	S	Ladekarl et al. (2005)
	50	1993	7.9 <sup>a</sup>	959	224	S	Ladekarl et al. (2005)
	50	1994	7.9 <sup>a</sup>	1004	264	S	Ladekarl et al. (2005)
	50	1995	7.9 <sup>a</sup>	770	262	S	Ladekarl et al. (2005)
	50	1996	7.9 <sup>a</sup>	578	230	S	Ladekarl et al. (2005)
	50	1997	7.9 <sup>a</sup>	835	365	S	Ladekarl et al. (2005)
	50	1998	7.9 <sup>a</sup>	1029	322	S	Ladekarl et al. (2005)
	50	1999	7.9 <sup>a</sup>	974	351	S	Ladekarl et al. (2005)
Fontainebleau, C France <sup>i</sup>	136	1981	10 <sup>a</sup>	702	340	S	Nizinski and Saugier (1989)
	136	1982	10 <sup>a</sup>	718	241	S	Nizinski and Saugier (1989)
	136	1983	10 <sup>a</sup>	775	284	S	Nizinski and Saugier (1989)
Champenoux, E France <sup>i</sup>	237	1991	9.6	759	294	TD	Bréda et al. (1993a)

<sup>a</sup> Long-term average.<sup>b</sup> Evapotranspiration.<sup>c</sup> Annual evapotranspiration.<sup>d</sup> *F. sylvatica*, *Q. petraea*; beech dominating stand structure.<sup>e</sup> *Q. robur*, admixed *Acer pseudoplatanus*, *Fraxinus excelsior*.<sup>f</sup> *Q. robur*, admixed *Fraxinus excelsior*, *Tilia cordata*.<sup>g</sup> *Q. petraea*, *F. sylvatica*.<sup>h</sup> *Q. petraea*, *Q. robur* and hybrids.<sup>i</sup> *Q. petraea*.



## **Erklärung**

Hiermit erkläre ich, die vorliegende Arbeit selbstständig verfasst und keine anderen als die angegebenen Quellen und Hilfsmittel benutzt zu haben sowie weder diese noch eine gleichartige Doktorprüfung an einer anderen Hochschule endgültig nicht bestanden zu haben.

Markus Schmidt